TECHNISCHE UNIVERSITÄT MÜNCHEN
Integrative Research Center Campus Straubing für Biotechnologie und Nachhaltigkeit

Conversion of Monoterpenes and Isoprene to New Bio-Based Products

Paul Stockmann

Vollständiger Abdruck der von der promotionsführenden Einrichtung Campus Straubing für Biotechnologie und Nachhaltigkeit der Technischen Universität München zur Erlangung des akademischen Grades eines

Doktors der Naturwissenschaften (Dr. rer. nat.)

genehmigten Dissertation.

Vorsitzender:	Prof. Dr. Sebastian J. Goerg
Prüfer der Dissertation:	1. Prof. Dr. Volker Sieber
	2. Prof. Dr. Cordt Zollfrank
	3. Prof. Dr. Thomas Rosenau

Die Dissertation wurde am 30.08.2019 bei der Technischen Universität München eingereicht und von der promotionsführenden Einrichtung Campus Straubing für Biotechnologie und Nachhaltigkeit am 18.05.2020 angenommen.

Conversion of Monoterpenes and Isoprene to New Bio-Based Products

Prüfungsrechtliche Erklärung

Ich versichere, dass ich die Arbeit selbständig verfasst, nicht anderweitig für Prüfungszwecke vorgelegt, alle benutzten Quellen und Hilfsmittel angegeben sowie wörtliche und sinngemäße Zitate als solche gekennzeichnet habe.

Plagiarism Declaration in Accordance with Examination Rules

I herewith declare that I have worked on this thesis independently. Furthermore, it was not submitted to any other examining committee. All sources and aids used in this thesis, including literal and analogous citations, have been identified.

Straubing, 27.10.2020

Paul Stockmann

Acknowledgements

Foremost, I would like to express my gratitude to Prof. Volker Sieber for giving me the opportunity to work on this very interesting and important project and to be part of the CBR chair and the Fraunhofer IGB Electro and Chemocatalysis BioCat, Straubing branch.

Besides, I would like to thank the other professors of my thesis committee XX and XX.

My sincere thanks also go to my mentor Priv.-Doz. Dr. Malte Winnacker.

Furthermore, I want to thank my colleagues at BioCat, especially Dr. Harald Strittmatter, Marion Wölbing and Claudia Falcke and my PhD fellows Melanie Iwanow, Steffen (Stefan?) Roth and Sumanth Ranganathan (special thanks for proofreading!). I also want to thank all the students I supervised, especially Dominik Pastötter, Moritz Höhenberger and Johannes Raab for their valuable scientific contributions and their friendship.

I also want to thank the best football club in Bavaria and the world, the Grasshoppers Straubing, for the great team spirit and the outstanding football performances I was allowed to witness. Hopp! Hopp! Hopp!

Most important, I want to thank my parents for their unlimited support, my sister for being a great example in self-discipline and toughness, and Kati for enriching my life with her love.

Abstract

Plastics and fuels are used in multimillions of tons every year, and the consumption is constantly increasing. This demand is met by fossil oil as raw material for monomers and gasoline, diesel, kerosene, etc. In agreement with the principles of green chemistry, resources such as biomass or side streams of industrial processes are considered as a sustainable alternative. During the last decades various bio-based fuels, for example bio-ethanol and bio-diesel, have been established. In addition, bio-based polymers were introduced to the market, representatively polyamides based on castor oil and polyesters from lactic acid. However, challenges remain as these "green" alternatives often suffer from low availability of the bio-source, comparably low performance, high costs, competition with the food industry, and others.

In the first part of this work, isoprene is converted to a β-lactam that is successfully converted into a polyamide with a side chain barring a terminal alkene, which could be further functionalized to tailor the polymer properties. The T_g was 97 °C and T_m was 240 °C. A δ-lactone and isoprene epoxide for polyester or polyether were also produced.

The potential of bio-based isoprene as precursor for fuels is evaluated in a review, focusing on the chemical methods for linear dimer- and trimerization. Palladium catalysts, Ziegler Natta catalysts and other methods, such as ionic liquids, are the reported methods for this reaction. Although some promising processes were described, the costs and relatively low selectivity are challenges that need resolving before isoprene can be considered as a bio-precursors for fuels.

Within the second part of this work, monoterpenes were identified as a highly abundant class of bio-molecules with outstanding structural variety, enabling chemical modification for the generation of new monomers. As the unique chemical structures lead to new substituent patterns in the polymer backbone, new properties compared to classical polyesters and polyamides were expected. Thermal high-performance properties, caused by rigid cyclic structures in the polymer backbone, were focused on in particular. Some of their most prominent representatives, namely limonene, α-pinene, and (+)-3-carene were investigated. Limonene and (+)-3-carene were converted to diols, which are considered as one of the most important class of monomers as they are used in polyesters and polyurethanes. The first step of the conversion was an oxidative olefin cleavage, leading to ketoaldehydes which were subsequently reduced to the desired diols. Exemplary enzymatically and chemically catalyzed polymerizations were successfully performed with commercial aromatic and aliphatic dicarboxylic acids, underlining the general potential of terpene-based diols. The application of the obtained ketoaldehydes as platform chemical for hydroxy carboxylic acids, amido acids and diamines was also outlined.

(+)-3-carene and α-pinene were also utilized as precursor for β- and ε-lactams, which can be used as monomers for polyamides of the type polyamide 2 (PA 2) and polyamide 6 (PA 6). The β-lactams were obtained in a one-step reaction with chlorosulfonyl isocyanate. The anionic ring opening polymerization was accomplished; however – in particular the α-pinene based polyamide – was challenging to characterize, and the obtained materials seemed unsuitable for classical polyamide applications. Nonetheless, their potential as co-monomer for classical polyamides is worth exploring. The synthesis of the ε-lactams was achieved in a multi-step reaction following the synthesis pathway of caprolactam, which is the monomer of polyamide 6. These steps are: initial oxidation of an olefin to an alcohol, ketone formation, conversion to the corresponding oxime and Beckmann rearrangement to the lactam. The α-pinene based ε-lactam could only be oligomerized, and the polymerization conditions need to be optimized for better results. Poly-3R-caranamide, obtained from the (+)-3-carene based 3R-caranlactam was amorphous and possessed a glass transition (T_g) at 120 °C and molecular weights above 30 kg/mol, which is well in the range of industrial polyamides.

The synthesis of the (+)-3-carene based lactam was optimized, the key step being the ketone formation by epoxidation and subsequent rearrangement instead of hydroxylation and oxidation. Depending on the epoxidation method, stereoisomeric epoxides were obtained. The establishment of a diastereoselective rearrangement led to the selective synthesis of two different lactams; the previously mentioned 3R-caranlactam and a methyl-group diastereomer, 3S-caranlactam. The corresponding polyamides poly-3R-caranamide and poly-3S-caranamide highly differ in their properties, as poly-3S-caranamide is semi-crystalline instead of amorphous, with a high-performance melting temperature (T_m) of up to 280 °C. The production of 3S-caranlactam was scaled to four liter in a sustainable one-vessel process, reaching a total yield of 25w% over four steps. Co-polymerizations with caprolactam and laurolactam were also investigated, and the integration of the bulky three-membered ring of 3S-caranlactam in the polymer backbone led to increasing amorphousness and T_g.

“When we see that we may produce hundreds of compounds from simple hydrocarbons and chlorine and that from each one of them we may obtain a great number of others… we ask with some anxiety whether, in a few years’ time, it will be possible to find our way in the labyrinth of organic chemistry.” Auguste Laurent, 1854

List of contents

1 Introduction 1
1.1 Isoprene: General background 1
1.2 Biosynthesis of isoprene 1
1.3 Biotechnological isoprene production 4
1.4 Industrial chemical isoprene production 4
1.5 Recent applications of isoprene 5
1.6 General background: Polyesters and polyamides 7
1.7 Polycondensation of polyesters and polyamides 12
1.8 Ring opening polymerization of polyesters and polyamides 14
1.9 Bio-based polyesters and polyamides 17
1.10 General background: Monoterpenes 20
1.11 Monoterpenes as resource for polyesters: Selected examples 22
1.12 Monoterpenes as resource for polyamides: Selected examples 26
1.2 Objectives 29
1.2.1 Isoprene as precursor for bio-fuels 29
1.2.2 Isoprene as starting material for monomers for new isoprene-based polymers 29
1.2.3 Synthesis and polymerization of monoterpene-based lactams 29
1.2.4 Synthesis of diols from terpenes 30
2 Results 31
2.1 Oligomerization of isoprene to linear dimers and trimers for advanced bio-fuels 31
2.2 Isoprene derivatives as valuable monomers 67
2.2.1 Reactions of isoprene with chlorosulfonyl isocyanate (CSI) 68
2.2.2 Synthesis of 4-methyl-4-vinylazetidin-2-one (2) 70
2.2.3 Initial polymerization of 4-methyl-4-vinylazetidin-2-one (2) 72
2.2.4 Synthesis of 4-methyl-1,6-dihydropyridin-2(3H)-one (3) and 4-methyl-5,6-dihydropyridin-2(1H)-one (4) 75
2.2.5 Synthesis of 4-methyl-1,6-dihydropyridin-2(3H)-one (5) and 4-methyl-5,6-dihydropyridin-2(1H)-one (6) 77
2.2.6 Synthesis of 2-methyl-2-vinyloxirane (7) 77
2.3 New Bio-Polyamides from Terpenes: α-Pinene and (+)-3-Carene as Valuable Resources for Lactam Production 80
2.4. Biobased chiral semi-crystalline or amorphous high-performance polyamides and their scalable stereoselective synthesis 90
2.5 Limonene, α-pinene, and (+)-3-carene as precursor for diol monomers 105
2.5.1 Oxidative cleavage of limonene, α-pinene, and (+)-3-carene 105

2.5.2 Initial polymerizations of 3-(prop-1-en-2-yl)heptane-1,6-diol (11) 108

3. Discussion 112

3.1 Isoprene as precursor for bio-fuels 112

3.2. Isoprene as precursor for β-lactams, δ-lactams, and δ-lactones 114

3.3 Conversion of α-pinene and (+)-3-carene to PA6-type bio-polyamides 115

3.4 Conversion of (+)-3-carene and limonene to polymerizable diols 122

3.5 Conclusion 124

4. Methods 125

4.1 Methods section 2.2 “Isoprene derivatives as valuable monomers” 125

4.2 Methods section 2.3 “New Bio-Polyamides from Terpenes: α-Pinene and (+)-3-Carene as Valuable Resources for Lactam Production 141

4.3 Methods section 2.4 “Biobased Chiral Semi-Crystalline or Amorphous High-Performance Polyamides and their Scalable Stereoselective Synthesis 186

4.4 Methods section 2.5 “Limonene, α-pinene, and (+)-3-carene as precursor for diol monomers” 296

5 Lists 308

7. References 314

1 Introduction

During the last decades, as a consequence of dwindling resources, the investigation of alternative raw materials for a medium-term replacement of fossil-oil based fuels and plastics has become a focus of research. In this regard, isoprene, which probably will be industrially accessible from bio-resources or CO_2 on medium-term, was identified as a promising C5-diolefine. In this context, biogenic dimers of isoprene, which are called monoterpenes, are another high abundant 'green' feedstock that could be utilized, especially for bio-based plastics. The following section describes the general properties and applications of these compounds and outlines the potential in the context of new bio-based products. For this, some relevant aspects of polymer chemistry are briefly addressed, as well as a state-of-the-art overview of already existing monoterpene-based polymers.

1.1 Isoprene: General background

Isoprene (2-methylbuta-1,3-diene) is a colorless, volatile liquid with a boiling point of 34 °C. It is one of the most abundant organic substances in nature, as it is produced by animals, plants, bacteria or fungi. Over 500 Mt are released into the atmosphere each year, accounting for 40% of all biogenic isoprenoid emissions.[1] However, its concentration in these organisms is relatively low.[1–3] The reasons for organisms to emit isoprene are still a topic of ongoing research. The self-cooling of plants could be involved, as heat-stress has been shown to induce the release of isoprene.[4] Apart from its role as a building block for terpenes, the functions in the organisms seem to be diverse. Isoprene has been suggested as a trait against thermal and oxidative stresses and drought or as electron-transfer support in the photosystem II.[4–8] Despite the great variety of isoprene producing organisms, only two different pathways for natural occurring isoprene have been identified so far– the methylerythritol phosphate (MEP) and the mevalonate (MVA) pathway.

1.2 Biosynthesis of isoprene

The MEP pathway is found in plants, bacteria, and eukaryotic parasites, whereas the MEP pathway occurs in archaea, bacteria, and most eukaryotes. The usual initial carbon source are sugars.[2] Both ways lead to isopentenyl pyrophosphate (IPP) and dimethylallyl pyrophosphate (DMAPP), which are isomers interconverted by an isomerase (Scheme 1.1).[2,7] In the MEP pathway, the first reaction step is the formation of an oxidized C6 molecule from pyruvate and glyceraldehyde, which is subsequently reduced and rearranged by various enzymes to give the desired product.[9] From a chemists' perspective, the formation of an eight-membered ring in 2-C-methyl-D-erythritol-2,4-cyclodiphosphate is worth mentioning, as a similar synthesis would be very challenging with chemical methods. The strategy in the MVA pathway is different, as the C6 molecule mevalonate is built up from identical C2-units (3 x Acetyl-CoA) and is then reduced to IPP/DMAPP under application of adenosine triphosphate (ATP). In the last step, DMAPP is converted to isoprene by isoprene synthase.[2,7,9]

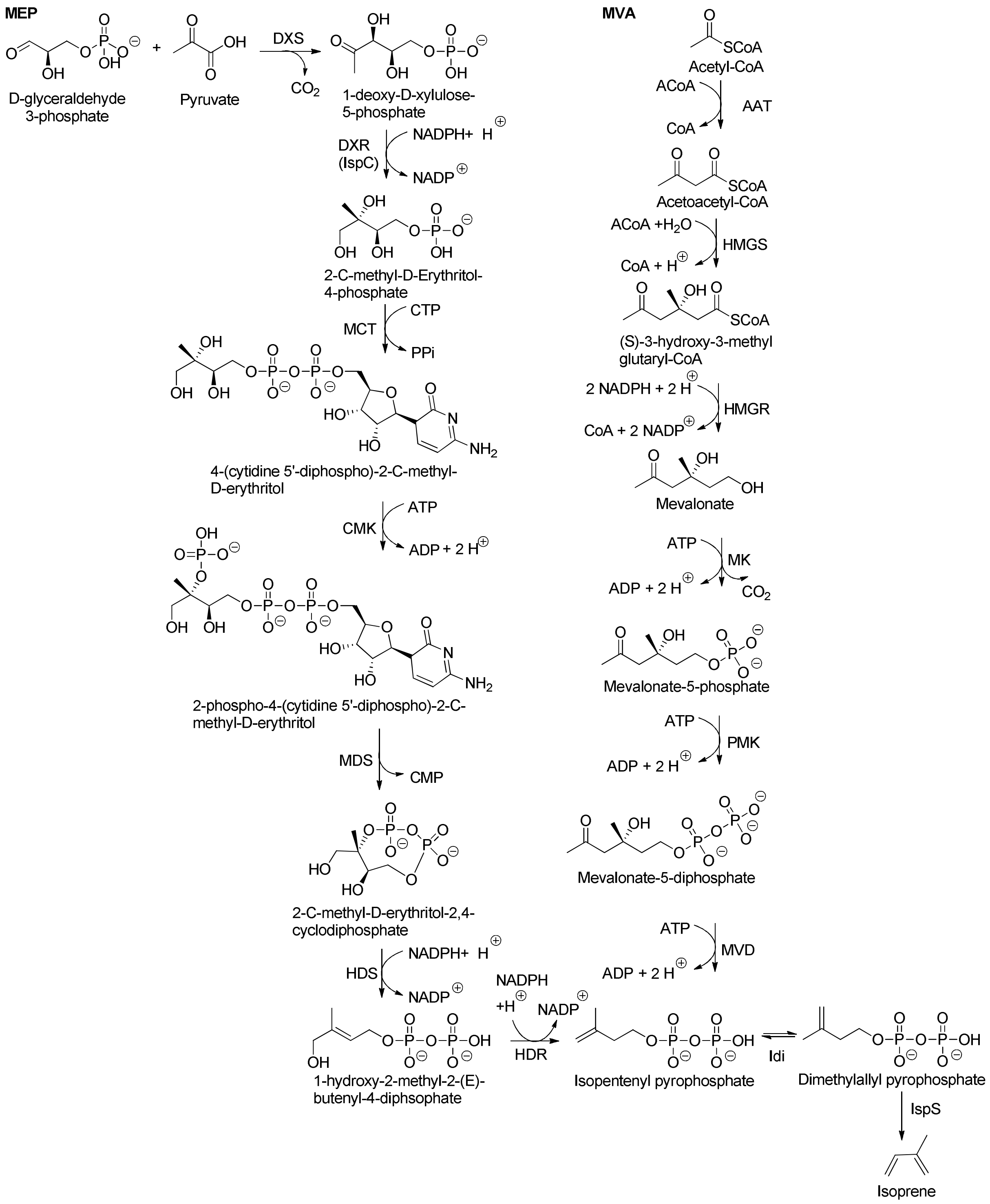
MEP
D-glyceraldehyde 3-phosphate
Pyruvate
DXS
CO2
1-deoxy-D-xylulose-5-phosphate
DXR (IspC)
NADPH+ H
NADP
2-C-methyl-D-Erythritol-4-phosphate
MCT
CTP
PPi
4-(cytidine 5'-diphospho)-2-C-methyl-D-erythritol
CMK
ATP
ADP + 2 H
2-phospho-4-(cytidine 5'-diphospho)-2-C-methyl-D-erythritol
MDS
CMP
2-C-methyl-D-erythritol-2,4-cyclodiphosphate
HDS
NADPH+ H
NADP
1-hydroxy-2-methyl-2-(E)-butenyl-4-diphsophate
NADPH +H
NADP
HDR
Isopentenyl pyrophosphate
Idi
Dimethylallyl pyrophosphate
IspS
Isoprene
MVA
Acetyl-CoA
ACoA
AAT
CoA
Acetoacetyl-CoA
ACoA +H2O
HMGS
CoA + H
(S)-3-hydroxy-3-methyl glutaryl-CoA
2 NADPH + 2 H
HMGR
CoA + 2 NADP
Mevalonate
ATP
MK
ADP + 2 H
CO2
Mevalonate-5-phosphate
ATP
PMK
ADP + 2 H
Mevalonate-5-diphosphate
ATP
MVD
ADP + 2 H

Scheme 1.1 Biosynthesis of isoprene following the methylerythritol phosphate (MEP) and the mevalonate pathway (MVA). MEP: DXS 1-deoxyxylulose-5-phosphate synthase, DXR 1-deoxy-Dxylulose-5-phosphate reductoisomerase, CMK 4-diphophocytidyl-2-C-methyl-D-erythritol kinase, MCT 4-diphosphocytidyl-2-C-methyl-D-erythritol synthase, MDS 2-C-methyl-Derythritol 2,4-cyclodiphosphate synthase, HDS 1-hydroxy-2-methyl-2-(E)-butenyl 4-diphosphate synthase, HDR hydroxymethylbutenyl diphosphate reductase. MVA: AAT Acetyl-CoA C-acetyltransferase, HMGS hydroxymethylglutaryl-CoA synthase, HMGR hydroxymethylglutaryl-CoA reductase, MK mevalonate kinase,, PMK phosphomevalonate decarboxylase, MVD diphosphomevalonate decarboxylase.[2,7,9]

1.3 Biotechnological isoprene production

Several procedures for isoprene production in various organisms have been described.[2] Relevant organisms are *B. subtilis*, *E. coli*, *cyanobacteria* and *S. cerevisiae.*[10] The most successful approach at present was reported by Goodyear.[11] An *E. coli* strain was engineered to produce 60g/L isoprene in a continuous process with a volumetric productivity of 2.0 g L^{-1} h^{-1} and a cell productivity of 0.85 g L^{-1} h^{-1} isoprene/g dry cell. Still, the yield with respect to glucose was only 11w% (theoretical maximum: 38w%). The documented challenges of the biotechnological isoprene production are plasmid instability, multi-gene integration, the use of cost-increasing antibiotics and glucose as carbon source, as it is competitive to food industry and comparably expensive.[2] Although several big companies such as Goodyear, DuPont or Bridgestone are involved in the research for bio-based isoprene production, only GlycosBio has built a commercial facility so far. The maximum capacity is 40 kt isoprene annually.[12]

1.4 Industrial chemical isoprene production

Isoprene is almost exclusively produced from fossil feedstocks, with an annual volume of close to 1.0 Mt in 2011.[3] For the industrial chemical production of isoprene there are three major methods currently available:[13,14]

- Recovery of isoprene from C_5 streams
- Dehydrogenation of iC_5H_{12}
- Synthesis from iC_4H_8 and formaldehyde

Isoprene can be obtained from waste streams of cracking processes. In the pyrolysis of hydrocarbons to ethylene, a C_5 side stream is formed (10w% with respect to ethylene) that contains 15w%-20w% isoprene, which can be separated by advanced distillation methods. The total yield of isoprene is only about 3w%.[13] Therefore, it is challenging to produce enough of the C_5 fraction for the distillation plant. Additionally, the amount of side-stream isoprene will be decreased by technical improvements of the ethylene production process, and the method will probably lose its importance.

The catalytic dehydrogenation of iC_5H_{12} is another approach for isoprene production that utilizes C_5 fractions from cracking. The dehydrogenation is achieved by several different strategies, including one-step-, two-step- or oxidative dehydrogenation.[14] An example for the one-step process is the Houdry-catadiene procedure that uses Cr_2O_3/Al_2O_3-catalysts at about 850 K and a pressure of 7 kPa, yielding 52w% isoprene in appreciable quality.[15] Other catalysts such as Fe_2O_3-Cr_2O_3-K_2CO_3 – at about 800 K – achieve a yield of 85w%.[3] In all cases, high temperatures are required and considerable amounts of side products are generated. Another drawback is the use of iC_5H_{12}, high-quality gasoline, leading to comparably high substrate costs and low availability.

The reaction of iC_4H_8 and formaldehyde to isoprene can be achieved by different strategies, namely the Kuraray-method, the DMD-method and the Eurochim-method.[13] As the Kuraray-method is not open to the public and the DMD-method has several disadvantages like bad atom economy or high energy consumption, only the Eurochim-method is discussed briefly (Scheme 1.2).

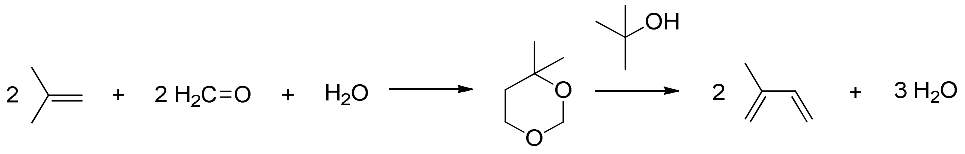

Scheme 1.2 Eurochim-method for the synthesis of isoprene from iC_4H_8 and formaldehyde.

Two molecules of iC_4H_8, two molecules of formaldehyde and water form a substituted dioxane compound that subsequently reacts with *t*BuOH to two molecules of isoprene and water. All reactions are carried out in the liquid phase. This method was developed in the 1990ies by the Russian company EuroChim and reached 39% of total isoprene production in 2013 in Russia, as proclaimed by the developer.[13,16] The advantages compared to the DMD-process are: (I) decreased energy consumption, (II) increased atom economy, (III) less emissions and (IV) useful side products.

To summarize, the EuroChim method seems to possess the highest potential for isoprene production and the most promising future opportunities when compared to the production methods currently available.

1.5 Recent applications of isoprene

Isoprene is mainly utilized as a monomer for elastomers for gloves, shoes or rubber bands. The most commonly used elastomer derived from isoprene is poly(*cis*-1,4-isoprene, Figure 1.1 a). This synthetic rubber is the most suitable substitute for natural rubber, which is most commonly used in the tire industry.[15] The *trans*-isomer is used mainly for cable insulations. Other than that, isoprene is also a component of styrene-isoprene-styrene (SIS) block copolymers, an important thermoplastic elastomer (Figure 1.1 a). SIS contain up to 88w% isoprene. Butyl rubber is a copolymer of isoprene and isobutene. Only 3w% of isoprene is typically used in butyl rubbers, but this is sufficient to lower the gas permeability significantly. About 95% of the annual isoprene consumption is for these polymers; the remaining 5% are used as precursors for pharmaceuticals, perfumes or additives (Table 1.1, Figure 1.1 b).

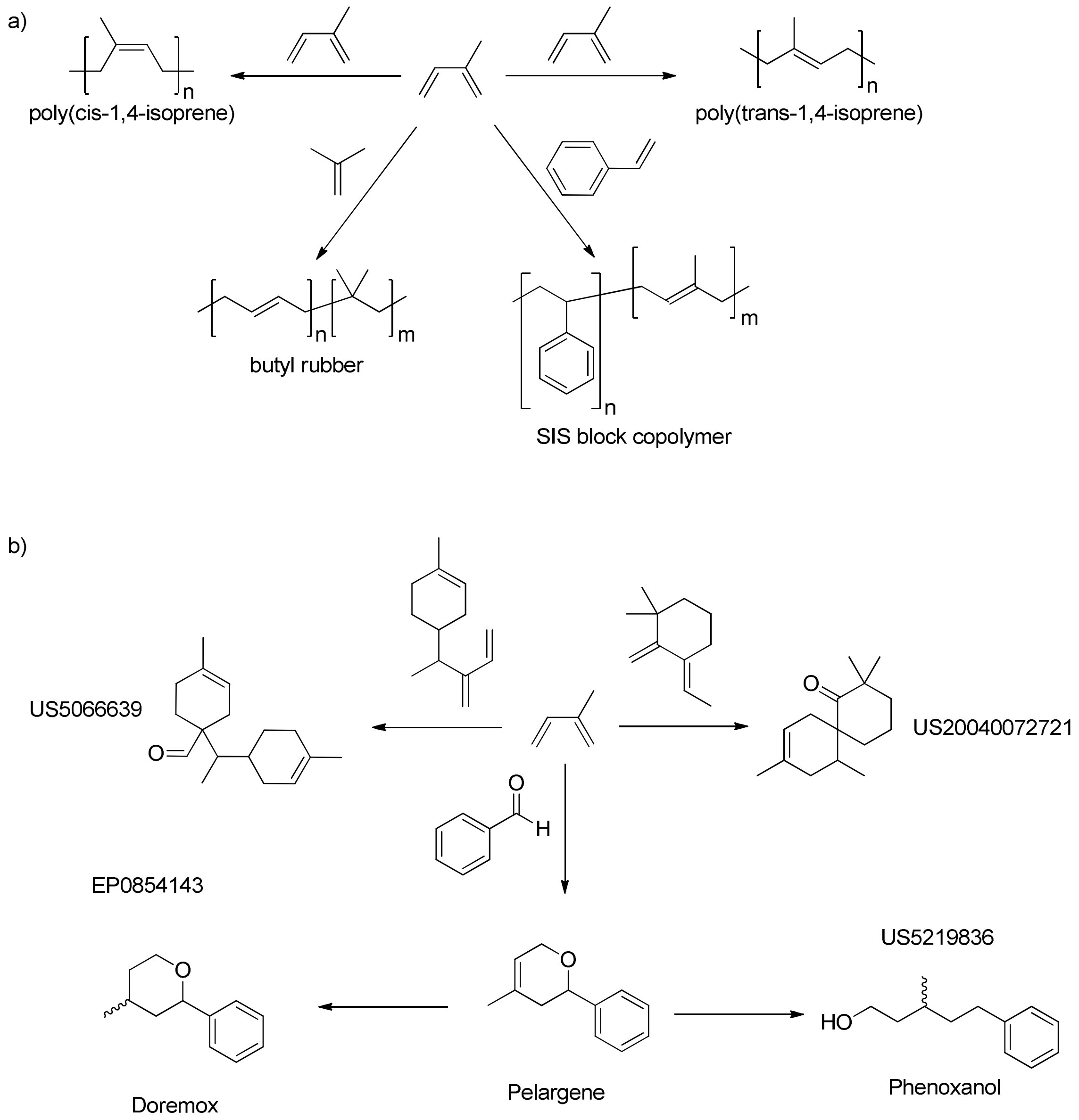
a)
poly(cis-1,4-isoprene)
poly(trans-1,4-isoprene)
n
m
butyl rubber
SIS block copolymer
b)
US5066639
US20040072721
EP0854143
US5219836
O
H
HO
Doremox
Pelargene
Phenoxanol

Figure 1.1 a) Important isoprene polymers and b) Several perfumes derived from isoprene.[17]

Table 1.1 Isoprene (**1**)-based fine chemicals and their applications as commercialized by Kuraray Co., Ltd.

Structure	Name	Applications (selection)
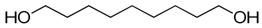	nonane-1,9-diol	Pharmaceuticals
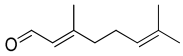	3,7-dimethylocta-2,6-dienal	Vitamin A
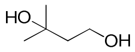	3-methylbutane-1,3-diol	Cosmetics
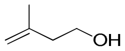	3-methylbut-3-en-1-ol	Aroma chemicals
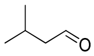	3-methylbutanal	Aroma chemicals
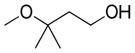	3-methoxy-3-methylbutan-1-ol	Cleaners
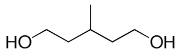	3-methylpentane-1,5-diol	Polymer additive
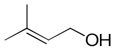	3-methylbut-2-en-1-ol	Aroma chemicals

1.6 General background: Polyesters and polyamides

Polyesters and polyamides are thermoplastic materials, which means they can be reversibly reformed as they are malleable or moldable at certain temperatures without degradation. Thermoplastics are usually divided in groups: commodity-, engineering-, and high-performance polymers.[18] This can be seen in the polymer pyramid diagram (Figure 1.2). As a rule, polymers with high heat resistance and exceptional mechanic properties – associated with high prices – are on top of the pyramid. However, depending on the focused properties, the categorization is not fixed, and commodity materials are counted to the engineering plastics and *vice versa*.

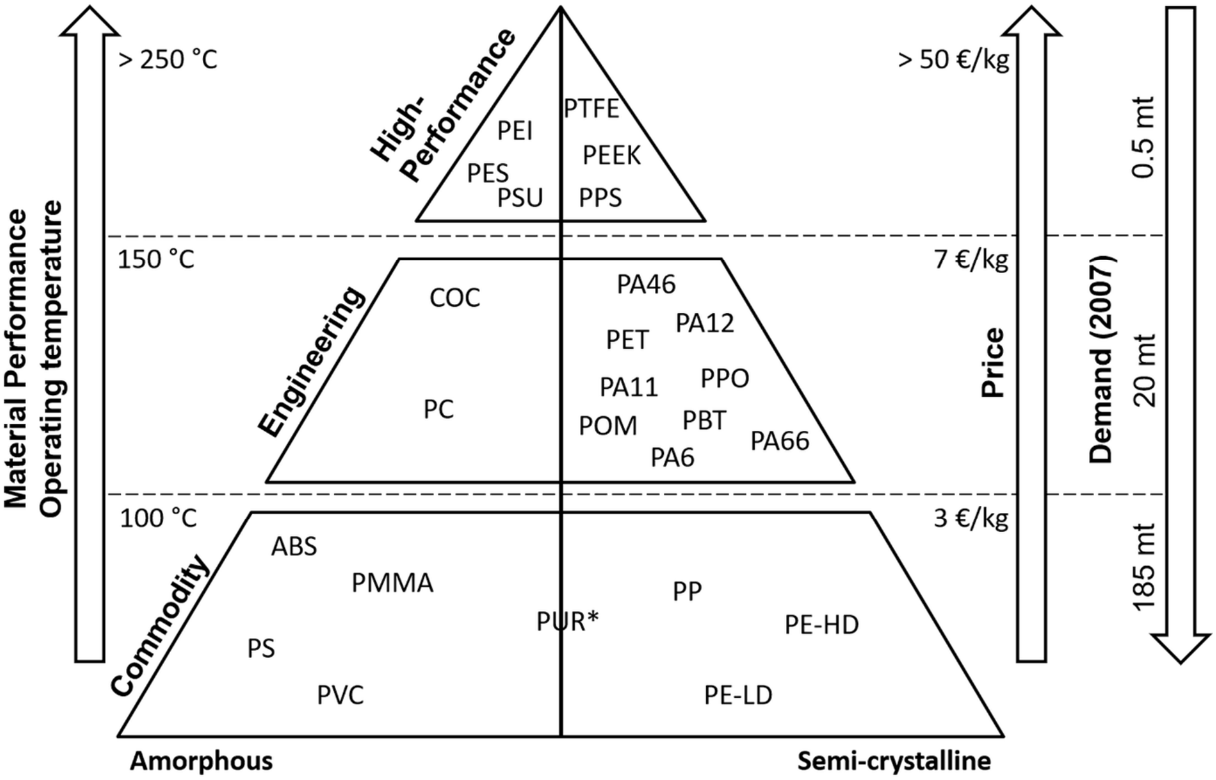
Material Performance
Operating temperature
> 250 °C
150 °C
100 °C
High-Performance
Engineering
Commodity
PEI
PES
PSU
PTFE
PEEK
PPS
COC
PC
PA46
PA12
PET
PA11
PPO
POM
PBT
PA6
PA66
ABS
PMMA
PUR*
PP
PE-HD
PS
PVC
PE-LD
Amorphous
Semi-crystalline
> 50 €/kg
7 €/kg
3 €/kg
Price
Demand (2007)
0.5 mt
20 mt
185 mt

Figure 1.2 Polymer pyramid. Amorphous high-performance: Polyetherimide (PEI), poly(ether sulfone) (PES), polysulfone (PSU); Amorphous engineering: Cyclic olefin copolymer (COC), polycarbonate (PC); Amorphous commodity: Acrylonitrile butadiene styrene (ABS), poly(methyl methacrylate) (PMMA), polystyrene (PS), poly(vinyl chloride) (PVC); Semi-crystalline high-performance: Poly(tetrafluoro ethylene) (PTFE) , poly(ether ketone) (PEEK), poly(phenylene sulfide) (PPS); Semi-crystalline engineering: Polyamide 46 (PA46), polyamide 12 (PA12), poly(ethylene terephthalate) (PET), poly(*p*-phenylene oxide), poly(butylene terephthalate) (PBT), poly(oxy methylene), polyamide 6 (PA6), polyamide 66 (PA66); Semi-crystalline commodity: Polypropylene (PP), polyethylene high-density (PP-HD), polyethylene low-density (PP-LD);*Depending on polyurethane (PUR) type.[18–20]

Polyesters are defined by their repetitive ester group in the polymer backbone, whereas polyamides contain an amide group instead. In general, polyesters are synthesized by a polycondensation reaction between a diacid and a diol; in polyamides, a diamine replaces the alcohol. The resulting polymers are so-called AA/BB-types, with AA/BB describing the pattern of the functional groups in the main chain. Alternatively, cyclic esters (lactones) or amides (lactams) can be converted to their corresponding polymer by ring-opening polymerization (ROP)[21] to produce AB-type polymers.

In most polyesters, either the acid or the diol contains an aromatic domain to enhance the thermal and mechanic properties. The most abundant polyester resin is poly(ethylene terephthalate) (PET), with a total consumption of almost 2.2 Mt in 2018 in western Europe alone. The global demand was 76.8 Mt.[22] PET is mainly used for fibers and in the packaging industry, e.g. for bottles, but also for high quality construction materials. In general, especially because of their low prices, polyesters are by far the most used synthetic fibers; for engineering applications, the contribution is more balanced (Figure 1.3).[23]

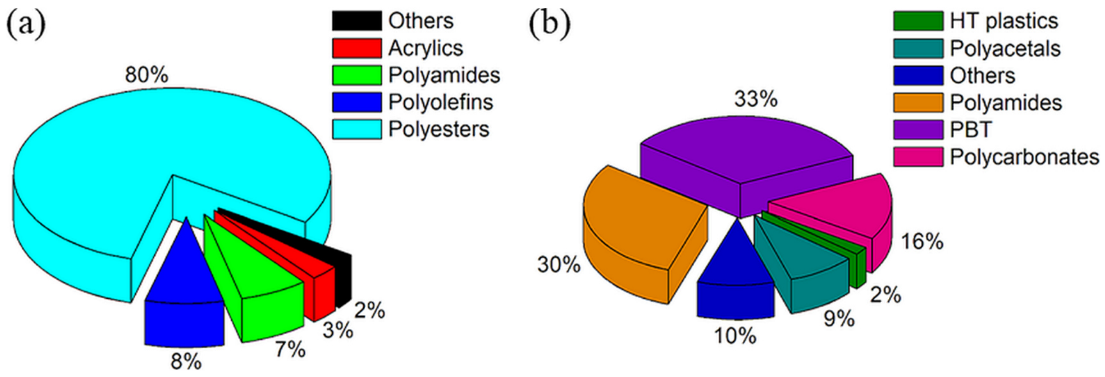

Figure 1.3 Contribution of plastics for synthetic fibers (a) and engineering applications (b).[23]

Other polyesters containing aromatic diacids are poly(butylene terephthalate) (PBT) – with an annual consumption of almost one Mt worldwide,[22] poly(ethylene naphthalate) (PEN), or Tritan, consisting of terephthalic acid, 2,2,4,4-tetramethyl-1,3-cyclobutanediol, and cyclohexanedimethanol (Figure 1.4).[22] As can be seen by comparison of the properties of PET and PBT (Table 1.2), increasing the chain length of the aliphatic linear monomer unit (ethylene glycol *versus* 1,4-dibutanol) results in a decreasing glass transition temperature (T_g) and melting temperature (T_m). Purely aliphatic examples are polycaprolactone (PCL), polylactic acid (PLA), and polyhydroxy butyrate (PHB). A special case is polycarbonate (PC) – derived from phosgene and diols – that are often considered to be polyesters as well,[24] although the carbon atom of the repeating functional group possesses a higher oxidation state.

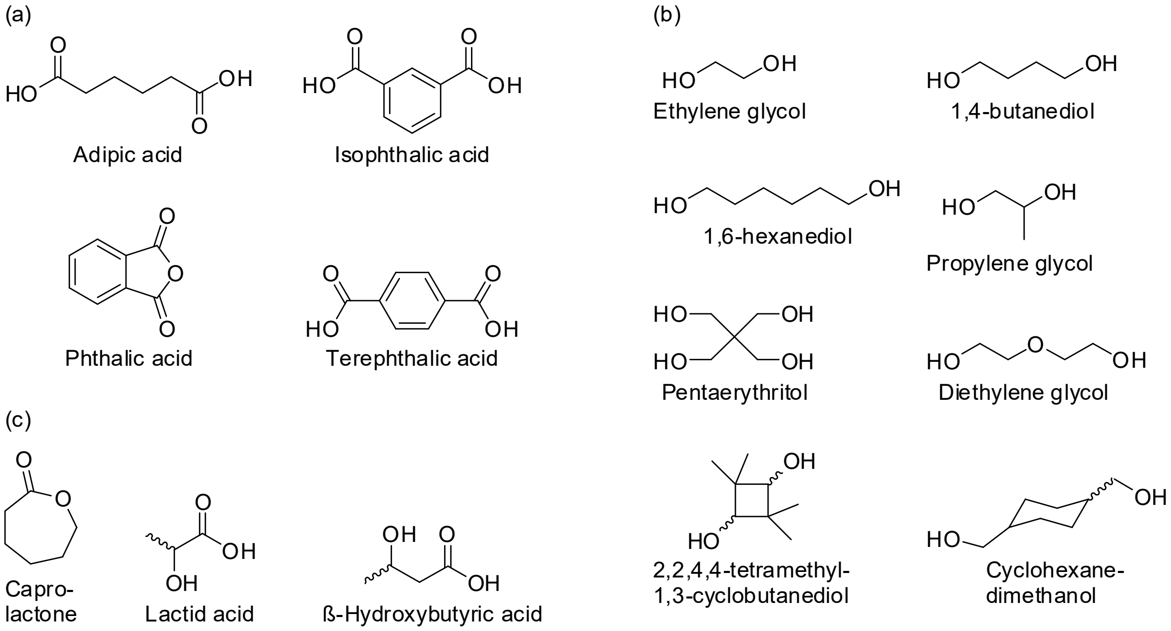
(a)
Adipic acid
Isophthalic acid
Phthalic acid
Terephthalic acid
(b)
Ethylene glycol
1,4-butanediol
1,6-hexanediol
Propylene glycol
Pentaerythritol
Diethylene glycol
2,2,4,4-tetramethyl-1,3-cyclobutanediol
Cyclohexane-dimethanol
(c)
Capro-lactone
Lactid acid
ß-Hydroxybutyric acid

Figure 1.4 Selection of typical diacids (a) and diols (b) for AA/BB-type polyester and AB-type monomers (c).[22]

Table 1.2 Technical data of PET, PBT and PC.[21,25]

Property [unit]	**PET (crystalline)**	**PBT**	**PC**
Tensile modulus [MPa]	2800	2500	2400
Stress at yield [MPa]	80	60	66
Elongation at break [%]	70	200	>80
Glass transition [° C]	70	47	147
Melting Point [° C]	250	225	-
Deflection temperature at 1.8 MPa [° C]	60-70	50-65	125-135
Minimal use temperature [° C]	-50	-50	-100
Density [g/cm^3]	1.40	1.30	1.20
Transparency	Opaque	Opaque	Clear
Resistance to chemicals[25]			
Aliphatic solvents	+	+	+
Aromatic solvents	+	0	-
Acetone	0	-	-
Hot water (hydrolysis resistance)	-	-	-
Weak/strong mineral acids	+/0	+/0	+/0
Weak/strong organic acids	+/-	+/-	+/0
Weak/strong alkalis	0/-	0/-	-/-
UV light and weathering	0	0	0

Although aromatic high-performance polyamides (usually called aramids, such as Kevlar® or Nomex®) exist,[26,27] by far the most common polyamides are aliphatic and linear. The most prominent examples are PA6 and PA66, formed from caprolactam or the polycondensation of hexamethylene diamine and adipic acid, respectively. The worldwide demand for polyamides was 7.4 Mt in 2016, the sales reached almost 25 billion US dollars (USD) in 2014, and the predicted annual increase is 2.3%-5.4% until 2022.[23] In general, polyamides are engineering or high-performance polymers that are characterized by their toughness, chemical resistance, high strength, temperature stability, and good processability (Table 1.3); they are used in all types of industry (Figure 1.5).[28]

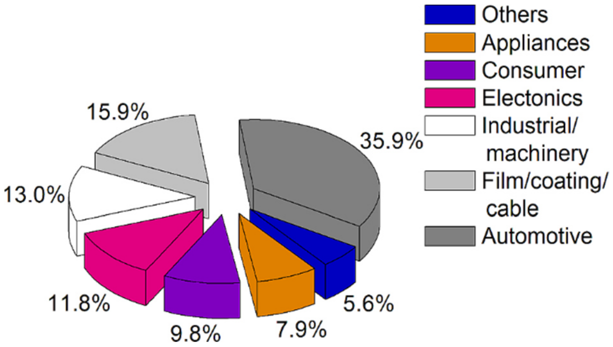

Figure 1.5 Applications of polyamides.[28]

PCL and PA6 are structurally similar, apart from the ester/amide group. Nonetheless, the melting temperature of PCL is only 60 °C, which is 160 °C below PA6. This is caused by the hydrogen-bonding of the amide groups. The ability to form -NH···O=C- bonds between the polymer chains is the key aspect of polyamides. Many of their properties, e.g. melting temperature and water uptake, can directly be attributed to these bonding and the ratio of CNOH to CH_2 in the main chain, as illustrated by comparison of the melting temperature of PA610 and PA46 (Table 1.3, Figure 1.6). Additionally, the structure of the main chain is important, which can be described by comparing PA6 and PA66. Both polyamides possess the same CH_2/CNOH ratio, but the increased symmetry of PA66 facilitates the formation of hydrogen bonds. Consequently, the melting temperature also reaches higher values.

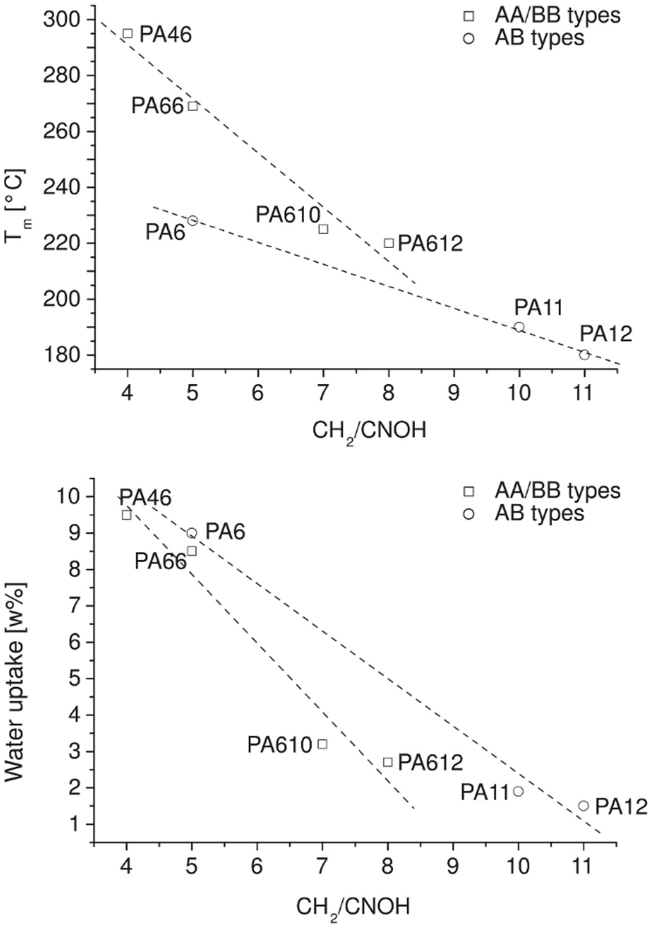

Figure 1.6 Dependence of T_m (upper) and the water uptake (lower) of the CH_2/CNOH ratio for various polyamides.[21,28]

Table 1.3 Technical data of AA/BB and AB type polyamides.[21,25] ND = no data.

Property [unit]	**PA46**	**PA66**	**PA610**	**PA6**	**PA12**
Tensile modulus [MPa]	3300	3100	2400	3000	1500
Stress at yield [MPa]	100	85	70	80	46
Elongation at break [%]	30	40	ND	70	280
Glass transition [° C]	74	50	45	47	38
Melting Point [° C]	295	260	210	220	180
Deflection temperature at 1.8 MPa [° C]	160	70-100	60	55-80	40-50
Minimal use temperature [° C]	ND	-40	ND	-40	-70
Density [g/cm^3]	1.18	1.14	1.08	1.14	1.01
Transparency	Opaque	Opaque	Opaque	Opaque	Opaque
Resistance to chemicals[25]					
Aliphatic solvents	ND	+	ND	+	+
Aromatic solvents	ND	+	ND	+	+
Acetone	ND	+	ND	+	+
Hot water (hydrolysis resistance)	ND	0	ND	0	0
Weak/strong mineral acids	ND	0/-	ND	0/-	+/-
Weak/strong organic acids	ND	0/-	ND	0/-	+/-
Weak/strong alkalis	ND	+/0	ND	+/0	+/+
UV light and weathering	ND	0	ND	0	0

1.7 Polycondensation of polyesters and polyamides

Polyamides and polyesters synthesized by the polycondensation reaction of AA/BB-type monomers (diacids, diols, diamines, etc.) or AB-type monomers (hydroxy- or amino carbonic acids).[29] The monomers form a polymer-chain under the loss of a small molecule, usually water or methanol (Figure 1.7).

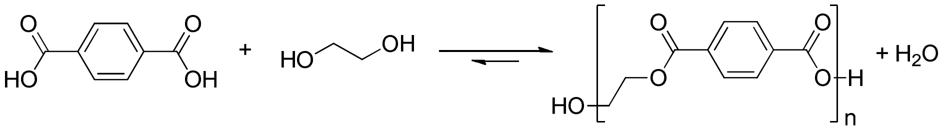

Figure 1.7 Polycondensation of terephthalic acid and ethylene glycol to PET under release of water.

Polycondensation reactions are so-called step-growth reactions.[30] These types of reaction can be defined by several characteristics:[24]

I. No initialization of the reaction by additional, highly reactive starting reagents
II. All molecules possess the same reactivity and participate at the reaction, leading to many similar-growing polymer chains
III. To reach high weight- or number average molecular weight (M_w and M_n), a very high conversion is necessary (Carothers' equation (1))
IV. The polydispersity index (PDI, ratio of M_w and M_n) of an ideal polycondensation (100% selectivity and conversion) is 2.00.

Characteristic III is described by Carothers' equation (1.1) for an AA/BB-type polycondensation.[24,29,31,32]

$$P_n = \frac{r+1}{r-2rp+1} \qquad (1.1)$$

with P_{n} = Average number degree of polymerization, $r = n_{AA}/n_{BB}$ with $n_{BB} \geq n_{AA}$, p = conversion.

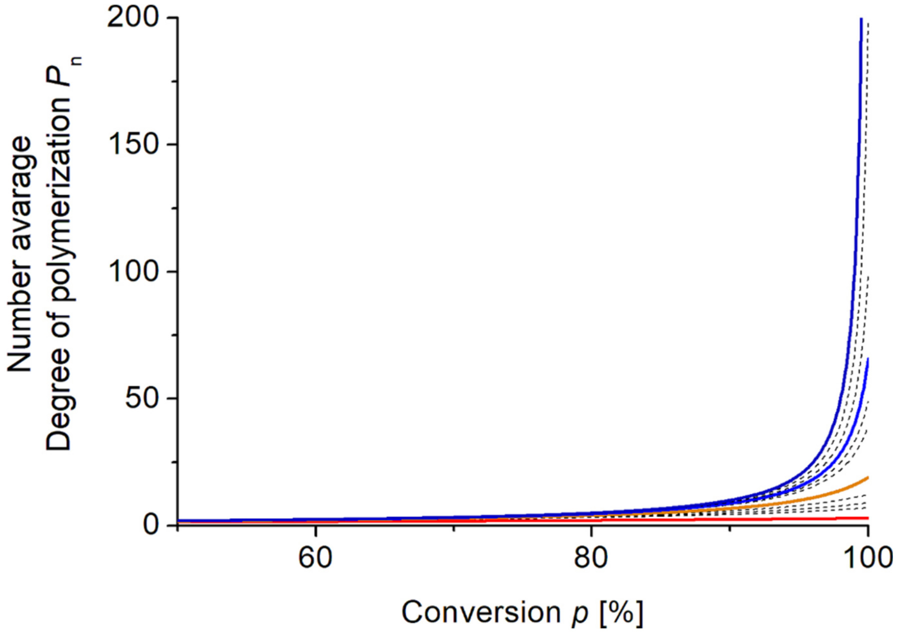

Figure 1.8 Graphs of Carothers' equation for differing r-values; r = 0.5 (red), r = 0.9 (orange), r = 0.97 (blue), r = 1.0 (dark blue).

The previously formed oligomers will react with each other to reach high molecular weights only at conversions above 99%. Hence, a crucial parameter for a high conversion and a major challenge for AA/BB-type polycondensations is the stoichiometry. If the AA reactant is used in excess, at full conversion of the BB compound only oligomers of the type AA-(BB-AA)$_n$-BB-AA will be present, and the reaction is terminated (Figure 1.8).

Polycondensations are equilibrium reactions (Figure 1.7). To reach high values for P_{n}, the equilibrium needs to be shifted to the polymer side. This can be achieved by separation of the released small molecule, e.g. by distillation during the polymerization process. The polymer can also be removed from the equilibrium, for example in precipitation polymerization reactions.

For the synthesis of PA66, the first step is the formation of a so-called AH salt (hexamethylene diamine adipate) in aqueous solution and the subsequent polycondensation under the loss of water in an autoclave at 270 °C – 280 °C.[28] A positive effect is that the AH-salt can be precipitated in perfect stoichiometry. To control the degree of polymerization, a monofunctional acid is added that terminates the chain growth.[24]

For polyesters, metal catalysts (antimony, aluminum, titanium, and others) are widely used. The amount depends on the catalyst but is typically 20 ppm - 300 ppm.[33] In a classical vacuum-melt process, the diacid is mixed with a diol (in excess) under inert atmosphere at 125 °C and 220 °C for the formation of oligomers.[22] In a second step, the temperature is raised to 270 °C and the pressure is decreased. In addition to the removal of water, the excess diol is separated, and the oligomers are converted into polyesters by transesterification.

For the last 30 years, the application of enzymes – mostly lipases and cutinases – as catalyst for polycondensation has been investigated.[34,35] The features are lower reaction temperatures, less toxicity and high selectivity. The major drawbacks are the long reaction times and high costs. Additionally, whereas the molecular weight for linear, aliphatic polyesters are in the range of their classically synthesized counterparts,[36] enzymatically polymerized polyamides with sufficient molecular weight have yet to be developed. Furthermore, the reaction conditions required for enzymes, especially the low temperature and solvents, lead to precipitation at oligomer level if aromatic monomers are used.[35] For the synthesis of linear, aliphatic polyesters of high molecular mass, an interesting strategy was reported: In the first step, dimethyl succinate formed a cyclic compound with butanediol in toluene, catalyzed by a lipase. In the second step, the polyester was formed by ROP in bulk, catalyzed by the same lipase.[37]

1.8 Ring opening polymerization of polyesters and polyamides

Lactams and lactones can be converted in the corresponding polymeric form by ROP. The three major routes are the hydrolytic, the cationic, and the anionic ROP. In ROPs, an equilibrium between the opened, incorporated monomers and the closed rings can be described (Figure 1.9).

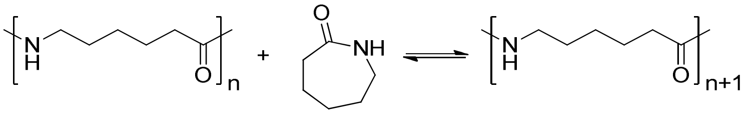

Figure 1.9 Polymerization equilibrium of caprolactam and PA6.[38]

According to Flory's assumption[39] that the functional groups of the growing chain ends are independent of the chain length and equally reactive, the free enthalpy of the polymerization ΔG is defined by equation (1.2) with ΔH_0 and ΔS_0 as standard polymerization enthalpy and entropy, temperature T, gas constant R and monomer concentration [M].[40]

$$\Delta G = \Delta H_0 - T(\Delta S_0 + Rln[M]) \qquad (1.2)$$

A polymerization is generally possible for $\Delta G_0 < 0$ kJmol^{-1}, and the signs of ΔH_0 and ΔS_0 define the range of temperature for polymerization under standard conditions (Table 1.4).

Table 1.4 Impact of the signs of ΔH_0 and ΔS_0 on the polymerization temperature.

ΔH_0 [kJmol^{-1}]	ΔS_0 [kJmol^{-1}]	Polymerization
< 0	< 0	Possible if T < T_c (celling temperature) $T_c = \frac{\Delta H_0}{\Delta S_0 + R\ln{[M]_0}}$
< 0	> 0	Always possible
> 0	> 0	Possible if T > T_f (floor temperature) $T_f = \frac{\Delta H_0}{\Delta S_0 + R\ln{[M]_0}}$
> 0	< 0	Never possible

At equilibrium state ($\Delta G = 0$), the concentration of the closed monomers $[M]_e$ is expressed by equation (1.3)[40]

$$[M]_e = exp\left[\frac{\Delta H_0}{RT} - \frac{\Delta S_0}{R}\right] \qquad (1.3)$$

A strategy to decrease the reaction temperature and therefore lower $[M]_e$ for $\Delta H_0, \Delta S_0 < 0$ is the activated anionic polymerization as described for the synthesis of PA6 from caprolactam (Figure 1.10).

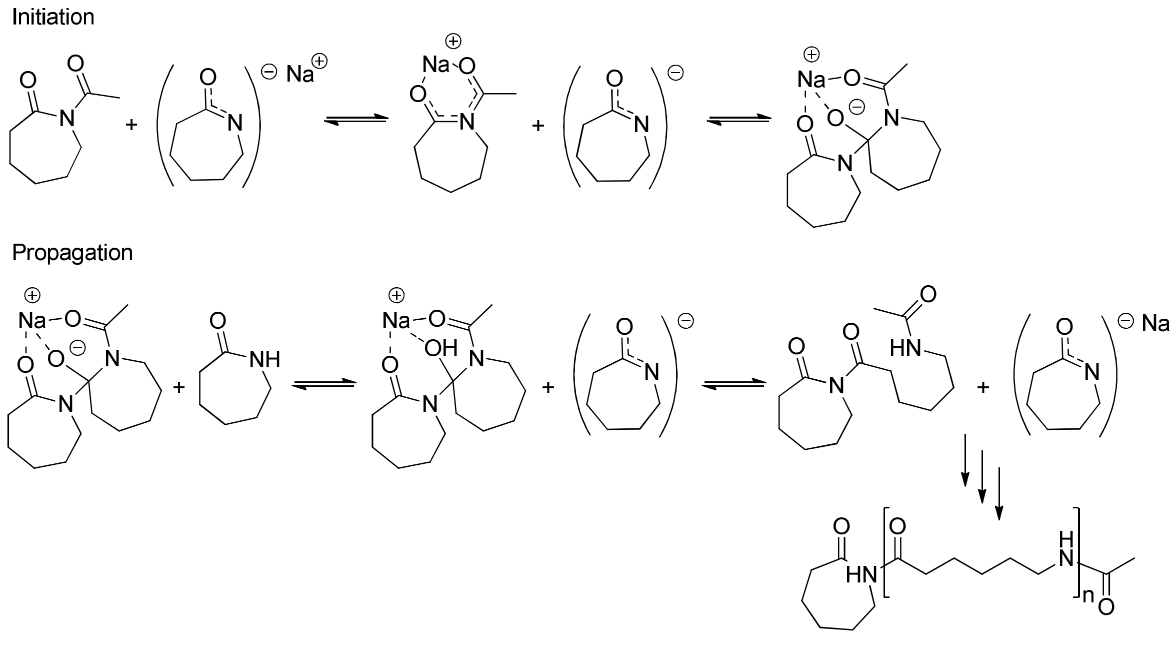

Figure 1.10 Initiation (dimer formation) and propagation of the activated aROP of caprolactam with acetyl-caprolactam as activator and sodium caprolactamate as initiator.[38]

The initiation step – which is also the rate-determining step of the polymerization – is the nucleophilic attack of a lactamate (e.g. sodium lactamate) on the carbonyl group of the amide. The lactamate, which is usually referred to as initiator, can be formed *in situ* by adding hydrides or alkalis, or they can be pre-synthesized. In activated anionic ROP (aROP), small amounts of an additional activator such as acetylated lactams (imides) or other highly reactive electrophiles are added. The rate of the initiation step is therefore much increased as the formation of the initial dimer (attack of the lactamate at the electrophilic center) is more facile compared to the attack at the carbonyl group of a regular lactam. As these dimers are the starting points of the growing polymer chain, the molecular weight can be adjusted by the initial concentration of lactamate and activator. The propagation occurs as a sequence of nucleophilic attacks at the newly-formed imide groups after addition and subsequent ring-opening of each lactamate *via* a tetrahedral bicyclic intermediate (Figure 1.10). The negatively charged lactam group in the main chain deprotonates a lactam monomer and subsequently the ring opens, leading to a constant regeneration of the lactamate concentration. In the initiation and the propagation, the cation of the lactamate coordinates the imide/amide groups and facilitates the reaction.[38] As the temperature and the reaction time of the activated aROP are considerably reduced compared to standard methods, the amount of side reaction is drastically decreased.[41]

Besides the temperature, many additional parameters influence the ROP, such as the ring size, substituents, ring strain, polymer/monomer miscibility, catalysts, solvents, and others.[38] Especially substituents are crucial, as even a small methyl group and its position in the ring considerably affects the conversion (Figure 1.11).[42] In general, substituents shift the polymerization equilibrium to the monomer side, increasing $[M]_e$: (I) substitution at tetragonal atoms favors ring-closure (increase of ΔH_0), (II) the rate of the initial dimerization may be lowered due to steric effects, and (III) substituents restrict the rotation in the polymer chain (decrease of ΔS_0).

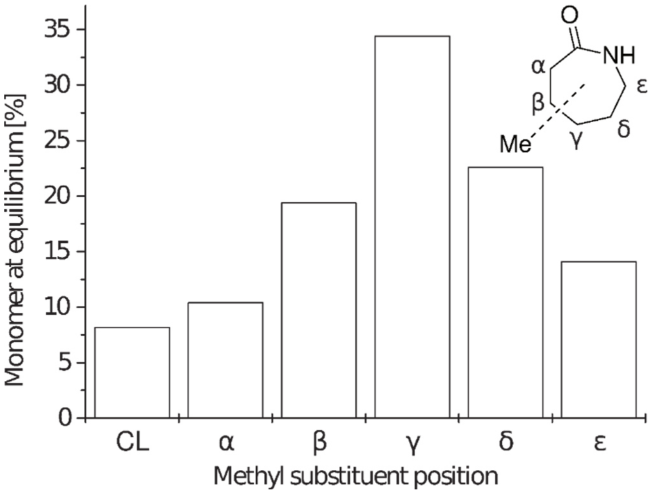

Figure 1.11 Influence of a methyl substituent on $[M]_e$ at the α-ε positions in a bulk polymerization at 250 °C.[43]

Polyesters are formed by ROP from lactones of all ring sizes. For small (four- to six-membered rings) and medium rings (seven- to twelve-membered rings), various kinds of chemical and enzymatic catalysts are applied, such as Sn-catalysts, metal aliphatic alkoxides, carboxylates, alkali metals, and lipases from mammals (porcine pancreatic lipase, PPL), fungi (*Candida antarctica*, CA; *Aspergillus niger*, AN; *Rhizopus delemar*, RD, and others) or bacteria (manly *Pseudomonas* family).[40] For ring-sizes above 13, functionalized monomers, and enantioselective polymerizations, lipases are the commonly preferred catalysts as they are superior in terms of large-ring lactam conversion, chemo-, and enantioselectivity.[40,44] However, with the exception of PCL, these aliphatic polyesters are of little industrial significance.

1.9 Bio-based polyesters and polyamides

Polymers, formed either partially or entirely from renewable (carbon) sources other than fossil oil are called bio-based polymers.[45] This includes naturally occurring polymers such as polysaccharides or lignin and also polymers from chemically modified biogenic monomers. Sometimes, bio-polymers that have been developed in the last 30 years are referred to as “new economy plastics”.[46] Consequently, well established bio-based polymers such as rubber, cellulose acetate, celluloid, and others are often excluded from market research. Polyurethanes (PUR) are also sometimes neglected, as the actual amounts of bio-compounds in polyurethanes remains to be unclear.[47] As a result, the market data is not always consistent and comparable. However, the future of bio-polymers is generally estimated to be positive.[46,48–50]

In 2018 – according to the German nova institute GmbH – the consumption of all bio-plastics combined was about 2% (7.5 mt) of the total plastic consuumption.[50] For fossil oil and bio-based polymers, the forecasted compound annual growth rate is about 4%. Bio-based polymers are used in various industries; consumer goods, building and construction, and automotive and transports are the three dominating sectors (Figure 1.12).[50]

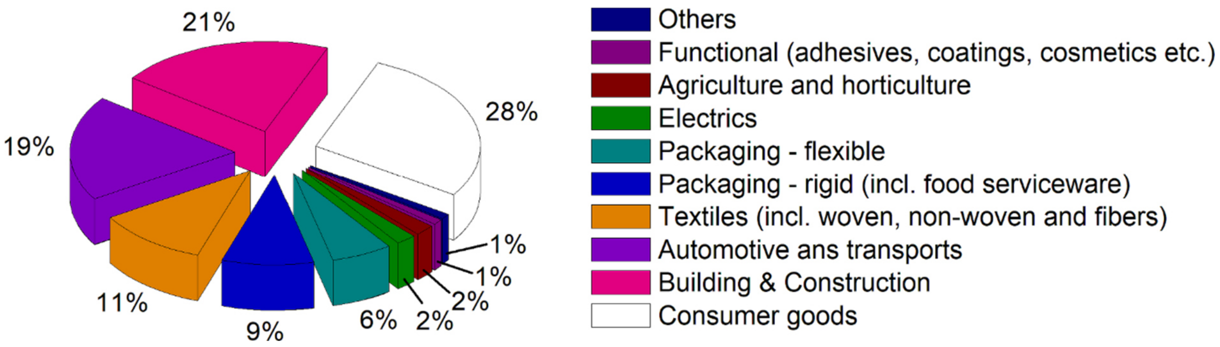

Figure 1.12 Bio-based polymers and their fields of application.[50]

Polyesters are high-volume bio-based polymers (Figure 1.13) and are mainly used as commodities (price-driven). Polyamides only reach comparably small volumes but are used as engineering or high-performance materials (performance-driven).

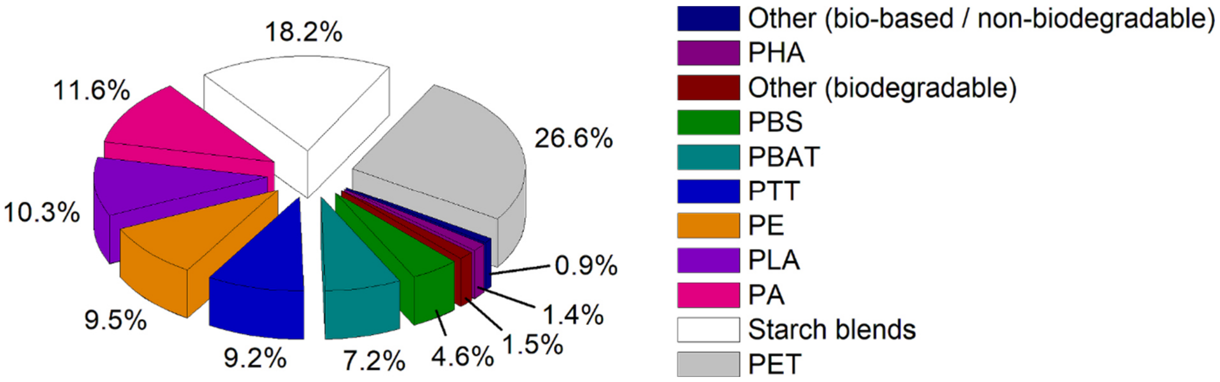

Figure 1.13 Global production capacities of bio-based polymers 2018 (only new economy plastics, without PUR). Poly(butylene succinate) (PBS); poly (butylene adipate terephthalate) (PBAT); poly (trimethylene terephthalate) (PTT); polyethylene (PE); poly (hydroxy alkanoate) (PHA).[47]

They can be either completely new polymers or so-called drop-in polymers. Drop-ins are structurally equivalent to their fossil-oil-based counterparts and therefore exhibit the same properties. Common examples are bio-polyethylene from bio-ethanol or PET with bio-based ethylene glycol (Figure 1.14); however, the mass content of the green diol is only 27%. Nonetheless, bio-ethylene glycol is the most-used sustainable building-block for bio-based polymers.

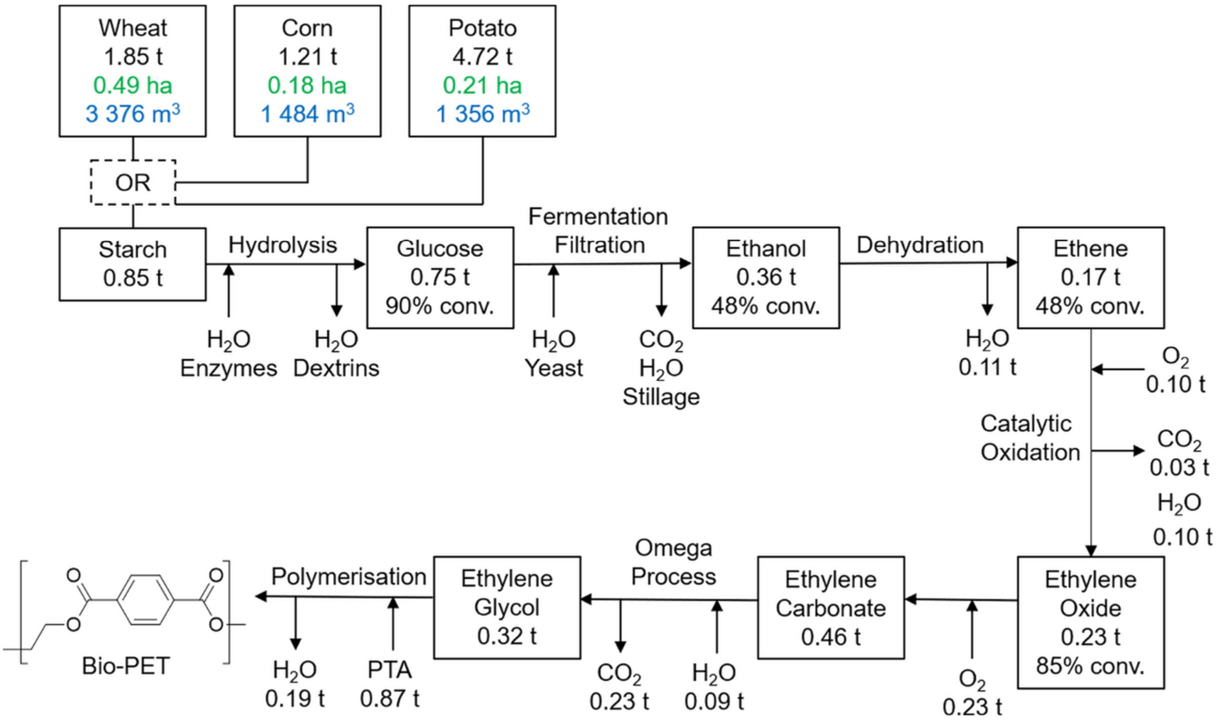
Wheat
1.85 t
0.49 ha
3 376 m3
Corn
1.21 t
0.18 ha
1 484 m3
Potato
4.72 t
0.21 ha
1 356 m3
OR
Starch
0.85 t
Hydrolysis
H2O
Enzymes
H2O
Dextrins
Glucose
0.75 t
90% conv.
Fermentation
Filtration
H2O
Yeast
CO2
H2O
Stillage
Ethanol
0.36 t
48% conv.
Dehydration
H2O
0.11 t
Ethene
0.17 t
48% conv.
O2
0.10 t
Catalytic
Oxidation
CO2
0.03 t
H2O
0.10 t
Ethylene
Oxide
0.23 t
85% conv.
O2
0.23 t
Ethylene
Carbonate
0.46 t
Omega
Process
CO2
0.23 t
H2O
0.09 t
Ethylene
Glycol
0.32 t
Polymerisation
H2O
0.19 t
PTA
0.87 t
Bio-PET

Figure 1.14 Synthesis pathway to bio-based ethylene glycol. Green: Land use; blue: Water use.[46]

The advantage of drop-in candidates is that starting from the monomer level, all established processes – processing, value chains, recycling, etc. – can be used without any adaptions.[45] In addition, long-term ecological aspects and toxicities are well-known. However, no new fields of application can be addressed with drop-in solutions, and the crucial factor for commercialization is the overall production price. Therefore, no polyamide drop-in has been commercialized to date, even though caprolactam is accessible from renewable feedstocks.[51,52]

The most relevant non-drop-in, 100% bio-based polyester is PLA. Glucose from corn, wheat or potatoes is usually used as raw material.[46,48] It is used in medical, textile, packaging and plasticulture.[53]

Other important building blocks for polyesters are 2,5-furandicarboxylic acid and the diols ethylene glycol, 1,3-propanediol and 1,4-butanediol, being the main drivers for future market growth.[50]

Bio-based AA/BB-type polyamides usually contain C10 or C12 di-acids or -amines from castor beans. The only currently available AB-type is PA11 from the same feedstock (Figure 1.15);

although bio-based routes from palm kernel oil by one-step fermentation to the PA12 monomer 12-aminodedaconicacid exist,[54] they have not been commercialized to date.

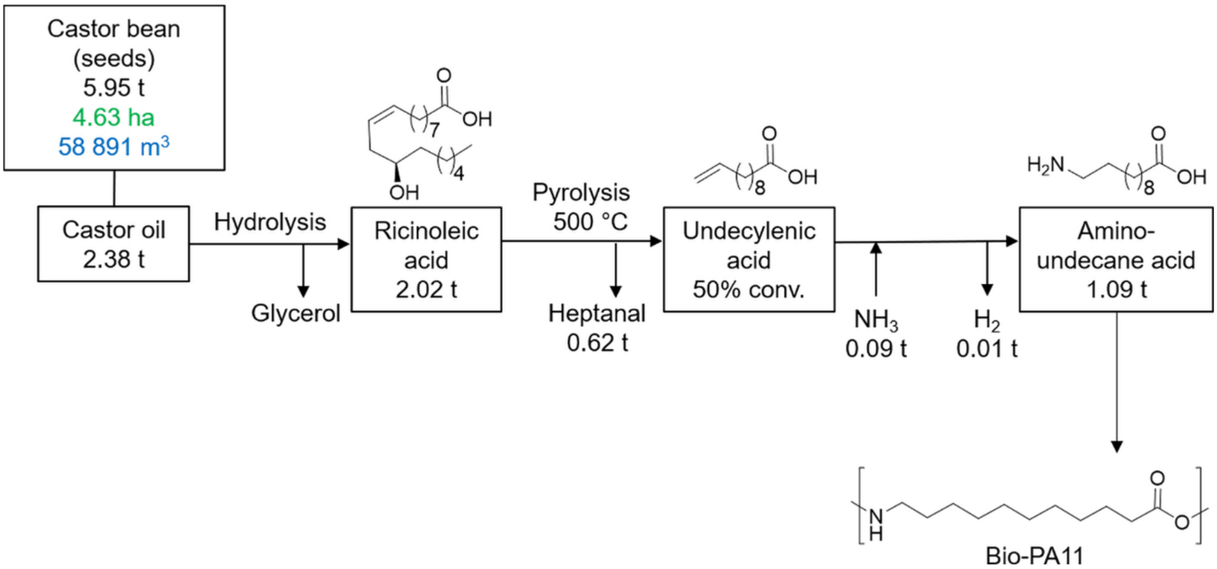

Figure 1.15 Conversion of ricinoleic acid from castor oil to bio-PA11. Green: Land use; blue: Water use.[46]

The commercial bio-polyamides and bio-polyesters are, with the exception of the chiral hydroxyl group in PLA and PHB, aliphatic linear polymers that differ only in chain length from the fossil-based materials. Therefore, the differences are rather small. For example, the polyamides PA410, PA1010, PA1012 are "property bridges" between the small chain PA46 and the long chain PA1212;[48] they are essentially "bio-replacement" materials.[45] They can be used instead of fossil-based polyamides in some applications, but do not offer real novelty. Naturally occurring, more complex molecules contain structural elements that might lead to polymers with completely new, outstanding properties – "bio-advantaged" polymers.[45]
Monoterpenes often contain motifs that are not easily synthesized from fossil oil, such as bicyclic structures, well-defined aliphatic side chains, or enantiopure substances. The utilization of these compounds could greatly enhance the portfolio of common bio-based polyesters and polyamides.

1.10 General background: Monoterpenes

Monoterpenes belong to the compound class of terpenes. Terpenes are non-essential metabolites of plants, insects, fungi, and others.[55] They share a common bio-synthetic pathway with isoprene (see above) as the general precursor (Figure 1.16): two or more isoprene units form the corresponding terpene structures, mostly by 'head-to-tail' condensations ('isoprene rule').[56] Hence, terpenes can be classified as isoprene-oligomers – however, because of different carbon skeletons, aliphatic substituents, olefinic structures, chiral centers, and functional groups, the structural diversity is immense. In addition, hydroxyl- or keto-groups are often introduced during the bio-synthesis.

Over 8000 terpenes and 30000 terpenoids have been identified so far.[55] As mentioned previously, monoterpenes are isoprene-dimers. They are the smallest isoprene oligomer, containing ten carbon atoms, and are still a good example for structural variety. The central dimer from which cyclic monoterpenes are formed is the α-terpinyl-cation (Figure 1.16).[57]

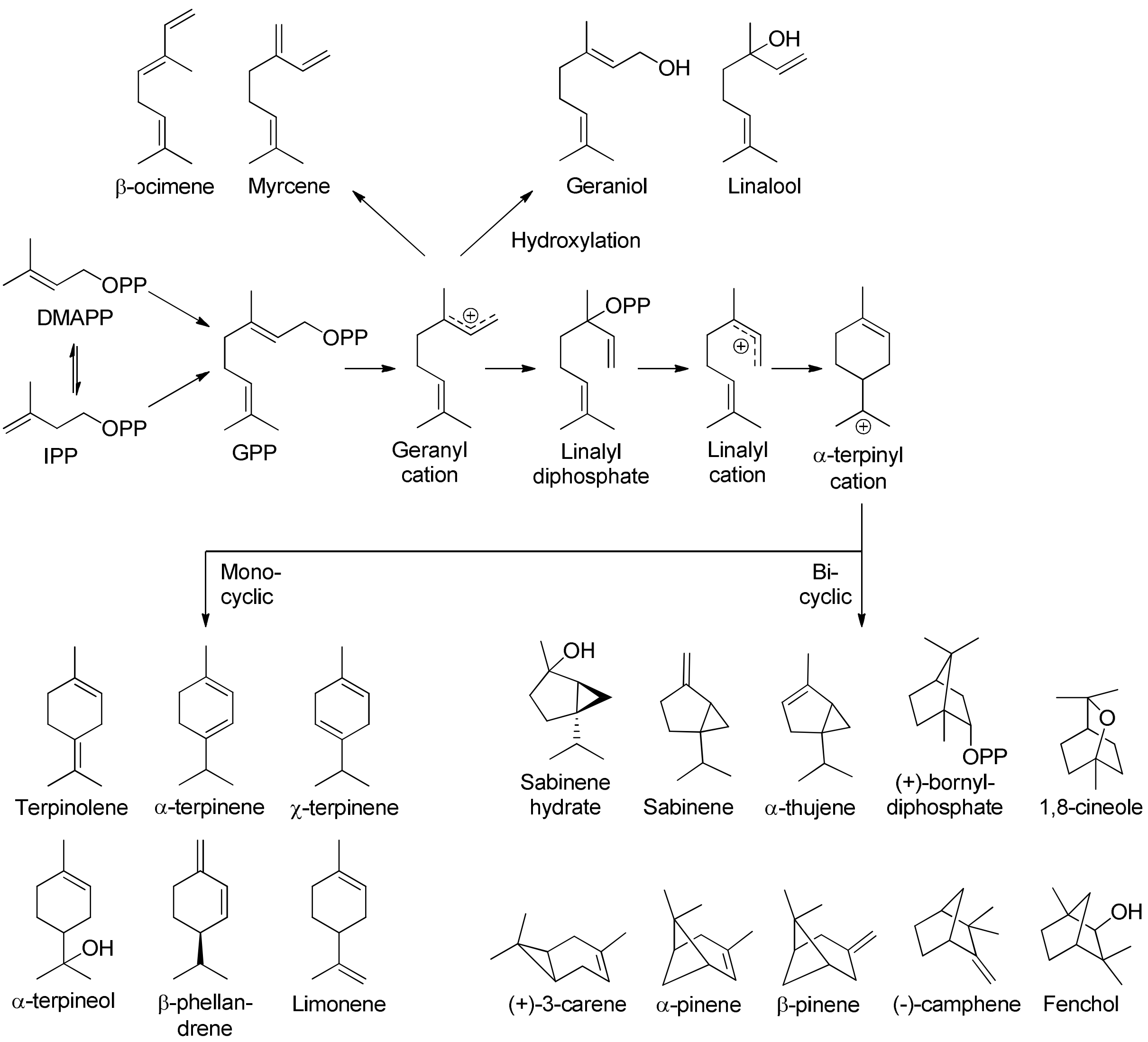
β-ocimene
Myrcene
Geraniol
Linalool
OH
OH
Hydroxylation
OPP
DMAPP
OPP
IPP
OPP
GPP
Geranyl cation
OPP
Linalyl diphosphate
Linalyl cation
α-terpinyl cation
Mono-cyclic
Bi-cyclic
Terpinolene
α-terpinene
χ-terpinene
OH
Sabinene hydrate
Sabinene
α-thujene
OPP
(+)-bornyl-diphosphate
O
1,8-cineole
OH
α-terpineol
β-phellan-drene
Limonene
(+)-3-carene
α-pinene
β-pinene
(-)-camphene
OH
Fenchol

Figure 1.16 Pathway from isoprene-precursors dimethylallyl pyrophosphate (DMAPP) and isopentenyl pyrophosphate (IPP) to hydroxylated and purely aliphatic linear, mono-cyclic, and bi-cyclic monoterpenes.

All monoterpenes that are formed from the same biosynthetic pathway can be converted into each other by rearrangements, condensations, cyclization, etc. (‘biogenic isoprene rule’).[58] However, as the cyclic structures rearrange relatively easily, selective conversions are generally challenging in terpene chemistry. Especially common are Wagner-Meerwein rearrangements, a reaction discovered during investigations of the reaction of the monoterpene isoborneol to camphene.[59]

Mixtures of monoterpenes have been used as ‘essential oils’, pharmaceuticals, and solvents since millennia. Carvone, limonene, menthol, and others are used in cosmetics because of their odour.[60] In macromolecular chemistry, polyterpene resins, mainly from β-pinene and usually with a molecular weight below 1.0 kDa, are used as thermoplastic adhesives.[61–63]

The first polyamide from a monoterpene (β-pinene) was synthesized by Hall in 1963,[64] during his investigations about the polymerizability of cyclic and bicyclic structures,[65–68] but the material was not investigated in detail. Since then, the potential of terpenes for thermoplastic polymers has been forecasted and explored in scientific research, but commercialization of the new polymers has not been realized yet.[69–72]

1.11 Monoterpenes as resource for polyesters: Selected examples

Monoterpenes for terpene-based polyesters have to be functionalized before polymerization. A suitable strategy is the conversion to anhydrides that can be polymerized with polyols or epoxides. Deivasagayam *et al.* functionalized α-phellandrene with maleic anhydride in a solvent-free Diels-Alder reaction, obtaining yields of more than 99%. The new monomer was polymerized with diglycerol and catalytic *para*-toluene sulfonic acid (Scheme 1.3).[73]

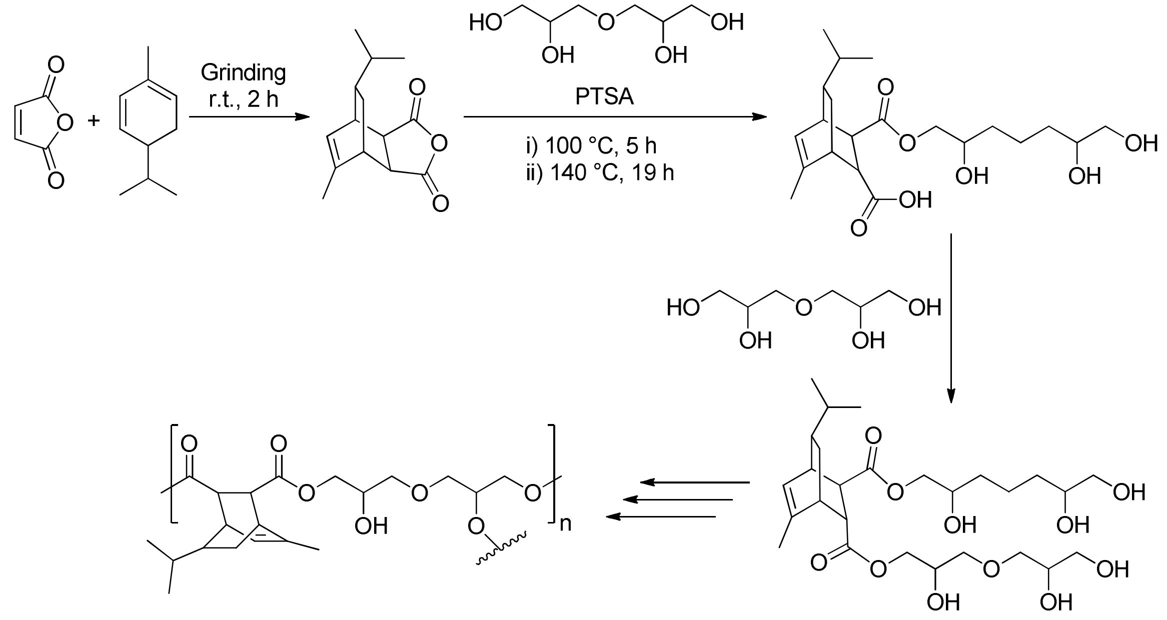

Scheme 1.3 Synthesis of a terpene-based co-polyester starting from the Diels-Alder reaction of α-phellandrene with malic anhydride.

M_w was above 40 kDa, but the reaction time exceeded 28 h. T_g was between 0 °C - 30 °C, depending on the dehydration and esterification during the reaction. The final polyester consisted of 70%-100% renewable carbon, depending on the maleic anhydride source.[73]

In a similar approach, the terpene-based anhydrides were copolymerized with propylene oxide catalyzed by complexes of Cr, Co or Al and aromatic ligands and a PNP-cation containing co-catalyst.[74] The conversion to amorphous polyesters was above 99%, M_n surpassed 50 kDa and the PDI was between 1.1 and 1.7. The T_g reached 109 °C, which is more than 30 °C above the T_g of PET (Table 1). This underlines that bulky substituents can shift the T_g to high values, and aromatic compounds are not necessarily required in this regard. However, the bio-based content is only 47%.[74]

Finally, Carrodeguas *et al.* used phthalic anhydride and terpene-based epoxides from 2-menthene, limonene, (+)-3-carene, and others.[75] With *cis*-limonene oxide, the T_g was 141 °C, M_n was 16.4 kDa and the conversion was above 99%. The reaction time in THF at 65 °C catalyzed by a homogenous iron catalyst and a PNP-cation co-catalyst was 24 h. In this case too, the bio-based carbon was only about 50%.

Another strategy is the conversion of terpenes to ketones, subsequent Baeyer-Villiger oxidation to the corresponding lactone and ROP. Starting from carvone,[76,77] limonene,[76] or menthone,[78] the resulting monomers are lactons containing an *iso*-propylene substituent and a methyl substituent. Even when β-pinene was used,[79] rearrangements during the synthesis led to a similar structure, barring the methyl group (Scheme 1.4 c). Another similarity worth mentioning is that in all cases, stereoisomers of the *iso*-propylene group or the methyl group were formed; consequently, the obtained polyesters were atactic, which can greatly influence the properties compared to an isotactic structure.

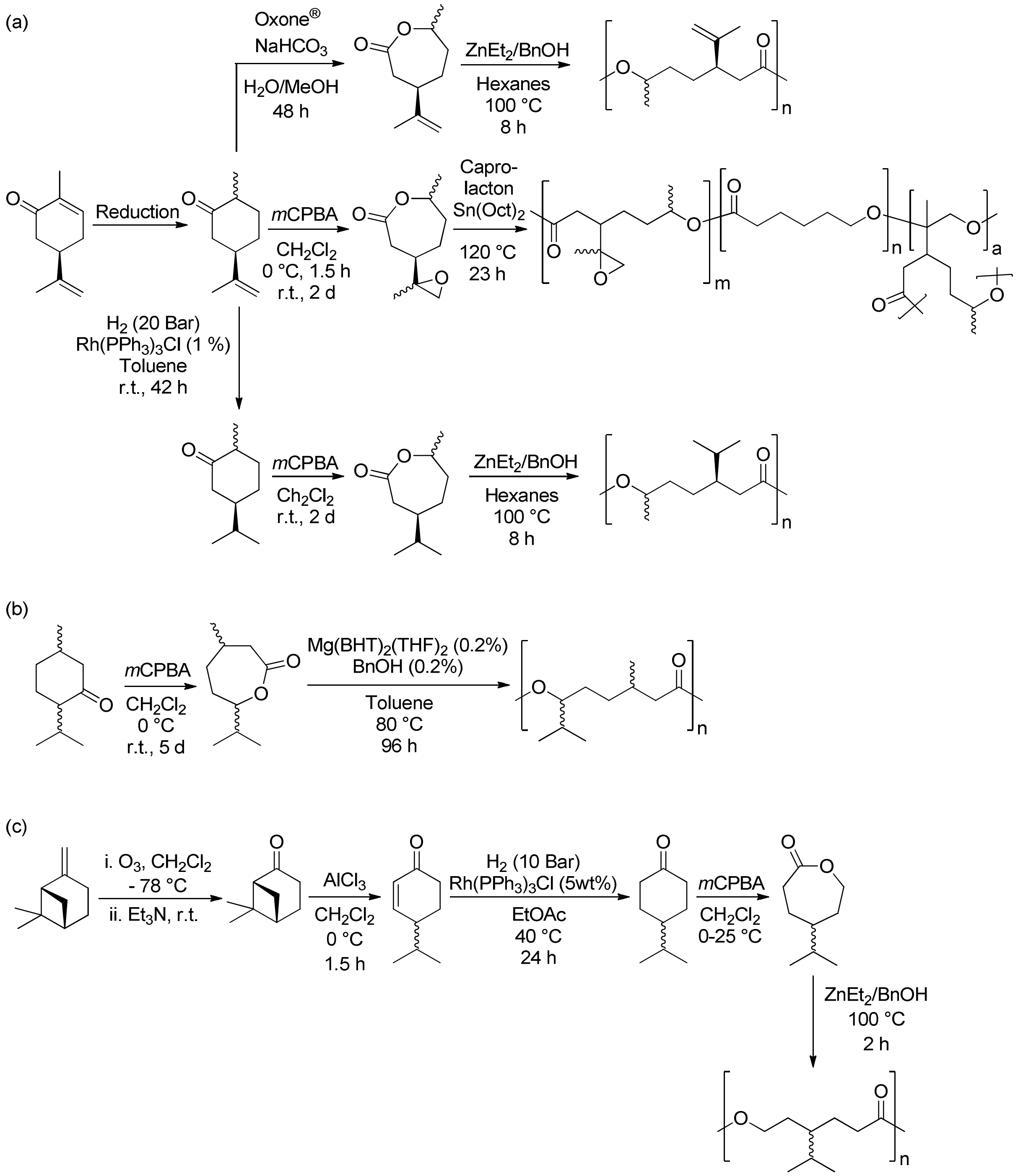
(a)
Oxone®
NaHCO$_3$
H$_2$O/MeOH
48 h
ZnEt$_2$/BnOH
Hexanes
100 °C
8 h
n
Reduction
mCPBA
CH$_2$Cl$_2$
0 °C, 1.5 h
r.t., 2 d
Capro-lacton
Sn(Oct)$_2$
120 °C
23 h
m
n
a
H$_2$ (20 Bar)
Rh(PPh$_3$)$_3$Cl (1 %)
Toluene
r.t., 42 h
mCPBA
CH$_2$Cl$_2$
r.t., 2 d
ZnEt$_2$/BnOH
Hexanes
100 °C
8 h
n
(b)
mCPBA
CH$_2$Cl$_2$
0 °C
r.t., 5 d
Mg(BHT)$_2$(THF)$_2$ (0.2%)
BnOH (0.2%)
Toluene
80 °C
96 h
n
(c)
i. O$_3$, CH$_2$Cl$_2$
- 78 °C
ii. Et$_3$N, r.t.
AlCl$_3$
CH$_2$Cl$_2$
0 °C
1.5 h
H$_2$ (10 Bar)
Rh(PPh$_3$)$_3$Cl (5wt%)
EtOAc
40 °C
24 h
mCPBA
CH$_2$Cl$_2$
0-25 °C
ZnEt$_2$/BnOH
100 °C
2 h
n

Scheme 1.4 Synthesis of terpene lactones from carvone (a),[76,77] menthone (b)[78] and β-pinene (c)[79] and subsequent ROP to polyesters. BHT = [4-[bis[4-[(3-sulfophenyl)amino]phenyl]methylidene]-1-cyclohexa-2,5-dienylidene]-(4-sulfophenyl)azanium.

Lowe *et al.* epoxidized the terminal double bond of the *iso*-propylene unit before[76] and after[77] the polymerization (Scheme 1.4 a). The epoxidized monomer was also co-polymerized with caprolactone; in both cases, Sn- and Zn-catalysts were used. The T_g was between -3 °C and -62 °C, and T_m reached 25 °C – 55 °C. Cross-linking *via* the epoxide led to gel formation in a solvent, with the volume increasing above ten times the original size. These gels reshaped after repeated deformation and are probably biodegradable, making them promising candidates for biomedical devices.[76] It is worth mentioning that the lactone formation of the carvone lactone could be achieved with environmental benign $KHSO_5$ (Oxone®) in 42% yield, instead of *meta*-chloroperoxybenzoic acid (Scheme 1.4 a).

Wilson *et al.* polymerized the menthone-based lactone by cationic ROP with a magnesium catalyst in THF (Scheme 1.4 b).[78] M_n did not surpass 8.5 kDa, and the highest conversion was below 80%. Co-polyesters with ω-pentadecalactone lead to increased molecular weight (20 kDa - 79 kDa). The T_g of these co-polyesters varied depending on the monomer ratio, but never exceeded 75 °C.

Quilter *et al.* converted β-pinene in a monocyclic lactone to establish a bio-based alternative to PCL (Scheme 1.4 c).[79] The polymerization of these monomers led to thick, colorless gels. The T_g was about -50 °C, and the highest M_n was 32.1 kDa. The polymerization time was only two hours, and 91% conversion was observed. Co-polymerizations with lactic acid were proven to be possible and gave semi-crystalline polyesters with a T_m of about 138 °C, but the resulting polyesters did not surpass a M_n above 10 kDa.

As described above, bio-based diols are a main driver of the future market growth of bio-based polyesters. A recent example is the application of a limonene derived diol in polymerization with adipic acid, catalyzed by Sn or Ti catalysts.[80] T_g and M_n varied between -7 °C – 23 °C and 9.0 kDa – 23 kDa, respectively. The diol was also converted into a hydroxylic acid for the generation of AB-type polyesters, but the attempt did not reach M_n above 2.6 kDa; one of the two stereoisomers obtained even preferred ring-closure (Scheme 1.5).

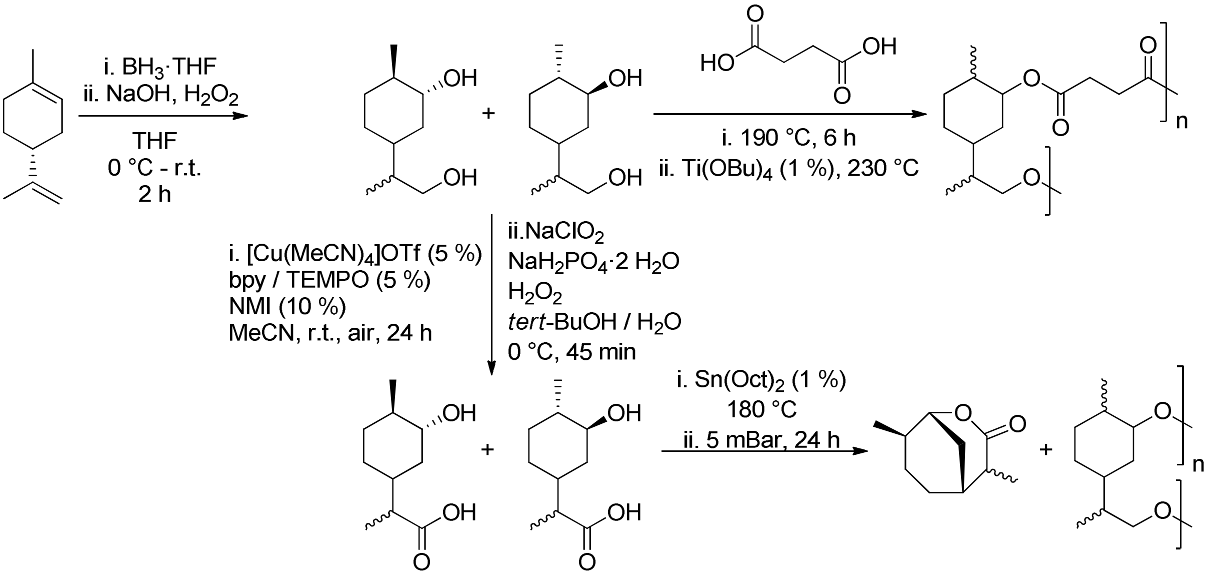

Scheme 1.5 Synthesis of limonene-based AB- and AA/BB-type homo-polyesters. TEMPO = 2,2,6,6-tetramethylpiperidin-1-yl)oxyl; bpy = 2,2′-bipyridine; NMI = N-methylimidazole.[80]

Another elegant approach was the whole-cell catalytic biotransformation of borneol to hydroxyborneol by Roth *et al.*[81] The bicyclic diol was polymerized with succinic acid dimethyl ester. M_w did not reach more than 4.0 kDa; the T_g was around 70 °C, which is caused by the rigid bicyclic structure. One particular detail that distinguishes this work from the others is the synthesis and polymerization of an enantiopure monomer that is directly gained from the synthesis, without the effort of a chiral purification. As no isomerization occurs during the polymerization process, the polyester is also chiral (Scheme 1.6).

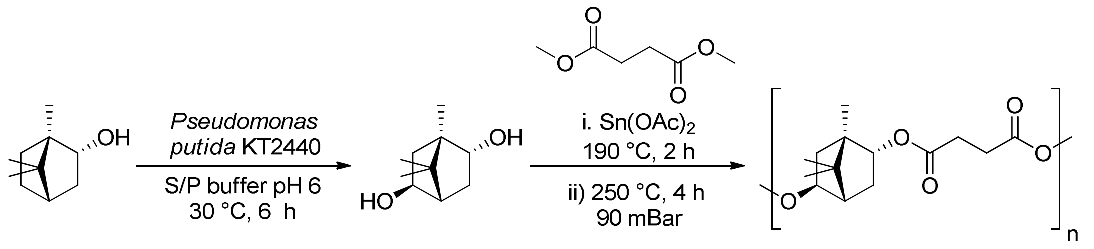

Pseudomonas putida KT2440
S/P buffer pH 6
30 °C, 6 h
i. Sn(OAc)2
190 °C, 2 h
ii) 250 °C, 4 h
90 mBar
OH
HO
O
n

Scheme 1.6 Synthesis of hydroxyborneol and polymerization with succinic acid to a chiral terpene-based polyester.[81]

1.12 Monoterpenes as resource for polyamides: Selected examples

Examples of polyamides from terpenes are rare.[82] An example for the utilization of a limonene derivative was reported by Firdaus *et al.*[83] Limonene was converted into diamines or diacids by addition of amino- or carboxyl ethanethiol to the double bonds (Scheme 1.7). Therefore, the resulting polymers can be classified as poly(thioether amides). The new monomers were used for homo-polymerizations and for the formation of co-polyamides with succinic acid, 1,6-diaminohexane, and other long-chain monomers.

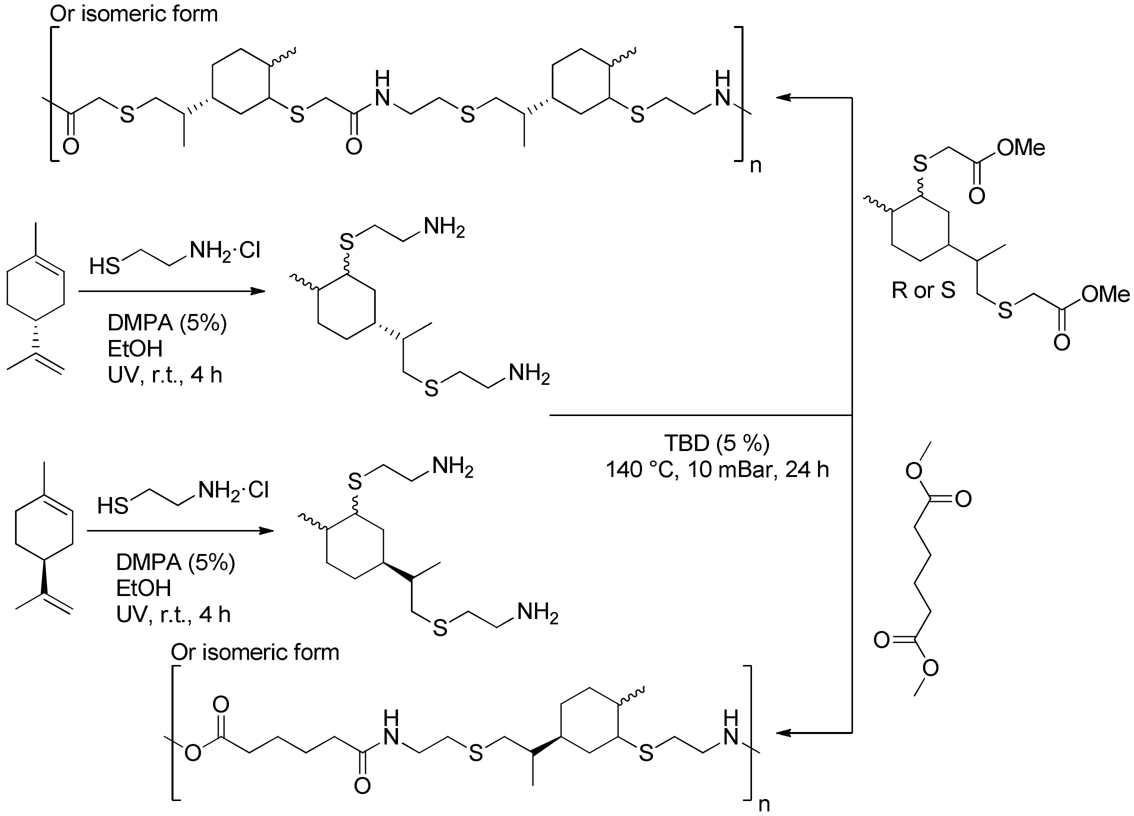

Or isomeric form
HS NH2·Cl
DMPA (5%)
EtOH
UV, r.t., 4 h
TBD (5 %)
140 °C, 10 mBar, 24 h
R or S
OMe
NH2
S
H N
O
n
Or isomeric form

Scheme 1.7 Synthesis of limonene-based poly(thioether amides). DMPA = 2,2-dimethoxy-2-phenylacetophenone (photoinitiator); TBD = 1,5,7-triazabicyclo-[4.4.0]dec-5-ene.[83]

T_g of amorphous limonene AA/BB-type homopolyamides was about 42 °C. Interestingly, the stereo-configuration of the monomers had no impact on the thermal properties or M_n (6.4 kDa – 7.9 kDa). The co-polyamides with various linear diacids or diamines preferably resulted in semi-crystalline polyamides with a similar T_g and T_m between 50 °C and 240 °C.

The first homopolyamide of a terpene was reported by Hall.[64] In the first step, the terminal double bond of β-pinene was oxidatively cleaved. The ketone was then converted to a lactam by oximation and Beckmann rearrangement (which is the rearrangement of a ketoxime to a lactam)[84] in basic media under application of benzenesulfonyl chloride. The cationic ROP with phosphoric acid was successful. A melting point of 358 °C was observed, but a detailed investigation of the polymer properties was not reported. Winnacker *et al.* re-investigated the synthesis and polymerization (Scheme 1.8).[85]

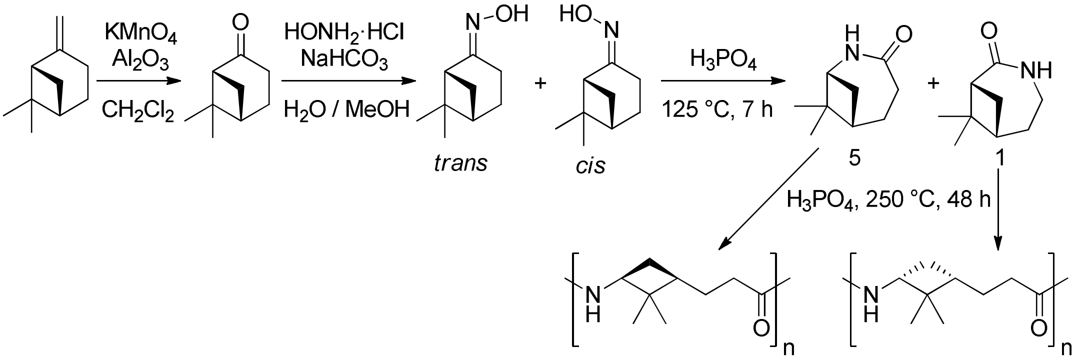

Scheme 1.8 Synthesis of β-pinene based homopolyamides.[85]

The Beckmann rearrangement was not completely selective, as the configuration of the oxime is crucial for the direction of the nitrogen insertion; a 5:1 mixture in favor of the trans-oxime was observed. Both lactams were polymerized by cationic ROP, using HCl , phosphoric acid, and others at different reaction times and temperatures. However, M_n did not surpass 7.7 kDa. In addition, only at long reaction times (> 16 h) yields of 80% - 90% were reached. T_m was remarkable 322 °C, and T_g was at 160 °C. The expected optic activity was confirmed by light-polarization experiments. The potential of this polyamide blended with poly(ethylene glycol) for cell adhesion and growth was recently explored.[86]

Before that, the same research group had already converted menthone into the corresponding lactam, either by reaction with hydroxylamine sulfonic acid (HOSA)[87] or by oximation and Beckmann rearrangement.[88] The selectivity of the rearrangement also depended on the configuration of the oxime, but the *trans*-oxime crystallized selectively in a yield of 56%. If HOSA was applied, only one of the lactam isomers was obtained (Scheme 1.9). The polymerization of the menthone-derives lactams was initially performed by anionic ROP with *in-situ* generated N-benzoyl-lactam and potassium,[88] and later optimized as the activator was separately synthesized and added in a controlled manner.[87] However, M_n was below 3.0 kDa, also if a cationic protocol was applied.[89] T_m reached temperatures of up to 290 °C, and a weak T_g was observed at about 50 °C.

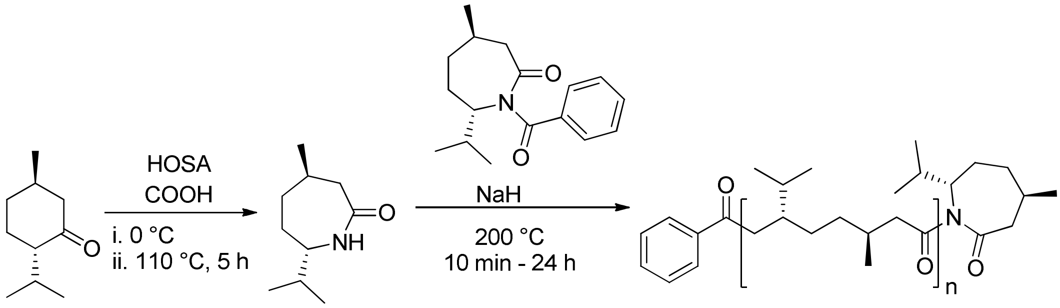

Scheme 1.9 Synthesis and polymerization of a menthone-derived lactam by anionic ROP.[87,89]

The general co-polymerizability of menthone lactam with caprolactam was also mentioned and verified by a few experiments, but no detailed investigation was conducted.[89]

In general, the reported methods for homopolyamides from terpene lactams highlighted the potential, but also suffered from low polymerization conversions, long reaction times, unsustainable or expensive monomer synthesis, and purification issues.

1.2 Objectives

The double bonds of isoprene and some monoterpenes can be chemically modified to convert these precursors to new bio-products. For bio-fuels from isoprene, a linear dimer- or trimerization, preferably with high selectivity, is required. To convert isoprene and olefinic monoterpenes to new building blocks for polymers, hetero-atoms for polyesters, polyamides, and others need to be integrated. The obtained monomers should be polymerized, and the polymers should be analyzed in terms of structure and thermal properties. These aims are addressed in five sections (Section 2.1-2.5). Within each section, the numbers of compounds are re-assigned.

1.2.1 Isoprene as precursor for bio-fuels

The potential synthesis of isoprene oligomers as precursor for bio-fuels is addressed in a literature review, which focuses on different catalytic methods for dimer- and trimer production (Section 2.1). The originally reported mechanisms of these methods are also discussed briefly. The contributions of the co-authors are listed at the beginning of the section.

1.2.2 Isoprene as starting material for monomers for new isoprene-based polymers

As described above, polyesters and polyamides are very important thermoplastics. To verify the potential of isoprene-based polymers in this context and beyond the standard application in rubbers, lactams and lactones should be specifically focused. A promising strategy might be the conversion with chlorosulfonyl isocyanate in a cyclo-addition reaction, or the double bond epoxidation. The results are discussed in Section 2.2.

1.2.3 Synthesis and polymerization of monoterpene-based lactams

Bio-based polyamides also have a huge future potential, especially as high-performance materials. The structural variety of monoterpenes offers several possible lactams; the previously mentioned bicyclic structures are of high interest as the thermal properties are strongly influenced by these sterically demanding and rigid structures. The introduction of non-linear, non-aromatic, bio-based polyamides would remarkably broaden the field of polyamides. Appropriate lactam-monomers from (+)-3-carene and α-pinene might be accessible by reaction with chlorosulfonyl isocyanate (β-lactams) or by a multi-step synthesis to the corresponding ε-lactams (Figure 1.17). The results are discussed in the sections 2.3 and 2.4.

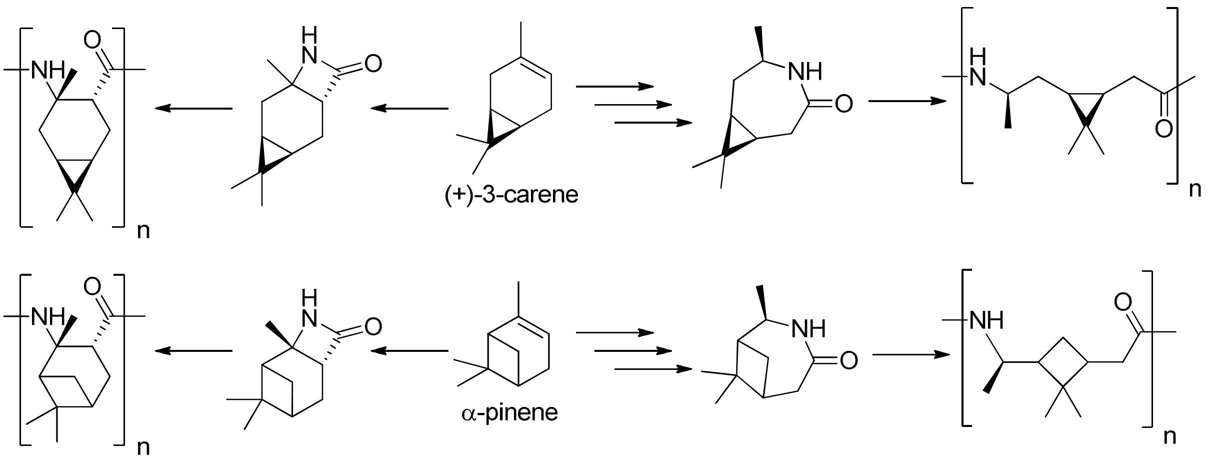
NH
O
n
H
N
O
(+)-3-carene
NH
O
H
N
O
n
α-pinene

Figure 1.17 Synthesis of β-lactams and ε-lactams starting from (+)-3-carene and α-pinene.

1.2.4 Synthesis of diols from terpenes

Polyesters from natural resources are a very important class of bio-based polymers. This is true especially for diols of AA/BB-type polymers, which are expected to be a major driving force for future market growth. Terpenes are suitable precursors for bio-based polyesters, but diols are still rare. Therefore, the conversion of abundant terpenes such as limonene, (+)-3-carene, and α-pinene are of interest. This is addressed in Section 2.5. The diols are produced by an oxidative cleavage and subsequent reduction of the cyclo-olefins (Figure 1.18). The polymerization of a limonene-based diol to verify the general polymerizability with diacids is also described.

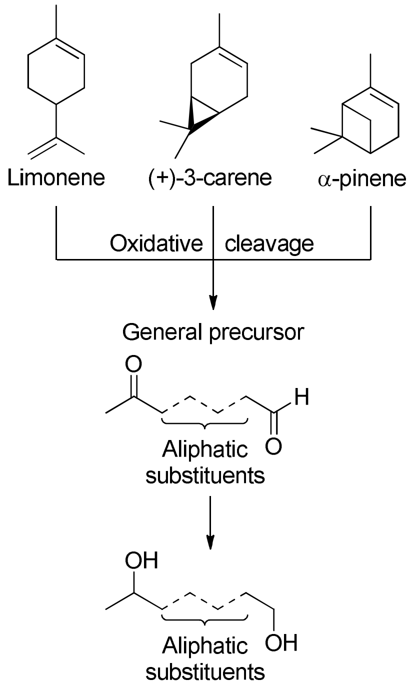
Limonene
(+)-3-carene
α-pinene
Oxidative cleavage
General precursor
O
H
O
Aliphatic substituents
OH
OH
Aliphatic substituents

Figure 1.18 Oxidative cleavage of limonene, (+)-3-carene, and α-pinene and subsequent conversion to diols.

2 Results

2.1 Oligomerization of isoprene to linear dimers and trimers for advanced bio-fuels

Title:	Oligomerization of isoprene to linear dimers and trimers for advanced bio-fuels
Status:	Manuscript draft
Journal:	-
Publisher:	-
DOI:	-
Authors:	Paul N. Stockmann, Prof. Olga Garcia Mancheño, Prof. Volker Sieber

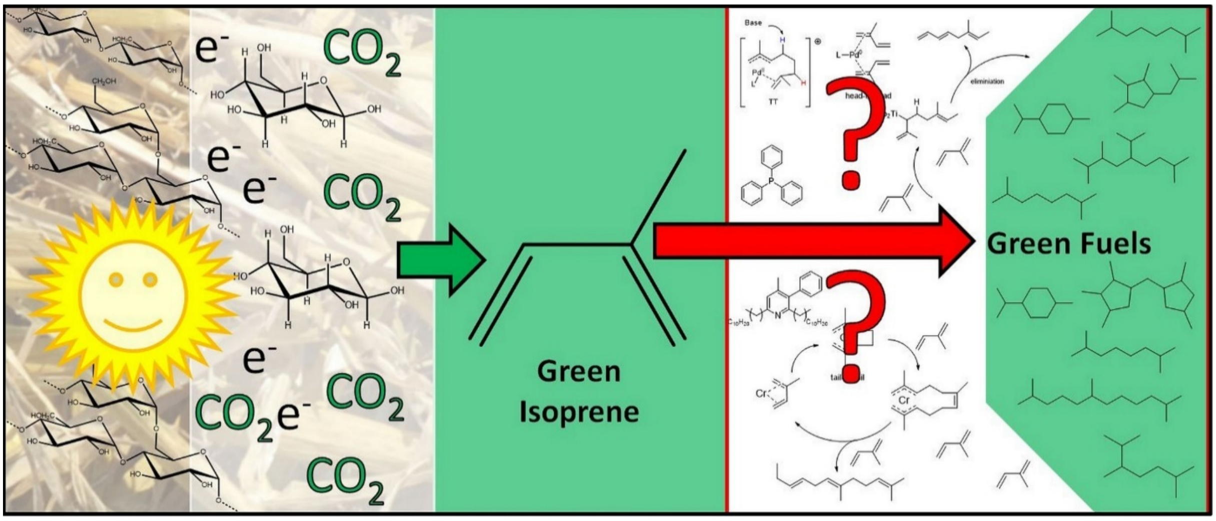

This manuscript draft comprises the methods for the linear dimerization and trimerization of isoprene accessible from renewable feedstock as precursor for advanced bio-fuels. Academic literture as well as patents have been included. The methods were categorised in three sections; palladium catalysts, Ziegler-Natta catalysts and other methods. The results reported in the literature were summarized and the originally published mechanisms were briefly discussed. As major draw-backs, unsufficient selectivity towards linear oligomerization and complex and expensive reaction systems were identified.

Paul N. Stockmann reviewed and categorized the literature and wrote the manuscript and made all tables, figures and schemes. Olga Garcia Mancheño and Volker Sieber revised the work.

Authors	Contributions
Paul N. Stockmann	Conceived the work; wrote the manuscript.
Prof. Olga Garcia Mancheño	Revised the manuscript.
Prof. Volker Sieber	Conceived the work, revised the manuscript, general supervision.

Oligomerization of isoprene to linear dimers and trimers for advanced bio-fuels

Paul N. Stockmann[a], Olga García Mancheño[b] and Volker Sieber* [a, c]

a. Paul N. Stockmann, Prof. Volker Sieber, Fraunhofer IGB, Straubing branch, Bio, Electro and Chemocatalysis BioCat, Schulgasse 11a, 94315 Straubing, Germany, paul.stockmann@igb.fraunhofer.de

b. Prof. Dr. Olga Garcia Mancheño, Organic chemistry institute, University of Münster, Corrensstraße 40, 48149 Münster, Germany, ogarc_01@uni-muenster.de

c. Prof. Volker Sieber, Chair of Chemistry for Biogenic Resources, Technical University of Munich, Campus Straubing for Biotechnology and Sustainability, Schulgasse 16, 94315 Straubing, Germany; Catalysis Research Center, Technical University of Munich, 85748 Garching bei München, Germany, sieber@tum.

Email: Volker Sieber sieber@tum.de

* Corresponding author

The production of sustainable, bio-based isoprene (2-methyl-but-1,3-diene) as a precursor for bio-fuels has been a matter of recent intense research.[1–11] Usually, synthetic strategies from bio-resources to access isoprene under the application of chemical or biotechnological methods are investigated. As hydrogenated, linear dimers or trimers of isoprene are structurally similar to fuels and its handling to produce fine chemicals and synthetic rubber is already established in the industry in scales of hundred thousands of tons per year, isoprene oligomers indeed seem to be a valuable drop-in candidate to replace fossil-based fuels.[12] A patent from 2012 describes a complete production chain from bio-based isoprene to fuels.[13] The physical data of some of these isoprene oligomers are displayed in Table 1.[13] To use isoprene oligomers as a fossil fuel replacement, a convenient chemical method to convert isoprene to fuel candidates in a scale of industrial relevance and sufficient selectivity is required. Despite isoprene's high abundance and industrial importance, isoprene-based fuel has not been commercialized yet. One reason for this might be the challenging selective synthesis of isoprene dimers and trimers. Although numerous articles concerning the conversion of isoprene to rubber (polyisoprene) or about the telomerization of isoprene to hetero-atom containing oligomers have been published, a high-yielding selective method to produce pure C_{10}-C_{15} oligomers is still a topic of ongoing research. The general draw-back of the established methods are the use of expensive or toxic (metal) catalysts, the low selectivity due to the formation of higher oligomers (> C_{20}), the formation of cyclic by-products and high production costs. The crucial reason, however, are the high costs of isoprene. Nonetheless, some recent publications point out the value of isoprene as a fuel precursor instead of a building block for polymers or terpenes.[13–15]

Table 1 Overview about selected isoprene dimers and trimers and their physical properties relevant for their application as fuels.[13]

Formula	**Boiling point (°C)**	**Density (g/cm³)**	**Vapor pressure (hPa, 25 °C)**	**ΔHc (kJ/mol)**	**Lower heating value (kBtu/gal)**	**Higher heating value (kBtu/gal)**	**Octane** ***Cetane***
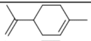	177	0.848	2.05	6167	130.6	137.9	88
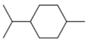	170	0.806	2.16	6531	126.5	134.9	75
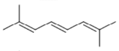	186	0.782	1.22	6196	121.1	127.8	110
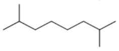	160	0.728	4.47	6778	116.5	124.7	97
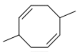	183	0.860	1.45	6234	134.0	414.4	95
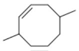	179	0.830	1.77	6464	131.6	139.4	90
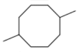	159	0.800	1.85	6527	125.4	133.8	85
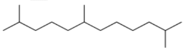	247	0.766	0.05	10040	121.7	130.1	*65*
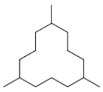	278	0.850	0.010	9957	135.7	144.6	*40*
3:1 mixture of linear : cyclic C_{15} (BIF-15)	255	0.787	0.043	10020	125.2	133.7	*59*

Figure 1 is a process scheme of how isoprene, its linear oligomers and the cyclic structures might be utilized as a fuel replacement or additive.[14] This review covers the years 1959-2018 and focuses on the chemical conversion of isoprene to linear dimers and trimers by Palladium (Pd) catalysts (Section 1), Ziegler-Natta catalysts (ZNc) with various metals including Titanium (Ti), Nickel (Ni) or Zirconium (Zr) (Section 2), and other methods (Section 3). The proposed mechanisms for these transformations are also shortly discussed, while the oligomerization of other light olefins by chemical methods is not included since it has been reviewed extensively elsewhere.[16]

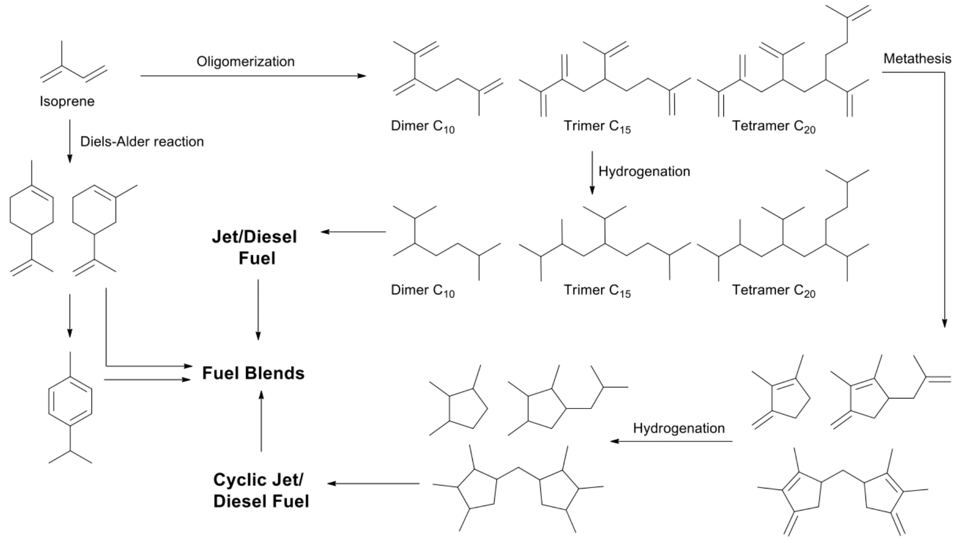
Isoprene
Oligomerization
Diels-Alder reaction
Dimer C_{10}
Trimer C_{15}
Tetramer C_{20}
Metathesis
Hydrogenation
Jet/Diesel Fuel
Dimer C_{10}
Trimer C_{15}
Tetramer C_{20}
Fuel Blends
Hydrogenation
Cyclic Jet/ Diesel Fuel

Figure 1 Oligomerization and subsequent hydrogenation of isoprene for the formation of fuel and fuel blends.[16]

1 Palladium catalysts

One of the most studied and versatile approaches for the dimerization of isoprene (**1**) rely on the use of palladium catalysis. This might be due to the fact that the palladium metal provides many possibilities for the right choice of the appropriate catalytic system, including both the ligand and reaction conditions adjustments, permitting the tuning or control of the selectivity of the process. A possible mechanism for the palladium catalyzed dimerization of two isoprene (**1**) molecules is shown in Figure 2.[17,18]

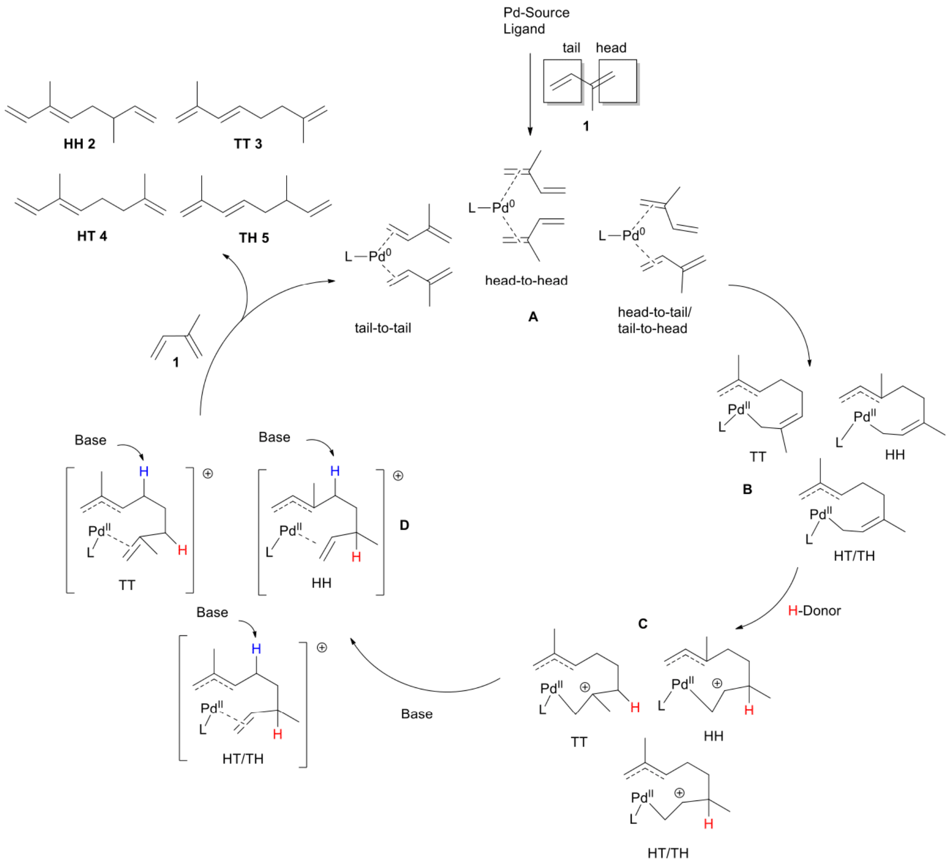
Pd-Source
Ligand
tail
head
1
HH 2
TT 3
HT 4
TH 5
L—Pd0
head-to-head
A
tail-to-tail
head-to-tail/
tail-to-head
1
PdII
L
TT
HH
B
HT/TH
H-Donor
C
H
TT
HH
HT/TH
Base
D
HT/TH

Figure 2 Proposed mechanism for the Pd-catalyzed dimerization of isoprene (**1**) to 3,6-dimethylocta-1,3,7-triene (**HH 2**), 2,7-dimethylocta-1,3,7-triene (**TT 3**), 3,7-dimethylocta-1,3,7-triene (**HT 4**) and 2,6-dimethylocta-1,3,7-triene (**TH 5**).[17,18]

For the linear dimerization, there are four competing mechanisms leading to isomeric 2-methyl-octatrienes **2**-**5**. Two isoprene (**1**) molecules coordinate to Pd to form an *in situ* generated Pd(O)-complex (**A**) that is stabilized by electron donating ligands such as phosphines or N-heterocyclic carbenes, among others. The subsequent C-C coupling leads – heavily depending on the reaction conditions such as solvents, temperature, ligands and others – to head-to-head, head-to-tail or tail-to-tail dimers forming a ligand-Pd(II)-(η^1, η^3-dimethyloctadienyl)-complex (**B**). The presence of a proton donor, usually alcohols or organic acids, leads to the formation of the intermediate (**C**) that subsequently forms the positively charged η^1, η^3-Pd(II) complex (**D**). At this stage, two competing reactions can occur: Either the addition of a nucleophile such as alkoxides or amines at the allylic positions to form a telomer, or deprotonation to form the $C_{10}H_{16}$

dimers **2**-**5.** The β-hydrogen elimination is promoted by an additional base or the corresponding conjugated base of the proton donor.

In 1972, the direct dimerization of alkyl-substituted dienes, such as isoprene (**1**), was patented by DuPont.[19] Palladium complexes of reactive alkenes such as maleic anhydride and $(Ph_3)P$ were used as catalysts in acetone at 105 °C in an autoclave for 10 h under autogenous pressure. The yield of linear dimers was 75% and consisted to 98% of 2,7-dimethylocta-1,3,7-triene (**TT 3**). This publication is one of only a few examples where the amount of substrate exceeded the usual laboratory scale, as 500 g of isoprene (**1**) were used. The authors also claim that, in this case, an organic solvent is not mandatory.

A more detailed follow-up publication dealt with mechanistic details and the reusability of the catalyst, revealing that the yield was almost unchanged in a second run.[18]

It could also be shown that by the use of 10% Pd/C, a saturated C_{10} dimer is built with a yield of 83%. An increased selectivity could be observed if tetrakis(triphenylphosphite)palladium(0) $[(Ph_3)_4Pd]$ was applied as catalyst. In this case, isoprene (**1**) was converted into its dimers without an additional solvent at 115 °C for 7 h.[20] The yield of the linear dimers was 97% with a product distribution of 71% **TT 3**, 28.4% **TH 5** and 0.6% **HH 2**.

The effect of various electron donating organophosphorus ligands was investigated by J. Berger; in fact, the nature of the ligand was shown to be crucial for the selectivity of the reaction (Table 2).[21]

Table 2 Influence of electronic and steric effects of various ligands on the dimerization and telomerization of isoprene (**1**). Reaction conditions: $Pd(acac)_2$ 0.05%, ligand 0.4%, isoprene (**1**) 100%: methanol 300%, 80 °C, 10 h.[21]

Entry	**1**	**2**	**3**	**4**	**5**	**6**
Ligand	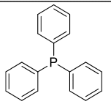	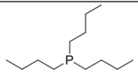	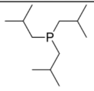	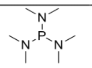	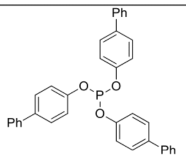	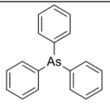
Conversion [%]	100	100	100	75	70	65
Dimers [%]	40	36	36	67	66	38
Telomers [%]	60	64	64	33	34	62

Whereas the steric demands of the ligands seem to be of little importance, a strong electron donating character of the Pd coordinating P-ligand increases the homo-dimer selectivity by over 50% (Table 2, entries 1-3 compared to entries 4 and 5). $(Ph)_3P$ has also been used as a ligand to convert isoprene (**1**) using dioxane as solvent and $Pd(acac)_2$ as pre-catalyst.[22] Then, the isomer **TT 3** was produced selectively with a yield of 76%. Similar results were achieved with $Pd(acac)_2$, $(Ph)_3P$ and *m*-methoxybenzaldehyde (70% yield).[22] In both cases, no additional base was needed. Moreover, in the latter case, the exchange of the aldehyde to triethylamine decreased the yield drastically.[22] In another catalytic system, the reaction using $(Ph)_3P$ as ligand was shown to be less active and selective than the aliphatic ligands Et_3P or $(C_6H_{11})_3P$. In this case, the reaction was carried out under CO_2 pressure (9-10 bar) at 110 °C (Table 3).[23]

Table 3 Influence of different Pd-catalysts on the tail-to-tail dimerization of isoprene (**1**) in the presence of CO_2. Reaction conditions: Catalyst 0.24%, isoprene (**1**) 100%, CO_2 (9-10 bar), 110 °C. [a]Missing to 100% = other dimers.[23]

Entry	Catalyst·CO_2	t [h]	Conversion [%]	Dimers [%]	Distribution of dimers [%][a]		
					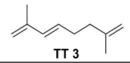 TT 3	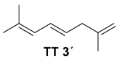 TT 3´	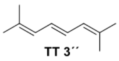 TT 3´´
1	$Pd[(Ph)_3P]_3$	7	No data	16	53	3	0
2	$Pd[PEt_3]_3$	3	70	58	86	1	Traces
3	$Pd[PEt_3]_3$	27	86	60	2	35	52
4	$Pd[P(C_6H_{11})_3]_2$	5	71	58	75	11	Traces
5	$Pd[P(C_6H_{11})_3]_2$	29	87	67	1	23	59

After a reaction time of 7 hours using $(Ph_3)P$ as ligand, 16% of isoprene (**1**) was converted into the dimers with a selectivity to the tail-to-tail **TT 3** of 53% (Table 2.5, entry 1) - whereas for Et_3P a conversion of 70% and a selectivity of 58% was observed within 3 h (Table 2.3, entry 2). If the reaction time was raised to over 25 h, **TT 3** was almost completely isomerized into mostly the 2,7-dimethyl-2,4,6-octatriene (**TT 3´´**, 52%) and 2,7-dimethyl-2,4,7-octatriene (**TT 3´**, 35%) derivatives (Table 2.3, entry 3). A similar behavior was observed for $P(C_6H_{11})_3$ (Table 2.3, entries 4 and 5) As this had not been described before under Pd-catalysis, **TT 3** was directly tested for the isomerization at 110 °C in the presence of $[PEt_3]_3Pd$ and $[P(C_6H_{11})_3]_2Pd$ in the absence of a CO_2 atmosphere. In this case, no isomerization occurred. However, the recycled catalyst from the initial reaction using the $[P(C_6H_{11})_3]_2Pd/CO_2$ system was still able to isomerize the double bonds, also in the absence of CO_2. The authors conclude that CO_2 assists the formation of the catalytically active species and suggest the formation of an adduct of the form $[P(C_6H_{11})x(CO_2)_x]Pd$. Unfortunately, all attempts to isolate this proposed adduct failed. More reasonable is the assumption that carboxylic acids are formed from CO_2, which are able to stabilize Pd^0 and Pd^{II}. Interestingly, although lacking experimental data, the use of CO_2 as a suitable ligand for the dimerization of isoprene (**1**) had been mentioned before.[24]

In a more recent work, an excellent selectivity for the formation of tail-to-tail dimers was described by Kellner et al.[17] Again, simple $(Ph)_3P$ was used as most selective ligand. The use of $Pd(OAc)_2$ as palladium source in THF at 90°C for 48 h lead to **TT 3** in an isolated yield of 85% (total amount of dimer: 91%, Table 2.4, entry 4). Interestingly, no additional proton donor was necessary. The authors suggested that the acetate acts as a proton acceptor/donor shuttle, mediated by the present Et_3N that was used as base. In this system, Et_3N was revealed to be a more suitable base than KOH or $KHCO_3$ (Table 4, entries 7-9). Also, THF hugely increased the selectivity compared to toluene, methanol or EtOAc (Table 2.4, entries 9-11).

Table 4 Screening of the solvent, base and catalyst/ligand ratio for the highly selective formation of **TT 3** and the hypothetical role of the acetate anion as an in situ generated proton source. Reaction conditions: isoprene (**1**) 100%, base 10%, 48 h.[17]

Entry	**Catalyst [%]**	**$(Ph)_3P$ [%]**	**Base**	**Solvent**	**T [°C]**	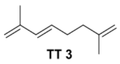 TT 3 **/others**	**Dimers [%]**
1	$Pd(OAc)_2$ (5)	-	Et_3N	THF	90	1:9	15
2	$(Ph_3P)_2PdCl_2$ (2)	-	Et_3N	THF	90	-	traces
3	$(Ph_3P)_4Pd$ (2)	-	Et_3N	THF	90	-	traces
4	$Pd(OAc)_2$ (2)	6	Et_3N	THF	90	16:1	91
5	$Pd(OAc)_2$ (2)	6	Et_3N	THF	70	-	traces
6	$Pd(OAc)_2$ (1)	3	Et_3N	THF	90	16:1	90
7	$Pd(OAc)_2$ (1)	3	KOH	THF	90	-	traces
8	$Pd(OAc)_2$ (1)	3	K_2CO_3	THF	90	4:3	-
9	$Pd(OAc)_2$ (1)	3	$KHCO_3$	MeOH	90	1:8	46
10	$Pd(OAc)_2$ (1)	3	Et_3N	EtOAc	90	9:1	30
11	$Pd(OAc)_2$ (1)	3	Et_3N	toluene	90	7:1	89
12	$Pd(OAc)_2$ (0.02)	0.06	Et_3N	THF	90	-	traces

A new class of ligands for this reaction was introduced by H. Beller and co-workers in 2007.[25] *In situ* generated palladium-carbene catalysts converted isoprene (**1**) to the homo-dimers almost quantitatively (98% yield, Table 5, entries 8 and 10). The N-heterocyclic carbenes (NHCs) were generated from various imidazolium salts (Table 5, IS-A – IS-E). The NHCs were initially considered as a promising class of ligands for telomerization due to their electron-richer character with respect to phosphines. However, it was additionally revealed that by an increase of the steric demand of the applied NHCs, the selectivity of the reaction was shifted to a considerable extent from the telomerization to the dimerization. Moreover, if isopropanol was applied instead of methanol, no telomerization was observed. In the system described, temperatures of more than 90 °C lead to polymerization, but this effect could be reduced by a decrease of the concentration of isoprene (**1**). Furthermore, a full conversion without diffusion control could be realized using liquid isoprene (**1**) at a reaction pressure of more than 50 bar.

Table 5 Imidazolium salts AS1-5 as source for in situ generated N-heterocyclic Pd-carbenes and their catalytic activity for isoprene (**1**) dimerization under varying parameters. Reaction conditions: Isoprene (**1**) 100% (10 mL, $c_{isorene\,(1)}$= 4 M), Pd(acac)$_2$, Pd : L = 1 : 10, 0.5% Na*i*PrO/*i*PrOH 15 mL, 24 h, 30 bar. [a]Isoprene (**1**) 100% (5 mL, $c_{isoprene\,(1)}$= 2M), NaiPrO/iPrOH 20 mL. [b] 50 bar.[25]

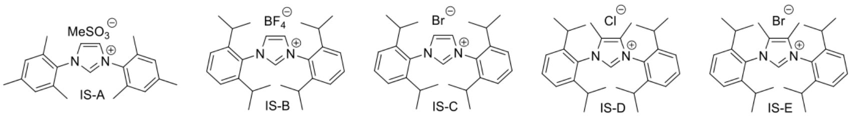

Entry	Ligand	Pd(acac)$_2$ [%]	T [°C]	Dimers [%]	Distribution of dimers [%] 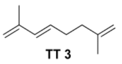 TT 3	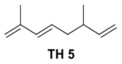 TH 5	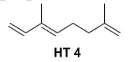 HT 4 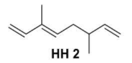 HH 2
1	Cy$_3$P	0.02	90	14	84	<1	15
2	IS-A	0.02	90	87	70	22	8
3	IS-A	0.01	70	69	47	37	16
4	IS-B	0.01	70	82	74	16	10
5	IS-B	0.005	70	76	71	15	14
6	IS-C	0.02	90	62	71	16	13
7	IS-D	0.01	70	93	72	17	11
8	IS-D[a]	0.02	90	98	75	16	9
9	IS-E	0.02	90	72	58	26	16
10	IS-E[b]	0.02	90	98	60	25	15
11	IS-E	0.01	130	69	55	11	34

The homo-dimer formation also strongly depends on the proton donor used in the reaction, e.g. various alcohols. It was shown that nucleophilic alcohols (that is, small and unbranched alcohols) react to telomers in a fast manner (Table 6 A, entries 1-4), whereas branched alcohols favor the formation of the homo-dimers (Table 7, entries 5-10). This is accompanied by an increase of the reaction time. Moreover, as expected, if the amount of alcohol is reduced, the formation of telomers also decreases drastically (Table 6 B, entries 1 and 2).[21,26]

Table 6 Influence of different alcohols (A) and the MeOH : isoprene (**1**) ratio (B) on the isoprene (**1**) conversion and (hetero)-dimer formation. Reaction conditions Table 6A): Isoprene (**1**) 100%, $Pd(acac)_2$ 0.05%, $(Ph)_3P$ 0.1%, alcohol 300%, 80 °C, 10 h. Reaction conditions Table 6B): Isoprene (**1**) 100%, $Pd(acac)_2$ 0.1%, $(Ph)_3P$ 0.2%, alcohol 300%, 80 °C, 5 h.[21]

A)

Entry	Alcohol	T [°C]	Conversion [%]	Dimers [%]	Telomers [%]	Trimers [%]
1	MeOH	60	100	21	79	-
2	MeOH	80	100	43	57	-
3	MeOH	100	100	46	54	-
4	EtOH	80	100	73	27	-
5	*n*PrOH	80	55	88	12	-
6	*i*PrOH	80	50	53	47	-
7	*n*BuOH	80	48	88	12	-
8	*i*BuOH	80	42	100	-	-
9	*s*BuOH	80	32	100	-	-
10	*t*BuOH	80	24	89	-	11

B)

Entry	MeOH : Isoprene (1)	Conversion [%]	Dimers [%]	Telomers [%]
1	0.2	95	86	14
2	0.5	100	78	22
3	1	100	65	35
4	3	100	50	50
5	5	100	48	54
6	10	100	42	58

The distribution of the homo-dimers, as well as the formation of trimers, is also influenced by the addition of phenol.[26] Various ratios of isoprene (**1**) : phenol were investigated. The selectivity for the formation of linear dimers decreased with an increasing amount of phenol. A total yield of 77% (90% conversion, 86% dimer selectivity) on the homo-dimers could be obtained with 3% phenol (Table 7 A, entry 2), whereas it was only 24% if 67% phenol was applied (Table 7 A, entry 5). Interestingly, the complete absence of phenol (Table 7 A, entry 1) also had a very negative effect on the conversion and selectivity as only 8% dimers where formed, from which only 26% were linear (**TT 3**). It was also revealed that the selectivity for dimer formation changed if different phenol derivatives were used. Apparently, methyl phenols with a higher pKa value favor the dimerization (Table 7 B, entries 1 and 2), whereas more acidic phenol derivatives such as 4-chloro-phenol lower both selectivity and conversion (Table 7 B entry 4). The exact role of phenol in the reaction mechanism has yet to be explored.

Table 7 Influence of various phenol amounts (A) and phenol derivatives (B) on the dimer formation and distribution. Reaction conditions: $PdBr_2(Ph_2PCH_2CH_2PPh_2)_2$ 0,08%, NaOPh 0,8%, benzene ($c_{Isoprene\ (\mathbf{1})}$= 1.8 M), 150 °C, 1 h.[27]

A)

Entry	**Phenol [%]**	**Conversion [%]**	**Dimers [%]**	**Distribution of dimers [%]** 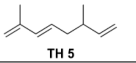 **TH 5**	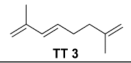 **TT 3**	**Others [%]**	**Trimers [%]**
1	0	19	43	-	26	74	20
2	3	90	86	6	89	5	12
3	17	96	72	37	55	8	22
4	33	95	57	60	28	12	24
5	67	75	32	34	9	57	34

B)

Entry	**Phenol derivative [33%]**	**Conversion [%]**	**Dimers [%]**	**Distribution of dimers [%]** 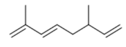 **TH 5**	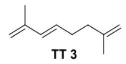 **TT 3**	**Others [%]**	**Trimers [%]**
1	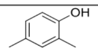	94	82	26	64	10	12
2	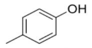	93	74	46	38	16	24
3	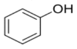	95	57	60	27	13	24
4	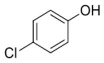	13	46	1	1	98	-

Generally, the homo-dimerization is favored by increasing the reaction temperature.[21,26,28] The distribution of the dimers can also be adjusted by defined heating profiles. Hidai et. al. observed that in a reaction system with $(n\mathrm{Bu}_3\mathrm{P})_2\mathrm{PdCl}_2$-NaOMe (1:3) and isoprene (**1**) without additional solvent lead to the formation of 65% of **TH 5** if it was kept at 25 °C for two days and then heated for 8 h at 80 °C.[29] Conversely, without the pretreatment at room temperature, **TT 3** was produced selectively. A more detailed investigation of this observation revealed that a temperature-controlled two-stage reaction leads to the formation of 75 % **TH 5** and 14 % **TT 3** (figure 3).[26]

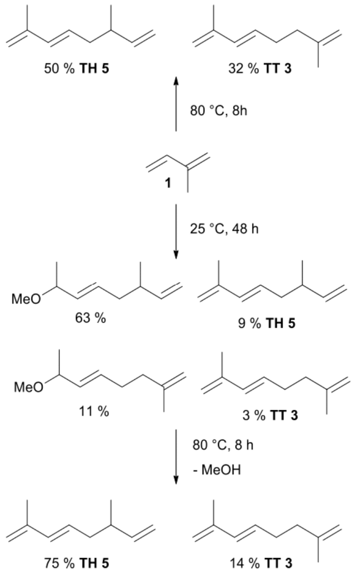

Figure 3 Two-stage temperature controlled telomerization and demethoxylation to the homo-dimers **TH 5** and **TH 3**.[26]

During the first stage, isoprene (**1**), $[(\eta^3\text{-}C_3H_5)PdCl]_2$ and $(Ph)_3P$ were stirred in a 1 : 1 mixture of methanol and isopropanol for 48 h at room temperature using NaOMe as a base. The analysis of the reaction mixture before the second stage showed that 74% of the dimers are methoxy-dimers. After the second stage (80 °C, 8 h), however, all methoxy-telomers are converted to the homo-dimers by elimination of methanol. The strategy to deliberately synthesize telomers and subsequent elimination of the attached nucleophile was reported before as one of the first strategies of isoprene (**1**) dimerization.[30] Phenol and isoprene (**1**) were telomerized catalyzed by $[(\eta^3\text{-}C_3H_5)PdCl]_2$ in the presence of sodium phenolate to 1-phenoxy-2,7-octadienes in a yield of 70% within 20 h. Degradation of the telomers to **HH 2** and **HT 4** was achieved via elimination of phenol catalyzed by a $[(\eta^3\text{-}C_3H_5)PdCl]_2/(Ph)_3P$ complex and concomitant separation of the dimers by distillation at 80 °C and a pressure of 1 mbar to shift the reaction equilibria towards the homo-dimers. An adjustment of the reaction equilibrium was not described for the afore mentioned elimination of methanol.[26,29] The yield of the second step was 75%, resulting in a total dimer yield of about 50%. Although similar isoprene (**1**) dimer acetates have been synthesized, their degradation to dimers has not been described yet.[31]

In addition to the formation of octatrienes, isoprene (**1**) can also be dimerized to dienes under reductive conditions. Heck and co-workers investigated this reaction in detail.[32] In the presence of 1.0 mol% of $[(C_3H_5)PdOAc]_2$, 1.0 mol% of $[2,5\text{-}C_6H_3(i\text{Pr})_2]P$ and stoichiometric amounts of formic acid and NEt_3 at 40 °C in THF, isoprene (**1**) was converted to four isomeric octadienes (3x**HT**, 1x**HH**) in a total yield of 98%. Two mechanisms for this reaction were suggested and are exemplarily displayed for the formation of the HT-dimers 2,6-dimethylocta-1,7-diene (**HT 6**) and 3,7-dimethylocta-1,6-diene (**HT 7**) in Figure 4.

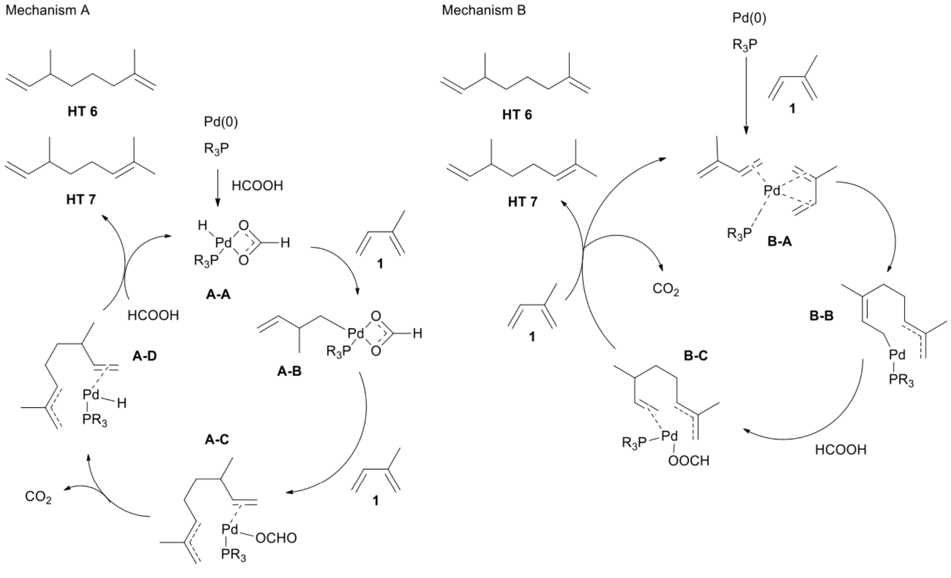

Figure 4 Reductive isoprene (**1**) head-to-tail dimerization as proposed by Heck and co-workers.[32]

In mechanism A, a hydridoformatopalladium(II) complex is formed by oxidative addition of formic acid to an *in situ* generated Pd(0) phosphine complex (**A-A**). Isoprene (**1**) then reacts with this complex to a formato(methylbutenyl) palladium complex (**A-B**). By addition of a second isoprene (**1**) molecule, a chelated complex is formed (**A-C**) that reductively eliminates the octadiene under loss of CO_2. Finally, the Pd-π complex intermediate (**A-D**) reacts with formic acid, liberating the product and regenerating the catalytic active hydridoformatopalladium(II) species (**A-A**).

Alternatively, the mechanism B favors the coordination and coupling of two isoprene (**1**) molecules to the Pd(0) catalyst (**B-A**) as initial step to form a dimethyloctadienediylpalladium(II) complex (**B-B**) that reacts with formic acid (**B-C**) and isoprene (**1**) under the loss of CO_2, HT **6** and HT **7**, thereby regenerating the Pd(0) catalyst (**B-A**).

In both cases, the base Et_3N can be considered as an equilibrium buffer to control the formic acid concentration, as an increase of the concentration of the acid may lead to the reduction of the monomer instead of the coupling product. To further decrease the concentration of formic acid, only one equivalent was used and added portion-wisely throughout the reaction. This led to an optimized yield and the formation of only small amounts of methyl-butene was observed. Other reaction parameters also had significant effects on the reductive dimerization, which can be summarized as follows: (I) ligands with increased electron donating capacity decreased the dimer formation (Table 10, entries 4, 5, 7-10) ; (II) ligands with increased electron donating capacity increased the reaction rate; (III) steric effects of the ligands showed no trend regarding the total yield, but large ligands preferably lead to tail-to-tail dimers; (IV) the ideal ratio of ligand : palladium was 1 : 1; (V) the formation of head-to-tail dimers was supported by low temperature; (VI) the anion of the palladium source was crucial to the reaction rate and dimer selectivity (acetate increases reaction rate and head-to-tail formation); and (VII) THF increased the reaction rate.

Table 8 Influence on the reductive dimerization of isoprene (**1**) of various catalysts, solvent and reaction time. Reaction conditions: catalyst 0.7%, $\mathrm{Et_3N}$ 110%, formic acid 130%, 40-45 °C. [a] $[2,5\text{-}\mathrm{C_6H_3}(i\mathrm{Pr})_2]\mathrm{P}$ 1.3%, 20-25 °C, formic acid added in aliquots.[32]

Entry	Catalyst	Solvent	Reaction time [h]	linear dimers [%]
1	$[(p\mathrm{C_6H_4CF_3})_3\mathrm{P}]_2\mathrm{PdCl_2}$	-	24	91
2	$[(p\mathrm{C_6H_4CF})_3\mathrm{P}]_2\mathrm{PdCl_2}$	-	10	59
3	$[(p\mathrm{C_6H_4Cl})_3\mathrm{P}]_2\mathrm{PdCl_2}$	-	10	73
4	$[(\mathrm{C_6H_5})_3\mathrm{P}]_2\mathrm{PdCl_2}$	-	24	24
5	$[(p\mathrm{C_6H_4OCH_3})_3\mathrm{P}]_2\mathrm{PdCl_2}$	-	24	27
6	$[(\mathrm{OCH_3})_2(\mathrm{OCH_2CH_3})\mathrm{P}]_2\mathrm{PdCl_2}$	-	24	55
7	$[(\mathrm{OCH_3})_3\mathrm{P}]_2\mathrm{PdCl_2}$	-	24	33
8	$[(\mathrm{O}o\mathrm{C_6H_4CH_3})_3\mathrm{P}]_2\mathrm{PdCl_2}$	-	24	28
9	$[(o\mathrm{C_6H_4OCH_3})(\mathrm{C_6H_4})_2\mathrm{P}]_2\mathrm{PdCl_2}$	-	24	16
10	$[(o\mathrm{C_6H_4CH_3})_3\mathrm{P}]_2\mathrm{PdCl_2}$	-	24	23
11	$[(\mathrm{C_6H_{11}})_3\mathrm{P}]_2\mathrm{PdCl_2}$	-	24	60
12	$[(\mathrm{C_6H_{11}})_3\mathrm{P}]_2\mathrm{Pd(OAc)_2}$	-	7	96
13	$[(\mathrm{C_6H_8})_3\mathrm{P}]_2\mathrm{Pd(OAc)_2}$	-	4	56
14	$[(\mathrm{OCH_3})_2(\mathrm{OCH_2CH_3})\mathrm{P}]_2\mathrm{PdCl_2}$	THF	24	89
15	$[(p\mathrm{C_6H_4Cl})_3\mathrm{P}]_2\mathrm{PdCl_2}$	THF	24	83
16[a]	$[(\mathrm{C_3H_5})\mathrm{PdOAc}]_2 + [2,5\text{-}\mathrm{C_6H_3}(i\mathrm{Pr})_2\mathrm{P}$	THF	12	98

An examination of Heck's system showed that the recovered catalyst was inactive. To minimize the amount of palladium, THF was then replaced by dimethylacetamide.[33] The change of the solvent enabled the use of only 0.01% of palladium catalyst with otherwise similar conditions and results, decreasing the palladium consumption by a factor of 100.

2 Ziegler-Natta catalysts

Ziegler-Natta catalysts (ZNc) are combinations of transition metal salts (group III to VIII, mainly IV, V and VI) and metal-organic compounds (group I to III, mainly organyl-aluminium species or Grignard reagents) that show activity as polymerization catalysts. These catalysts are commonly used for the polymerization of olefins or the highly selective industrial cyclo-trimerization of 1,3-butadiene and have also been applied for the dimerization of isoprene (**1**) several times. A simplified mechanism of this reaction with the ZNc system $\mathrm{Cp_2TiCl_2}/i\mathrm{PrCl}$ is displayed in Figure 5.[34–36]

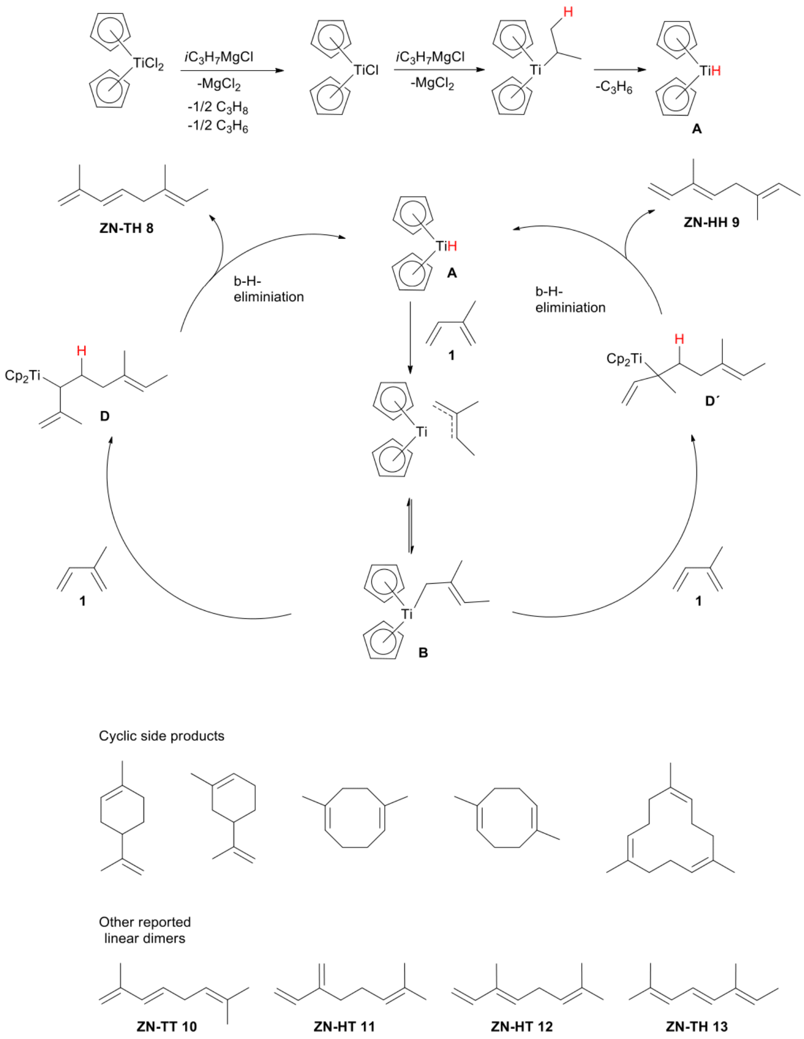
TiCl2
iC3H7MgCl
-MgCl2
-1/2 C3H8
-1/2 C3H6
TiCl
iC3H7MgCl
-MgCl2
H
Ti
-C3H6
TiH
A
ZN-TH 8
ZN-HH 9
TiH
A
b-H-
eliminiation
b-H-
eliminiation
1
H
Cp2Ti
D
H
Cp2Ti
D´
Ti
1
1
Ti
B
Cyclic side products
Other reported
linear dimers
ZN-TT 10
ZN-HT 11
ZN-HT 12
ZN-TH 13

Figure 5 Proposed (simplified) mechanism of the dimerization of isoprene (**1**) by the Ziegler-Natta system Cp_2TiCl_2/*i*PrMgCl.[34–36]

As various double bond isomers have been reported, other mechanisms also occur and the determination of the mechanisms is aggravated by the fact that most Ziegler-Natta systems are heterogeneous.[37] Additionally, the elaborated complex structures that have been detected for this and similar systems are neglected for the sake of simplicity.[38–40] However, at the time the catalysts were often not characterized sufficiently, and very little spectroscopic data was gathered. The complete mechanism of the dimerization of isoprene (**1**) by ZNcs is still unclear.

For this type of oligomerization, there are two competing mechanisms leading to two isomeric dimethyl-1,3,6-ocatatrienes. Hence, these dimers are also isomers to the Pd-catalyzed isoprene (**1**) dimers **2**-**5**. The reactive Ti-hydride catalyst (**A**) is formed by the *in-situ* reduction of Cp_2TiCl_2 by two equivalents of *i*PrMgCl under the loss of propene and propane. The active complex (**A**) then coordinates the head of isoprene (**1**) to form a η^3-allyldipentadienyltitanium (III) complex (**B**) which is more stable than the corresponding tail-complex. After insertion of another isoprene (**1**) unit and C-C bond formation (tail to head: **D**, head-to-head **D´**), the Ti-hydride complex (**A**) is reformed by β-H-elimination under release of the linear dimer products 2,6-dimethylocta-1,3,6-triene (**ZN-TH 8**) and 3,6-dimethylocta-1,3,6-triene (**ZN-HH 9**).

In 1959, Wilke used the combination of $CrCl_3$ and Et_2AlCl to oligomerize isoprene (**1**) into a mixture of cyclic dimers (from Diels-Alder reaction), linear dimethyloctatrienes – the structures **ZN-TH 8** and 2,7-dimethylocta-1,3,6-triene (**ZN-TT 10**) were postulated – and a mixture of isomeric dimethylcyclooctatrienes; yields were not given in this publication.[41] It was also mentioned that Ti was a suitable metal, but no experimental details were described for isoprene (**1**). Zakharkin then applied $TiCl_4$ (0.2 mol%) and *i*Bu_3Al (0.5 mol%) in toluene at 25 °C for 2 h, which gave a 41% of a mixture of linear and cyclic dimers, a similar amount of trimers, and about 20% of C_{20} (or higher) oligomers.[42] The $Ti(O\textit{n}Bu)_4$-Et_2AlCl system led to 36% of trimers and 21% of the **ZN-TH 8**.[43] N-vinylpyrrolidone (NVP), tosylate and carbonates have also been investigated as Ti coordinating ligands.[44] All these new ligands were easily obtained by precipitation from solutions of $TiCl_4$ and the respective ligands in benzene. They were then screened in the dimerization of isoprene (**1**) as described in Table 9.

Table 9 Influence of different amide, tosyl and carbonate ligands on the dimer formation and distribution. Reaction conditions: Ti-catalyst 0.38%, Et_2AlCl 1.5%, isoprene (**1**) 100%, c = 5 M, 50 °C, 2 h. [a]Missing to 100%: unreacted isoprene (**1**) or higher oligomers (>C_{15}). Reaction conditions: [b]80 °C, [c]Et_2AlCl 0.6%.[44]

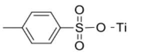
tosyl

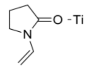
NVP

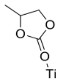
PC

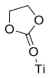
EC

Entry	Ti-catalyst	DMSO [%]	Dimers [%]	Trimers [%]	Distribution of dimers [%][a]		
					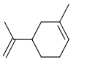	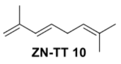 ZN-TT 10	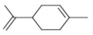
1	(tosyl)$_2$TiCl$_2$	-	34	-	40	58	2
2	(tosyl)$_2$TiCl$_2$	0.3	52	8	61	39	-
3[b]	(tosyl)$_2$TiCl$_2$	0.3	56	12	46	49	5
4[b]	(tosyl)$_2$TiCl$_2$	0.9	90	6	54	41	5
5[b]	(tosyl)$_2$TiCl$_2$	1.2	-	-	-	-	-
6	$TiCl_4$·NVP	-	62	5	49	49	2
7	$TiCl_4$·NVP	0.6	88	5	54	43	4
8	$TiCl_4$·2NVP	-	28	6	49	48	3
9	$TiCl_4$·2PC	-	52	12	54	44	6
10	$TiCl_4$·2EC	-	52	18	50	42	4
11[c]	$TiCl_4$	0.3	-	-	-	-	-
12	$TiCl_4$	0.3	29	42	38	58	5

Interestingly, the authors also suggested **ZN-TT 10** as the linear dimer structure based on chemical degradation experiments, as well as IR and NMR measurements. As for the cyclic dimers, the Diels-Alder products were identified, with the 1-methyl-3-isopropylene substitution pattern as very dominant major cyclic compound. The trimers were also cyclic, forming a 12-membered ring system. If bulky and electron-supplying ligands such as NVP (Table 9, entries 6-8) or toluene sulfonate (Table 9, entries 1-5) were used, dimerization was preferred. Alternatively, for the system $TiCl_4$-Et_2AlCl without ligands, trimers were formed as the main product (Table 9, entry 11). As it was verified that the ligands form a stable coordination bond with the Ti metallic center in the active species *via* their carbonyl oxygen, the authors hypothesized that, additionally to the mentioned coordinative ligands, two isoprene (**1**) molecules predominantly form a *cis-trans* coordination complex, followed by either a Diels-Alder reaction (tail-to-head complex) or the linear dimer **ZN-TT 10** (tail-to-tail complex, Figure 6).

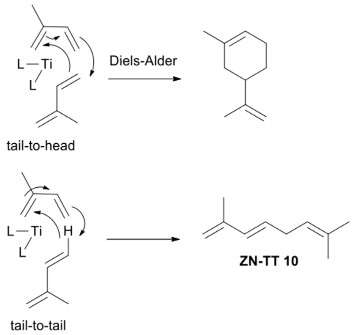

Figure 6 Cyclic dimer formation by Diels-Alder reaction compared to the tail-to-tail linear dimerization.[44]

Since the 1-methyl-4-isopropylene compound was only detected in traces, the hydride shift seems to be highly preferred compared to the Diels-Alder reaction in the tail-to-tail complex.

Head-to-head dimers such as **ZN-HH 9** were not detected, indicating that under the conditions described no corresponding complex was formed. The role of DMSO in this reaction is not clear, although it considerably increased the yield as long as the molecular ratio Ti : DMSO was not higher than 1 : 3. If more DMSO was used, no reaction was observed. It could also be demonstrated that a pure alkyl-aluminum base such as Et_3Al is unreactive. Pyridines with long alkyl substituents as ligands have also been used for the dimerization of isoprene (**1**) with Ti and Ni as applied transition metals.[37] Pyridines in general are suitable ligands as they can form σ-donor as well as η^6-π-complexes. The long alkyl chains were attached to the pyridine to increase the solubility of the formed complex in organic solvents. A selection of these catalysts and the results of their application are presented in Table 10. Under these conditions, Ni showed a higher tendency for linear dimerization (65.3% linear and 27.7% cyclic dimers, Table 10, entry 1) than Ti, which led mostly to the formation of various linear and cyclic trimers and higher oligomers. If the ratio of Ni : ligand was switched from 1 : 1.5 to 1 : 2.5, the distribution of the dimers changed drastically, leading to the preferred formation of the cyclic dimers (linear dimer 8.4%, cyclic dimer 65.5%, Table 10, entry 2). Ti was only tested with the 1 : 2.5 ratio, therefore it is unclear if a lower amount of ligand might shift the distribution towards the linear dimers. The alkyl-chain also had a considerable effect on the reaction selectivity. The alkyl pyridine A (**AP**-**A**) led to 65.3% of linear dimers, whereas with **AP**-**B** only 17.1% of linear dimers were produced (Table 10, entries 1 and 4). A second side chain as in **AP**-**C** resulted in an increase of the formation of cyclic dimers and various trimers (Table 10, entry 6), while the use of aryl substituents (**AP**-**D**) resulted in over 80% yield of the trimers (Table 10, entry 7). Again, the obtained linear trimers were isomers of the dimers discussed above, revealing the structures 7-methyl-3-methyleneocta-1,6-diene (**ZN-HT 11**), 3,7-dimethylocta-1,3,6-triene (**ZN-HT 12**) and 2,6-dimethylocta-2,4,6-triene (**ZN-TH 13**). This underlines the great variety of linear isoprene (**1**) dimers.

Table 10 Influence of different alkyl substituted pyridine ligands on the dimer formation and distribution. Reaction conditions: metal 0.3%, isoprene (**1**) 100%, iBu$_3$Al 1.7-3.0%, - 5 °C – 10 °C, 10 h. [a]Missing to 100%: unreacted isoprene (**1**) or higher oligomers ($>C_{15}$).[37] L = ligand; M = metal.

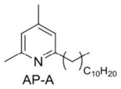

AP-A

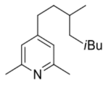

AP-B

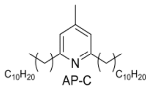

AP-C

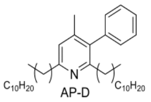

AP-D

Entry	L [%]	M	Linear dimer [%]	Distribution of linear dimers [%][a]			Cyclic dimers [%]	Trimer [%]
				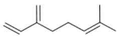 ZN-HT 11	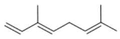 ZN-HT 12	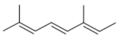 ZN-TH 13		
1	AP-A 0.45	Ni	65.3	71	16.4	12.6	27.7	7.0
2	AP-A 0.70	Ni	8.4	45.2	34.5	20.3	65.5	18.9
3	AP-A 0.70	Ti	8.4	77.4	20.6	-	17.8	49.9
4	AP-B 0.45	Ni	17.1	31.6	46.6	22.8	22.9	44.1
5	AP-B 0.70	Ti	5.3	52.8	47.2	-	11.8	13.0
6	AP-C 0.45	Ni	52.7	68.7	16.9	14.4	31.5	11.9
7	AP-D 0.45	Ni	4.2	28.6	-	71.4	8.6	82.8

Ni was used as transition metal in Ziegler-Natta catalysts before, with a maximum yield of 15% for linear dimers in a $Ni(acac)_2PPh(NEt_2)_2/Et_3Al$ system and 51% for linear trimers.[45] A more effective method was described in a patent from 1981, where the metal organyl was buthyl lithium (BuLi).[46] Table 2.11 displays the results from these experiments. Also, the new dimer 2,7-dimethylocta-1,6-diene (**dihydro-TT 3´**) was found in a considerable amount, which structurally is similar to **TT 3´** but with a saturated C4-C5 bond (Table 11, e.g. entry 2).

In addition to the reduced **dihydro-TT 3´**, also a hydrogenated form of isoprene (**1**), 2-methyl-but-2-en, was detected as side product (up to 17%). The influence of a very bulky H-donor resulted in the increased formation of linear trimers. With a maximum yield of 82% **TT 3**, the application of BuLi improved the yield by over 500% compared to Al-bases or alcoholates (Table 11, entry 3). The addition of π-electron donors also had a positive impact regarding the conversion and selectivity.

Table 11 BuLi as metal organyl in combination with various Ni catalysts. Reaction conditions: Ni-catalyst 1%, 90 °C. [a]80 °C. [b]Main side-product: linear trimer 57%.[46]

Entry	**Catalyst**	**Ligand** [%]	**BuLi** [%]	**Alcohol** [%]	**t** [h]	**Conversion** [%]	**Distribution of linear dimers** [%]	
							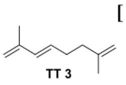 TT 3	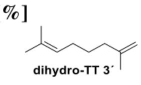 dihydro-TT 3´
1	$[(n\text{Bu})_3\text{P}]_2\text{NiCl}_2$	-	3	*i*PrOH [50]	8	39	30	-
2	$\text{Ni}(\text{C}_8\text{H}_{12}\text{O}_2)_2$	$(n\text{Bu})_3\text{P}$ [1.0]	4	*i*PrOH [66]	5	100	60	20
3	Ni(acac)_2	$(n\text{Bu})_3\text{P}$ [1.0]	4	*i*PrOH [100]	4	100	82	-
4	Ni(acac)_2	$(n\text{Bu})_3\text{P}$ [1.0]	4	pent-3-ol [50]	2	100	64	7
5	Ni(acac)_2	$(n\text{Bu})_3\text{P}$ [1.0]	4	menthol [50]	2	70	72	8
6	$\text{Ni}(\text{C}_8\text{H}_{12}\text{O}_2)_2$	$(\text{NMe}_2)_3\text{PO}$ [1.0]	3	*i*PrOH [33]	2	86	48	10
7	$\text{Ni}(\text{C}_8\text{H}_{12}\text{O}_2)_2$	$(\text{Ph}_3)\text{P}$ [1.0]	3	*i*PrOH [33]	2	92	45	15
8[a]	Ni(acac)_2	$(\text{NMe}_2)_3\text{PO}$ [1.0]	4	*i*PrOH [100]	3	89	52	-
9[b]	Ni(acac)_2	$(\text{NMe}_2)_3\text{PO}$ [1.0]	4	*t*-pentanol	5	100	35	-

Titanocene (dichloridobis(η^5-cyclopentadienyl)titanium, Figure 5) and alkyl-titanocene complexes have also been investigated for the dimerization of isoprene (**1**) in a R-Cp_2TiCl_2/ *i*PrMgCl system.[35] In this attempt, Grignard reagents were used as reducing agents. The reaction parameters such as the nature and the amount of the applied solvent, reaction time and temperature, as well as the catalyst : isoprene (**1**) ratio have been addressed. The results can be summarized as follows: (I) THF is the most suitable solvent for the isoprene (**1**) dimerization compared to diethyl ether and dioxane. This can be explained by the low solubility of the catalyst system in these solvents. (II) Increasing the solvent volume lead to longer reaction times, but also increased the dimer selectivity. (III) The reaction time of 10 h lead to 70% conversion; longer reaction times resulted in an increased formation of higher oligomers. (IV) The temperature optimum was 65 °C, whereas lower or higher reaction temperatures stopped the reaction or led to polymerization, respectively. (V) A catalyst : isoprene (**1**) ratio of 1 : 55 proved to be superior in terms of dimer formation (27% yield) and selectivity (39%).The results of various alkylated titanocene dichlorides under the optimized conditions are displayed in Table 12.

Table 12 Effect of different alkyl-substituents for isoprene (**1**) dimerization in the Cp_2TiCl_2/*i*PrMgCl system. Reaction conditions: Ti-catalyst 1.8%, *i*PrMgCl 10%, isoprene (**1**) 100%, THF, 65 °C, 10 h.[35]

Entry	Catalyst	Conversion [%]	Higher oligomer yield [%]	Dimer yield [%]	Distribution of dimers [%] 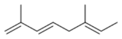 **ZN-TH 8**	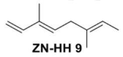 **ZN-HH 9**
1	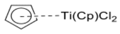	70	43	27	67	33
2	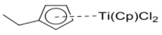	46	31	15	75	25
3	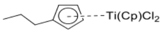	30	25	5	64	36
4	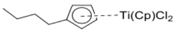	35	28	7	56	44
5	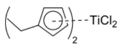	38	29	9	86	14
6	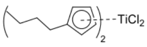	35	26	9	74	36
7	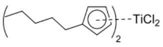	40	32	11	73	27

Both the yield and the distribution of **ZN-TH 8** and **ZN-HH 9** were affected by different alkyl substituents. Alkylation of one or both cyclopentadiene (Cp) ligands led to a decrease of the conversion and yield of the dimer. This effect is more dominant if both Cps were alkylated. The yields decreased with a growing alkyl chain until C_3 was reached (Table 12, entry 3); then, a minor increase was observed for C_4- and C_5-alkylation. Interestingly, the ratio **ZN-TH 8** : **ZN-HH 9** was rather similar in all cases, with the exception of the ethyl-Cp, reaching a 86% selectivity for **ZN-TH 8** (Table 12, entry 5). In total, a maximum yield of 27% for the linear dimers was reached for the non-alkylated Cp_2TiCl_2 catalyst (Table 12, entry 1). In a follow-up publication, the effect of alkenyl-substituted Cps was described as illustrated in Table 13.[47] The conversion was increased by over 14% up to 84% for the *n*-butenyl substituted Cp (Table 13, entry 2). Also, the other alkenyl substituents proved to be more effective than their alkyl counter parts (e.g. Table 12, entry 3 and Table 13, entry 5 for a propyl/propenyl substituent).

Table 13 Effect of different alkenyl-substituents for isoprene (**1**) dimerization in the Cp_2TiCl_2/*i*PrMgCl system. Reaction conditions: see Table 12.[47]

Entry	Catalyst	Conversion [%]	Higher oligomer yield [%]	Dimer yield [%]	Distribution of products [%]	
					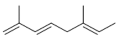 ZN-TH 8	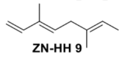 ZN-HH 9
1	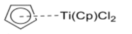	70	43	27	67	33
2	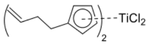	84	53	31	63	37
3	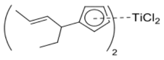	68	39	29	72	28
4	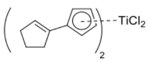	62	47	15	63	27
5	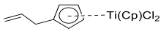	64	40	24	68	32
6	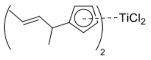	72	44	28	69	31

The authors explained these results by an additional stabilization of the *in situ* generated Ti-hydride complex by the coordinating double bonds as shown in Figure 7.

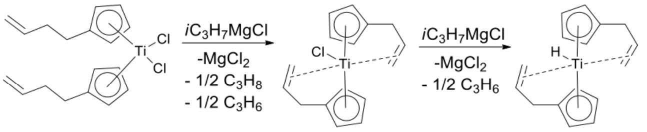

Figure 7 Assumed stabilization of the active state due to the coordination of Ti by alkenes.[47]

Nonetheless, with an isolated yield of only 31% for the linear dimers, competitive conditions for titanocene complexes are yet to be found. Other transition metals such as Fe, Ni, Co, Cr and Ni as Ziegler-Natta catalyst in combination with a Grignard reagent as reducing agent instead of the commonly used alkyl-Al compounds have also been investigated.[48] The influence of different electron donors was also described. For all combinations, the maximum yield was only 38% (Table 14, entry 12). The results are displayed in Table 14.

Table 14 The dimerization of isoprene (**1**) with a Grignard compound as reducing agent in combination with various metal catalysts and electron donors. Reaction conditions: 100% isoprene (**1**), 2.2% catalyst, 2.2% electron donor, 6.6% Grignard reagent, 50-60 °C, 5 h; dipy = dipyridyl; phen = o-phenanthroline. [a]Missing to 100%: unidentified products. [b]Mixing order: $[(Ph)_3P])_2NiBr_2$, THF, isoprene (**1**), Grignard reagent. [c]Mixing order: $[(Ph)_3P])_2NiBr_2$, THF, Grignard reagent, isoprene (**1**). [d]linear dimer 80%.[48]

					Distribution of products [%][a]		
Entry	**Catalyst**	**Electron donor**	**Grignard reagent**	**Dimer yield [%]**	**Cycloocta-dienes**	**Cyclohexa-dienes**	**Linear Dimers**
1	$Fe(acac)_3$	dipy	BuMgBr	30	93	7	-
2	$Fe(acac)_3$	dipy	*i*PrMgBr	33	90	10	-
3	$Ni(acac)_2$	dipy	EtMgBr	8	-	100	-
4	$Ni(acac)_2$	$(Ph)_3P$	EtMgBr	10	-	100	-
5	$Ni(acac)_2$	phen	EtMgBr	10	-	90	-
6	$Co(acac)_2$	$(Ph)_3P$	EtMgBr	8	-	100	-
7	$Cr(acac)_3$	dipy	EtMgBr	5	-	100	-
8	$Cr(acac)_3$	$(Ph)_3P$	EtMgBr	3	-	100	-
9	$Mg(acac)_2$	$(Ph)_3P$	EtMgBr	3	-	100	-
10	$NiBr_2$	-	BuMgBr	-	-	-	-
11	$Co_2(CO)_8$	-	BuMgBr	5	-	100	-
12[b,d]	$[(Ph)_3P])_2NiBr_2$	-	EtMgBr	38	-	-	80
13[c]	$[(Ph)_3P])_2NiBr_2$	-	EtMgBr	5	-	-	80

All tested systems led to the formation of cyclooctadienes or cyclohexadienes, except for the $[(Ph)_3P)_2]NiBr_2$/EtMgBr system, which led to a conversion of 38% of isoprene (**1**) with a selectivity of 80% towards the linear dimers **ZN-TH 8** (75%), a 2,7-dimethyloctane (15%) and a 3,6-dimethyloctane (10%) that were not examined in detail (Table 14, entry 12). Another interesting finding was the big impact of the mixing order of the reactants (Table 14 entries 12 and 13). The yield of the dimers was greatly increased when isoprene (**1**) was added to the reaction mixture before the Grignard reagent (Table 14, entry 12 compared to entry 13). This indicates an interaction of isoprene (**1**) with the catalyst that facilitates the dimerization, which is decreased by the presence of the Grignard reagent. A mixing order of THF, isoprene (**1**), Grignard reagent and catalyst to exclude a direct dimerization of isoprene (**1**) by the Grignard reagent was not reported. The complete absence of a Grignard reagent in this system was also not described.

The application of Zr as transition metal in Ziegler-Natta catalysts for the oligomerization of isoprene (**1**) has also been reported several times.[49–5149–51] Misono *et al.* investigated various Zr-compounds and different reaction conditions, including the influence of additives.[50] In contrast to the Ti-compounds that formed several dimer isomers, Zr selectively produced **ZN-TH 8** and higher oligomers. These results can be summarized as follows: (I) For the Zr compound, $Zr(OnBu)_4$ and $Zr(C_3H_5)_4$ led to dimerization and polymerization, whereas the use of $ZrCl_4$ resulted in low yields due to a low solubility. Moreover, $Zr(acac)_4$ selectively polymerized isoprene (**1**). (II) The most suitable Al-base was Et_2AlCl in a molar ratio of Et_2Al : Zr-compound of 1 : 10. Within 2 h at a reaction temperature of 100 °C and with 1 mol% of the Zr-catalyst and 10 mol% of Et_2AlCl, 50% of **ZN-TH 8** was isolated, representing the highest yield reported in this series of experiments. An increase of the amount of the Al-base led to a conversion of almost 100%, but the dimers also exhibited an increased tendency to polymerize and, therefore, the isolated yield strongly decreased. Other tested Al-bases either led to polymerization (Et_3Al, Et_2AlCl_2) or no reaction (Et_2AlOEt). (III) The reaction time of 1 h showed the best selectivity, as an increased reaction time led to polymerization. The best compromise between reaction time and conversion was 2 h. (IV) Additives had no positive effect on the reaction. $(Ph_3)P$ improved the selectivity to a minor extent, but the conversion was reduced. THF and 2,2´dipyridyl suppressed the reaction drastically. The authors explained these results by the valence state of Zr during the reaction, which was assumed to be four due to magnetic measurements (diamagnetic during all reaction stages).

As Zr is in the d^0 configuration in the tetra-valent state, the back donation to ligands is of little relevance for the reaction outcome. (V) The yield of the trimer was about 10%, and analysis of the trimer fraction revealed three different trimers; for two of them, a linear structure was identified.

In a follow-up publication, $Zr(C_3H_5)_4$ was re-investigated in combination with other Al-compounds, revealing a positive effect on the conversion and the selectivity, in which the isolated yield was increased by 32% up to 66% for the $Zr(C_3H_5)_4/Et_{1.5}AlCl_{1.5}$ system (Table 15, entry 3).[52]

Table 15 Effect of Al-compounds at optimized Al : Zr ratios on the dimerization of isoprene (**1**) by $Zr(C_3H_5)_4$. Reaction conditions: catalyst 1.0%, isoprene (**1**) 100%, benzene ($c_{isoprene\ (1)}$= 6 M), 100 °C, 2 h.[52]

Entry	**Aluminum compound**	**Al : Zr ratio**	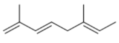 **ZN-TH 8**
1	Et_3Al	1 - 11	-
2	Et_2AlCl	4.5 - 10	40
3	$Et_{1.5}AlCl_{1.5}$	2	66
4	$EtAlCl_2$	1	51
5	$AlCl_3$	0.46	17
6	none	-	12

Zr-catalysts were also patented by Mitsubishi Petrochemical in the aspect of isoprene (**1**) dimerization.[49] Various Zr-catalysts and Al-compounds were investigated. The results are listed in Table 16. The best combined yield of linear dimers was 75%, accomplished with a $Zr(OEt)_2Cl_2$/ *i*Bu_2AlCl and $(Ph)_3P$ system dissolved in benzene (Table 16, entry 5). As suitable solvents, hydrocarbons such as benzene, xylene or heptane were described. Alternatively, the solvent free reaction was mentioned to be possible, but no experimental data was reported. In contrast to the afore mentioned selective synthesis of **ZN-HT 8**, in this case **ZN-HH 9** was also detected in considerable amounts. The trimer yield was up to 19% (Table 16, entry 1 and 2), and trimer formation was favored at lower temperatures combined with sterically demanding ligands.

Table 16 Dimerization and trimerization of isoprene (**1**) by Zr-catalysts in combination with various Al-compounds and P-additives. Reaction conditions: Zr-catalyst 0.2%, isoprene (**1**) 100%, $c_{isoprene\,(1)}$: 4.2 M, solvent: [a]benzene, [b]toluene, [c]xylene, 8 h. [d]Missing to 100% = higher oligomers. [49]

Entry	Catalyst	T [°C]	P- [%]	Al- [%]	Distribution of products [%][d]		
					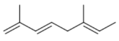 ZN-TH 8	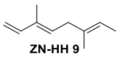 ZN-HH 9	Trimers [%]
1[a]	$Zr(OnBu)_3Cl$	80	$(Ph)_3P$ [0.45]	Et_2AlCl [1.4]	60	7	19
2[a]	$Zr(nOiPr)_3Cl$	80	$P(OC_7H_8)_3$ [0.9]	Et_2AlCl [1.8]	63	6	19
3[b]	$Zr(nOPh)_3Cl$	100	$PnBu_3$ [0.45]	Et_2AlCl [2.7]	61	6	14
4[c]	$Zr(OnBu)_2Cl_2$	110	$P(OPh)_3$ [0.45]	Et_2AlCl [1.8]	57	10	12
5[a]	$Zr(OEt)_2Cl_2$	80	$(Ph)_3P$ [0.68]	iBu_2AlCl [2.3]	61	14	9
6[b]	$Zr(OnBu)_3Br$	100	$P(OPh)_3O$ [0.68]	Et_2AlBr [3.6]	45	5	14
7[b]	$Zr(OnBu)_2Br_2$	100	$(Ph)_3P$ [0.45]	Et_2AlCl [2.3]	47	7	13

Trimers:

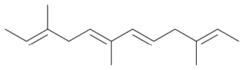

ZN-HHTH 14

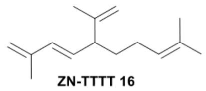

ZN-TTTT 16

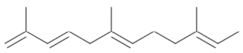

ZN-THTH-15

Contrary to Misono´s observations, the additives such as $(Ph)_3P$ had no negative influence on the result of the reaction; in fact, the best results were achieved by their addition. The trimers were isolated and analyzed regarding their structure, revealing to be linear unbranched C_{12}-chains in the case of **ZN-HHTH 14** and **ZN-THTH 15**, and a C_{10} chain with an *iso*-propylene-branch for **ZN-TTTT 16** that arises from a di-substitution at the tail double bond of the center-located isoprene (**1**) unit.

Hf, V, Co and Fe as Ziegler-Natta catalysts have also been investigated by Misono, Uchida *et al.* in a very similar approach as the previously described Zr-catalysts.[50,51,53,54] For Hf and V the results were comparable to the experiments achieved by Zr catalysis, although in both cases another linear dimer (probably **ZN-HH 9**) was observed additionally to the main dimer **ZN-HT 8**.[52,53] Although many temperatures, isoprene (**1**) : catalyst ratios and Al-compounds were tested, the combined dimer yield never exceeded 60%. This indicates that Ti is the most suitable metal for the Ziegler-Natta catalyzed dimerization of isoprene (**1**). This assumption is also supported by the results of Co and Fe based catalysts, which exclusively formed cyclo-dimers in almost quantitative yields.[52] For the $Co(acac)_2/Et_3Al\text{-}(Ph)_3P$ system in benzene at 80 °C, the formation of **TT 3´´** has been reported, but the yield was only 10%.[55] Methylaluminoxane (MAO) is a very active co-catalyst for Kaminsky-catalysts (that is, Ziegler-Natta metallocene-type catalysts). MAO can be used for the selective dimerization and, in particular, trimerization of isoprene (**1**) in combination with symmetric chromium *N,N*-bis(diarylphosphino)amine catalysts (PNP-catalysts). In a subsequent publication of the same group, non-symmetric chromium PNP and *N,N*-bis(diarylphosphino)dimethylhydrazine (PNNP) catalysts were reported (Table 17).[56,57]

Table 17 Symmetric and asymmetric PNP- and PNNP-ligands in combination with MAO for the trimerization of isoprene (**1**). Reaction conditions: 100% isoprene ($c_{isoprene\,(1)}$= 6.8 M), toluene, 0.007% $(THF)_3CrCl_3$, 0.007% ligand, 2% MAO, 70 °C, 1 h.[56,57]

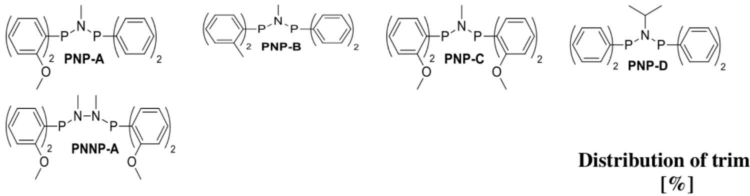

Entry	Ligand	$g(g_{Cr}h)^{-1}$	Total trimer	Distribution of trimers [%]		
				Linear	Cyclic	Other
1	PNP-A	585	98	99	1	2
2	PNP-B	669	86	87	13	14
3	PNP-C	826	79	70	30	21
4	PNP-D	298	95	74	26	5
5	PNNP-A	1103	100	87	13	0

The ratio of linear to cyclic trimer was depended on the concentration of isoprene (**1**). On the one hand, at 0.5 M of substrate concentration the formation of the cyclic trimer (linear : cyclic = 32% : 68%) was favored. On the other hand, at a concentration of 6.8 M the product distribution was inverted to a 88 : 12 linear : cyclic ratio. This was explained by the postulated mechanism (Figure 2.8), where the trimer ratio depends on the rate of the reductive elimination, which is assumed to be facilitated by isoprene (**1**) in the case of the linear trimer formation.

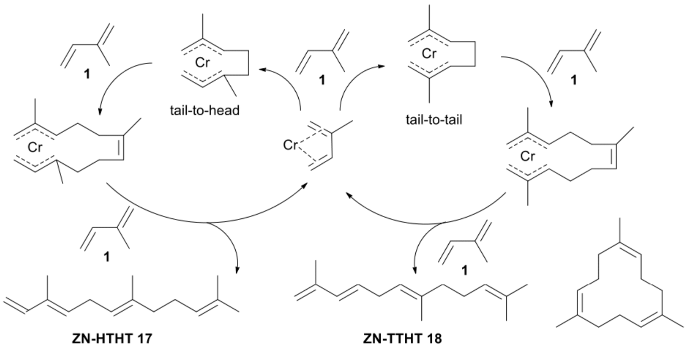

Figure 8 Proposed mechanism for the trimerization of isoprene (**1**) by Cr-PNP/PNNP-MOA catalysis.[56,57]

The productivity of the reaction was increased by heating, whereas the trimer selectivity decreased in favor of higher oligomers (79% at 70 °C, 100% at 25 °C). In control experiments it was verified that the Cr-compound, as well as the ligands and MAO, were crucial for the reaction. The application of the most suitable reaction conditions achieved a yield of 98% of the trimers with a distribution of 99% linear and 1.0% cyclic, marking the most selective trimerization of isoprene (**1**) reported to date (Table 17, entry 1). The asymmetric **PNP-A** clearly increased the selectivity towards the linear trimers compared to the symmetric **PNP-C** (Table 17, entry 3) Analysis of the linear trimers revealed a mixture of **ZN-HTHT 17** and **ZN-TTHT 18**. The PNNP-motif increased the productivity of the reaction, obtaining 100% yield (Table 17, entry 5).

3 Other methods

Nickel has been used in the dimerization and trimerization of isoprene (**1**) not only as part of a Ziegler-Natta system, but also in other catalytic systems.[46,58,59] Isoprene (**1**) was converted to dimers with the carbon structure of **TT 3** (the double bond pattern was not investigated) in 79% yield (82% conversion) within 10 h at 80 °C in an inert system containing 0.4% $(COD)_2Ni$ as catalyst and 1.4% $(n\mathrm{Bu})_3P$ as ligand and *i*PrOH as proton donor/solvent ($c_{\mathrm{isoprene}\ (\mathbf{1})}$= 7 M). The alcohol was crucial for this reaction; the same was reported for Pd-catalysis (see section 1).[58] Ni salts of organic acids or halides have also been tested under various conditions that are summarized in Table 18.

Table 18 Results of the oligomerization of isoprene (**1**) to **TT 3**, **ZN-TT 10** and **ZN-TTHT 18** by a Ni-catalyst. Reaction conditions: $[(n\text{Bu})_3\text{P}]_2\text{NiCl}_2$ 1.0%, 90 °C, 8 h. [a]*i*Pr/H_2O = 1:1.5. [b]Missing to 100% = higher oligomers.[59]

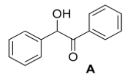
A

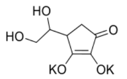
B

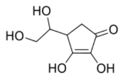
C

Entry	1	2	3	4	5	6	7	8
Additive [%]	A [1]	B [1]	C [1]	B [1]	B [3]	B [2]	C [1]	C [2]
Base [%]	KOH [4.0]	KOH [4.0]	KO*t*Bu [2.0]	KO*t*Bu [2.0]	KOH [2.0]	KO*t*Bu [3.0]	KO*t*Bu [4.0]	KO*t*Bu [4.0]
Solvent	MeOH	*i*PrOH/ H_2O[a]	*t*BuOH	*t*BuOH	*i*PrOH	*t*BuOH	*t*BuOH	*t*BuOH
$c_{\text{Isoprene}\,(\mathbf{1})}$ [M]	7.1	5.5	6.8	6.8	5.6	6.8	6.8	6.8
Conversion [%]	50	60	100	100	60	100	100	100
	Distribution of products [%][b]							
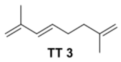 **TT 3**	75	76	65	84	78	76	7	4
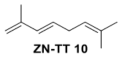 **ZN-TT 10**	22	14	5	12	20	3	5	7
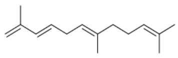 **ZN-TTHT 18**	-	-	-	-	-	14	72	87

With this method, very good results for both the dimer (up to 96% yield for combined **TT 3** and **ZN-TT 10**, Table 18, entry 5) and the trimer (87% yield, Table 18, entry 8) formation could be obtained. Other methods with Ni as catalytic metal and combinations of various bases such as Et_3N or $C_{15}H_{31}ONa$ and non-P-based ligands such as $(i\text{Pr})_3\text{As}$ have been reported. However, the yield and selectivity never exceeded 30%.[45,60]

In$(acac)_3$ has also been used for the Lewis acid catalyzed isoprene (**1**) oligomerization, reaching a yield of 89% as a mixture of dimers and trimers (6% catalyst, solvent free, 72 h at 30 °C). The obtained complex product mixture was not investigated in detail, although head-to-tail bonds were verified by NMR.[61]

The reductive dimerization of isoprene (**1**) was also achieved using Li-naphthalene, in which the **TH 25** and **TT 26** isomers were isolated with a total yield of 40% (Table 19, entry 1).[62] As a side reaction, a polymerization process was observed for all tested reaction conditions. The ratio of Li : isoprene (**1**) defined the contribution of dimers, trimers and tetramers. Unfortunately, the structural information of the trimers was not provided. Use of other alkali metal dispersions led to yields of oligomers below 30%.

Table 19 Li-naphthalene as reagent for the dimerization of isoprene (**1**) and the influence of the amount on the oligomer distribution.[62]

				Distribution of dimers [%]				
Entry	**Isoprene (1) [%]**	**Li-naphthalene [%]**	**Dimers [%]**	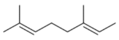 TH 25	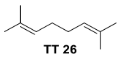 TT 26	**Trimers [%]**	**Tetramers [%]**	**Others [%]**
1	100	50	40	50	50	5	-	30
2	100	33	7	50	50	35	7	40
3	100	25	2	50	50	5	40	50
4	100	17	-	-	-	-	2	80

In 2018, isoprene (**1**) was successfully oligomerized and hydrogenated over a NiMoS/Al_2O_3 catalyst from a spent commercial hydrotreater.[15] The reaction conditions implied 2.4 w% of isoprene (**1**) in decalin, 250 °C, 3.4 MPa of H_2, liquid hourly space velocity of 2 h^{-1} and H_2/feed ratio 392 mL(STP)/mL, leading to the dimer on a 15% yield. The authors proposed a mechanism for the formation of the four detected isomers **HH 2**, **TT 3**, **HT 4** and **TT 21** (Figure 9).

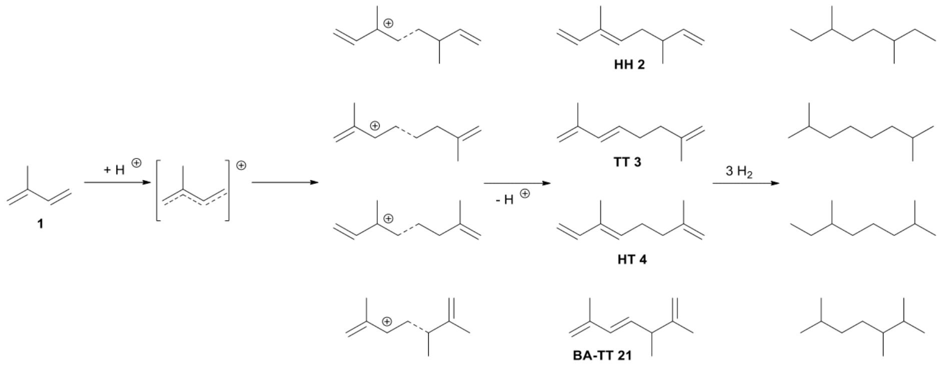

Figure 9 Dimerization and complete hydrogenation of the product dimers by a NiMoS/Al_2O_3-H_2 catalyst system.[15]

Due to a Brønsted acid function of the NiMoS/Al_2O_3 catalyst, isoprene (**1**) forms an allylic carbocation that is stabilized by resonance. In a next step, another isoprene (**1**) molecule attacks to the allyl cation, resulting in a dimer with a secondary or tertiary carbocation, which then reacts with a proton acceptor to form the specific dimer. Hence, for other alkenes without stabilization by conjugation such as penta-1,4-diene, dimers were not detected. In another control experiment, oct-1-ene was added to the reaction mixture, but no isoprene (**1**)-octene heterodimer was observed.

Although the oligomerization of isoprene (**1**) can also be carried out with metal-free Brønsted acids, the selectivity is very low.[63] Thus, H_2SO_4, CH_3CO_3H and Nafion-H have been tested, giving a product mixture consisting mostly of cyclic dimers or higher oligomers up to C_{25}; the best selectivity was 11% at a conversion of 52%. The authors suggested the structures of the hydrogenated dimers; presenting each a carbon-backbone structure that differed from the ones reported for the metal coordination catalysts (Figure 10). The positions of the double bonds before the hydrogenation were not reported.

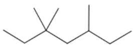
hydroBA-HH 19

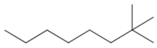
hydroBA-HT 20

Figure 10. Proposed from the isoprene (**1**)dimers formed by Brønsted acid catalysis after hydrogenation.[63]

Another metal free strategy is the utilization of SO_3H-functionalized imidazolium ionic liquids (IL, Table 20).[64] A great advantage of this method is that the products were insoluble in the ionic liquid and could be separated by simple decantation. Additionally, the IL was reused seven times with only minor loss of selectivity and an almost unchanged conversion.

Table 20 Dimerization and trimerization with SO_3H-functionalyzed imidazolium ionic liquids. Reaction conditions: 25% ionic liquid, 100% isoprene (**1**), 120 °C, 6 h.[64]

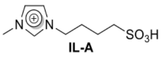
IL-A

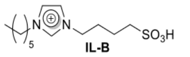
IL-B

Entry	**Ionic liquid**	**Conversion [%]**	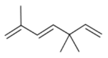 **BA-TS 22**	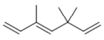 **BA-HH 23**	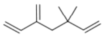 **BA-HH 24**	**Others**	**Trimer**	**Tetramer**
1	IL-A	100	21	15	23	22	11	8
2	IL-B	100	4	2	3	1	79	11

As can be concluded from the results for the short-chain and long-chain alkylated imidazolium salt, the selectivity of the reaction highly depended on the polarity of the IL. The longer aliphatic chain of **IL-B** probably leads to a better solubility of the produced dimers, which can then be converted to higher oligomers before the layers segregate. Especially, the selectivity for trimers (79% yield) and for head-to-head dimers **BA-HH 23** and **BA-HH 24** (38%) was remarkable. All in all, this metal-free method with adjustable selectivity is a very interesting alternative to coordination catalysis as it is green, comparably robust towards moisture, easy to handle and requires only moderate reaction conditions (120 °C, 6 h).

4 Conclusion

The application of isoprene (**1**) as building block for bio-fuels faces major challenges such as selective synthesis of linear C_{10}-C_{15} oligomers, competitive costs compared to fossil fuels or scalability of laboratory preparation methods. The reviewed coordination metal catalysts require an inert atmosphere, are hard to recycle and the reusability – if investigated at all – does not meet industrial demands yet. For example, Heck´s Pd-catalyzed dimerization proved to be highly effective, achieving an overall dimer yield of up to 98%, but either high amount of catalyst (e.g. 1.0 mol%) or the toxic and expensive solvent dimethylacetamide had to be applied. Other Pd protocols are also hard to handle and use complex ligands (P-ligands, carbenes and others). Cheaper metals such as Ti, Fe or Co have been applied in Ziegler-Natta catalysis, but selectivity, conversion and yield are considerably decreased. Neither the standard protocols applying Ti salts and Al organyl compounds nor the advanced catalysts (alkenyl-cyclopentadienyl-Ti compounds, alkylated pyridine ligands etc.) lead to a satisfactory dimerization. For the linear trimerization, Ni and Cr can be used with excellent yields under application of PNP-ligands, probably representing the most promising method presented in this review. Heterogeneous catalysts have not been investigated in detail up to date, and gas-phase reactions are yet to be explored. For metal-free methods, acidic ionic liquids are promising. However, ionic liquids are still not widely accepted in industry and open new problem-sets on their own (e.g. high costs, end-of-life disposal). Taking all this into account, many challenges in the field of catalysis need to be addressed in the future in order to bring the synthesis of bio-based isoprene (**1**) derivatives to a level in which they can start truly competing with fossil-based fuels.

5 References

1. Morais, A. R.C. *et al.* Chemical and biological-based isoprene production. Green metrics. *Catalysis Today* **239,** 38–43; 10.1016/j.cattod.2014.05.033 (2015).
2. Wang, S. *et al.* Production of isoprene, one of the high-density fuel precursors, from peanut hull using the high-efficient lignin-removal pretreatment method. *Biotechnology for biofuels* **10,** 297; 10.1186/s13068-017-0988-5 (2017).
3. Riazi, B., Karanjikar, M. & Spatari, S. Renewable Rubber and Jet Fuel from Biomass. Evaluation of Greenhouse Gas Emissions and Land Use Trade-offs in Energy and Material Markets. *ACS Sustainable Chem. Eng.* **6,** 14414–14422; 10.1021/acssuschemeng.8b03098 (2018).
4. Beller, H. R., Lee, T. S. & Katz, L. Natural products as biofuels and bio-based chemicals. Fatty acids and isoprenoids. *Natural product reports* **32,** 1508–1526; 10.1039/c5np00068h (2015).
5. Lu, X. *Biofuels. From microbes to molecules* (Caister Academic Press, Norfolk, 2014).
6. Chaves, J. E. & Melis, A. Biotechnology of cyanobacterial isoprene production. *Appl. Microbiol. Biotechnol.* **102,** 6451–6458; 10.1007/s00253-018-9093-3 (2018).
7. Chaves, J. E. & Melis, A. Engineering isoprene synthesis in cyanobacteria. *FEBS letters* **592,** 2059–2069; 10.1002/1873-3468.13052 (2018).
8. Wilson, J., Gering, S., Pinard, J., Lucas, R. & Briggs, B. R. Bio-production of gaseous alkenes. Ethylene, isoprene, isobutene. *Biotechnology for biofuels* **11,** 234; 10.1186/s13068-018-1230-9 (2018).
9. Li, M. *et al.* Improvement of isoprene production in Escherichia coli by rational optimization of RBSs and key enzymes screening. *Microbial cell factories* **18,** 4; 10.1186/s12934-018-1051-3 (2019).
10. Pahima, E., Hoz, S., Ben-Tzion, M. & Major, D. T. Computational design of biofuels from terpenes and terpenoids. *Sustainable Energy Fuels* **3,** 457–466; 10.1039/C8SE00390D (2019).
11. Li, M., Nian, R., Xian, M. & Zhang, H. Metabolic engineering for the production of isoprene and isopentenol by Escherichia coli. *Applied microbiology and biotechnology*; 10.1007/s00253-018-9200-5 (2018).

12. Ezinkwo, G. O., Tretjakov, V. F., Talyshinky, R. M., Ilolov, A. M. & Mutombo, T. A. Overview of the Catalytic Production of Isoprene from different raw materials; Prospects of Isoprene production from bio-ethanol. *Catalysis for Sustainable Energy* **1**; 10.2478/cse-2013-0006 (2013).
13. McAuliffe, J. C. *Fuel Compositions Comprising Isoprene Derivatives* (2012).
14. Harvey, B. C. *High Density Fuel from Isoprene* (2017).
15. Alzaid, A., Wiens, J., Adjaye, J. & Smith, K. J. Impact of molecular structure on the hydrogenation and oligomerization of diolefins over a Ni-Mo-S/γ-Al 2 O 3 catalyst. *Fuel* **221,** 206–215; 10.1016/j.fuel.2018.02.030 (2018).
16. Nicholas, C. P. Applications of light olefin oligomerization to the production of fuels and chemicals. *Applied Catalysis A: General* **543,** 82–97; 10.1016/j.apcata.2017.06.011 (2017).
17. Kellner, D., Weger, M., Gini, A. & Mancheño, O. G. Pd(OAc)2/Ph3P-catalyzed dimerization of isoprene and synthesis of monoterpenic heterocycles. *Beilstein journal of organic chemistry* **13,** 1807–1815; 10.3762/bjoc.13.175 (2017).
18. Josey, A. D. Palladium-catalyzed linear dimerization of conjugated dienes. *J. Org. Chem.* **39,** 139–145; 10.1021/jo00916a004 (1974).
19. Josey, A. D. & Kirchner, J. R. *1,3,7-Octatriene und ihre Herstellung* (1972).
20. Young, E. L. de. *Dimerization of olefinic compounds* (1972).
21. Beger, J., Duschek, C. & Reichel, H. Dienoligomerisierung. VIII. Palladiumkomplexkatalysierte Dimerisierung und Telomerisierung von methylsubstituierten Butadienen im alkoholischen Medium. *J. Prakt. Chem.* **315,** 1077–1089; 10.1002/prac.19733150611 (1973).
22. ANTEUNIS, M. & SMET, A. de. Synthesis of 2,7-Dimethyl-1,3, trans -7-octatriene (Tail-to-Tail Isoprene Dimer). *Synthesis* **1974,** 800–801; 10.1055/s-1974-23433 (1974).
23. Musco, A. Tail-to-tail dimerization of isoprene catalyzed by Pd0—phosphine complexes in the presence of CO2. *Journal of Molecular Catalysis* **1,** 443–445; 10.1016/0304-5102(76)85007-9 (1976).
24. Ploner, K.-J. *Verfahren zur Herstellung ungesättigter Kohlenwasserstoffe* (1974).
25. Jackstell, R., Grotevendt, A., Michalik, D., El Firdoussi, L. & Beller, M. Telomerization and dimerization of isoprene by in situ generated palladium–carbene catalysts. *Journal of Organometallic Chemistry* **692,** 4737–4744; 10.1016/j.jorganchem.2007.06.039 (2007).
26. Yagi, H., Tanaka, E., Ishiwatari, H., Hidai, M. & Uchida, Y. Synthesis of 2,6-Dimethyl-1,3- trans ,7-octatriene (Head-to-tail Isoprene Dimer) by a Temperature-Controlled Two-Stage Reaction. *Synthesis* **1977,** 334–335; 10.1055/s-1977-24387 (1977).
27. Takahashi, K., Hata, G. & Miyake, A. Dimerization of Isoprene by Palladium-Diphosphine Complex Catalyst. *BCSJ* **46,** 600–602; 10.1246/bcsj.46.600 (1973).
28. Zakharkin, L. I. & Babich, S. A. Dimerization of isoprene in methanol using palladium complexes. *Russ Chem Bull* **25,** 1967–1968; 10.1007/BF00921735 (1976).
29. Hidai, M. *et al.* Synthesis of (+)- or (–)-citronellol from isoprene. *J. Chem. Soc., Chem. Commun.* **0,** 170–171; 10.1039/C39750000170 (1975).
30. Smutny, E. J. *Octatriene Production* (1966).
31. Suga, K., Watanabe, S. & Hijikata, K. The reaction of isoprene with acetic acid catalysed by palladium dichloride. *Aust. J. Chem.* **24,** 197; 10.1071/ch9710197 (1971).
32. Neilan, J. P., Laine, R. M., Cortese, N. & Heck, R. F. Monoterpene syntheses via a palladium catalyzed isoprene dimerization. *J. Org. Chem.* **41,** 3455–3460; 10.1021/jo00883a030 (1976).
33. Chalk, A. J. & Magennis, S. A. A Comparison of Transition Metal and non-Transition Metal Oligomerisations of Isoprene for the Synthesis of Terpenes. *Ann NY Acad Sci* **333,** 286–301; 10.1111/j.1749-6632.1980.tb53648.x (1980).
34. Martin, H. A. & Jellinek, F. Synthesis of allyldicyclopentadienyltitanium(III) complexes from dienes. *Journal of Organometallic Chemistry* **12,** 149–161; 10.1016/S0022-328X(00)90908-2 (1968).
35. Tao, X., Qian, F., Yong, L. & Qian, Y. Substituent effect on oligomerization of isoprene catalyzed by ring-substituted (RCp)2TiCl2/i-C3H7MgCl system. *Journal of Molecular Catalysis A: Chemical* **156,** 121–126; 10.1016/S1381-1169(99)00418-5 (2000).
36. Sato, F., Urabe, H. & Okamoto, S. Synthesis of Organotitanium Complexes from Alkenes and Alkynes and Their Synthetic Applications. *Chem. Rev.* **100,** 2835–2886; 10.1021/cr990277l (2000).
37. Bogatian, M. V. *et al.* Pyridines with long alkylsubstituents as ligands in oligomerization of isoprene. *Revue Roumaine de Chimie* **51,** 735–741 (2006).
38. Stephan, D. W. Titanium/magnesium complexes. Intermediates in the reduction of titanocene dichloride by magnesium. *Organometallics* **11,** 996–999; 10.1021/om00038a081 (1992).
39. Troyanov, S. I., Antropiusová, H. & Mach, K. Direct proof of the molecular structure of dimeric titanocene; The X-ray structure of μ(η5. H5-fulvalene)-di-(μ-hydrido)-bis(η5-cyclopentadienyltitanium)· 1.5 benzene. *Journal of Organometallic Chemistry* **427,** 49–55; 10.1016/0022-328X(92)83204-U (1992).
40. Varga, V., Petrusová, L., Cejka, J. & Mach, K. Fermethyltitanocene(III) diacetylide - magnesium tweezer complexes, intermediates in the catalysis of linear head-to-tail dimerization of terminal acetylenes. *Journal of Organometallic Chemistry* **532,** 251–259; 10.1016/S0022-328X(96)06806-4 (1997).
41. Wilke, G. Oligomerization of 1,3-diolefines with ziegler-type catalysts. *J. Polym. Sci.* **38,** 45–50; 10.1002/pol.1959.1203813305 (1959).
42. Zakharkin, L. I. Formation of linear dimer of isoprene over a complex (iso-C4H9)3Al-TiCl4 catalyst. *Dokl. Akad. Nauk SSSR,* 1069–1071 (1960).
43. Takahashi, D. & Yamaguchi, M. *Daikoshi Kiho,* 271 (1964).

44. Itakura, J. & Tanaka, H. The Oligomerization of isoprene with modified Ziegler Catalysts. *Makromol. Chem.* **123,** 274–285; 10.1002/macp.1969.021230126 (1969).
45. Akutagawa, S., Taketomi, T. & Otsuka, S. METAL-ASSISTED TERPENOID SYNTHESIS II. CATALYTIC CONVERSION OF ISOPRENE INTO FARNESENE AND ITS ISOMER, 2,6-DIMETHYL-10-METHYLENE-1,6-TRANS,11-DODECATRIENE. *Chem. Lett.* **5,** 485–490; 10.1246/cl.1976.485 (1976).
46. Alder, E., Fuellbier, H. & Gaube, W. *Verfahren zur selektiven Herstellung von acyclischen Isoprenoligomeren* (1981).
47. Yong, L., Tao, X., Qian, F. & Qian, Y. Organotitanium chemistry. Substituent effects on the dimerization of isoprene catalyzed by alkenyl-substituted cyclopentadienyl titanium complexes. *Journal of Molecular Catalysis A: Chemical* **184,** 147–150; 10.1016/S1381-1169(02)00008-0 (2002).
48. Watanabe, S., Suga, K. & Kikuchi, H. Dimerization of isoprene by transition metal complexes and Grignard reagents. *Aust. J. Chem.* **23,** 385; 10.1071/CH9700385 (1970).
49. Morikawa, Hiroyuki & Ibaraki. *Verfahren zur Herstellung von Isoprenoligomeren* (1971).
50. Misono, A., Uchida, Y., Furuhata, K.-i. & Yoshida, S. Oligomerization of Isoprene by Zirconium Catalysts. *BCSJ* **42,** 2303–2307; 10.1246/bcsj.42.2303 (1969).
51. Uchida, Y., Furuhata, K.-i. & Yoshida, S. Oligomerization of Isoprene by the Catalyst Systems Consisting of Tetraallylzirconium and Aluminum Compounds. *BCSJ* **44,** 1966–1967; 10.1246/bcsj.44.1966 (1971).
52. Misono, A., Uchida, Y., Hidai, M. & Ohsawa, Y. The Oligomerization of Isoprene by Cobalt or Iron Complex Catalysts. *BCSJ* **39,** 2425–2429; 10.1246/bcsj.39.2425 (1966).
53. Misono, A., Uchida, Y., Furuhata, K.-i. & Yoshida, S. Oligomerization of Isoprene by Hafnium Catalysts. *BCSJ* **42,** 1383–1386; 10.1246/bcsj.42.1383 (1969).
54. Uchida, Y., Furuhata, K.-i. & Ishiwatari, H. Oligomerization of Isoprene by Vanadium Catalysts. *BCSJ* **44,** 1118–1121; 10.1246/bcsj.44.1118 (1971).
55. Beger, J., Duschek, C. & Paul, D. Dienoligomerisierung; Isoprenoligomerisierung durch ein Kobalt-Ziegler-Natta-Katalysatorsystem. *Z. Chem.* **13,** 133–134; 10.1002/zfch.19730130408 (1973).
56. Bowen, L. E. *et al.* Ligand effects in chromium diphosphine catalysed olefin co-trimerisation and diene trimerisation. *Dalton transactions (Cambridge, England : 2003),* 560–567; 10.1039/b913302j (2010).
57. Bowen, L. E., Charernsuk, M. & Wass, D. F. The selective trimerisation of isoprene with chromium N,N-bis(diarylphosphino)amine catalysts. *Chemical communications (Cambridge, England),* 2835–2837; 10.1039/B702331F (2007).
58. Someya, T., Sakaguchi, T., Akutagawa, S. & Komatsu, A. *Verfahren zur Herstellung von Kohlenwasserstoffen vom Squalen-Typ* (1974).
59. Gaube, W., Füllbier, H. & Alder, E. *Verfahren zur selektiven Herstellung von acyclischen Oligomeren 1,3-Dienen* (1977).
60. Akutagawa, S. *et al.* Metal-Assisted Terpenoid Synthesis. V. The Catalytic Trimerization of Isoprene to trans -β-Farnesene and Its Synthetic Applications for Terpenoids. *BCSJ* **51,** 1158–1162; 10.1246/bcsj.51.1158 (1978).
61. Rodriguez, J. G. Acetylacetonate of indium. Structure and reactivity with 1,3-dienes. *React Kinet Catal Lett* **36,** 91–96; 10.1007/BF02071146 (1988).
62. Suga, K., Watanabe, S., Kikuchi, H. & Watanabe, T. Oligomerization of isoprene. *Can. J. Chem.* **46,** 2619–2623; 10.1139/v68-426 (1968).
63. Audisio, G., Priola, A. & Rossini, A. Cationic oligomerization of isoprene and structure of its oligomers. *Makromolekulare Chemie. Macromolecular Symposia* **47,** 263–270; 10.1002/masy.19910470121 (1991).
64. Gu, Y., Shi, F. & Deng, Y. SO3H-functionalized ionic liquid as efficient, green and reusable acidic catalyst system for oligomerization of olefins. *Catalysis Communications* **4,** 597–601; 10.1016/j.catcom.2003.09.004 (2003).

2.2 Isoprene derivatives as valuable monomers

As extensively outlined in Section 1, bio-based thermoplastics derived from isoprene (**1**) are of interest. The corresponding lactams **2**-**4** for polyamides and lactones **5**-**6** for polyesters are accessible from the conversion of isoprene (**1**) with chlorosulfonyl isocyanate (CSI, Figure 2.1). Epoxide **7** could be used as a building block for polyethers by polymerization of the terminal alkene or for polyethers by polymerization of the oxirane.

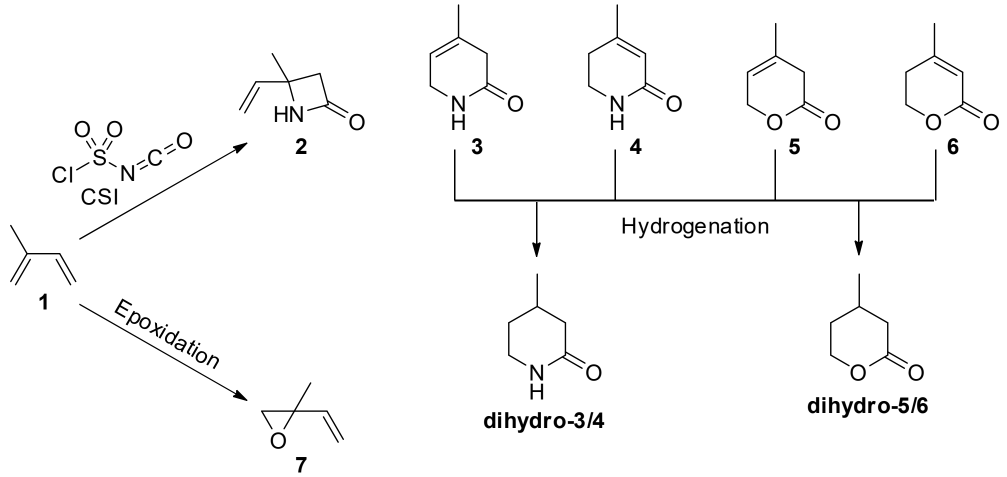

Figure 2.1 Selected isoprene (**1**)-based building blocks for polymers.

Works regarding the hydrogenated form of lactone **6** – lactone **dihydro-5/6** – have already been reported, and it is considered as valuable monomer that is also accessible from glucose (Figure 2.2 a).[90] It has been used as a component of sustainable graft block copolymer thermoplastics,[91] polyurethans,[92] copolymer with polylactic acid,[93] and – after conversion to isoprene carboxylic acid – functionalized polyethylene for superabsorbent hydrogels.[94] Because of these broad application spectrum, an alternative synthesis from (bio-based) isoprene that does not compete with food production is desirable.

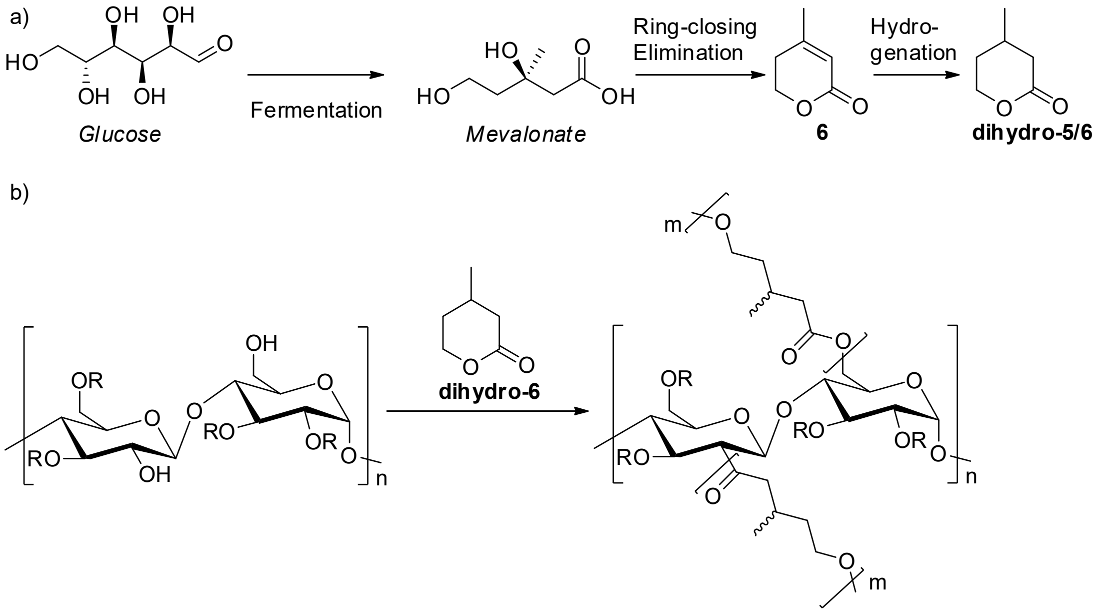

Figure 2.2 Pathway from glucose to **dihydro-5/6** (a) and application of **dihydro-5/6** in a polysaccharide copolymer (b).

For the lactams **2**, **3** and **4**, no polymerizations have been reported. However, copolymerizations of piperidin-2-on, which is structurally the same as a hydrogenated lactam **3** or **4** but misses the methyl group, have been successfully performed. These polyamides possess new properties, such as a decreased melting point in a PA4/PA5-type copolyamide.[95,96] A similar approach with **dihydro-3/4** is therefore of interest, though the additional methyl group might lead to a challenging polymerization.[38,95,96] Poly-β-amides are usually investigated in terms of their bioactivity, and antibacterial polyamides from various β-lactams have been reported (Figure 2.3).[97–105] Since a polyamide of lactam **2**, **poly2**, would still possess a terminal alkene in the side chain, many post-polymerization modifications could be applied, including chiral modifications. In addition, the terminal olefin of **2** was copolymerized with ethylene, styrene, and other alkenes to give side-chain containing polyethylene derivatives.[106]

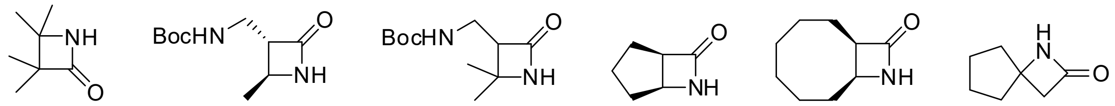

Figure 2.3 Various β-lactams which have successfully been polymerized to the corresponding poly-β-amides.

Isoprene epoxide **7** has also already been applied as a precursor or for direct polymerization to vinyl-polyethers.[107–112]

2.2.1 Reactions of isoprene with chlorosulfonyl isocyanate (CSI)

After Graf discovered the formation of chlorosulfonyl-lactams by the reaction of olefins with chlorosulfonyl isocyanate (CSI),[113] the reaction of isoprene with CSI has been investigated in the literature for the synthesis of δ-lactones **5** and **6** and β- and δ-lactams **2-4**.[113–117] Hoffmann suggested the formation of a linear sulfonyl amide, where a new bond is formed between the

C1 of isoprene and the carbonyl group of CSI in diethyl ether at room temperature.[118] However, this compound could only be isolated after subsequent reaction with 4-chloroaniline. At 0 °C reaction temperature, the sulfonyl beta lactam was synthesized and isolated after reaction with aniline. Moriconi and others investigated the reaction in detail and suggested a complex temperature-dependent sequence of rearrangements and hydrolysis equilibria (Scheme 2.1).[119,120]

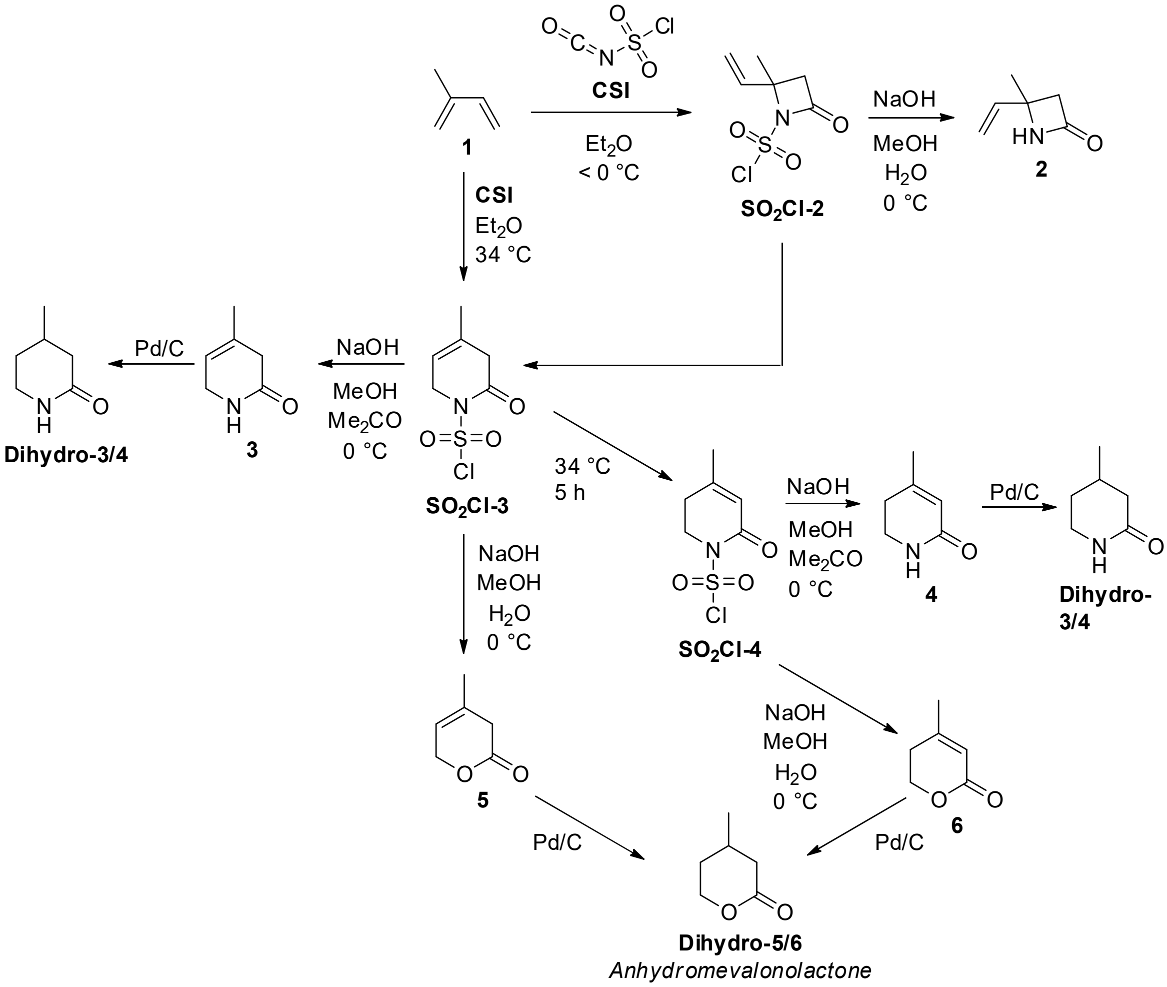
CSI
Et$_2$O
< 0 °C
1
NaOH
MeOH
H_2O
0 °C
2
SO$_2$Cl-2
CSI
Et$_2$O
34 °C
Pd/C
NaOH
MeOH
Me$_2$CO
0 °C
Dihydro-3/4
3
SO$_2$Cl-3
34 °C
5 h
NaOH
MeOH
Me$_2$CO
0 °C
Pd/C
4
Dihydro-3/4
SO$_2$Cl-4
NaOH
MeOH
H_2O
0 °C
5
NaOH
MeOH
H_2O
0 °C
6
Pd/C
Pd/C
Dihydro-5/6
Anhydromevalonolactone

Scheme 2.1 Reaction pathway for the synthesis of lactams **2-4** and lactones **5-6** as precursor for **dihydro-5/6**.

If the reaction was carried out in diethyl ether at temperatures below 0 °C, the 2,2' substituted double bond of isoprene (**1**) reacted with CSI in a 2+2 cycloaddition. The resulting chlorosulfonyl isoprene β-lactam **SO$_2$Cl-2** was reported to precipitate at -65 °C, but was unstable to recrystallization. Hydrolysis at 0 °C in a mixture of H_2O, EtOH and NaOH gave lactam **2** in 50% yield. A similar approach led to 76% yield, whereas a reaction temperature of -20 °C in a pressure vessel and a reaction time of two days resulted in over 90% yield.[121,122] Subsequent heating at 35 °C rearranges lactam **SO2-Cl-2** to lactam **SO$_2$Cl-3**. If the reaction was carried out in diethyl ether at reflux temperature from the beginning on, the 4,5 unsaturated chlorosulfonyl isoprene δ-lactam **SO$_2$Cl-3** was produced directly. This rather unstable lactam then rearranges into the more stable 3,4 unsaturated chlorosulfonyl isoprene δ-lactam **SO_2Cl-4** (31% yield after recrystallization). **SO_2Cl-3** was converted into lactone **5** by hydrolysis in aqueous MeOH/NaOH solution (22% yield). The double bond of lactone **5** was stable towards isomerization to the 3,4 unsaturated lactone **6**. This lactone was accessible by hydrolysis of lactam **SO_2Cl-4** in a yield of 30%.[119] The challenges described in all reports are the temperature-sensitive reaction conditions, little selectivity, low yields and unsatisfying purity of the products. This is due to several aspects of this reaction cascade: (I) considerable temperature sensitivity, (II) isomerization of the initially formed C5-C6 double bond to the more stable Michael-type system for the δ-structures, (III) parallel reactions despite temperature control, and (IV) sensitive hydrolysis leading to irrepressible lactone formation.

2.2.2 Synthesis of 4-methyl-4-vinylazetidin-2-one (2)

The target compound was synthesized using CSI in Et_2O at a reaction temperature of -70 °C up to -10 °C in an argon atmosphere. The hydrolysis was conducted at 0 °C in basic media with Na_2SO_3 and $NaHCO_3$. The isolated yield was 72%. During the synthesis it was detected that the 2+2 cycloaddition was the preferred mechanism and almost no δ-structures were formed at low temperatures. If the temperature surpassed -10 °C, the β-lactam **SO_2Cl-2** started to rearrange to the δ-structure; this was in agreement with literature.[120,123] As Et_2O is not a suitable solvent for industry applications, the reaction was screened in various solvents (Table 2.1). In general, screening of the reaction conditions was challenging as neither isoprene (**1**) nor the sulfonyl chloride species are detectable by GCMS and an uncontrolled micro-hydrolysis for in-process control (IPC) was not reliable and hard to reproduce. Therefore, thin-layer chromatography (TLC) was used for IPC, which is not a quantitative method. Nonetheless, relative comparisons gave information about the influence of the solvent polarity.

Table 2.1 Influence of solvent polarity on the product distribution of the reaction of isoprene (**1**) with CSI. Reaction conditions: T = -70 – -30 °C, t = 2 – 3 h. *reaction temperature 0 °C.

Solvent	Polarity[124]	SO_2Cl-2	SO_2Cl-3	SO_2Cl-4	Side products
Hexane	0.009	-	-	-	-
Toluene	0.099	++	+	-	-
Diethyl ether	0.117	+++	+	-	-
MTBE	0.124	-	-	-	-
Dioxane	0.164	+	++	+	+
THF	0.207	+	++	++	+
EtOAc	0.228	+	++	++	+
MeCN	0.460	+	+++	++	+
Toluene/ EtOAc (5:1)*	-	+++	+	-	-

For hexane, no reaction was detected at low temperatures and the CSI and hexane formed two layers. If the reaction temperature exceeded 0 °C, CSI started to dissolve in the hexane and a very exothermic uncontrolled reaction with isoprene resulted in a wild mixture of products that where not further investigated. **SO_2Cl-2** was formed in toluene to similar extent as in Et_2O, but TLC indicated a decreased reaction rate. Solvents with an increased polarity such as dioxane, THF and MeCN led to an increased reaction rate, and the direct formation as well as the rearrangement to **SO_2Cl-3** occurred at the same time. Additionally, the isomerization of **SO_2Cl-3** to **SO_2Cl-4** was preferred in polar solvents. If the reaction was performed in methyl *t*-butyl ether (MTBE), an unsuspected product was formed almost exclusively and NMR and GCMS analysis verified the formation of 4,4-dimethylazetidin-2-one (**8**, Figure 2.4).

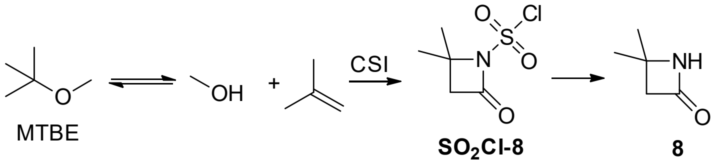

Figure 2.4 Proposed reaction pathway for the synthesis of lactam **8** from MTBE.

Hypothesizing, MTBE – catalyzed by acidic conditions from traces of isocyanate sulfonic acid – may form an equilibrium with MeOH and isobutylene that subsequently reacts with CSI to **SO_2Cl-8**. Hydrolysis then leads to the β-lactam **8**.

In all pure polar solvents, the δ-structures were formed at temperatures above -10 °C – 0 °C. At low reaction rates due to nonpolar solvents, the already formed **SO_2Cl-2** started to rearrange to the δ-structures before all isoprene was consumed. Therefore, diethyl ether was the most suitable solvent, as the reaction rate was satisfying at a temperature low enough to ensure a high selectivity to the β-lactam **2**. Another approach was using a mixture of a polar and a nonpolar solvent to adjust the reaction rate to acceptable conversion, but to decrease the rearrangement to the δ-structure at the same time. A mixture of toluene and EtOAc (5:1) led to the formation of **SO_2Cl-2** with a selectivity of > 90% within three hours at 0 °C and no detectable isoprene residues, representing a suitable replacement for Et_2O. Another advantage is the increased reaction temperature that does not require intensive cooling.

2.2.3 Initial polymerization of 4-methyl-4-vinylazetidin-2-one (2)

Although the synthesis was the main objective, and not the polymerization of potential monomers, lactam **2** was polymerized by anionic ring-opening polymerization (aROP, Section 1.8) for the proof of concept (Scheme 2.2)

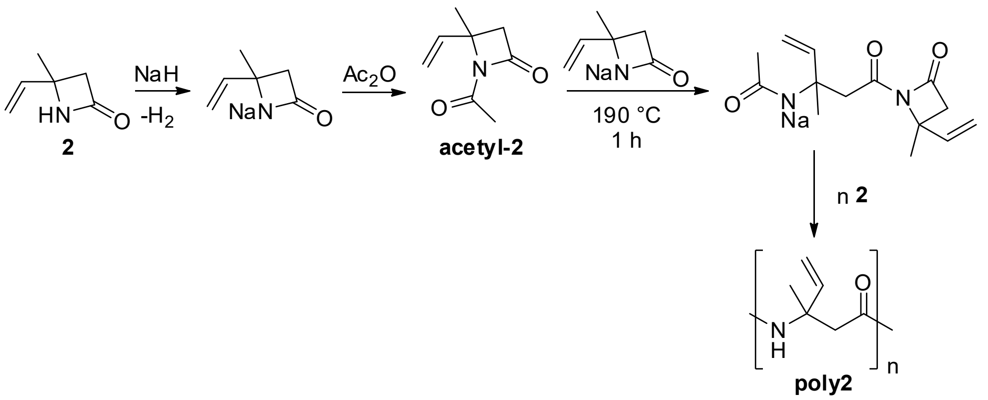

Scheme 2.2 AROP of lactam **2** to **poly2** with NaH and Ac_2O.

As a first try, polymerization was achieved using NaH (60% on paraffin wax) as initiator and in-situ generated **N-acetyl-2** at 190 °C in an argon atmosphere. Lactam **2** was melted in the reaction flask under inert atmosphere before NaH was added, followed by Ac_2O. The resulting brown and very brittle solid was crushed and stirred in EtOH/H_2O to remove residual monomers and was then frequently washed with EtOAc. Analysis by NMR showed that the lactam bond was indeed the reacting functional group, and the terminal double bond was still present. ^{13}C analysis revealed – as expected for a racemic monomer mixture – that the polyamide was atactic as the side-chain carbons directly attached to the chiral center in the polymer backbone gave more than one signal (Figure 2.5).

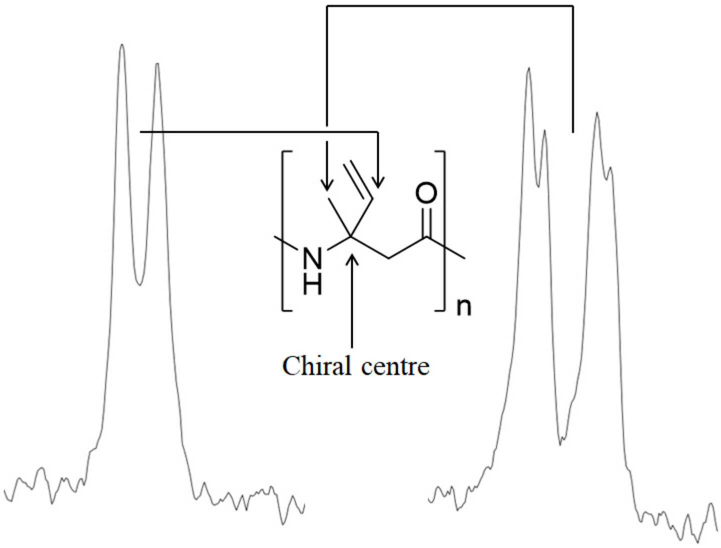

Figure 2.5 ^{13}C-NMR of **poly2** and signal-splitting of carbons attached to the chiral center as expected for an atactical polymer.

In a more controlled approach, the polymerization system of Section 2.4 was used (N-benzoyl-3S-Caranlactam as activator and NaH as initiator). All components were mixed in a glass vial under inert atmosphere and then heated in a heating block for 15 min. **Poly2** generated with this protocol was only slightly yellow and less brittle. The residual monomers were removed as described above.

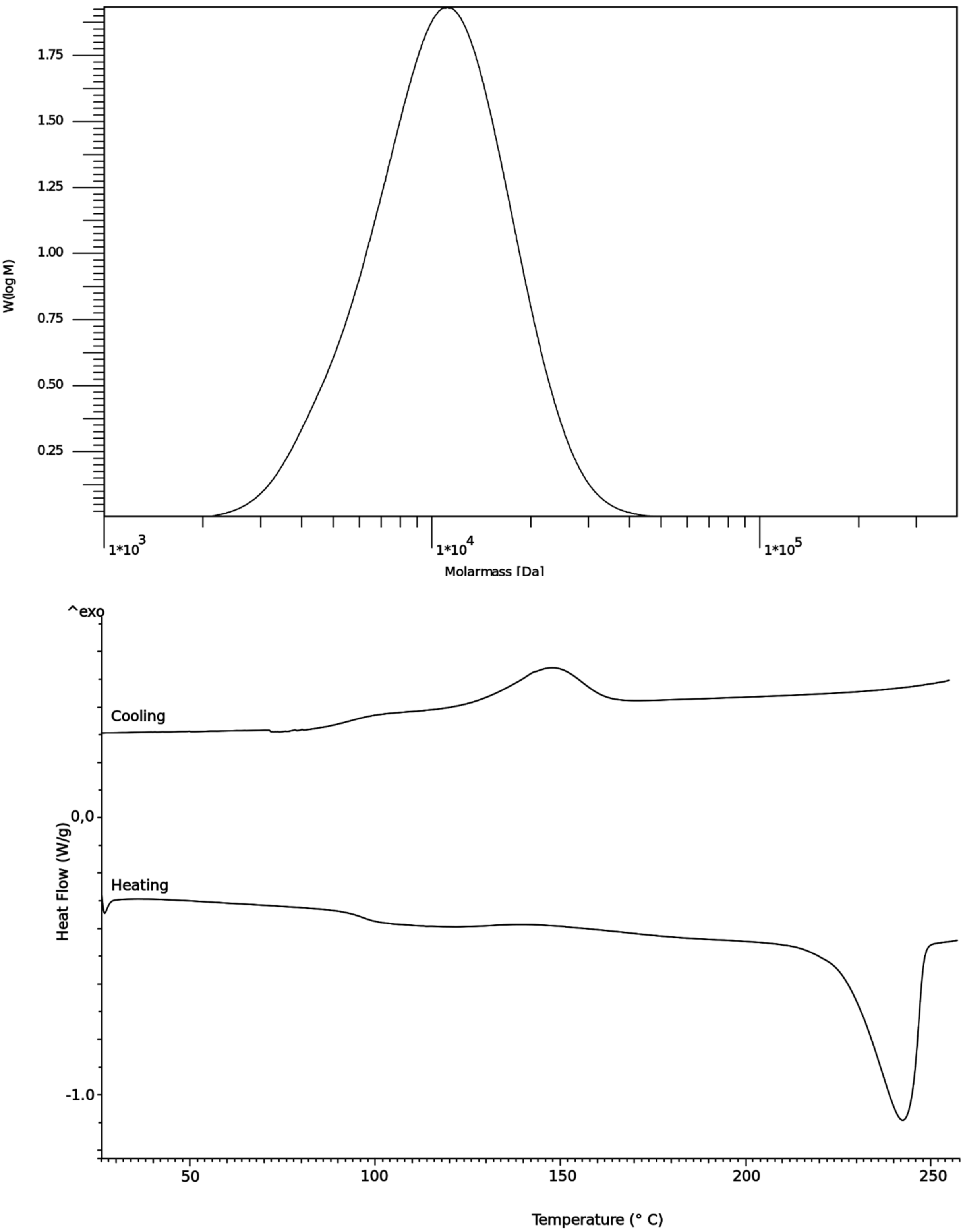

Figure 2.6 GPC curve (upper) and DSC curve (lower) of **poly2**.

NMR-analysis once again revealed an intact terminal double bond and a molecular weight M_n of 9.2 and M_w 11.6 kDa was confirmed by GPC (Figure 2.6, upper). DSC showed a T_g of 97 °C and a T_m of 240 °C (Figure 2.6, lower). One distinct feature of the polymer was the 'sintering-window' of 60 °C between the crystallization onset of about 165 °C and the melting onset at 225 °C. As this window is a crucial parameter for selective laser sintering (SLS), the suitability of **poly2** in this additive manufacturing technique might be worth exploring.

The radical polymerization of the terminal double bond was tested with azobisisobutyronitrile (AIBN) as radical starter in toluene at different temperatures (Figure 2.7), but no conversion was observed; however, more sophisticated methods might be successful.[106]

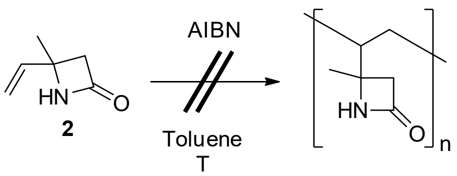

Figure 2.7 Unsuccessful radical polymerization of β-lactam **2** with AIBN.

2.2.4 Synthesis of 4-methyl-1,6-dihydropyridin-2(3H)-one (3) and 4-methyl-5,6-dihydropyridin-2(1H)-one (4)

As the synthesis of the lactams **3** and **4** was unselective and of low yield, a first approach to enhance the selectivity of the δ-structure formation was the synthesis of the β-lactam **2** and a subsequent acetylation or tosylation followed by a more controlled rearrangement to the δ-lactams **acetyl/tosyl-3** and **acetyl/tosyl-4**. After that, the free lactams should be formed by hydrolysis. **Acetyl-2** and **tosyl-2** were successfully synthesized (Scheme 2.3).

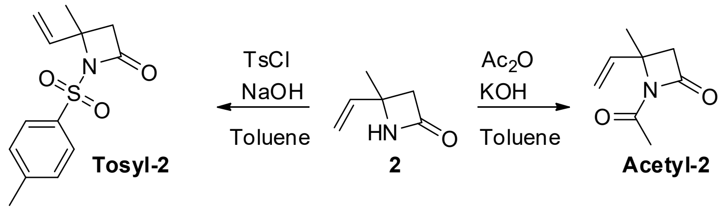

Scheme 2.3 Acetylation and tosylation of β-lactam **2**.

Acetyl-2 was formed by conversion of lactam **2** with Ac_2O and solid KOH in toluene.[125] For **tosyl-2**, two methods were tested: The direct conversion of isoprene (**1**) with 4-methylbenzenesulfonyl isocyanate (*p*TSI) and the reaction of lactam **2** with 4-methylbenzene-1-sulfonyl chloride (TsCl) and NaOH in toluene.[125,126] Although several reaction conditions were tested for the 2+2 cycloaddition of isoprene (**1**) and *p*TSI, the selectivity of the reaction was low and the δ-species as well as unidentified side products were observed. The application of TsCl was successful, and **tosyl-2** was isolated with a yield of 58%. However, neither thermal activation nor the application of various Lewis- or Brønsted acids in polar solvents led to formation of the lactams **3** or **4**. From solvent screening for the synthesis of lactam **2** (Table 2.2), it was established that polar solvents and an increased temperature preferably lead to the formation of the δ-lactams. If the reaction was carried out initially in EtOAc at -50 °C for 7 h (formation of **SO_2Cl-2**) and then stirred at 40 °C for 12 h (rearrangement to the δ-structure **SO_2Cl-3** and double bond isomerization), **SO_2Cl-4** could be isolated as colorless crystals (19% yield). Similar results were achieved with MeCN. Several Lewis acids were screened for catalytic activity for the 4+2 cycloaddition of CSI, the direct formation of lactam **SO_2Cl-3**, or the rearrangement of β-lactam **SO_2Cl-2** to the δ-structure (Table 2.2).

Table 2.2 Lewis acids as catalysts for the synthesis of lactams **SO_2Cl-3** and **SO_2Cl-4** in relative comparison to a catalyst-free standard reaction. + = increased product formation; - = decreased product formation; / = no change. Reaction conditions: Isoprene (**1**) 2 mmol, 0.3 mmol Lewis acid, MeCN 5 mL, 50 °C, 3 h.

Lewis acid	SO_2Cl-2	SO_2Cl-3	SO_2Cl-4	Side products
Al_2O_3	-	/	+	/
$Fe(OAc)_2$	-	/	/	+
$CuCO_3$	-	/	/	++
$AlCl_3$	-	/	/	+
H_4O_4Zr	/	/	+	+
$ZnCl_2$	/	/	/	/
CeO	-	-	-	++
$Sn(OAc)_2$	-	-	-	+
$Al(O\textit{i}Pr)_3$	-	+	-	+
$CoCl_2 \cdot 6\,H_2O$	-	-	++	+
$ZnBr_2$	/	/	/	++
$CuCl_2$	-	+	+	/
$MnCl_2 \cdot 4\,H_2O$	-	+	++	+
ZnO	/	/	/	+
$ZnCO_3$	-	/	/	+
LiOAc	/	/	/	+
$CaCl_2$	/	/	+	+
$SnCl_2$	/	/	+	+
Cp_2TiCl_2	-	-	+++	-
$Ti(\textit{i}OPr)_4$	-	-	+	++
$NbCl_5$	/	/	/	+

The screening was analyzed by TLC in comparison to a catalyst-free standard reaction and the relative comparisons between the TLCs revealed that $MnCl_2 \cdot 4\,H_2O$ and Di(cyclopentadienyl)titanium(IV) dichloride (Cp_2TiCl_2) were the most selective catalysts. On using $MnCl_2 \cdot 4\,H_2O$ in MeCN at room temperature for a period of 72 h, 52% of lactam **SO_2Cl-4** could be isolated, which is an increase of yield by more than 150%. However, the hydrolysis of lactam **SO_2Cl-4** was not possible in considerable yield although several pH-values, co-solvents, nitrogen bases and temperatures were tested. The desired lactam **4** was only isolated in yields beneath 10%. Hydrolysis almost exclusively led to the formation of lactone **6** if a base or acid in water or EtOH was used. In water-free systems, the free lactam **4** was formed as verified by GCMS, but product isolation failed. The same phenomenon was observed for lactam **SO_2Cl-3** – which was not isolated but directly hydrolyzed – to a minor extent; 70% of lactone **5** was formed and 30% of lactam **3**.

2.2.5 Synthesis of 4-methyl-1,6-dihydropyridin-2(3H)-one (5) and 4-methyl-5,6-dihydropyridin-2(1H)-one (6)

As described above, the lactones **5** and **6** were accessible by hydrolysis of **SO_2Cl-3** and **SO_2Cl-4** with aqueous solutions of NaOH or Na_2SO_3. **SO_2Cl-4** was converted to lactone **6** by stirring in a mixture of NaOH, H_2O, DCM and EtOH at room temperature in 88% yield. In a direct approach without isolation of the δ-structure, isoprene (**1**) and CSI were stirred in MeCN at room temperature for 2 h. After subsequent hydrolysis with an aqueous solution of Na_2SO_3, 57% of crude lactone **5** was isolated; the by-products were lactam **2** and lactone **6**. These side products underlined the draw-back of the synthesis, as a full conversion of β-lactam **SO_2Cl-2** to δ-lactam **SO_2Cl-3** was impossible before the double bond isomerization to **SO_2Cl-3** started. Purification was accomplished by distillation to yield 40% of lactone **5**. As a solid was formed in the distillation bubble during the process, it is possible that uncontrolled polymerization decreased the yield. For the synthesis of lactone **6**, Cp_2TiCl_2 and a reaction time of six days was tested in a small-scale reaction. The crude yield was 89% and GCMS and NMR analysis verified a purity of over 90%.

2.2.6 Synthesis of 2-methyl-2-vinyloxirane (7)

Several methods for the synthesis of **7** have been reported in the literature. If moderate oxidation reagents are used, the higher-substituted double bond reacts more readily with the epoxidizing reagent, and a selective epoxidation without excessive formation of the regioisomeric epoxide or the di-epoxide is possible. Application of *t*BuOOH lead to a decrease of regioselectivity, for instance. Other described protocols apply *m*CPBA in DCM or chloroform, which is neither economical nor ecological.[127] However, the epoxidation with other established methods such as enzyme-mediated systems,[128] diluted AcOOH,[129] or acetone-Oxone® ($KHSO_5$) systems[130] (for the *in-situ* generation of dimethydioxirane) is prone to opening of the epoxide and post-epoxidation rearrangements, as the acids – especially in aqueous media – catalyze unwanted side reactions (Figure 2.8). Therefore, the yield is usually below 50%. More elaborated methods applying homogeneous metal catalysis lead to increased yields but are expensive.[131,132] Side reactions are a general challenge in epoxidation reactions, even more for the vinyl-group containing epoxide **7**. All tested acidic aqueous methods led to the formation of highly polar substances – probably polyols and aldehydes – that where not further investigated. For an enzyme-mediated approach with H_2O_2·urea to reduce the amount of water, no conversion was observed. Other reported methods applying *Mycobacterium* are low-yielding (< 25%).[133]

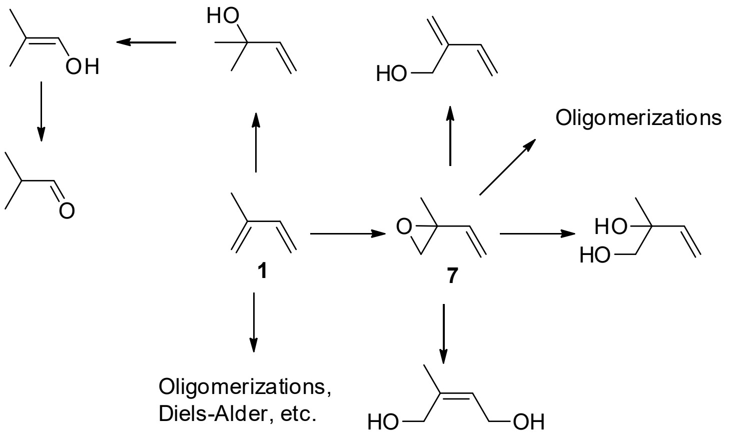

Figure 2.8 Possible side reactions of the isoprene (**1**) epoxidation.

An industrially relevant strategy for the epoxidation of light olefins is the direct conversion with O_2 over Ag-catalysts at 200-300 °C at 10 bar, or the oxidation with H_2O_2 over Ti-catalysts. Both techniques require an advanced infrastructure and the selectivity in asymmetric dienes might be unsatisfactory. Before these methods were established, a two-step strategy was applied for the synthesis of ethylene- and propylene oxide: The double bond was treated with ClOH (from the reaction of Cl_2 and H_2O) to give the corresponding chlorohydrine, which was subsequently converted to the epoxide by an elimination reaction under strong basic conditions from NaOH or $Ca(OH)_2$ (Scheme 2.4 a). For the preparation of **7**, the synthesis of bromohydrine **9** with N-Bromosuccinimide (NBS) followed by a base-induced elimination has proven to be high-yielding (70% isolated yield) and very selective.[134] However, the use of NBS is not economic. For the synthesis of **7**, a similar approach was investigated, but the formation of the bromohydrine **9** was replaced by NH_4Br as inorganic bromide source and Oxone® as oxidation reagent.

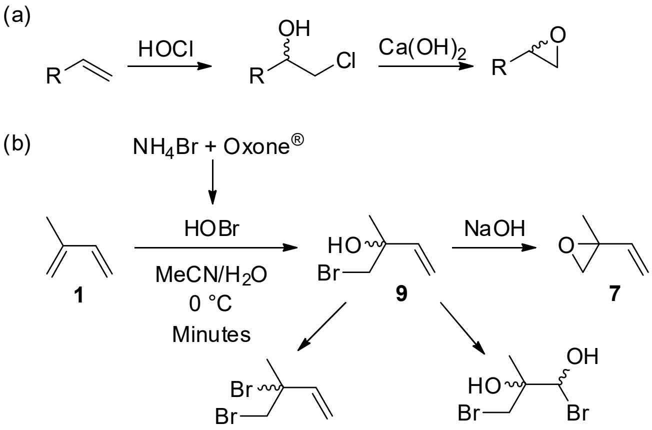

Scheme 2.4 General epoxidation via the chlorohydrine (a) and adjusted synthesis of **7** using in-situ generated HOBr (b).

For the lab-scale synthesis, it has proven suitable to convert isoprene (**1**) in a bromohydrine and to promote the elimination to **7** in aqueous NaOH (Scheme 2.4 b). The bromohydrine was formed by *in-situ* generated BrOH – from the oxidation of NH_4Br with Oxone® – using an adjusted protocol that was successfully applied for other alkenes (Scheme 2.4 b).[107,135,136] The reaction medium was a mixture of MeCN and H_2O (5:3) to guaranty a sufficient solubility of isoprene (**1**). The challenging aspect of this method was the chemo- and regioselectivity. If an excess of BrOH was formed, side reactions such as uncontrolled bromination or the conversion of the vinyl double bond were observed. In addition, an increased reaction temperature decreased the selectivity. The best result was obtained when Oxone® and isoprene were dissolved in a mixture of MeCN, H_2O, and ice before a precooled solution of NH_4Br was added drop-wise within a few minutes under vigorous stirring. The crude yield was 87% with a purity of over 90%, and bromohydrin **9** could directly be converted to **7** by slow addition to a cooled solution of NaOH (10 M). The purification was facile as the upper layer (organic phase) consisted almost exclusively of **7**. To verify the stability of **7**, a sample of the pure compound was stored at -20 °C for four months and then compared by NMR with a freshly produced sample; no degradation was observed.

2.3 New Bio-Polyamides from Terpenes: α-Pinene and (+)-3-Carene as Valuable Resources for Lactam Production

Title: New Bio-Polyamides from Terpenes: α-Pinene and (+)-3-Carene as Valuable Resources for Lactam Production
Status: Published (2019)
Journal: Macromolecular Rapid Communications
Publisher: Wiley-VCH Verlag GmbH & Co. KGaA
DOI: 10.1002/marc.201800903
Authors: Paul N. Stockmann, Dominik L. Pastoetter, Marion Woelbing, Claudia Falcke, Dr. Malte Winnacker, Dr. Harald Strittmatter, Prof. Volker Sieber

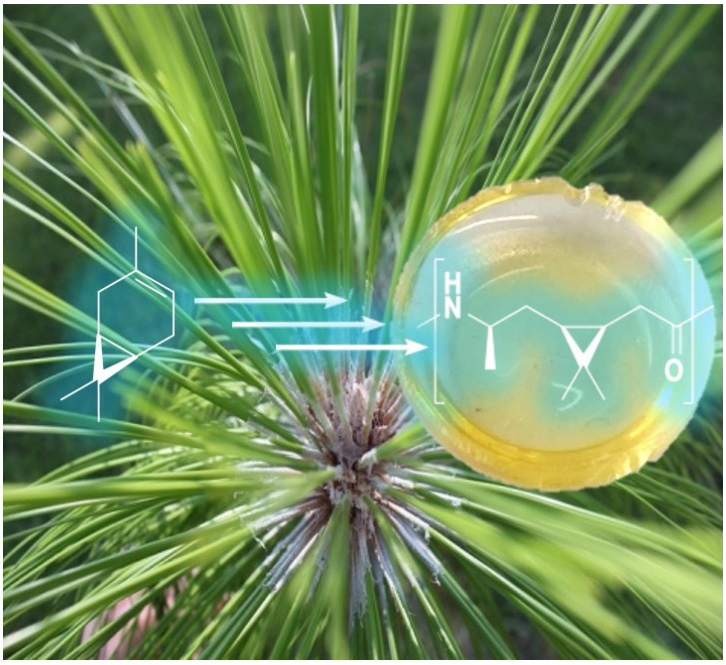

The publication describes the conversion of the monoterpenes α-pinene and (+)-3-carene to β- and ε-lactams and initial polymerization reactions. β-lactams were synthesized by a 2+2 cycloaddition of the terpenes with chlorosulfonylisocyanate (CSI). 19 % yield was obtained for the (+)-3-carene β-lactam and 74 % for the α-pinene β-lactam. Synthesis of the ε-lactams was achieved by a four-step synthesis protocol. The initial double bond oxidation by hydroboration gave the trans-anti-Markovnikov alcohols in excellent selectivity. Oppenauer oxidation under application of $Al(OiPr)_3$ and 3-niotrobenzaldehyde as redox equivalent gave the corresponding ketones that were then converted to ketoximes with $HONH_2 \cdot HCl$. Finally, the lactams were accessible by Beckmann rearrangement in basic media and tosyl chloride as oxime-activating, highly active leaving group. The overall yields for the (+)-3-carene ε-lactam and the α-pinene ε-lactam were 17 % and 15 %, respectively. All monomers were characterized by NMR, IR, GCMS, and DSC. Anionic ring-opening polymerization was used for the polymerization of the β- and ε-lactams. Several reaction conditions were tested. Typically, NaH on paraffin wax or potassium were applied as initiators. The activator was formed *in situ* from sodium lactamate and benzoyl chloride or acetic anhydride. β-lactams are usually highly reactive, thus the reaction proceeded in a rather uncontrolled manner, and only partially soluble oligomers were formed. NMR and IR confirmed the formation of PA2-type oligomers, and no rearrangement of the bicyclic structures were observed. Both polymers showed no glass transition (T_g) or melting temperature (T_m) in thermal analysis and only started to decompose at temperatures as high as 350 °C. The number average molecular weight (M_n) did not exceed 3.3 kDa. Polymerization of the ε-lactam from α-pinene under similar conditions yielded oligomers that could not fully be characterized due to insolubility. DSC revealed the absence of T_m and T_g. From the ε-lactam based on (+)-3-carene, a hard and transparent polyamide was formed very rapidly that reached a M_n of 33 kDa and a T_g of 115-120 °C. For the first time, a high-yielding, high-mass, transparent, 100 % bio-based polyamide was synthesized from terpene feedstock.

The authors, Paul N. Stockmann and Dominik L. Pastoetter, contributed equally to this work and both wrote the manuscript. Paul Stockmann synthesized and polymerized the lactams from α-pinene, polymerized the β-lactam from (+)-3-carene, and investigated the polymerization of (+)-3-carene ε-lactam in detail. He fully characterized all monomers and polymers, performed water-uptake experiments and supervised Dominik Pastoetter. Dominik Pastoetter synthesized the (+)-3-carene ε-lactam and performed initial polymerization experiments. Marion Woelbing, Claudia Falcke, and Malte Winnacker gave advice in polymerization reactions and polymer characterization. Harald Strittmatter supported in organic synthesis. Paul Stockmann, Harald Strittmatter and Volker Sieber conceived the work. Volker Sieber revised the manuscript and supervised the research project.

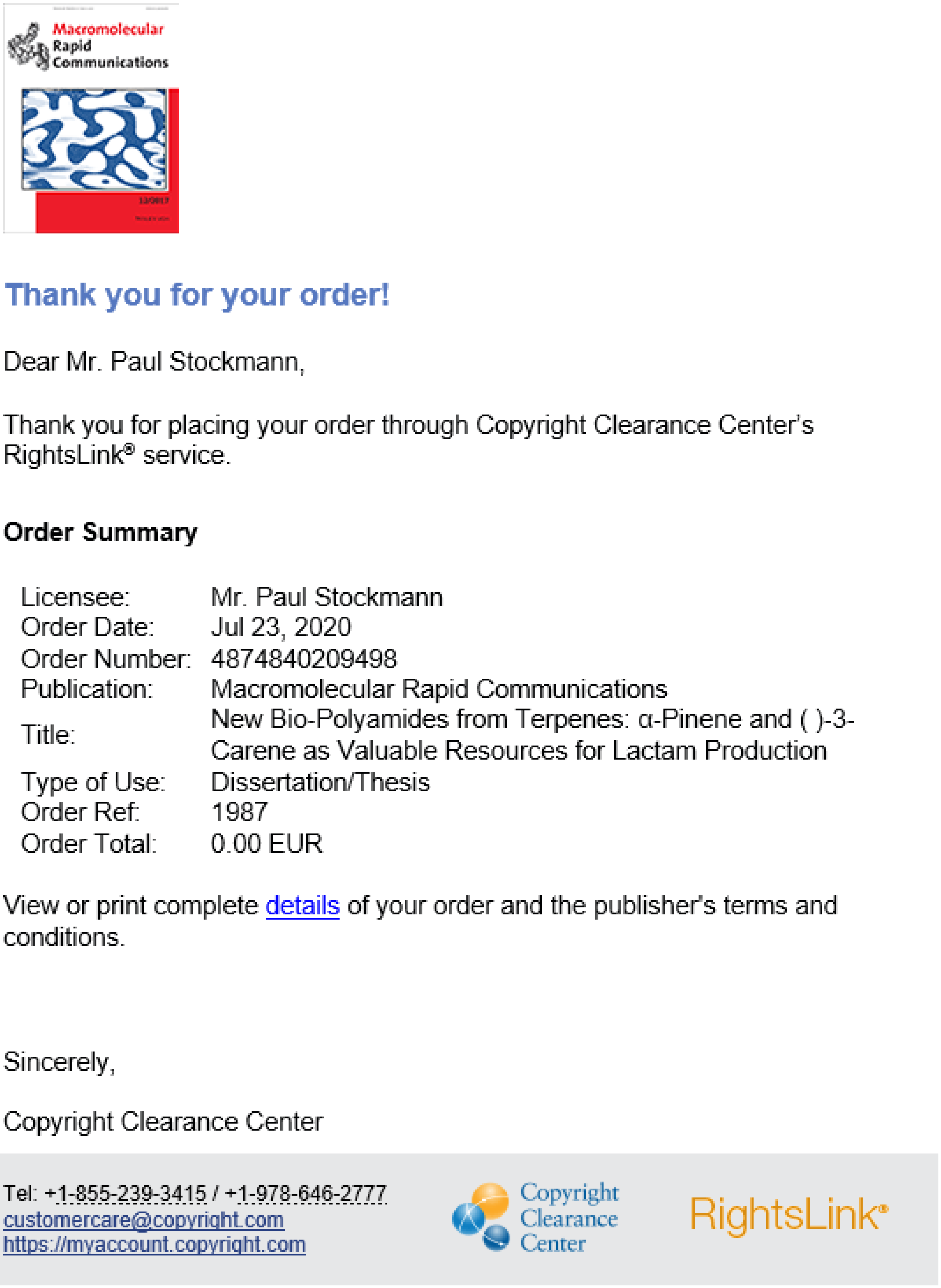

Thank you for your order!

Dear Mr. Paul Stockmann,

Thank you for placing your order through Copyright Clearance Center's RightsLink® service.

Order Summary

Licensee:	Mr. Paul Stockmann
Order Date:	Jul 23, 2020
Order Number:	4874840209498
Publication:	Macromolecular Rapid Communications
Title:	New Bio-Polyamides from Terpenes: α-Pinene and ( )-3-Carene as Valuable Resources for Lactam Production
Type of Use:	Dissertation/Thesis
Order Ref:	1987
Order Total:	0.00 EUR

View or print complete details of your order and the publisher's terms and conditions.

Sincerely,

Copyright Clearance Center

Tel: +1-855-239-3415 / +1-978-646-2777
customercare@copyright.com
https://myaccount.copyright.com

COMMUNICATION
Polyamides
Macromolecular
Rapid Communication
www.mrc-journal.d

New Bio-Polyamides from Terpenes: α-Pinene and (+)-3-Carene as Valuable Resources for Lactam Production

*Paul N. Stockmann, Dominik L. Pastoetter, Marion Woelbing, Claudia Falcke, Malte Winnacker, Harald Strittmatter, and Volker Sieber**

The synthesis and polymerization of two β-lactams and two ε-lactams derived from the terpenes α-pinene and (+)-3-carene are reported. The new biopolymers can be considered as polyamide 2 (PA2) and polyamide 6 (PA6)-types with aliphatic stereoregular side chains, which lead to remarkable new properties. The macromolecules are investigated by gel permeation chromatography (GPC), nuclear magnetic resonance (NMR), differential scanning calorimetry (DSC), and infrared (IR). The (+)-3-carene-derived PA6-type is of particular interest, since it reaches a molecular weight of over 30 kDa, which is the highest value for lactam-based polyamides derived from terpenes reported to date. Additionally, a glass transition temperature (T_g) of 120 °C is observed, surpassing the glass transition temperature of PA6 by 60 °C. The absence of a melting point (T_m) indicates high amorphicity, another novelty for terpene-based polyamides, which might give transparent bio-polyamides access to new fields of application.

Bio-based polymers are polymers synthesized from renewable resources that have been recently attracting attention due to the increasing awareness of green chemistry.[1] For the preparation of various types of such polymers, monoterpenes, which are naturally occurring dimers of isoprene, have been used with or without prior chemical modifications. Monoterpenes provide a variety of structural elements such as bicyclic motifs, olefins, alcohols, or ketones that enable the production of monomers that would be challenging to synthesize from fossil oil. From these monomers, polyolefins, polyesters, polycarbonates, and PAs have been prepared.[2,3]

Due to its high impact strength, mechanical resistance, and superior thermal properties, PA is probably the most used semicrystalline technical thermoplastic, with applications in commodities, automotive, medicine, and aviation.[3,4] An example for the industrial demand of bio-based PAs is PA11, which is obtained from ricinoelic acid derived from castor beans and commercialized by Arkema under the trade name Rilsan.[5]

In comparison to the linear PA11, the polymers derived from terpene lactams having substituted ring structures comprise branched side chains and backbones. For instance, Winnacker et al. reported the polymerization of the ε-lactam obtained from the conversion of (–)-menthone.[6,7] Some monoterpenes such as pinenes or camphor also yield PAs with a cyclic motif in the backbone. Although the polymerization of many of these lactams is challenging due to the occurrence of unfavorable monomer–polymer equilibria and low reaction rates,[8] a β-pinene-based bicyclic lactam was synthesized and converted to a PA by Hall in 1963.[9] Since the properties of that PA were not reported in detail, Winnacker et al. recently reproduced and optimized its synthesis and analyzed the structural and thermal properties of this new PA.[10,11] **Table 1** gives an overview of some properties of terpene-based and conventional AB-type PAs.

T_g and T_m of terpene-based PAs are in the range of high-performance polymers and surpass the thermal properties of PAs with a linear backbone.[3,11,12] For example, the bulky four-membered ring of poly-β-pinanamide and the isopropyl substituent of polymenthoneamide decrease the ability of the polymer chains to slide past one another, thereby increasing the T_g of the polymers.

Apart from these promising features, a major drawback of the reported terpene-based PAs is their rather low molecular weights, which may be due to precipitation of the growing polymer chain during the ring-opening polymerization (ROP) (Table 1).[6]

Interestingly, α-pinene and (+)-3-carene, two bicyclic, abundant, and comparably cheap monoterpenes that are accessible

---

P. N. Stockmann, D. L. Pastoetter, M. Woelbing, C. Falcke,
Dr. H. Strittmatter, Prof. V. Sieber
Fraunhofer IGB, Straubing Branch Bio
Electro and Chemocatalysis BioCat
Schulgasse 11a, 94315 Straubing, Germany
E-mail: sieber@tum.de

Dr. M. Winnacker
WACKER-Chair of Macromolecular Chemistry
Technical University of Munich
Lichtenbergstraße 4, 85748 Garching bei München, Germany

Prof. V. Sieber
Chair of Chemistry for Biogenic Resources
Campus Straubing for Biotechnology and Sustainability
Technical University of Munich
Schulgasse 16, 94315 Straubing, Germany

Prof. V. Sieber
Catalysis Research Center
Technical University of Munich
85748 Garching bei München, Germany

The ORCID identification number(s) for the author(s) of this article can be found under https://doi.org/10.1002/marc.201800903.

DOI: 10.1002/marc.201800903

© 2019 WILEY-VCH Verlag GmbH & Co. KGaA, Weinheim

Table 1. Thermal properties of several bio- and fossil-based AB-type PAs.

PA	Structure	Biosourcing [%]	T_g [°C]	T_m [°C]	M_n [kDa] M_w [kDa]	Ref.
PA6	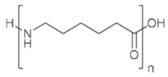	0	47	218	Adjustable Adjustable	[3]
PA11	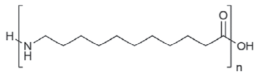	100	42	183	Adjustable Adjustable	[3]
PA12	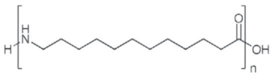	0	38	176	Adjustable Adjustable	[3]
Poly-β-pinanamide	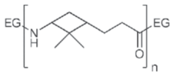	100	160	322	7.7 (adjustable) 20 (adjustable)	[10,11]
Polymenthone amide	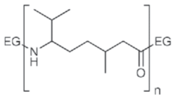	100	50	300	2.8 (adjustable) 3.3 (adjustable)	[6,7]

Biosourcing, C-content from biosources; EG, end-group; Ref., reference.

from industrial waste streams or from turpentine oil, have not been examined as ε-lactam monomers yet.[13] Analogous to the findings for (–)-menthone and β-pinene PAs, promising thermal properties can be expected for the polymers obtained from these monoterpenes. Since bulky side chains enhance the thermal properties of terpene PAs, we hypothesized that PA3-type PAs obtained from β-lactams might exhibit even higher T_g and T_m.

We herein report the synthesis and the first polymerization of two ε- and two β-lactams derived from (+)-3-carene and α-pinene into new PAs. In the case of the ε-lactam derived from 3-carene, a number-average molar mass (M_n) up to 33 kDa was reached, representing the first terpene-based high-molecular-mass PA.

The conversion of racemic α-pinene (**1a**, only one enantiomer is shown throughout this report for clarity) and enantiopure (+)-3-carene (**1b**) into ε-lactams **5a** and **5b** was achieved by the four-step reaction sequence displayed in **Scheme 1**, which involves formation of alcohols of type **2**, subsequent oxidation to the corresponding ketones **3a** and **3b**, conversion to oximes **4a** and **4b**, and finally, Beckmann rearrangement. A similar reaction pathway from (+)-3-carene was previously reported by Stanislaw Lochyński.[14]

The initial oxidation of the double bond to alcohols **2a** and **2b** was performed by hydroboration, and the anti-Markovnikov structures were obtained selectively in good yields of up to 82%.[14,15] The purity was sufficient for the subsequent reactions, and further purification was not required. Although the conversion to ketones **3a** and **3b** has been previously performed with chromium salts,[15,16] to avoid hazardous chemicals we used an adapted Oppenauer reaction reported by Christopher R. Graves et al. for the oxidation of the monoterpene hydroxyborneol.[17] We replaced the usually applied redox equivalent acetone with 3-nitrobenzaldehyde (3-NBA). The electron withdrawing effect of the nitro group in the meta-position creates a reduction potential that is sufficiently low for the desired oxidation to proceed. However, since Lewis acids such as $Al(OiPr)_3$ facilitate rearrangements of α-pinene (**1a**) and (+)-3-carene (**1b**), several side products were obtained, affording a product yield of only 60%. Furthermore, product isolation was challenging due to the presence of unidentified side products with similar polarity and boiling points, hence only ketone **3b** could be purified in a small scale by column chromatography. Nevertheless, product isolation was again not necessary for the synthesis of the next intermediate. The oximes of type **4** were synthesized by reacting **3a** and **3b** with hydroxylamine hydrochloride at 65 °C within 4 h in yields up to 90%.

The most challenging step of the synthesis was the Beckmann rearrangement. Most procedures for this reaction require acidic conditions, which lead to several unknown side products. Besides hydrolysis of the oxime to ketone **3b** and, probably, a stereoisomer with an inverted methyl group at C3, the GCMS

© 2019 WILEY-VCH Verlag GmbH & Co. KGaA, Weinheim

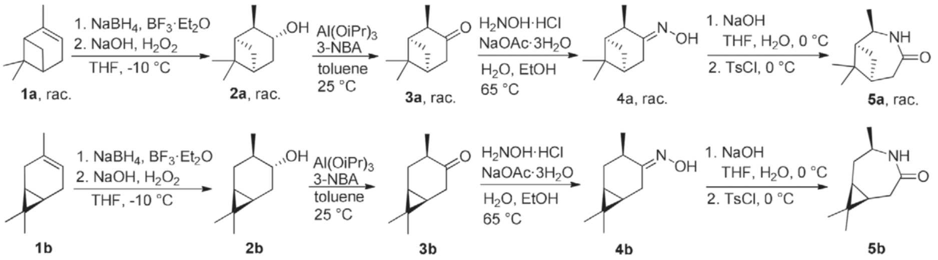

Scheme 1. Reaction pathway of ε-lactams **5a** and **5b** derived from racemic α-pinene (**1a**, total yield 15%) and (+)-3-carene (**1b**, total yield 17%).

database suggested the occurrence of a rearrangement of the three-membered ring affording limonene derivatives. Additionally, the formation of ortho- and para-cymol was observed. Several mineral acids such as HCl or H_2SO_4 were tested, as well as the Lewis acids $BF_3 \cdot Et_2O$ and $AlCl_3$. The selectivity was low in all cases. More elaborate approaches involving the activation of the oximes with leaving groups such as acetic anhydride or trichlorotriazine also failed. The direct conversion of ketones **3a** and **3b** by application of hydroxylamine-*O*-sulfonic acid—as reported for the lactam synthesis from (−)-menthone or camphor—also led to unsatisfying results.[6] Acidic conditions in aqueous and organic media and high temperatures were identified as the main limiting factors for lactam formation. Stanislaw Lochyński et al. previously used TsCl in basic media for the rearrangement of oxime **4b**, although no yield was reported. To our delight, following a slightly modified approach and decreasing the amount of TsCl from 100% to 10% excess reduced the amount of side reactions, leading to isolated yields of about 40% for the desired lactam monomers **5a** and **5b** after recrystallization. The regioselectivity regarding the nitrogen insertion was excellent, which is most likely due to the in situ formation of a tosylated trans-oxime caused by the repulsion of the tosyl and the methyl group, leading to an exclusive C3 migration. The side products and impurities from previous reactions did not prevent the lactams from crystallizing. The overall yield after the four reaction steps was about 15% for lactam **5a** and 17% for lactam **5b**. Further reaction optimizations were not the focus of our research at this point but will be required in the future for high-yielding and sustainable lactam production.

β-Lactam monomers **6a** and **6b** were synthesized directly from alkenes **1a** and **1b** by [2 + 2] cycloaddition of chlorosulfonyl isocyanate following a previously reported procedure.[18] Interestingly, the yield for **6a** (74%) was considerably higher than for **6b** (19%).

For the small-scale synthesis of PAs, we selected the alkali-initiated anionic ring-opening polymerization (AROP) and the HCl-initiated cationic ring-opening polymerization (CROP) procedures. Hydrolytically initiated polymerizations or polycondensations have not been investigated in this work. **Table 2** displays the applied reaction conditions and analytical data of the obtained polymers.

All AROP reactions were carried out under inert gas atmosphere with temperatures varying from 150 to 270 °C, using NaH or potassium as initiators and benzoyl chloride (BzCl) or acetic anhydride (Ac_2O) as pre-activators (in both cases, the in situ generated sodium lactamates are assumed to react with the pre-activator to afford the corresponding imide with the concomitant formation of the activator). The polymerization of the bicyclic lactam **5a** using the alkali–AROP method was quite challenging, albeit achievable with NaH (5.4 mol%) and BzCl (0.4 mol%) at 230–270 °C (Table 2, entry 2). All attempts involving less NaH or BzCl did not lead to the corresponding polymer **poly5a**. Utilizing potassium or Ac_2O at moderate temperatures also failed. Another drawback was the strong sublimation of monomer **5a**, which hindered setting a specific monomer/activator ratio. It was observed that oligomers precipitated during the reaction, which led to the formation of brittle clusters. The crude polymer **poly5a** was brown, very brittle, and transparent. After residual monomer separation (RMS) by heating in a mixture of water and ethanol, and subsequent washing with acetone, polymer **poly5a** was obtained as a yellow powder in a 24% yield. GPC analysis confirmed the formation of oligomers with a molecular weight of 2.9 kDa, which is equal to an average of 17 repeating units. Hence, PA **poly5a** was not completely soluble in hexafluoroisopropanol (HFIP, used as GPC solvent). Therefore, the GPC information is incomplete, and longer polymer chains might be present. This poor solubility can be attributed to the rearrangement of the four-membered ring under the present conditions causing cross-linking. However, (+)-3-carene-derived lactam **5b** could successfully be converted to PA **poly5b**, which has high molecular weight. Using potassium (6 mol%) and BzCl (3 mol%) at 150 °C leads to the formation of PA **poly5b** as a transparent brown solid within 4 h. After RMS, the polymer was obtained as a yellow powder in 68% yield. GPC analysis revealed a M_n of 22.3 kDa. Furthermore, a combination of Ac_2O and NaH decreased the polymerization time and gave a M_n of over 30 kDa, which corresponds to an average of 200 repeating units. Decreasing the amount of activator and initiator resulted in higher M_n (entries 7 and 8, Section S8, Supporting Information). In both cases, an exceptionally short reaction time of 30 s was sufficient to yield over 70% of isolated **poly5b**. In contrast, CROP of **5a** and **5b** with HCl was less successful; the yield of **poly5a** was low (11%), and the polymers were very viscous and contained only few hard and transparent domains, which is indicative of oligomerization. In the case of lactam **5b**, CROP using HCl failed. Since the

© 2019 WILEY-VCH Verlag GmbH & Co. KGaA, Weinheim

Table 2. Polymerization of lactams **5a**, **5b**, **6a**, and **6b** under various conditions.

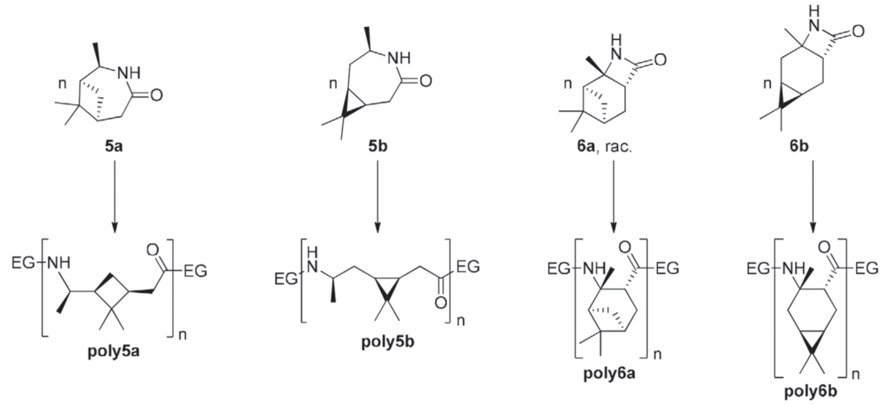

Entry	Monomer	Initiator [mol%]	Activator [mol%]	Conditions	Yield [%]	M_n [kDa]	M_W [kDa]	T_g [°C]	T_m [°C]
1	5a	K (6.0)	BzCl (0.8)	150 °C, 4 h	—	—	—	—	—
2	5a	NaH (5.4)	BzCl (0.4)	230 °C 1 h, 270 °C 1 h	24	2.9	4.3	—	dec.
3	5a	NaH (4)	Ac_2O (3)	160 °C, 2 h	—	—	—	—	—
4	5a	HCl (2.4)	—	270 °C, 1 h	40	1.5	1.9	—	dec.
5	5b	K (6.0)	BzCl (2.5)	150 °C, 4 h	70	22.3	38.1	X	dec.
7	5b	NaH (4.1)	Ac_2O (1.6)	165 °C, 0.5 h	71	29.5	55.1	X	dec.
8	5b	NaH (2.7)	Ac_2O (0.5)	170 °C, 0.5 s	77	33.3	64.6	X	dec.
9	5b	HCl (2.4)	—	150 °C, 4 h	—	—	—	—	—
10	6a	NaH (2.0)	—	160 °C, 30 s	72	3.3	3.3	—	dec.
11	6b	NaH (2.0)	—	160 °C, 30 s	78	1.4	1.5	—	dec.

dec., decomposing.

anionic approach was more successful, cationic methods were not further investigated.

The reason for the different polymerization abilities of lactams **5a** and **5b** under the described conditions remains unclear. Since both monoterpene lactams possess a methyl group next to the N atom, a crucial steric effect of this methyl group on ROP can be excluded. The (+)-3-carene-based lactam **5b** contains a three-membered ring, in contrast to the four-membered ring of lactam **5a**. The sterically demanding quaternary C atom bearing two methylene groups blocks the lactam moiety due to the rigid [4.1.1]-bicyclic structure of lactam **5a**, thereby hindering the nucleophilic attack of the carbonyl function on the C atom. The lowered steric hindrance and the increased flexibility of the [5.1.0]-bicyclic structure along with ring-strain effects can be invoked as the factors improving the polymerization ability of lactam **5b**. Moreover, the presence of two enantiomers in the case of lactam **5a** probably leads to an atactic oligomer with an increased tendency to precipitate, which might limit the chain growth.

The obtained PAs were also characterized by IR (**Figure 1**), NMR, and DSC (**Figure 2**). As can be seen in Figure 1, the IR spectra show the characteristic amide II bands at 1545/1503 cm^{-1} (**poly5a**) and 1559 cm^{-1} (**poly5b**). These bands only occur in noncyclic amides, which confirm the polymerization by opening of the cyclic lactam bond.

The poor solubility of PA **poly5a** in deuterated formic acid and other common NMR solvents prevented us from conducting NMR analysis. Although the powder of **poly5a** could be partially dissolved in a 1:5 mixture of DMSO-d_6 and formic acid, a clear solution could not be obtained even at low concentrations. ^{13}C NMR and 2D NMR experiments were not performed due to the low polymer concentration. A complete structure determination was therefore not possible, and only a few signals could be assigned (Section S4.1, Supporting Information). ^1H NMR revealed that residual monomers remained even after repeated washing of the polymer. Conversely, PA **poly5b** was readily dissolved in deuterated formic acid, and the proposed structure was confirmed by ^1H, ^{13}C, and 2D NMR experiments (Section S4.2, Supporting Information). The proton spectrum of **poly5b** was compared to that of the hydrolyzed lactam **hyd5b** (Section S4.3, Supporting Information) to find that, as expected, both the polymer and

© 2019 WILEY-VCH Verlag GmbH & Co. KGaA, Weinheim

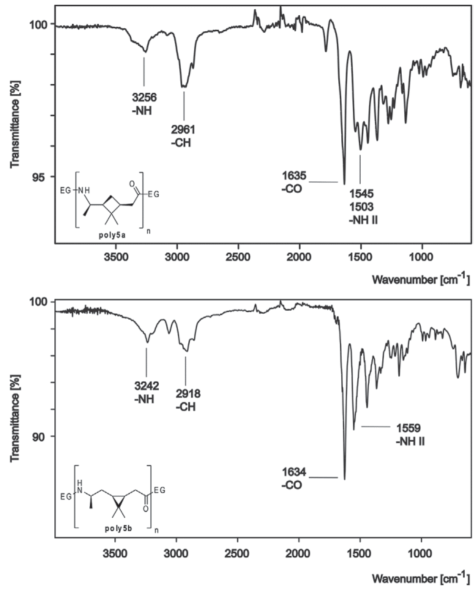

Figure 1. IR analysis of **poly5a** and **poly5b**. The wavenumbers for PA identification are highlighted.

the open monomer give rise to very similar chemical shifts. A difference worth mentioning is the broadening of signals in the polymer spectrum, which is typical of a long polymer chain.

The thermal properties of PA **poly5a** and **poly5b** were determined by DSC, which confirmed that the presence of bulky cyclic substituents increases the glass transition T_g and T_m. In the case of **poly5a**, no phase transitions could be detected at all, contrary to the reports by Hall and Winnacker on a similar polymer derived from β-pinene.[9–11] This PA lacks the methyl group and possesses a $-CH_2-CH_2-$ motif in the backbone, which enhances the flexibility of the polymer chains, causing a shift in the melting point below the decomposition temperature. However, PA **poly5b** exhibits a T_g at 120 °C, but no T_m was detected before decomposition at 400 °C. Considering that the bulky motifs in the polymer chains might increase the crystallization time, a DSC method including a tempering step of 20 min at 220 °C was applied. Even so, no characteristic change was observed (Section S9, Supporting Information), contrary to what is stated for terpene-based PAs in the literature. The comparably higher molecular weight of **poly5b** slowing down the formation of crystals could be invoked as the reason for this result; however, after extending the tempering to 3 h, no melting was observed, and the sample still remained transparent (Section S5, Supporting Information). An alternative explanation could be the repulsion of the methyl group and the three-membered ring resulting in an arbitrary rotation of the polymer backbone that would prevent the formation of hydrogen bonds.

The polymerization of β-lactams **6a** and **6b** was achieved in the absence of an activator. At 160 °C, the ring opening and subsequent chain growth were instantly initiated in an uncontrollable manner, even if minimal amounts of NaH were used. In the case of **6a**, powder-like nontransparent particles were formed in 19% yield after the residual monomers were removed. DSC analysis revealed the absence of T_g or T_m before decomposition (Section S9, Supporting Information). IR analysis showed the bands expected for PAs (amide I 1652 cm^{-1}, amide II 1503 cm^{-1}; Section S7, Supporting Information). Nevertheless, the insolubility of **poly6a** in deuterated solvents prevented us from obtaining a complete structural characterization. For PA2-type polymers, insolubility is well known in the literature.[19] Similarly to **poly5a**, polymer **poly6a** was just partly soluble even in HFIP. Consequently, the GPC results are not completely reliable; the soluble oligomers consisted of 18 monomer units (3.3 kDa) on average. These results come to confirm the literature showing that the polymerization of highly substituted β-lactams is a challenging task.[20]

For the (+)-3-carene-based β-lactam **6b**, the polymerization also occurred directly after NaH addition. However, the resulting polymer was neither brittle nor powdery, but a hard and transparent colorless block (Section S5, Supporting Information). Contrary to **poly6a**, **poly6b** was partly soluble in deuterated toluene, and its structure could be confirmed by solution NMR spectroscopy (Section S4.4, Supporting Information). Unfortunately, HFIP was not suitable as solvent, and only oligomers with a molecular weight of 1.5 kDa, which represents an average of nine monomer units, were detected in the GPC analysis (Section S8, Supporting Information). The DSC measurement did not show either T_g or T_m before the decomposition temperature was reached (Section S9, Supporting Information). There is strong evidence for the aforementioned assumption that an extremely bulky side chain for PA2-type PAs will lead to a shift of phase transitions to very high temperatures.

Apart from thermal properties, the water uptake is important for PAs, as the increase of moisture may lead to changes in the material behavior such as reduction of strength, stiffness, and T_g.

To verify our hypothesis that the increased aliphatic density of **poly5b** compared to PA6 might decrease the water uptake, we synthesized PA6 samples by the same methods as applied for the terpene-based PAs and determined the masses after stirring in water for 3 days and subsequent drying steps (Section S5.4, Supporting Information). The water uptake of **poly5b** was only 40% of the value observed for PA6, and the drying time was remarkably reduced (Table S4 and Figure S4, Supporting Information).

Four lactams have been synthesized from racemic α-pinene and (+)-3-carene. The PA2-type macromolecules **poly6a** and **poly6b** built up through the AROP of these β-lactams possess a bicyclic system as side chain that completely suppresses T_g or melting processes. This renders (thermoplastic) processing probably impossible, thereby limiting the application of these homopolymers. Another challenge is the uncontrolled polymerization of the very active β-lactams. Nonetheless, they might be used as comonomers for the polymerization with caprolactam

© 2019 WILEY-VCH Verlag GmbH & Co. KGaA, Weinheim

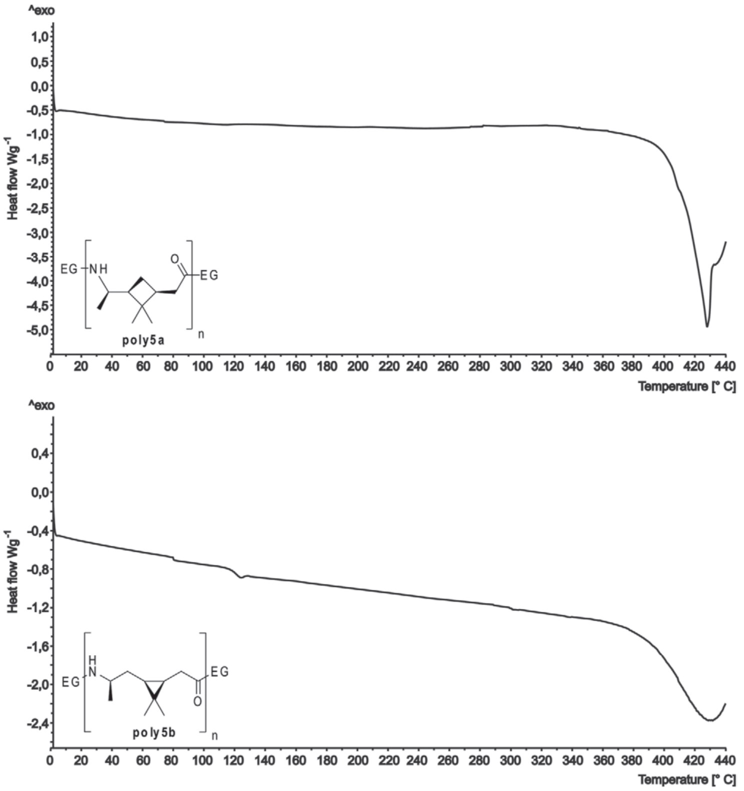

Figure 2. DSC analysis of **poly5a** and **poly5b** up to decomposition temperature at about 380 °C.

or laurolactam, which might shift the glass transition of PA6 and PA12 to higher temperatures. Similar conclusions can be drawn for the PA6-type oligomer **poly5a** obtained from the *ε*-lactam of *α*-pinene, **5a**. In all three cases, analysis of the macromolecules was limited due to poor solubility; therefore, accurate molecular weights cannot be provided at this point. The structure of the carene-based PA2 **poly6b** was elucidated using NMR spectroscopy, whereas the structure of both pinene-based PAs **poly5a** and **poly5b** remains unclear.

The *ε*-lactam of (+)-3-carene, **5b**, polymerized smoothly, and the resulting PA **poly5b** could be analyzed. The molecular weight achieved by a nonoptimized polymerization method surpassed 30 kDa, which is the highest molecular weight reported to date for terpene-based PAs obtained by ROP and is well in the range of industrial PAs. Compared to the *α*-pinene-based lactam **5a**, the easily accessible amide bond and the more suitable dissolution properties of **5b**—no precipitation was observed during the polymerization—might explain these findings. In addition, there are indications that the water uptake of **poly5b** might be lower than of PA6, although that finding needs a more detailed investigation under application of specimen and experiment setups meeting industry standards. Further studies regarding the polymerization ability of (+)-3-carene-based lactams and the development of a more sustainable synthesis are currently underway in our facility. Although more advanced DSC protocols as well as X-ray diffraction measurements are necessary to get additional information on the crystallinity of **poly5b**, the transparent polymer obtained directly after polymerization and the DSC analysis suggest amorphousness, microcrystallinity, or a considerably long crystallization time. To the best of our knowledge, this is also a novelty for terpene-based PAs. In combination with a T_g 60 °C above that of PA6, this may be used for applications requiring transparency as well as thermal resistance. The intriguing observations regarding **poly5b** are beyond the scope of this communication and will be investigated in detail in a separate publication.

To summarize, this work underlines the potential of terpenes as sustainable monomer sources for polymers that not only match but also enhance the profile of their oil-based counterparts.

Experimental Section

Detailed synthesis protocols and analytical data are given in Supporting information.

Supporting Information

Supporting Information is available from the Wiley Online Library or from the author.

Acknowledgements

P.N.S. and D.L.P. contributed equally to this work.

Conflict of Interest

The authors declare no conflict of interest.

Keywords

amorphicity, bio-based, polyamides, ring-opening polymerization, terpenes

Received: December 17, 2018
Revised: March 3, 2019
Published online: March 20, 2019

---

[1] a) S. A. Miller, *ACS Macro Lett.* **2013**, *2*, 550; b) R. Mülhaupt, *Macromol. Chem. Phys.* **2013**, *214*, 159; c) N. Hernández, R. C. Williams, E. W. Cochran, *Org. Biomol. Chem.* **2014**, *12*, 2834.
[2] a) M. A. Hillmyer, W. B. Tolman, *Acc. Chem. Res.* **2014**, *47*, 2390; b) M. Winnacker, *Angew. Chem., Int. Ed.* **2018**, *57*, 14362; c) J. Zhao, H. Schlaad in *Adv. Polym. Sci.* Vol. *253* (Ed.: H. Schlaad), Springer, Berlin **2013**, p. 151; d) W. J. Roberts, A. R. Day, *J. Am. Chem. Soc.* **1950**, *72*, 1226; e) T. Higashimura, J. Lu, M. Kamigaito, M. Sawamoto, Y.-X. Deng, *Makromol. Chem.* **1993**, *194*, 3441; f) *Monomers, Polymers and Composites from Renewable Resources* (Eds: A. Gandini, M. N. Belgacem), Elsevier, Oxford **2008**; g) P. A. Wilbon, F. Chu, C. Tang, *Macromol. Rapid Commun.* **2013**, *34*, 8; h) M. Firdaus, M. A. R. Meier, *Green Chem.* **2013**, *15*, 370; i) L. Peña Carrodeguas, C. Martín, A. W. Kleij, *Macromolecules* **2017**, *50*, 5337; j) H. C. Quilter, M. Hutchby, M. G. Davidson, M. D. Jones, *Polym. Chem.* **2017**, *8*, 833; k) N. J. van Zee, G. W. Coates, *Angew. Chem., Int. Ed.* **2015**, *54*, 2665; l) F. Parrino, A. Fidalgo, L. Palmisano, L. M. Ilharco, M. Pagliaro, R. Ciriminna, *ACS Omega.* **2018**, *3*, 4884; m) O. Hauenstein, S. Agarwal, A. Greiner, *Nat. Commun.* **2016**, *7*, 11862; n) O. Hauenstein, M. Reiter, S. Agarwal, B. Rieger, A. Greiner, *Green Chem.* **2016**, *18*, 760.
[3] M. Winnacker, B. Rieger, *Macromol. Rapid Commun.* **2016**, *37*, 1391.
[4] a) M. Pervaiz, M. Faruq, M. Jawaid, M. Sain, *Curr. Org. Synth.* **2017**, *14*, 146; b) S. Russo, E. Casazza in *Polymer Science: A Comprehensive Reference* (Eds.: K. Matyjaszewski, M. Moeller), Elseiver, Amsterdam **2012**, p. 331; c) K. Marchildon, *Macromol. React. Eng.* **2011**, *5*, 22; d) S. Koltzenburg, M. Maskos, O. Nuyken, R. Mülhaupt, K. Matyjaszewski, *Polym. Chem.*Springer, Berlin **2017**; e) T. S. Jahnke, *J. Am. Chem. Soc.* **1996**, *118*, 8186; f) C. Bonten, *Kunststofftechnik: Einführung und Grundlagen*, Hanser, München **2014**.
[5] https://www.extremematerials-arkema.com/en/product-families/rilsan-polyamide-11-family/(accessed: March 2019).
[6] M. Winnacker, S. Vagin, V. Auer, B. Rieger, *Macromol. Chem. Phys.* **2014**, *215*, 1654.
[7] M. Winnacker, M. Neumeier, X. Zhang, C. M. Papadakis, B. Rieger, *Macromol. Rapid Commun.* **2016**, *37*, 851.
[8] a) H. K. Hall, *J. Am. Chem. Soc.* **1958**, *80*, 6412; b) H. K. Hall, *J. Am. Chem. Soc.* **1958**, *80*, 6404; c) H. K. Hall, *J. Am. Chem. Soc.* **1960**, *82*, 1209; d) H. Hall, *Polymers* **2012**, *4*, 1674.
[9] H. K. Hall, *J. Org. Chem.* **1963**, *28*, 3213.
[10] M. Winnacker, J. Sag, *Chem. Commun.* **2018**, *54*, 841.
[11] M. Winnacker, J. Sag, A. Tischner, B. Rieger, *Macromol. Rapid Commun.*1600787, **2017**, *38*.
[12] J. Pagacz, K. N. Raftopoulos, A. Leszczyńska, K. Pielichowski, *J. Therm. Anal. Calorim.* **2016**, *123*, 1225.
[13] a) M. Eggersdorfer, *Ullmann's Encyclopedia of Industrial Chemistry*, Wiley-VCH Verlag GmbH & Co. KGaA, Weinheim **2000**; b) M. Gscheidmeier, H. Fleig, *Ullmann's Encyclopedia of Industrial Chemistry*, Wiley-VCH Verlag GmbH & Co. KGaA, Weinheim **2000**.
[14] S. Lochyński, J. Kułdo, B. Frąckowiak, J. Holband, G. Wójcik, *Tetrahedron: Asymmetry* **2000**, *11*, 1295.
[15] B. Kilbas, A. Azizoglu, M. Balci, *Helv. Chim. Acta.* **2006**, *89*, 1449.
[16] D. G. Cooper, R. A. Jones, *J. Chem. Soc. C* **1971**, 3920.
[17] C. R. Graves, B.-S. Zeng, S. T. Nguyen, *J. Am. Chem. Soc.* **2006**, *128*, 12596.
[18] Z. Szakonyi, T. Martinek, A. Hetényi, F. Fülöp, *Tetrahedron: Asymmetry* **2000**, *11*, 4571.
[19] J. Zhang, D. A. Kissounko, S. E. Lee, S. H. Gellman, S. S. Stahl, *J. Am. Chem. Soc.* **2009**, *131*, 1589.
[20] H. Bestian, *Angew. Chem., Int. Ed. Engl.* **1968**, *7*, 278.

© 2019 WILEY-VCH Verlag GmbH & Co. KGaA, Weinheim

2.4. Biobased chiral semi-crystalline or amorphous high-performance polyamides and their scalable stereoselective synthesis

Title:	Biobased chiral semi-crystalline or amorphous high-performance polyamides and their scalable stereoselective synthesis
Status:	Published (2020)
Journal:	Nature Communications
Publisher:	Nature Research
DOI:	10.1038/s41467-020-14361-6
Authors:	Paul N. Stockmann, Dr. Daniel Van Opdenbosch, Dr. Alexander Poethig Dominik L. Pastoetter, Moritz Hoehenberger, Sebastian Lessig, Johannes Raab, Marion Woelbing, Claudia Falcke, Dr. Malte Winnacker, Prof. Cordt Zollfrank, Dr. Harald Strittmatter, Prof. Volker Sieber

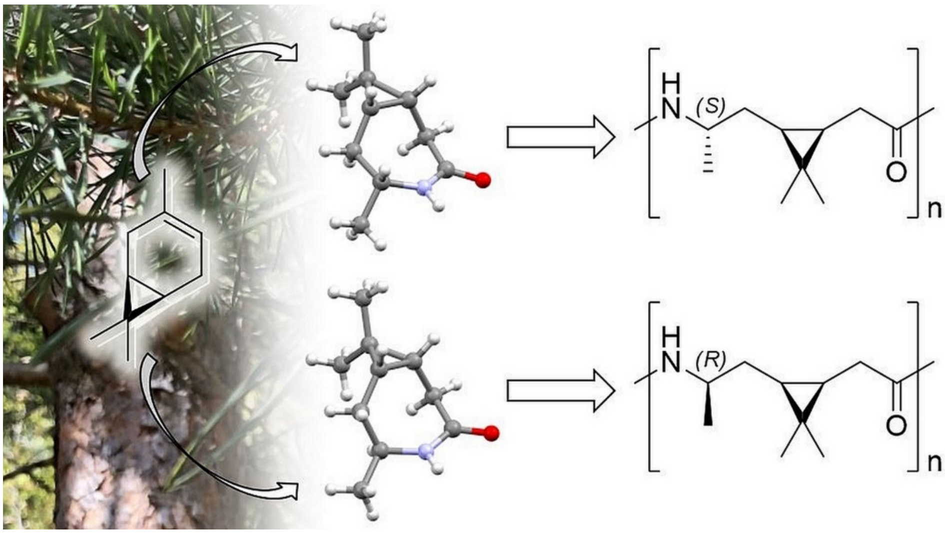

The publication describes the synthesis and characterization of the two novel 100 % bio-based 3S-polycaranlactam and 3R-polycaranlactam. The polyamides are diastereomers with respect to a methyl group which leads to considerably different polymer properties. Starting from (+)-3-carene, the diastereomeric monomers 3S-caranlactam and 3R-caranlactam were accessible in a four-step reaction sequence. Starting from (+)-3-carene, 3S-caranlactam was formed by epoxidation with peracetic acid. For 3R-selectivity, N-bromo-succinimide for the formation of a bromo hydrine and subsequent epoxide formation in basic media was used. Conversion of the epoxide by Meinwald rearrangement in nonpolar solvents in combination with strong acids gave the corresponding carbonyl compounds under retention of configuration. After conversion to oximes with $HONH_2 \cdot HCl$, Beckmann rearrangement in basic media with tosyl chloride as oxime activation reagent yielded about 20 % 3S-caranlactam or 3R-caranlactam. 3R-lactam reacted more facile than 3S-caranlactam in anionic ring-opening polymerization under application of N-benzoyl-caranlactam as activator and NaH on paraffin wax as initiator.

However, the conversion of both stereoisomers was between 85-90 %. The average number molecular weight (M_n) was over 20 kDa for 3R-polycaranlactam and 15 kDa for polycaranlactam as verified by GPC. The three-membered ring in the main chain was maintained throughout the polymerization. DSC confirmed the visual impression of the transparent 3R-polycaranlactam to be amorphous as only a T_g at 120 °C and no T_m was detected. Surprisingly, the opaque 3S-polycaranlactam exhibited a T_m at 280 °C and is therefore semi-crystalline. The crystal structures of the monomers and of 3S-polycaranlactam were investigated with XRD. Copolymerisation of 3S-caranlactam with caprolactam and laurolactam resulted in a loss of long-range order and transparent copolyamides in a range of about 25-80 % built-in 3S-caranlactam. Solvent-cast transparent films were produced to underline the modification of standard semi-crystalline polyamides to amorphous copolyamides. Additionally, the T_g of the copolyamides increased depending on the amount of rigid three-ring structures in the main chain. Two 100 % bio-based polyamides with varying crystallinity and transparency and high-performance thermal properties were produced in a scalable fashion that have the potential to considerably broaden the scope of bio-based, as well as fossil-based polyamides.

Paul N. Stockmann wrote the manuscript and the supplementary information except for crystallography-related sections. He synthesized 3S-caranlactam, optimized the synthesis of 3R-caranlactam, developed and scaled the one-vessel process and designed all synthesis and polymerization experiments. He analyzed and characterized all intermediates, monomers and polymers with the exception of XRD experiments and supervised Dominik Pastoetter, Moritz Hoehenberger, Johannes Raab, and Sebastian Lessig. Daniel Van Opdenbosch performed the polymer related XRD experiments and interpreted the data together with Paul Stockmann. He wrote the polymer related XRD sections. Alexander Poethig performed the monomer related XRD experiments, interpreted the data, and wrote the corresponding sections. Dominik Pastoetter synthesized 3R-caranlactam and performed initial polymerization experiments. Moritz Hoehenberger synthesized 3S-caranlactam. Johannes Raab investigated the epoxidation of (+)-3-carene in detail and performed initial Meinwald rearrangement experiments. Sebastian Lessig investigated the Meinwald rearrangement in detail. Marion Woelbing, Claudia Falcke and Malte Winnacker supported in polymer analysis and polymerization techniques. Paul Stockmann, Harald Strittmatter, Malte Winnacker and Volker Sieber conceived the work. Cordt Zollfrank and Volker Sieber revised the manuscript. Volker Sieber supervised the project.

Rights and permissions

Open Access This article is licensed under a Creative Commons Attribution 4.0 International License, which permits use, sharing, adaptation, distribution and reproduction in any medium or format, as long as you give appropriate credit to the original author(s) and the source, provide a link to the Creative Commons license, and indicate if changes were made. The images or other third party material in this article are included in the article's Creative Commons license, unless indicated otherwise in a credit line to the material. If material is not included in the article's Creative Commons license and your intended use is not permitted by statutory regulation or exceeds the permitted use, you will need to obtain permission directly from the copyright holder. To view a copy of this license, visit http://creativecommons.org/licenses/by/4.0/.

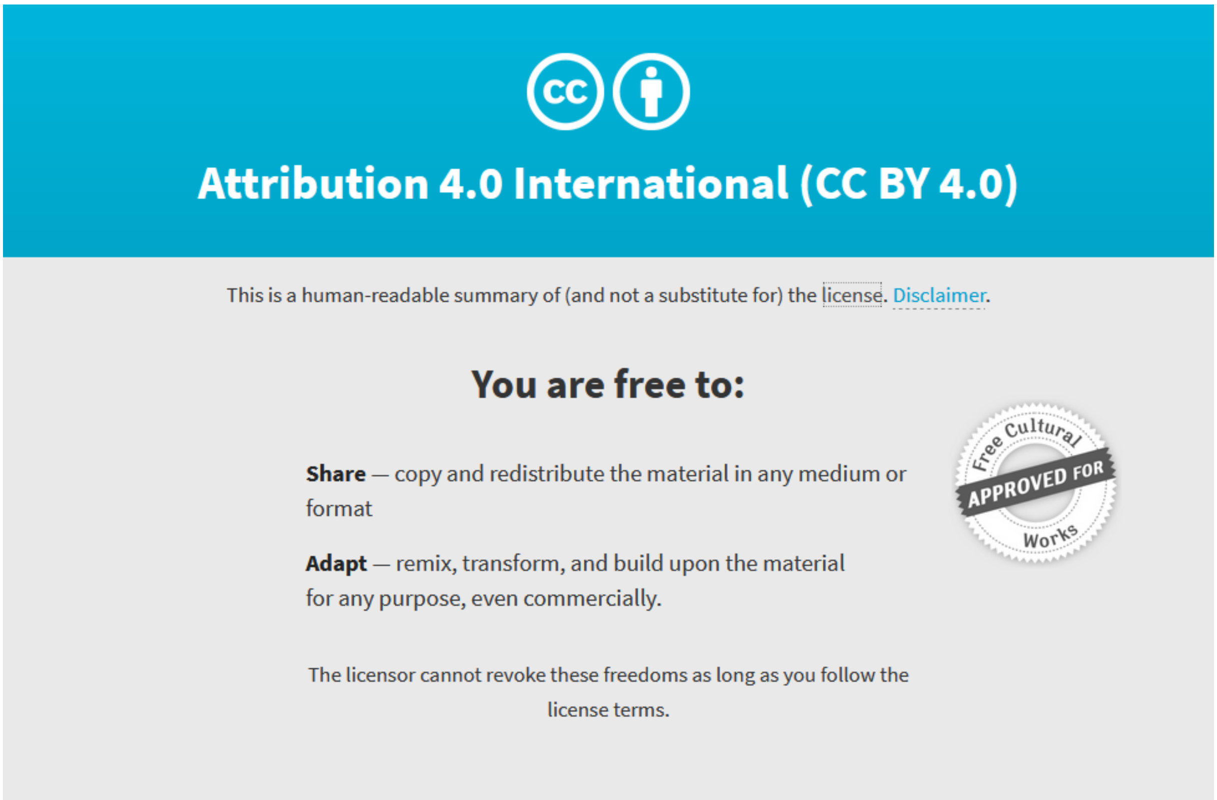

Attribution 4.0 International (CC BY 4.0)

This is a human-readable summary of (and not a substitute for) the license. Disclaimer.

You are free to:

Share — copy and redistribute the material in any medium or format

Adapt — remix, transform, and build upon the material for any purpose, even commercially.

The licensor cannot revoke these freedoms as long as you follow the license terms.

nature COMMUNICATIONS

ARTICLE

https://doi.org/10.1038/s41467-020-14361-6 OPEN

Biobased chiral semi-crystalline or amorphous high-performance polyamides and their scalable stereoselective synthesis

Paul N. Stockmann[1], Daniel Van Opdenbosch[2], Alexander Poethig[3,4], Dominik L. Pastoetter[1], Moritz Hoehenberger[1], Sebastian Lessig[1], Johannes Raab[1], Marion Woelbing[1], Claudia Falcke[1], Malte Winnacker[3,4], Cordt Zollfrank[2], Harald Strittmatter[1] & Volker Sieber[1,2,4*]

The use of renewable feedstock is one of the twelve key principles of sustainable chemistry. Unfortunately, bio-based compounds often suffer from high production cost and low performance. To fully tap the potential of natural compounds it is important to utilize their functionalities that could make them superior compared to fossil-based resources. Here we show the conversion of (+)-3-carene, a by-product of the cellulose industry into ε-lactams from which polyamides. The lactams are selectively prepared in two diastereomeric configurations, leading to semi-crystalline or amorphous, transparent polymers that can compete with the thermal properties of commercial high-performance polyamides. Copolyamides with caprolactam and laurolactam exhibit an increased glass transition and amorphicity compared to the homopolyamides, potentially broadening the scope of standard polyamides. A four-step one-vessel monomer synthesis, applying chemo-enzymatic catalysis for the initial oxidation step, is established. The great potential of the polyamides is outlined.

---

[1] Fraunhofer IGB, Bio, Electro and Chemocatalysis BioCat, Straubing Branch, Schulgasse 11a, 94315 Straubing, Germany. [2] Technical University of Munich, Campus Straubing for Biotechnology and Sustainability, Schulgasse 16, 94315 Straubing, Germany. [3] Department of Chemistry, Technical University of Munich, Lichtenbergstr. 4, 85748 Garching, Germany. [4] Catalysis Research Center, Technical University of Munich, Ernst-Otto-Fischer-Straße 1, 85748 Garching, Germany. *email: sieber@tum.de

olyamides (PA) are an important class of high-performance polymers and have been used in various industries (automotive, textile, medical, etc.) since the first industrial polyamide PA-6.6 was developed by Carothers in 1936 (refs. [1,2]). They are either produced by condensation of diacids with diamines, leading to AABB-type polymers, or amino acids for the AB-type, respectively. This type can alternatively be produced by ring-opening polymerization (ROP) of lactams. The most famous example for a lactam used as a monomer is ε-caprolactam, a seven-membered cyclic amide which was first polymerized to PA-6 by Schlack in 1938 (ref. [3]). It is usually produced from fossil oil-based cyclohexane after the oxidation to cyclohexanone, oxime formation, and subsequent Beckmann rearrangement. Recently, bio-based ways to synthesize caprolactam starting from glucose and fructose via hydroxymethylfurfural (HMF) have been described[4,5]. Due to the increasing awareness of dwindling fossil resources and environmental problems that arise using fossil oil as basis for plastics, alternative monomer resources for polymers in general and for polyamides specifically have become a major focus of research[6–19]. Sustainable monomer sources can be serious alternatives to fossil oil, as demonstrated by the commercially available bio-based polyamides PA1010, PA11, or PA410. These examples are linear, non-chiral condensation polyamides composed of diacids or amino acids derived from castor oil. In this context, we consider especially monoterpenes from renewable feedstocks to be a promising source for biogenic polymers. Monoterpenes such as limonene, camphor, menthone, α- and β-pinene, or 3-carene provide valuable carbon structures such as aliphatic rings and can be isolated from waste streams of biomass-utilizing processes in high volumes[20]. The latter three are the main components of turpentine oil with a combined annual production volume of about 350 kt per year, primarily isolated from the kraft pulping process (sulfate turpentine, 200 kt) or by distillation of resins extracted from conifers (gum turpentine, 100 kt). The composition highly depends on the species and origin of the utilized conifers. In Southeast USA, α-pinene (60–75%) and β-pinene (20–25%) are more common, whereas turpentine from Scandinavia and Russia contains considerable amounts of (+)-3-carene (40%)[21]. Chemically functionalized terpenes used for polyolefins, polyesters, polycarbonates, polyacrylates, and others with promising properties have been reported, underlining their enormous potential for bio-polymers[22–37]. However, terpene-based polyamides are still rare. The first terpene-based bio-polyamide was synthesized by Hall[38] in 1963 via the cationic ROP of a β-pinene based lactam. Recently, Winnacker et al.[39,40] reproduced, investigated, and optimized the synthesis and polymerization and tested the application of the new polyamide in cell growth control. Another approach by the same group was the oligomerization of a menthone-derived lactam[41,42]. For both the commercial polyamides, such as PA6, PA11, PA12, and the lactam-based bio-polyamides, factors limiting broader fields of application remain: relatively low glass transition temperatures (T_g) and melting temperatures (T_m) or low molecular weights (M_n and M_w) in addition to a costly or unscalable synthesis. However, the terpene-based polyamides possess thermal properties in the range of high-performance polymers. We recently described the synthesis of 3R-caranlactam from (+)-3-carene and its polymerization to poly-3R-caranamide[43]. This new polyamide has interesting thermal properties and a molecular weight in the range of commercial PA6 and PA12, but the monomer synthesis was challenging and involved toxic and expensive chemicals.

In this work, we report the synthesis of the new diastereomeric 3S-caranlactam and an optimized synthesis for 3R-caranlactam. 3S-caranlactam is a methyl group diastereoisomer of 3R-caranlactam with considerable different properties and polymerizability. The isomers are selectively prepared by an epoxide-ketone rearrangement and a suitable kinetic or thermodynamic control of the intermediates. A facile and straightforward one-vessel synthesis of 3S-caranlactam in a 4.0 L reactor is presented. Over four steps, an overall yield of 25% is reached. The monomers are polymerized to poly-3R-caranamide and poly-3S-caranamide, and the co-polymerization of 3S-caranlactam with caprolactam (CL) and laurolactam (LL) is also performed. The polymerizations are investigated regarding reaction time, temperature, and other factors. A crucial effect of the amount of applied activator is detected, which is in accordance with polymerization theory. Thermal properties of the homo- and co-polyamides are characterized by differential scanning calorimetry (DSC). Bio-based semi-crystalline or amorphous polyamides and co-polyamides with unique high-performance thermal properties are obtained. The amorphicity of poly-3R-caranmide and several co-polyamides is underlined by the preparation of transparent, sonlvent-cast films. A crystal structure of the semi-crystalline poly-3S-caranamide is also presented. As a conclusion, the great potential of these polyamides is shortly outlined.

Results

Monomer synthesis. Compared to reported literature, the initial oxidation of the double bond of (+)-3-carene (**1**) is achieved by an epoxidation instead of the challenging alcohol synthesis by hydroboration[45,46]. In pathway A (Fig. 1), application of immobilized Cal-B lipase, an industrial enzyme from *Candida antarctica*, or buffered diluted peracetic acid exclusively leads to epoxide **2-3S** (where “S” is the configuration of the stereo-centre of C3)[47–49]. The metal free enzymatic method generates epoxides in high yields under mild conditions, can be conducted in green solvents such as ethyl acetate, and prevents the potentially dangerous aggregation of peracetic acid. In both cases, the epoxidation—which is rather uncommon—was only little exothermic and therefore easily controlled. The yield after distillation was over 80%. As a next step, the rearrangement of the epoxide to a ketone was performed. A literature protocol using high amounts of $ZnBr_2$ in EtOAc resulted in 59% yield, consisting of a mixture of the diastereoisomeric ketones **3-3S** and **3-3R**, which can be identified by Gas chromatography mass spectrometry (GCMS), (Supplementary Methods, Supplementary Fig. 1, Supplementary Table 1)[50]. A diastereoselective rearrangement has not been reported to date. As a mixture of stereoisomers would eventually result in an atactic polyamide, we were interested in a stereoselective catalysis which would enable the synthesis of the pure isomers—but complex[51,52] and costly[53–56] catalysts should be avoided. We assumed that a concerted mechanism leads to inversion of the methyl group, whereas an ionic two-step mechanism results in a mixture[53,57–59]. After screening for optimized reaction conditions (Supplementary Tables 2–8) with respect to solvent polarity, concentrations of reactants, and temperatures, we identified several trends: (I) with decreasing polarity of the solvent, inversion of the methyl group to isomer **3-3S** is preferred; (II) increasing substrate concentration leads to formation of high-boiling molecules, presumably oligomers; (III) oligomer formation decreases at higher temperatures; (IV) various side products are formed under aqueous acidic conditions; and (V) very acidic conditions under exclusion of water are most promising.

The solvent polarity is crucial for the regioselectivity and the stereoselectivity. Hydrocarbons are most suited, whereas application of polar ethers, such as THF, and nucleophilic alcohols drastically reduce the yield (Supplementary Table 2). The role of the anion is also important, as the reaction was comparably unsuccessful with other iron salts ($FeCl_3{\cdot}6H_2O$: 22% ketone selectivity, Supplementary Table 3, entry 9; $Fe(OAc)_2$: no

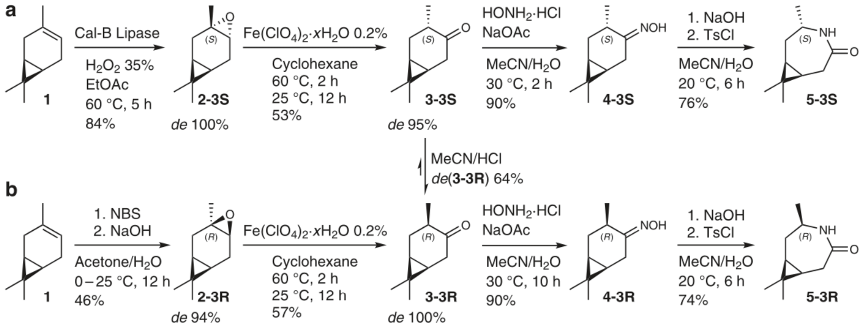

Fig. 1 Monomer synthesis overview. Synthesis pathway with yields and diastereomeric excess (de) of intermediates for the production of the lactam isomers **5-3S** and **5-3R** (yields refer to the small-scale experiments from purified starting material). The labelling of the stereo-centre C3 at all intermediates follows the recommendation for terpene carbon skeleton numbering of M. W. Grafflin, which suggest that the initial carbon labels of (+)-3-carene are fixed also in case of functionalization[44].

conversion, Supplementary Table 4, entry 4). $Zn(OTf)_2$ also gave satisfying results (Supplementary Table 4, entry 2); however, the reaction time was long even at comparably high catalyst concentration. A control reaction with $NH_4(ClO_4)$ showed no conversion. Alternatively, sulfonic acids in cyclohexane or toluene are suitable (Supplementary Table 5). The combination of non-polar solvents and very strong acids can also be applied for the stereoselective rearrangement of other epoxides and will be investigated in more detail in the future. For the synthesis of **3-3R**, **2-3R** was synthesized via the bromohydrine and base-induced epoxide formation, following an adjusted protocol of limonene epoxide production[11]. Application of the $Fe(ClO_4)_2·H_2O$/cyclohexane system gave isomer **3-3R** in excellent selectivity (de 95%). However, the work-up by distillation led to isomerization and 18% of **3-3S** were formed. As **3-3S** is the kinetic product, whereas isomer **3-3R** is thermodynamically favoured, an isomerization under protic acidic conditions (Supplementary Table 9) is possible and the equilibrium is 80:20 in favour of **3-3R**[45,60]. An allyl alcohol was identified as intermediate by GCMS (Supplementary Fig. 1). The synthesis of the oximes **4-3S** and **4-3R** was realized by conversion with hydroxylamine hydrochloride in over 80% yield. In both cases, the *trans*-oxime was the major isomer. Surprisingly, the reaction time was considerably longer for **3-3R** than for the S-isomer. We used that observation to produce **3-3R** from the 3R-enriched equilibrium mixture—thereby making the use of NBS obsolete—with an isomeric purity of over 97%: Addition of small amounts of hydroxylamine hydrochloride led to selective conversion of **3-3S** to **4-3S** in the presence of **3-3R**, which was then separated by distillation (Supplementary Fig. 2). The overall yield starting from (+)-3-carene (**1**) was 47%. Initial experiments indicated that the formation of acetals by the reaction of **3-3S** with alcohols such as glycerol could be used accordingly. The last step of the synthesis was the Beckmann reaction of **4-3S** and **4-3R** to the corresponding lactams 3S-caranlactam (**5-3S**) and 3R-caranlactam (**3-3R**). The yield was over 70% in both cases. As reported before for **5-3R**[43], the selectivity with respect to the nitrogen insertion was over 90%, and crystallization from EtOAc afforded pure **5-3S** or **3-3R**, respectively. Surprisingly—as other Lewis acids were proven unsuitable[43]—some of the perchlorate Lewis acids showed potential for a catalytic Beckmann rearrangement of **4-3S**, with the optimum reaction conditions being investigated at the moment.

We then scaled the reaction to 2.50 mol—or 1.25 mol for the enzymatic epoxidation—of **1** in a 4.0 L reactor and conducted the synthesis as a one-vessel process (Fig. 2, Supplementary Methods, Supplementary Figs. 3 and 4). As only washing steps and solvent changes were required, all intermediates remained in the reactor throughout the whole process. The crystallization was partly achieved in the reactor at 15 °C (approximately 50%), and the formed crystals could be filtered effortlessly. The remaining product was then isolated by crystallization at −20 °C separately. The crystallization protocol was not optimized so far, and a complete crystallization within the reactor might well be possible. In general, the crystallization of **5-3S** was not affected by the accumulated side products (e.g. cymene and unidentified high-boiling aliphatic compounds). The yield after recrystallization was 24% over four reaction steps. **5-3S** was synthesized accordingly with 20% overall yield; the enriched **3-3R** had to be purified separately by vacuum distillation and was then re-transferred to the reactor for the oximation. The process will be upscaled to the 100 L reactor shortly.

Although the synthesis is not fully optimized, several sustainable aspects are worth mentioning. The presented process requires only moderate reaction conditions and no elaborate reaction equipment. Only little amounts of metal are used during the process. In addition—as no low-boiling, interfering side products are formed—cyclohexane is retrieved during the process and can be reused; EtOAc and MeCN can also be recovered from the mother liquor by distillation after product crystallization. Finally, the product purity that is required for polymerization is reached by crystallization, avoiding material- or energy-consuming methods. However, for a fully sustainable synthesis, the amount of washing solutions—which were used in great excess so far—must be reduced, a catalytic method for the Beckmann rearrangement needs to be implemented, and an increase of the overall yield is required.

Preparation and investigation of the homopolyamides. As mentioned before, **5-3R** polymerizes by anionic ROP under application of NaH as initiator and in situ generated N-acetylated **5-3R** to poly-3R-caranamide (**poly5-3R**), reaching an average molecular weight number (M_n) over 30 kDa[43]. The addition of Ac_2O during this process is challenging to control and to reproduce due to reaction temperatures reaching values above the boiling point of Ac_2O and monomer sublimation. Therefore, we used *N*-benzoyl-3R-caranlactam (**Bz5-3R**) and *N*-benzoyl-3S-caranlactam (**Bz5-3S**,) as solid, high-boiling activators (Fig. 3). Gel permeation chromatography (GPC, Supplementary Methods,

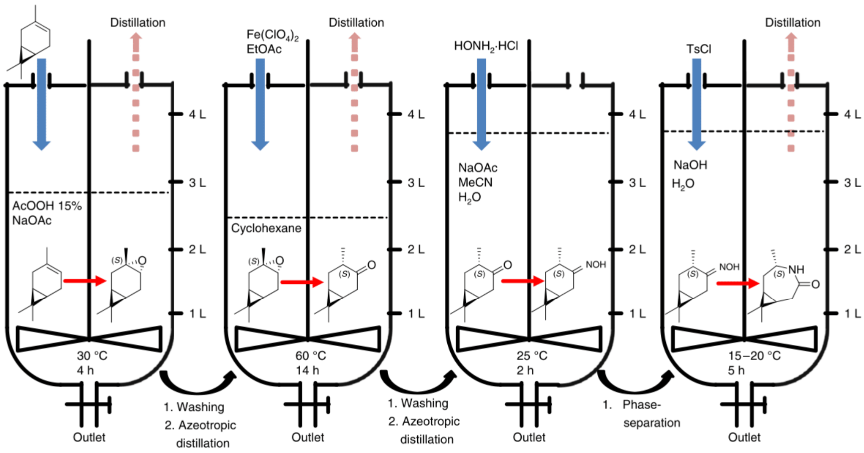
Distillation
Fe(ClO$_4$)$_2$
EtOAc
Distillation
HONH$_2$·HCl
TsCl
Distillation
4 L
3 L
2 L
1 L
AcOOH 15%
NaOAc
Cyclohexane
NaOAc
MeCN
H$_2$O
NaOH
H$_2$O
(S)
NOH
NH
30 °C
4 h
60 °C
14 h
25 °C
2 h
15–20 °C
5 h
Outlet
1. Washing
2. Azeotropic distillation
1. Washing
2. Azeotropic distillation
1. Phase-separation

Fig. 2 Up-scale of 5-3S. Schematic one-vessel reaction cascade in a 4.0 L scale for the synthesis of lactam **5-3S**. (1) Addition of **1** to the epoxidation reagent AcOOH, washing, addition of cyclohexane and subsequent azeotropic distillation; (2) Meinwald rearrangement of **2-3S** to **3-3S** with Fe(ClO$_4$)$_2$, washing, and solvent exchange to MeCN; (3) oximation to **4-3S** using a buffered solution of HONH$_2$·HCl; and (4) Beckmann rearrangement to **5-3S** in basic media with tosyl chloride (TsCl).

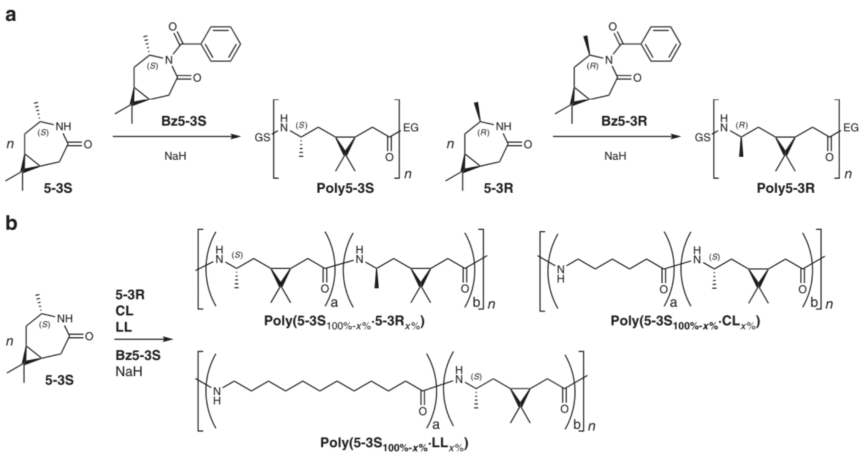
a
n
5-3S
Bz5-3S
NaH
Poly5-3S
GS
EG
5-3R
Bz5-3R
Poly5-3R
b
5-3R
CL
LL
Bz5-3S
NaH
Poly(5-3S$_{100\%-x\%}$·5-3R$_{x\%}$)
Poly(5-3S$_{100\%-x\%}$·CL$_{x\%}$)
Poly(5-3S$_{100\%-x\%}$·LL$_{x\%}$)

Fig. 3 Polymerization overview. Anionic ring-opening polymerization of the (+)-3-carene based lactams **5-3S** and **5-3R** (**a**) and co-polymers of the general structures poly(5-3S$_{100\%-x\%}$·5-3R$_{x\%}$) from **5-3S** and **5-3R**, poly(5-3S$_{100\%-x\%}$·CL$_{x\%}$) from **5-3S** and CL, and poly(5-3S$_{100\%-x\%}$·LL$_{x\%}$) from **5-3S** and LL (**b**).

Supplementary Fig. 5, Supplementary Table 10) was chosen for determination of the molecular weight as measurements of **poly5-3R** and **poly5-3S** with MALDI-TOF did show the characteristic peak distance of 167*m*/*z*, but only oligomers up to 6.5 kDa could be detected (Supplementary Fig. 6). This is a known phenomenon for polyamides[39,61]. The initial polymerization reactions of lactam **5-3S** were carried out in an evacuated glass vial equipped with a metal screw cap with a rubber septum, a magnetic stir bar, NaH on paraffin wax as an initiator, and **Bz5-3S** as an activator (Polymerization method A, Fig. 4, Supplementary Fig. 7). The activator concentration was varied, and the effect of the reaction temperature was evaluated at 180 and 220 °C.

At 180 °C, an M_n of over 10 kDa and an M_w over 16 kDa are observed, whereas at 220 °C the values do not exceed 7.5 kDa. For both temperatures, the decreasing amount of **Bz5-3S** results in an increasing molecular weight, as expected. However, this effect is stronger at 180 °C and M_n increases over 70%; at 220 °C, only 35% average chain growth is observed. At a starting monomer/activator ratio (ratio$_{A/M\ start}$) of approximately 50, the rise of the molecular weights attenuates considerably in both cases. The polydispersity

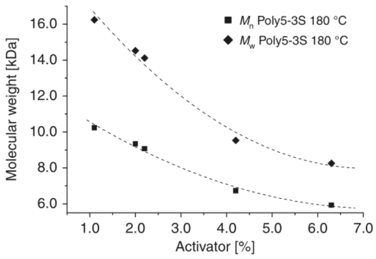

Fig. 4 Polymerization of 5-3S. Effect of the reaction temperature and the activator concentration on M_n and M_w (Supplementary Figs. 8 and 9, Supplementary Table 11). Conditions: 1.8 mmol **5-3S**, 2.0–5.5 mol% NaH on paraffin, 180 or 220 °C, 1 h. Molecular weights refer to masses over 1.0 kDa (GPC).

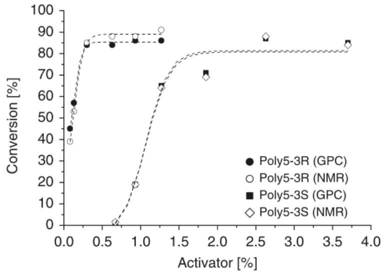

Fig. 5 NMR and GPC investigations of the monomer conversion. Conversion of the lactams and illustrative sigmoidal Boltzmann Fit depending on an increasing amount of activator **Bz5-3S** determined by NMR and GPC (Supplementary Figs. 11–16, Supplementary Table 13). Conditions: 3.0 mmol **5-3S** or **5-3R**, 3.0 mol% NaH on paraffin, 190 °C, 1 h.

index (PDI) is between 1.2 and 1.6 for all ratio$_{A/M\ start}$, being a typical value for ROP which usually yields polymers with a narrow mass distribution[62]. DSC revealed T_gs of 111–115 °C and T_ms of 245–285 °C (Supplementary Fig. 10, Supplementary Tables 11 and 12) for a reaction temperature of 180 °C, whereas the melting onset was as low as 230 °C for a reaction temperature of 220 °C. To remove the residual monomers and oligomers, the polyamides were grinded to powders and stirred in a water/ethanol solution for several hours (Polymer work-up method A). Though this process was successful, it became clear that the conversion of **5-3S** could not be calculated from the isolated polymer yield, as uncontrolled polymer losses during the process (filtering, grinding, etc.) are unavoidable. The yield of isolated poly-3S-caranamide (**poly5-3S**) was 60–80%. In addition, sublimation of the monomer during the polymerization was detected particularly at long reaction times, which distorts the monomer/activator ratio. Similar challenges were observed during the polymerization of lactam **5-3R**.

Therefore, we changed the polymerization set up and used a heating block covered with an aluminium foil to guarantee homogeneous temperature inside the polymerization vial and used nitrogen instead of vacuum for inert reaction conditions—this prevented sublimation almost completely (polymerization method B, Supplementary Fig. 17). To determine the conversion without the described drawbacks, **poly5-3S** and **poly5-3R** were dissolved in hexafluoro-2-isopropanol (HFIP) in the polymerization vial directly after the reaction. After complete dissolution of the polymer, samples of the homogeneous solution were analysed by GPC and NMR to measure the ratio of unreacted and incorporated monomer (Fig. 5). In both cases, the NMR and GPC analysis were in good agreement. NMR revealed that no isomerisation of the methyl group or side reactions of the three-membered ring occurred (Supplementary Figs. 18 and 19). This is worth mentioning, as the defined relative (and absolute) configuration gives rise—as indicated by chemical logic and demonstrated for other chiral lactams[39]—to chiral polyamides. **Poly5-3R** was formed more readily and at lower activator concentrations than **poly5-3S**; 0.3 mol% activator was enough to surpass 80% conversion of **5-3R**, whereas 2.5 mol% were required for **5-3S**. The lactams reached a conversion of almost 90%, which is surprisingly high for substituted lactams, especially as aliphatic side-chains are attached at the β- and γ-position[63]. Substituents in these positions usually set the Gibbs energy to less negative values and lead to ring closure, therefore lowering the reactivity. Consequently, aliphatic substituents such as methyl- or propyl groups in the γ-position lead to an unfavourable polymer–monomer equilibrium and decreased conversion[10,63,64]. However, although several examples have been published, detailed predictions about the polymerizability and polymer–monomer equilibrium of bicyclic lactams are challenging[65–67]. For lactam **5-3S**, no significant conversion was observed beneath a ratio$_{A/M\ start}$ of approximately 1:100, whereas even a ratio$_{A/M\ start}$ as small as 1:1200 (<0.1%) lead to a conversion of over 40% within 1 h for the stereoisomeric lactam **5-3R**. If 1% activator was applied, the polymerization was completed in seconds. The M_n of **poly5-3R** and, at high conversion levels, the M_n of **poly5-3S** increased at decreasing amounts of the activator. However, below a certain activator concentration and conversion, the observed molecular weights are low for **poly5-3S** (Fig. 6).

As the formation of **poly-5S** was considerably slower than of **poly-5R**, we investigated the conversion at a given activator concentration (3.3%) at different reaction times at 180 °C.

The conversion reached a maximum of 80% after 2 h; 94% of that was completed after about 50 min (Supplementary Fig. 20, Supplementary Table 14). As reported by us previously, **poly5-3R** did not possess a melting point in the DSC analysis (Supplementary Methods, Supplementary Table 15, Supplementary Fig. 21)[43]. We presume that the high degree of aliphatic substitution prevents the polymer chains to crystallize, even at long tempering times. This has not been reported for terpene-based polyamides before, but has been reported for other alkyl-chain-substituted short-chain bio-polyamides[10]. DSC of **poly5-3S** revealed that the polyamide is semi-crystalline with a comparably weak T_g at around 105 °C and a T_m of up to 280 °C, surpassing the T_g and T_m of unsubstituted PA6 by 50 and 60 °C, respectively. The decomposition temperature under nitrogen atmosphere was around 360 °C. The high T_gs are caused by the three-membered ring in the polymer backbone and the resulting reduction in one degree of rotational freedom in the

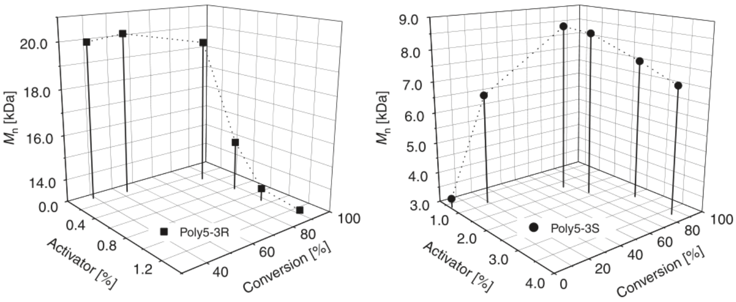

Fig. 6 Effects of the amount of activator. Influence of the activator concentration on the conversion and M_n of **poly5-3R** and **poly5-3S** (Supplementary Figs. 11–14, Supplementary Table 13). Conditions: 3.0 mmol **5-3S** or **5-3R**, 3.0 mol% NaH on paraffin, 190 °C, 1 h.

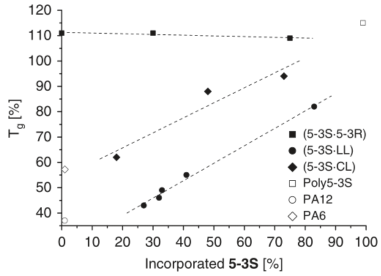

Fig. 7 Co-polymerization effects. Influence of the inclusion of **5-3S** on the T_g of co-polyamides with CL and LL (Supplementary Figs. 23–27, conditions: Supplementary Table 16).

polymer backbone. To rule out the possibility that the lower molecular weight enables the, therefore, shorter polymer chains to form crystals, a short-chain **poly5-R** (M_n = 10 kDa; Supplementary Fig. 22) was synthesized and analysed by DSC—still, no melting was observed. As no other differences in the monomer or the polymer chain are present, this finding can directly be attributed to the diastereomeric methyl group that, consequently, causes not only a different ring structure in the lactam but also strong structural changes in the polymer chain. To support these findings, we investigated the monomers and both polyamides with XRD (Supplementary Methods, Supplementary Notes 1 and 2).

Preparation and investigation of the co-polyamides. As the three-membered ring of **5-3S** might decrease the segmental chain motion[68], we hypothesized that the random inclusion of this motif in the more regular chains of PA6 and PA12 could not only result in an increased T_g but also in a decrease or even complete loss of long-range order. Apart from that, the copolymerizability of **5-3R** and **5-3S** was tested (Fig. 3b).

The co-polymerization was successful by applying similar reaction conditions as for the homopolyamides and could be verified by NMR. In all cases a complete consumption of **5-3S** was not achieved. If equimolar amounts of **5-3S**, CL or LL were used, the integration in the backbone was 96% (CL) and 89% (LL). The T_g of the co-polyamides with CL and LL was shifted to higher temperatures with increasing amount of **5-3S** (Fig. 7). For example, a built-in of 48% in the regular PA6 chain in **copoly(5-3S$_{48\%}$·CL$_{52\%}$)** resulted in a T_g of 88 °C, whereas the T_g of **copoly (5-3S$_{41\%}$·LL$_{59\%}$)** is shifted to 55 °C (Supplementary Table 16, entries E10 and E7). In both cases, no melting point was observed in DSC and the polymers were clear, yellow blocks. If only 18% of **5-3S** were integrated in the PA6-backbone, a broad melting area between 160 and 190 °C caused by cold crystallization (110–150 °C, Supplementary Fig. 26 i) was observed, indicating that this amount is not enough to completely suppress the establishment of a long-range order. **Copoly(5-3S$_{83\%}$·LL$_{17\%}$)** has a T_g of 82 °C and a melting range of 220–250 °C. The broad melting ranges suggest that **5-3S** is not regularly distributed in the polymer chain and that the different reaction kinetics of the monomers lead to a gradual increase of the slow-reacting lactam in the growing chain throughout the polymerization reaction. As only one melting range is observed, the parallel formation of the homopolyamides PA6/12 and **poly5-3S** can be excluded[69]. It is worth mentioning that the T_g seems to increase in a linear manner in a certain incorporation-range of **5-3S**, approximately between 25% and 80%. We hypothesize that outside of this range, effects arising from crystallinity affect the T_g. As the crystallinity is drastically reduced within the range, the increasing T_g can be directly attributed to the amount of **5-3S** in the polymer backbone.

Investigation of the co-polymerization of 1:1 mixtures of **5-3S** and CL/LL revealed that the monomers were consumed at different rates (Supplementary Figs. 28 and 29, Supplementary Table 17). The co-polymerization of **3-5S** and CL almost exclusively starts with the conversion of CL before **3-5S** is also incorporated. Some examples for intermediate **poly(5-3S·CL)** were: **poly(5-3S$_{18\%}$·CL$_{72\%}$)** at 60 s (6.7% total conversion), **poly(5-3S$_{37\%}$·CL$_{63\%}$)** at 240 s (41% total conversion) and **poly (5-3S$_{49\%}$·CL$_{51\%}$)** at 60 min (82% total conversion). The co-polymerization with LL proceeded vice versa, and the co-polymer composition was **poly(5-3S$_{66\%}$·LL$_{34\%}$)** at 60 s (7.9% total conversion), **poly(5-3S$_{58\%}$·LL$_{42\%}$)** at 240 s (34.5% total conversion) and **poly(5-3S$_{52\%}$·LL$_{48\%}$)** at 60 min (64.4% total conversion). From this, it can be concluded that the relative rates of consumption are CL > **5-3S** > LL.

To further evaluate the optical properties, we fabricated films of the co-polyamides and **poly5-3R** by dissolving them in HFIP and slow evaporation of the solvent. Commercial and self-made PA6 and PA12 resulted in colourless non-transparent films. From the amorphous co-polymers, however, relatively transparent foil-like films could be produced (Fig. 8). Although some of the films show little amounts of residual monomers and—due to the preparation method—inclusions of solvent and other irregularities, the increasing transparency is obvious.

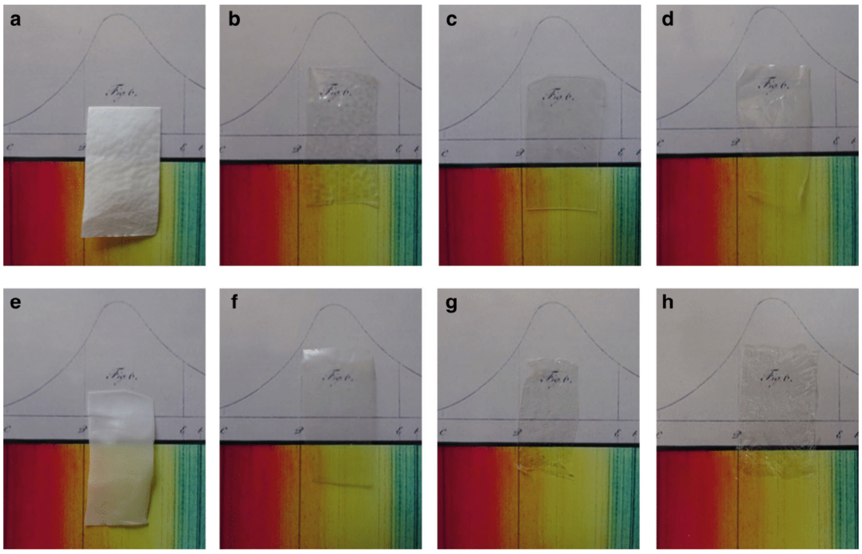

Fig. 8 Transparent polyamide films. Photographs taken under identical conditions of pure polymers and co-polymers in front of a sector of the Fraunhofer lines. **a** PA12; **b copoly(5-3S$_{32\%}$·LL$_{68\%}$)**; **c copoly(5-3S$_{33\%}$·LL$_{67\%}$)**; **d copoly(5-3S$_{41\%}$·LL$_{59\%}$)**; **e** PA6; **f copoly(5-3S$_{18\%}$·CL$_{82\%}$)**; **g copoly(5-3S$_{48\%}$·CL$_{52\%}$)**; **h** poly5-3R.

Crystal structures of the monomers. Comparison of the structures of the monomers, determined by single-crystal X-ray diffractometry (details see Supplementary Note 1), shows that the methyl-group inversion at C3 leads to a changed conformation of the seven-membered ring. This might explain the different properties of the monomers: **5-3S** has a higher melting point (about 170 °C instead of 140 °C as observed for **5-3R**, Supplementary Fig. 30); increased monomer sublimation was detected during the heating process, and **5-3S** crystallizes more rapidly from EtOAc.

The higher quality low-temperature (100 K) data obtained for **5-3R** (CCDC 1938733) agree with published values for a room temperature measurement (CCDC 145220)[46]. The crystal structures derived from the diffraction patterns (Fig. 9, Supplementary Fig. 31a, b, Supplementary Table 18) illustrate that hydrogen bonds are formed between symmetry-identical molecules in **5-3S** (CCDC 1938732), as well as between the two independent molecules in the asymmetric unit of **5-3R**. In case of **5-3R** a dimer formation via classic hydrogen bonding through antiparallel arrangement of the amide groups is observed and non-classic hydrogen bonding to the methyl groups at C9 and C10 leads to an extended hydrogen bonding through the crystal. The independent molecules of **5-3R** have identical absolute configurations (Supplementary Figs. 32–34). In case of **5-3s** the bonding network is different, since each amide oxygen atom forms hydrogen bonds to an amide hydrogen atom of one symmetry generated molecule, as well as a non-classic hydrogen bond to one of the C5-bound hydrogen atoms of another symmetry generated molecule in the crystal structure. Comparison of the lactam structures with their respective energy-minimized shapes (MOPAC, PM7, singlet) yields the root mean square displacements 0.032 Å (*S*) and 0.042 Å (*R*). This confirms the expected low-energy conformation of the unconstrained monomeric species. The amide motif (C3–N1–C4–C5) is almost planar for both isomers, reflecting the partial double bond character. In contrast, the absolute configuration of the stereogenic centre C3 significantly influences the different conformations of the seven-membered ring. In case of **5-3R**, derived from the thermodynamically favoured ketone **3-3R**, the seven-membered ring can be divided in two groups of coplanar arranged atoms: one plane spanned by C1–C2 and C5–C6 and the other by C2–C5 including N1. In case of **5-3S** the situation is different since one plane is spanned by C3–C5 including N1 and the other plane by C5–C6 and C1–C3.

Crystal structure of poly5-3S. The diffraction patterns recorded from **poly5-3S** were characteristic of a semi-crystalline polymer (Supplementary Data 1, Supplementary Fig. 31c), allowing structural determination by the direct space method simulated annealing (SA, Supplementary Methods, Supplementary Note 2, Fig. 10, Supplementary Figs. 35 and 36). By scaling the amorphous reference patterns to match them at 2Θ values outside the range of Bragg peaks, we obtained a fraction of crystalline phase (f_c) of 0.42 from the ratios of the integrated intensities. Patterns from **poly5-3R** showed no distinct reflexes, except those from residual monomers (Supplementary Fig. 31d).

In **poly5-3S**, the arrangement of N1 and O1 within the polymer chain is similar to that found in β-peptides[70]. Within crystallites of **5-3S**, hydrogen bonds are formed between pairs of antiparallel chains (Fig. 10, Supplementary Fig. 35). Consequently, the obtained crystal structure for **poly5-3S** is one of antiparallel two-strand β-sheets. The inter-sheet distances are $a/2 = 4.90(3)$ Å, and the repeat distances along the chain $c = 6.44(6)$ Å (Fig. 10, Supplementary Table 18). The distance from N1 to O1 of 2.79 Å corresponds well to the distances typically found in polyamides[71]. Further, the density of the crystalline phase of 1.167 g cm^{-3} is a good match for the densities of the **5-3S** monomer crystalline phase of 1.147 g cm^{-3} and well in the range of standard polyamides[2]. Finally, the bond angle C5–C6–C1 of

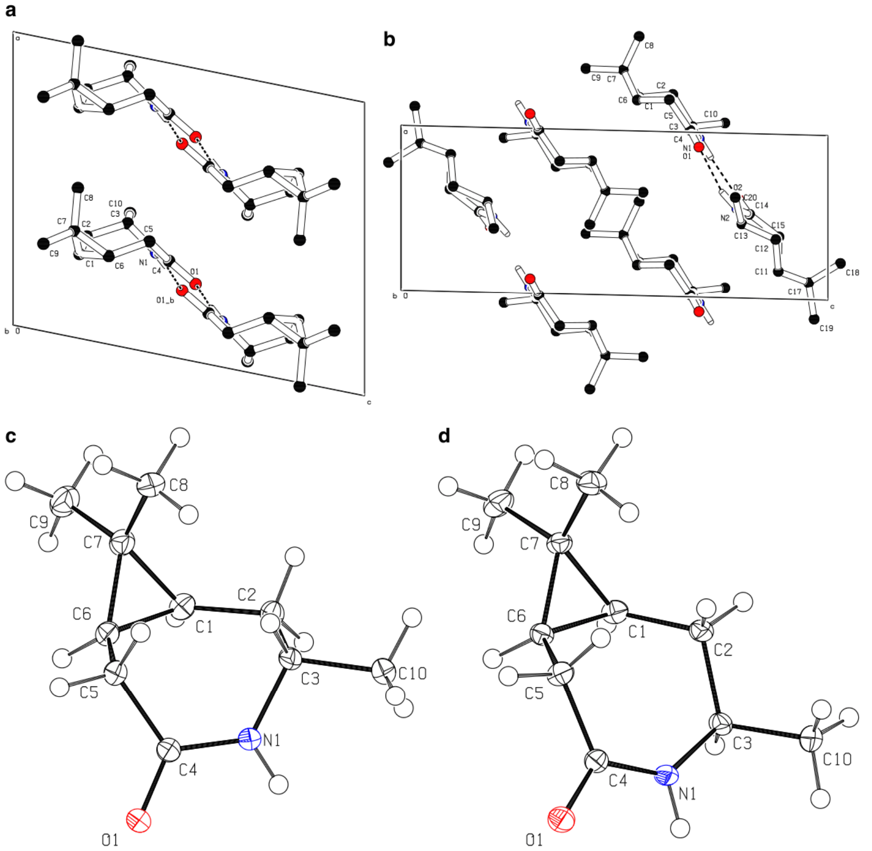

Fig. 9 Crystal structures of the monomers. Crystal structures and monomer molecule conformations of each **5-3R** (**a, c**) and **5-3S** (**b, d**) with bonding hydrogens only viewed in unit cell direction *b*.

104.49° is within a realistic margin to the ideal tetrahedron angle of 109.28°. The view of the expanded repeating unit demonstrates that the chain conformation is strongly influenced by the three-membered ring C1–C6–C7–C1 (Fig. 10). The crystal structure view in the same figure shows that the "bend" shape of the C2–C3–N1–C4O1–C5 segment results from the hydrogen bonds across chains, in conjunction with the angle imposed by the three-membered ring.

Discussion

To summarize, a stereoselective reaction sequence for two stereoisomeric lactams—starting from the chiral biomolecule (+)-3-carene—was developed. The selective Meinwald rearrangement enables the deliberate synthesis of **5-3S** or **5-3R**—new bio-based building blocks for either amorphous (transparent) or semi-crystalline polyamides. **5-3S** can be produced in an at least partly sustainable one-vessel process without purification of any intermediates. The final product was effortlessly purified by crystallization. The initial oxidation step could be achieved by in situ generated peracetic acid, formed by a lipase, H_2O_2, and acetic acid, a considerably environmentally benign and safe method for epoxidation.

The results of our small-scale basic polymerization experiments show that **5-3S** and **5-3R** polymerize comparably facile and that the molecular weight can be adjusted by variation of the activator amount. Additionally, the general potential to form co-polyamides with CL and LL allows the formation of new partially bio-based materials. The homopolymers and the co-polymers have very intriguing characteristics, regarding thermal properties, crystallinity, and transparency. These properties can be attributed to the three-membered ring and the methyl group at C3, which—according to NMR analysis—maintain their configuration throughout the polymerization. Especially the co-polymers are of high interest as the properties of these new polymers highly differ from PA6 and PA12, possibly giving way to new fields of application without the need of additional additives to introduce similar effects. Furthermore, all produced polyamides are, by chemical logic, chiral as the starting material (+)-3-carene consists of only one enantiomer and the three-membered ring is unable to isomerize. This might enable applications in chiral separation techniques.

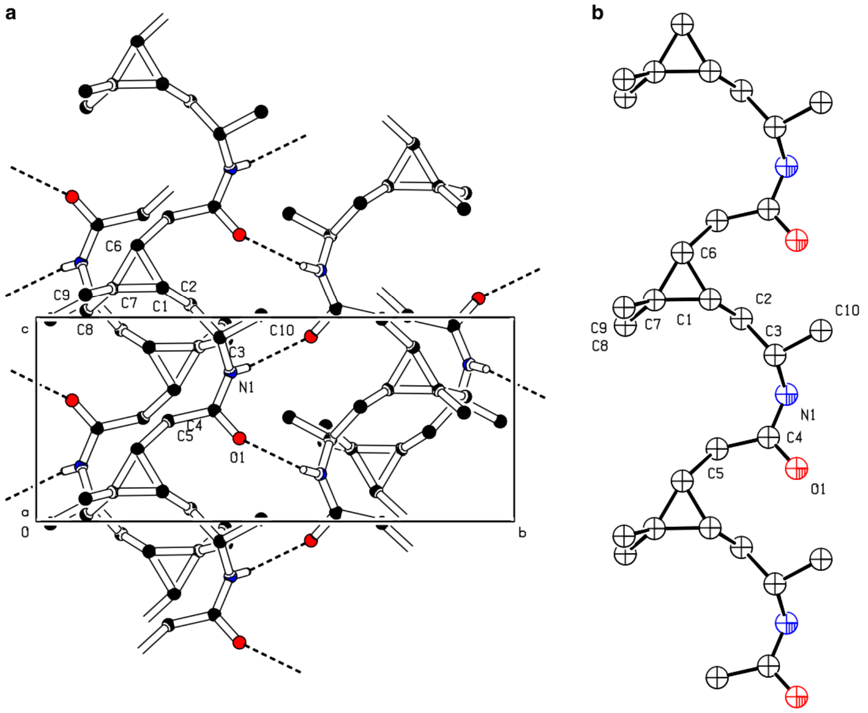

Fig. 10 Crystal structure of poly5-3S. Structure of **poly5-3S**, viewed in unit cell direction *a* (**a**) and the expanded repeating unit (**b**). In the unit cell view, only bonding hydrogens are shown.

In the future, we plan to scale-up the polymerization of the homo- and co-polymers, the investigation of the hydrolytic polymerization, compatibility tests with commercial polymerization systems and additives, and polymer processing to produce standardized specimen to further demonstrate that high-performance bio-polyamides can not only keep up with their fossil-based counterparts but also that bio can be better.

Methods

Instrumental and characterization. GCMS was performed using GC-2010 Plus (Shimadzu) with an auto-injector AOC-5000 (Jain, Combi PAL), a GC capillary column (BPX 5: 5% phenyl, 95% methyl polysilphenylene/siloxane; SGE), and MS-QO2010 Plus (Shimadzu) at 70 eV. NMR measurements were carried out on a JNM-ECA 400 MHz spectrometer from JEOL. Chemical shifts δ are indicated in parts per million with respect to residual solvent signals. SEC was performed using a SECcurity GPC system with an autosampler (1260 Infinity; Agilent Technologies) and a TCC6000 column oven (Polymer Standards Service, PSS). DSC was performed on a DSC 1 from Mettler Toledo with the software STARe V. 16.00. MALDI-TOF was conducted on a Bruker Ultra Flex TOF/TOF mass spectrometer. Single-crystal analysis was performed by single-crystal X-ray diffractometry (SC-XRD, D8 Venture, Bruker AXS, Madison, WI, USA) equipped with a 4-circle goniometer (Kappa geometry), a CMOS detector (Photon 100, Bruker AXS), a rotating anode (TXS, Bruker AXS) with MoKα radiation ($\lambda = 0.71073$ Å), and a multilayer mirror monochromator (HELIOS, Bruker AXS). Powder X-ray diffraction was carried out using Bragg-Brentano geometry (PXRD, Miniflex, Rigaku, Japan, with silicon strip detector D/teX Ultra) and copper Kα radiation. Detailed information about applied methods and sample preparation is described in the Supplementary Methods.

Monomer synthesis. All applied chemicals, including solvents, were purchased in industrial grade and used as received. All monomer synthesis reactions were carried out under air without inert atmosphere. For the enzymatic epoxidation, Novozyme-435 (CALB lipase immobilized on acrylic resin) was applied. The reaction progress was monitored by GCMS or TLC. Purification of the products was achieved by distillation, crystallization, or column chromatography. Product characterization was realized by NMR and GCMS. The exact structure of **5-3S** and **5-3R** was determined by XRD. TLC was performed using aluminium plates coated with SiO_2 (Merck 60, F-254) and the spots were visualized with a $KMnO_4$ stain. Flash column was performed using SiO_2 (0.06–0.2 mm, 230–400 mesh ASTM) from Roth. NMR assignments of all intermediates are provided beneath the synthesis protocol, NMR data are displayed in Supplementary Figs. 37–46.

One-vessel scale-up. The reaction cascade was performed under application of the METTLER TOLEDO LaBMax Automatic Lab Reactor equipped with a 4.50 L reaction vessel with a bottom outlet, a stirrer (shaft stirrer blade), a condenser, a distillation bridge, and active water cooling (minimum temperature: 15 °C). A detailed step-by-step protocol is described in the Supplementary Methods.

Polymerization method A. 3S-caranalctam (**5-3S**), 3R-caranlactam (**5-3R**), **CL** or **LL** and the specific amount of activator (N-Bz-caranlactams **Bz5-3S** and **NBz5-3R**) and NaH (60% on paraffin) were put into a glass vial (10 mL) equipped with a magnetic stir bar. The vial was closed with a screw lid with a rubber septum and vacuum was applied via a syringe connected to a vacuum pump for 10 min before the vial was vortexed for 30 s. The vial was placed in an oil bath and stirred at a specific temperature. When the reaction time was over, the vial was removed from the oil bath and cooled down to room temperature without external cooling.

Polymerization method B. 3S-caranalctam (**5-3S**), 3R-caranlactam (**5-3R**), **CL** and **LL**, and the specific amount of activator (*N*-Bz-caranlactams **Bz5-3S** and **NBz5-3R**) and NaH (60% on paraffin) were put into a glass vial (10 mL), flushed with nitrogen and closed with a screw lid with a rubber septum and vortexed for 30 s. The vial was then placed into a heating block at different temperatures for the respective amount of time. The heating block was covered with aluminium foil to decrease the temperature gradient. After the reaction time was reached, the vial cooled down to room temperature without external cooling.

Polymer work-up method A. The glass vial was destroyed and glass residues sticking to the polymer were removed before it was broken down to small pieces under application of scissors, hammering and liquid nitrogen if necessary. The polymers from lactam **5-3S** were more brittle than the polymers from **5-3R**, whereas the poly-3R-caranlactam (**poly5-3R**) was at least partly soluble in EtOH. The polymer pieces were transferred to a mortar and grinded in the presence of a few millilitres of organic solvent (EtOAc for **poly5-3R**, EtOH for **poly5-3S**) until a fine powder was produced. In cases of non-homogeneous particles, the powder was refluxed in a mixture of EtOH and water (1:1) for at least 12 h, filtered off, and washed several times with water, acetone, and EtOAc and grinded again. Finally, the colourless or slightly yellow powders were dried under reduced pressure and analysed by IR, NMR, DSC, and GPC.

Polymer work-up method B. The polymers were dissolved in HFIP within the polymerization glass vial and a sample of the homogeneous solution was analysed by GPC. Another sample was dried under reduced pressure, re-dissolved in DCOOD and investigated by NMR. Specific NMR signals as well as the GPC elugrams were used for the determination of monomer conversion.

Effect of temperature and activator concentration on *M*. Lactam **53-S** was converted to **poly5-3S** at 180 and 220 °C at different concentrations of activator **Bz5-3S**. Monomer (300 mg, 1.8 mmol, 1.00 equiv.), NaH (60% on paraffin, 1.6–4.0 mg, 0.04–0.10 mmol, 0.02–0.05 equiv.), and activator **Bz5-3S** was polymerized for 1 h as described in polymerization method A. Polymer work-up A was used for further investigations. The results are displayed in Supplementary Figs. 8 and 9 and Supplementary Table 11.

Impact of the activator concentration on the conversion. Monomer (500 mg, 3.0 mmol, 1.00 equiv.), NaH (60% on paraffin, 3.5 mg, 0.09 mmol, 0.03 equiv.), and a varying amount of activator was polymerized at 190 °C for 1 h as described in polymerization method B. Polymer work-up B was used for further investigations. The results are displayed in Supplementary Figs. 11–16 and Supplementary Table 13.

Impact of the reaction time on the conversion. 3S-caranlactam (**5-3S**, 300 mg, 1.80 mmol, 1.00 equiv.), NaH (60% on paraffin, 6.0 mg, 0.15 mmol, 0.08 equiv.), and **Bz5-3S** (15.0 mg, 0.06 mmol, 0.03 equiv.) was polymerized by polymerization method B several times. Each polymerization experiment was terminated after a specific reaction time. The polymers were dissolved in a mixture of HFIP and EtOH, and a sample was dried under reduced pressure. The remaining residue was re-dissolved in DCOOD and analysed by NMR as displayed in Supplementary Fig. 20 and Supplementary Table 14.

Copolymerizations of 3S-caranlactam (5-3S). Lactam **5-3S** was co-polymerized with **5-3R**, **LL,** and **CL** under various conditions as displayed in Supplementary Table 8. The ratio of lactam **5-3S** and the specific co-monomer (Built-in) of the polyamides copoly(**5-3S·5-3R**), copoly(**5-3S·LL**), and copoly(**5-3S·5-CL**) was investigated by NMR. The protons used for integration and comparison are highlighted in Supplementary Fig. 27; the results are displayed in Supplementary Figs. 23–25 and Supplementary Table 16. ^{1}H and ^{13}C spectra showing the full ppm range are displayed for an example of each type of co-polyamide as Supplementary Figs. 47–49.

Time-dependent integration of 5-3S in the CL/LL co-polymers. The time-dependent integration of **5-3S**, **CL**, and **LL** in the growing co-polymer chain was investigated. 1:1 mixtures of the monomers were polymerized as follows: The monomers were melted in a round bottom flask equipped with a magnetic stirrer bar in a nitrogen atmosphere. NaH was added, followed by **Bz5-3S**. Samples from the melt were taken at different reaction times until the reaction mixture became solid. A final sample was taken from the solid after 60 min. The samples were analysed by NMR and the conversion and integration were determined (Supplementary Figs. 28, 29 and Supplementary Table 17).

Film-cast experiments. 0.5 g of PA6, PA12, **copoly(5-3S·CL)**, or **copoly(5-3S·LL)** were dissolved in HFIP (20 mL) for at least 12 h. The solution was filtered and transferred in a crystallizing dish (diameter: 11 or 5.5 cm) and left under a fume hood until a clear film was formed. The film was carefully separated from the dish and dried in an oven at 85 °C for 3 h to remove residual solvent. For **poly5-3R**, this method proved unsuitable as the dried polyamide film could not be separated from the glass. Therefore, a PTFE foil was used as an inlay. Films of **poly5-3R** could then be separated from the PTFE inlay after drying.

Single-crystal production of the lactams. Single crystals were obtained by crystallization at 4 °C within 3 days. The crystals were separated by filtration, washed with cold acetone, and dried under air atmosphere.

Data availability

The authors declare that the data supporting the findings of this study are available within the article (and its Supplementary Information files). The X-ray crystallographic coordinates for structures reported in this study have been deposited at the Cambridge Crystallographic Data Centre (CCDC), under deposition numbers 1938732 (**5-3S**) and 1938733 (**5-3R**). These data can be obtained free of charge from The Cambridge Crystallographic Data Centre via www.ccdc.cam.ac.uk/data_request/cif. Crystallographic data of the polymers are available from Daniel Van Opdenbosch (daniel.van-opdenbosch@tum.de) at reasonable request.

Received: 8 August 2019; Accepted: 16 December 2019;
Published online: 24 January 2020

References

1. Smith, J. K. & Hounshell, D. A. Wallace H. Carothers and fundamental research at Du Pont. *Science* **229**, 436–442 (1985).
2. Deopura, B. L. ed. *Polyesters and Polyamides* (Woodhead Pub. in association with the Textile Institute, Cambridge, England, Boca Raton, FL, 2008).
3. Schlack P. Verfahren zur Herstellung verformbarer hochmolekularer Polyamide, IG Farbenindustrie AG, DE748253TA (1938).
4. Buntara, T. et al. Caprolactam from renewable resources: catalytic conversion of 5-hydroxymethylfurfural into caprolactone. *Angew. Chem. Int. Ed.* **50**, 7083–7087 (2011).
5. Wedde, S. et al. An alternative approach towards poly-ε-caprolactone through a chemoenzymatic synthesis. Combined hydrogenation, bio-oxidations and polymerization without the isolation of intermediates. *Green. Chem.* **19**, 1286–1290 (2017).
6. Winnacker, M. & Rieger, B. Recent progress in sustainable polymers obtained from cyclic terpenes: synthesis, properties, and application potential. *ChemSusChem* **8**, 2455–2471 (2015).
7. Winnacker, M. & Rieger, B. Biobased polyamides: recent advances in basic and applied research. *Macromol. Rapid Commun.* **37**, 1391–1413 (2016).
8. Meier, M. A. R. Plant-oil-based polyamides and polyurethanes. Toward sustainable nitrogen-containing thermoplastic materials. *Macromol. Rapid Commun.* **40**, 1800524–1800624 (2019).
9. Peña Carrodeguas, L., Martín, C. & Kleij, A. W. Semiaromatic polyesters derived from renewable terpene oxides with high glass transitions. *Macromolecules* **50**, 5337–5345 (2017).
10. Kühlborn, J. et al. Examples of xylochemistry: colorants and polymers. *Green Chem.* **19**, 3780–3786 (2017).
11. Hauenstein, O., Reiter, M., Agarwal, S., Rieger, B. & Greiner, A. Bio-based polycarbonate from limonene oxide and CO2 with high molecular weight, excellent thermal resistance, hardness and transparency. *Green Chem.* **18**, 760–770 (2016).
12. Biermann et al. New syntheses with oils and fats as renewable raw materials for the chemical industry. *Angew. Chem. Int. Ed.* **39**, 2206–2224 (2000).
13. Bolton, J. M., Hillmyer, M. A. & Hoye, T. R. Sustainable thermoplastic elastomers from terpene-derived monomers. *ACS Macro Lett.* **3**, 717–720 (2014).
14. Kristufek, S. L., Wacker, K. T., Tsao, Y.-Y. T., Su, L. & Wooley, K. L. Monomer design strategies to create natural product-based polymer materials. *Nat. Prod. Rep.* **34**, 433–459 (2017).
15. Jasinska, L. et al. Novel, fully biobased semicrystalline polyamides. *Macromolecules* **44**, 3458–3466 (2011).
16. Mülhaupt, R. Green polymer chemistry and bio-based plastics: dreams and reality. *Macromol. Chem. Phys.* **214**, 159–174 (2013).
17. Nguyen, H. T. H., Qi, P., Rostagno, M., Feteha, A. & Miller, S. A. The quest for high glass transition temperature bioplastics. *J. Mater. Chem. A* **6**, 9298–9331 (2018).
18. van Velthoven, J. L. J., Gootjes, L., Noordover, B. A. J. & Meuldijk, J. Bio-based, amorphous polyamides with tunable thermal properties. *Eur. Polym. J.* **66**, 57–66 (2015).
19. Brehmer, B. In *Bio-Based Plastics* (ed. Kabasci, S.) 275–293 (John Wiley & Sons Ltd, Chichester, UK, 2013).
20. Gscheidmeier M. & Fleig H. *Ullmann's Encyclopedia of Industrial Chemistry* (Wiley-VCH Verlag GmbH & Co. KGaA, Weinheim, Germany, 2000).
21. Zhu, J., Zhang, X. & Pan, X. *Sustainable Production of Fuels, Chemicals, and Fibers from Forest Biomass* (American Chemical Society, Washington, DC, 2011).
22. Byrne, C. M., Allen, S. D., Lobkovsky, E. B. & Coates, G. W. Alternating copolymerization of limonene oxide and carbon dioxide. *J. Am. Chem. Soc.* **126**, 11404–11405 (2004).
23. Thomsett, M. R., Moore, J. C., Buchard, A., Stockman, R. A. & Howdle, S. M. New renewably-sourced polyesters from limonene-derived monomers. *Green Chem.* **21**, 149–156 (2019).

24. Roth, S., Funk, I., Hofer, M. & Sieber, V. Chemoenzymatic synthesis of a novel borneol-based polyester. *ChemSusChem* **10**, 3574–3580 (2017).
25. Sanford, M. J., Peña Carrodeguas, L., van Zee, N. J., Kleij, A. W. & Coates, G. W. Alternating copolymerization of propylene oxide and cyclohexene oxide with tricyclic anhydrides. Access to partially renewable aliphatic polyesters with high glass transition temperatures. *Macromolecules* **49**, 6394–6400 (2016).
26. Schlaad, H. ed. *Bio-synthetic Polymer Conjugates* (Springer Berlin Heidelberg, Berlin, Heidelberg, 2013).
27. van Zee, N. J. & Coates, G. W. Alternating copolymerization of propylene oxide with biorenewable terpene-based cyclic anhydrides: a sustainable route to aliphatic polyesters with high glass transition temperatures. *Angew. Chem. Int. Ed.* **54**, 2665–2668 (2015).
28. Wilbon, P. A., Chu, F. & Tang, C. Progress in renewable polymers from natural terpenes, terpenoids, and rosin. *Macromol. Rapid Commun.* **34**, 8–37 (2013).
29. Zhang, D., Hillmyer, M. A. & Tolman, W. B. Catalytic polymerization of a cyclic ester derived from a “cool” natural precursor. *Biomacromolecules* **6**, 2091–2095 (2005).
30. Quilter, H. C., Hutchby, M., Davidson, M. G. & Jones, M. D. Polymerisation of a terpene-derived lactone. A bio-based alternative to ε-caprolactone. *Polym. Chem.* **8**, 833–837 (2017).
31. Miyaji, H., Satoh, K. & Kamigaito, M. Bio-based polyketones by selective ring-opening radical polymerization of α-pinene-derived pinocarvone. *Angew. Chem. Int. Ed.* **55**, 1372–1376 (2016).
32. Sainz, M. F. et al. A facile and green route to terpene derived acrylate and methacrylate monomers and simple free radical polymerisation to yield new renewable polymers and coatings. *Polym. Chem.* **7**, 2882–2887 (2016).
33. Firdaus, M. & Meier, M. A. R. Renewable polyamides and polyurethanes derived from limonene. *Green. Chem.* **15**, 370–380 (2013).
34. Hauenstein, O., Agarwal, S. & Greiner, A. Bio-based polycarbonate as synthetic toolbox. *Nat. Commun.* **7**, https://doi.org/10.1038/ncomms11862 (2016).
35. Parrino, F. et al. Polymers of limonene oxide and carbon dioxide: polycarbonates of the solar economy. *ACS Omega* **3**, 4884–4890 (2018).
36. Roberts, W. J. & Day, A. R. A study of the polymerization of α- and β-pinene with Friedel-Crafts type catalysts. *J. Am. Chem. Soc.* **72**, 1226–1230 (1950).
37. Robert, C., de Montigny, F. & Thomas, C. M. Tandem synthesis of alternating polyesters from renewable resources. *Nat. Commun.* **2**, https://doi.org/10.1038/ncomms1596 (2011).
38. Hall, H. K. Synthesis and polymerization of 3-azabicyclo-[4.3.1]decan-4-one and 7,7-dimethyl-2-azabicyclo[4.1.1]octan-3-one. *J. Org. Chem.* **28**, 3213–3214 (1963).
39. Winnacker, M., Sag, J., Tischner, A. & Rieger, B. Sustainable, stereoregular, and optically active polyamides via cationic polymerization of epsi lon-lactams derived from the terpene beta-pinene. *Macromol. Rapid Commun.* 38, https://doi.org/10.1002/marc.201600787 (2017).
40. Winnacker, M. et al. Polyamide/PEG blends as biocompatible biomaterials for the convenient regulation of cell adhesion and growth. *Macromol. Rapid Commun.* **40**, e1900091 (2019).
41. Winnacker, M., Vagin, S., Auer, V. & Rieger, B. Synthesis of novel sustainable oligoamides via ring-opening polymerization of lactams based on (−)-menthone. *Macromol. Chem. Phys.* **215**, 1654–1660 (2014).
42. Winnacker, M., Neumeier, M., Zhang, X., Papadakis, C. M. & Rieger, B. Sustainable chiral polyamides with high melting temperature via enhanced anionic polymerization of a menthone-derived lactam. *Macromol. Rapid Commun.* **37**, 851–857 (2016).
43. Stockmann, P. N. et al. New bio-polyamides from terpenes. A-pinene and (+)-3-carene as valuable resources for lactam production. *Macromol. Rapid Commun.* **40**, e1800903 (2019).
44. Grafflin, M. W. In *System of Nomenclature for Terpene Hydrocarbons* 1–11 (American Chemical Society, 1955).
45. Brown, H. C. & Suzuki, A. Hydroboration of terpenes. IV. Hydroboration of (+)-3-carene. Configuration assignments for the 4-caranols and 4-caranones. An unusual stability of 4-isocaranone with a cis relationship of the methyl and gem -dimethyl groups. *J. Am. Chem. Soc.* **89**, 1933–1941 (1967).
46. Lochyński, S., Kułdo, J., Frąckowiak, B., Holband, J. & Wójcik, G. Stereochemistry of terpene derivatives. Part 2. Synth. N. chiral amino acids potential neuroactivity. *Tetrahedron Asymmetry* **11**, 1295–1302 (2000).
47. Ranganathan, S., Gärtner, T., Wiemann, L. O. & Sieber, V. A one pot reaction cascade of in situ hydrogen peroxide production and lipase mediated in situ production of peracids for the epoxidation of monoterpenes. *J. Mol. Catal. B Enzym* **114**, 72–76 (2015).
48. Ścianowski, J. & Wełniak, M. Syntheses of the optically active terpene hydroxyphenylselenides. *Phosphorus Sulfur Silicon Relat. Elem.* **184**, 1440–1447 (2009).
49. Ranganathan, S., Zeitlhofer, S. & Sieber, V. Development of a lipase-mediated epoxidation process for monoterpenes in choline chloride-based deep eutectic solvents. *Green Chem.* **19**, 2576–2586 (2017).
50. Settine, R. L. & McDaniel, C. Rearrangement of 3-carene oxide. *J. Org. Chem.* **32**, 2910–2912 (1967).
51. Lamb, J. R., Jung, Y. & Coates, G. W. Meinwald-type rearrangement of monosubstituted epoxides to methyl ketones using an [Al porphyrin] + [Co (CO) 4] − catalyst. *Org. Chem. Front.* **2**, 346–349 (2015).
52. Reiter, M., Vagin, S., Kronast, A., Jandl, C. & Rieger, B. A Lewis acid β-diiminato-zinc-complex as all-rounder for co- and terpolymerisation of various epoxides with carbon dioxide. *Chem. Sci.*, https://doi.org/10.1039/c6sc04477h (2017).
53. Kulasegaram, S. & Kulawiec, R. J. On the mechanism of the palladium(0)-catalyzed isomerization of epoxides to carbonyl compounds. *Tetrahedron* **54**, 1361–1374 (1998).
54. Karamé, I., Tommasino, M. L. & Lemaire, M. Iridium-catalyzed alternative of the Meinwald rearrangement. *Tetrahedron Lett.* **44**, 7687–7689 (2003).
55. Gudla, V. & Balamurugan, R. AuCl3/AgSbF6-catalyzed rapid epoxide to carbonyl rearrangement. *Tetrahedron Lett.* **53**, 5243–5247 (2012).
56. Umeda, R. et al. Rhenium complex-catalyzed Meinwald rearrangement reactions of oxiranes. *Tetrahedron Lett.* **58**, 2393–2395 (2017).
57. Grigg, R. & Shelton, G. Thermal and catalysed rearrangement of olefinic epoxides. *J. Chem. Soc. D* **20**, 1247–1248 (1971).
58. Fraile, J. M., Mayoral, J. A. & Salvatella, L. Theoretical study on the BF3-catalyzed Meinwald rearrangement reaction. *J. Org. Chem.* **79**, 5993–5999 (2014).
59. Jamalian, A., Rathman, B., Borosky, G. L. & Laali, K. K. Catalytic, regioselective, and green methods for rearrangement of 1,2-diaryl epoxides to carbonyl compounds employing metallic triflates, Brønsted-acidic ionic liquids (ILs), and IL/microwave; experimental and computational substituent effect study on aryl versus hydrogen migration. *Appl. Catal. A* **486**, 1–11 (2014).
60. Paquette, L. A., Ross, R. J. & Shi, Y. J. Regioselective routes to nucleophilic optically active 2- and 3-carene systems. *J. Org. Chem.* **55**, 1589–1598 (1990).
61. Choi, H., Choe, E. K., Yang, E. K., Jang, S. & Park, C. R. Characterization of synthetic polyamides by MALDI-TOF mass spectrometry. *Bull. Korean Chem. Soc.* **28**, 2354–2358 (2007).
62. Dubois, P., Coulembier, O. & Raquez, J.-M. *Handbook of Ring-Opening Polymerization* (Wiley, 2009).
63. Matyjaszewski K., Möller M., Russo, S. & Casazza, E. In *Polymer Science: A Comprehensive Reference* 331–396 (2012).
64. Hall, H. K. Structural effects on the polymerization of lactams. *J. Am. Chem. Soc.* **80**, 6404–6409 (1958).
65. Hall, H. K. Synthesis and polymerization of atom-bridged bicyclic lactams. *J. Am. Chem. Soc.* **82**, 1209–1215 (1960).
66. Hall, H. K. Polymerization and ring strain in bridged bicyclic compounds. *J. Am. Chem. Soc.* **80**, 6412–6420 (1958).
67. Hall, H. Synthesis and polymerizability of atom-bridged bicyclic monomers. *Polymers* **4**, 1674–1686 (2012).
68. Temin, S. C. Effect of structure on the glass temperature of polyamides. *J. Appl. Polym. Sci.* **9**, 471–481 (1965).
69. Budín, J., Brožek, J. & Roda, J. Polymerization of lactams, anionic copolymerization of ε-caprolactam with ω-laurolactam. *Polymer* **47**, 140–147 (2006).
70. Astbury, W. T. The hydrogen bond. The hydrogen bond in protein structure. *Trans. Faraday Soc.* **36**, 871–880 (1940).
71. Bragg, W. L., Kendrew, J. C. & Perutz, M. F. Polypeptide chain configurations in crystalline proteins. *Proc. R. Soc. Lond. A* **203**, 321–357 (1950).

Acknowledgements

We would like to thank the Ministerium für Ernährung und Landwirtschaft (BMEL) and the Fachagentur Nachwachsende Rohstoffe e. V. (FNR) for generous funding (FKZ 22015916).

Author contributions

P.N.S., M. Winnacker, H.S., and V.S. conceived the work. P.N.S., D.L.P., M.H., S.L., J.R., M. Woelbling, and C.F. performed the synthetic experiments and characterization. X-ray experiments, structure determinations, and related manuscript/supplementary sections were conducted by A.P. (monomers), D.V.O. (polymers), and C.Z. (polymers). P.N.S. wrote the manuscript and supplementary except X-ray sections by A.P. and D.V.O. C.Z. and V.S. revised the manuscript.

Competing interests

The authors declare no competing interests.

Additional information

Supplementary information is available for this paper at https://doi.org/10.1038/s41467-020-14361-6.

Correspondence and requests for materials should be addressed to V.S.

Peer review information *Nature Communications* thanks the anonymous reviewer(s) for their contribution to the peer review of this work. Peer reviewer reports are available.

Reprints and permission information is available at http://www.nature.com/reprints

Publisher's note Springer Nature remains neutral with regard to jurisdictional claims in published maps and institutional affiliations.

Open Access This article is licensed under a Creative Commons Attribution 4.0 International License, which permits use, sharing, adaptation, distribution and reproduction in any medium or format, as long as you give appropriate credit to the original author(s) and the source, provide a link to the Creative Commons license, and indicate if changes were made. The images or other third party material in this article are included in the article's Creative Commons license, unless indicated otherwise in a credit line to the material. If material is not included in the article's Creative Commons license and your intended use is not permitted by statutory regulation or exceeds the permitted use, you will need to obtain permission directly from the copyright holder. To view a copy of this license, visit http://creativecommons.org/licenses/by/4.0/.

© The Author(s) 2020

2.5 Limonene, α-pinene, and (+)-3-carene as precursor for diol monomers

2.5.1 Oxidative cleavage of limonene, α-pinene, and (+)-3-carene

The cleavage of the double bond of limonene (**1**), α-pinene (**2**), and (+)-3-carene (**3**) has been extensively reported in literature so far (Figure 2.20).[137–142] The three dominating strategies are: (I) the conversion of the double bond into a diol (or epoxide) that is then treated with sodium periodate, (II) the direct reaction of the olefin with catalytic OsO_4 and *in-situ* regeneration of the catalyst, and (III) ozonolysis. As OsO_4 is very toxic[143] and ozonolysis requires a special set-up, the periodate cleavage was the chosen method. Racemic mixtures of limonene oxide (**5**) and α-pinene oxide (**6**) were purchased (synthesis grade) and used without further purification. (+)-3-carane oxide (**7**) was prepared with diluted peracetic acid as described in Section 2.4B. The epoxides **5** and **7** were cleaved oxidatively in a mixture of MeCN and H_2O with one equivalent of $NaIO_4$ at room temperature (Figure 18). The ketoaldehydes **8** and **9** were purified by distillation and yields were 50%-70%. However, GCMS and NMR analysis did not reveal side reactions to a considerable extent; therefore, the relatively low crude- and isolated yields might have been caused by the unoptimized work-up conditions. The reaction was observed to be rather slow, as three days of reaction time did not lead to a full conversion (51% for epoxide (**7**)). If 1.0 % of HCl was added, the reaction time decreased, and 70% conversion were observed within five hours. However, another addition of 1% HCl was required to complete the reaction, as the reaction rate dropped again at about 80%. This finding indicates that the conversion of the epoxide to a vicinal diol (**vic-diol**) is the rate-defining first step of the reaction, and small amounts of the dihydroxy-species **vic-diol-5** and **vic-ciol-7** were identified by GCMS as intermediate.

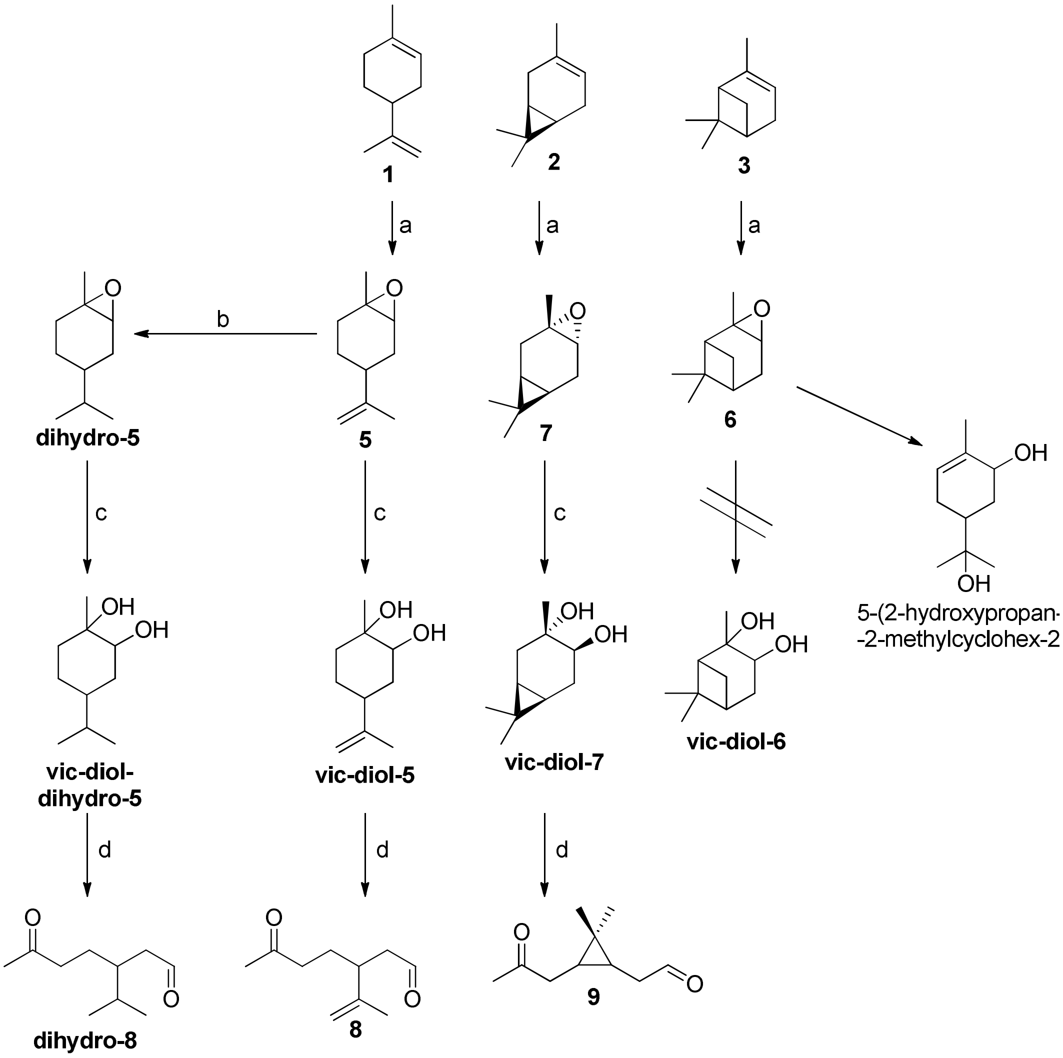

Figure 2.20 Synthesis of ketoaldehydes **8**, **dihydro-8** and **9** starting from the corresponding epoxides. (a) = epoxidation; (b) hydrogenation; (c) epoxide opening to the corresponding diol; (d) oxidative C-C bond cleavage with $NaIO_4$.

The pinene-based epoxide **6** could not be converted to the corresponding ketoaldehyde. The reaction turned out to be very unselective, and a mixture of various rearrangement products, which were then oxidized by $NaIO_4$, was obtained. The most commonly formed compound was 5-(2-hydroxypropan-2-yl)-2-methylcyclohex-2-enol (Figure 2.20), and a control reaction showed that even stirring of **6** in water at 40 °C led to this rearrangement.

Therefore, the synthesis of the required **vic-diol-6** (vicinal diol **6**) was not possible. Other attempts such as the basic opening of the epoxide or the formation of an ethoxy-hydrine and the subsequent oxidative cleavage were unsuccessful. Oxidation with $KMnO_4$ led – according to GCMS – to small amounts of **vic-diol-6**, the isolation failed.

Another observation was the significant difference in reaction rate for the *cis*- and *trans*-epoxide diastereomers (Figure 2.21). While the ratio is 1.5:1.0 at the beginning of the conversion of **5** to **8**, after 2.5 h the ratio of the remaining diastereoisomers is 8:1. More elaborate reaction conditions might lead to an almost exclusive conversion of only one diastereomer. This would lead to an increased isotacticity of the formed polymers.

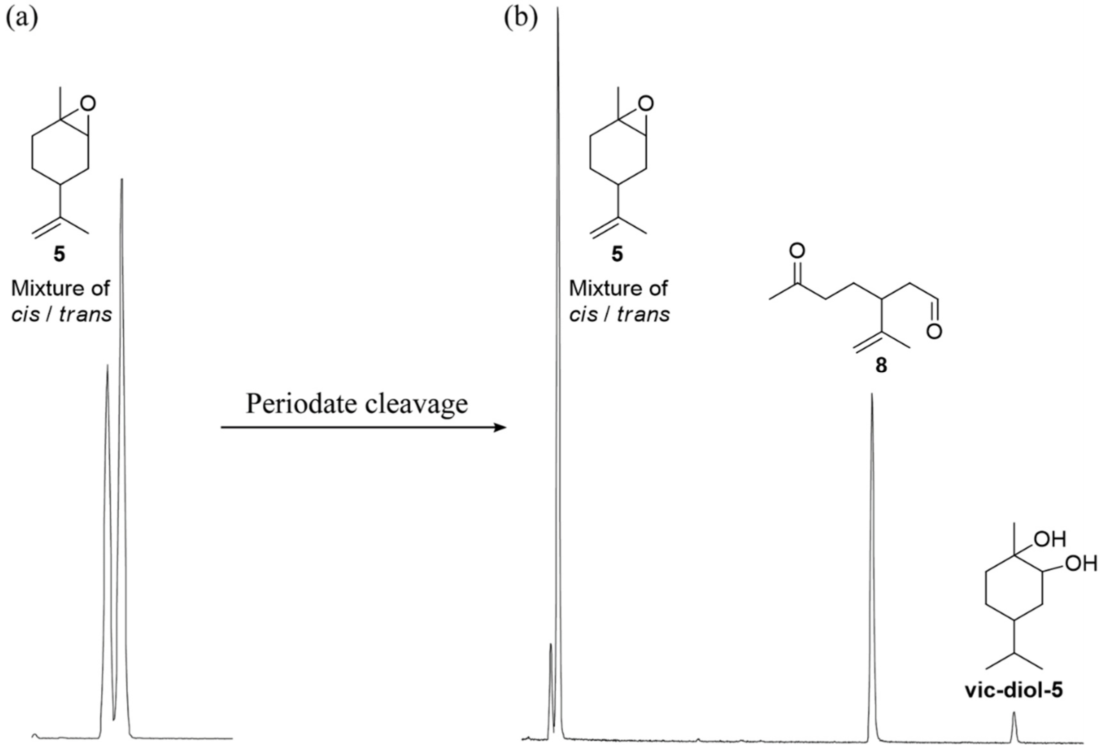

Figure 2.21 GCMS chromatogram displaying the kinetic resolution of the *cis*/*trans* mixture of **5** by periodate cleavage.

During the reaction, $NaIO_4$ was reduced to $NaIO_3$ which precipitated in the reaction mixture and was easily separated by filtration. The isolated $NaIO_3$ was dried and was 70%-80% of the initially used amount. Increasing the amount of MeCN after the reaction might even lead to a full isolation of $NaIO_3$. As the industrial synthesis of the periodate is done by electrochemical oxidation of the iodate, this is a facile way to regenerate the redox equivalent.

The terminal double bond of **5** and **8** was hydrogenated to the corresponding *iso*-propane to investigate differences in polymerization behavior of the olefinic and the purely aliphatic compound (Figure 2.20, Scheme 2.5). PtO_2 (0.1%) and hydrogen at atmospheric pressure in THF was sufficient for a complete reduction within 12 h to give **dihydro-5** and **dihydro-8** in good yields. If MeOH was used as a solvent, the double bond was also successfully converted, but the formation of an di-methoxy acetal was observed by GCMS.

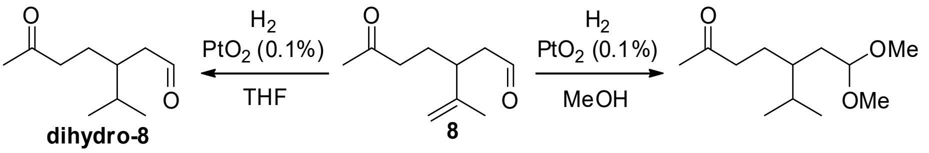

Scheme 2.5. Hydrogenation of the double bond of **8** in MeOH (acetal formation) or THF.

As a first attempt, a Meerwein-Ponndorf-Verley reaction[144] was used to reduce the ketoaldehydes to the corresponding alcohol as the catalyst and the redox equivalent – $Al(iOPr)_3$

and *iso*-propanol, respectively – are cheap, easy to handle and environmentally benign (Scheme 9). The aldehyde was fully converted to give alcohol **10**, but the carbonyl group was unreactive.

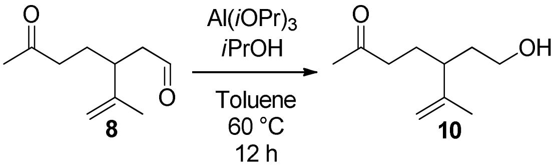

Scheme 2.6 Meerwein-Ponndorf-Verley reaction for the selective reduction of aldehyde **8**.

While this would be an useful way for a selective alcohol formation and the subsequent synthesis of hydroxy-amines for poly(ester amides), another method was required for diol synthesis. Although other variations of the Meerwein-Ponndorf-Verley reaction with stronger reducing agents than *iso*-propanol exist (for example, nitrobenzyaldehyde in Section 2.4B), the atom economy would drastically be reduced. Therefore, $NaBH_4$ was applied as an inorganic hydride donor following an adjusted protocol (Scheme 2.7).[145,146]

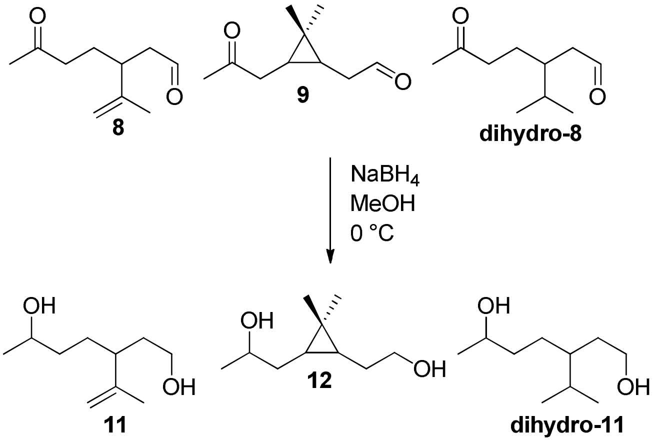

Scheme 2.7 Reduction of the limonene (**1**)-based ketoaldehydes **8**, dihydro **8**, and the (+)-3-carene (**2**)-based **9** to the corresponding diols.

The reactions were carried out in MeOH mixture at 0 °C. However – although the reaction seemed very selective in GCMS, NMR and thin-layer chromatography (TLC) – the isolated yields of the diols **11**,**12** and **dihydro-10** after column chromatography were only about 60%.

2.5.2 Initial polymerizations of 3-(prop-1-en-2-yl)heptane-1,6-diol (11)

To verify the polymerizability of the linear terpene diols in polycondensation reactions, the limonene-based candidate was polymerized with adipic acid methyl ester (**14**). The compatibility with an aromatic monomer was tested with terephthalic acid ethyl ester (**15**).

An enzymatic approach was used for the reaction with the aliphatic monomer **14.** Cal-B – which was already used for the epoxidation of (+)-3-carene (**2**) – was the enzyme used in a solvent-free two-stage reaction. In the first stage, the temperature was 50 °C at 50 mBar for 48 h. In the second stage, the temperature was 70 °C at 25 mBar for another 48 h. The resulting viscous, slightly yellow oil was analyzed by DSC; and no glass transition could be detected within the examined temperature range (-30 °C – 400 °C). The NMR analysis verified the reaction of **11** with **14** (Figure 2.22).

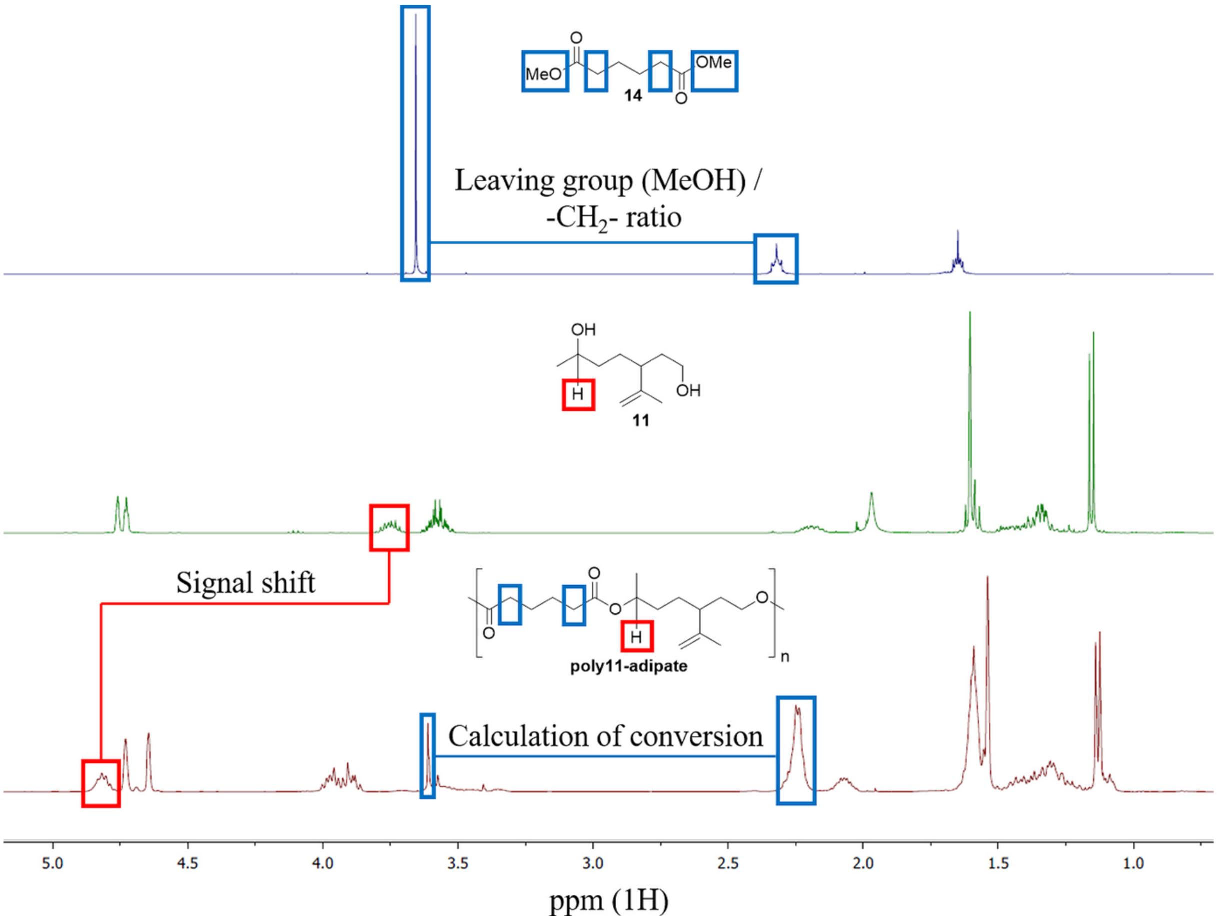

Figure 2.22 NMR comparison of the monomers **11** and **14** with **poly11-adipate**.

The methoxy ester was cleaved and MeOH was removed from the reaction mixture, which can be seen by the decreasing signal intensity at 3.66 ppm (*Me*O-, blue and red spectra). The conversion was calculated to be about 90% by comparison of the signal intensities of -CH_2-COOR and the methoxy-ester from the residual monomer **14** (red spectra, blue boxes). The conversion of the proton of Me-C*H*-OH (monomer alcohol) to Me-CH-O-CR=O (polyester) can be seen by the shift from 3.75 ppm to 4.79 ppm (green and red spectra, red boxes). Finally, the signal broadening also indicates a successful reaction to poly(1-methyl-4-iso-propenyl adipate) (**poly11-adipate**).

For the polymerization of **11** with **15**, Sn(OAc)$_2$ was used as catalyst in a solvent-free three-stage approach. In the first stage, the temperature was 180 °C for 4.5 h at atmospheric pressure. The sublimation of small amounts of **15** were detected, affecting the stoichiometry and resulting in a minor excess of diol **11**. In the second stage, the pressure was lowered to 2.5 mBar at

200 °C for 2.5 h. The viscosity of the mixture increased, and residual diol was evaporated from the mixture. Finally, the temperature was increased to 220 °C and the pressure was lowered to 1.4 mBar until the evaporation of excess diol was complete (1.5 h). The obtained poly(1-methyl-4-iso-propenyl terephthalate) (**poly11-terephthalate**) was investigated with DSC, revealing a T_g of 24 °C. The polyester decomposed at about 370 °C (Figure 2.23).

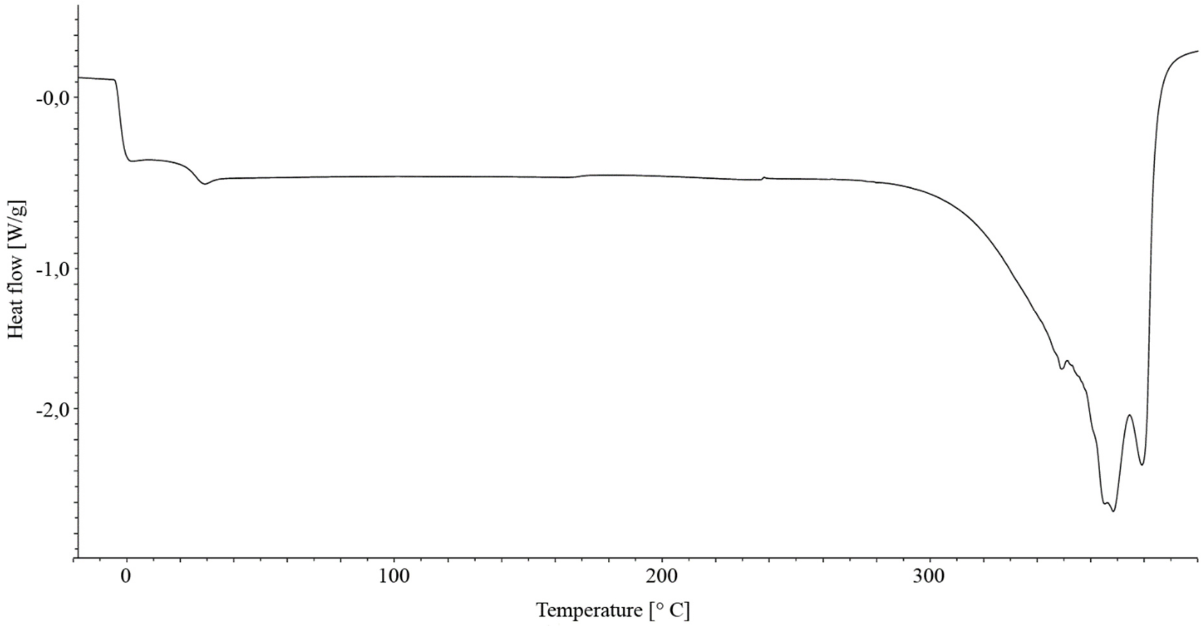

Figure 2.23 DSC of **poly11-terephthalate** (second run).

NMR analysis showed that 8.3% of **11** and 3.8% of **15** remained in the polymerization mixture. Again, signal broadening and a shift of Me-C*H*-OH (monomer alcohol) to 5.16 ppm was detected (Figure 2.24). As the reaction temperature and the low pressure led to partially evaporation of the monomers, a conversion could not be calculated by NMR.

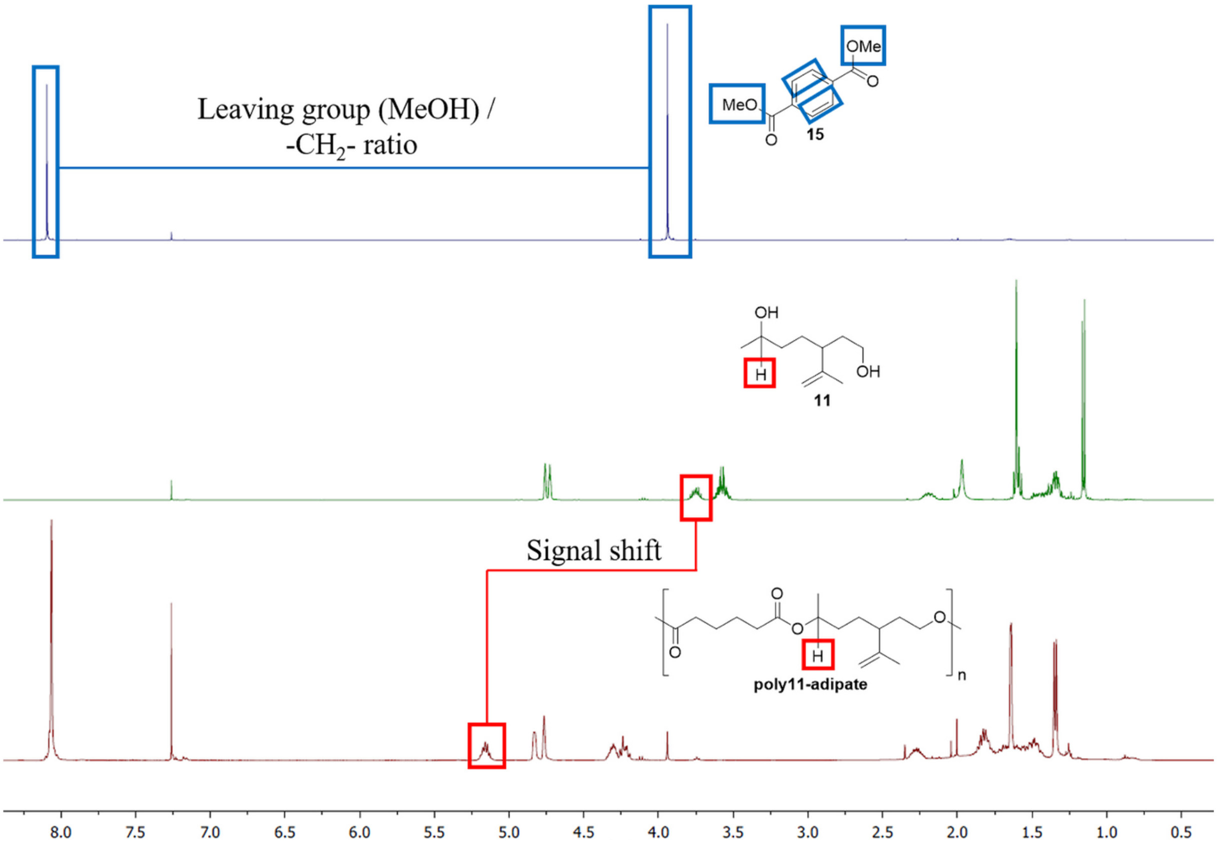

Figure 2.24 NMR comparison of the monomers **11** and **15** with **poly11-terephthalate**.

3. Discussion

3.1 Isoprene as precursor for bio-fuels

As fuels are the highest end volume application of fossil oil, many approaches to use bio-feedstocks as resources for bio-fuels have been undertaken. Different types and generations of bio-fuels have been established within the last decades (Table 3.1), and are nowadays produced in commercial amounts.

Table 3.1: The three bio-fuel generations and some of their characteristics.[147]

Characteristic	**Bio-fuels**		
	1st generation	2nd generation	3rd generation
Feedstock	Obtained from food crops: corn, wheat, sugar-cane, soybeans, animal fat, cooking oil	Obtained from non-food crops: Agricultural wastes, wood, municipal wastes, waste vegetable oil	Generated from algae and other microbes: Algae, sea weeds, cyanobacteria
Manufacturing method	Fermentation, trans-esterification, anaerobic fermentation	Enzymatic hydrolysis, thermo-chemical processes followed by synthesis	Biochemical and or thermochemical methods
Bio-fuels	Alcohols (ethanol, propanol, butanol), diesel	Cellulosic ethanol, methanol, Fischer-Tropsch diesel, dimethylfuran	Ethanol, Hydrogen
Energy density	Up to 48 MJ/kg	Up to 38 MJ/kg	Up to 123 MJ/kg
Greenhouse gas CO_2 (kg/kg)	Up to 3.4	Up to 2.85	Up to 3.4

As bio-fuels often suffer from production costs, varying quality or residual bio-impurities, the fermentation of olefins and subsequent oligomerization and hydrogenation to gain linear hydrocarbons as high-quality fuels seems reasonable.[148] The potential of one of these olefins, isoprene, was evaluated in a literature review (Section 2.1). The production of bio-based isoprene, especially from (poly-)saccharides, has been investigated thoroughly within the last decade, as isoprene is one of the most used monomers in the rubber industry.[3,10,148–155] In general, isoprene is accessible from many kinds of biomass and could be processed as a 1st, 2nd or 3rd generation bio-fuel. These studies mention the additional potential of isoprene as precursor for bio-fuels regularly, but there has been little research on the next step in this premise: the controlled linear oligomerization of isoprene to C10-C20 hydrocarbons. Less than 60 adequate papers or patents focusing on linear isoprene oligomerization were published since the 1950s, most of them without any context to fuels. Only within the last years, due to the improvements in bio-based isoprene production, several studies focus on isoprene oligomerization as a new route to bio-based fuels; however, the research output regarding selective and linear isoprene oligomerization remains low. This might change in the future as the price of bio-based isoprene will decrease. In addition, linear isoprene dimers and trimers possess properties that make them very suitable as fuel such as a high boiling point and an energy density of 47 MJ/kg (Section 2.1, Table 1). These characteristics are well in the range of other bio- or fossil-fuels.[147] In contrast to many other 1st, 2th or 3th generation bio-fuels, these oligomers do not contain heteroatoms and are structurally closely related to fossil-based fuel, which should guarantee an effortless integration in advanced internal combustion engine technology. The methyl group side chains, causing a decreased pour point, might enable low-temperature tank storage without the loss of flow characteristics. Another important aspect differing from other fermentation bio-fuel precursors is the facile downstream process, as isoprene is neither high-boiling nor water-soluble.

From a chemists' perspective, the major challenge is the linear conversion of isoprene to C10-C20 oligomers that could directly be used as a fossil-oil fuel replacement. Most methods from the 1950s until today use (transition) metal liquid phase catalysis for the oligomerization of isoprene. Even though this is similar to butadiene oligomerization, the significant difference is the unsymmetrical substitution pattern of the double bonds, leading to a decrease of selectivity and a high tendency for cyclization. As a result, complex mixtures of isoprene oligomers are usually obtained, comprising linear and cyclic structures of varying molecular weights, sometimes containing aromatic units. Methods with a high selectivity towards linear di- or trimers usually involve Pd accompanied by air sensitive and rather expensive phosphine ligands, which would lead to high fuel prices. Some Ziegler-Natta catalysts with a satisfying selectivity have also been reported, though several additional additives or co-catalysts were required as well. The use of ionic liquids was also mentioned, with outstanding selectivity; however, ionic liquids are industrially still not established due to issues in reusability, product isolation, end-of-life use, among other issues. Despite these draw-backs, if the bio-isoprene gets more affordable and accessible from various feedstocks and if major advances in the establishment of a selective linear dimer- or trimerization process are achieved, isoprene will find a new function as precursor for bio-fuels for modern internal combustion engines.

3.2. Isoprene as precursor for β-lactams, δ-lactams, and δ-lactones

The cycloaddition of isoprene and chlorosulfonylisocyanate (CSI), a reaction that has been reported several times,[113,114,118,119,123] was re-investigated as a one-step method for the formation of a β-lactam and δ-lactams and lactones. 2+2 cycloaddition of alkenes with CSI is the standard procedure for β-lactam synthesis, and conjugated dienes yield δ-structures after intramolecular rearrangement. The synthesis of the β-lactam could easily be reproduced, and the regioselectivity in favor of the methyl-group substituted double bond was 100 %. Aside from polymer science, hydrolysis and chiral separation would yield L-amino acids with terminal double bonds for functionalization – an intriguing precursor for artificial amino acids. The δ-lactam could only be isolated in trace amounts. Instead, a ring-opening followed by hydrolysis and subsequent ring closing gave the δ-lactones (Figure 3.1).

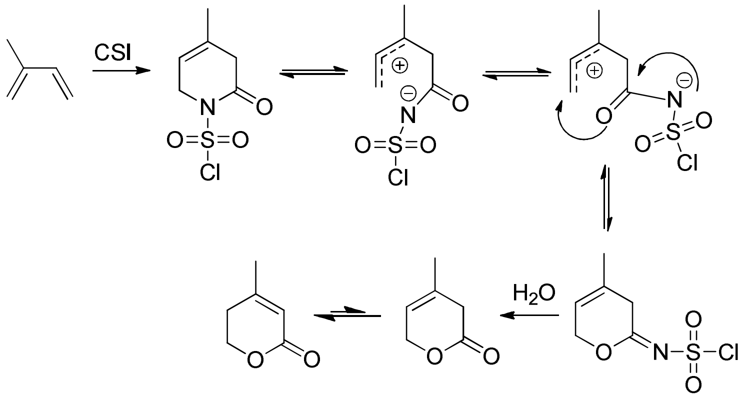

Figure 3.1 Proposed mechanism for the formation of δ-lactones from a chlorosulfonyl-δ-lactam.[119,123]

Application of Cp_2TiCl_2 optimized the yield to about 80 %. These lactones are also accessible from glucose and have been used as monomer (Section 2.2) and were therefore not further investigated. β-lactams are highly reactive and have been polymerized with advanced techniques.[97–99] In this case, simple anionic ring opening polymerization of the lactam was successful. NMR analysis confirmed a PA2-type polyamide. PA2-types are common in nature as proteins, and spidroin, the proteins of spider silk, is famous for its mechanical properties as a fiber. These properties arise from a highly ordered structure consisting of block copolymers of poly(alanine) and glycine enriched domains that are responsible for strength and elasticity, respectively. Modified isoprene β-lactams could be used in a similar way to produce semi-artificial PA2-fibers with tailor-made properties. The obtained polyamide possessed a T_g of almost 100 °C and a T_m of 240 °C, which is above the values of PA6. As mentioned above, the terminal double bond was intact in the side chain (Section 2.2.3). This provides several possibilities for post-polymerization functionalization, and tailor-made derivatives for all kinds of application. In addition, the isoprene-derived β-lactam could also be used for cross-linking in polyamides, polyesters, and polyurethane, enabling the production of thermoplastic elastomers. The terminal olefin could be used as an anchor for Diels-Alder reactions, click-chemistry, metathesis, and others as demonstrated for polylimonene carbonate (Figure 3.2).[156]

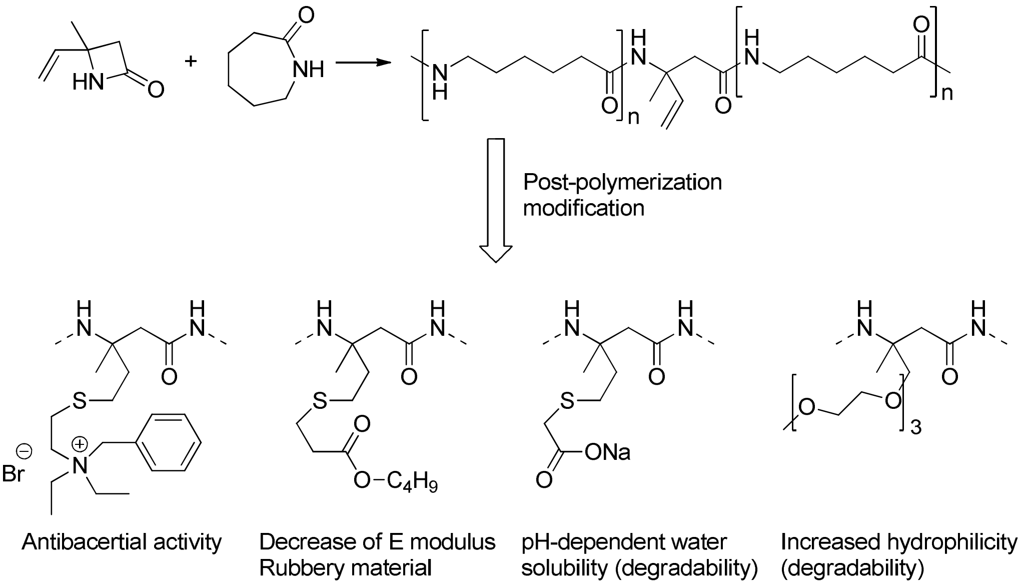
Post-polymerization modification
Antibacertial activity
Decrease of E modulus
Rubbery material
pH-dependent water solubility (degradability)
Increased hydrophilicity (degradability)

Figure 3.2 Co-polymer of isoprene β-lactam and caprolactam, post-polymerization modifications and proposed effects.

Despite these intriguing possibilities, the monomer synthesis needs optimization, and the use of toxic and expensive chlorosulfonyl isocyanate is a considerable economic and ecological drawback. The purification had to be achieved by column chromatography, which is expensive and laborious in production scales. A carefully designed distillation could also lead to satisfying results, but heat-induced uncontrolled polymerizations of the highly reactive β-lactam might occur.

To summarize, the isoprene based β-lactam and polyamides thereof are not sustainable at this point, but the double bond and the PA2-type structure itself are worth exploring in the future.

3.3 Conversion of α-pinene and (+)-3-carene to PA6-type bio-polyamides

The pivotal part of this work deals with the conversion of two bicyclic monoterpenes, α-pinene and (+)-3-carene, into ε-lactams that could be polymerized to PA6-type polymers. Both terpenes are to be chemically interpreted as aliphatic substituted and bridged cyclohexane derivative. Cyclohexane is the most used precursor to produce the most important industrial lactam of polyamides: caprolactam. Terpenoids such as camphor and menthone, naturally possessing a ketone motif, have already been converted to their corresponding lactams by oximation/Beckmann rearrangement or hydroxylamine sulfonic acid.[71] Additionally, α-pinene and (+)-3-carene possess a double bond that can be used as starting point for chemical modification. Thus, the oxidation of the double bond to generate a cyclohexanone derivative compound analogous to caprolactam synthesis was a reasonable approach. The first-generation synthesis was a four-step approach starting with (i) double bond epoxidation by hydroboration, (ii) alcohol oxidation, (iii) conversion to oxime using $HONH_2{\cdot}HCl$ and (iv) Beckmann rearrangement in basic media (Section 2.3) according to a literature protocol by Lochyński.[157] The hydroboration yielded the terpene alcohols in excellent trans-anti-Markovnikov selectivity and the stereoselectivity regarding the methyl group at C3 was 100 %. This is worth mentioning as diastereomeric mixtures eventually would result in atactic polymers, negatively influencing the mechanical properties as demonstrated in polypropylene, which exhibits a T_m of 240 °C in its isotactic configuration and is amorphous in its atactic configuration.[158]

To avoid toxic chromium agents for alcohol oxidation, the Oppenauer oxidation with 3-nitro benzaldehyde as redox equivalent was applied. Though the ketones were accessible by this method, the yield and the atom economy are moderate at best, and other methods using inorganic oxidation agents such as $NaOBr_3/NaSO_3$ or $NaHSO_5$ (Oxone®) might lead to superior results.[159,160] After conversion to the corresponding oximes, the Beckmann rearrangement in basic media was performed. The addition of at least stoichiometrically amounts of tosyl chloride proved crucial for the *in-situ* activation of the oxime. The nitrogen insertion was almost exclusively next to the methyl-group substituted C3. There are many methods for catalytic Beckmann rearrangement, but all of them are in strongly acidic media, causing the bridged bicyclic structures to rearrange.[84] This was particularly seen at the four-membered ring of α-pinene, which was labile under acidic conditions, rearranging to several unidentified species. The three-membered ring of (+)-3-carene showed similar tendencies, with the rearrangement to an isopropylene motif being the most dominant. Direct conversion of the ketones to lactams by application of hydroxyl sulfonic acid gave similar results. In all cases, in the presence of water, hydrolysis of the oxime and subsequent rearrangement to methyl cymene, probably by H_2O-addition-elimination mechanism, was observed. Extraordinarily, strong Lewis acids such as $Zn(OTf)_2$ in dry MeCN have shown some catalytic activity, but a high-yielding, highly active catalytic system is yet to be established. Fortunately, terpene lactams crystallize rather facile, and re-crystallization lead to purities sufficient for aROP. The same set of polymerization issues were observed for the α-pinene lactam as previously reported for the oligomerization of menthone[88] and β-pinene[161].These issues are (i) precipitation of oligomers from the monomer melt and (ii) the undesired cross-linking effects due to side reactions of the four-membered ring. 3R-caranlactam polymerized extremely fast and a hard, transparent polymer block was formed. Investigation by NMR, GPC and DSC revealed two unexpected novelties: The M_n was over 30 kDa, which is three times more as ever reported for terpene-based lactam polyamides, and no T_m was detected. The latter implies an amorphous polymer structure, which was verified with subsequent XRD experiments. In general, the most key intermediate in (industrial) caprolactam synthesis is cyclohexanone, and efforts to improve the monomer synthesis and avoiding expensive and nonecological hydroboration lead to a new reaction sequence: Epoxidation, Meinwald rearrangement to the corresponding ketone, Oximation, Beckmann rearrangement. Although the latter two steps remain unchanged, epoxidation and Meinwald reaction gave way to two diastereomeric ketones (Figure 3.3), eventually resulting in diastereomeric lactams with differing polymerization behavior and polymer properties.

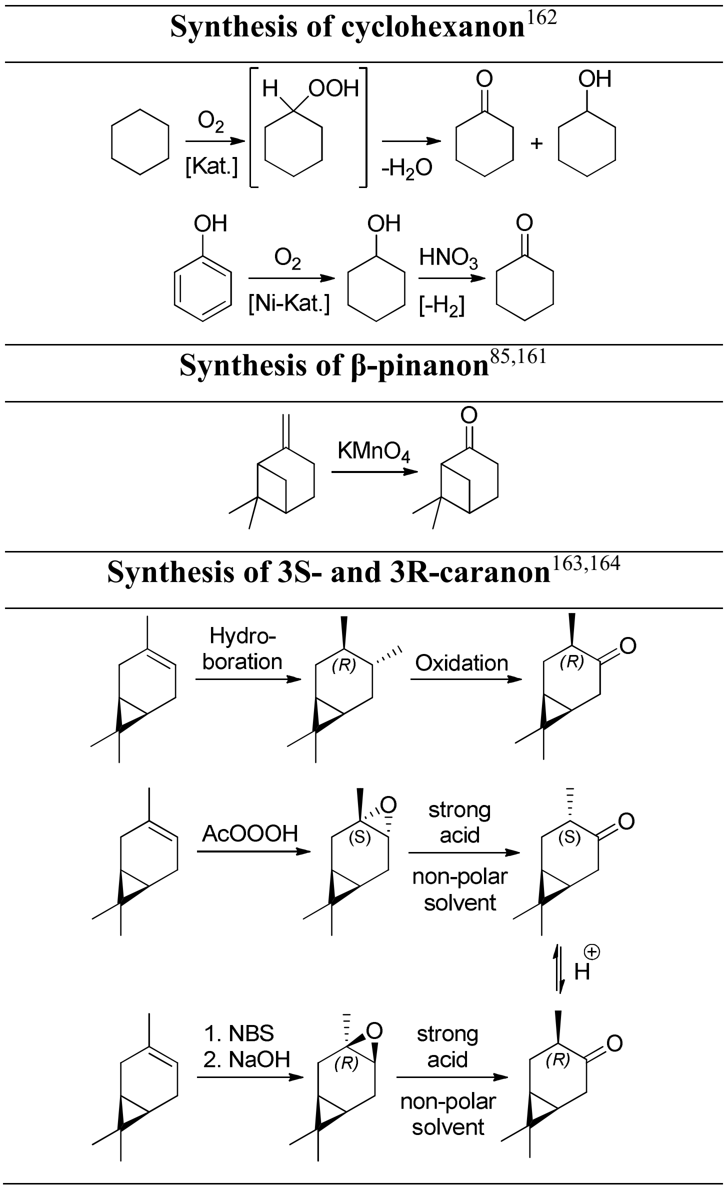
Synthesis of cyclohexanon[162]
O_2
[Kat.]
H OOH
$-H_2O$
O
OH
+
OH
O_2
[Ni-Kat.]
OH
HNO_3
$[-H_2]$
O
Synthesis of β-pinanon[85,161]
$KMnO_4$
O
Synthesis of 3S- and 3R-caranon[163,164]
Hydro-
boration
(R)
Oxidation
(R)
O
AcOOOH
(S)
O
strong
acid
non-polar
solvent
(S)
O
H
1. NBS
2. NaOH
O
(R)
strong
acid
non-polar
solvent
(R)
O

Figure 3.3 Synthesis strategies for ketones that are used as precursors for lactams.

The lactams are methyl group diastereomers at the C3 position, and XRD revealed that this causes the lactams to crystallize in non-identically distorted ring conformations. The stereo-configuration at C3 depends on the epoxidation method: peracetic acid, as a one-step method, attacks the double bond from the sterically more accessible side to form the space-demanding butterfly transition state, and exclusively yields the S-isomer. The R-isomer is formed by conversion with N-bromosuccinimide – also attacking from the sterically less demanding side – to form a bromo hydrine. In strong basic media, the epoxide is formed by the attack of the formed hydroxylate in a S_N2 reaction under the release of a bromide ion and the inversion of the methyl group. The subsequent Meinwald rearrangement in a non-polar solvent and strong acids proceeds under retention of configuration, as the concerted mechanism dominates in non-polar solvents and the ionic transition state is formed to a minor extent due to the absence of the stabilizing effect that a polar solvent would provide. Alternatively, the kinetically favored 3S-caranon can be isomerized in acidic media to the thermodynamically favored 3R-isomer, which eventually gives mixtures of 3R-caranlactam (80 %) and 3S-caranlactam (20 %). Oximation and Beckmann rearrangement were applied as before, and a one-vessel sequence was developed for the synthesis of 3S-caranlactam in mole scale. Both lactams were used for homopolymerization, and the resulting Caramid-R and Caramid-S were analyzed. In both cases, high-performance thermal properties (T_g 110-120 °C, T_m 280 °C for Caramid-S) and M_n surpassing all yet reported data of terpene-lactam based polyamides were detected. The ΔT_g is 60 °C higher compared to PA6, which is a direct result of the rigid ring structure, which causes and a decrease of the rotational degrees of freedom. Thermodynamically, at lower temperatures, the gauche conformation is favored as the energy barrier for gauche/trans transition is increased because of the ring-motif in the main chain. Thus, the unfolding of entropic random coils to form linear chains (trans configuration) that are rotationally active (T_g) and eventually begin to slide (melt-behavior) requires a higher energy input ΔE (equation 3.1) than the linear standard polyamides.

$$\frac{p(gauche)}{p(trans)} = \frac{2}{1}\, exp\left[\frac{\Delta E}{kbT}\right] \qquad (3.1)$$

The three-membered ring and the methyl group stereo-configuration remained fully unchained throughout the polymerization process. Both lactams could be used for copolymerization with caprolactam and laurolactam, increasing the T_g up to 90 °C and decreasing the crystallinity until long-range order is completely suppressed.

The ROP of the lactams was facile and high-yielding, particularly for Caramid-R. The differences in the polymerization behavior can most probably be attributed to the dissimilarities of the bridged ring systems caused by the configuration of the attached methyl group at C3. The reason for Caramid-R to not form long-range ordered, anti-parallel chains stabilized by hydrogen bonding in a similar way to Caramid-S, remains unclear. This kind of crystallization is known from PA6,[165] and was therefore expected of the terpene-based, aliphatic substituted

PA6 derivatives, especially as menthone-based polyamides and β-pinene based polyamides are also semi-crystalline. A more detailed exploration of this surprising finding should include solid state NMR, XRD investigation of various copolyamides of 3S-caranlactam and 3R-caranlactam and, most importantly, the synthesis of similar polyamides from (-)-3-carene and 2-carene to fully understand the stereo- and enantio-effects of the structures at hand. A retro-synthesis of a derivative without methyl-group at C3 might also be supportive to clarify the effects that lead to formation of long-range order and crystallinity (Figure 3.4).

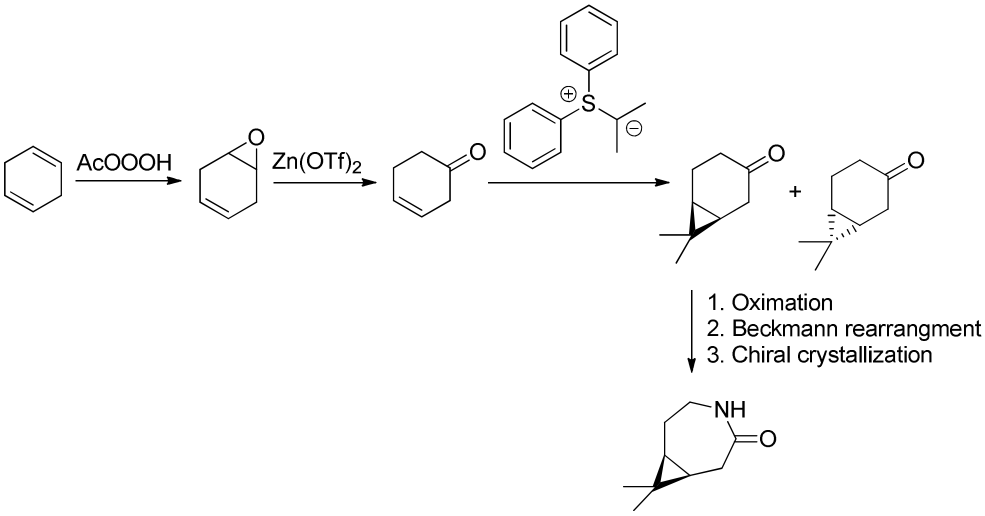

Figure 3.4 Synthesis approach of demethylated caranlactam starting from cyclohexa-1,4-diene under application of thio-ylide chemistry and enantioselective crystallization.

The production of terpene-based polyamides, as outlined in detail in Section 1.12, suffers from complex, hard-to-scale monomer synthesis, insufficient monomer purity unless chromatographic methods are applied, or low activity towards polymerization (Table 3.3). These challenges were overcome in this work by the development of a scalable, straight-forward one-vessel synthesis of monomers with satisfying polymerization properties. Although optimization is mandatory for the entire process, currently the yield of the Meinwald rearrangement and the catalytic Beckmann reaction needs immediate attention. The process yields moderate yields of the lactam in polymerization quality after crystallization. Synthesis in pre-industrial scale is reasonably possible, which has not been reported for a 100 % bio-based lactam yet.

As described above, Caramid-S/R differ from the commercialized PA11 and PA1010 due to the rigid ring containing main chain and the aliphatic substituents (Section 1.6, Section 1.9). Additionally, in the context of polyamides from biomass other than castor oil, Caramid-S and Caramid-R possess some real novelties (Table 3.2) worth further researching.

The utilization of starch, cellulose, xylose, and other biogenic resources results in diacids, diamines, or amino acids, and therefore only AA/BB types or polycondensation AB-types are possible. Mechanically superior cast polyamides are impossible to prepare from these monomers. Polycondensation of FDCA-polyamides is challenging due to decarboxylation and N-methylation,[166] and preparation of pre-polymers with 2,5-chlorofurandicarboxylic acid is required (Avantium/Solvay process).[167,168]

Characteristics	**Monoterpene (lactam precursor)**		
	Limonene[83]	β-pinene[72,85,161]	Menthone[88,89]
Structure	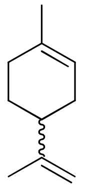	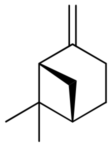	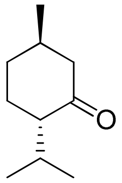
Availability	Waste stream Little alternative applications	Waste stream Little alternative applications	No waste stream Synthesis from myrcene Several alternative applications
Monomer synthesis	Few production steps Chromatographic monomer purification Elaborated reaction equipment	Chromatographic monomer purification Challenging initial olefin oxidation ($KMNO_4$)	Good yield (83%) Few production steps 8-10 times more expensive than other terpenes
Green carbon [%]	83	100	100
Polymer properties	*M*n < 8,0 kDa Exclusively amorphous polyamides *T*g = 42 °C	*M*n = 7,2 kDa Long reaction times Exclusively semi-crystalline, opaque polyamides	*M*n < 3,0 kDa Long reaction times Exclusively semi-crystalline, opaque polyamides
Scalability	Unknown	Unknown	Unknown
Processability	Unknown	Unknown	Unknown

Table 3.1 Terpene-based polyamides and their properties.

These methods usually apply terephthalic acids (TPA) as the additional, fossil-based comonomer. As far as rigid, cyclic structures are concerned, they are generally available from isosorbide or FDCA and contain heteroatoms or are aromatic, respectively. If no stabilizers are used as additives, these structures get oxidized in air after UV-light induced hydroperoxide formation, leading to yellow coloring, degradation, and loss of mechanical stability.[169] Especially for applications that need high transparency, coloring needs to be avoided, and the non-aromatic structures of Caramid-R or the copolyamides of Caramid-S might prove beneficial. Another aspect is the lowered T_g of about 120 °C in comparison to polycarbonates (PC, T_g = 148 °C). The lower working temperature of standard PC is at -40°C.[170] This is exceptionally low for amorphous polymers, and caused by so called secondary transition at -120 °C.[171] As Caramid-R is not brittle at room temperature, it most likely also possesses a secondary transition. If this secondary transition is – similar to the T_g – at a lower temperature compared to PC, this would enable applications at even lower temperatures.

Alternative bio-based polyamides[82,166,172–174]

Biomass	Starch, cellulose, xylose, turpentine
Processing	Enzymatic or chemical hydrolysis, distillation
Monomer precursors	Glucose, fructose, monoterpenes
Monomer types	Diamines, diacids, amino acids, lactams
Monomer examples	FDCA, 1,5-diamino pentane, isosorbide diamine, β-pinene lactam, menthone lactam
Food or feed application	Partially
Alternative applications	Yes
Polymer types	AABB/AB
Polymerization process	Polycondensation, ring-opening polymerization
Main chain structure	Linear non-branched, aromatic, aliphatic substituted, aliphatic cyclo-substituted
Green carbon	Up to 100 %
Status	Laboratory / pre-industrial
Engineering/High-Performance applications expected	Yes

Polymer properties

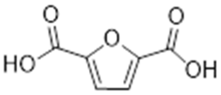	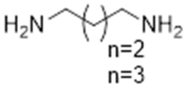	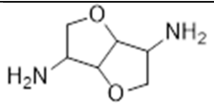
+ diamines + 1,6 diamino hexane Therephthalic acids (TPA)	+ Diacids	+ Sebacic acid + Diacids and diamino butane
M_n < 10 kDa (Standard techniques) Semi-crystalline / amorphous T_m up to 250 °C, T_g up to 110 °C	Example: Diamino pentane PA510: Semi-crystalline T_m = 215 °C T_g = 50 °C	M_n < 5 kDa 0% diamino butane Semi-crystalline T_m = 152 °C
M_n > 10 kDa (Avantium/Solvay-Process) - amorphous T_g up to 136 °C (0% TPA) - Semi-crystalline > 35 % TPA T_m = 336 °C (50% TPA)		M_n > 20 kDa 78% diamino butane Semi-crystalline T_m = 232 °C

Table 3.2 Bio-based polyamides from biomass other than terpenes and Ricinus oil and their properties.

High-mass polyamides from diamino isosorbide can only be formed as copolyamides with other diamines, and the monomer synthesis have low -yields and struggles from the formation of various stereo-isomers. The high amounts of chiral motifs – the methyl group at C3 and the three-membered ring – is unmatched, as well as the isotacticity of 100 %, resulting from the highly stereoselective synthesis and enantiopure starting material. This feature could be exploited in chiral technology, e.g. for chiral stationary phases in HPLC. In addition to the increased chemical and thermal stability compared to the usually applied chiral polysaccharides, this could enhance the established methods of enantioseparation.

3.4 Conversion of (+)-3-carene and limonene to polymerizable diols

Besides the exploration of hydrolytic polymerization of 3S- and 3R-caranlactam, the next steps required for the validation of Caramid-R and Caramid-S in an industrial application context are the processing parameters and the mechanical properties. Tensile and impact testing for E-modulus, elongation at break, impact resistance, etc. as well as melt-flow and water-uptake according to DIN are mandatory for the identification of suitable applications. For cast polyamides, the activation system needs optimization, and the machining process must be developed. To reach a price level that enables commercialization, the monomer synthesis must be optimized and a catalytic method for the Beckmann rearrangement must be developed. If 30 €/kg monomer accompanied by outstanding polymer properties can be achieved, Caramid-S and Caramid-R could well be the first terpene-based polyamides on the market in the future. For the synthesis of bio-based diols from monoterpenes, the double bond of limonene and (+)-3-carene was oxidized by epoxidation and cleaved with periodate (Section 2.5). The obtained ketoaldehydes were then reduced with $NaBH_4$ to diols. The yields were rather low (> 50%) but this is probably due to purification issues. In general, after optimization, this reaction pathway is sustainable as the epoxidation can be performed with H_2O_2 and a lipase, and neither the cleavage with $NaIO_4$ nor the reduction with $NaBH_4$ leads to organic waste. Application of $NaIO_4$ makes the application of toxic and expensive ozone obsolete. In addition, many alternative reduction methods could substitute the borohydride. However, a disadvantage of this process is the loss of stereo-information, leading to mixtures of diastereoisomers and enantiomers. The limonene-derived diol was polymerized with dimethyl adipate by a lipase and with dimethyl terephthalate by a Sn-catalyst (Section 2.5.2). As expected, the T_g of the aliphatic polyester was below -30 °C, whereas the aromatic polyester had a T_g of 24 °C. Again, the terminal double bond in the polymer backbone was maintained. The synthesis of diols from the cyclic monoterpenes limonene and (+)-3-carene was successful. Oxidative cleavage of the double bond by epoxidation and subsequent treatment with $NaIO_4$ led to the corresponding ketoaldehydes. The yields were about 60%, but NMR and GCMS suggest that the relatively low yields are caused by unoptimized work-up protocols, as almost no side-products were observed. The reduction to the diols was carried out with $NaBH_4$. Again, no side reactions were detected, but the yields after column chromatography were rather low. For α-pinene, the synthesis pathway is not suitable due to uncontrollable rearrangements. As described in the introduction, polymerization of the aromatic dimethyl terephthalate was not possible by means of enzyme catalysis.

In the future, the synthesis should be optimized, focusing on the complete isolation of $NaIO_3$ and electrochemical regeneration of $NaIO_4$. Enzyme-catalyzed reduction of the ketoaldehydes should also be worth exploring.[175] If the periodate cleavage is optimized, the ketoaldehydes can be used as platform chemicals not only for diols, but also for hydroxy carboxylic acids, amino acids, and diamines to establish a complete new set of AA/BB- and AB-type monomers for bio-based polyesters, polyamides and polyurethane (Figure 3.4).

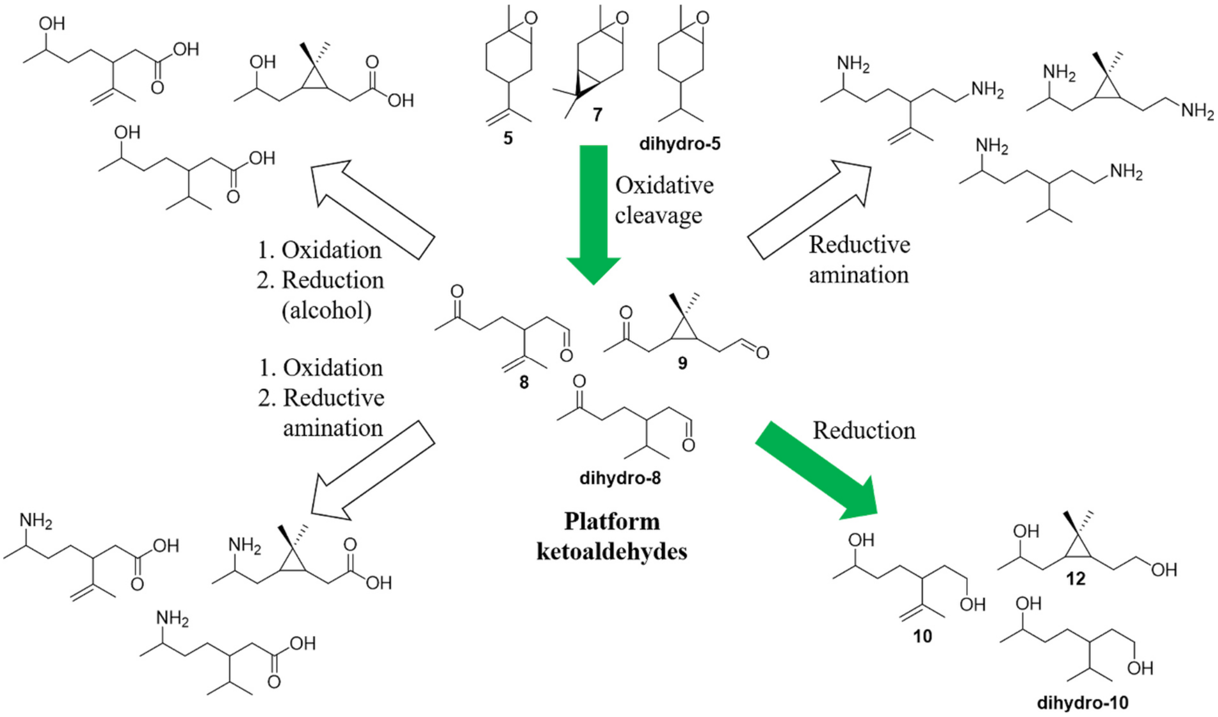
5
7
dihydro-5
Oxidative cleavage
1. Oxidation
2. Reduction (alcohol)
Reductive amination
1. Oxidation
2. Reductive amination
8
9
dihydro-8
Platform ketoaldehydes
Reduction
10
12
dihydro-10
OH
NH2
O

Figure 3.4 Terpene-based ketoaldehydes as platform chemicals for hydroxy carboxylic acids, amino acids, diamines, and diols.

3.5 Conclusion

To conclude, this work shows that isoprene can be used as a precursor for bio-fuels; though the existing oligomerization protocols might need some further improvements, the general feasibility has been outlined. However, from an economic point of view, the production and subsequent conversion to suitable hydrocarbons from isoprene is still too expensive to compete with fossil fuels presently. A more relevant application in the near future would be the utilization of isoprene and monoterpenes as feedstock for monomers. Chemical conversion to new polymer building blocks was demonstrated for isoprene (β-lactam), limonene (diol), α-pinene (β-lactam and ε-lactam) and (+)-3-carene (β-lactam and ε-lactam); in all cases, initial polymerizations were successful. The (+)-3-carene based polyamides possess exceptional features, especially in terms of thermal properties and crystallinity. Depending on the application, transparent or semi-crystalline (co-)-polyamides can be produced starting from the same monoterpene. In addition, the scalability of the monomer synthesis and the polymerization – which has meanwhile been demonstrated in 2.5 kg monomer production scale and 40 g polymerization scale – are very promising novelties in the field of bio-based polyamides. Though various other material parameters need validation and the synthesis still needs further optimization, the commercialization of (+)-3-carene-based polyamides seems within reach.

4. Methods

4.1 Methods section 2.2 “Isoprene derivatives as valuable monomers”

Synthesis *4-methyl-4-vinylazetidin-2-one* (**2**)

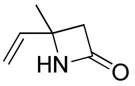

2

Isoprene (**1**, 13.6 g, 200 mmol) was dissolved in Et_2O (25 mL) in a three-necked flask (500 mL) equipped with a magnetic stirrer and a thermometer in an argon atmosphere and cooled to -65 °C under application of liquid nitrogen and an EtOH cooling bath in a dewar. CSI (29.3 g, 207 mmol) was dissolved in Et_2O and slowly dropped to the reaction mixture with a dropping funnel within 15 min. After stirring for 1.5 h, the internal temperature was -30 °C. It was cooled down to -65 °C and stirred for additional 2.5 h. The internal temperature was not allowed to exceed -30 °C at any point of time. For hydrolysis, solutions of Na_2SO_3 (2 M, 200 mL) and NaOH (4 M, 125 mL) were carefully added to the reaction mixture within 1.5 h. The temperature was kept between -10 °C and 0 °C during this exothermic reaction. IPC by GCMS revealed the selective formation of lactam **2**. It was stirred overnight, and a second IPC showed no further reaction. The reaction mixture was extracted with EtOAc until no product was detected in the aqueous phase. The organic fractions were combined, washed with saturated solutions of $NaHCO_3$ and NaCl and dried over Na_2SO_4. The solvent was removed under reduced pressure and lactam **2** (16.0 g, 144 mmol, 72%) was obtained as a slightly yellow oil.

^{1}H NMR (400 MHz, d6-DMSO): δ/ppm = 8.20 (s, $\mathrm{-CO{-}N\underline{\mathit{H}}{-}}$, 1H), 6.09 (dd, *J* = 17.3, 10.5 Hz, 1H, $\mathrm{H_2C{-}C\underline{\mathit{H}}{-}CCH_3{-}}$), 5.21 (dd, *J* = 17.2, 1.2 Hz, 1H, $\mathrm{\underline{\mathit{H_2}}C{-}CH{-}}$), 5.08 (dd, *J* = 10.5, 1.3 Hz, 1H, $\mathrm{\underline{\mathit{H_2}}C{-}CH{-}}$), 2.69 (qd, *J* = 14.3, 1.6 Hz, 2H, $\mathrm{-CO{-}C\underline{\mathit{H_2}}{-}CCH_3{-}}$), 1.40 (s, 3H, $\mathrm{-CH_2{-}CC\underline{\mathit{H_3}}{-}}$).

^{13}C NMR (101 MHz, d6-DMSO): δ/ppm = 165.9 ($\mathrm{-\underline{\mathit{C}}O{-}NH{-}}$), 142.5 ($\mathrm{H_2C{-}\underline{\mathit{C}}H{-}}$), 112.9 ($\mathrm{H_2\underline{\mathit{C}}{-}CH{-}}$), 53.0 ($\mathrm{-CH_2{-}\underline{\mathit{C}}CH_3{-}}$), 50.1 ($\mathrm{-\underline{\mathit{C}}H_2{-}CCH_3{-}}$), 24.8 ($\mathrm{-CH_2{-}C\underline{\mathit{C}}H_3{-}}$).

MS (EI, 70 eV): m/z (%) = 111 (0.2), 82 (7.9), 69 (6.5), 68 (100), 67 (63), 54 (48), 53 (29), 50 (2.6), 42 (42), 41 (14).

Synthesis of *4-methyl-1-(prop-1-en-2-yl)-4-vinylazetidin-2-one* (**acetyl-2**)

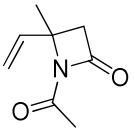

acetyl-2

Isoprene β-lactam **2** (1.10 g, 10.0 mmol) and TBAB (320 mg,1.0 mmol) were dissolved in toluene (150 mL) and cooled in an ice bath before NaOH (20 g, 500 mmol) was added. Ac$_2$O was dropped to the reaction mixture and it was stirred for 20 min until TLC showed the full conversion of lactam **2**. The reaction mixture was filtered and mixed with water. The layers were separated, and the aqueous phase was extracted with EtOAc. The solvent was removed under reduced pressure and **acetyl-2** (600 mg, 4.0 mmol, 40%) was obtained as a slightly yellow oil.

^{1}H NMR (400 MHz, d6-DMSO): δ/ppm = 6.12 (dd, *J* = 17.4, 10.7 Hz, 1H, H$_2$C-C*H*-CCH$_3$-), 5.28 – 5.13 (m, 2H, *H*$_2$C-CH-), 3.04 (s, 2H, -CO-C*H*$_2$-CCH$_3$-), 2.26 (s, 3H, -N-CO-C*H*$_3$), 1.61 (s, 3H, -CH$_2$-CC*H*$_3$-).

MS (EI, 70 eV): m/z (%) = 153 (0.7), 112 (5.9), 111 (46), 96 (17), 82 (29), 68 (57), 67 (85), 53 (32), 43 (100), 39 (16).

Synthesis of *4-methyl-1-tosyl-4-vinylazetidin-2-one* (**tosyl-2**)

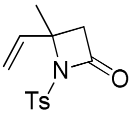

tosyl-2

Isoprene β-lactam **2** (330 mg, 3.0 mmol) was dissolved in toluene (15 mL) and added to a solution of TBAB (97 mg, 0.3 mmol), TsCl (1.72 g, 9.0 mmol) and NaOH (9.0 g, 360 mmol) in toluene (135 mL). It was stirred at room temperature until full conversion of lactam **2** (monitored by TLC). The reaction mixture was filtered and mixed with water. The layers were separated, and the aqueous phase was extracted with toluene. It was dried over Na$_2$SO$_4$, filtered and the solvent was removed under reduced pressure. The crude product was crystallized from EtOH at -20 °C and **tosyl-2** was obtained (460 mg, 1.74 mmol, 58%) as colorless crystals.

^{1}H NMR (400 MHz, d6-DMSO): δ/ppm = δ 7.80 (d, *J* = 8.3 Hz, 2H, 2xC*H* Ts), 7.48 (d, *J* = 8.1 Hz, 2H, 2xC*H* Ts), 6.03 (dd, *J* = 17.3, 10.7 Hz, 1H, H$_2$C-C*H*-CCH$_3$-), 5.32 (dd, *J* = 45.3, 14.0 Hz, 2H, *H*$_2$C-CH-), 3.13 (s, 1H, -CO-CH*H*-CCH$_3$-), 3.13 (s, 1H, -CO-C*H*H-CCH$_3$-), 2.42 (s, 3H, CH$_3$ Ts), 1.63 (s, 3H, -N-CO-C*H*$_3$).

Synthesis of *4-methyl-2-oxo-5,6-dihydropyridine-1(2H)-sulfonyl chloride* (**SO_2Cl-4**)

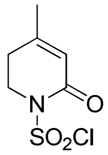

SO_2Cl-4

Method A:

Isoprene (**1**, 16,3 g, 240 mmol) was added drop-wise to a cooled solution of CSI (28.3 g, 200 mmol) in EtOAc (200 mL) within 30 min. The reaction temperature was maintained between -60 °C and -40 °C throughout the process. After stirring for additional 7 h at said temperature range, it was stirred for 12 h at 40 °C. The solvent was removed under reduced pressure. The remaining reaction mixture was dissolved in DCM (150 mL) and carefully washed with an aqueous solution of HCl (0.2 M, 3 x 100 mL). The aqueous layer was extracted with DCM (4 x 100 mL) and the combined organic layers were dried over Na_2SO_4. DCM was removed by distillation and the solid crude product (24.6 g) was crystallized from $ChCl_3$ (30 mL) at -20 °C within three days to give **SO_2Cl-4** (7.69 g, 40.0 mmol, 19%) as colorless crystals.

Method B:

Isoprene (**1**, 820 mg, 12 mmol) was added to a solution of CSI (1.63 g, 11.5 mmol) and $MnCl_2 \cdot 4\ H_2O$ (63 mg, 0.5 mmol) in MeCN (10 mL) at room temperature. After 14 h, TLC showed a mixture of **SO_2Cl-3** and **SO_2Cl-4**. After stirring for 5 days, the reaction mixture was filtered, and the solvent removed under reduced pressure and the work-up was performed as described in method A to give **SO_2Cl-4** (1.1 g, 5.2 mmol, 52%) as colorless crystals.

^{1}H NMR (400 MHz, d6-DMSO): δ/ppm = 5.74 – 5.69 (m, 1H, -CO-C*H*-CCH_3-), 4.29 (t, *J* = 6.2 Hz, 2H, -NSO_2Cl-C$\underline{H_2}$-), 2.37 (t, *J* = 6.2 Hz, 2H, -CH_2-C$\underline{H_2}$-CCH_3-), 1.95 (d, *J* = 1.1 Hz, 3H, -CH_2-CC$\underline{H_3}$-).

^{13}C NMR (101 MHz, d6-DMSO): δ/ppm = 164.1 (-$\underline{C}$O-), 159.8 (-$\underline{C}CH_3$-), 115.5 (-$\underline{C}$H-CO-), 65.8 (-$\underline{C}H_2$-NSO_2Cl-), 28.6 (-CH_2-$\underline{C}H_2$-CCH_3-), 22.6. (-CH_2-C$\underline{C}H_3$-).

Synthesis of *4-methyl-1,6-dihydropyridin-2(3H)-one* (**5**)

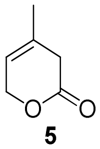

5

Isoprene (**1**, 6.80 g, 100 mmol) was dissolved in MeCN (15 mL) was dropped into a solution of CSI (13.0 g, 92 mmol) in MeCN (40 mL) at room temperature. The reaction temperature was kept below 30 °C. After stirring for 2 h, the reaction mixture was cooled in an ice bath and a solution of Na_2SO_3 (4.40 g) in water (20 mL) was added drop-wise. The mixture was stirred for 2 h and the temperature was kept below 5 °C. The layers were separated, and the aqueous layer was extracted with EtOAc. The combined organic fractions were washed several times with a saturated aqueous solution of $NaHCO_3$ until the pH-value of the washing solution was constant. After extraction of the aqueous layers with EtOAc, the combined organic layers were washed with saturated NaCl solution and dried over Na_2SO_4. The solvent was removed under reduced pressure and the crude product was purified by fractional distillation (1.5 mBar, 55 °C gas phase temperature) and lactone **5** (4.55 g, 41 mmol, 44%) was obtained as a colorless oil.

^{1}H NMR (400 MHz, d6-DMSO): δ/ppm = 5.69 – 5.60 (m, -O-CH$_2$-C$\underline{\mathit{H}}$-, 1H), 4.81 – 4.73 (m, 2H, -CO-C$\underline{\mathit{H}_2}$-CCH$_3$-), 2.98 (dd, *J* = 3.0, 1.8 Hz, 2H, -O-C$\underline{\mathit{H}_2}$-CH-), 1.73 (dd, *J* = 3.0, 2.1 Hz, 3H, -CH$_2$-CC$\underline{\mathit{H}_3}$-).

^{13}C NMR (101 MHz, d6-DMSO): δ/ppm = 169.2 (-$\underline{\mathit{C}}$O-), 130.7 (-CH$_2$-$\underline{\mathit{C}}$CH$_3$-), 116.2 (-O-CH$_2$-$\underline{\mathit{C}}$H-), 68.1 (-CO-$\underline{\mathit{C}}$H$_2$-), 34.7 (-O-$\underline{\mathit{C}}$H$_2$-CH-), 21.0 (-CH$_2$-C$\underline{\mathit{C}}$H$_3$-).

MS (EI, 70 eV): m/z (%) = 112 (43), 84 (63), 82 (10), 69 (75), 56 (50), 53 (73), 50 (15), 43 (13), 41 (100), 32 (30).

Synthesis of *4-methyl-5,6-dihydropyridin-2(1H)-one* (**6**)

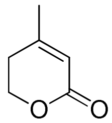

6

Isoprene (**1**, 680 mg, 10 mmol) was dissolved in MeCN (10 mL) and dropped into a solution of CSI (1.63 g, 11.5 mmol) and Cp_2TiCl_2 (12.5 mg, 0.5 mmol) in MeCN (10 mL) and stirred for 6 days in a sealed glass tube. The solvent was removed under reduced pressure, and the residue was dissolved in DCM (10 mL) before a solution of NaOH (440 mg, 11 mmol) in EtOH (5 mL) and H_2O (10 mL) was added. The reaction mixture was stirred overnight. Saturated brine (10 mL) was added and the product was extracted with DCM (2 x 10 mL). The organic layer as washed with an aqueous solution of NH_4Cl (saturated, 10 mL) before the organic solvent was removed under reduced pressure. Lactone **6** (1.0 g, 8.9 mmol, 89%) was obtained as a colorless oil.

^{1}H NMR (400 MHz, d6-DMSO): δ/ppm = 5.77 – 5.66 (m, -CO-C$\underline{\mathit{H}}$-, 1H), 4.29 (t, *J* = 6.2 Hz, -O-C$\underline{\mathit{H}_2}$-CH$_2$-, 2H), 2.38 (t, *J* = 6.2 Hz, -CH$_2$-C$\underline{\mathit{H}_2}$-CCH$_3$-, 2H), 1.96 (d, *J* = 0.9 Hz,-CH$_2$-CC$\underline{\mathit{H}_3}$-, 3H).

^{13}C NMR (101 MHz, d6-DMSO): δ/ppm = 164.0 ($-\underline{C}O-$), 160.0 ($-CH_2-CH_2-\underline{C}CH_3-$), 115.5 ($-CO-\underline{C}H-CCH_3-$), 65.7 ($-O-\underline{C}H_2-CH_2-$), 28.5 ($-CH_2-\underline{C}H_2-CCH_3-$), 22.5 ($-CH_2-C\underline{C}H_3-$).
MS (EI, 70 eV): % (m/z) = 112 (48), 111 (1), 83 (8), 82 (100).

Synthesis of *2-methyl-2-vinyloxirane* (**7**)

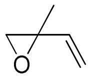

7

To a suspension of isoprene (**1**, 15.0 g, 220 mmol), Oxone (80 g, 260 mmol), H_2O (500 mL), MeCN (300 mL), and ice (100 g), a precooled solution of NH_4Br (19.6 g, 200 mmol) was added in a fast-dropping manner within 3 min. The reaction mixture was stirred for 6 additional min and was then poured through a suction filter. EtOAc was added, and the layers were separated. The aqueous layer was extracted with EtOAc (3 x 200 mL), and the combined organic phases were washed with saturated solutions of $NaHCO_3$, $NaSO_3$, and brine. After drying over $NaSO_4$ and subsequent filtration, the solvent was removed under reduced pressure to give 1-bromo-2-methylbut-3-en-2-ol (**8**, 28.5 g, 172 mmol, 86%).
A precooled solution of NaOH (14.4 mL, 10 M) was dropped to 1-bromo-2-methylbut-3-en-2-ol (**8**, 15.75 g, 95 mmol) at 0 °C and stirred for 2 h. The phases were separated, and the colorless upper layer (organic phase) consisted of almost pure epoxide **7** (purity > 90% as verified by GCMS, 6.9 g 83 mmol, 87%).
^{1}H NMR (400 MHz, d6-DMSO): δ/ppm = 5.62 (dd, *J* = 17.5, 10.7 Hz, 1H, $H_2C-C\underline{H}-CCH_3-$), 5.35 (dd, *J* = 17.4, 0.9 Hz, 1H, $\underline{H_2}C-CH-CCH_3-$), 5.22 (dd, *J* = 10.7, 1.0 Hz, 1H, $\underline{H_2}C-CH-CCH_3-$), 2.81 (t, *J* = 4.5 Hz, 1H, $-O-C\underline{H_2}-CCH_3-$), 2.69 (d, *J* = 5.4 Hz, 1H, $-O-C\underline{H_2}-CCH_3-$), 1.37 (s, 3H, $-O-CH_2-CC\underline{H_3}-$).
^{13}C NMR (101 MHz, d6-DMSO): δ/ppm = 140.0 ($H_2C-\underline{C}H-CCH_3-$), 117.0 ($H_2\underline{C}-CH-CCH_3-$), 55.3 ($H_2C-CH-\underline{C}CH_3-$), 54.4 ($-O-\underline{C}H_2-CCH_3-$), 18.6 ($H_2C-CH-C\underline{C}H_3-$).
MS (EI, 70 eV): m/z (%) = 84 (9.1), 83 (28), 69 (19), 56 (36), 55 (66), 54 (16), 53 (54), 42 (9.0), 41 (29), 39 (100), 37 (2.8).

Polymerization of *4-methyl-4-vinylazetidin-2-one* (**2**) to **poly2**

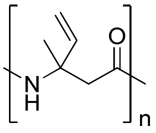

Lactam **2** (200 mg, 1.8 mmol), N-benzoyl-caranlactam (4.4 mg, 0.016 mmol, 0.8%, refer to Section 2.4B and 4.7) and NaH (60% on paraffin, 3.8 mg, 0.01 mmol, 0.6%) were mixed under

inert atmosphere and then heated to 170 °C. The polymerization started immediately. After 15 min at 170 °C, the polymer was cooled on air. **Poly2** was obtained as a yellow solid. 180 mg were stirred in a mixture of H_2O (20 mL) and EtOH (20 mL) at 70 °C for 12 h to remove residual monomers and oligomers. The resulting almost colorless powder was dried under reduced pressure to give pure **poly2** (120 mg, 67%) which was then analyzed by NMR, DSC and GPC.
^{1}H NMR (400 MHz, d6-DMSO): δ/ppm = 6.19 – 5.92 (1H, H_2C-CH-), 5.38 – 5.14 (2H, H_2C-CH-), 2.90 (2H, -CO-C$\underline{\mathit{H_2}}$-), 1.62 (3H, -NH-CC$\underline{\mathit{H_3}}$-).
^{13}C NMR (101 MHz, d6-DMSO): δ/ppm = 172.4 (-$\underline{\mathit{C}}$O-), 140.6 (H_2C-$\underline{\mathit{C}_{atak.}}$H-), 140.5 ($H_2C$-$\underline{\mathit{C}_{atak.}}$H-), 114.5 ($H_2\underline{C}$-CH-), 57.2 (-CO-$\underline{\mathit{C}}H_2$-), 45.6 -NH-$\underline{\mathit{C}}CH_3$-), 24.7 (-NH-C$\underline{\mathit{C}_{atak}}H_3$), 24.4 (-NH-C$\underline{\mathit{C}_{atak}}H_3$).

NMR spectra of 4-methyl-2-oxo-5,6-dihydropyridine-1(2H)-sulfonyl chloride (**SO_2Cl-4**)

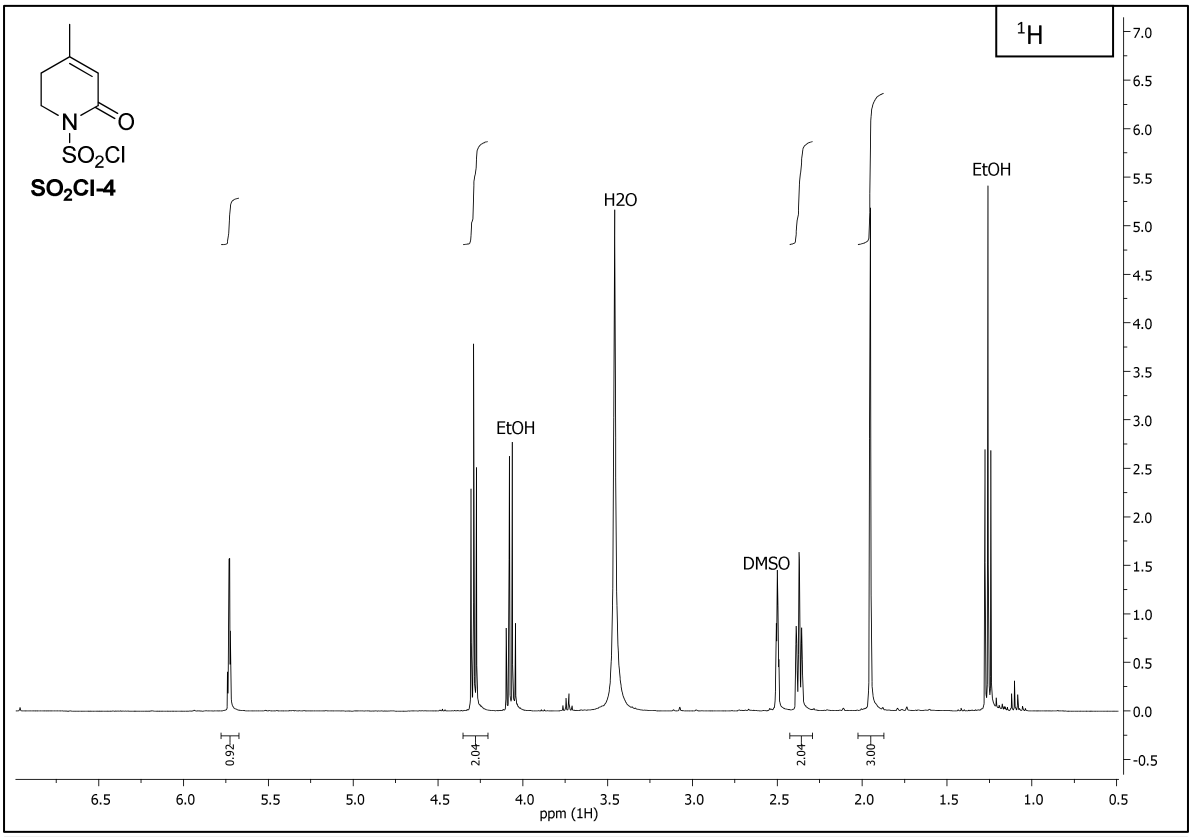

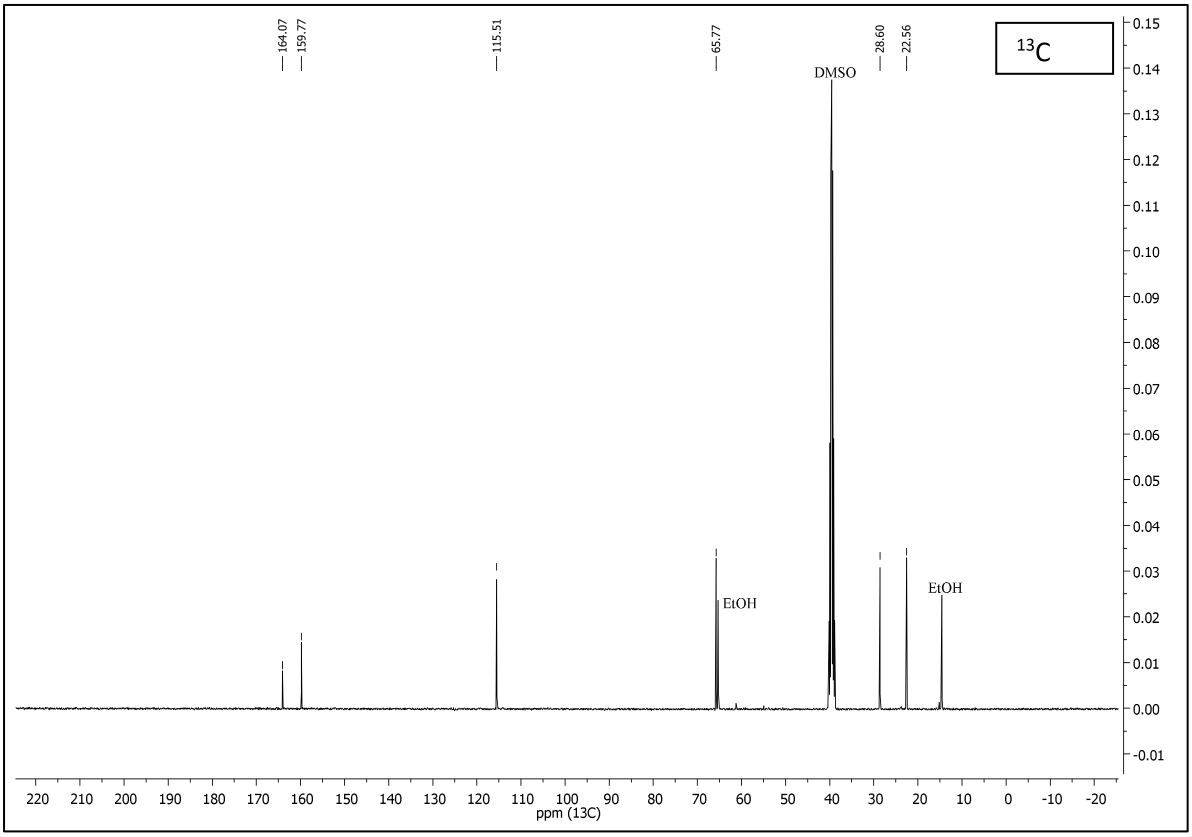

NMR spectra of 4-methyl-1,6-dihydropyridin-2(3H)-one (**5**)

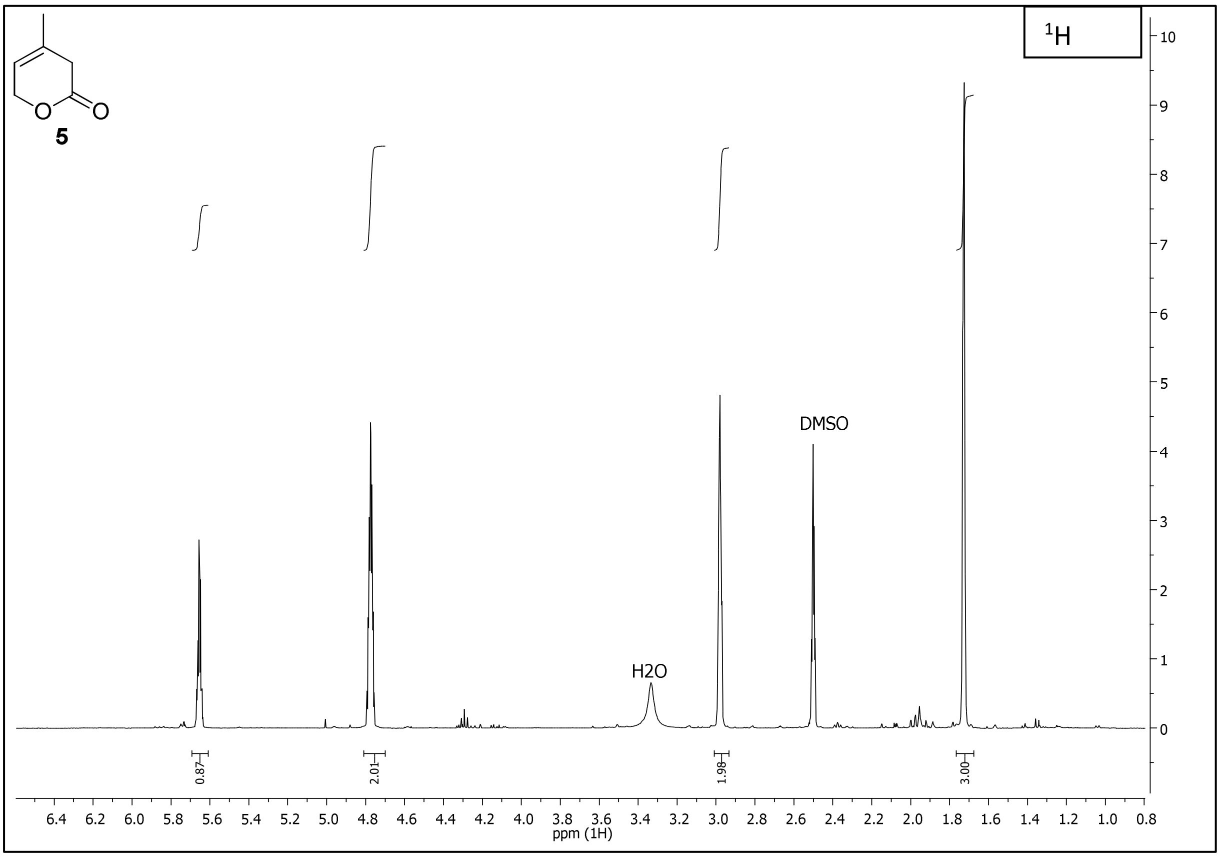

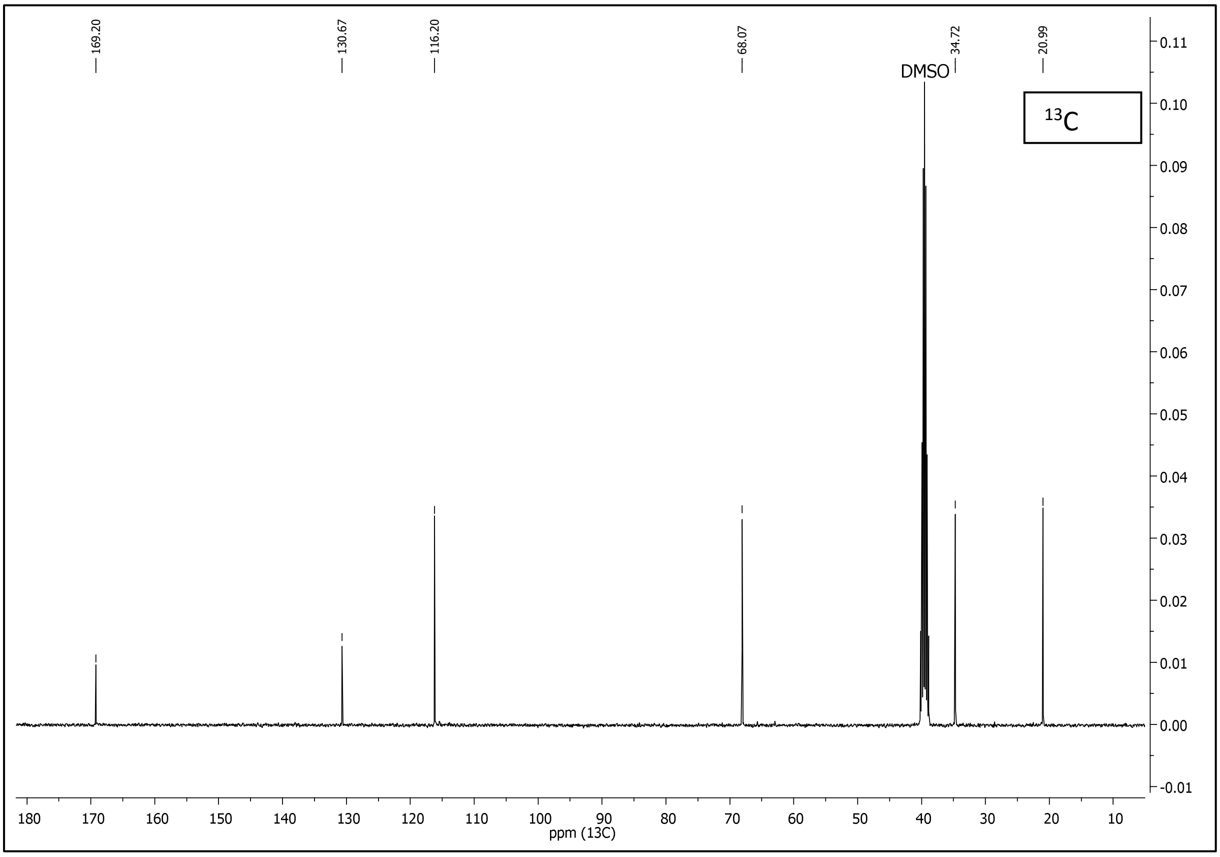

NMR spectra of 4-methyl-5,6-dihydropyridin-2(1H)-one (**6**)

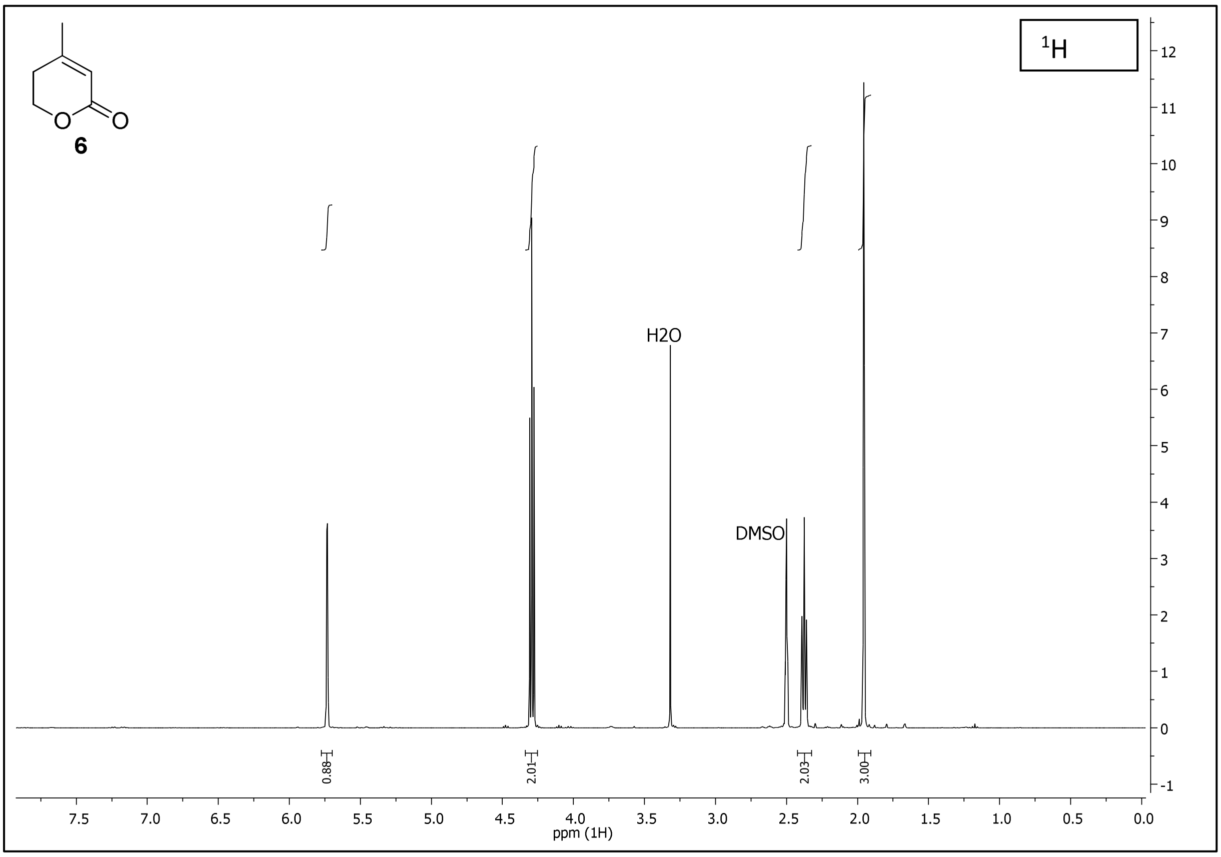

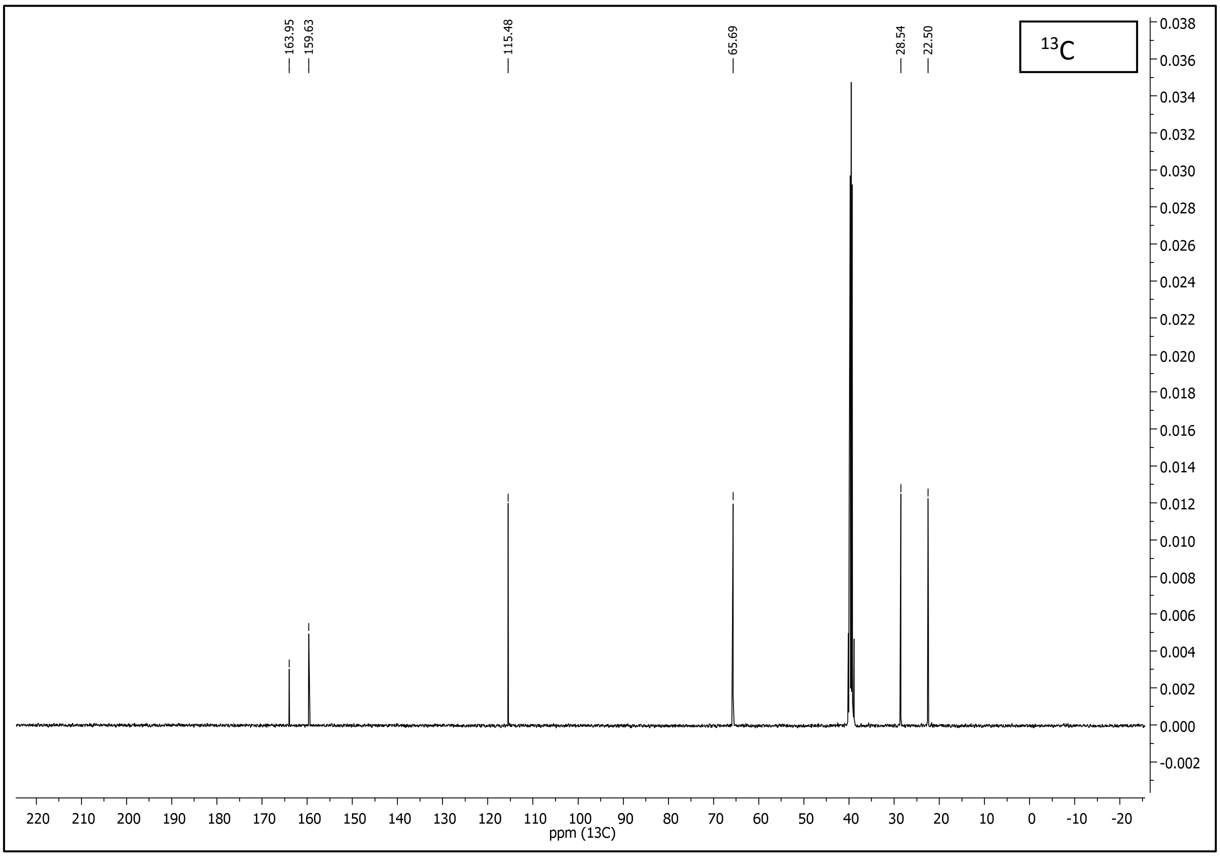

NMR spectra of 4-methyl-1-(prop-1-en-2-yl)-4-vinylazetidin-2-one (**acetyl-2**)

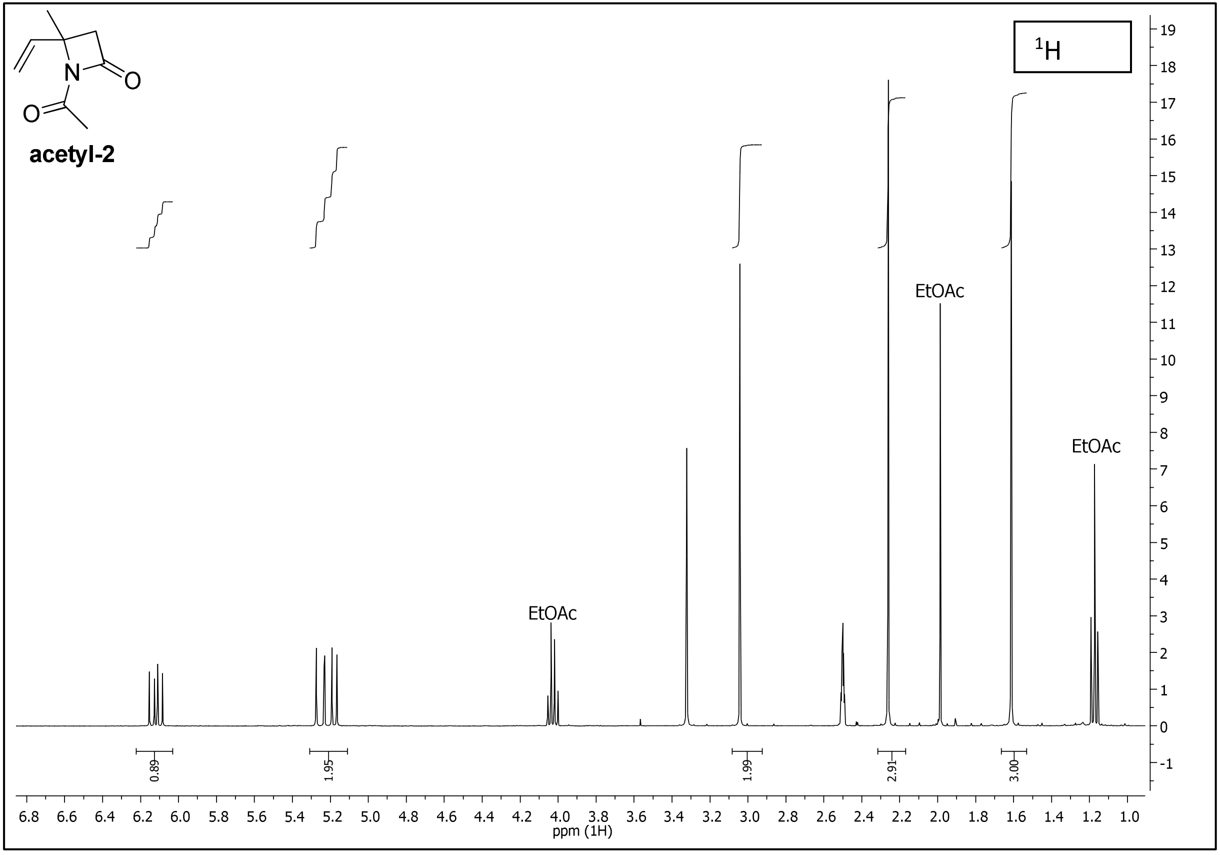

NMR spectra of 4-methyl-1-tosyl-4-vinylazetidin-2-one (**tosyl-2**)

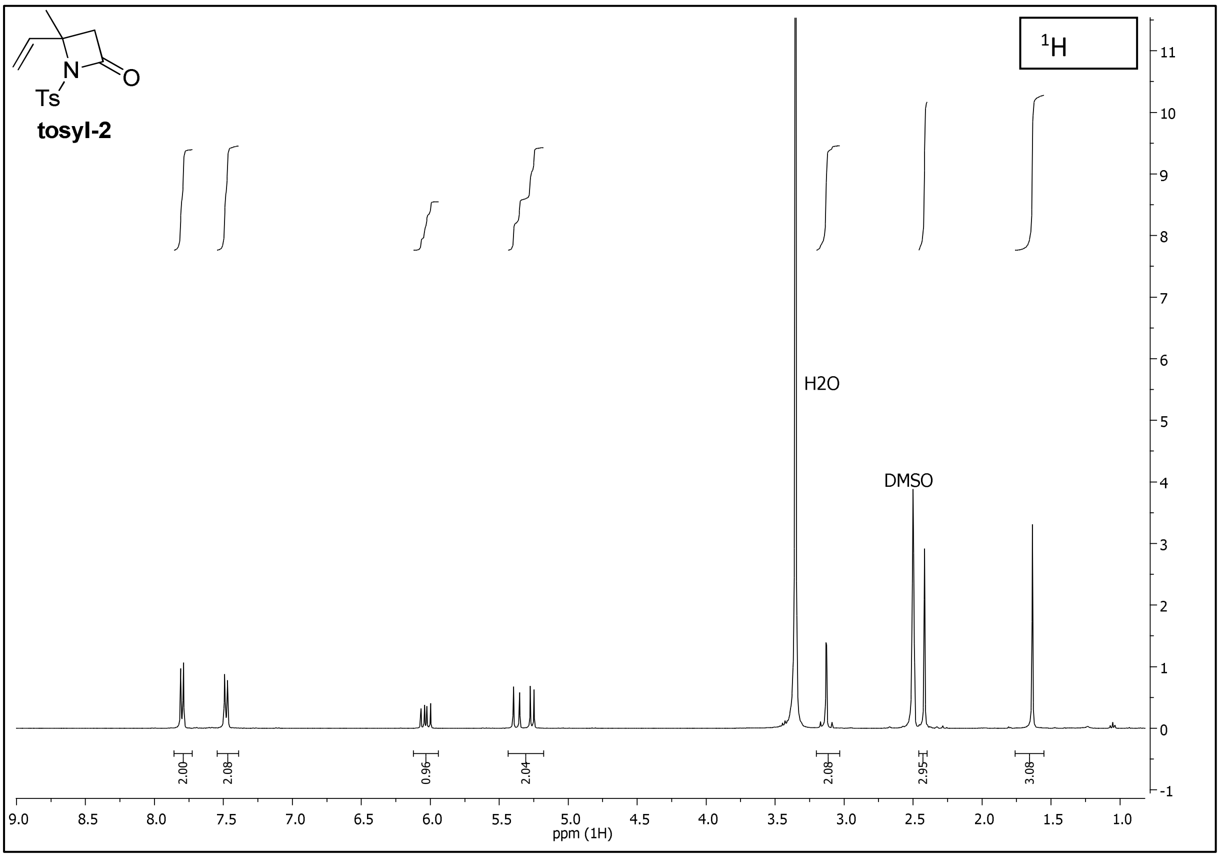

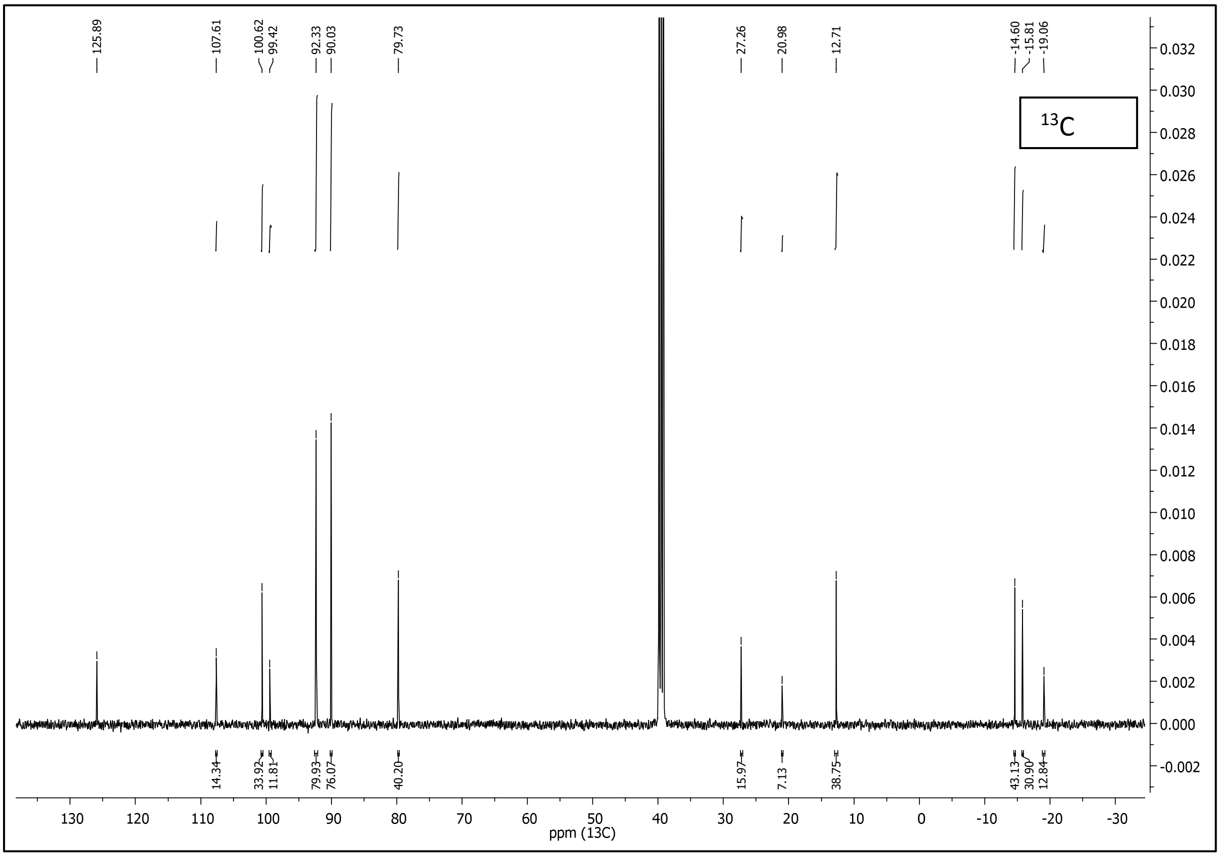

NMR spectra of 4-methyl-4-vinylazetidin-2-one (**2**)

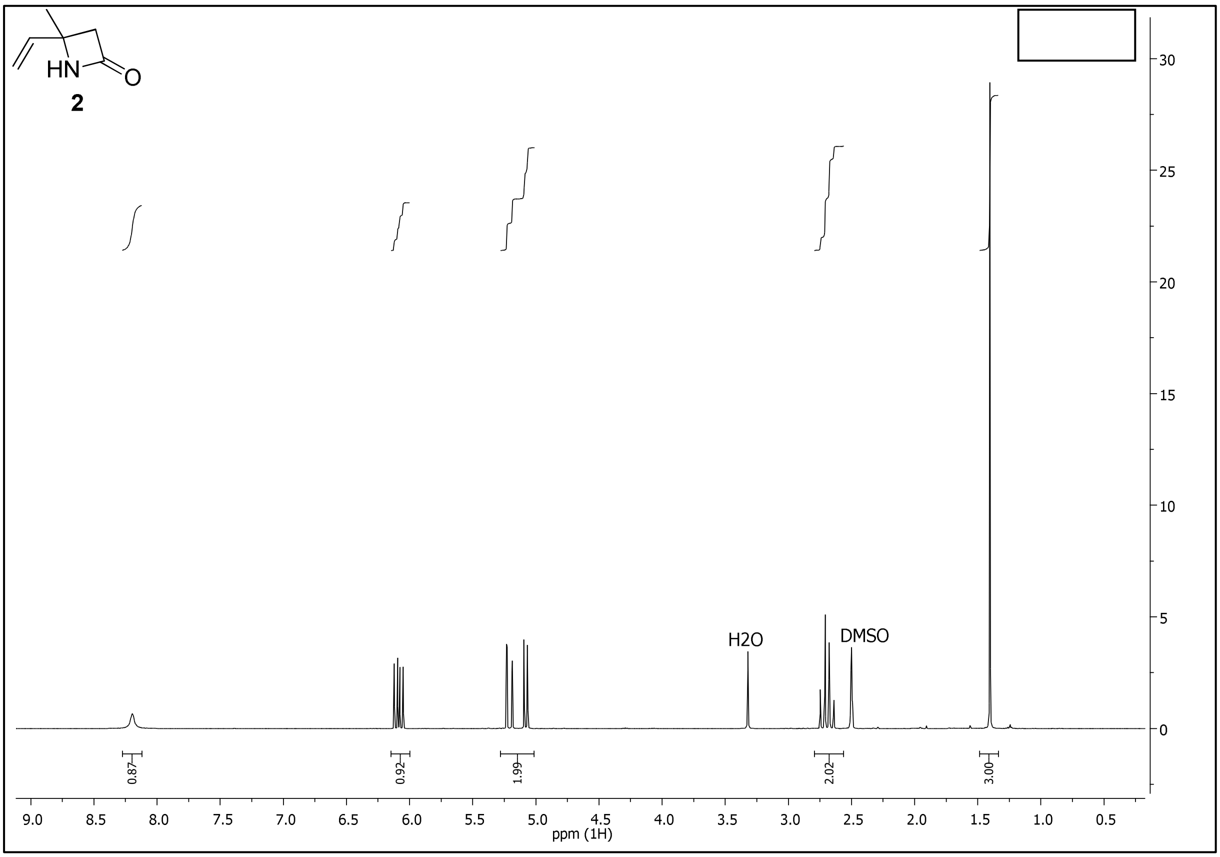

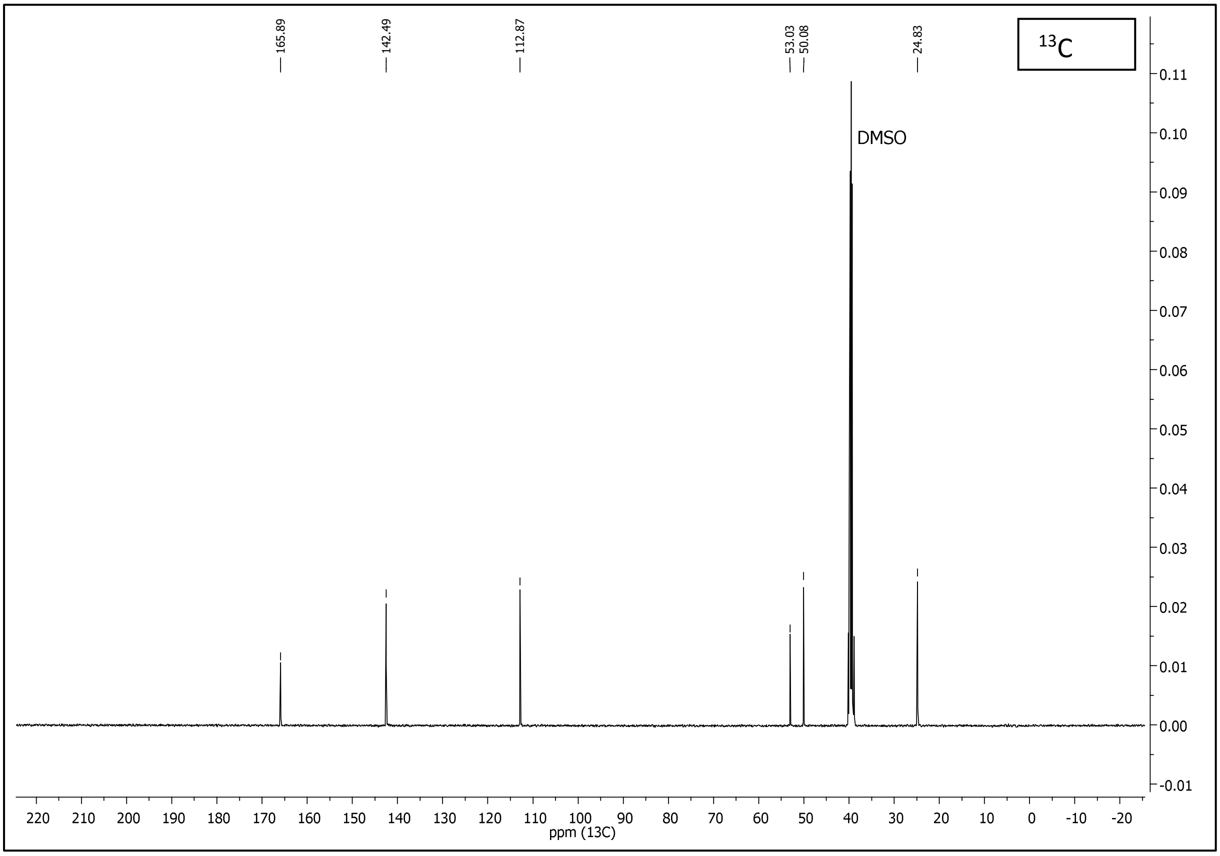

NMR spectra of 2-methyl-2-vinyloxirane (**7**)

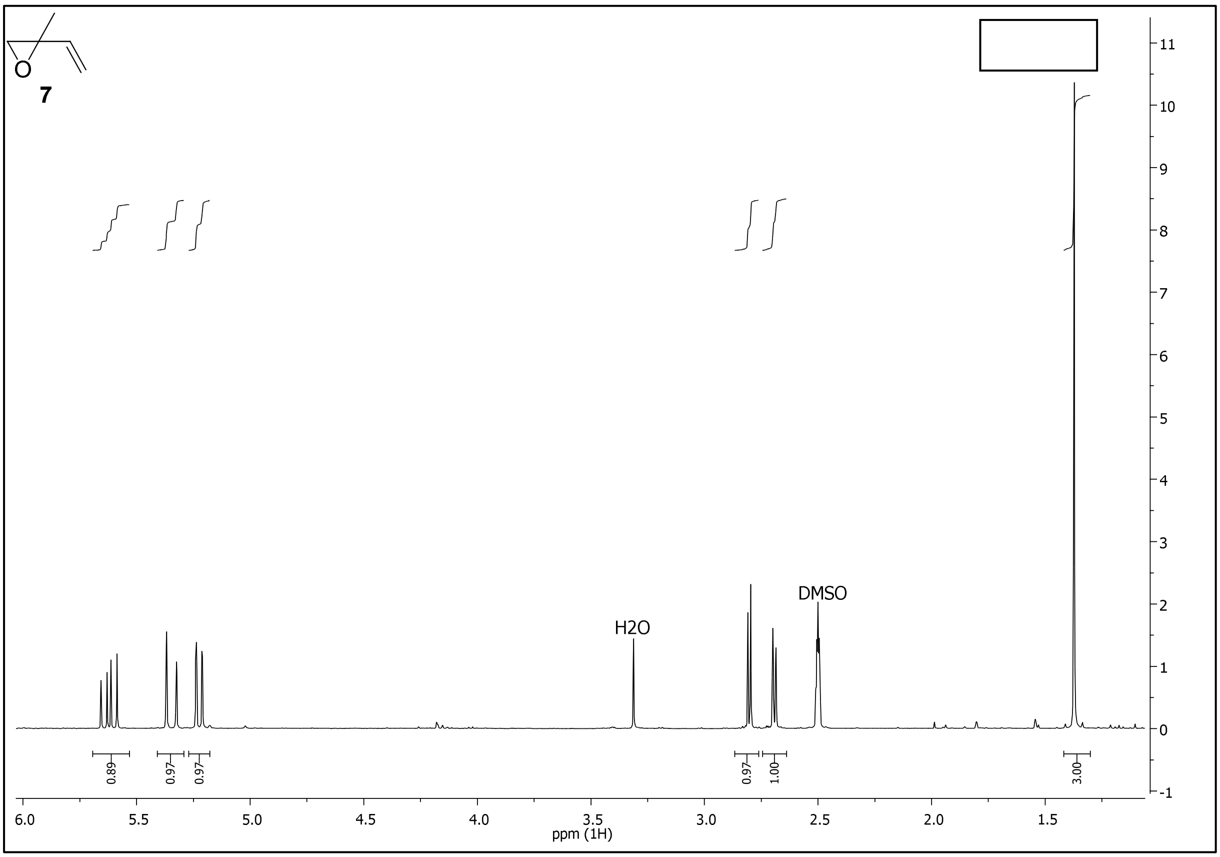

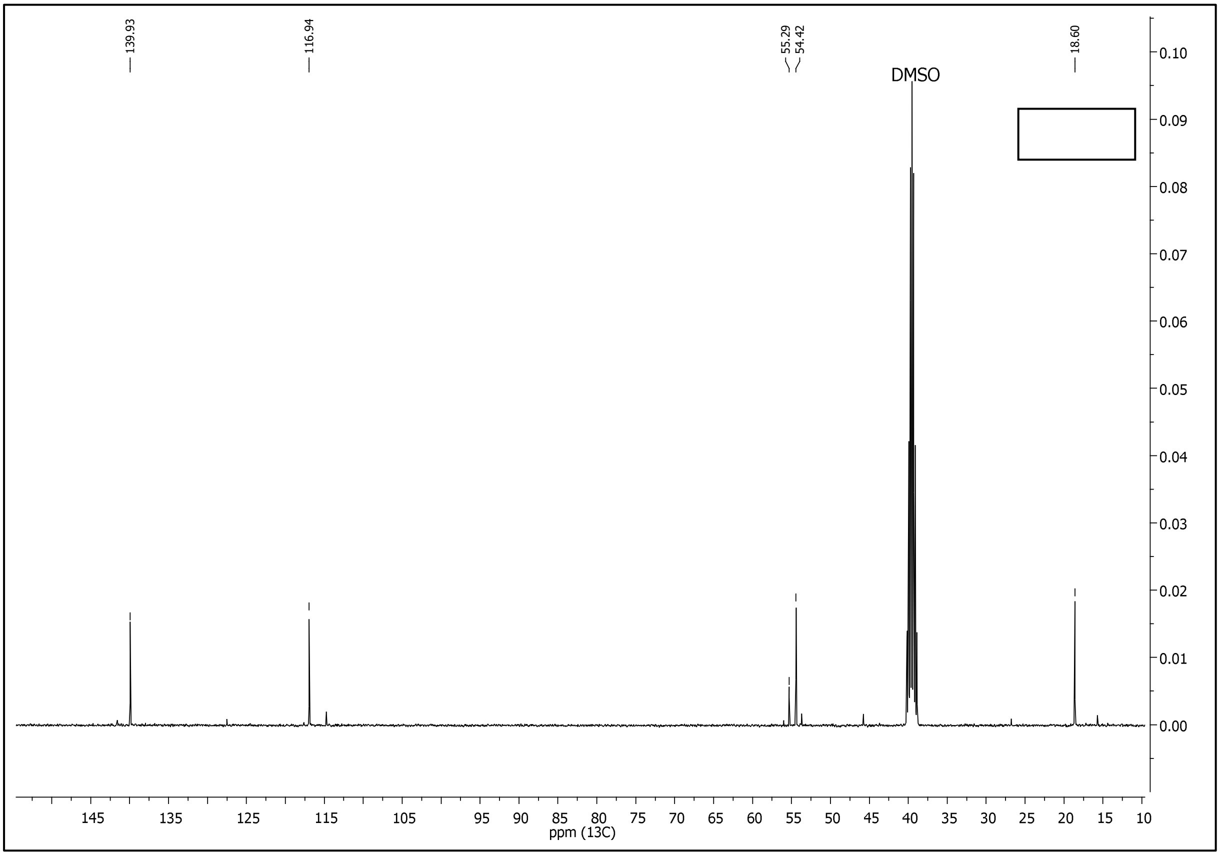

NMR spectra of polyisoprene-β-amide(**poly2)**

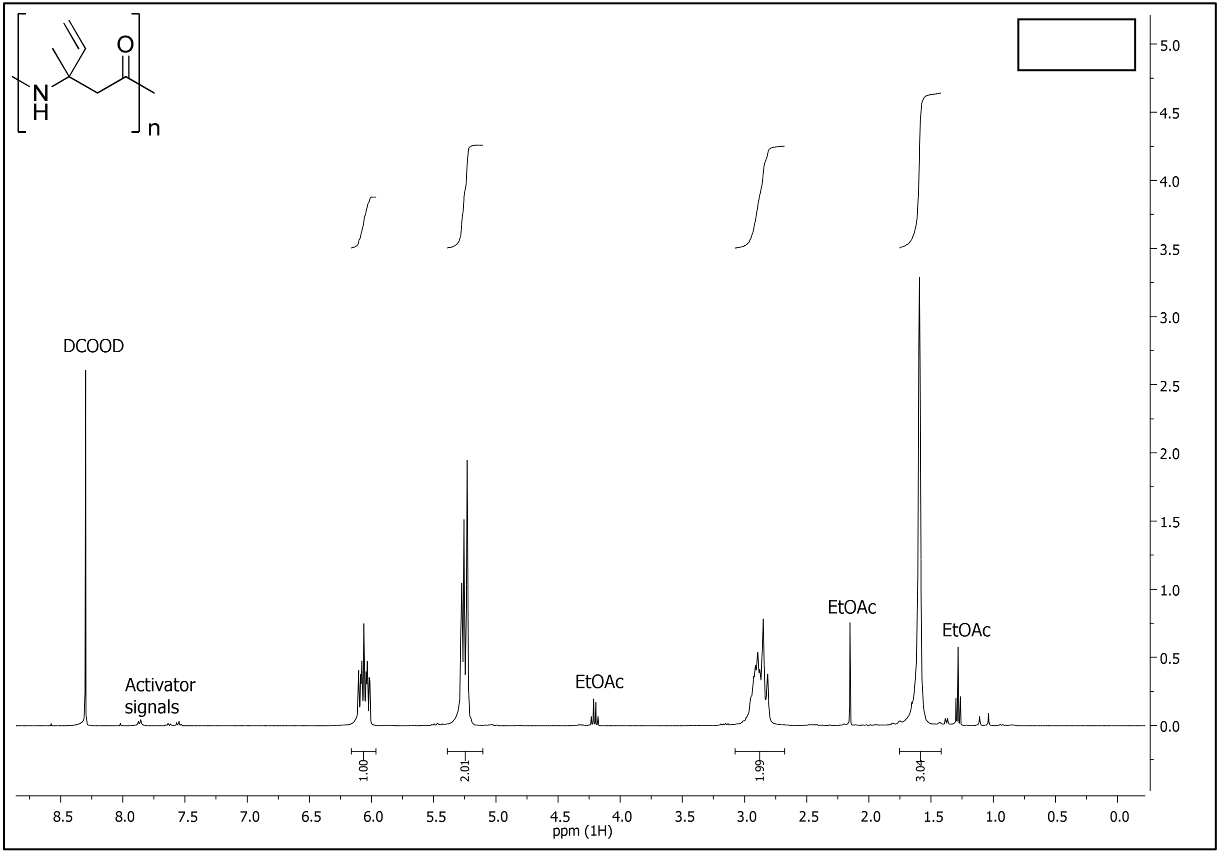

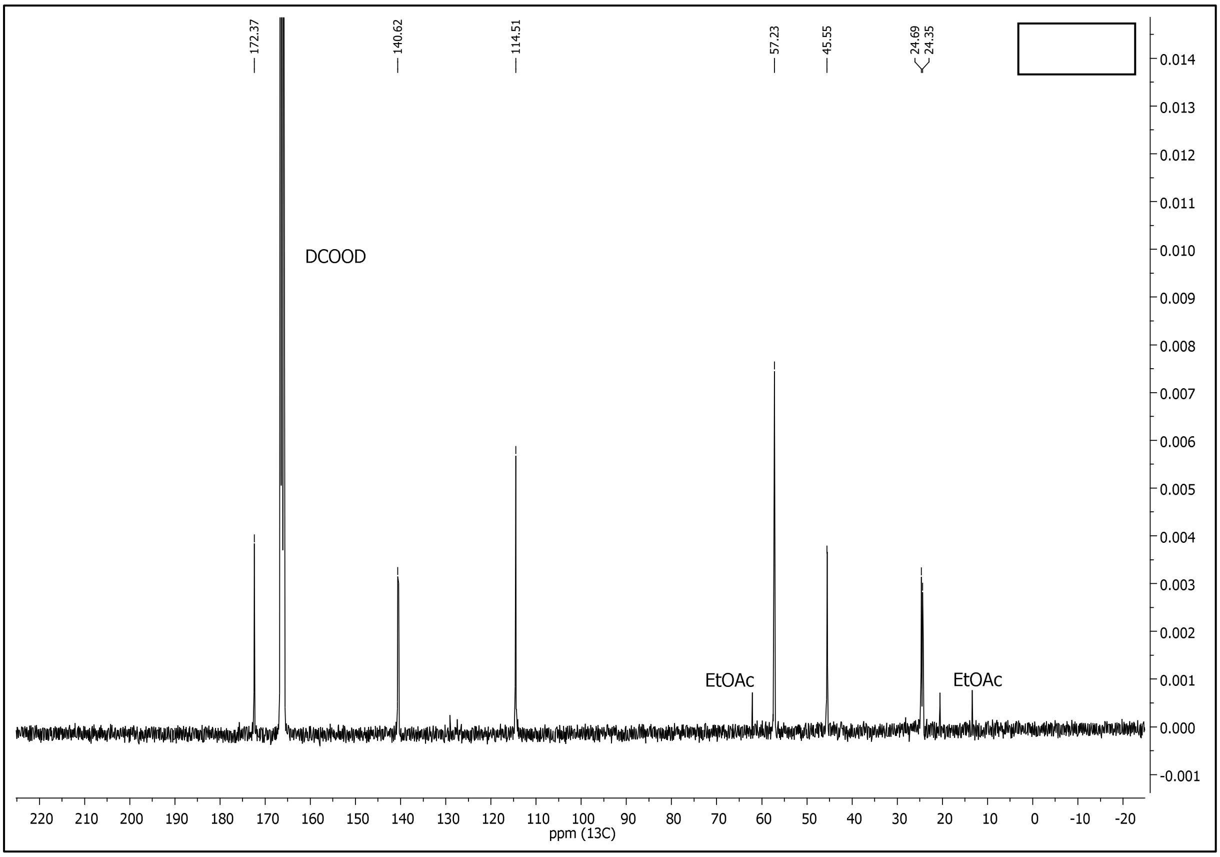

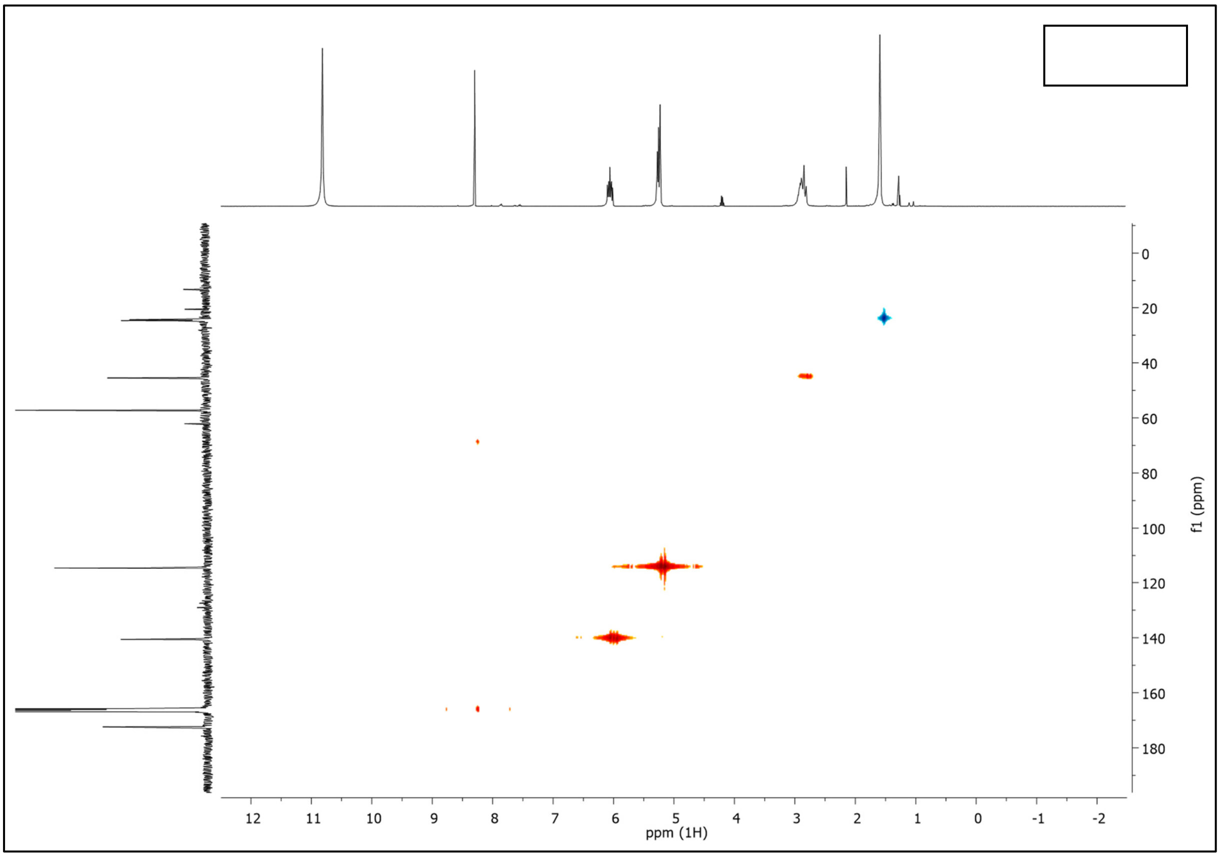
0
20
40
60
80
100
120
140
160
180
f1 (ppm)
12
11
10
9
8
7
6
5
4
3
2
1
0
-1
-2
ppm (1H)

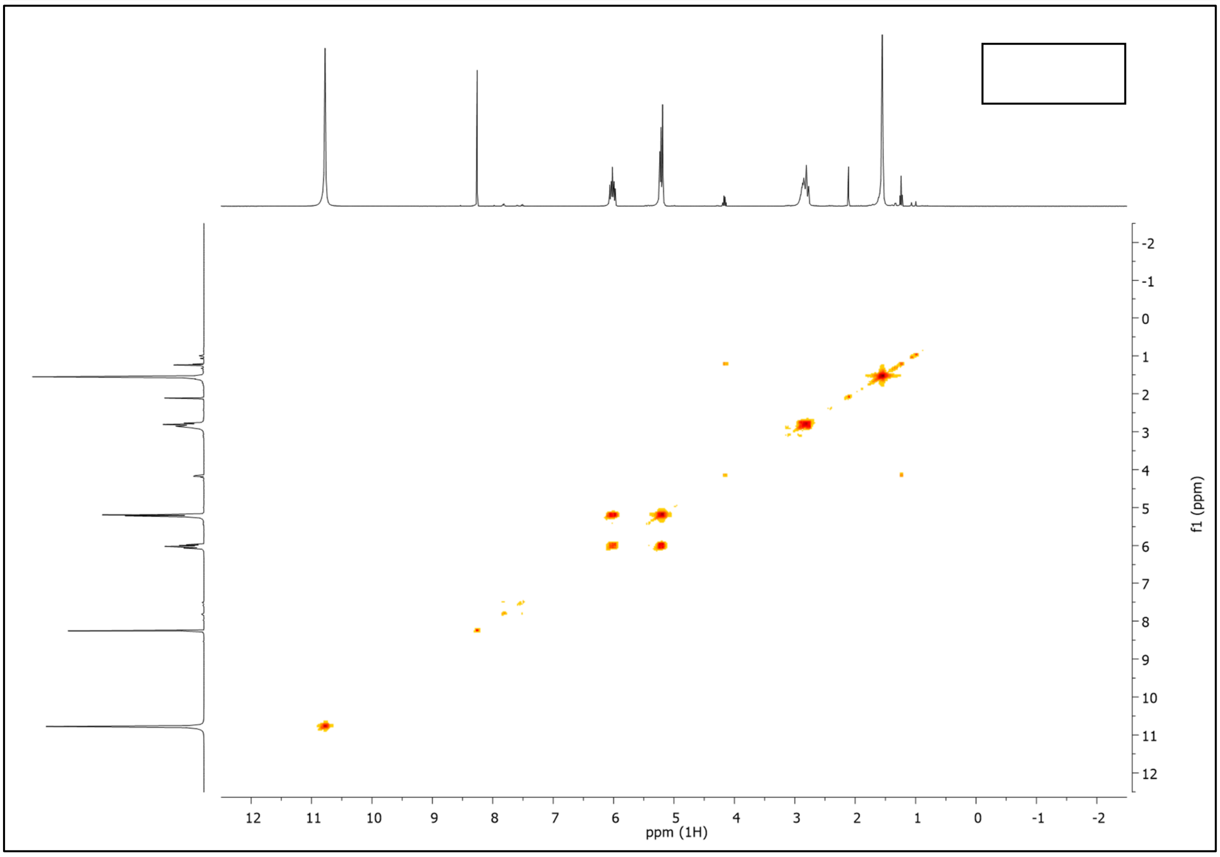
-2
-1
0
1
2
3
4
5
6
7
8
9
10
11
12
f1 (ppm)
12
11
10
9
8
7
6
5
4
3
2
1
0
-1
-2
ppm (1H)

GPC curve of Polyisoprene-β-amide (**poly2**)

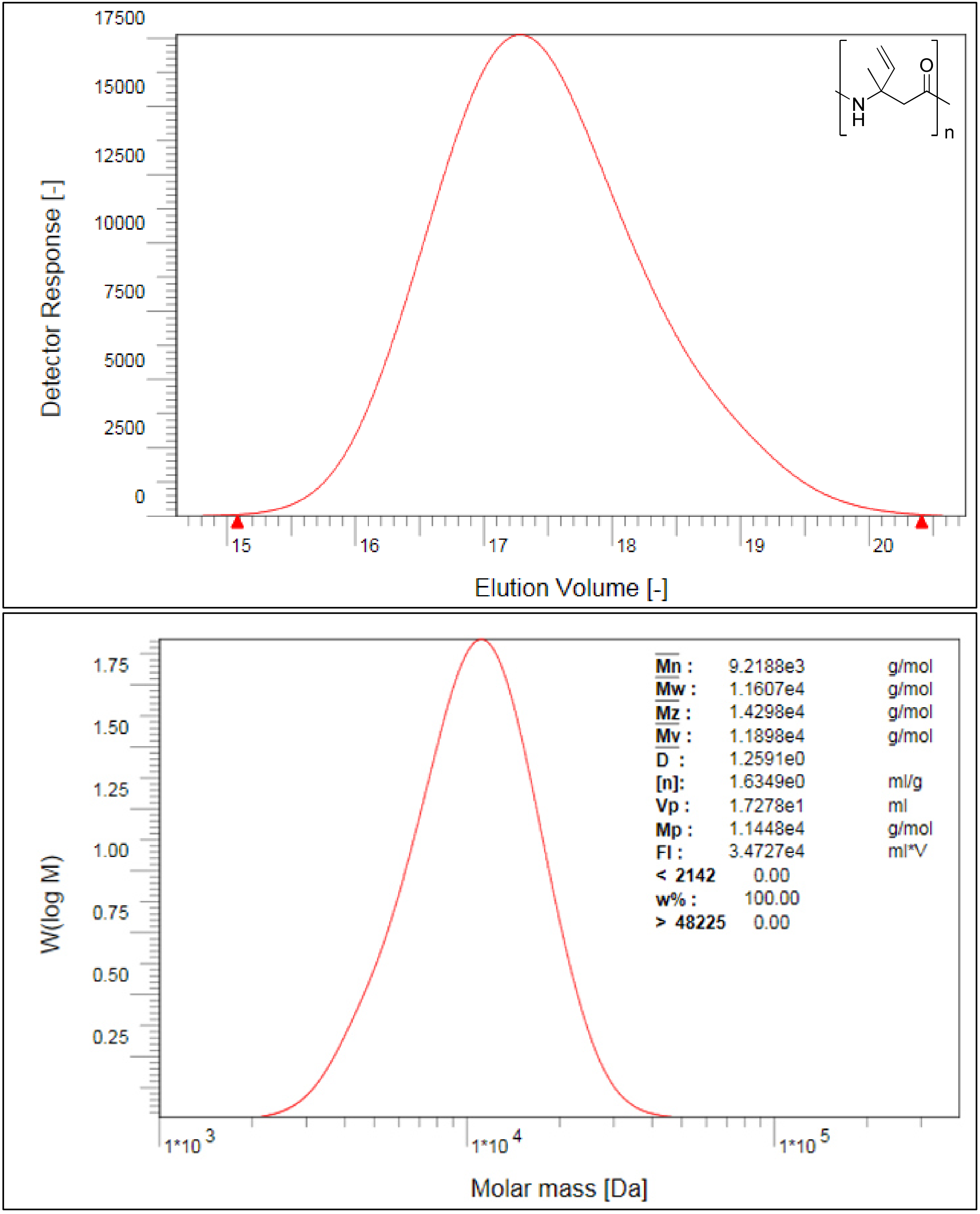

```
Mn :      9.2188e3     g/mol
Mw :      1.1607e4     g/mol
Mz :      1.4298e4     g/mol
Mv :      1.1898e4     g/mol
D  :      1.2591e0
[n]:      1.6349e0     ml/g
Vp :      1.7278e1     ml
Mp :      1.1448e4     g/mol
FI :      3.4727e4     ml*V
< 2142      0.00
w% :      100.00
> 48225     0.00
```

4.2 Methods section 2.3 “New Bio-Polyamides from Terpenes: α-Pinene and (+)-3-Carene as Valuable Resources for Lactam Production

Copyright WILEY-VCH Verlag GmbH & Co. KGaA, 69469 Weinheim, Germany, 2019.

Supporting Information

for *Macromol. Rapid Commun.,* DOI: 10.1002/marc.201800903

New Bio-Polyamides from Terpenes: #-Pinene and (+)-3-Carene as Valuable Resources for Lactam Production

Paul N. Stockmann, Dominik L. Pastoetter, Marion Woelbing, Claudia Falcke, Malte Winnacker, Harald Strittmatter, and Volker Sieber*

Copyright WILEY-VCH Verlag GmbH & Co. KGaA, 69469 Weinheim, Germany, 2018.

Supporting Information

New Bio-Polyamides from Terpenes: α-Pinene and (+)-3-Carene as Valuable Resource for Lactams

Paul N. Stockmann, Dominik L. Pastoetter, Marion Woelbing, Claudia Falcke, Malte Winnacker, Harald Strittmatter, Volker Sieber*

1 General information

1.1 Analytical methods and instruments

1.1.1 Gas chromatography/Mass spectrometry (GC/MS)

GC analysis was performed using GC-2010 Plus (Shimadzu) in combination with auto-injector AOC-5000 (Jain, Combi PAL). Separation was achieved via GC capillary column (BPX 5: 5% phenyl, 95% methyl polysilphenylene / siloxan; SGE). For coupled MS, MS-QP2010 Plus (Shimadzu) with electron ionization (70 eV) was used. Software analysis of measured data was accomplished with GC-MS Postrun Analysis (Shimadzu). Gathered data was compared with the National Institute of Standards and Technology database version 08. Table SI-1 displays the used parameters.

Table SI-1: Heating- and elution-parameters of the GC-MS analysis.

Parameters	**Values**
split rate	5
injection temperature	250 °C
carrier gas	helium
column flow-through	1.69 ml/min.
heating program	50 °C for 1 min.
	50-120 °C, heating 15 °C per min.
	120-170 °C, heating 5 °C per min.
	170-200 °C, heating 20 °C per min.
	200 °C for 7 min.
column	BPX5 (CS Chromatography), length 30 m, inner diameter 0.25 µm, diameter 0.25 mm

1.1.2 Nuclear magnetic resonance (NMR) spectroscopy

All NMR-measurements were carried out on a JNM-ECA 400 MHz spectrometer from JEOL at 25 °C using standard pulse programs. Chemical shifts are reported as δ-values in ppm. Coupling constants (J-values) are given in Hertz (Hz). The DEPT135° technique was used to assign CH_2-signales. 2D NMR methods (COSY, HSQC, HMBC) were applied if useful. Chemical shifts are reported as follows: value (multiplicity, coupling constant(s) where applicable, number of protons). NMR spectra assignation was supported by comparison with literature values for similar compounds. Only clearly identifiable peaks are assigned. For the characterization of observed signal multiplicities, the following abbreviations were applied: s (singlet), d (doublet), dd (double doublet), dt (double triplet), t (triplet), q (quartet), quint (quintet) and m (multiplet).

1.1.3 Fourier transform Infrared (FTIR) spectroscopy

For FTIR measurements, the Bruker Tensor 27 FT-IR with a diamond attenuated total reflectance (ATR) top plate was utilized. Software analysis of measured data was accomplished with OPUS 7.0. The absorption bands are reported in wavenumbers (cm^{-1}). For the band characterization, the following abbreviations were used: s (strong), m (medium), w (weak), and vw (very weak).

1.1.4 Thin layer chromatography (TLC)

TLC was performed using aluminum plates coated with SiO_2 (Merck 60, F-254) and the spots were visualized with a $KMnO_4$ stain. Flash column was performed using SiO_2 (0.06-0.2 mm, 230-400 mesh ASTM) from Roth.

1.1.5 Gel permeation chromatography (GPC)

GPC was performed by a SECcurity GPC system with an autosampler (1260 Infinity, Agilent Technologies) and a TCC6000 column oven (Polymer Standards Service, PSS). The data was evaluated using PSS WinGPC UniChrom (PSS). PMMA was chosen for narrow molar mass standard calibration and correlated to PA6 standards with a ready-call-kit (M_w/M_n = 31400/17400 kDa; 22000/13000 kDa; 17200/11300) broad calibration. For sample preparation, the polyamide was dissolved in a solution of 0.05 M sodium trifluoroacetate (NaTFA) and hexafluoro-iso-propanol (HFIP). Table SI-2 displays the applied GPC parameters.

Table SI-2: GPC-parameters applied for analysis of terpene-based polyamides.

Parameters	**Values**
column temperature	25 °C
flow	0.6 mL/min
elution solvent	0.05 M NaTFA in HFIP
sample concentration	3.0 mg/mL
injection volume	50 µL
elution time	51 min
elution volume	30.6 mL
column 1	PSS PFG pre-column
column 2	PSS PFG 100 A
column 3	PSS PFG 1000 A

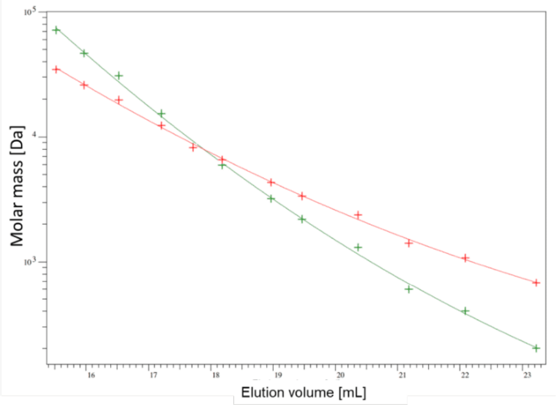

Figure SI-1: Narrow PMMA calibration (green) and PMMA/PA broad calibration (red).

1.1.6 Differential Scanning Calorimetry (DSC)

DSC was performed on a DSC 1 from Mettler Toledo with the software STARe V. 16.00. The samples (5-10 mg) were prepared in alumina crucibles. Table 3 displays the applied method. The usual tempering time (segment 4) was 20 min but was increased to 180 min for poly-3R-caranamide (**poly5b**). The last heating run (segment 8) was used for evaluation.

Table SI-3: DSC method for thermal analysis of polyamides.

Segment	**Temperature [°C] Start/End**	**heating rate [K/min]**	**N_2 [mL/min]**
1	20/350	20	50
2	350/20	-20	50
3	20/220	10	50
4	220 (20 min)	0	50
5	220/0	-10	50
6	0/370	10	50
7	370/0	-10	50
8	0/440	10	50

1.2 Chemicals

All applied chemicals were purchased commercially in technical grade if not otherwise stated.

2 Synthesis of lactam monomers

2.1 Synthesis of α-pinene derived lactams **5a** and **6a**

Remark: All α-pinene (**1a**) derivatives are racemic as racemic α-pinene (**1a**) was the starting material and no enatioselective reactions were performed. The entiomeric ratio has not been investigated. For clarity, only one enantiomer is discussed in text and schemes.

2.1.1 Synthesis of (1R,2R,5S)-2,6,6-trimethylbicyclo[3.1.1]heptan-3-one (**3a**)

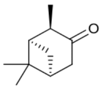

Pinanol (**2a**, 122 g, 0.79 mol, 1.0 eq.) and Al(OiPr)$_3$ (8.1 g, 40 mmol, 0.05 eq.) were dissolved in dry toluene and stirred for 10 min at room temperature. Then 3-nitrobenzaldehyde (144 g, 0.95 mol, 1.2 eq.) was added to toluene (400 mL). After 12 h, the solvent was removed under reduced pressure and the resulting yellow oil was filtered through silica gel using hexane (3.0 L) as the eluent to separate the catalyst from the reaction mixture. The organic layer was then reduced to 500 mL under reduced pressure and washed with solutions of HCl (1 M, 2x150 mL), saturated NaHCO$_3$ (2x150 mL) and water (150 mL). Total evaporation of the solvent yielded crude (1R,2R,5S)-2,6,6-trimethylbicyclo[3.1.1]heptan-3-one (**3a**, 135 g, estimated yield). Purification could not be achieved by flash column chromatography or fractional distillation. However, the structure of the desired product could be verified by GC-MS data base and $^{1}H/^{13}C$ NMR. The GC-MS purity was 70% (uncorrected values) and used as estimated yield for all calculations for the subsequent reactions. As the synthesis and isolation of the next intermediates was successful applying the crude ketone **3a**, a successful purification method was not developed.

^{1}H NMR (400 MHz, DMSO-d$_6$): δ/ppm = 2.61 – 2.53 (m, 1H), 2.52 – 2.41 (m, DMSO superposition), 2.06 (tt, J = 5.9, 2.8 Hz, 1H), 2.00 (td, J = 6.3, 1.8 Hz, 1H), 1.34 – 1.20 (m, 5H), 1.10 (d, J = 7.4 Hz, 3H), 0.80 (s, 3H).

^{13}C NMR (101 MHz, DMSO-d$_6$): δ/ppm = 213.3, 50.2, 44.4, 44.1, 38.7, 38.4, 33.5, 26.7, 21.5, 16.5.

MS (EI, 70 eV): m/z (%) = 152 (11), 97 (24), 95 (43), 83 (81), 81 (19), 69 (93), 67 (22), 55 (100), 41 (58) 39 (18).

2.1.2 Synthesis of (1R,2R,5S,E)-2,6,6-trimethylbicyclo[3.1.1]heptan-3-one oxime (**4a**)

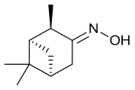

Crude pinanon (**3a**, 113 g, est. purity 70%, 0.52 mmol, 1.0 eq.) in EtOH (150 mL) was added to a mixture of hydroxylamine hydrochloride (77.4 g, 1.1x mol, 2.1 eq.) and NaOAc·3H_2O (150 g, 1.1x mol, 2.1 eq.) in EtOH (150 mL) and H_2O (150 mL) at 65 °C and stirred vigorously for 4 h. After the reaction was complete, the mixture was extracted with toluene (5x150 mL). The solvent was removed under reduced pressure to give crude (1R,2R,5S,E)-2,6,6-trimethylbicyclo[3.1.1]heptan-3-one oxime (**4a**, 107 g). 5.02 g of the yellow oil was dissolved in MeCN and pure oxime **4a** (2.8 g, 16 mmol, 65%) crystallized at -10 °C within several weeks. The crude mixture was used without further purification.

^{1}H NMR (400 MHz, DMSO-d$_6$): δ/ppm = 10.41 (s, 1H), 2.79 – 2.66 (m, 2H), 2.45 – 2.34 (m, 2H), 1.91 (tt, J = 5.8, 2.9 Hz, 1H), 1.84 (td, J = 5.9, 2.0 Hz, 1H), 1.20 (m, 6H), 0.90 (dd, J = 10.4, 6.5 Hz, 1H), 0.83 (s, 3H).

^{13}C NMR (101 MHz, DMSO-d$_6$): δ/ppm = 158.4, 45.5, 40.8, 38.5, 37.6, 33.0, 30.4, 27.1, 21.41, 19.4.

IR (diamond-ATR, neat): $\tilde{\nu}$/cm^{-1} = 3272 (m), 2985 (m), 2968 (m), 2951 (s), 2930 (m), 2886 (m), 1651 (vw), 1448 (m), 1369 (m), 1327 (w), 1262 (w), 1226 (w), 1155 (m), 1092 (w), 963 (m), 946 (s), 856 (m), 838 (m), 813 (m), 744 (s), 560 (m).

MS (EI, 70 eV): m/z (%) = 167 (6), 152 (100), 108 (29), 96 (24), 69 (45), 67 (33), 55 (77), 43 (34), 41 (63), 28 (57).

2.1.3 Synthesis of (1S,2R,6S)-2,7,7-trimethyl-3-azabicyclo[4.1.1]octan-4-one (**5a**)

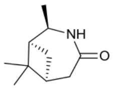

NaOH (75 mL, 4 M, 300 mmol, 3 eq.) was slowly added to a solution of pinanoxime (**4a**, 17.0 g, 0.1x mol, 1.0 eq.) in THF (80 mL) at 0 °C within 10 min. After stirring for 6 h at this temperature, 4-toluenesulfonyl chloride (21.0 g, 0.11 mol, 1.1 eq.) in THF (30 mL) was slowly added over a time of 45 min. The reaction mixture was kept at 0 °C for additional 2 h and was then allowed to warm up to room temperature overnight. As the reaction was complete, the organic layer of the two-phased mixture contained only little amounts of the desired product but various side-products from the previous intermediates and other unidentified impurities. The aqueous layer contained lactam **2a** in high purity. The organic layer was discarded, and the aqueous layer was extracted with toluene (5 x 100 mL). Toluene was removed under reduced pressure and the residue was dissolved in EtOAc for crystallization at -10 °C. (1S,2R,6S)-2,7,7-trimethyl-3-azabicyclo[4.1.1]octan-4-one (**5a**, 7.32 g, 44.0 mmol, 43%) was obtained as colourless crystals.

^{1}H NMR (400 MHz, DMSO-d$_6$): δ/ppm = 7.40 (s, 1H), 3.59 – 3.49 (m, 1H), 2.56 – 2.39 (DMSO superposition), 2.12 – 2.05 (m, 1H), 1.83 – 1.76 (m, 1H), 1.30 – 1.23 (m, 4H), 1.17 (d, J = 6.9 Hz, 3H), 1.01 (s, 3H).

^{13}C NMR (101 MHz, DMSO-d$_6$): δ/ppm = 172.6, 53.2, 46.8, 38.2, 38.0, 37.3, 30.2, 27.3, 21.7, 21.3.

IR (diamond-ATR, neat): $\tilde{\nu}$/cm^{-1} = 3270 (w), 3173 (m), 3038 (m), 2986 (m), 2951 (m), 2899 (m), 2867 (m), 1639 (s), 1491 (m), 1451 (m), 1439 (m), 1407 (m), 1355 (m), 1307 (m), 1228 (w), 1150 (w), 1121 (w), 1037 (w), 858 (m), 802 (m), 766 (m), 520 (s).

MS (EI, 70 eV): m/z (%) = 167 (4), 126 (38), 124 (33), 110 (33), 84 (60), 70 (63), 69 (71), 55 (100), 44 (93), 41 (68).

2.1.4 Synthesis of (2S,5R)-2,8,8-trimethyl-3-azatricyclo[5.1.1.02,5]nonan-4-one (**6a**)

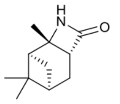

Chlorosulfonyl isocyanate (7.78 g, 55.0 mmol, 1.0 eq.) in dry THF (30 mL) was dropped into a solution of racemic *α*-Pinene (**1a**, 7.50 g, 55.0 mmol, 1.0 eq.) in dry THF (200 mL) at room temperature within 30 min. After stirring for 1 h, the reaction mixture was cooled to 0 °C. The pH value was raised from 2 to 7-8 by slow addition of KOH (3.5 M). A solution of Na_2SO_3 (1M, 100 mL) was dropped to the reaction mixture while the pH value was maintained at 7-8 using KOH. During the whole progress, the reaction temperature was kept below 5 °C. The reaction mixture was then stirred for 1 h at room temperature. After extraction with toluene (5x100 mL) and evaporation of solvents under reduced pressure, the obtained yellow oil was dissolved in n-hexane (10 mL) and stored at 5 °C overnight. The colourless crystals thus formed were washed with precooled n-hexane and dried in vacuo to give (2S,5R)-2,8,8-trimethyl-3-azatricyclo[5.1.1.02,5]nonan-4-one (**4a**, 7.28 g, 40.7 mmol, 74%).

^{1}H NMR (400 MHz, DMSO-d$_6$): δ/ppm = 7.66 (s, 1H), 2.58 – 2.53 (m, 1H), 1.94 – 1.83 (m, 2H), 1.25 (s, 3H), 1.08 – 0.92 (m, 8H), 0.60 – 0.48 (m, 2H).

^{13}C NMR (101 MHz, DMSO-d$_6$): δ/ppm = 169.5, 53.5, 51.6, 28.8, 28.0, 26.5, 18.2, 17.7, 17.4, 17.1, 15.7.

IR (diamond-ATR, neat): $\tilde{\nu}$/cm^{-1} = 2991 (w), 2981 (w), 2925 (m), 2912 (m), 2869 (w), 1742 (s), 1715 (s), 1473 (m), 1454 (m), 1378 (m), 1365 (m), 1297 (m), 1123 (m), 1108 (m), 1071 (m), 1028 (m), 711 (s), 690 (m), 585 (m).

MS (EI, 70 eV): m/z (%) = 179 (0.3), 136 (18), 94 (12), 93 (100), 92 (52), 91 (24), 79 (15), 77 (14), 70 (11), 41 (17).

2.2 Synthesis of (+)-3-carene derived lactams **5b** and **6b**

2.2.1 Synthesis of (1R,4R,6S)-4,7,7-trimethylbicyclo[4.1.0]heptan-3-one (**3b**)

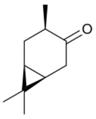

3b

Caranol (**2b**, 90.0 g, 0.46 mol, 1.0 eq.) and Al(OiPr)$_3$ (17.9 g, 87.x mmol, 0.2 eq.) were dissolved in toluene (400 mL) and stirred at room temperature for 0.5 h. 3-Nitrobenzaldehyde (105 g, 0.69 mol, 1.5 eq.) were added portion-wise and it was stirred for 14 h. Full conversion was verified by GC-MS and the solvent was removed under reduced pressure. The remaining viscous oil was poured into water and the resulting precipitate, which predominately consisted of 3-nitrophenol was filtered off and repeatedly washed with hexane. The aqueous layer was extracted with hexane (8x100 mL) and the combined extraction and washing fractions were washed with a saturated solution of NaHCO$_3$ (100 mL) and dried over Na$_2$SO$_4$. The solvent was removed under reduced pressure to give crude (1R,4R,6S)-4,7,7-trimethylbicyclo[4.1.0]heptan-3-one (**3b**, 75.7g, x mol, x%) as yellow oil. A small sample was purified by LC (hexane 12:1 ethyl acetate) and 57w% was obtained, corresponding to a total yield of 61% (0.28 mol).

^{1}H-NMR (DMSO-d$_6$, 400 MHz): δ (ppm) = 2.57 (dd, J = 17.6, 8.4 Hz, 1H), 2.41 – 2.23 (m, 2H), 2.12 (dd, J = 17.6, 2.1 Hz, 1H), 1.20 – 1.11 (m, 1H), 1.09 – 1.02 (m, 1H), 1.00 (s, 3H), 0.99 – 0.93 (m, 1H), 0.83 (d, J = 6.4 Hz, 3H), 0.78 (s, 3H).

^{13}C-NMR (DMSO-d$_6$, 101 MHz): δ (ppm) = 215.2, 41.0, 36.4, 29.2, 27.6, 22.5, 19.6, 18.9, 14.7, 14.1.

MS (EI, 70 eV): m/z (%) = 152 (40), 137 (19), 110 (46), 109 (44), 96 (25), 95 (43), 83 (13), 82 (51), 81 (100), 79 (24), 69 (27), 68 (16), 67 (97), 56 (14), 55 (27), 53 (16), 43 (12), 41 (45), 39 (22), 27 (13).

IR (Diamond-ATR, neat): $\tilde{\upsilon}$ (cm^{-1}) = 2930 (m), 1710 (vs), 1532 (m), 1456 (m), 1350 (m), 1165 (w), 1045 (w).

2.2.2 Synthesis of (1R,4R,6S,E)-4,7,7-trimethylbicyclo[4.1.0]heptan-3-one oxime (**4b**)

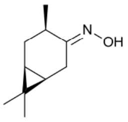

4b

Caranon (**4b**, 25.3 g, 0.17 mol, 1.0 eq.), NaOAc·3H_2O (26.9 g, 0.2x mol, 1.2 eq.) and hydroxylamine hydrochloride (17.1 g, 0.25 mol, 1.5 eq.) were dissolved in water (75 mL) and ethanol (105 mL) and stirred at 60 °C for 1 h. GC-MS showed full conversion of ketone **3b**. The mixture was extracted with toluene (4x100 mL) and the combined organic layers were extracted with a saturated solution of $NaHCO_3$ (225 mL) and brine (150 mL). Toluene was removed under reduced pressure to give crude (1R,4R,6S,E)-4,7,7-trimethylbicyclo[4.1.0]heptan-3-one oxime (**4b**, 27.0 g) as colourless oil. A small sample was purified by LC (hexane 4:1 ethyl acetate) and 91w% was obtained, corresponding to a total yield of 90% (0.18 mol). As crystallization failed, the crude oxime was used without further purification.

^{1}H NMR (400 MHz, DMSO-d$_6$): δ/ppm = 10.33 (s, 1H), 2.79 (dd, J = 18.1, 1.6 Hz, 1H), 2.25 – 2.07 (m, 3H), 1.01 – 0.92 (m, 7H), 0.91 – 0.82 (m, 1H), 0.79 – 0.70 (m, 4H).

^{13}C NMR (101 MHz, DMSO-d$_6$): δ/ppm = 160.2, 33.7, 29.4, 27.9, 19.8, 19.7, 19.3, 17.8, 16.5, 14.5.

MS (EI, 70 eV): m/z (%) = 167 (17), 136 (57), 134 (37), 112 (60), 108 (62), 107 (56), 106 (51), 95 (32), 94 (37), 93 (44), 91 (33), 81 (45), 79 (55), 69 (44), 67 (69), 55 (100), 53 (35), 43 (45), 41 (96), 39 (40), 28 (41).

IR: $\tilde{\nu}$ (cm^{-1}) = 3277 (w), 2929 (m), 2865 (w), 1375 (w), 939 (s), 819 (m).

2.2.3 Synthesis of (1R,5R,7S)-5,8,8-trimethyl-4-azabicyclo[5.1.0]octan-3-one (**5b**)

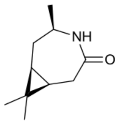

5b

Crude caranoxime (**4b**, 26.5 g, w = 91 %, 0.14 mol, 1.0 eq.) was dissolved in THF (120 mL) and cooled with an ice bath. Sodium hydroxide solution (4 M, 120 mL, 0.48 mol, 3.3 eq.) were dropped into the reaction mixture within 30 min. The resulting emulsion was stirred vigorously for 4.5 h at 5 °C. P-toluenesulfonyl chloride (33.0 g, 0.18 mol, 1.2 eq.) in THF (42 mL) was slowly added within 2 h and the temperature was kept below 10 °C. After stirring for additional 12 h at room temperature, the layers were separated, and the organic solvent was removed under reduced pressure. The remaining brown oil was poured into water and the aqueous layers were combined and extracted with toluene (5x100 mL). The combined organic layers were washed with a solution of saturated NaHCO$_3$ and toluene was removed under reduced pressure to give crude (1R,5R,7S)-5,8,8-trimethyl-4-azabicyclo[5.1.0]octan-3-one (**5b**, 24.3 g). After crystallization from a mixture of hexane (300 mL) and EtOAc (50 mL), lactam **5b** (9.2 g, 55 mmol, 38%) was yielded as colourless crystals.

^{1}H NMR (400 MHz, DMSO-d$_6$): δ/ppm = 0.71 – 0.78 (m, 2H); 0.99 und 1.03 (2s, 6 H); 1.06 (d, J = 6,4 Hz, 3H); 1.41 – 1.50 (m, 1H); 1.81-1.85 (m, 1H); 2.29-2.37 (m, 2H); 3.43 – 3.48 (m, 1H); 6.91 (s, 1H).

^{13}C NMR (101 MHz, DMSO-d$_6$): δ/ppm = 16.3, 19.2, 22.0, 23.8, 24.4, 28.7, 30.2, 33.5, 50.1, 173.5.

MS (EI, 70 eV): m/z (%) = 167 (11), 152 (30), 125 (14), 124 (17), 110 (60), 99 (18), 96 (11), 82 (38), 81 (47), 79 (15), 70 (11), 68 (11), 67 (66), 57 (20), 55 (19), 53 (14), 44 (100), 43 (14), 42 (14), 41 (37), 39 (18).

IR: $\tilde{\nu}$ (cm^{-1}) = 3205 (m), 3075 (w), 2924 (m), 1646 (vs), 1454 (m), 1378 (m), 1328 (s), 844 (s).

2.2.4 Synthesis of (1R,3R,5S)-4,4,7-trimethyl-8-azatricyclo[5.2.0.03,5]nonan-9-one (**6b**)

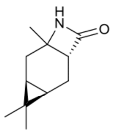

6b

(+)-3-carene (2.72 g, 18.x mmol, 1.0 eq.) was dissolved in dry THF (25 mL) and a solution of chlorosulfonyl isocyanate (2.84 g, 19.6 mmol, 1.1 eq.) in dry THF (25 mL) was added dropwise at room temperature. After stirring for 24 h, the mixture was cooled with an ice bath and the pH value was carefully set to 8 under application of a solution of KOH (3.5 M). A precooled solution of Na_2SO_3 (2 M, 50 mL, x mol, x eq.) was slowly added and the pH value was kept between 7 and 9 during this process. After the addition was complete, it was stirred for an hour before extraction with toluene (5x50 mL). The thereby formed precipitate was filtered off and discarded. Toluene was removed under reduced pressure and the residue was dissolved in hexane for crystallization. (1R,3R,5S)-4,4,7-trimethyl-8-azatricyclo[5.2.0.03,5]nonan-9-one (**6b**, 0.6 g, x mol, 18%) was yielded as colourless crystals.

^{1}H NMR (400 MHz, DMSO-d$_6$): δ/ppm = 0.48 – 0.62 (m, 2H); 0.94 (s, 3H); 1.01 (s, 3H); 1.00 – 1.11 (m, 2H); 1.25 (s, 3H); 1.84 – 1.94 (m, 2H); 2.53 (m, 1H), 7.66 (s, 1H).

^{13}C NMR (101 MHz, DMSO-d$_6$): δ/ppm = 15.7, 17.1, 17.4, 17.7, 18.2, 26.5, 28.0, 28.8, 51.6, 53.5, 169.5.

MS (EI, 70 eV): m/z (%) = 179 (2) [M$^+$], 136 (34), 121 (24), 108 (10), 107 (10), 94 (16), 93 (100), 92 (28), 91 (26), 84 (13), 81 (10), 80 (17), 79 (20), 77 (17), 70 (10), 67 (14), 55 (11), 43 (16), 42 (21), 41 (21), 39 (12).

IR: $\tilde{\nu}$ (cm^{-1}) 3229 (m), 2927 (m), 1759 (s), 1709 (s), 1446 (m), 666 (m), 643 (m).

2.2.5 Synthesis of 2-((1R,3S)-3-((R)-2-aminopropyl)-2,2-dimethylcyclopropyl)acetic acid (**hyd5b**)

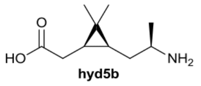

hyd5b

ε-Caranlactam (**5b**, 1.0 g, 6.0 mmol, 1.0 eq.), NaOH (0.48 g, 12 mmol, 2.0 eq.) and water (3.0 mL) were dissolved in EtOH (7.0 mL) and stirred for 1 h at 80 °C. The conversion of lactam **5b** was observed by GC-MS. The reaction mixture was cooled to room temperature and the pH value was set to 7 by addition of a solution of HCl (1 M). The formed precipitate was filtered off and the solvent was removed under reduced pressure. The residue was crystallized from EtOH and 2-((1R,3S)-3-((R)-2-aminopropyl)-2,2-dimethylcyclopropyl)acetic acid (**hyd5b**, 0.4x g, 2.2 mmol, 36%) was yielded as colourless crystals.

^{1}H-NMR (D$_2$O): *δ* (ppm) = 0.54 (dd, J = 15.4, 7.2 Hz, 1H); 0.72 – 0.90 (m, 1H); 0.92 (s, 3H); 1.06 (s, 3H); 1.30 (d, J = 6.6 Hz, 3H); 1.36 – 1.52 (m, 2H); 2.09 (dd, J = 16.1, 8.3 Hz, 1H); 2.20 (dd, J = 16.1, 7.1 Hz, 1H), 3.10 – 3.30 (m, 1H)

IR: $\tilde{\nu}$ (cm^{-1}) = 3041 (m), 2943 (m), 2880 (m), 1621 (s), 1521 (vs), 1418 (m), 1386 (vs), 674 (s)

3. Ring opening polymerization of the lactam monomers

3.1 General Polymerization method of the ε-lactams 5a and 5b

In a typical procedure, lactam **2a** or **2b** was stirred in a sealed argon-flushed glass tube at different temperatures between 150-280 °C. After complete melting at the given temperature, the initiator was added, directly followed by the activator. The reaction mixture was stirred at various temperatures and times. If a change of the viscosity was observed, the reaction mixture was kept at that temperature for at least 20 min. and then cooled to room temperature. The obtained solid or viscous oil was washed with acetone, ethanol and water. To remove the residual monomers and oligomers, the resulting solids were crushed (in case of very hard solids, liquid nitrogen was applied to facilitate the crushing) and stirred in a mixture of H_2O and MeOH (1:1) under reflux for 24 h. After filtration and repeated washing with acetone, the obtained yellow or colourless powders were dried in vacuo and analysed by GPC, IR and NMR if they were soluble.

3.2 Polymerization of the β-lactams 6a and 6b

The β-lactam based polymers were synthesized in the same set-up as the ε-lactams. NaH (0.02 eq.) were used as initiator and an activator was not required. The reaction temperature was 160 °C The residual monomers were removed by the same protocol as described above.

4. NMR analysis of the polyamides

4.1 Graphical NMR comparison of lactam 5a and poly5a

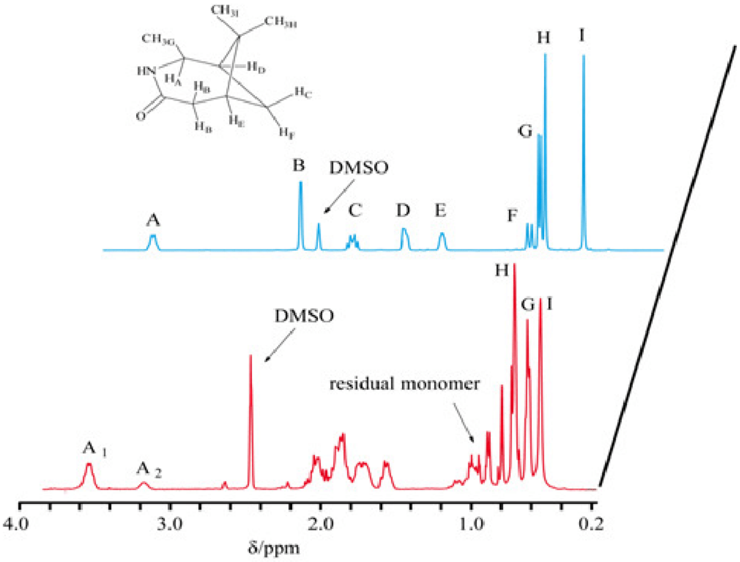

Figure SI-2: ^{1}H-spectra of lactam 5a and the corresponding poly6a in a mixture of formic acid and deuterated DMSO.

4.2 Complete NMR signal assignment of poly5b

For 2D spectra, see chapter 6.

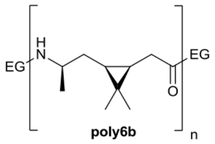

^{1}H NMR (400 MHz, DCOOD): δ/ppm = 4.13 – 3.99 (1H, -NH-C$\underline{H}$CH$_3$-CH$_2$-), 2.55 – 2.35 (2H, -HN-CO-C$\underline{H_2}$-CH-), 1.77 – 1.60 (1H, -NH-CHCH$_3$-C$\underline{H_2}$-CH-), 1.54 – 1.39 (1H, -NH-CHCH$_3$-C$\underline{H_2}$-CH-), 1.32 – 1.22 (3H, -NH-CHC$\underline{H_3}$-CH$_2$-), 1.18 – 1.07 (3H, -CO-CH$_2$-CH-CCHCH$_3$C$\underline{H_3}$-, methyl group facing carboxylic group), 1.06 – 1.00 (3H, -NH-CHCH$_3$-CH-CCHC$\underline{H_3}$CH$_3$-, methyl group turned away from carboxylic group), 0.99 – 0.88 (1H, -CO-CH$_2$-C$\underline{H}$-), 0.76 – 0.64 (1H, -NH-CHCH$_3$-CH$_2$-C$\underline{H}$-).

^{13}C NMR (100 MHz, DCOOD): δ/ppm = 176.6 (-$\underline{C}$O-), 47.5 (-NH-$\underline{C}$HCH$_3$-), 31.3 (-CO-$\underline{C}$H$_2$-), 30.7 (-CHCH$_3$-$\underline{C}$H$_2$-), 28.2 (-CCHCH$_3$$\underline{C}H_3$-, methyl group facing carboxylic group), 23.3 (-CO-CH$_2$-$\underline{C}$H-), 21.9 (-CHCH$_3$-CH$_2$-$\underline{C}$H-), 19.3 (-CH$\underline{C}$H$_3$-), 17.9 (-$\underline{C}$CHCHCH$_3$CH$_3$-), 14.5 (-CCH$\underline{C}$H$_3$CH$_3$-, methyl group facing turned away from carboxylic group).

4.3 Graphical NMR comparison of lactam 5b, hyd5b and poly5b

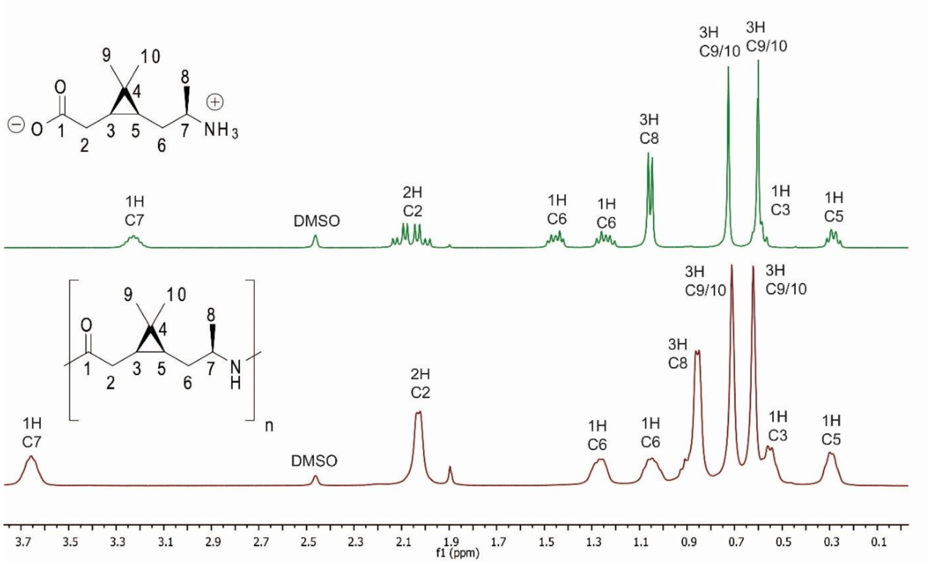

Figure SI-3: ^{1}H-spectra of hydrolysed monomer **hyd5b** and polyamide **poly5b**. The spectra were measured in a mixture of formic acid and deuterated DMSO.

4.4 Complete NMR signal assignment for poly6b

For 2D spectra, chapter 6.

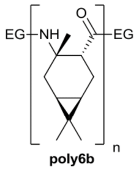

poly6b

^{1}H NMR (400 MHz, C_6D_6): δ/ppm = 8.36 – 8.08 (1H, $\mathrm{-N\underline{H}-}$), 3.73 (1H, $\mathrm{-CCH_3NH-C\underline{H}_2-CH-}$), 2.41 (1H, $\mathrm{-HCCO-C\underline{H}_2-CH-}$), 1.74 (1H, $\mathrm{-HCCO-C\underline{H}_2-CH-}$), 1.56 (1H, $\mathrm{-CCH_3NH-\underline{H}CCO-CH_2-}$), 1.41 (3H, $\mathrm{-CC\underline{H}_3NH-}$), 0.89 – 0.57 (8H superposition; $\mathrm{-CC\underline{H}_3C\underline{H}_3}$, 6H; $\mathrm{-CCH_3NH-C\underline{H}_2-CH-}$, 1H; $\mathrm{-CCH_3NH-CH_2-C\underline{H}-}$, 1H), 0.54 – 0.42 (1H,$\mathrm{-HCCO-CH_2-C\underline{H}-}$).

^{13}C NMR (101 MHz, C_6D_6): δ/ppm = 186.1($\mathrm{-\underline{C}O-}$), 63.6 ($\mathrm{-\underline{C}CH_3NH-}$), 61.5 ($\mathrm{-\underline{C}HCO-}$), 39.5-$\mathrm{CCH_3NH-\underline{C}H_2-CH-}$, 38.8 ($\mathrm{-C\underline{C}H_3CH_3-}$), 34.7 ($\mathrm{-C\underline{C}H_3NH-}$), 31.3 ($\mathrm{-HCCO-\underline{C}H_2-CH-}$), 29.3 ($\mathrm{-CCH_3NH-\underline{C}H_2-\underline{C}H-}$), 28.4 ($\mathrm{-CCH_3NH-CH_2-\underline{C}H-}$), 27.7 ($\mathrm{-\underline{C}CH_3CH_3}$), 25.4 ($\mathrm{-CCH_3\underline{C}H_3-}$).

5 Pictures of transparent Polyamides and water uptake measurement

5.1 Poly-3R-caranamide (poly5b) after tempering (220 °C/180 min)

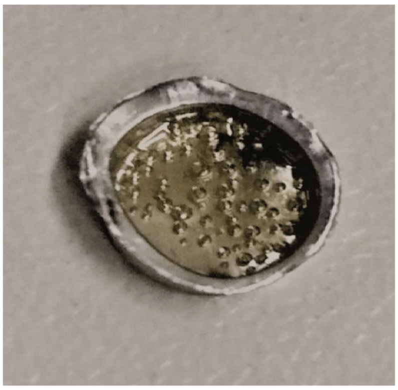

5.2 Poly-3R-caranamide (poly5b) crude polymer

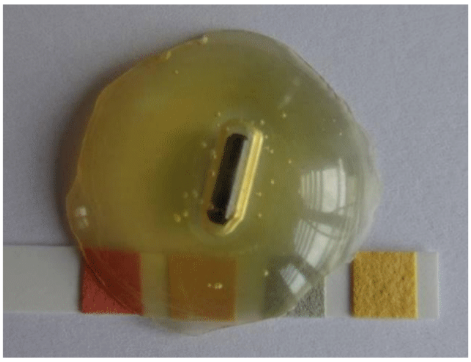

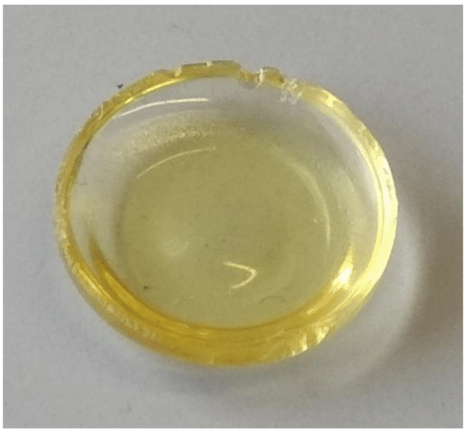

5.3 Polycaran-β-amide (poly6b)

5.4 Water-uptake of Poly-3R-caranamide (poly5b) compared to PA6

PA6 was polymerized and purified as described in section 3.1 (2.8 mmol caprolactam, 0.1 mmol NaH 60% on paraffin wax, 0.05 mmol Ac_2O, 180 °C). 30-42 mg of PA6 (3 samples, table SI-4 entry 1-3) or **poly5b** (2 samples, table SI-5 entry 4-5) were transferred in a DSC alumina crucible and tempered for 3 min at 230 °C in a nitrogen atmosphere to remove water from the polyamide powders and to produce solid polymer blocks. The masses were measured on an OHAUS Discovery DV215CD balance with a maximum error of 0.01 mg. The blocks were stirred in water at 25 °C for three days. The samples were then dried on air and scaled after 30 min and 4.5 h. The samples were then heated to 80 °C in an oven for three hours; this was sufficient to completely remove the residual water from the **poly5b** polymer blocks. The higher water uptake of **PA6** under saturation conditions and the increased drying time supports the suggestion that **poly5b** is less hydrophilic than PA6.

Table SI-:4 Pre-treatments: A = DSC sample polymer block; B = Water-bath (3 d) and Drying on air (0.5 h); C = Drying on air (4.5 h); D = Drying at 80 °C (3.0 h).

		A	B	C	D
Entry	**Polymer**	**Water uptake [w%] Weight [mg]**			
1	PA6-1	35.66	37.45	37.01	36.05
			5.4	4.0	1.5
2	PA6-2	37.78	39.57	39.36	38.16
			4.9	4.3	1.1
3	PA6-3	31.86	33.67	32.58	32.2
			5.7	2.3	1.1
4	Poly 5b-1	40.75	41.44	40.80	40.62
			2.0	0.44	0
5	Poly 5b-2	30.89	31.32	30.92	30.7
			2.3	0.75	< 0.1

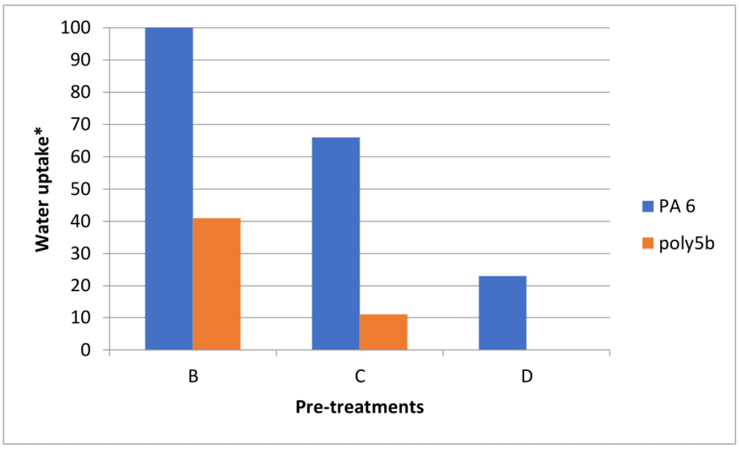

Figure SI-4: Average Water-uptake (B) and drying (C, D) of polymer blocks of **PA6** (blue) and **poly5b** (orange). * = Average water uptake of **PA6** samples, table SI-4, entries 1-3, after pre-tratment B was set to 100%.

6 NMR Spectra

6.1 NMR Spectra of (1R,2R,5S)-2,6,6-trimethylbicyclo[3.1.1]heptan-3-one (**3a**) in DMSO-d_6

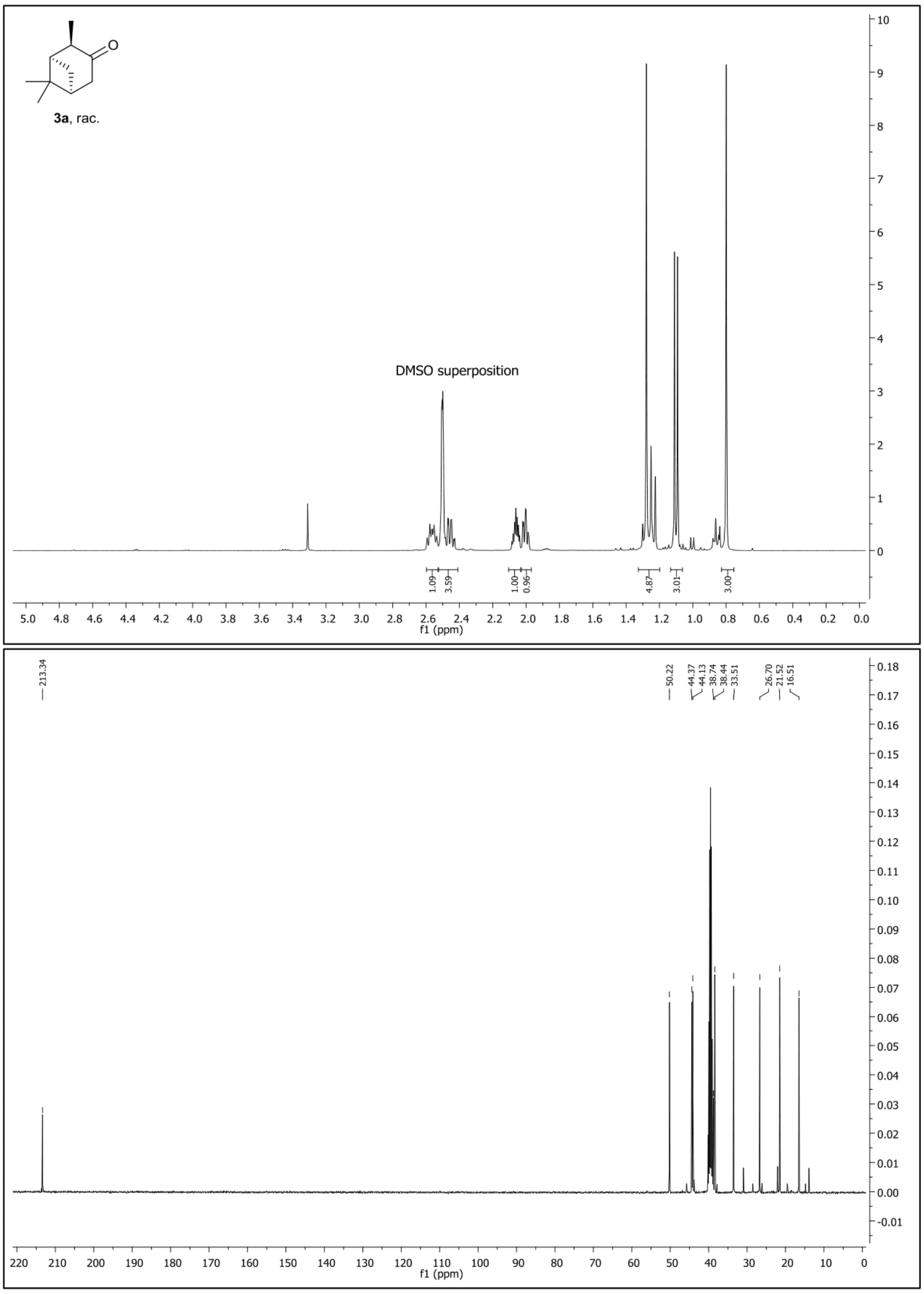

6.2 NMR-Spectra of (1R,2R,5S,E)-2,6,6-trimethylbicyclo[3.1.1]heptan-3-one oxime (**4a**) in DMSO-d_6

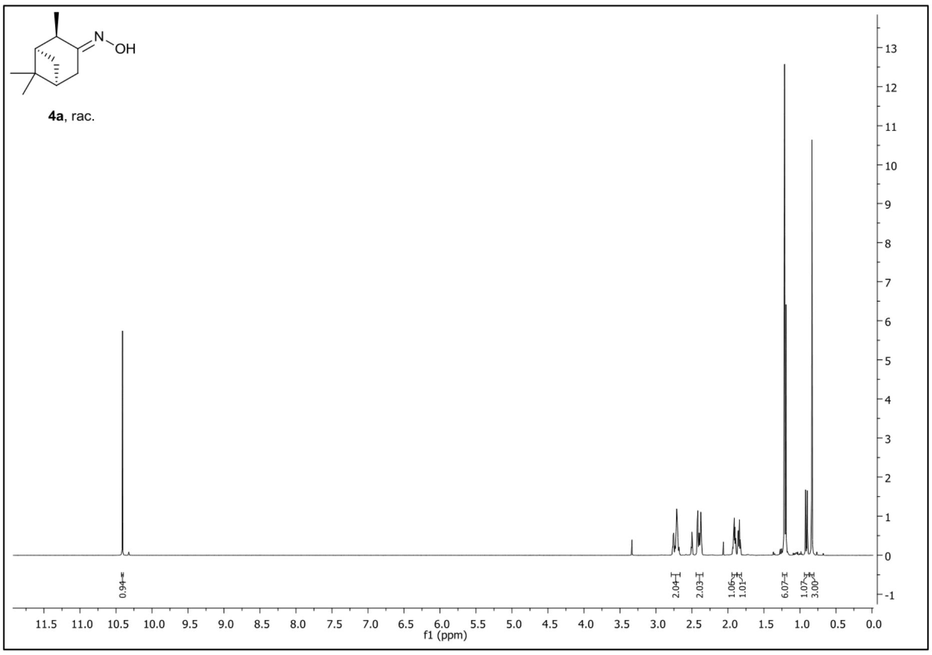

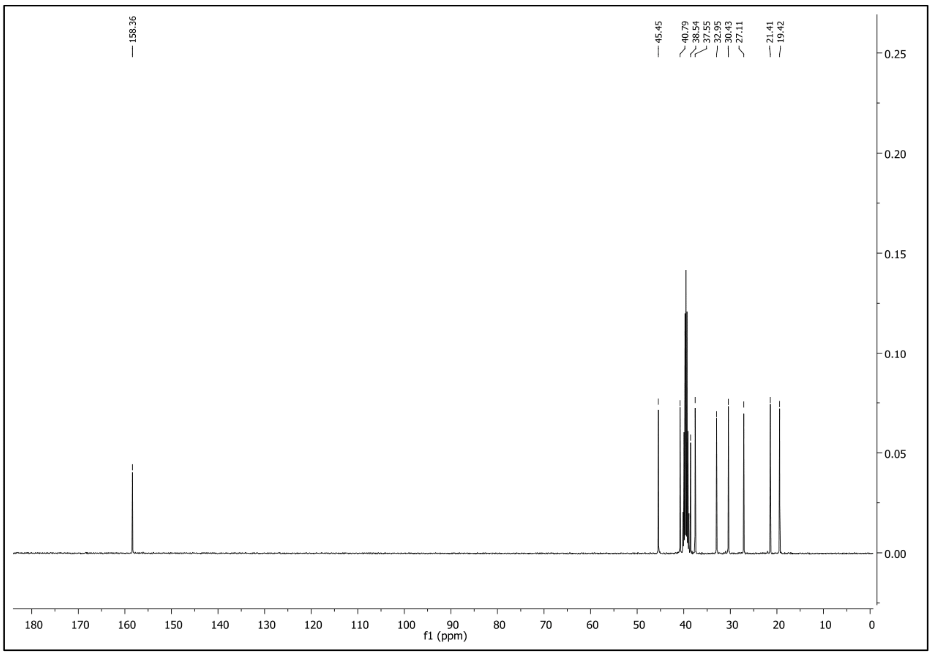

6.3 NMR-Spectra of (1S,2R,6S)-2,7,7-trimethyl-3-azabicyclo[4.1.1]octan-4-one (**5a**) in DMSO-d_6

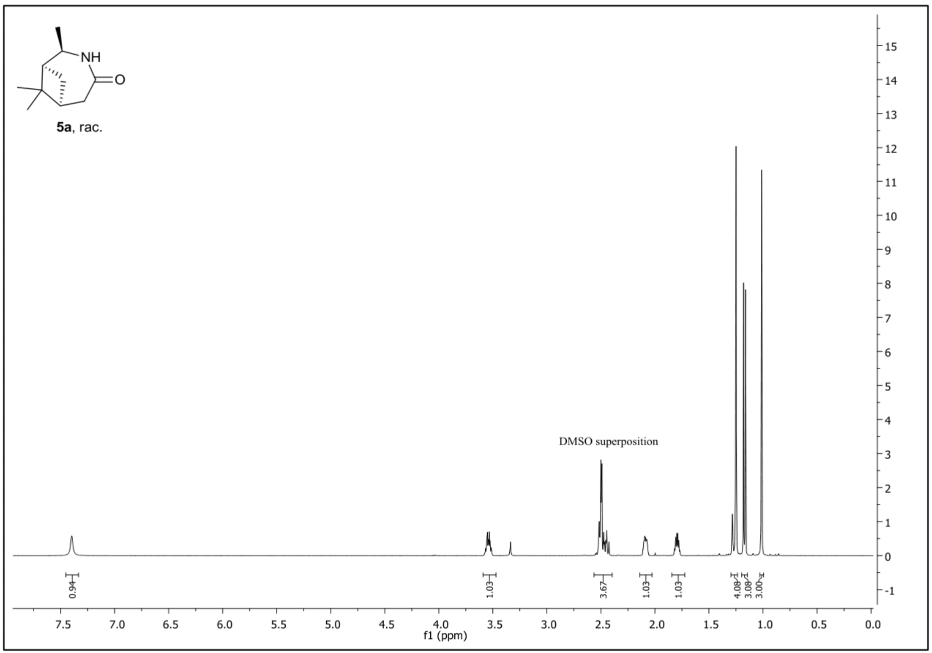

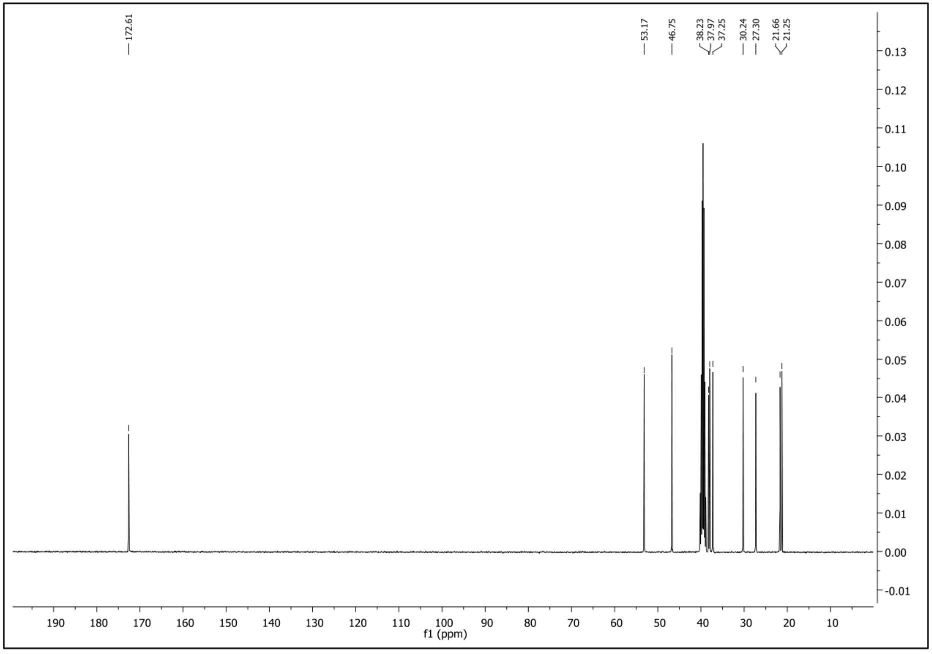

6.4 NMR Spectra of (2S,5R)-2,8,8-trimethyl-3-azatricyclo[5.1.1.02,5]nonan-4-one (**6a**) in DMSO-d_6

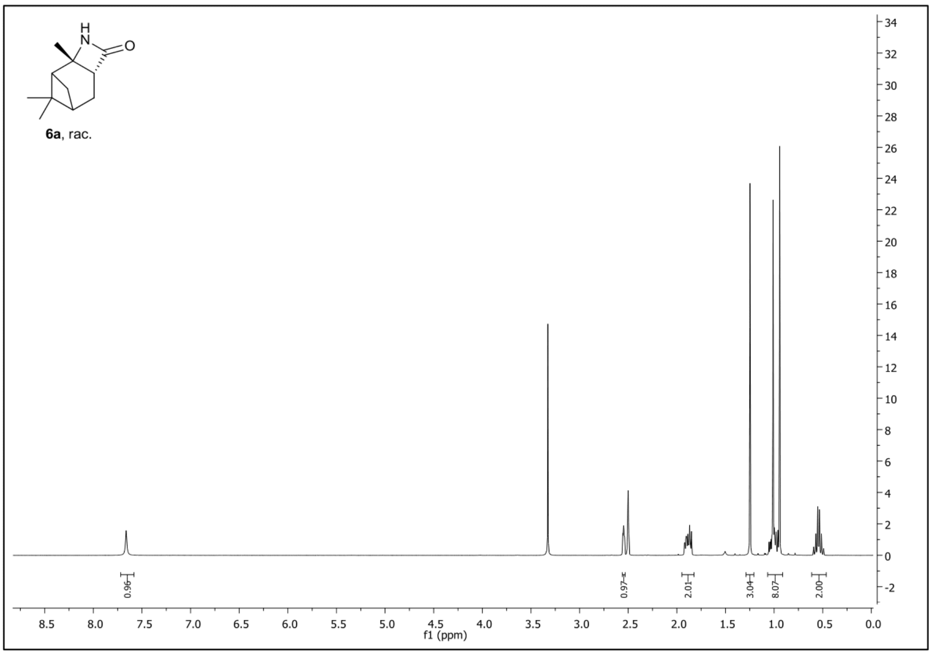

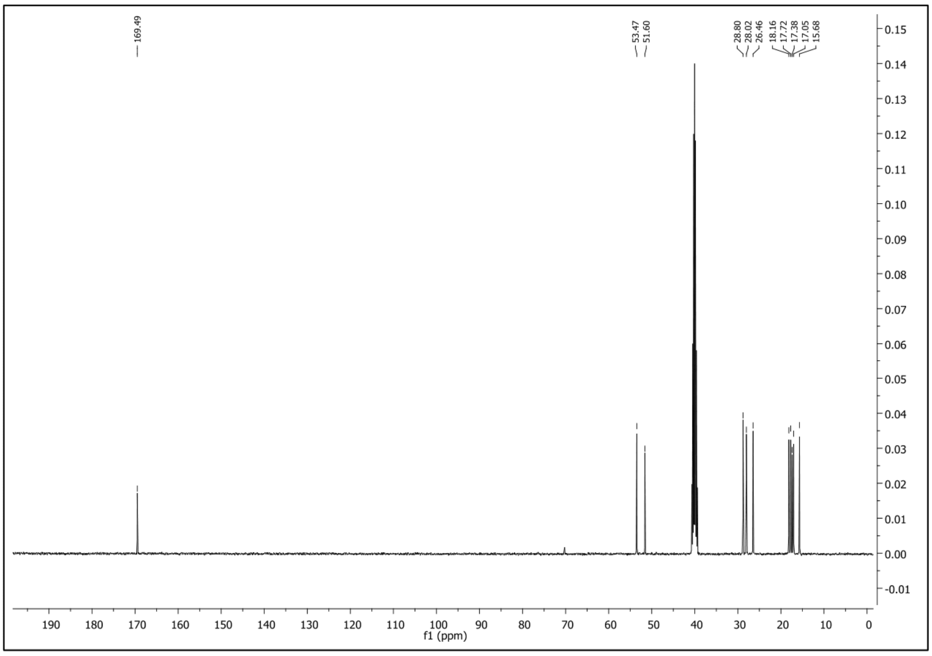

6.5 NMR-Spectra of (1R,4R,6S)-4,7,7-trimethylbicyclo[4.1.0]heptan-3-one (**3b**) in DMSO-d_6

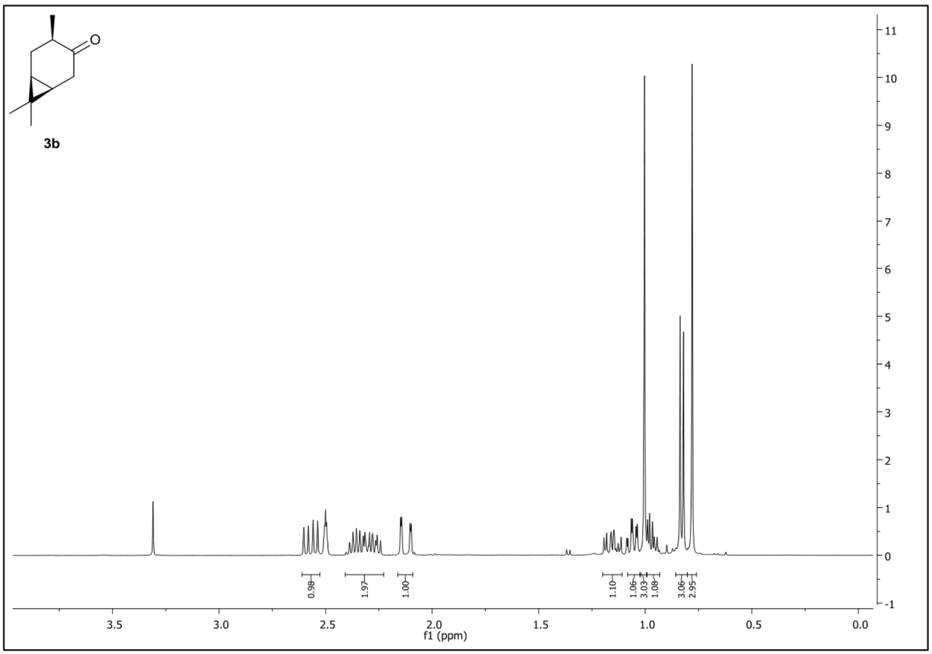

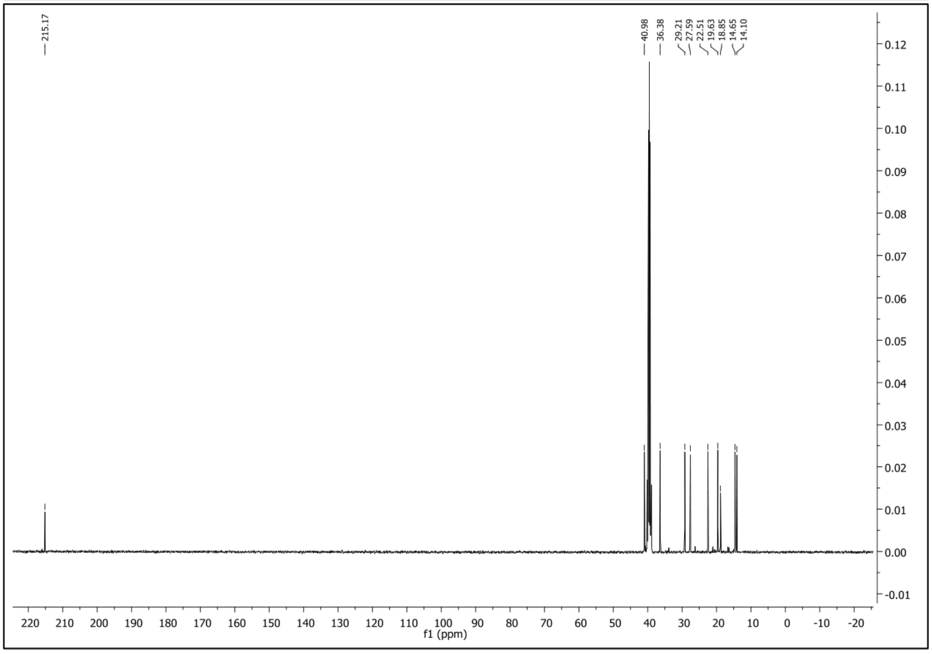

6.6 NMR-Spectra of (1R,4R,6S,E)-4,7,7-trimethylbicyclo[4.1.0]heptan-3-one oxime (**4b**) in DMSO-d_6

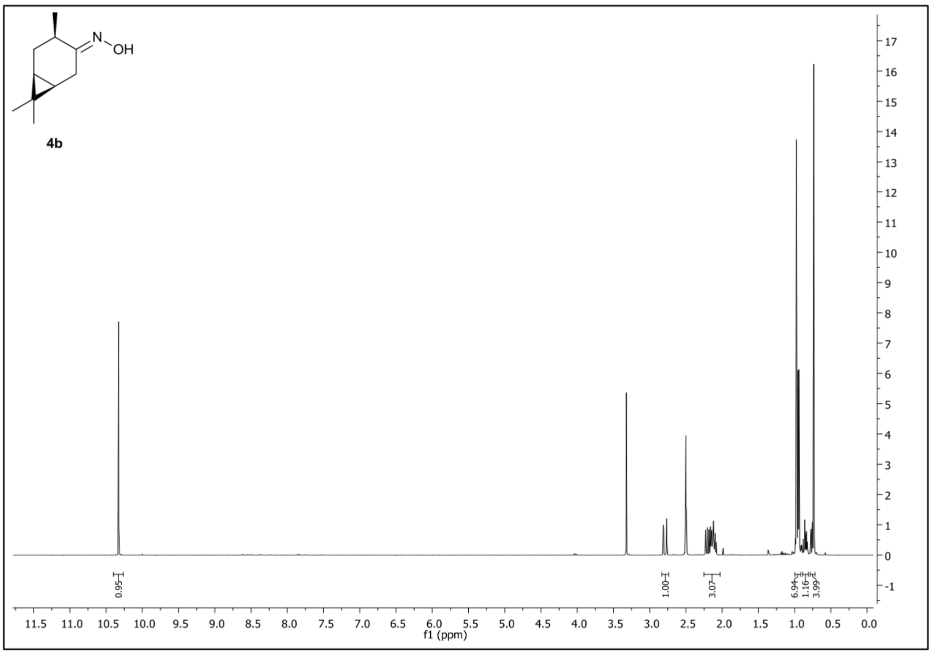

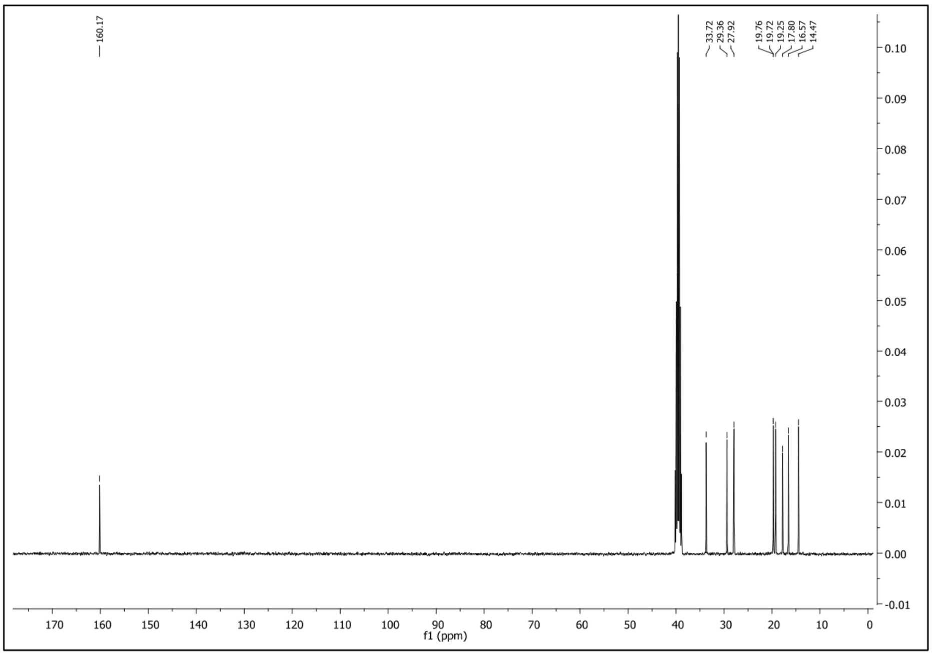

6.7 NMR-Spectra of (1R,5R,7S)-5,8,8-trimethyl-4-azabicyclo[5.1.0]octan-3-one (**5b**) in DMSO-d_6

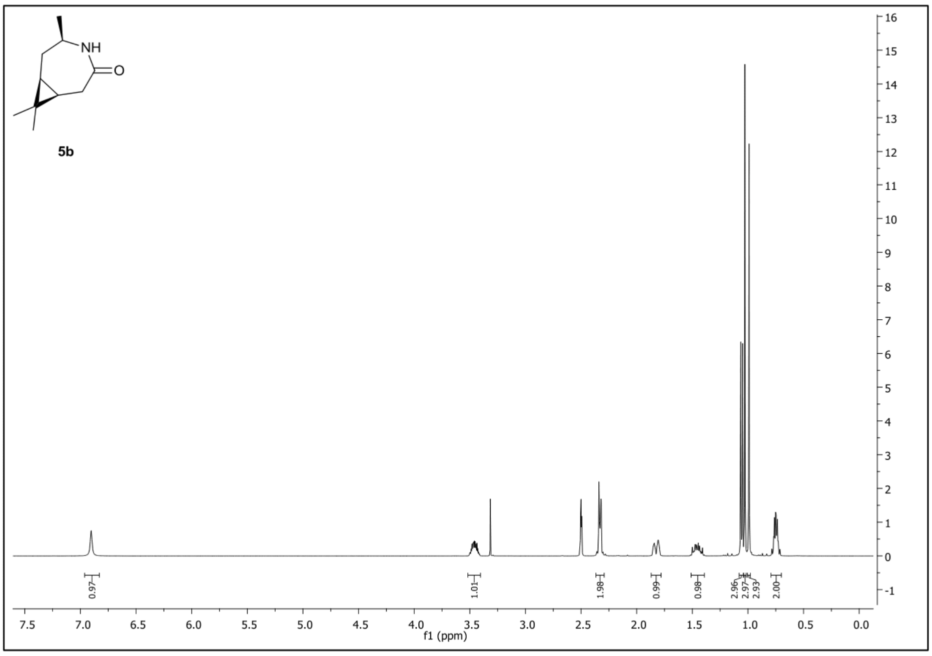

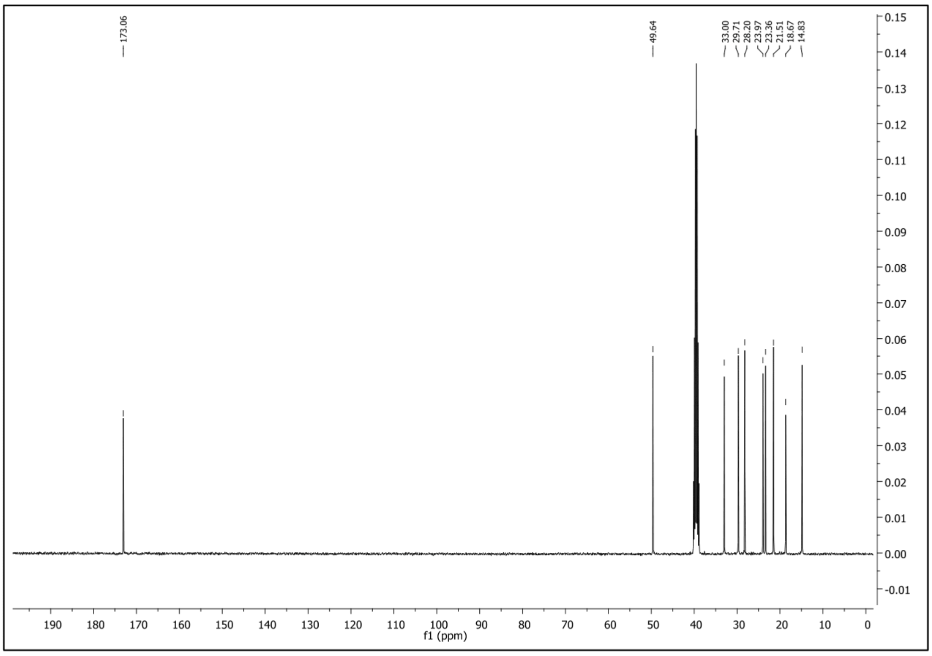

6.8 NMR-Spectra of (2S,5R)-2,8,8-trimethyl-3-azatricyclo[5.1.1.02,5]nonan-4-one (**6a**) in DMSO-d_6

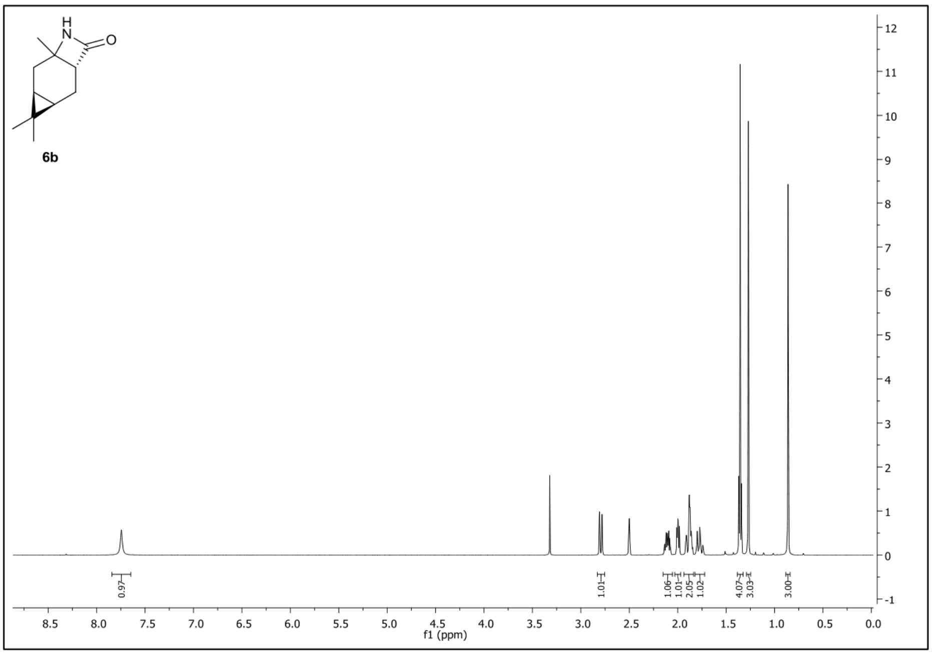

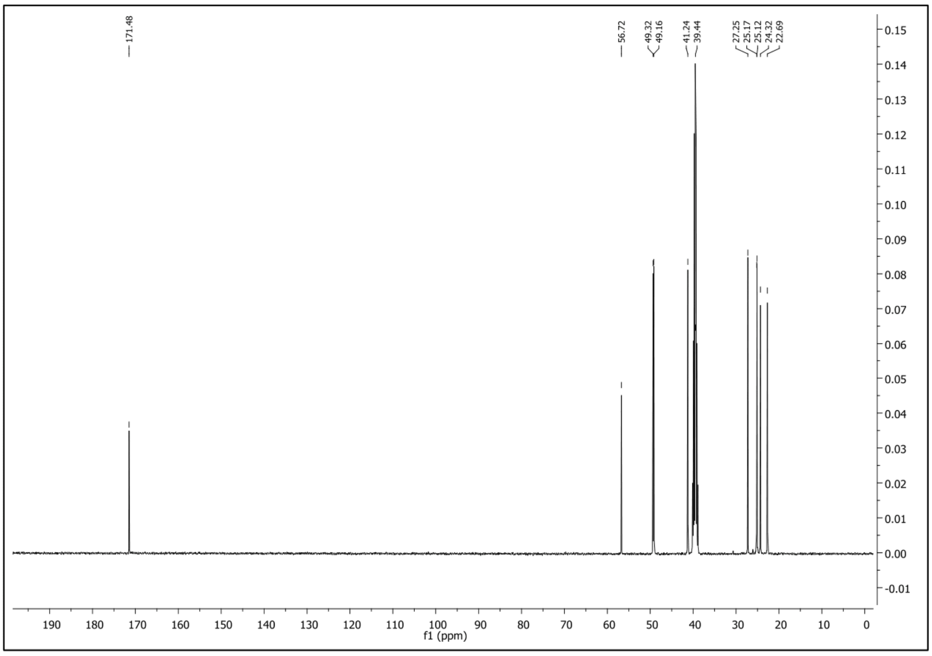

6.9 NMR Spectra of **poly5b** in DMSO-d_6

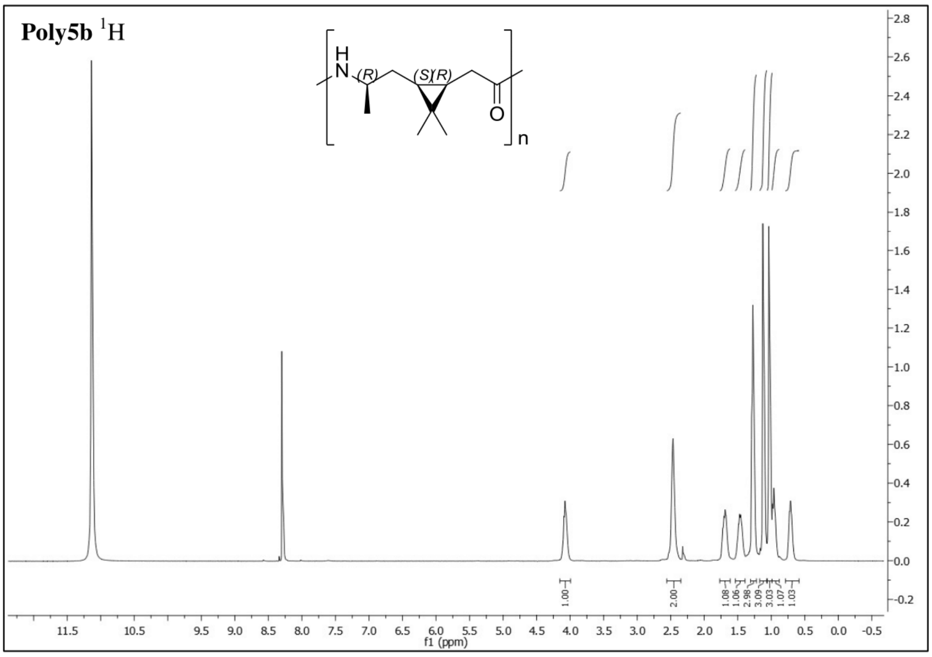

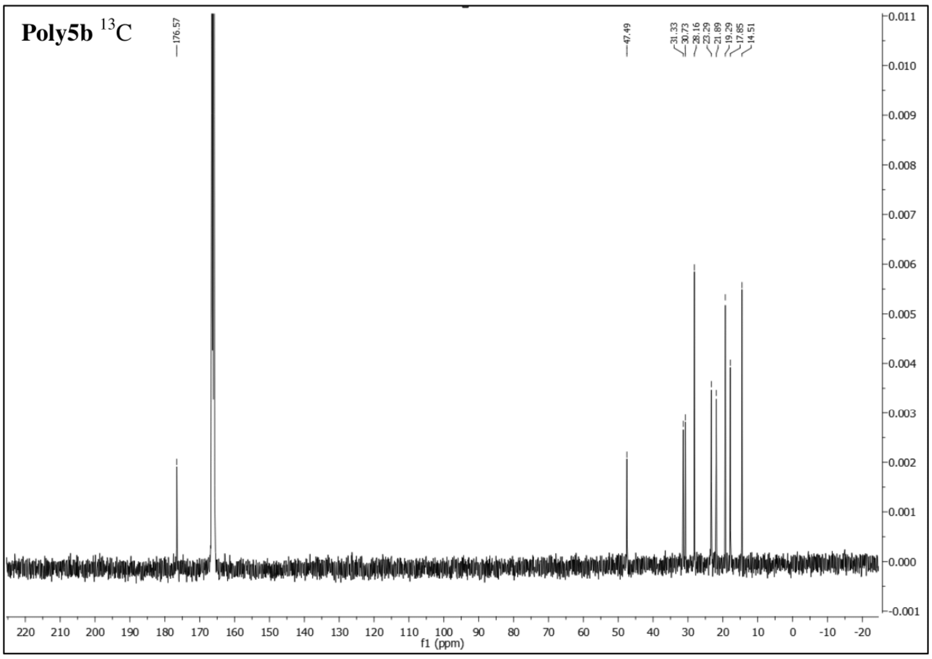

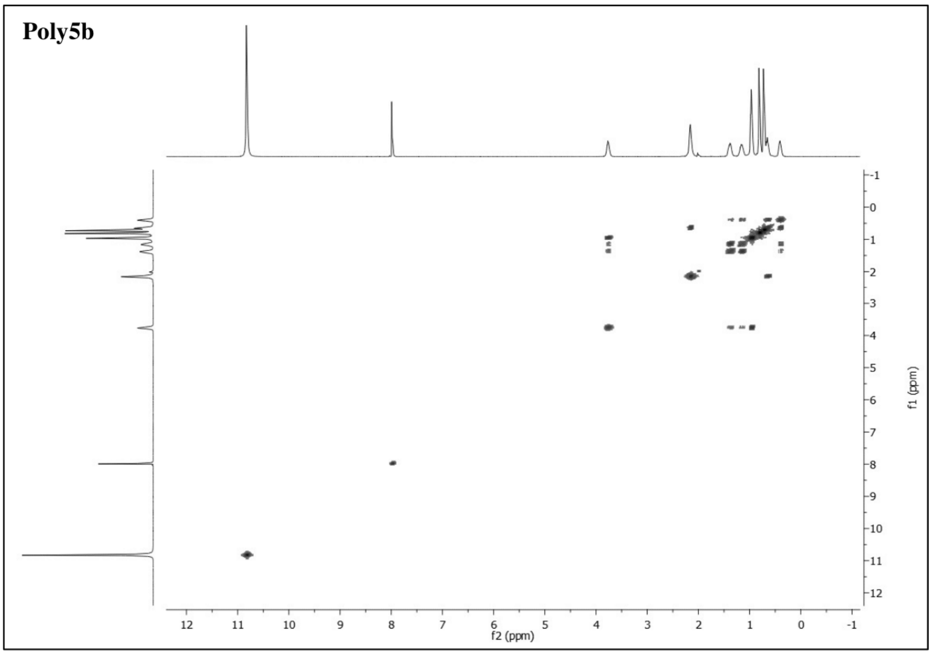

Poly5b

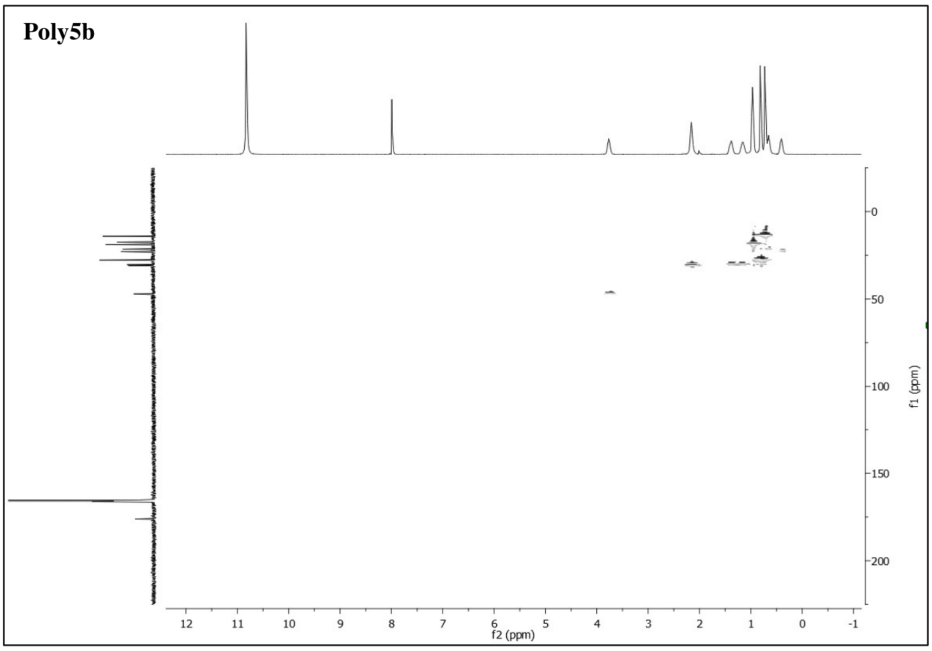

Poly5b

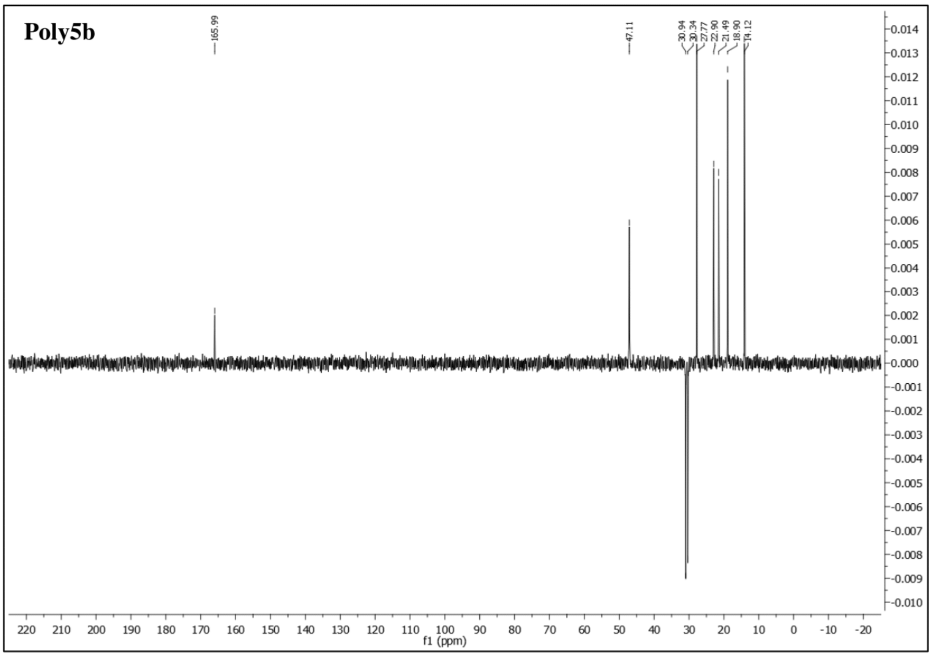
Poly5b

165.99
47.11
30.94
30.34
27.77
22.90
21.49
18.90
14.12
0.014
0.013
0.012
0.011
0.010
0.009
0.008
0.007
0.006
0.005
0.004
0.003
0.002
0.001
0.000
-0.001
-0.002
-0.003
-0.004
-0.005
-0.006
-0.007
-0.008
-0.009
-0.010
220 210 200 190 180 170 160 150 140 130 120 110 100 90 80 70 60 50 40 30 20 10 0 -10 -20
f1 (ppm)

6.10 NMR Spectra of **poly6b** in DMSO-d_6

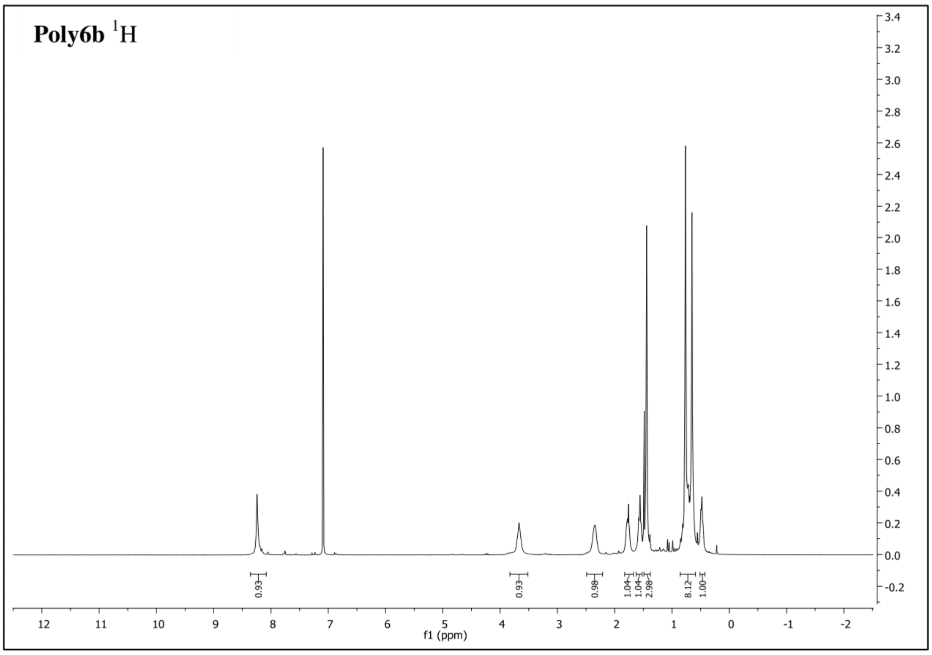

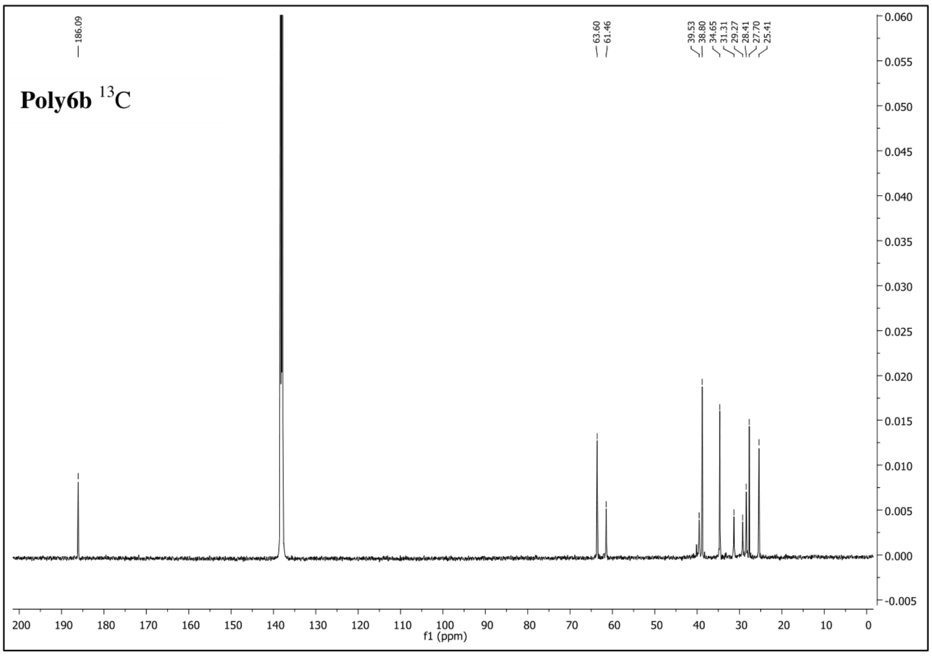

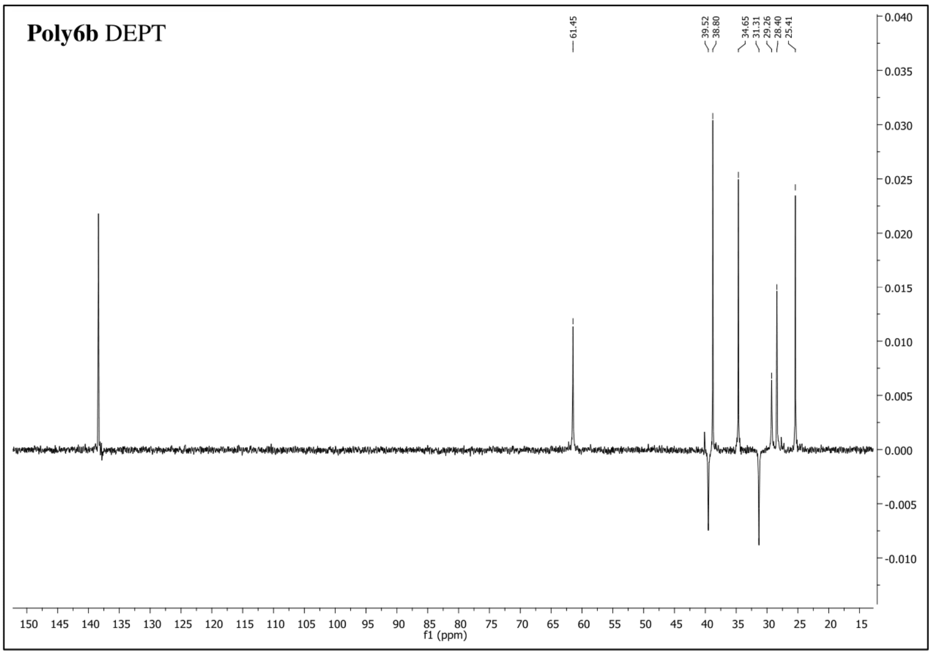

Poly6b DEPT

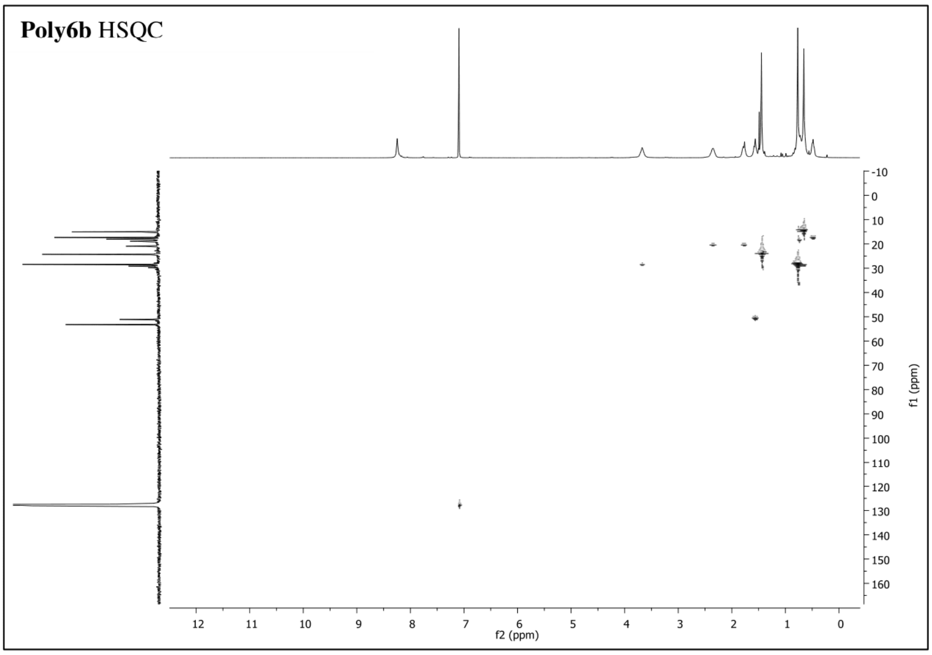

Poly6b HSQC

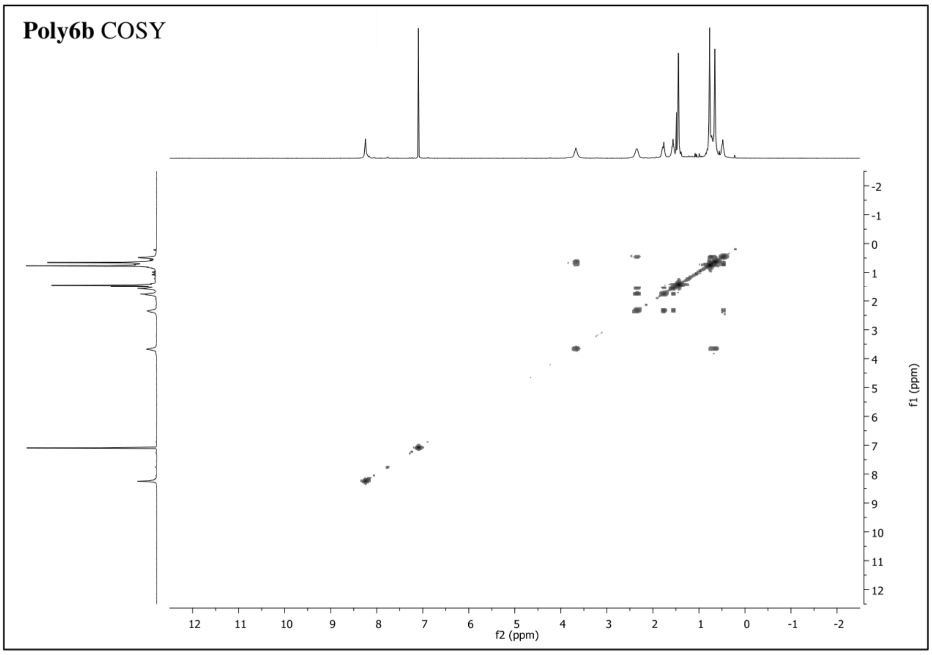

Poly6b COSY

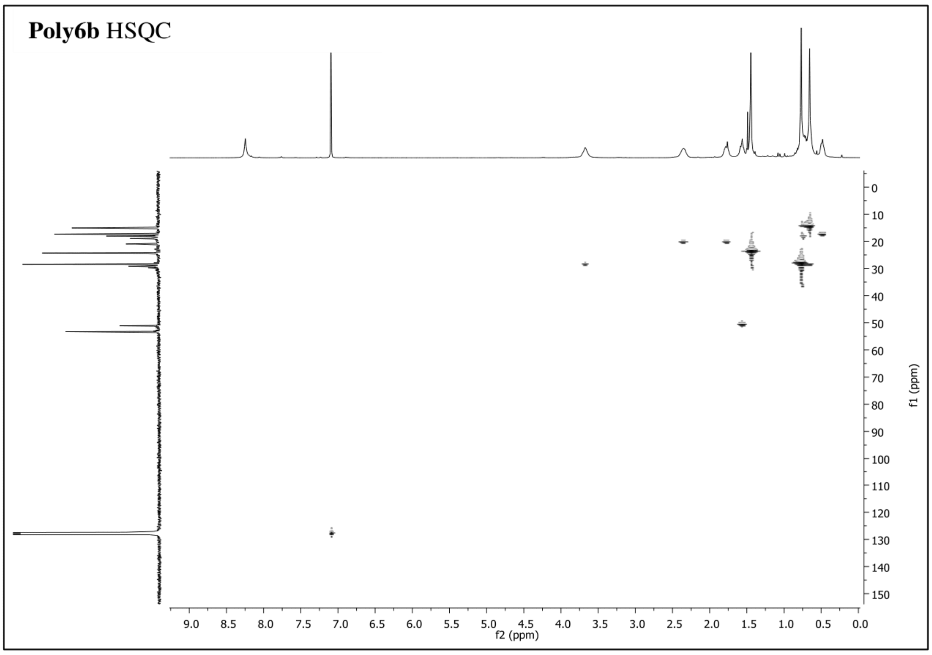

Poly6b HSQC

7. IR Spectra

7.1 poly5a

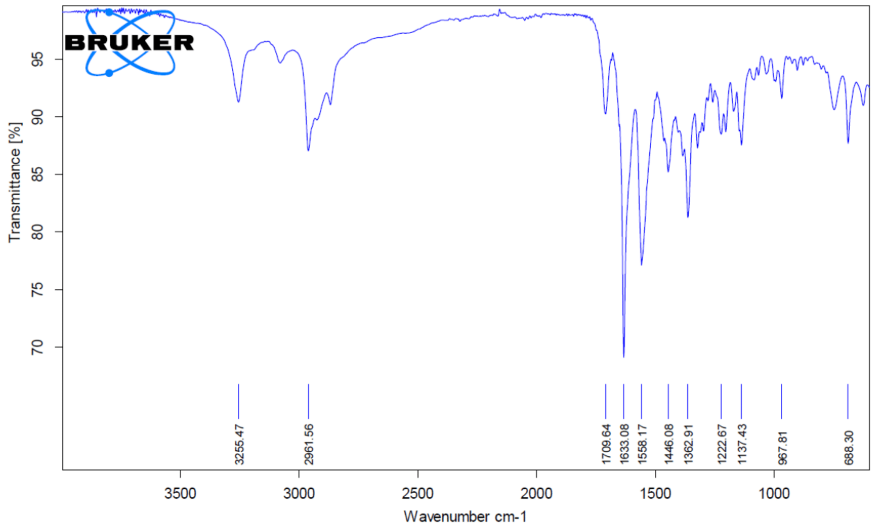

7.2 poly5b

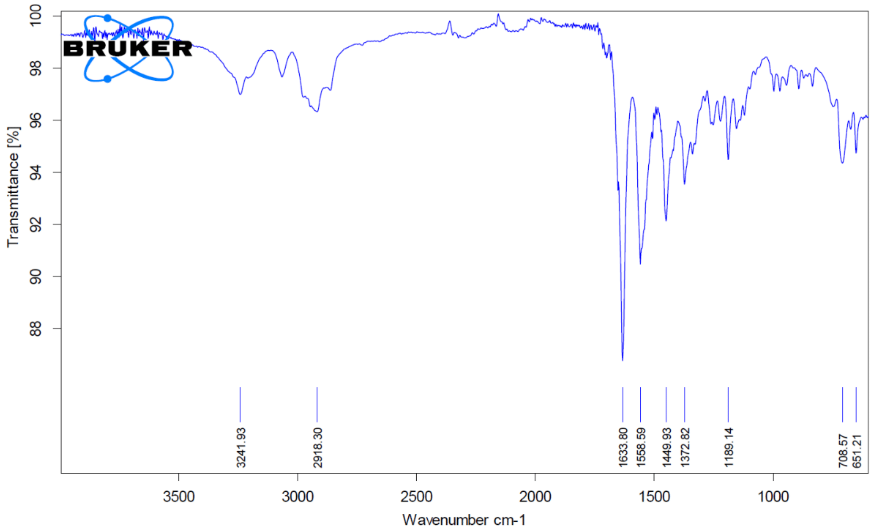

I

7.3 poly6a

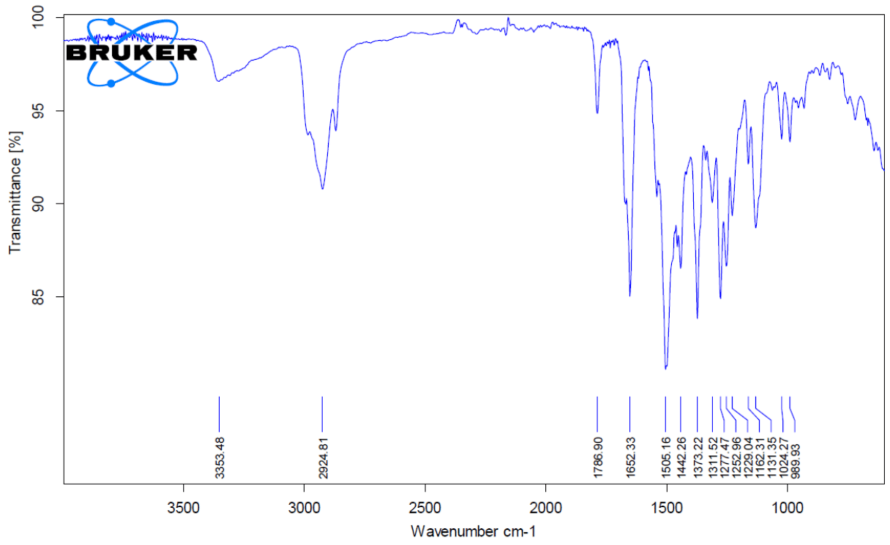

7.4 poly6b

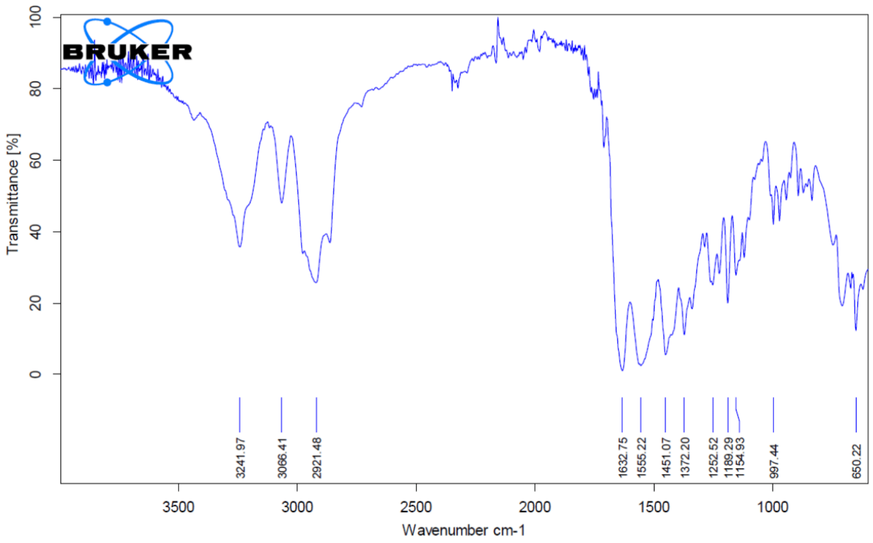

8. GPC molar mass distribution

8.1 **poly5a** (entry 2)

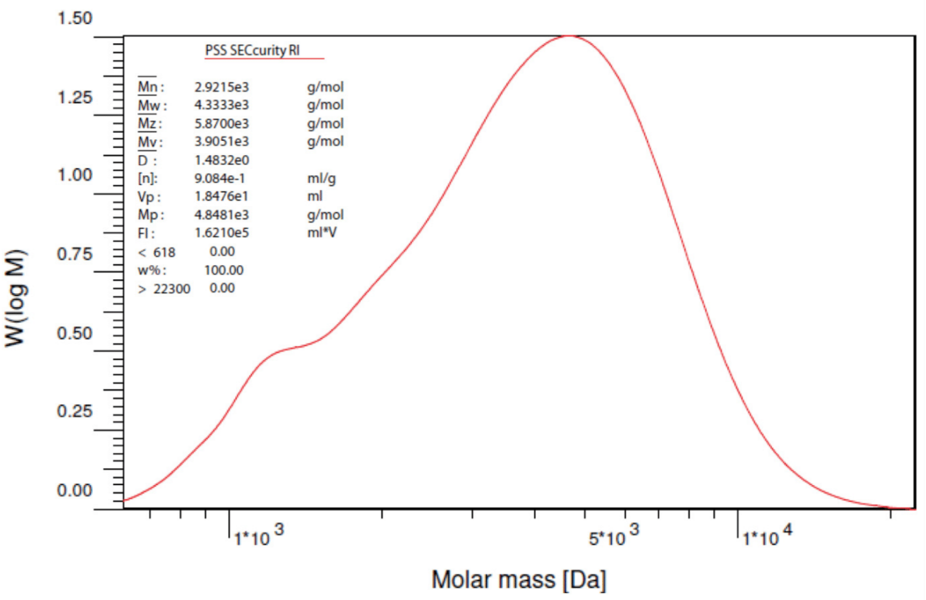

8.2 **poly5a** (entry 4)

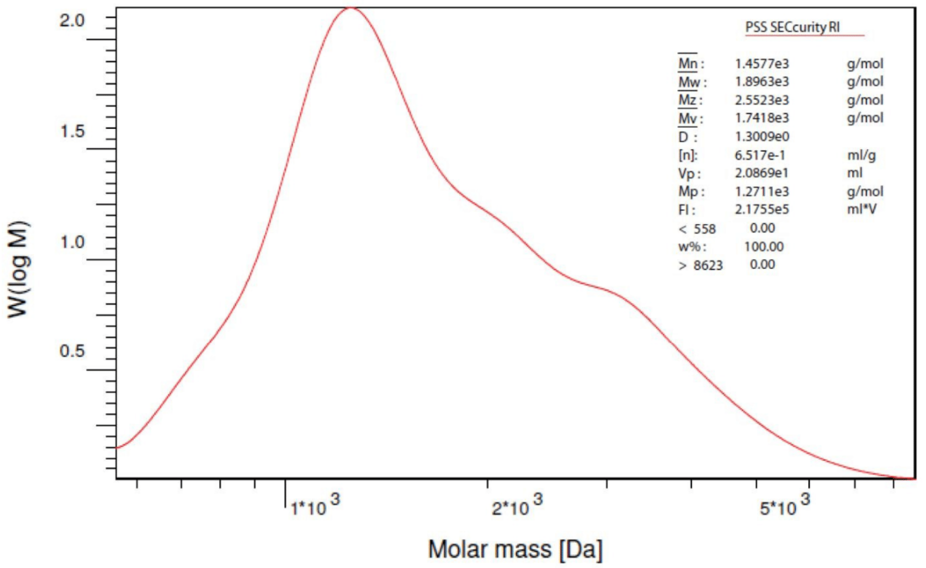

8.3 **poly5b** (entry 5)

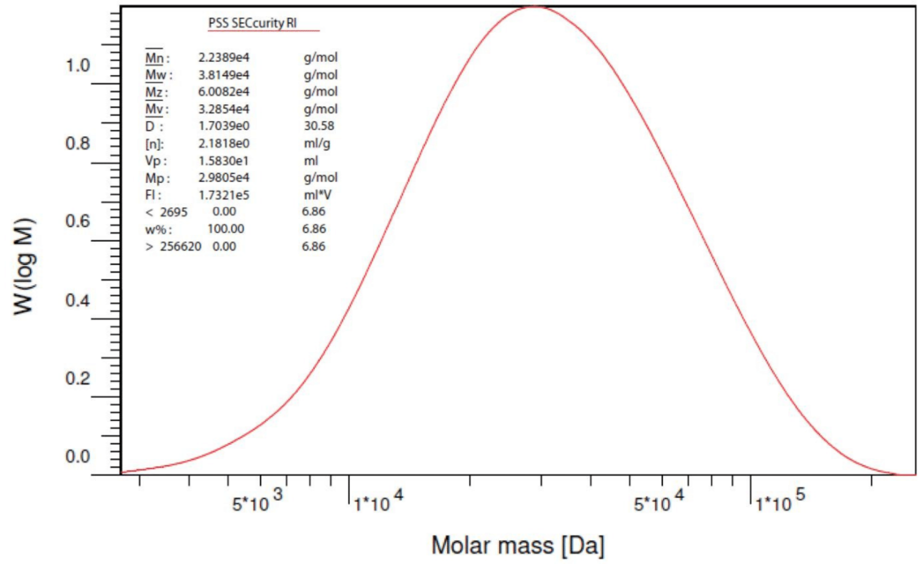

```
Mn :     2.2389e4      g/mol
Mw :     3.8149e4      g/mol
Mz :     6.0082e4      g/mol
Mv :     3.2854e4      g/mol
D  :     1.7039e0      30.58
[n]:     2.1818e0      ml/g
Vp :     1.5830e1      ml
Mp :     2.9805e4      g/mol
FI :     1.7321e5      ml*V
< 2695     0.00        6.86
w% :      100.00       6.86
> 256620   0.00        6.86
```

8.4 **poly5b** (entry 7)

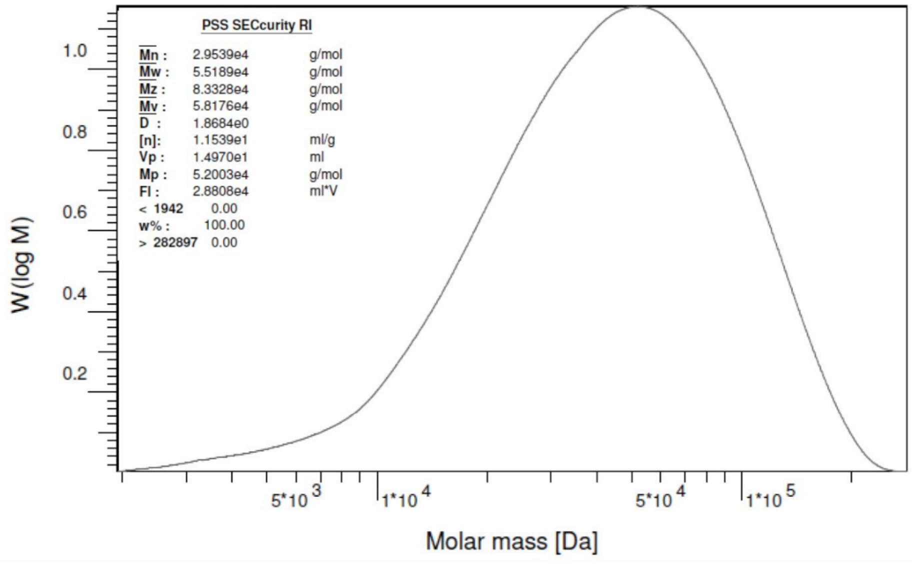

```
Mn :     2.9539e4       g/mol
Mw :     5.5189e4       g/mol
Mz :     8.3328e4       g/mol
Mv :     5.8176e4       g/mol
D  :     1.8684e0
[n]:     1.1539e1       ml/g
Vp :     1.4970e1       ml
Mp :     5.2003e4       g/mol
FI :     2.8808e4       ml*V
< 1942     0.00
w% :      100.00
> 282897   0.00
```

8.5 **poly5b** (entry 8)

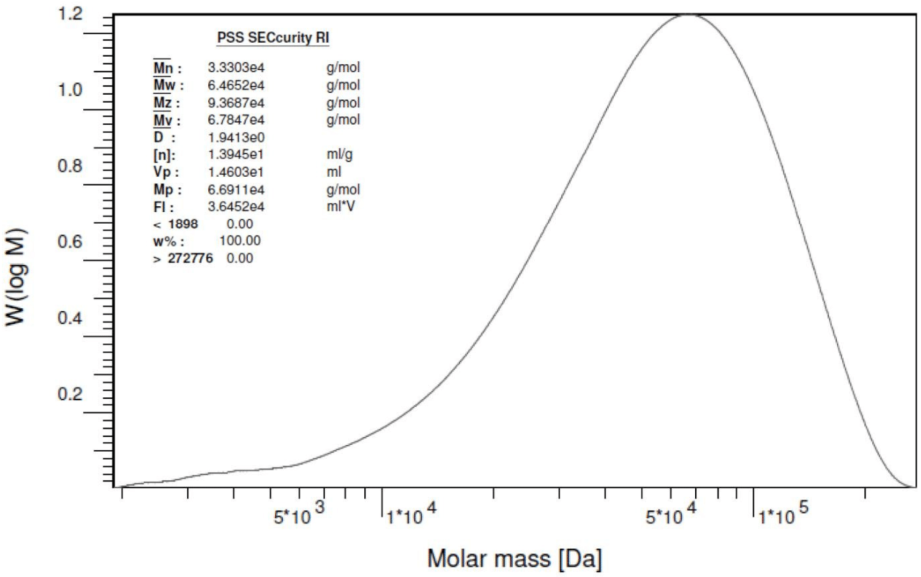

8.6 **poly6a** (entry 10)

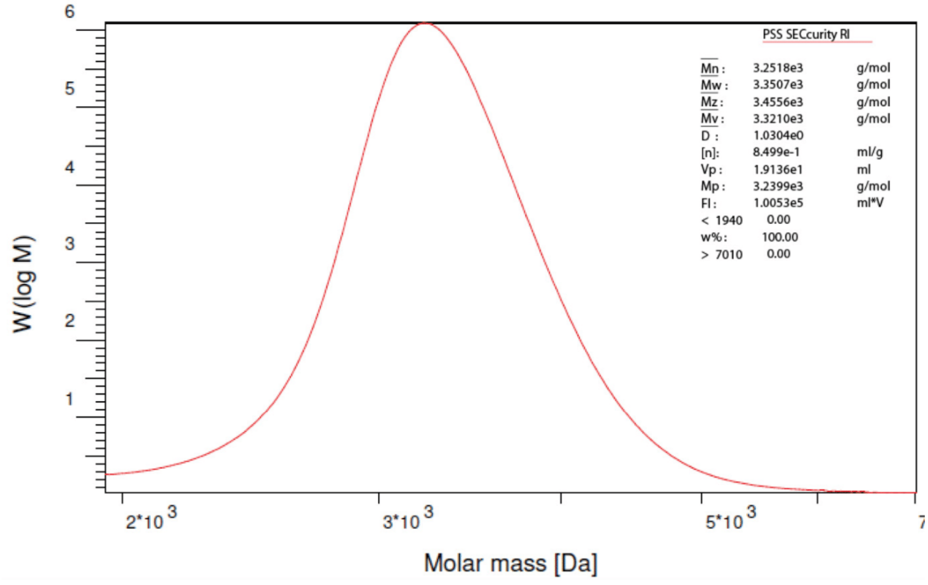

8.7 **poly6b** (entry 11)

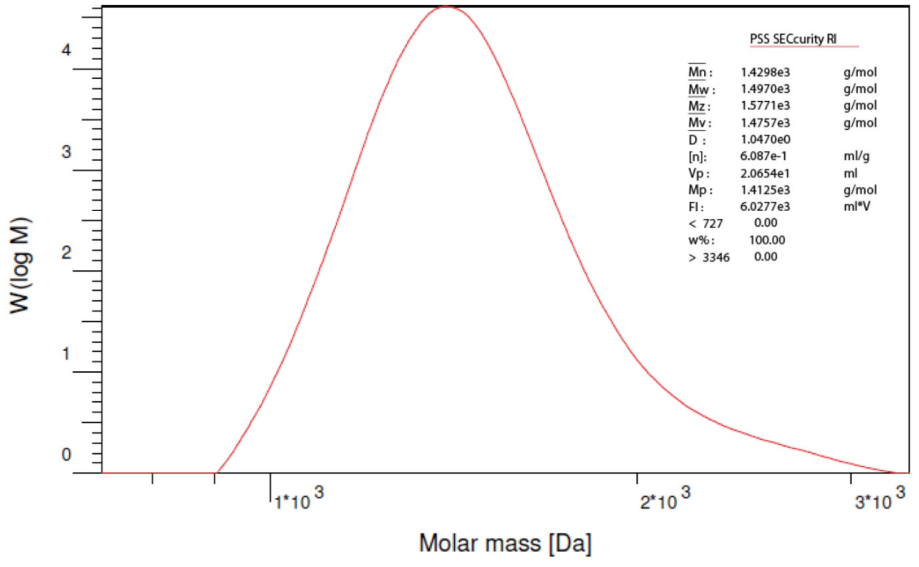

Mn :	1.4298e3	g/mol
Mw :	1.4970e3	g/mol
Mz :	1.5771e3	g/mol
Mv :	1.4757e3	g/mol
D :	1.0470e0	
[n]:	6.087e-1	ml/g
Vp :	2.0654e1	ml
Mp :	1.4125e3	g/mol
FI :	6.0277e3	ml*V
< 727	0.00	
w% :	100.00	
> 3346	0.00	

9. DSC spectra

9.1 **poly5a**

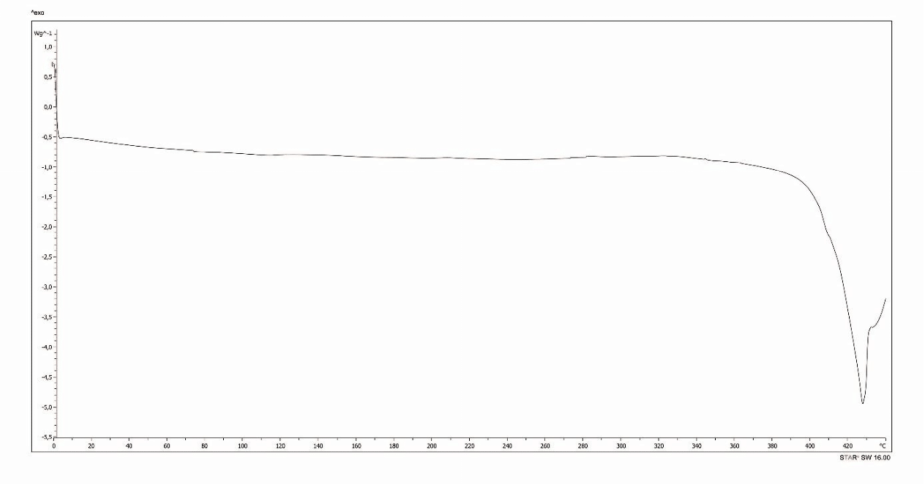

9.2 **poly5b** (220 °C / 20 min)

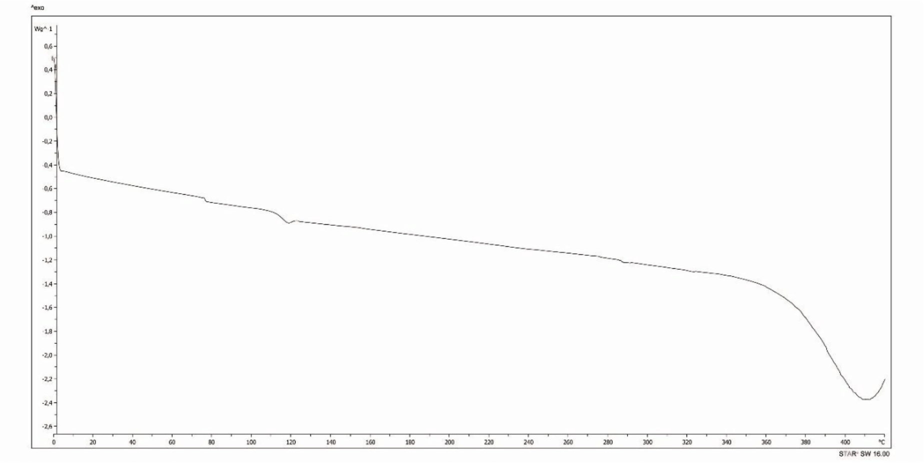

9.3 **poly5b** (220 °C / 180 min)

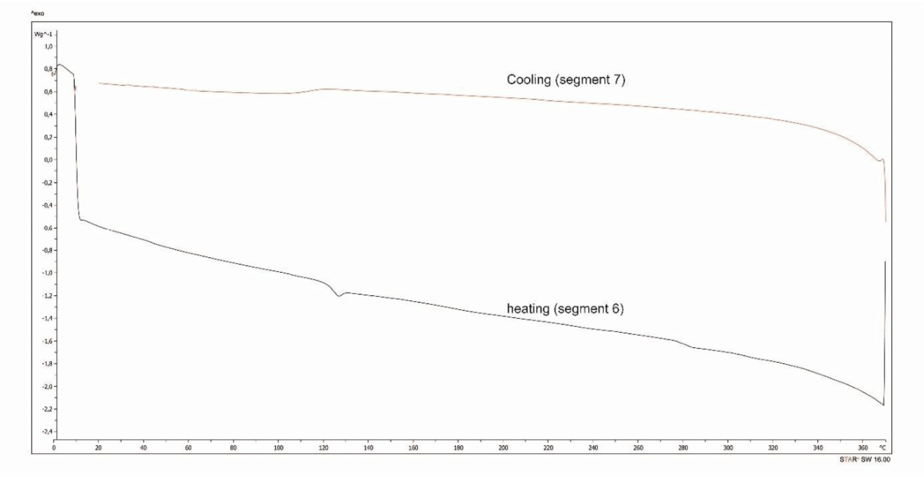

9.3 **poly6a**

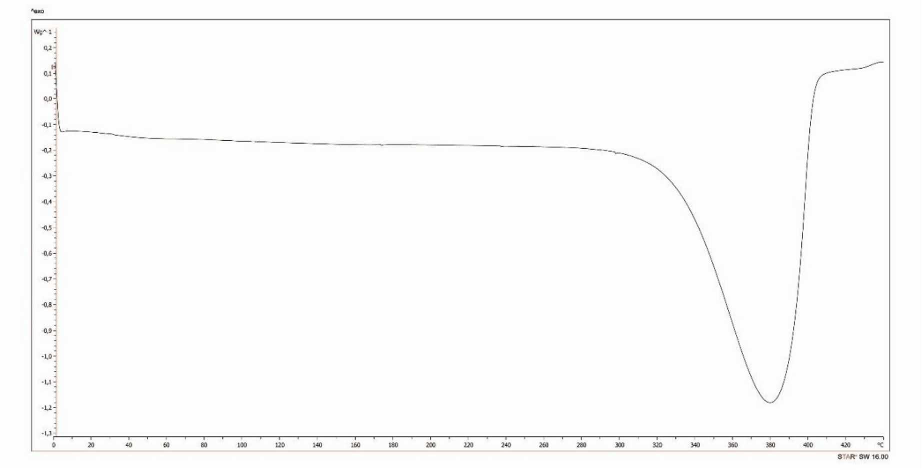

9.4 **poly6b**

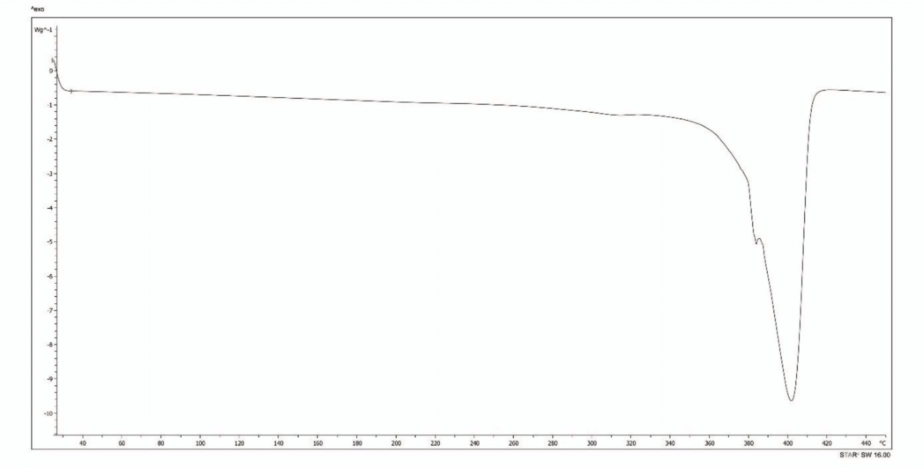
^exo
Wg^-1
0
-1
-2
-3
-4
-5
-6
-7
-8
-9
-10
40
60
80
100
120
140
160
180
200
220
240
260
280
300
320
340
360
380
400
420
440
°C
STARᵉ SW 16.00

4.3 Methods section 2.4 “Biobased Chiral Semi-Crystalline or Amorphous High-Performance Polyamides and their Scalable Stereoselective Synthesis

Supplementary Information

V. Sieber et al.

Biobased Chiral Semi-Crystalline or Amorphous High-Performance Polyamides and their Scalable Stereoselective Synthesis

1. Supplementary Figures

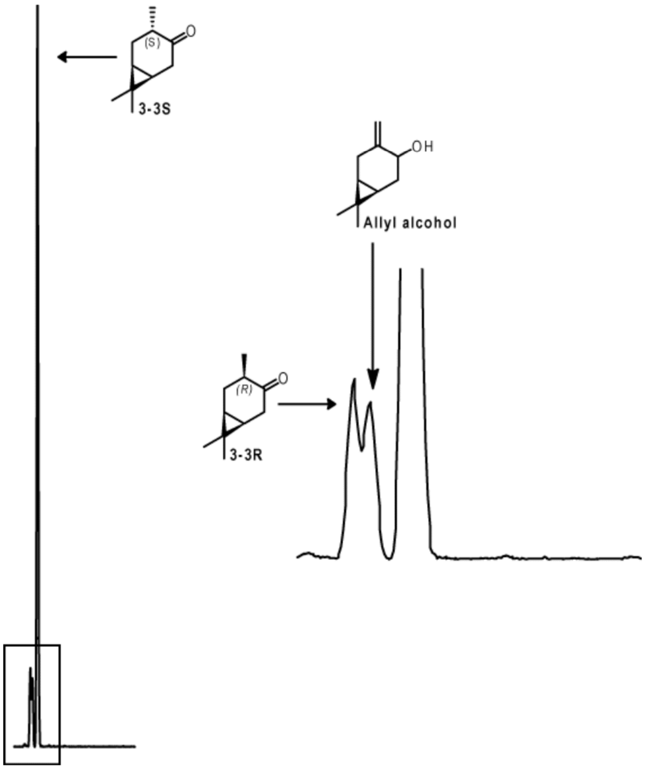

Supplementary Figure 1: Isomeric ketones **3-3S** and **3-3R** and the intermediate allyl alcohol.

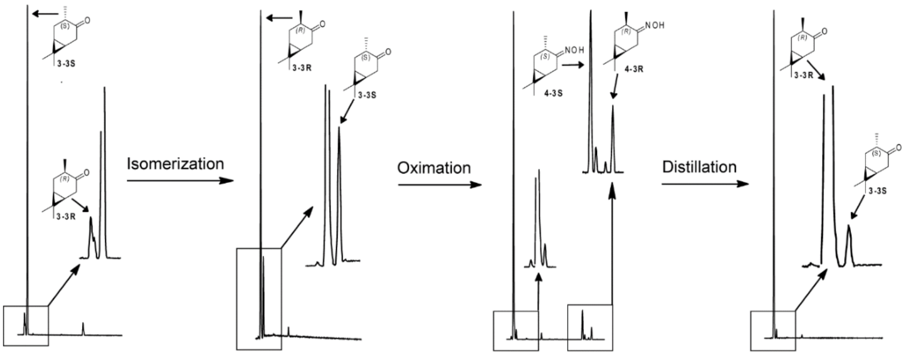

Supplementary Figure 2: GCMS-spectra of the enrichment of ketone **3-3R** by acidic isomerization of ketone **3-3S**, kinetic resolution by oximation with $HONH_2 \cdot HCl$ and subsequent distillation.

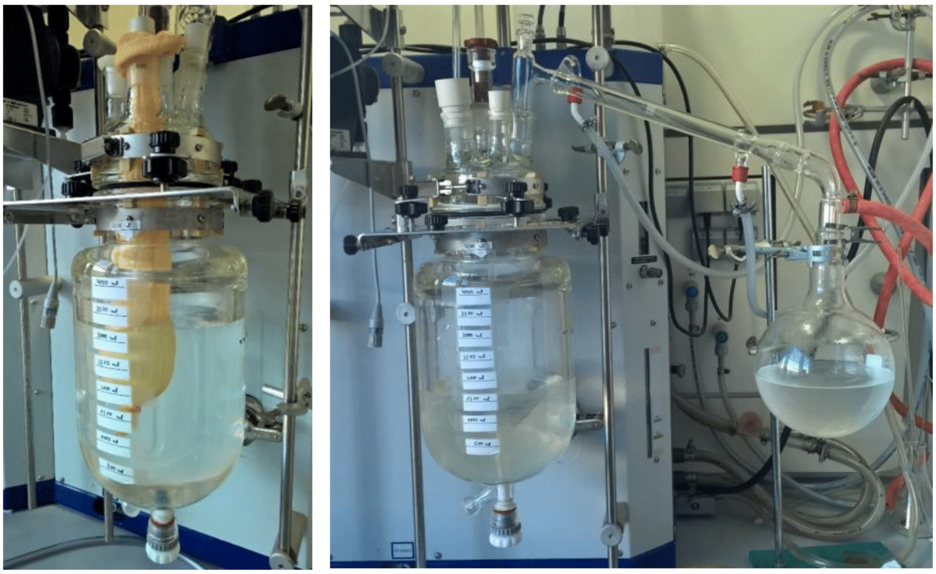

Supplementary Figure 3: Enzyme bag loaded with Novozyme-435 for epoxidation of (+)-3-carene (**1**) to epoxide **2-3S** (left) and azeotropic distillation of cyclohexane before the Meinwald rearrangement of epoxide **2-3S** to ketone **3-3S** catalysed by $Fe(ClO_4)_2 \cdot H_2O$ (right) in the 4.0 L scale.

Supplementary Figure 4: Lactam **5-3S** synthesized in the 4.0 L scale after crystallization at -20 °C.

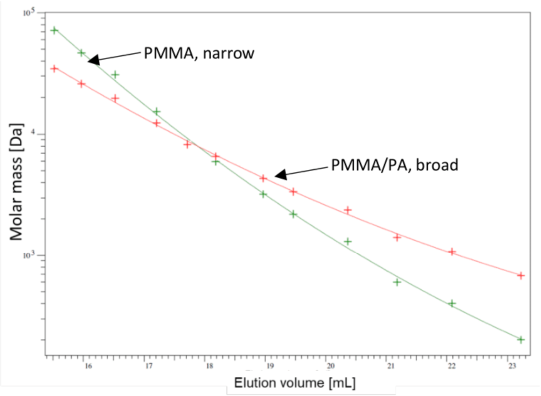

Supplementary Figure 5: Calibration curve for GPC measurements with narrow PMMA calibration (green) and PMMA/PA broad calibration (red).

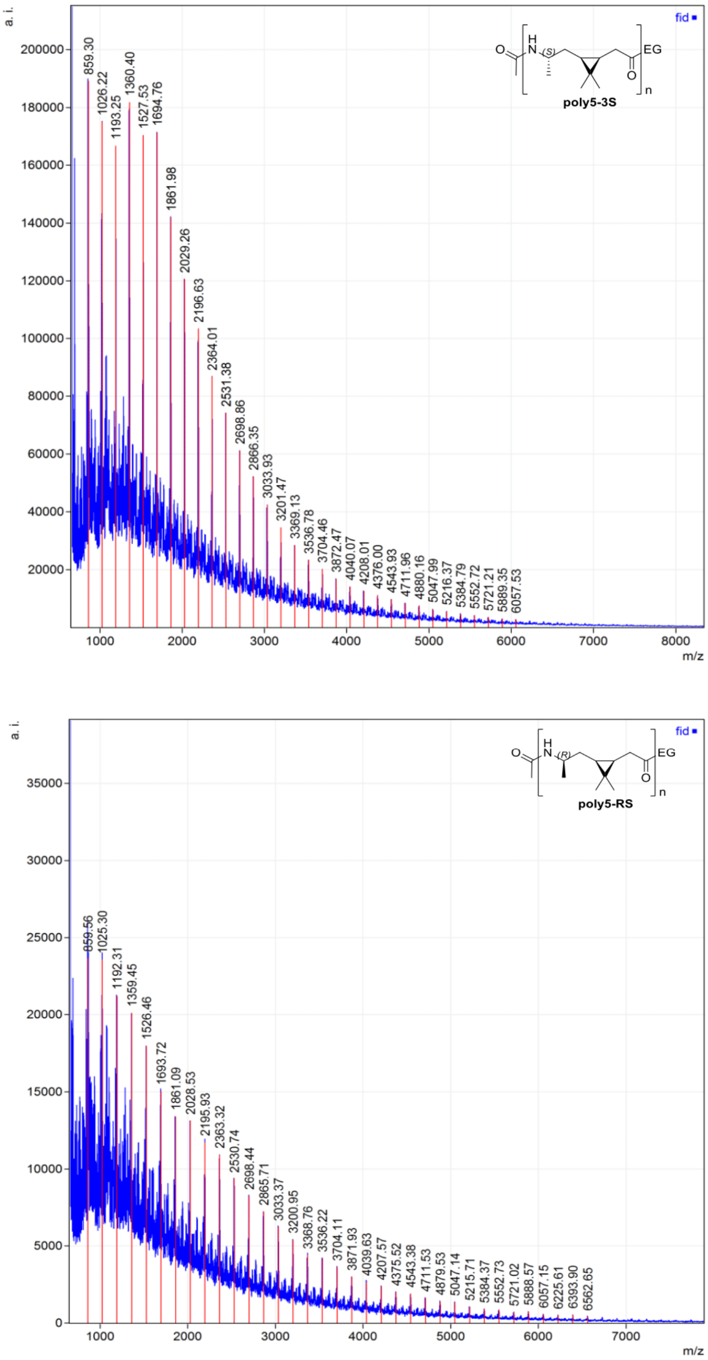

Supplementary Figure 6: MALDI-TOF measurements of **poly5-3S** and **poly5-3R**.

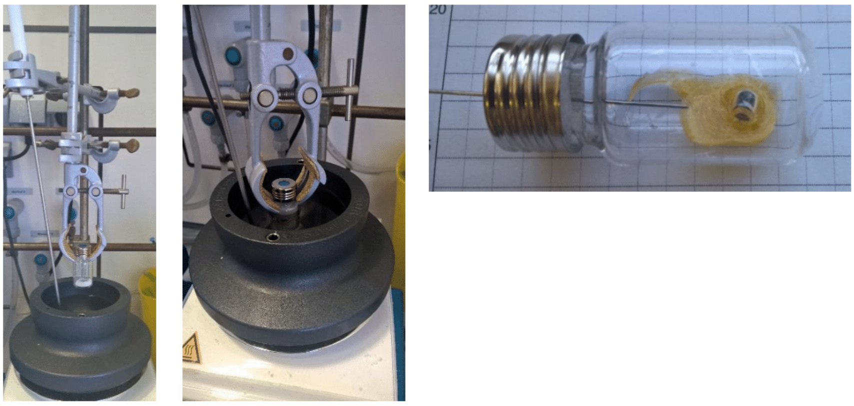

Supplementary Figure 7: Pictures of polymerizations under application of polymerization method A.

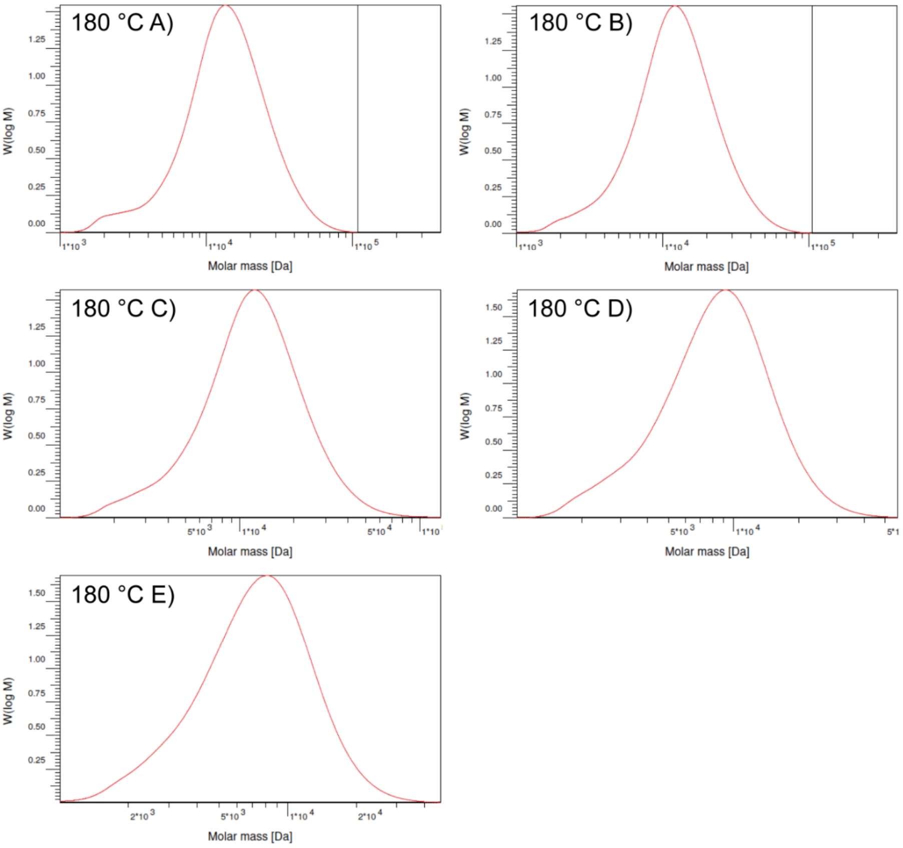

Supplementary Figure 8: Molecular weight of **poly5-3S** at different activator concentrations at 180 °C.

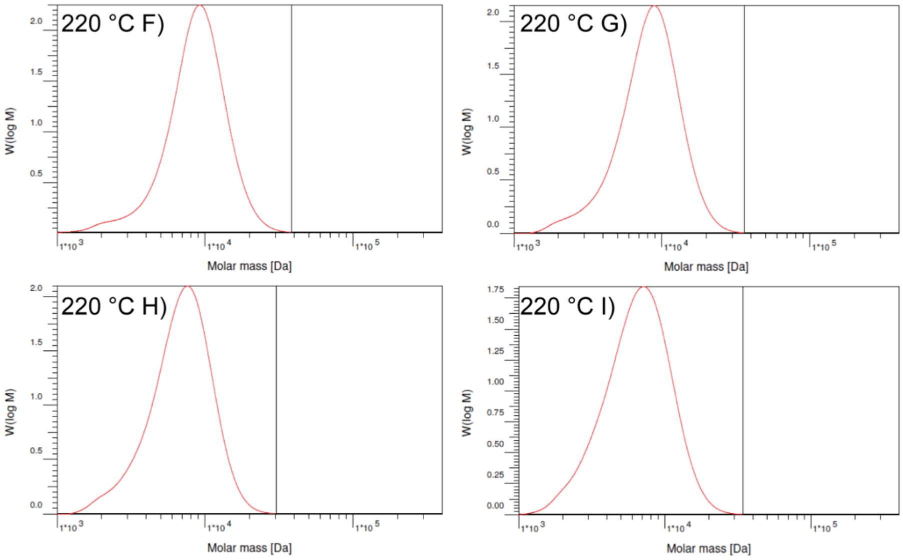

Supplementary Figure 9: Molecular weight of **poly5-3S** at different activator concentrations at 220 °C.

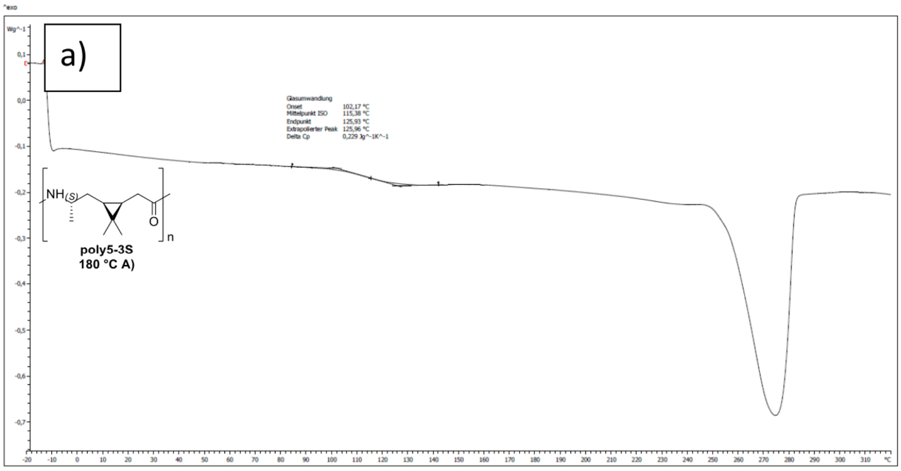
^exo
Wg^-1
0,1
0,0
-0,1
-0,2
-0,3
-0,4
-0,5
-0,6
-0,7
-20
-10
0
10
20
30
40
50
60
70
80
90
100
110
120
130
140
150
160
170
180
190
200
210
220
230
240
250
260
270
280
290
300
310
°C
a)
Glasumwandlung
Onset 102,17 °C
Mittelpunkt ISO 115,38 °C
Endpunkt 125,93 °C
Extrapolierter Peak 125,96 °C
Delta Cp 0,229 Jg^-1K^-1
NH
(S)
O
n
poly5-3S
180 °C A)

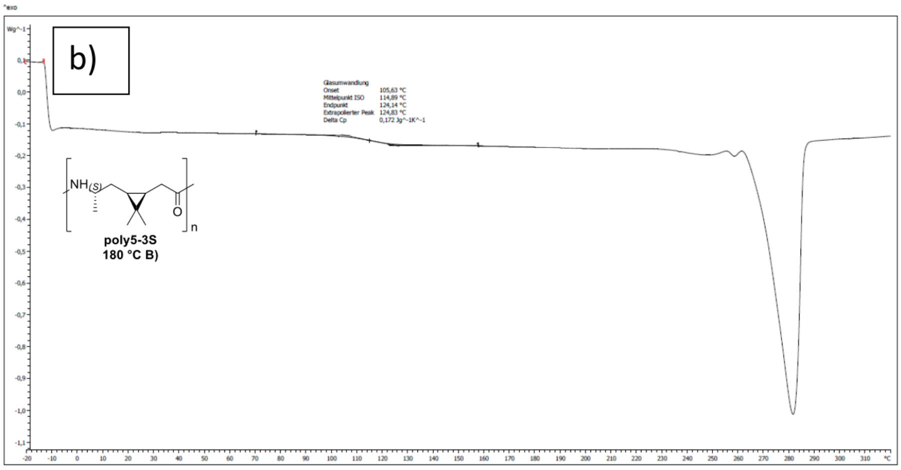
^exo
Wg^-1
0,1
0,0
-0,1
-0,2
-0,3
-0,4
-0,5
-0,6
-0,7
-0,8
-0,9
-1,0
-1,1
-20
-10
0
10
20
30
40
50
60
70
80
90
100
110
120
130
140
150
160
170
180
190
200
210
220
230
240
250
260
270
280
290
300
310
°C
b)
Glasumwandlung
Onset 105,63 °C
Mittelpunkt ISO 114,89 °C
Endpunkt 124,14 °C
Extrapolierter Peak 124,83 °C
Delta Cp 0,172 Jg^-1K^-1
NH
(S)
O
n
poly5-3S
180 °C B)

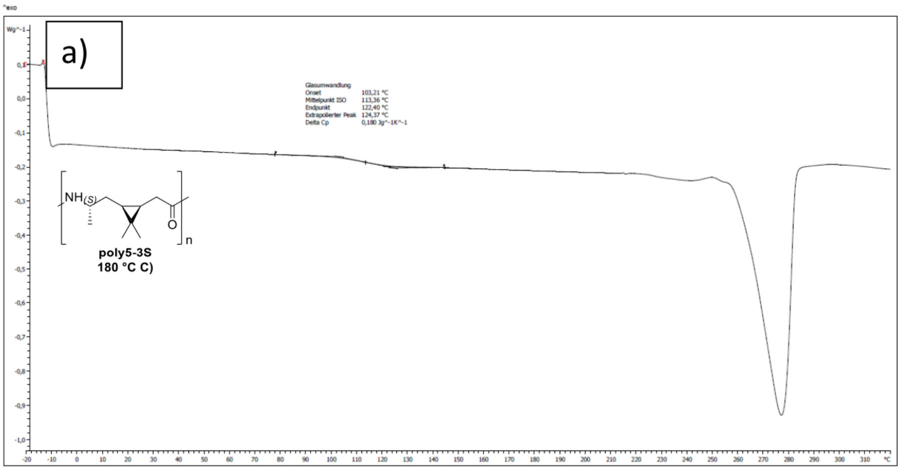
^exo
Wg^-1
a)
Glasumwandlung
Onset 103,21 °C
Mittelpunkt ISO 113,36 °C
Endpunkt 122,40 °C
Extrapolierter Peak 124,37 °C
Delta Cp 0,180 Jg^-1K^-1
NH
(S)
O
n
poly5-3S
180 °C C)
0,1
0,0
-0,1
-0,2
-0,3
-0,4
-0,5
-0,6
-0,7
-0,8
-0,9
-1,0
-20 -10 0 10 20 30 40 50 60 70 80 90 100 110 120 130 140 150 160 170 180 190 200 210 220 230 240 250 260 270 280 290 300 310 °C

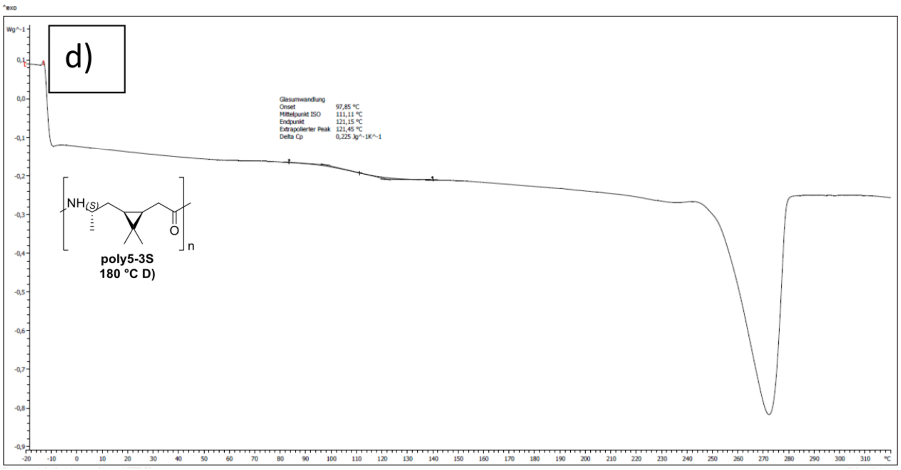
^exo
Wg^-1
d)
Glasumwandlung
Onset 97,85 °C
Mittelpunkt ISO 111,11 °C
Endpunkt 121,15 °C
Extrapolierter Peak 121,45 °C
Delta Cp 0,225 Jg^-1K^-1
NH
(S)
O
n
poly5-3S
180 °C D)
0,1
0,0
-0,1
-0,2
-0,3
-0,4
-0,5
-0,6
-0,7
-0,8
-0,9
-20 -10 0 10 20 30 40 50 60 70 80 90 100 110 120 130 140 150 160 170 180 190 200 210 220 230 240 250 260 270 280 290 300 310 °C

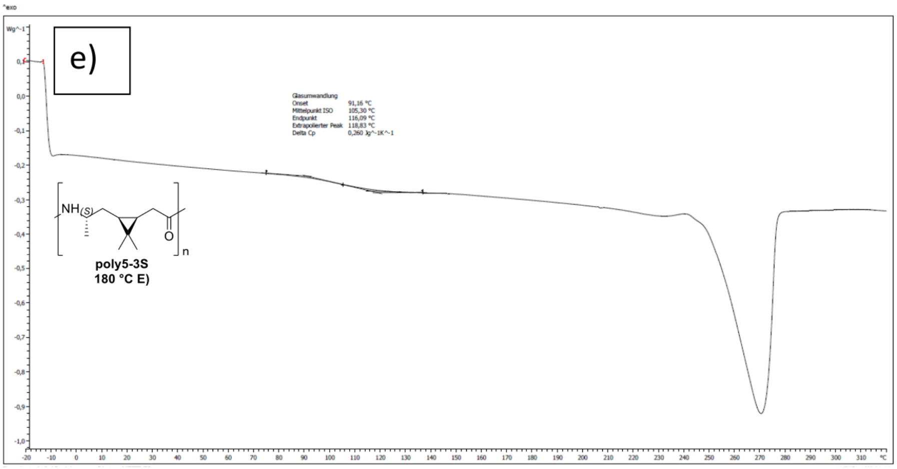
e)
^exo
Wg^-1
0,1
0,0
-0,1
-0,2
-0,3
-0,4
-0,5
-0,6
-0,7
-0,8
-0,9
-1,0
-20 -10 0 10 20 30 40 50 60 70 80 90 100 110 120 130 140 150 160 170 180 190 200 210 220 230 240 250 260 270 280 290 300 310 °C
Glasumwandlung
Onset 91,16 °C
Mittelpunkt ISO 105,30 °C
Endpunkt 116,09 °C
Extrapolierter Peak 118,83 °C
Delta Cp 0,260 Jg^-1K^-1
NH
(S)
O
n
poly5-3S
180 °C E)

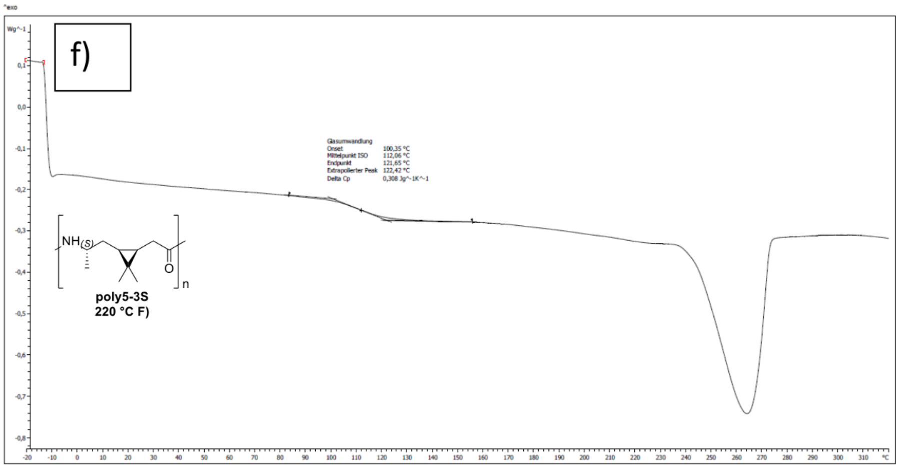
f)
^exo
Wg^-1
0,1
0,0
-0,1
-0,2
-0,3
-0,4
-0,5
-0,6
-0,7
-0,8
-20 -10 0 10 20 30 40 50 60 70 80 90 100 110 120 130 140 150 160 170 180 190 200 210 220 230 240 250 260 270 280 290 300 310 °C
Glasumwandlung
Onset 100,35 °C
Mittelpunkt ISO 112,06 °C
Endpunkt 121,65 °C
Extrapolierter Peak 122,42 °C
Delta Cp 0,308 Jg^-1K^-1
NH
(S)
O
n
poly5-3S
220 °C F)

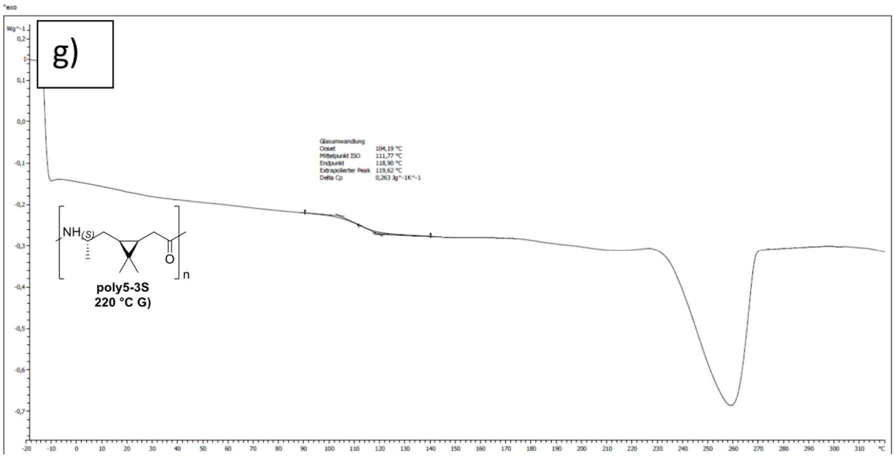
^exo
Wg^-1
g)
Glasumwandlung
Onset 104,19 °C
Mittelpunkt ISO 111,77 °C
Endpunkt 118,90 °C
Extrapolierter Peak 119,62 °C
Delta Cp 0,263 Jg^-1K^-1
NH
(S)
O
n
poly5-3S
220 °C G)
0,2
0,1
0,0
-0,1
-0,2
-0,3
-0,4
-0,5
-0,6
-0,7
-20 -10 0 10 20 30 40 50 60 70 80 90 100 110 120 130 140 150 160 170 180 190 200 210 220 230 240 250 260 270 280 290 300 310 °C

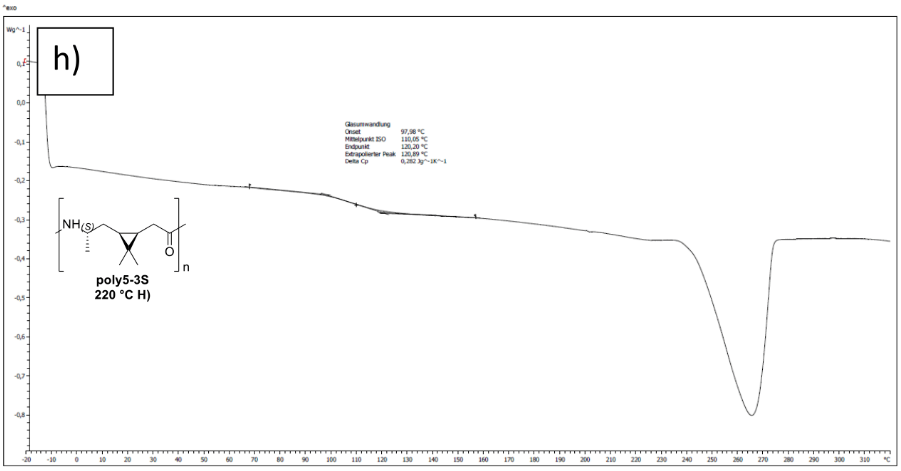
^exo
Wg^-1
h)
Glasumwandlung
Onset 97,98 °C
Mittelpunkt ISO 110,05 °C
Endpunkt 120,20 °C
Extrapolierter Peak 120,89 °C
Delta Cp 0,282 Jg^-1K^-1
NH
(S)
O
n
poly5-3S
220 °C H)
0,1
0,0
-0,1
-0,2
-0,3
-0,4
-0,5
-0,6
-0,7
-0,8
-20 -10 0 10 20 30 40 50 60 70 80 90 100 110 120 130 140 150 160 170 180 190 200 210 220 230 240 250 260 270 280 290 300 310 °C

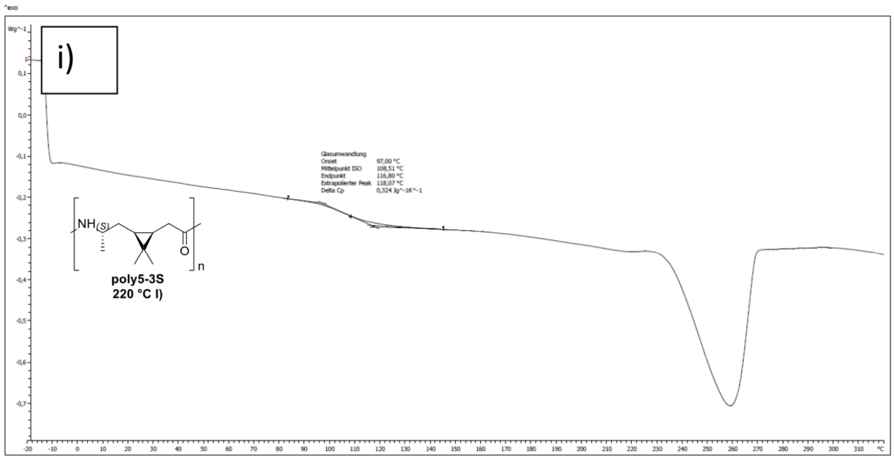

Supplementary Figure 10: DSC curves of various poly-3S-caranamides a)-i) as described in Supplementary Table 12, measured using DSC method B, segment 10 (heating, black).

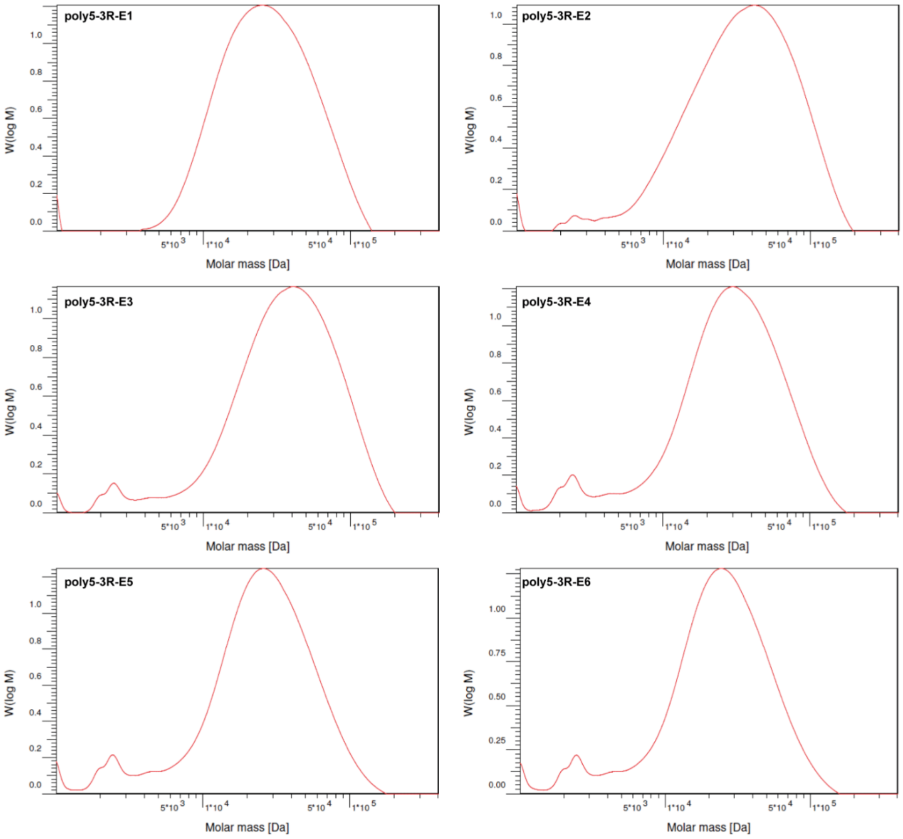

Supplementary Figure 11: Molecular weight of **poly5-3R** at different activator concentrations.

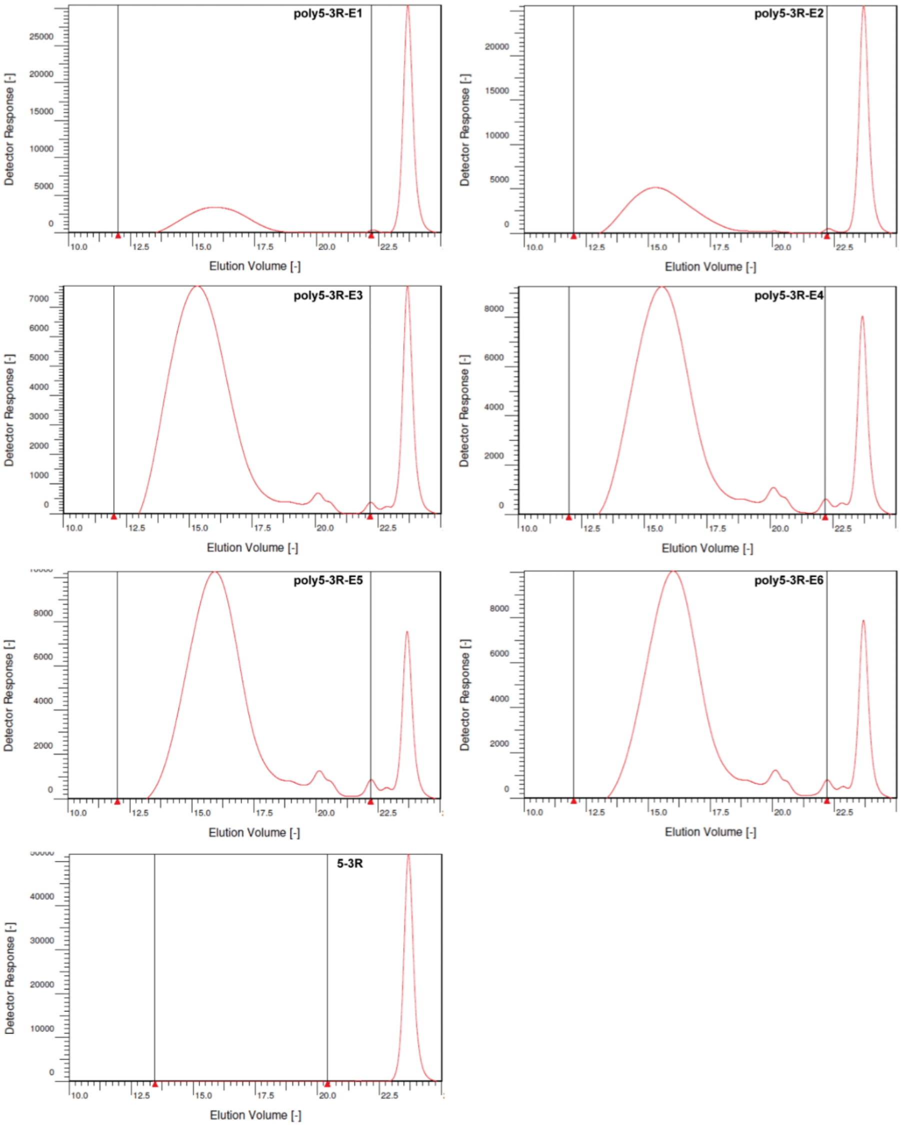

Supplementary Figure 12: GPC elugrams of **poly5R** displaying the monomer conversion at different activator concentrations

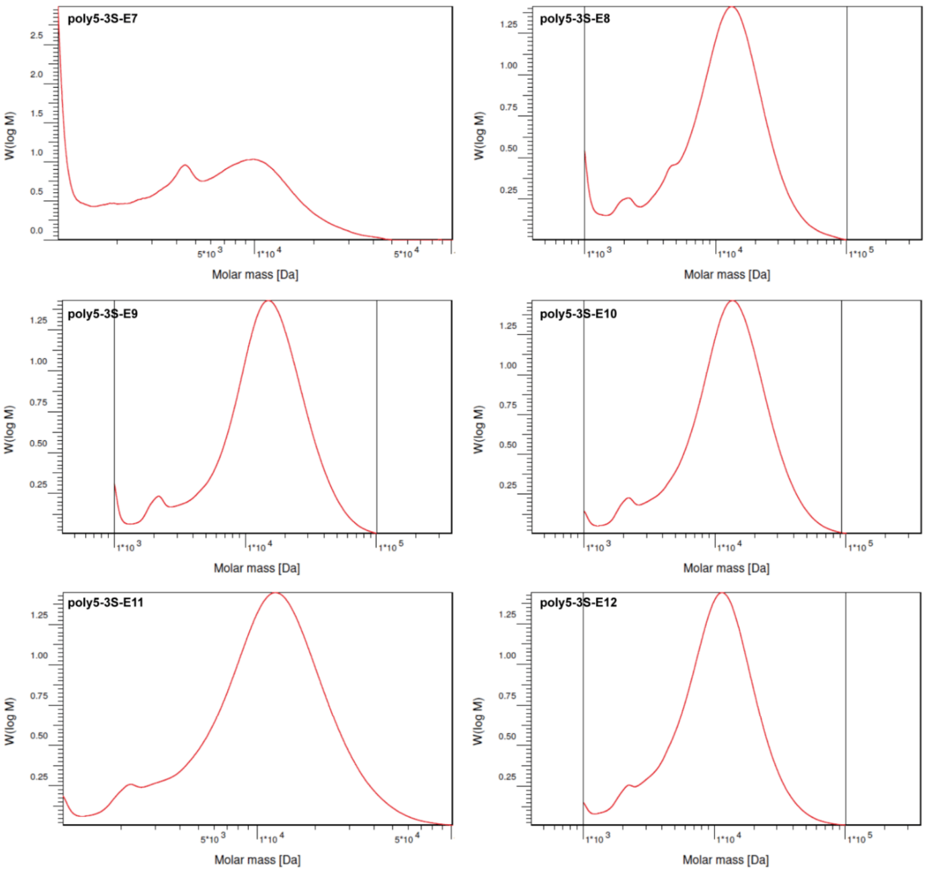

Supplementary Figure 13: Molecular weight of **poly5-3S** at different activator concentrations.

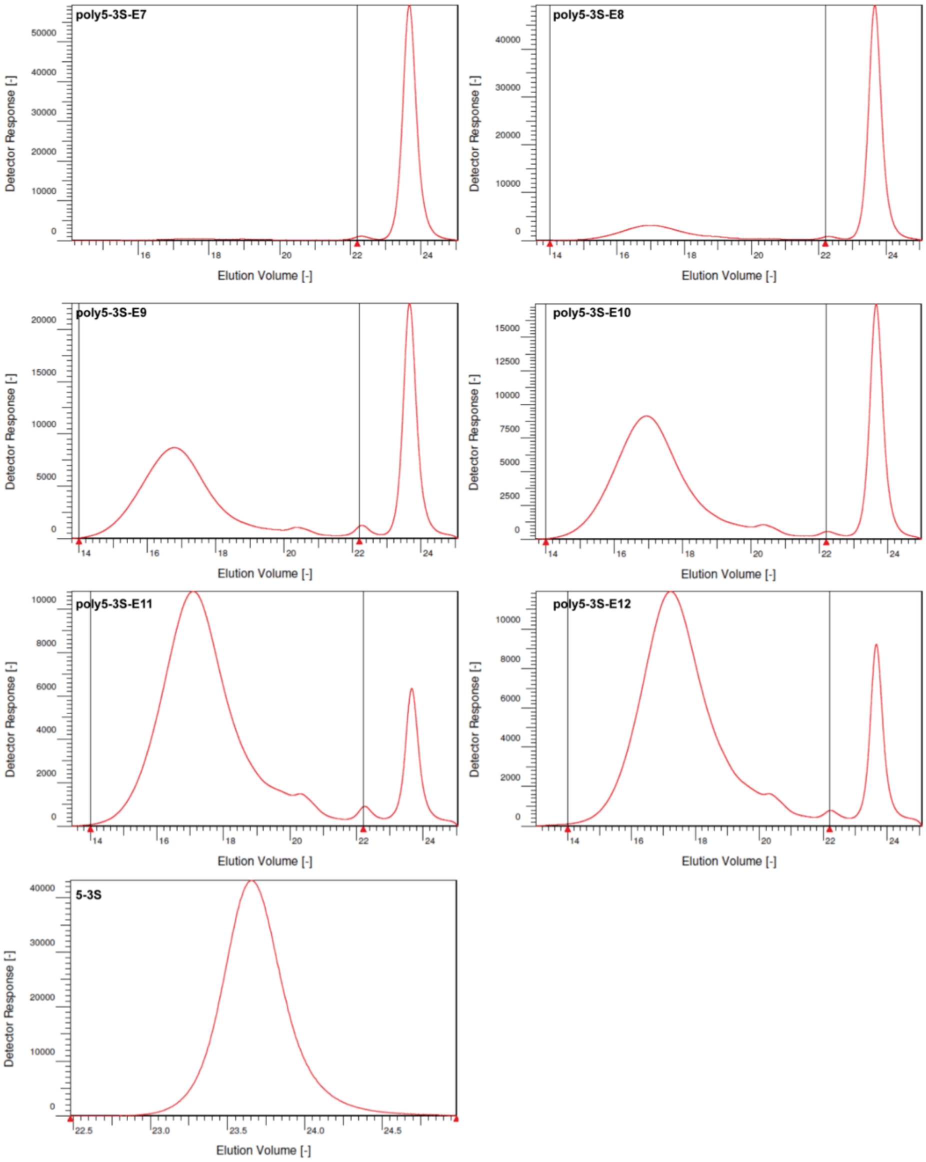

Supplementary Figure 14: GPC elugrams of **poly5R** displaying the monomer conversion at different activator concentrations.

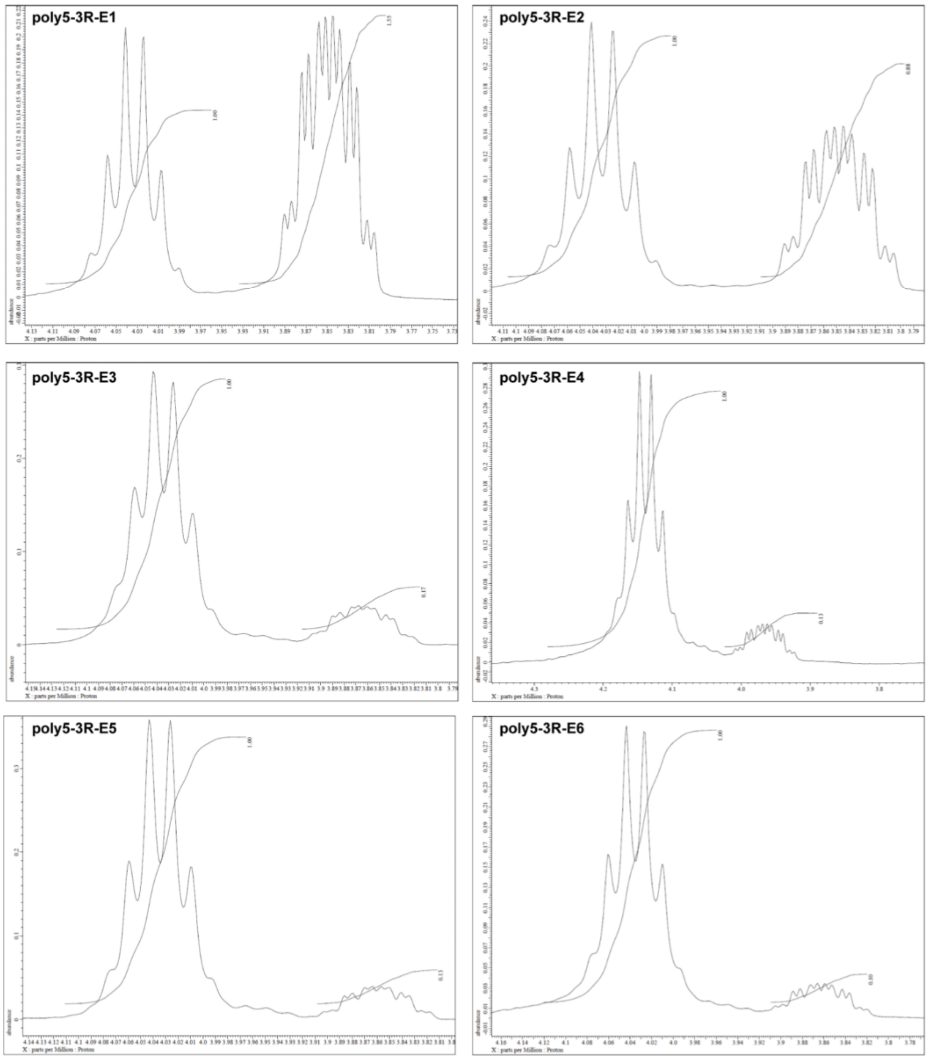

poly5-3R-E1

poly5-3R-E2

poly5-3R-E3

poly5-3R-E4

poly5-3R-E5

poly5-3R-E6

Supplementary Figure 15: Evaluation of the conversion of monomer **5-3R** at different concentrations of activator.

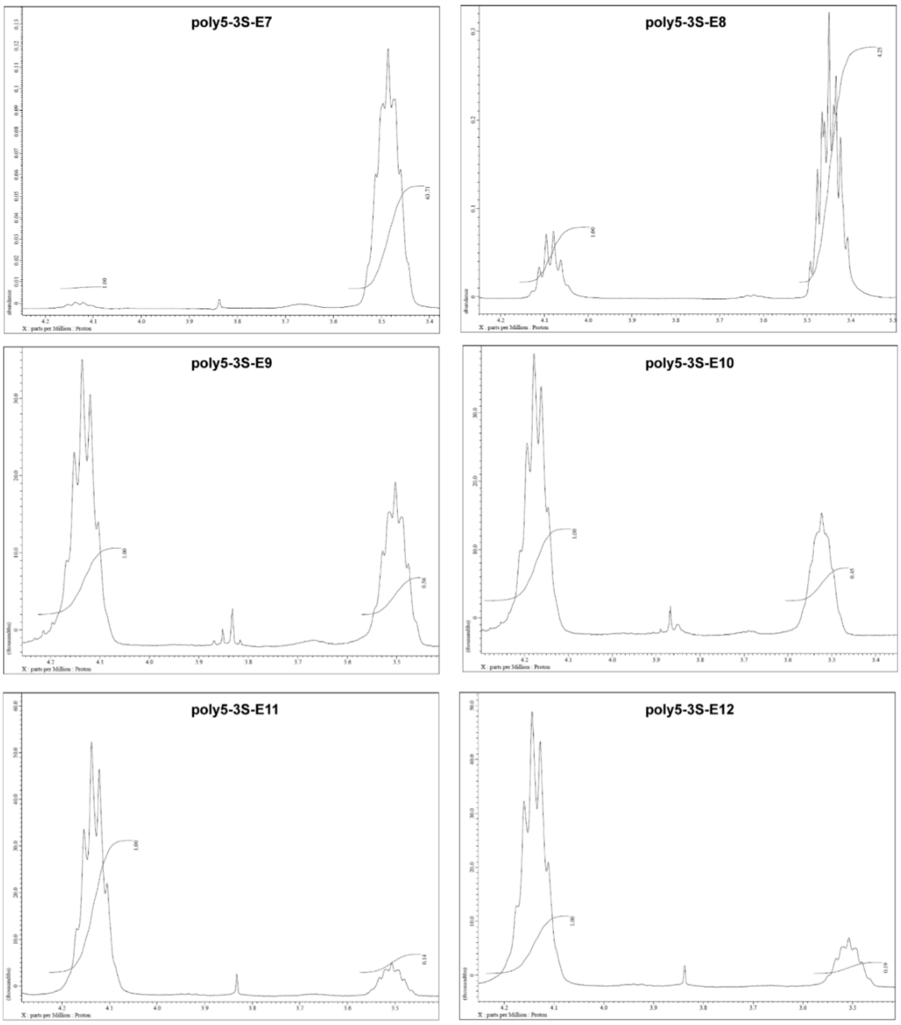
poly5-3S-E7

poly5-3S-E8

poly5-3S-E9

poly5-3S-E10

poly5-3S-E11

poly5-3S-E12

Supplementary Figure 16: Evaluation of the conversion of monomer **5-3S** at different concentrations of activator.

Supplementary Figure 17: Pictures of the reaction vial and oven for polymerization method B.

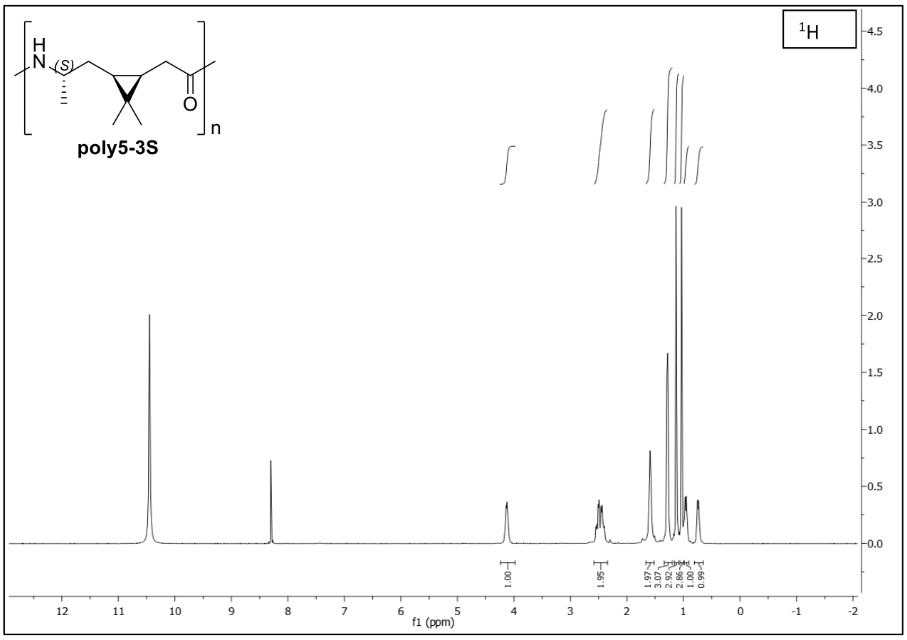
H
N
(S)
O
n
poly5-3S
1H
4.5
4.0
3.5
3.0
2.5
2.0
1.5
1.0
0.5
0.0
1.00
1.95
1.97
3.07
2.92
2.86
1.00
0.99
12
11
10
9
8
7
6
5
4
3
2
1
0
-1
-2
f1 (ppm)

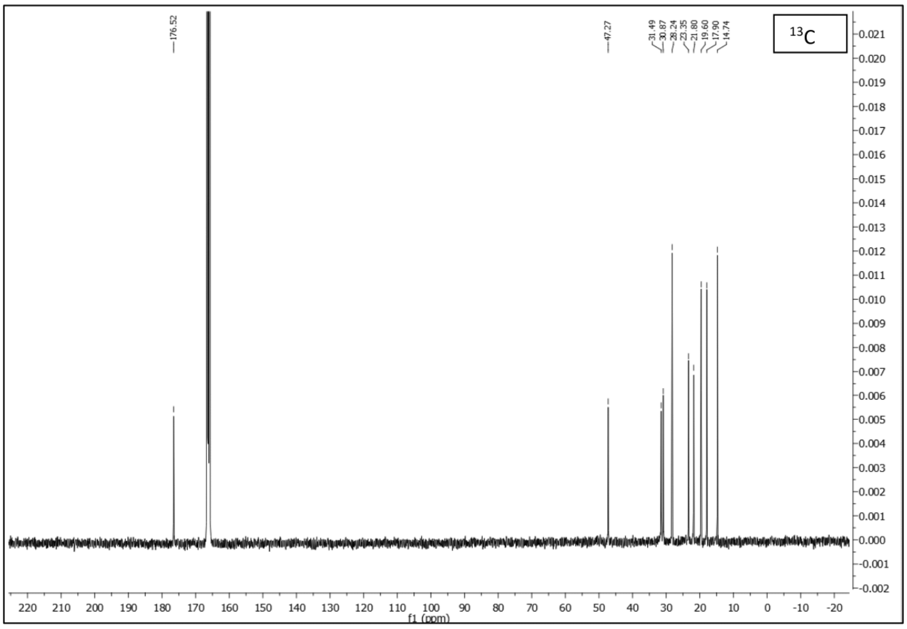
176.52
47.27
31.49
30.87
28.24
23.35
21.80
19.60
17.90
14.74
13C
0.021
0.020
0.019
0.018
0.017
0.016
0.015
0.014
0.013
0.012
0.011
0.010
0.009
0.008
0.007
0.006
0.005
0.004
0.003
0.002
0.001
0.000
-0.001
-0.002
220
210
200
190
180
170
160
150
140
130
120
110
100
90
80
70
60
50
40
30
20
10
0
-10
-20
f1 (ppm)

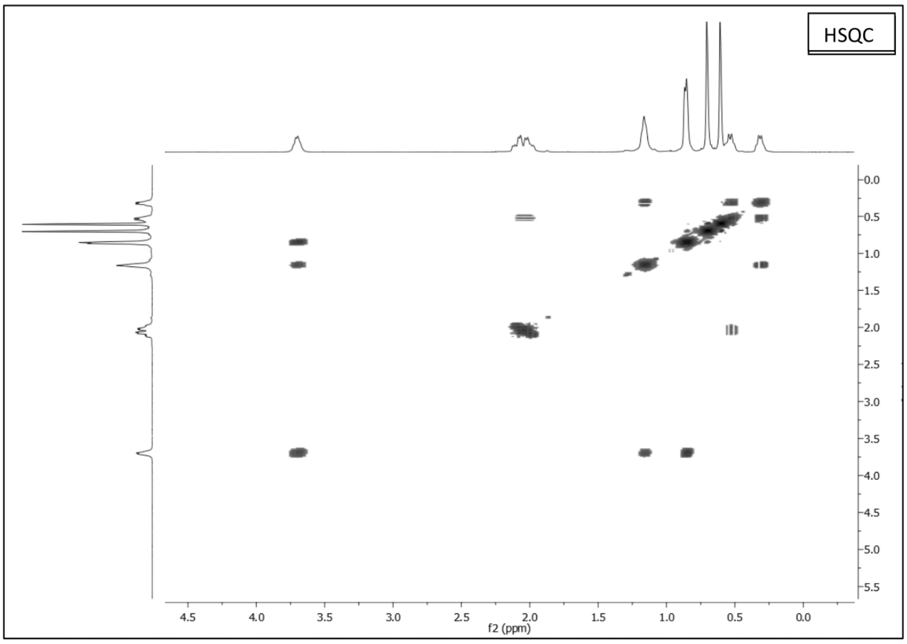
HSQC
4.5
4.0
3.5
3.0
2.5
2.0
1.5
1.0
0.5
0.0
f2 (ppm)
0.0
0.5
1.0
1.5
2.0
2.5
3.0
3.5
4.0
4.5
5.0
5.5

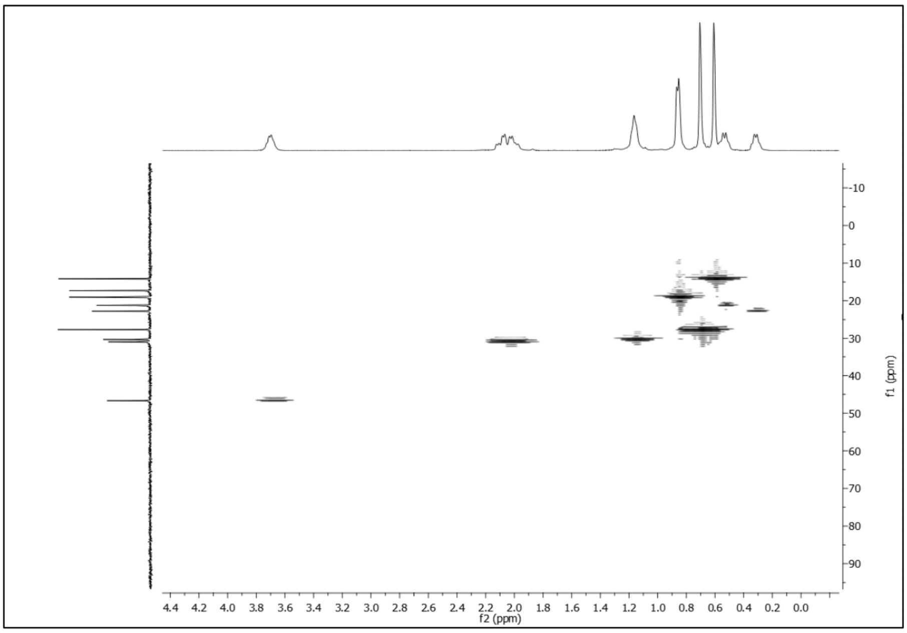
4.4
4.2
4.0
3.8
3.6
3.4
3.2
3.0
2.8
2.6
2.4
2.2
2.0
1.8
1.6
1.4
1.2
1.0
0.8
0.6
0.4
0.2
0.0
f2 (ppm)
-10
0
10
20
30
40
50
60
70
80
90
f1 (ppm)

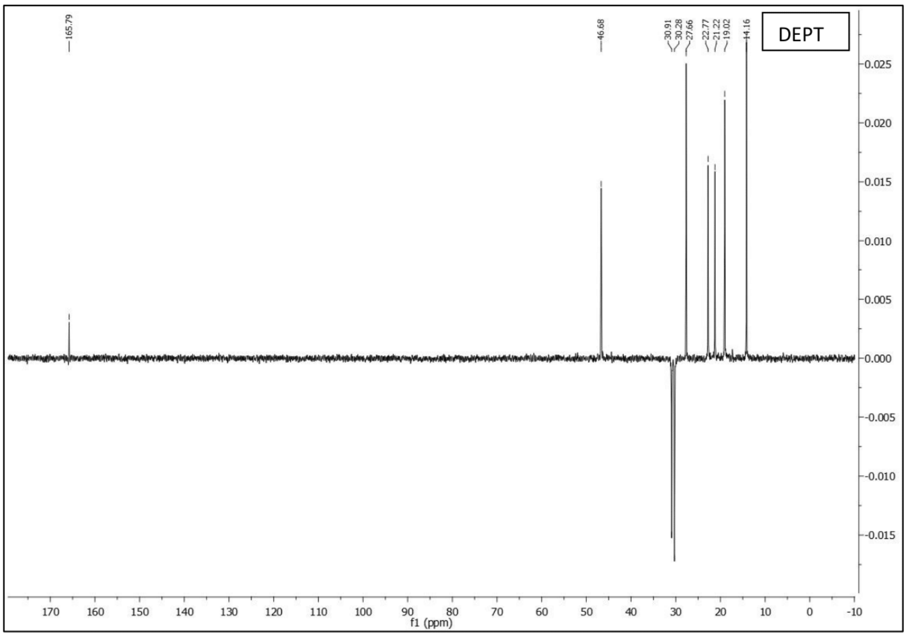

Supplementary Figure 18: NMR-spectra of Poly-3S-caranamide (DCOOD, 1H 400 MHz, 13C 100 MHz).

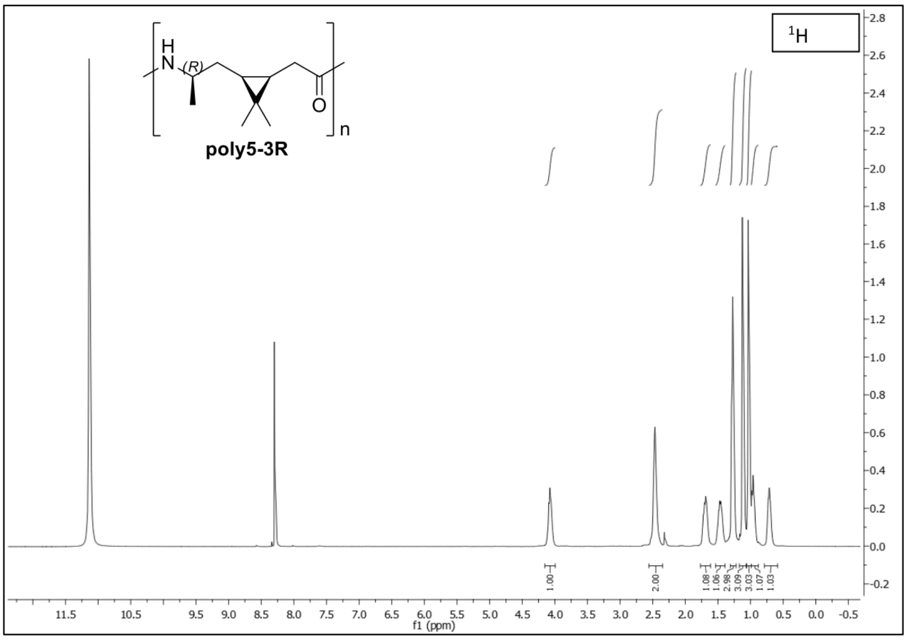
poly5-3R
(R)
n
1H
1.00
2.00
1.08
1.06
2.98
3.09
3.03
1.07
1.03
f1 (ppm)
11.5
10.5
9.5
9.0
8.5
8.0
7.5
7.0
6.5
6.0
5.5
5.0
4.5
4.0
3.5
3.0
2.5
2.0
1.5
1.0
0.5
0.0
-0.5

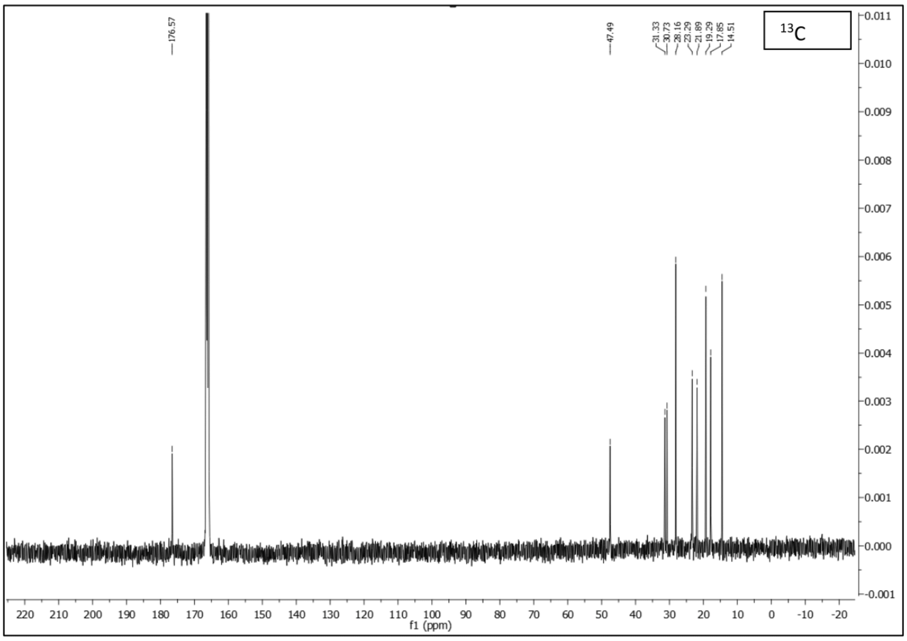
13C
176.57
47.49
31.33
30.73
28.16
23.29
21.89
19.29
17.85
14.51
f1 (ppm)
220
210
200
190
180
170
160
150
140
130
120
110
100
90
80
70
60
50
40
30
20
10
0
-10
-20

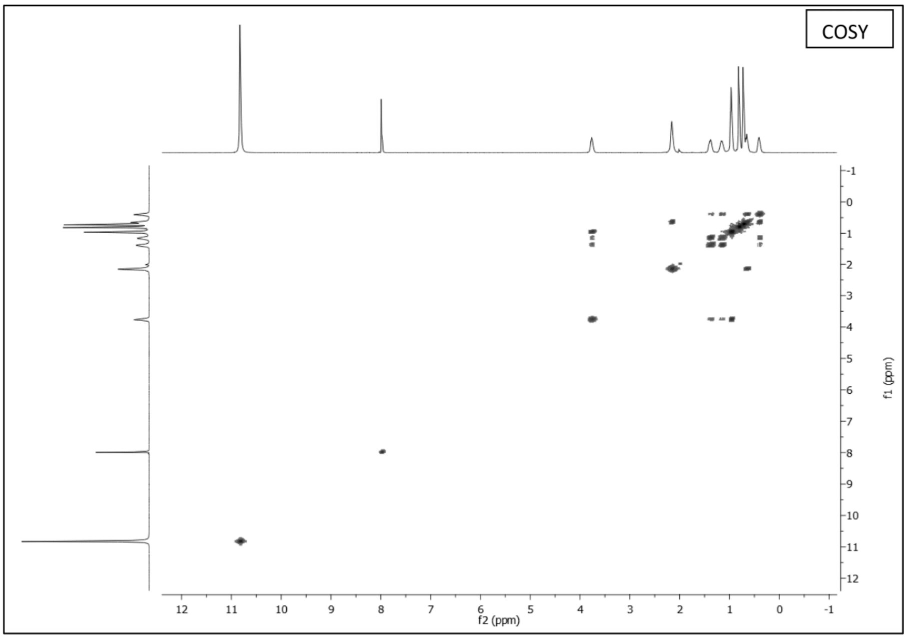
COSY
f2 (ppm)
12 11 10 9 8 7 6 5 4 3 2 1 0 -1
f1 (ppm)
-1 0 1 2 3 4 5 6 7 8 9 10 11 12

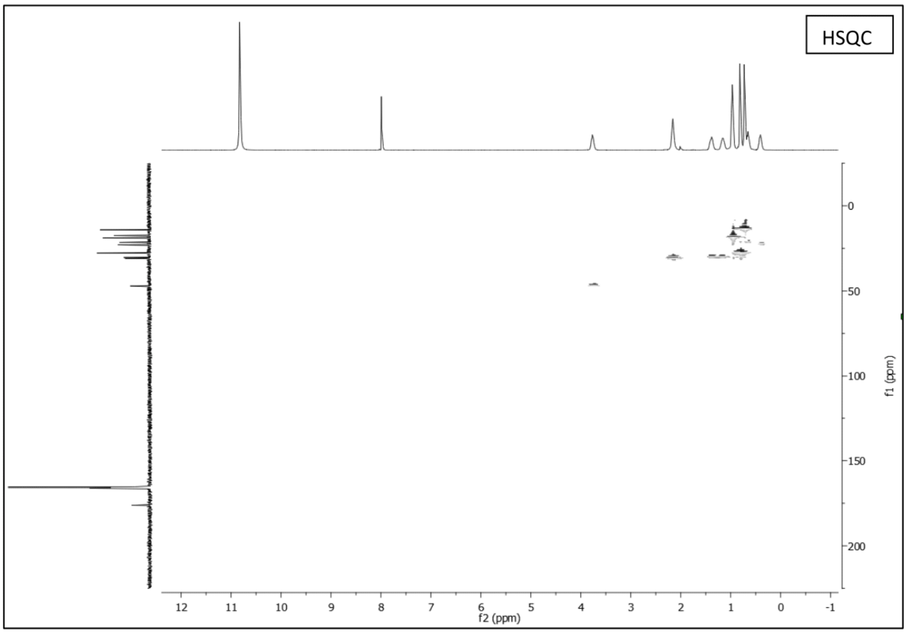
HSQC
f2 (ppm)
12 11 10 9 8 7 6 5 4 3 2 1 0 -1
f1 (ppm)
0 50 100 150 200

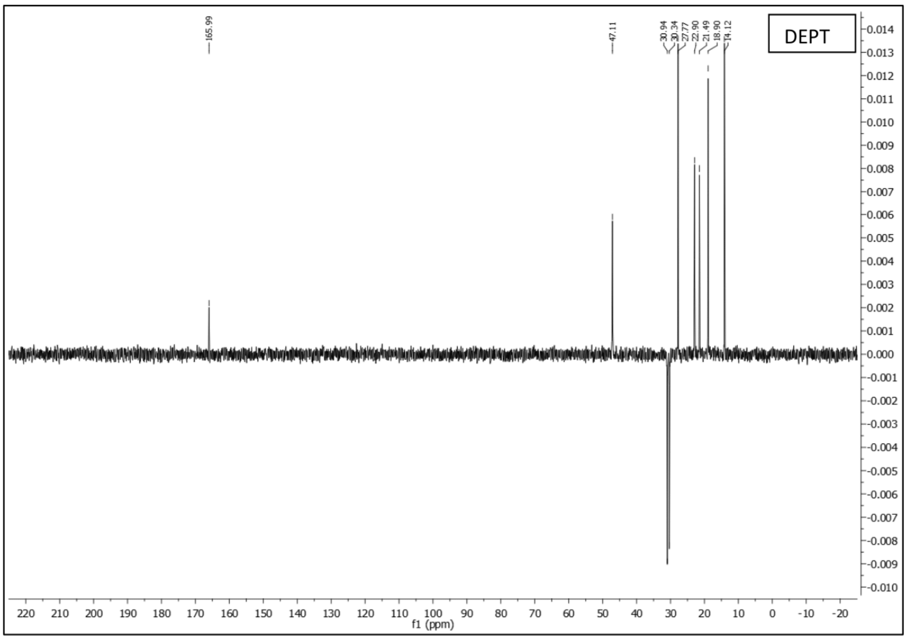

Supplementary Figure 19: NMR-spectra of Poly-3R-caranamide (DCOOD, 1H 400 MHz, 13C 100 MHz).[12]

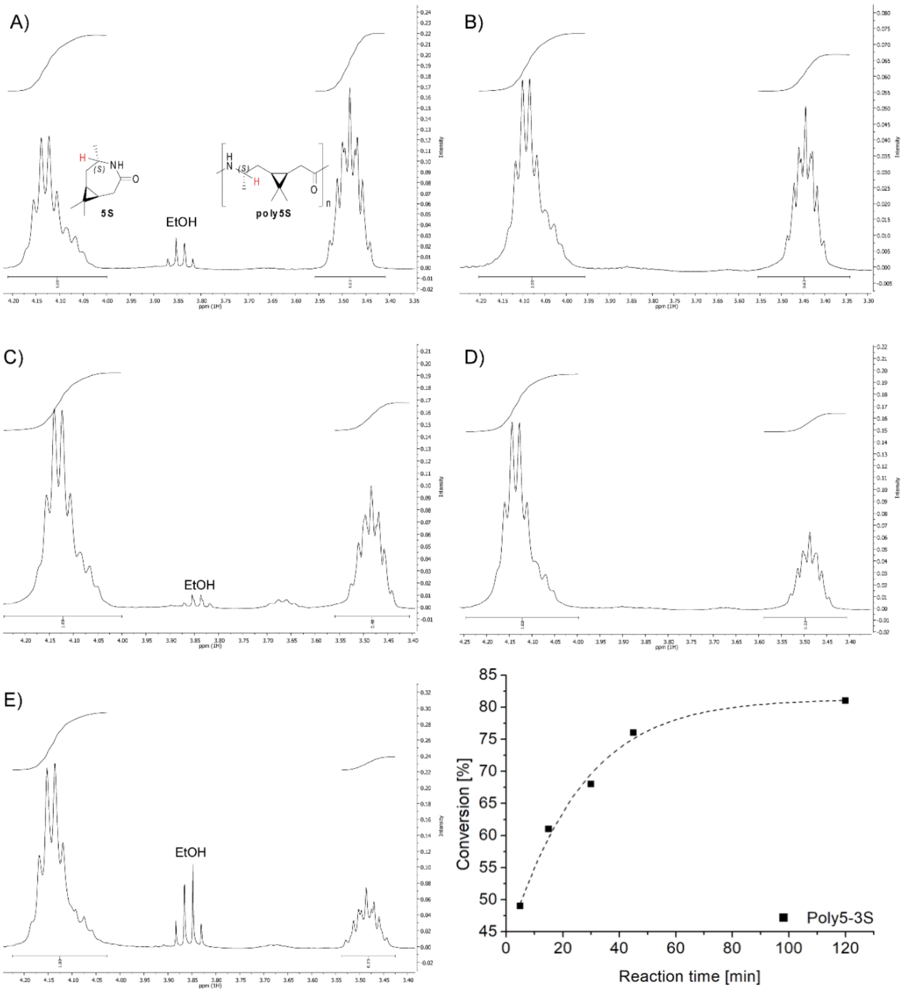

Supplementary Figure 20: Influence of the reaction time on the conversion.

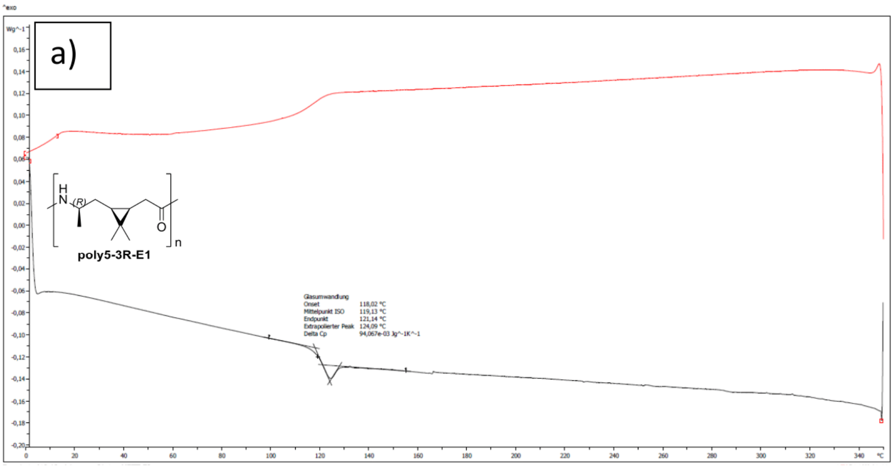
^exo
Wg^-1
a)
0,16
0,14
0,12
0,10
0,08
0,06
0,04
0,02
0,00
-0,02
-0,04
-0,06
-0,08
-0,10
-0,12
-0,14
-0,16
-0,18
-0,20
H
N
(R)
O
n
poly5-3R-E1
Glasumwandlung
Onset 118,02 °C
Mittelpunkt ISO 119,13 °C
Endpunkt 121,14 °C
Extrapolierter Peak 124,09 °C
Delta Cp 94,067e-03 Jg^-1K^-1
0
20
40
60
80
100
120
140
160
180
200
220
240
260
280
300
320
340
°C

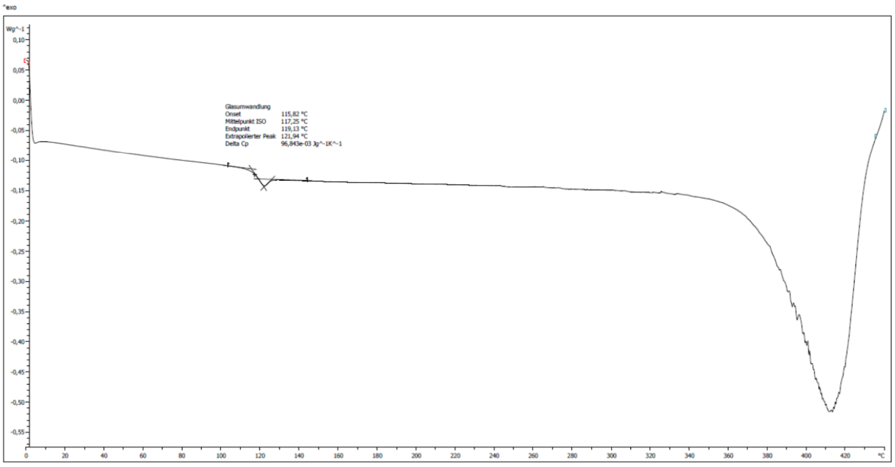
^exo
Wg^-1
0,10
0,05
0,00
-0,05
-0,10
-0,15
-0,20
-0,25
-0,30
-0,35
-0,40
-0,45
-0,50
-0,55
Glasumwandlung
Onset 115,82 °C
Mittelpunkt ISO 117,25 °C
Endpunkt 119,13 °C
Extrapolierter Peak 121,94 °C
Delta Cp 96,843e-03 Jg^-1K^-1
0
20
40
60
80
100
120
140
160
180
200
220
240
260
280
300
320
340
360
380
400
420
°C

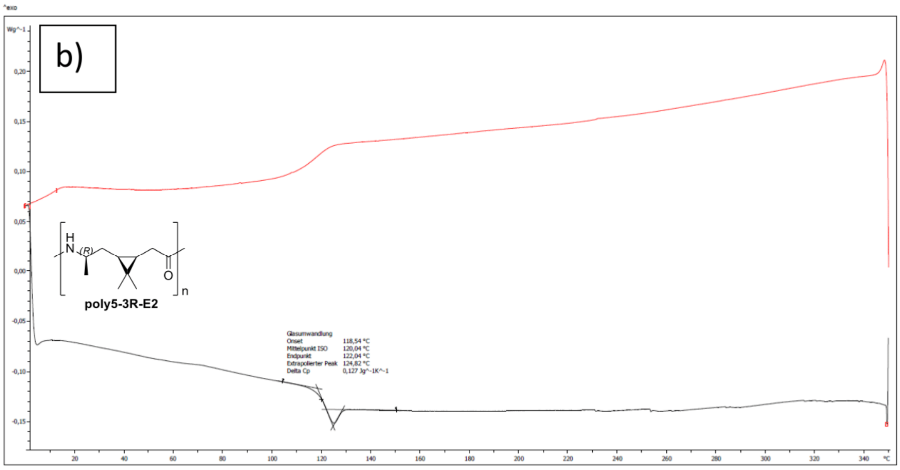
^exo
Wg^-1
b)
0,20
0,15
0,10
0,05
0,00
-0,05
-0,10
-0,15
H
N
(R)
O
n
poly5-3R-E2
Glasumwandlung
Onset 118,54 °C
Mittelpunkt ISO 120,04 °C
Endpunkt 122,04 °C
Extrapolierter Peak 124,82 °C
Delta Cp 0,127 Jg^-1K^-1
20
40
60
80
100
120
140
160
180
200
220
240
260
280
300
320
340
°C

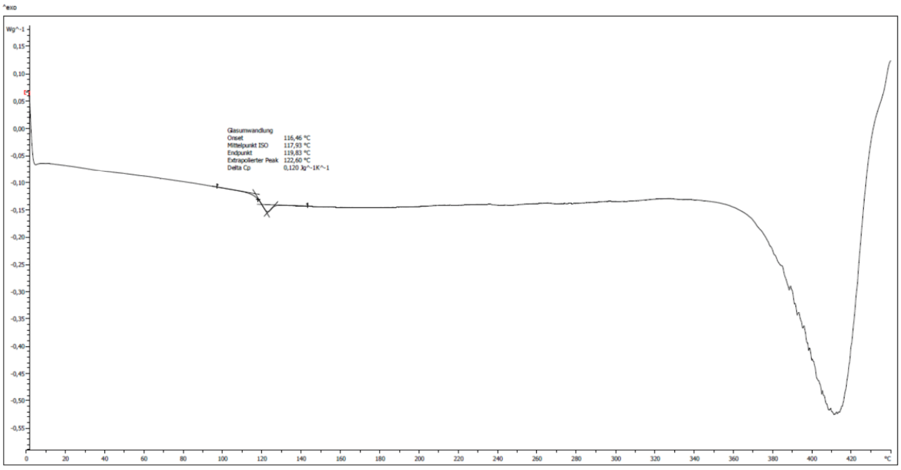
^exo
Wg^-1
0,15
0,10
0,05
0,00
-0,05
-0,10
-0,15
-0,20
-0,25
-0,30
-0,35
-0,40
-0,45
-0,50
-0,55
Glasumwandlung
Onset 116,46 °C
Mittelpunkt ISO 117,93 °C
Endpunkt 119,83 °C
Extrapolierter Peak 122,60 °C
Delta Cp 0,120 Jg^-1K^-1
0
20
40
60
80
100
120
140
160
180
200
220
240
260
280
300
320
340
360
380
400
420
°C

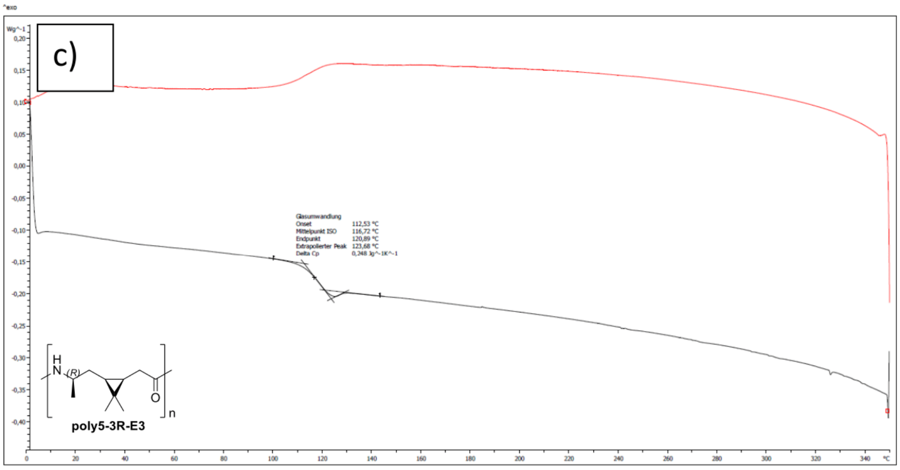
^exo
Wg^-1
c)
0,20
0,15
0,10
0,05
0,00
-0,05
-0,10
-0,15
-0,20
-0,25
-0,30
-0,35
-0,40
Glasumwandlung
Onset 112,53 °C
Mittelpunkt ISO 116,72 °C
Endpunkt 120,89 °C
Extrapolierter Peak 123,68 °C
Delta Cp 0,248 Jg^-1K^-1
H
N
(R)
O
n
poly5-3R-E3
0
20
40
60
80
100
120
140
160
180
200
220
240
260
280
300
320
340
°C

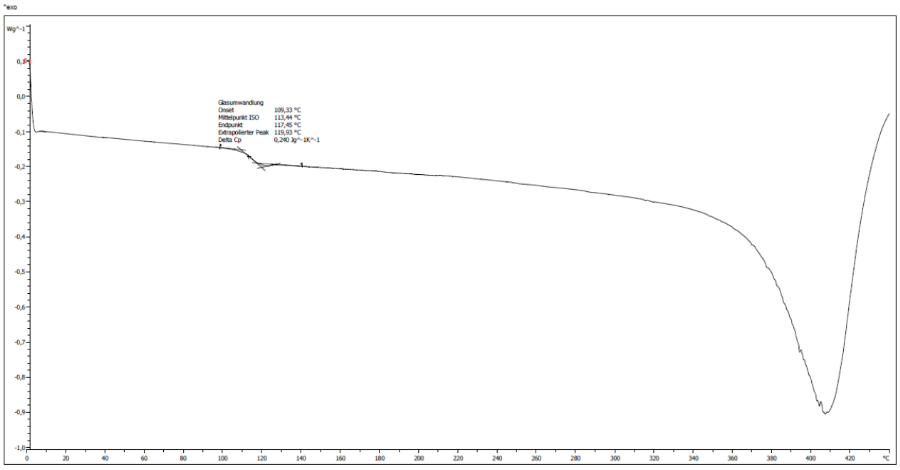
^exo
Wg^-1
0,1
0,0
-0,1
-0,2
-0,3
-0,4
-0,5
-0,6
-0,7
-0,8
-0,9
-1,0
Glasumwandlung
Onset 109,33 °C
Mittelpunkt ISO 113,44 °C
Endpunkt 117,45 °C
Extrapolierter Peak 119,93 °C
Delta Cp 0,240 Jg^-1K^-1
0
20
40
60
80
100
120
140
160
180
200
220
240
260
280
300
320
340
360
380
400
420
°C

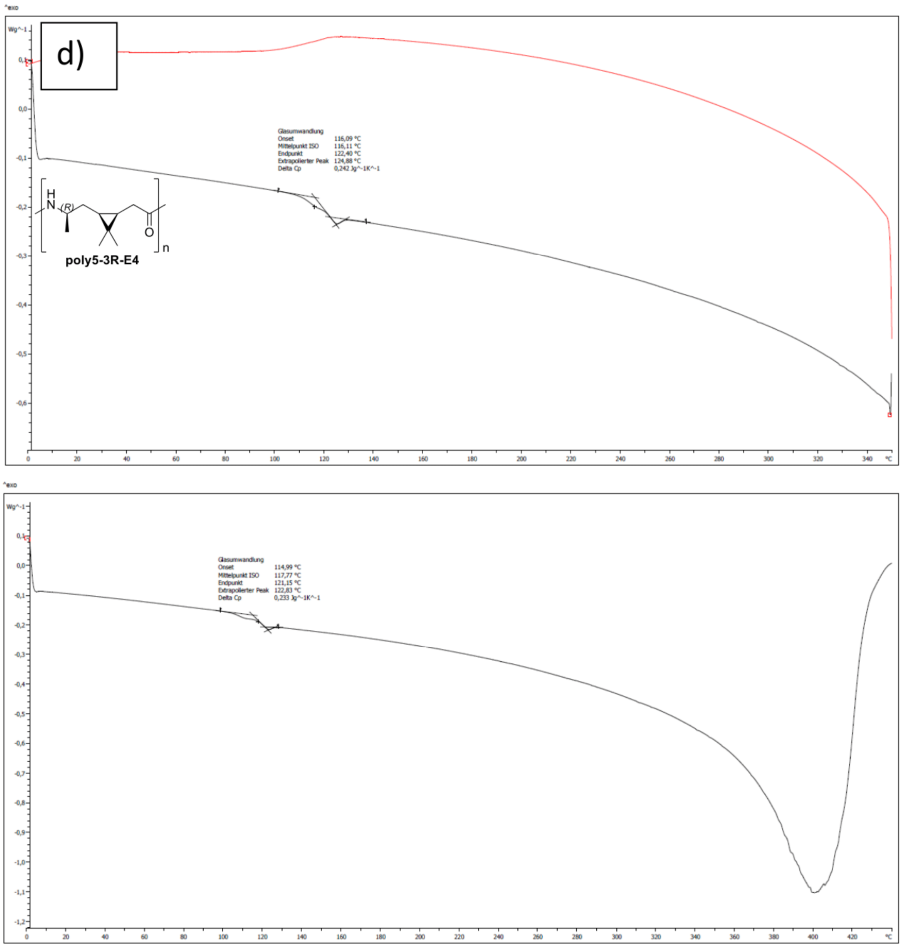
d)
^exo
Wg^-1
poly5-3R-E4
H
N
(R)
O
n
Glasumwandlung
Onset 116,09 °C
Mittelpunkt ISO 116,11 °C
Endpunkt 122,40 °C
Extrapolierter Peak 124,88 °C
Delta Cp 0,242 Jg^-1K^-1
0,1
0,0
-0,1
-0,2
-0,3
-0,4
-0,5
-0,6
0 20 40 60 80 100 120 140 160 180 200 220 240 260 280 300 320 340 °C
^exo
Wg^-1
Glasumwandlung
Onset 114,99 °C
Mittelpunkt ISO 117,77 °C
Endpunkt 121,15 °C
Extrapolierter Peak 122,83 °C
Delta Cp 0,233 Jg^-1K^-1
0,1
0,0
-0,1
-0,2
-0,3
-0,4
-0,5
-0,6
-0,7
-0,8
-0,9
-1,0
-1,1
-1,2
0 20 40 60 80 100 120 140 160 180 200 220 240 260 280 300 320 340 360 380 400 420 °C

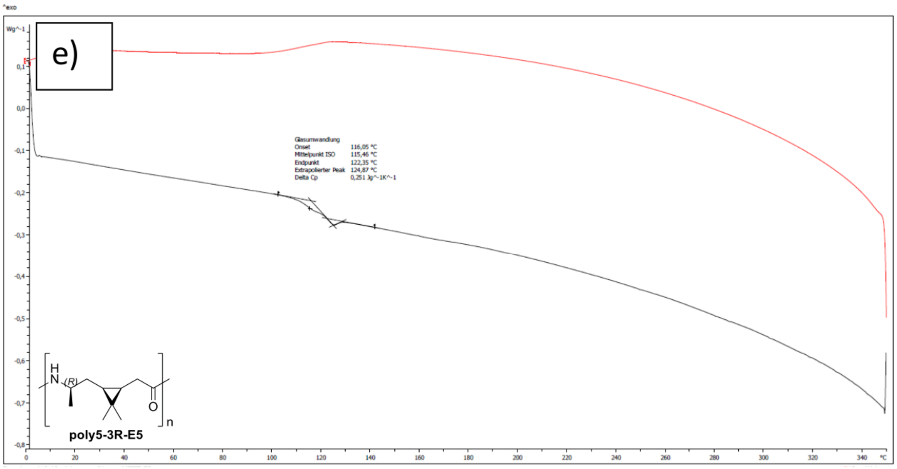

Glasumwandlung
Onset 116,05 °C
Mittelpunkt ISO 115,46 °C
Endpunkt 122,35 °C
Extrapolierter Peak 124,87 °C
Delta Cp 0,251 Jg^-1K^-1

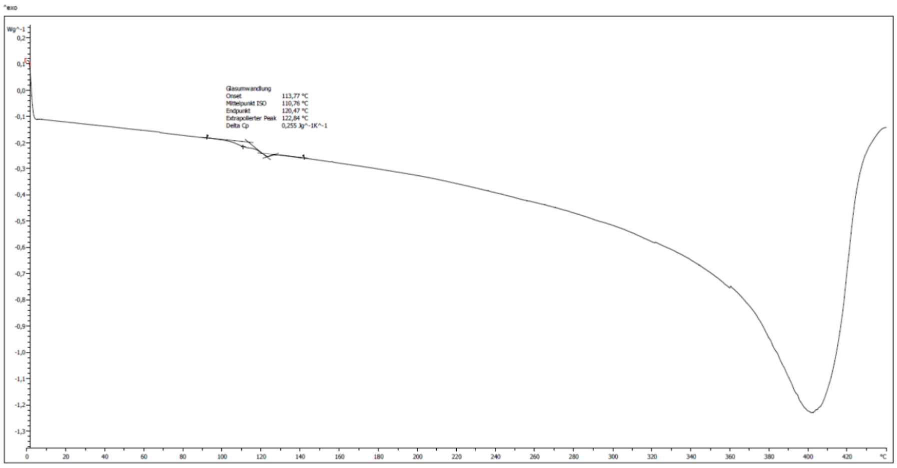

Glasumwandlung
Onset 113,77 °C
Mittelpunkt ISO 110,76 °C
Endpunkt 120,47 °C
Extrapolierter Peak 122,84 °C
Delta Cp 0,255 Jg^-1K^-1

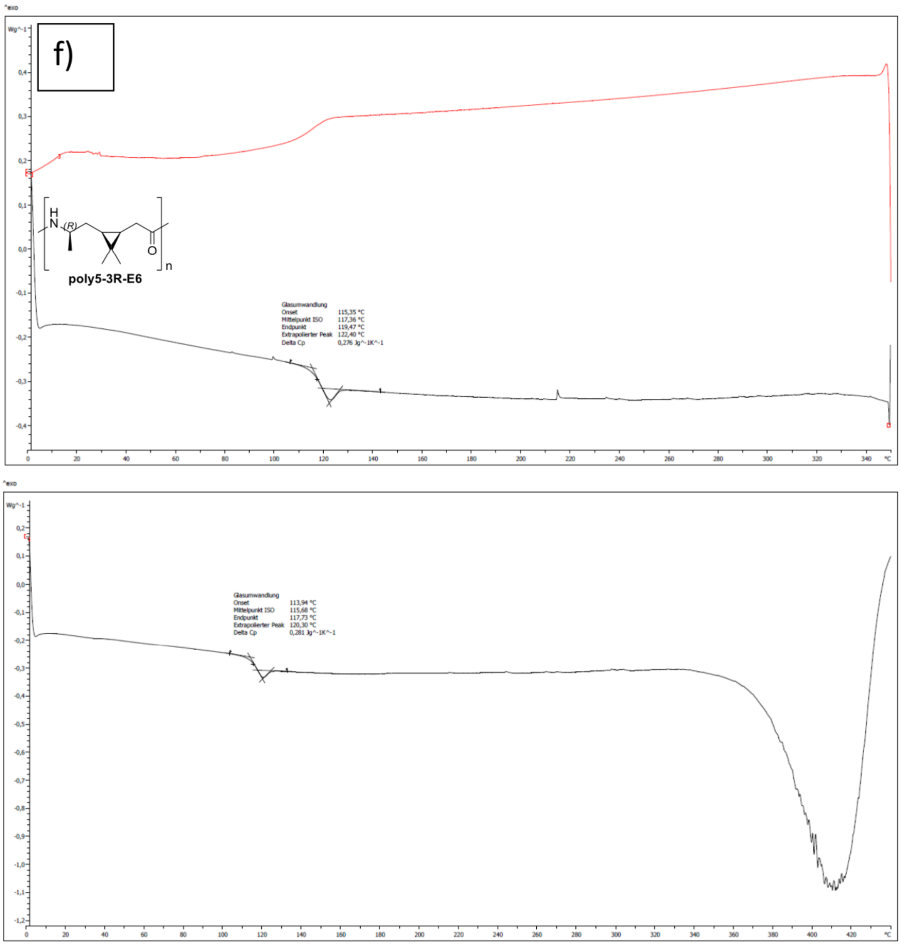

Supplementary Figure 21: DSC curves of various poly-3R-caranamides e)-f) as described in Supplementary Table 13, measured using DSC method A, segment 6 (heating, black, upper), segment 7 (cooling, red, upper) and segment 8 (black, heating to decomposition, lower).

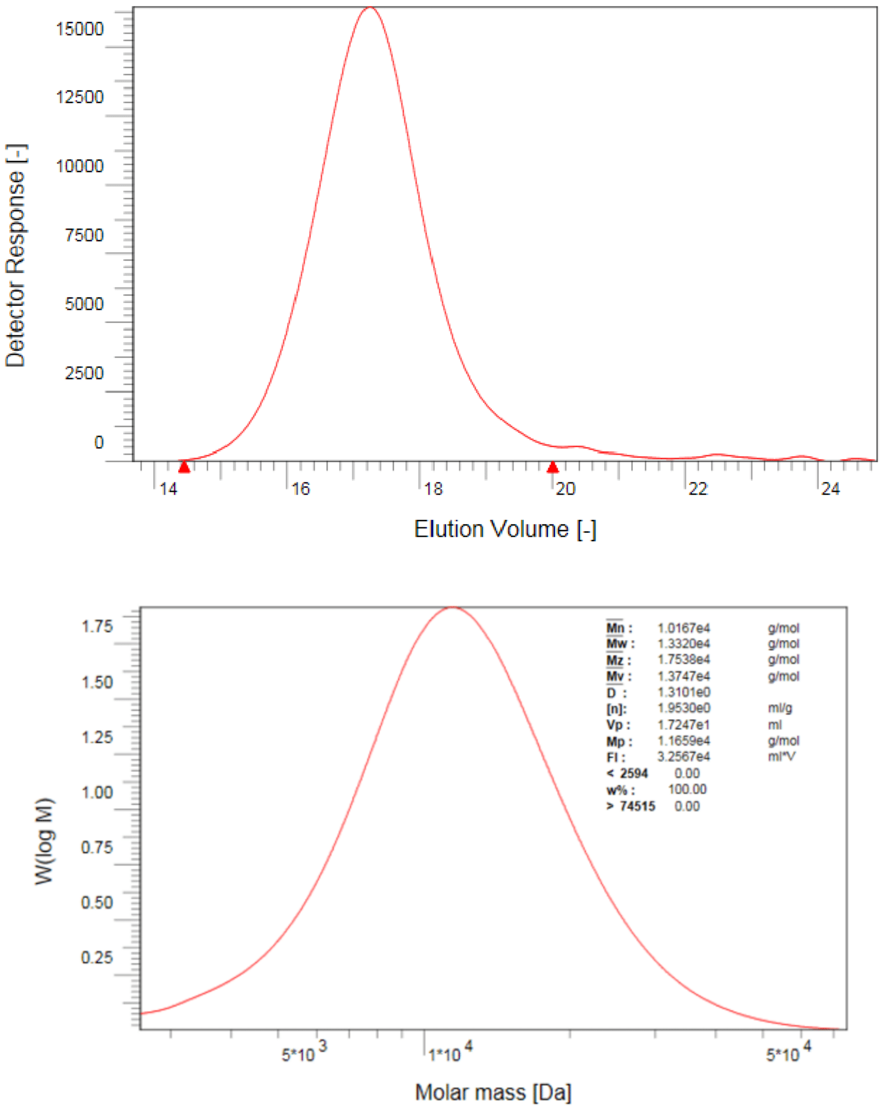

Supplementary Figure 22: GPC analysis **poly5-3R** with 10 kDa.

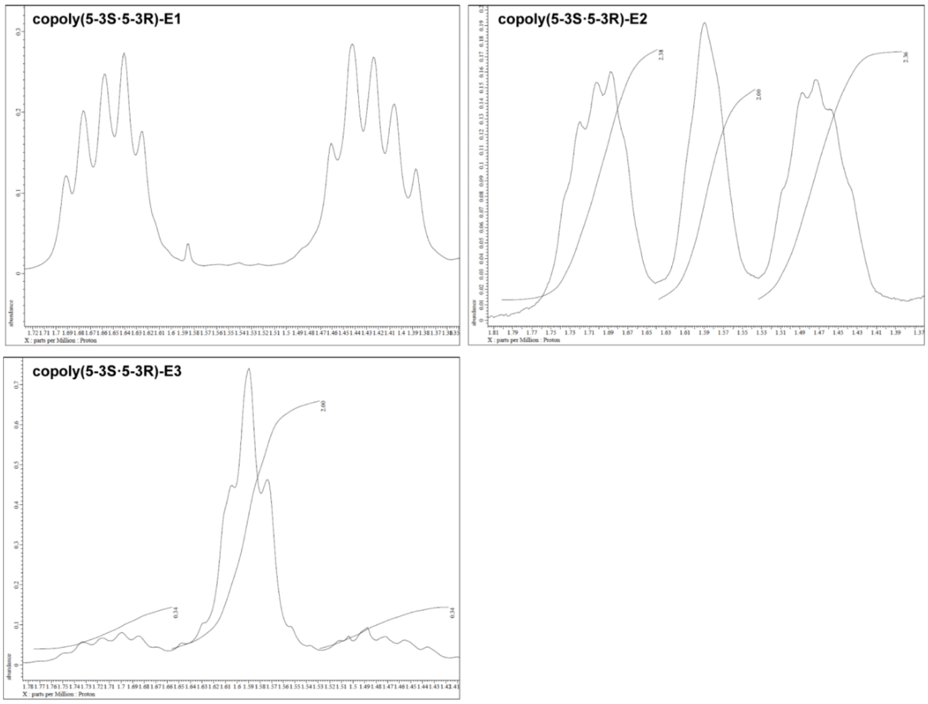

Supplementary Figure 23: Ratio of 3S-caranlactam (**5-3S**) and 3R-caranlactam (**5-3R**) in co-polymers synthesized as displayed in Supplementary Table 16 entries E1-E3.

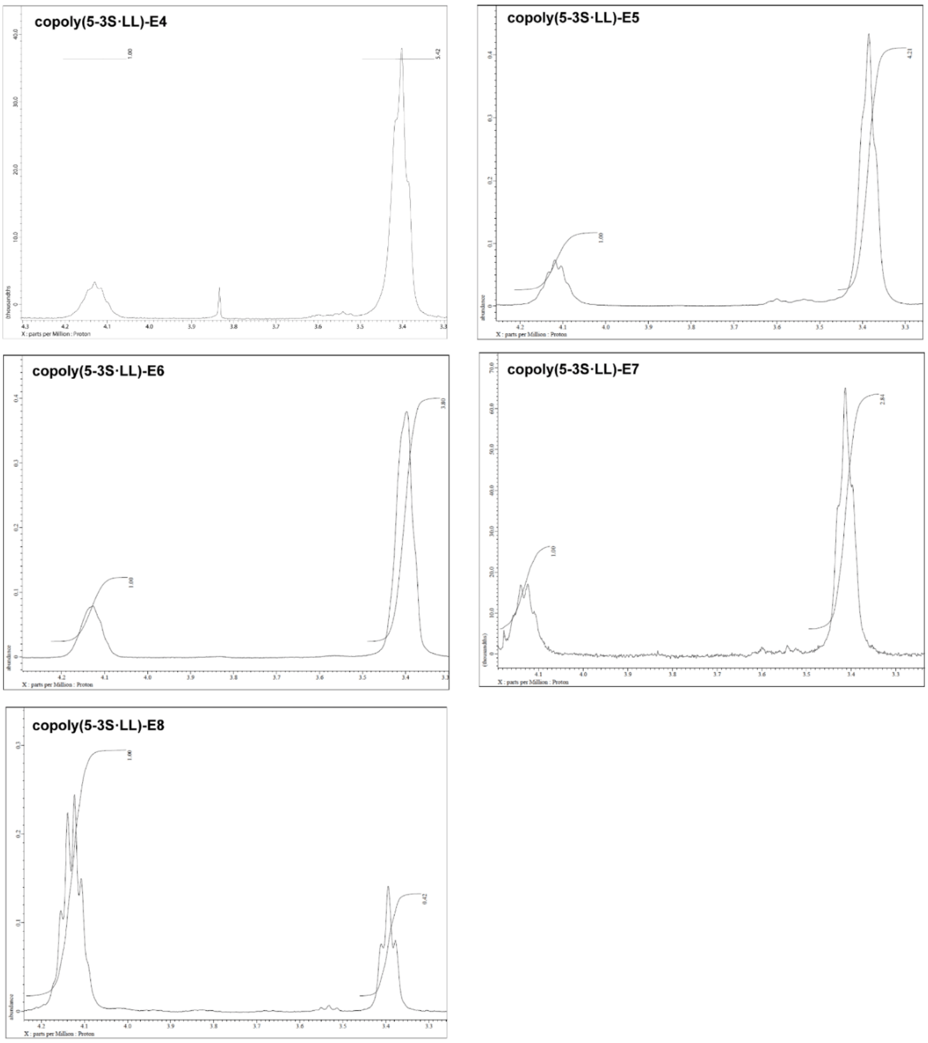

Supplementary Figure 24: Ratio of 3S-caranlactam (**5-3S**) and laurolactam (**LL**) in co-polymers synthesized as displayed in Supplementary Table 16 entries E4-E8.

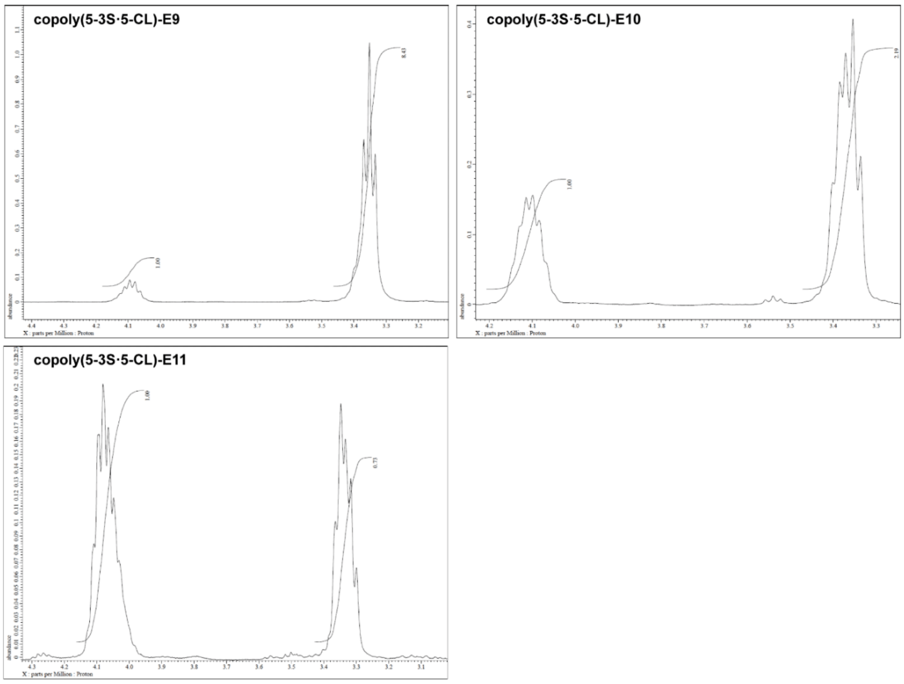

Supplementary Figure 25: Ratio of 3S-caranlactam (**5-3S**) and caprolactam (**CL**) in co-polymers synthesized as displayed in Supplementary Table 16 entries E9-E11.

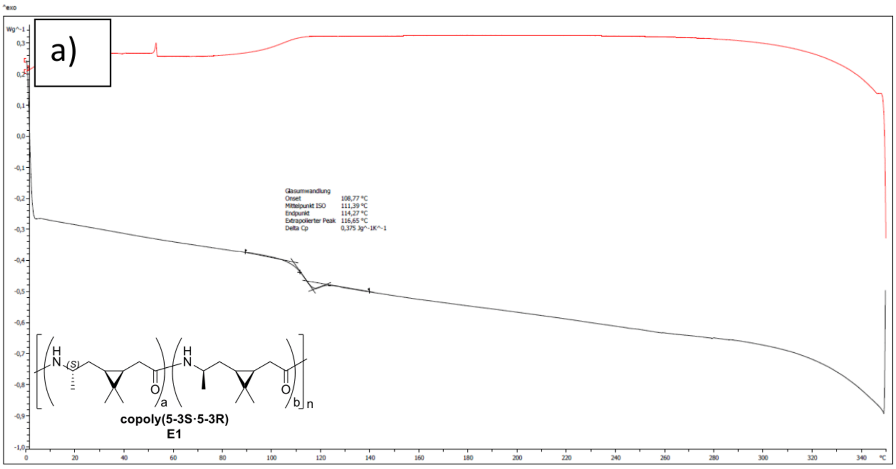
a)
^exo
Wg^-1
0,3
0,2
0,1
0,0
-0,1
-0,2
-0,3
-0,4
-0,5
-0,6
-0,7
-0,8
-0,9
-1,0
0
20
40
60
80
100
120
140
160
180
200
220
240
260
280
300
320
340
°C
Glasumwandlung
Onset 108,77 °C
Mittelpunkt ISO 111,39 °C
Endpunkt 114,27 °C
Extrapolierter Peak 116,65 °C
Delta Cp 0,375 Jg^-1K^-1
H
N
(S)
O
a
H
N
O
b
n
copoly(5-3S·5-3R)
E1

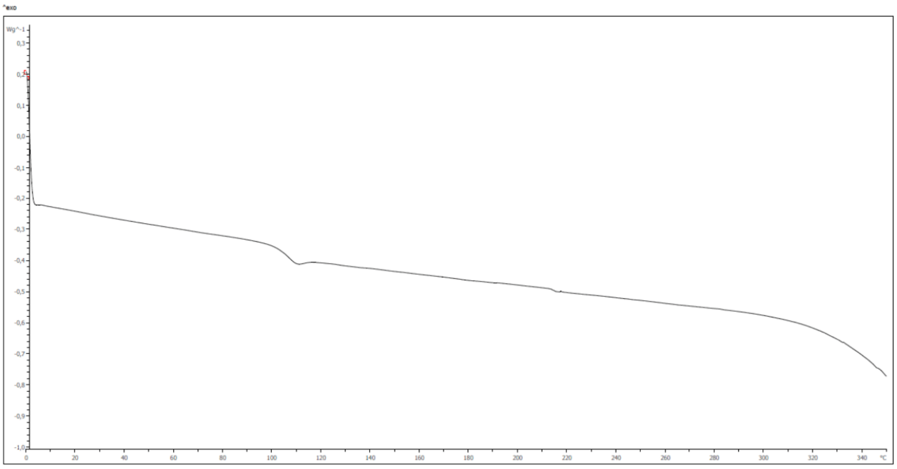
^exo
Wg^-1
0,3
0,2
0,1
0,0
-0,1
-0,2
-0,3
-0,4
-0,5
-0,6
-0,7
-0,8
-0,9
-1,0
0
20
40
60
80
100
120
140
160
180
200
220
240
260
280
300
320
340
°C

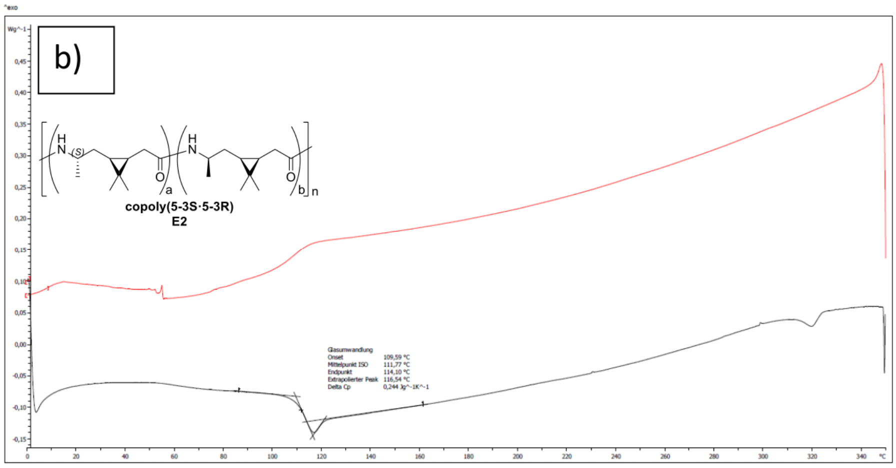
^exo
Wg^-1
b)
0,45
0,40
0,35
0,30
0,25
0,20
0,15
0,10
0,05
0,00
-0,05
-0,10
-0,15
H
N
(S)
O
a
H
N
O
b
n
copoly(5-3S·5-3R)
E2
Glasumwandlung
Onset 109,59 °C
Mittelpunkt ISO 111,77 °C
Endpunkt 114,10 °C
Extrapolierter Peak 116,54 °C
Delta Cp 0,244 Jg^-1K^-1
0
20
40
60
80
100
120
140
160
180
200
220
240
260
280
300
320
340
°C

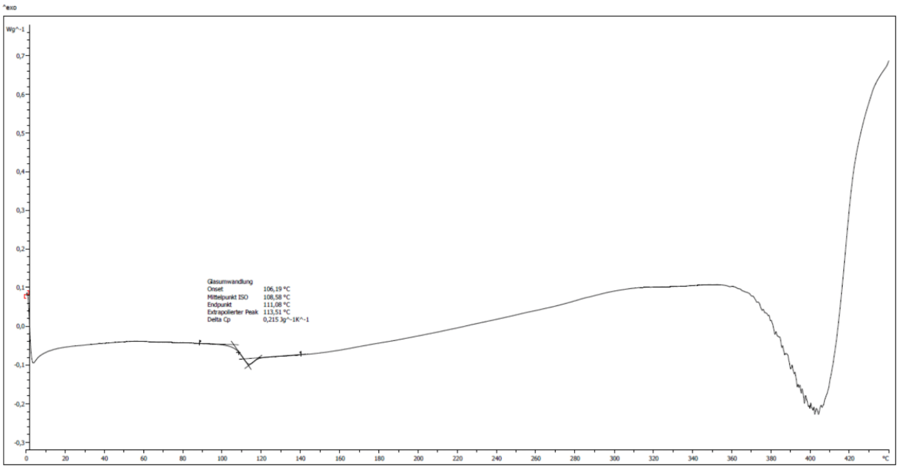
^exo
Wg^-1
0,7
0,6
0,5
0,4
0,3
0,2
0,1
0,0
-0,1
-0,2
-0,3
Glasumwandlung
Onset 106,19 °C
Mittelpunkt ISO 108,58 °C
Endpunkt 111,08 °C
Extrapolierter Peak 113,51 °C
Delta Cp 0,215 Jg^-1K^-1
0
20
40
60
80
100
120
140
160
180
200
220
240
260
280
300
320
340
360
380
400
420
°C

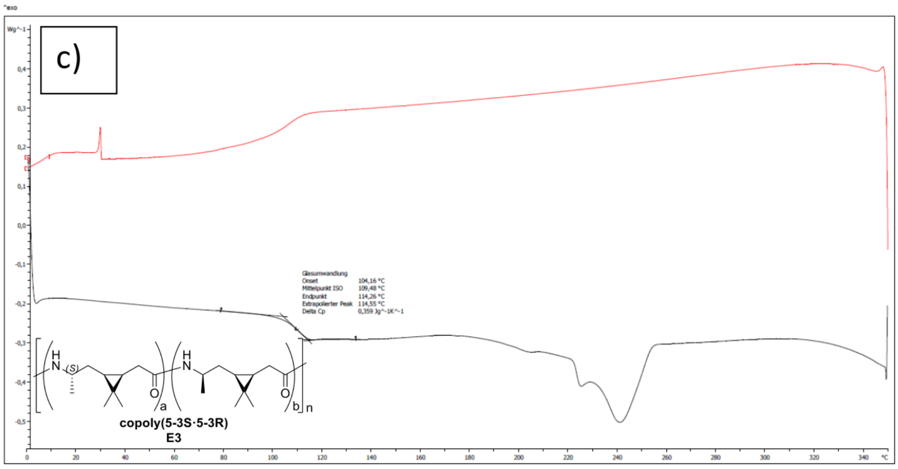
^exo
Wg^-1
c)
0,4
0,3
0,2
0,1
0,0
-0,1
-0,2
-0,3
-0,4
-0,5
Glasumwandlung
Onset 104,16 °C
Mittelpunkt ISO 109,48 °C
Endpunkt 114,26 °C
Extrapolierter Peak 114,55 °C
Delta Cp 0,359 Jg^-1K^-1
H
N
(S)
O
a
H
N
O
b
n
copoly(5-3S·5-3R)
E3
0
20
40
60
80
100
120
140
160
180
200
220
240
260
280
300
320
340
°C

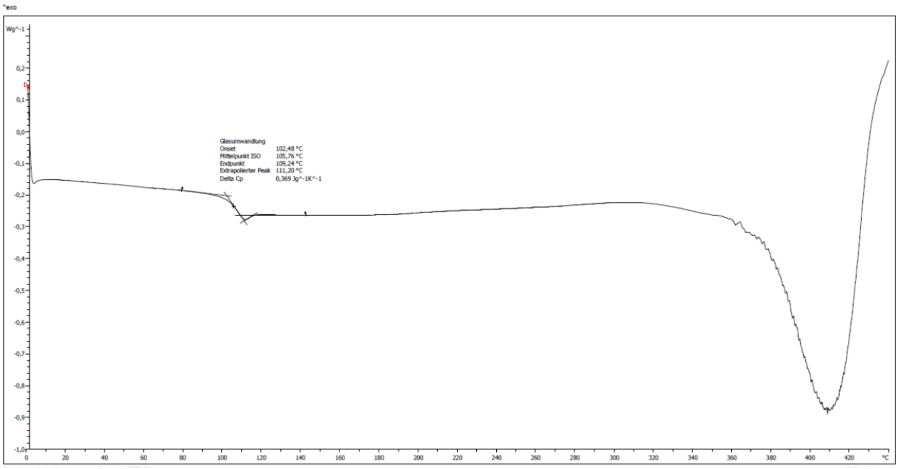
^exo
Wg^-1
0,2
0,1
0,0
-0,1
-0,2
-0,3
-0,4
-0,5
-0,6
-0,7
-0,8
-0,9
-1,0
Glasumwandlung
Onset 102,48 °C
Mittelpunkt ISO 105,76 °C
Endpunkt 109,24 °C
Extrapolierter Peak 111,20 °C
Delta Cp 0,369 Jg^-1K^-1
0
20
40
60
80
100
120
140
160
180
200
220
240
260
280
300
320
340
360
380
400
420
°C

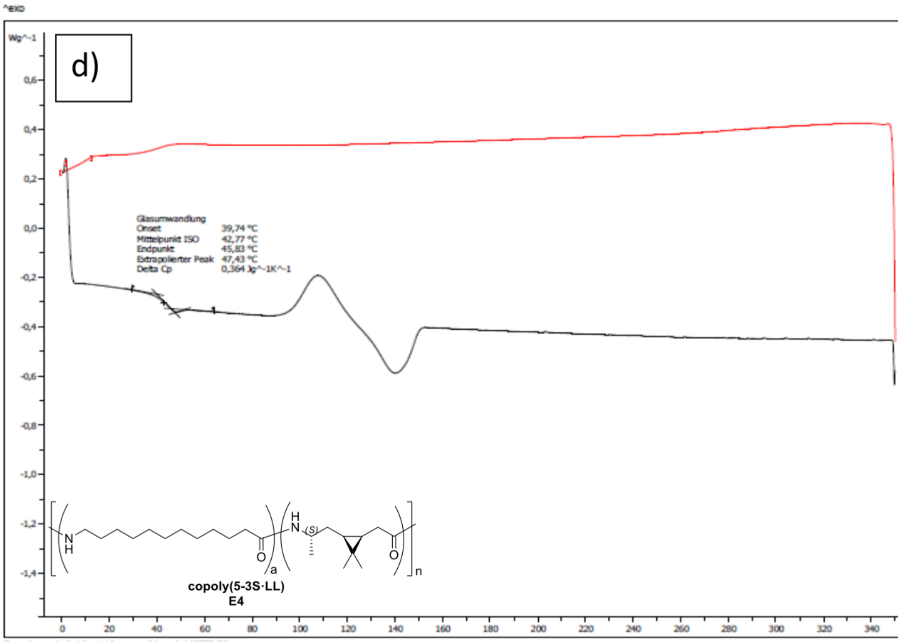
^exo
Wg^-1
d)
0,6
0,4
0,2
0,0
-0,2
-0,4
-0,6
-0,8
-1,0
-1,2
-1,4
Glasumwandlung
Onset 39,74 °C
Mittelpunkt ISO 42,77 °C
Endpunkt 45,83 °C
Extrapolierter Peak 47,43 °C
Delta Cp 0,364 Jg^-1K^-1
N
H
O
a
H
N
(S)
O
n
copoly(5-3S·LL)
E4
0
20
40
60
80
100
120
140
160
180
200
220
240
260
280
300
320
340

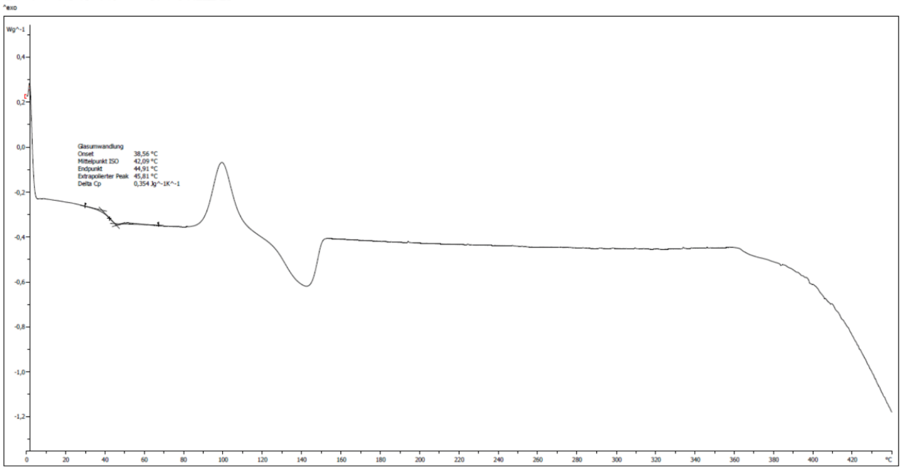
^exo
Wg^-1
0,4
0,2
0,0
-0,2
-0,4
-0,6
-0,8
-1,0
-1,2
Glasumwandlung
Onset 38,56 °C
Mittelpunkt ISO 42,09 °C
Endpunkt 44,91 °C
Extrapolierter Peak 45,81 °C
Delta Cp 0,354 Jg^-1K^-1
0
20
40
60
80
100
120
140
160
180
200
220
240
260
280
300
320
340
360
380
400
420
°C

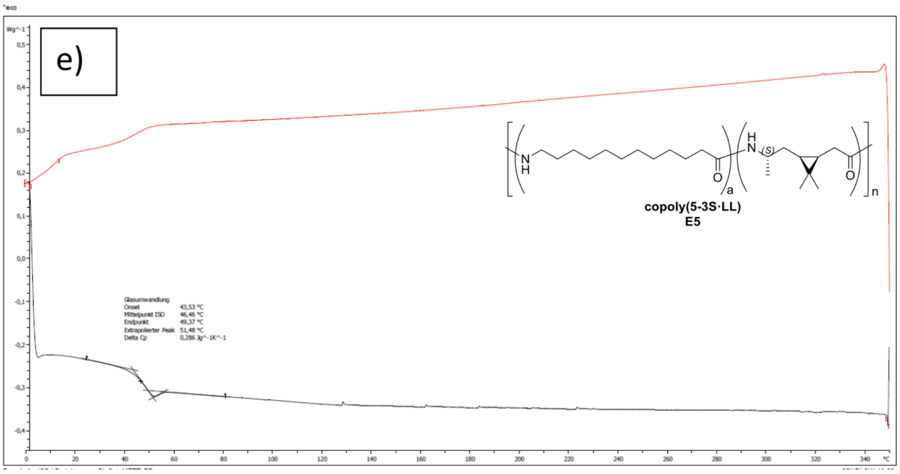
e)
^exo
Wg^-1
0,5
0,4
0,3
0,2
0,1
0,0
-0,1
-0,2
-0,3
-0,4
Glasumwandlung
Onset 43,53 °C
Mittelpunkt ISO 46,46 °C
Endpunkt 49,37 °C
Extrapolierter Peak 51,48 °C
Delta Cp 0,286 Jg^-1K^-1
H
N
(S)
O
a
n
copoly(5-3S·LL)
E5
0
20
40
60
80
100
120
140
160
180
200
220
240
260
280
300
320
340
°C

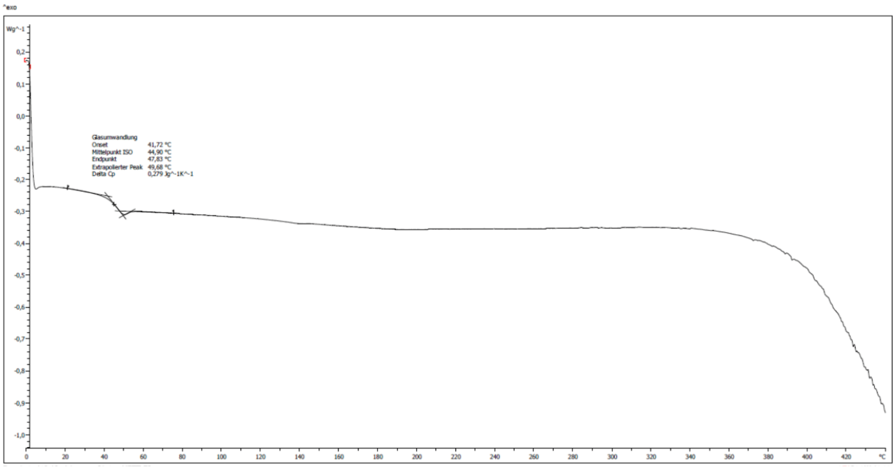
^exo
Wg^-1
0,2
0,1
0,0
-0,1
-0,2
-0,3
-0,4
-0,5
-0,6
-0,7
-0,8
-0,9
-1,0
Glasumwandlung
Onset 41,72 °C
Mittelpunkt ISO 44,90 °C
Endpunkt 47,83 °C
Extrapolierter Peak 49,68 °C
Delta Cp 0,279 Jg^-1K^-1
0
20
40
60
80
100
120
140
160
180
200
220
240
260
280
300
320
340
360
380
400
420
°C

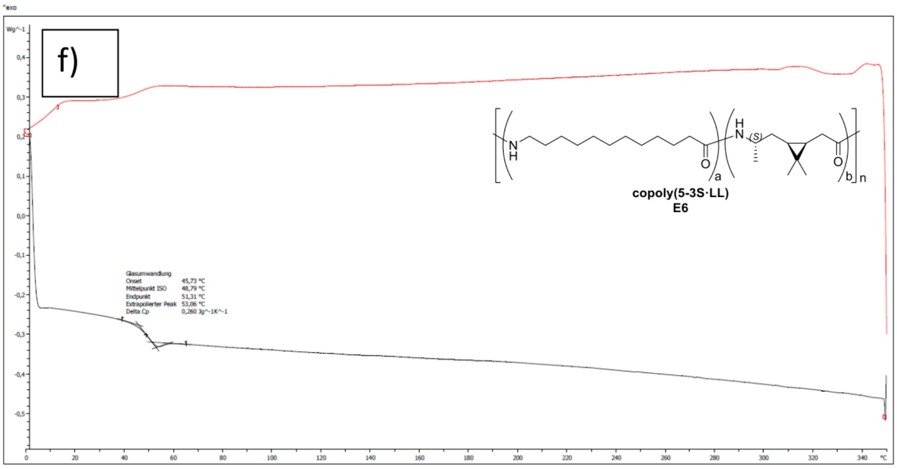
^exo
Wg^-1
f)
0,4
0,3
0,2
0,1
0,0
-0,1
-0,2
-0,3
-0,4
-0,5
0
20
40
60
80
100
120
140
160
180
200
220
240
260
280
300
320
340
°C
NH
H
O
a
H
N
(S)
O
b
n
copoly(5-3S·LL)
E6
Glasumwandlung
Onset 45,73 °C
Mittelpunkt ISO 48,79 °C
Endpunkt 51,31 °C
Extrapolierter Peak 53,06 °C
Delta Cp 0,260 Jg^-1K^-1

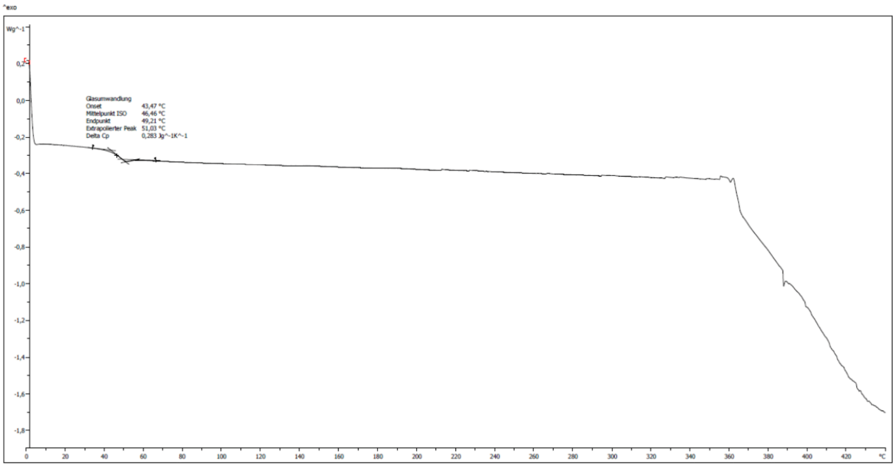
^exo
Wg^-1
0,2
0,0
-0,2
-0,4
-0,6
-0,8
-1,0
-1,2
-1,4
-1,6
-1,8
0
20
40
60
80
100
120
140
160
180
200
220
240
260
280
300
320
340
360
380
400
420
°C
Glasumwandlung
Onset 43,47 °C
Mittelpunkt ISO 46,46 °C
Endpunkt 49,21 °C
Extrapolierter Peak 51,03 °C
Delta Cp 0,283 Jg^-1K^-1

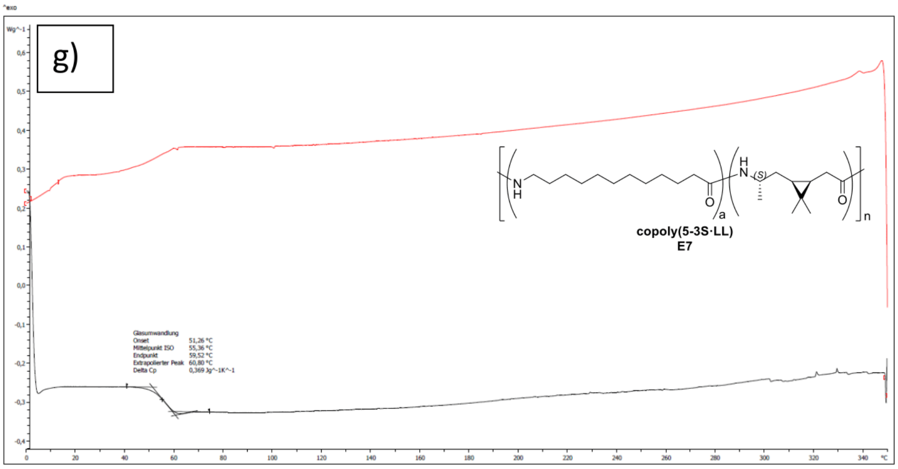
^exo
Wg^-1
g)
0,6
0,5
0,4
0,3
0,2
0,1
0,0
-0,1
-0,2
-0,3
-0,4
copoly(5-3S·LL)
E7
Glasumwandlung
Onset 51,26 °C
Mittelpunkt ISO 55,36 °C
Endpunkt 59,52 °C
Extrapolierter Peak 60,80 °C
Delta Cp 0,369 Jg^-1K^-1
0
20
40
60
80
100
120
140
160
180
200
220
240
260
280
300
320
340
°C

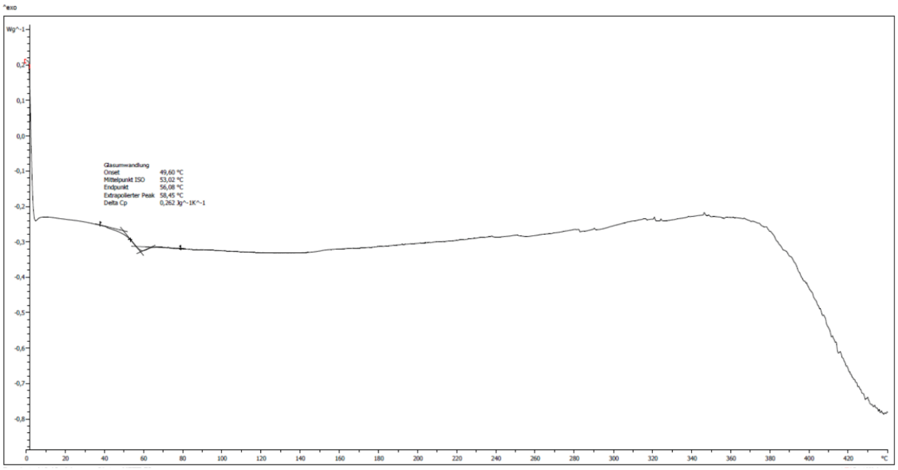
^exo
Wg^-1
0,2
0,1
0,0
-0,1
-0,2
-0,3
-0,4
-0,5
-0,6
-0,7
-0,8
Glasumwandlung
Onset 49,60 °C
Mittelpunkt ISO 53,02 °C
Endpunkt 56,08 °C
Extrapolierter Peak 58,45 °C
Delta Cp 0,262 Jg^-1K^-1
0
20
40
60
80
100
120
140
160
180
200
220
240
260
280
300
320
340
360
380
400
420
°C

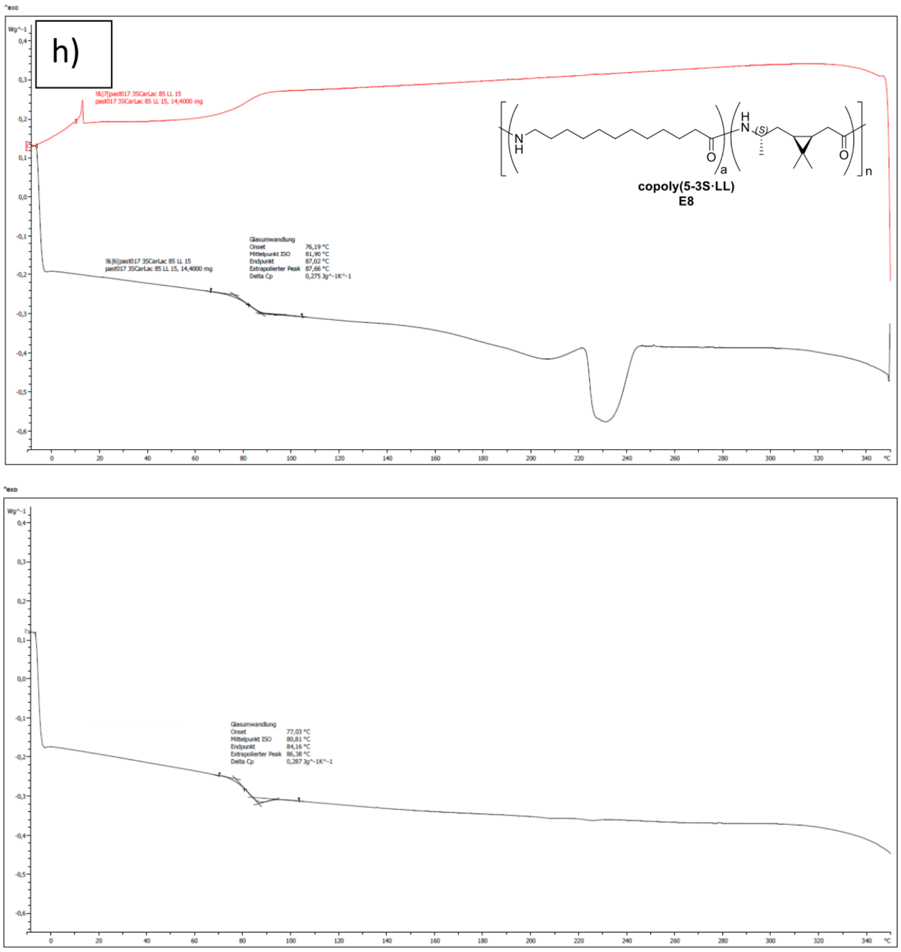
^exo
Wg^-1
h)
0,4
0,3
0,2
0,1
0,0
-0,1
-0,2
-0,3
-0,4
-0,5
-0,6
!&]7[past017 3SCarLac 85 LL 15
past017 3SCarLac 85 LL 15, 14,4000 mg
!&]6[past017 3SCarLac 85 LL 15
past017 3SCarLac 85 LL 15, 14,4000 mg
Glasumwandlung
Onset 76,19 °C
Mittelpunkt ISO 81,90 °C
Endpunkt 87,02 °C
Extrapolierter Peak 87,66 °C
Delta Cp 0,275 Jg^-1K^-1
H
N
H
N
(S)
O
O
a
n
copoly(5-3S·LL)
E8
0
20
40
60
80
100
120
140
160
180
200
220
240
260
280
300
320
340
°C
^exo
Wg^-1
0,4
0,3
0,2
0,1
0,0
-0,1
-0,2
-0,3
-0,4
-0,5
-0,6
Glasumwandlung
Onset 77,03 °C
Mittelpunkt ISO 80,81 °C
Endpunkt 84,16 °C
Extrapolierter Peak 86,38 °C
Delta Cp 0,287 Jg^-1K^-1
0
20
40
60
80
100
120
140
160
180
200
220
240
260
280
300
320
340
°C

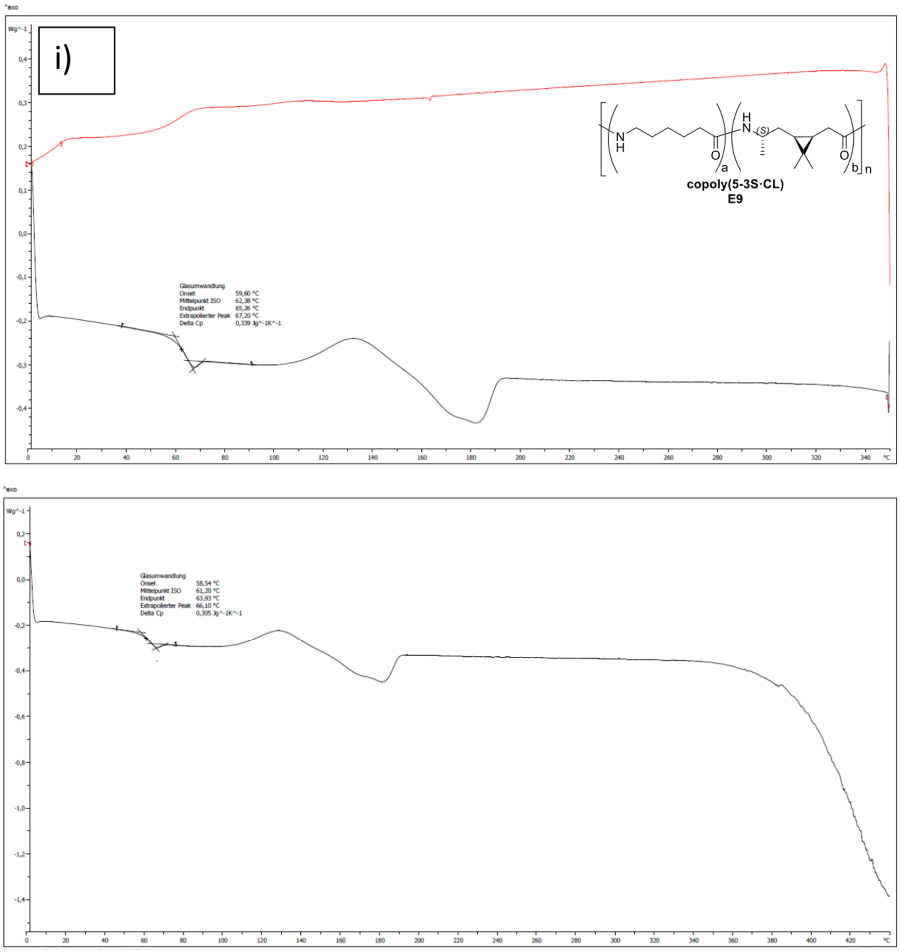
i)
^exo
Wg^-1
0,4
0,3
0,2
0,1
0,0
-0,1
-0,2
-0,3
-0,4
0 20 40 60 80 100 120 140 160 180 200 220 240 260 280 300 320 340 °C
H
N
H
N
(S)
O
O
a
b
n
copoly(5-3S·CL)
E9
Glasumwandlung
Onset 59,60 °C
Mittelpunkt ISO 62,38 °C
Endpunkt 65,26 °C
Extrapolierter Peak 67,20 °C
Delta Cp 0,339 Jg^-1K^-1
^exo
Wg^-1
0,2
0,0
-0,2
-0,4
-0,6
-0,8
-1,0
-1,2
-1,4
0 20 40 60 80 100 120 140 160 180 200 220 240 260 280 300 320 340 360 380 400 420 °C
Glasumwandlung
Onset 58,54 °C
Mittelpunkt ISO 61,20 °C
Endpunkt 63,93 °C
Extrapolierter Peak 66,10 °C
Delta Cp 0,305 Jg^-1K^-1

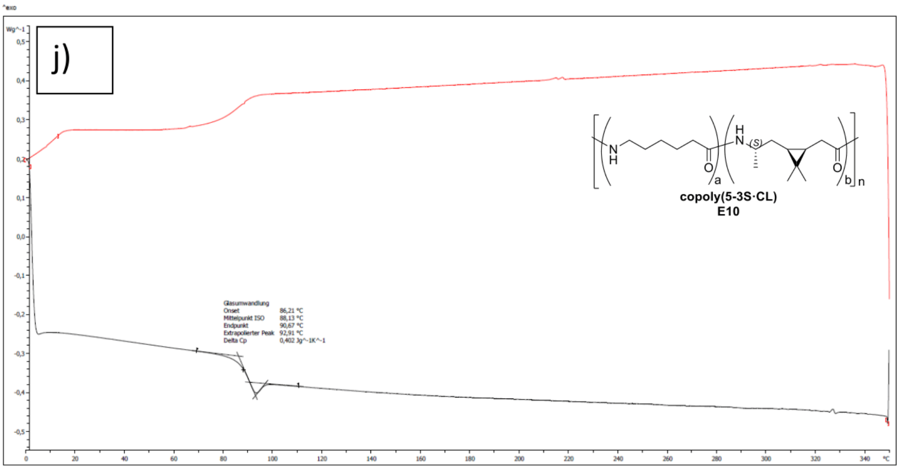
^exo
Wg^-1
j)
0,5
0,4
0,3
0,2
0,1
0,0
-0,1
-0,2
-0,3
-0,4
-0,5
N
H
O
a
H
N
(S)
O
b
n
copoly(5-3S·CL)
E10
Glasumwandlung
Onset 86,21 °C
Mittelpunkt ISO 88,13 °C
Endpunkt 90,67 °C
Extrapolierter Peak 92,91 °C
Delta Cp 0,402 Jg^-1K^-1
0
20
40
60
80
100
120
140
160
180
200
220
240
260
280
300
320
340
°C

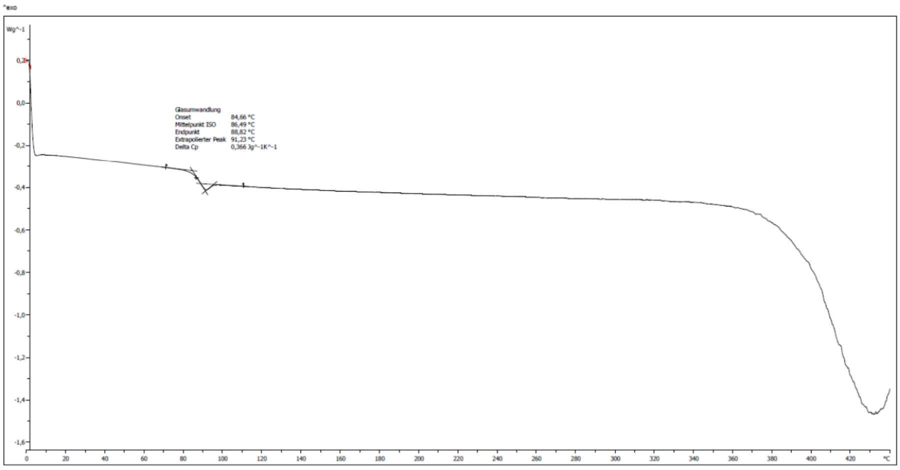
^exo
Wg^-1
0,2
0,0
-0,2
-0,4
-0,6
-0,8
-1,0
-1,2
-1,4
-1,6
Glasumwandlung
Onset 84,66 °C
Mittelpunkt ISO 86,49 °C
Endpunkt 88,82 °C
Extrapolierter Peak 91,23 °C
Delta Cp 0,366 Jg^-1K^-1
0
20
40
60
80
100
120
140
160
180
200
220
240
260
280
300
320
340
360
380
400
420
°C

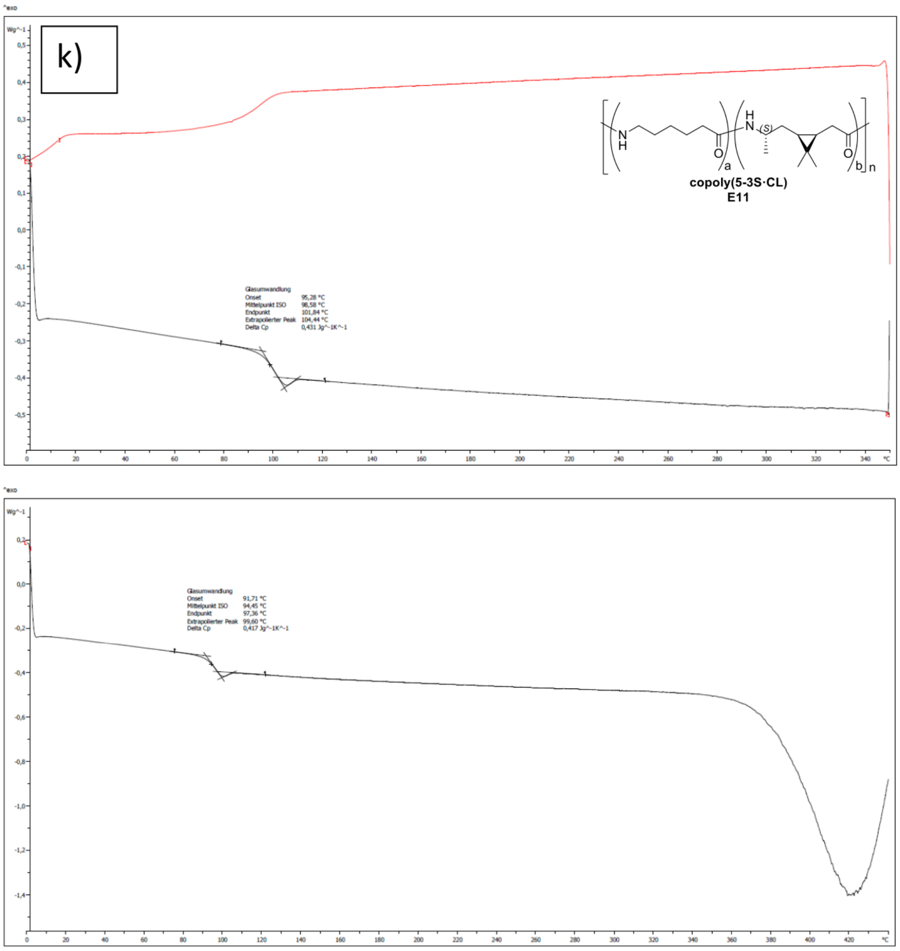

Supplementary Figure 26: DSC curves of various co-polyamides a)-k) as described in Supplementary Table 16, measured using DSC method A, segment 6 (heating, black, upper), segment 7 (cooling, red, upper) and segment 8 (black, heating to decomposition, lower).

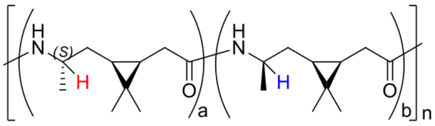
H
N
(S)
H
O
a
H
N
H
O
b
n

copoly(5-3S·5-3R)

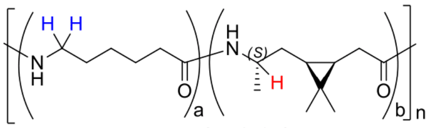
H H
N
H
O
a
H
N
(S)
H
O
b
n

copoly(5-3S·CL)

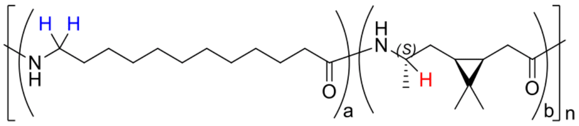
H H
N
H
O
a
H
N
(S)
H
O
b
n

copoly(5-3S·LL)

Supplementary Figure 27: Selected protons (red: **5-3S**, blue: co-monomer) for the determination of different built-ins under various reaction conditions by NMR.

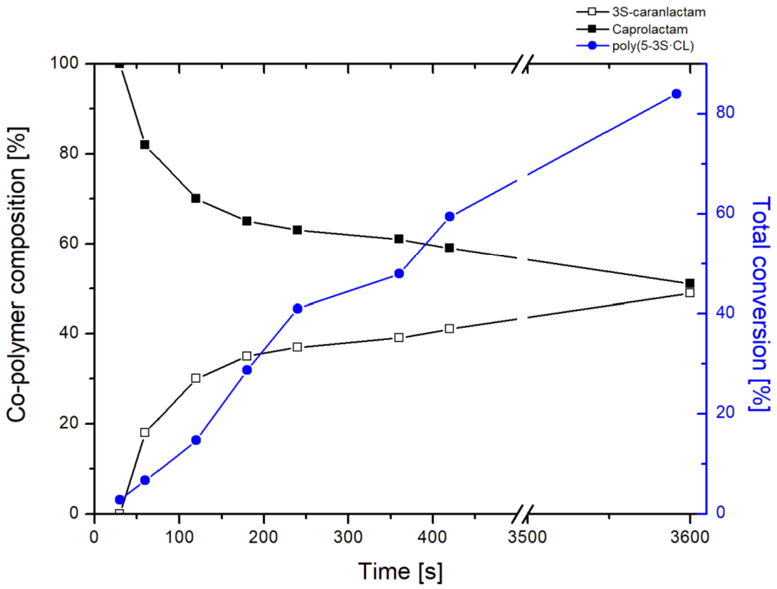

Supplementary Figure 28: Incorporation of **5-3S** and **CL** at different reaction times. Reaction conditions: 3S-caranlactam (**5-3S**, 2.36 g, 14.1 mmol), caprolactam (**CL**, 1.64 g, 14.5 mmol, NaH (60% on paraffin, 10.0 mg, 0.25 mmol) and **Bz5-3S** (54.0 mg, 0.22 mmol), 190 °C

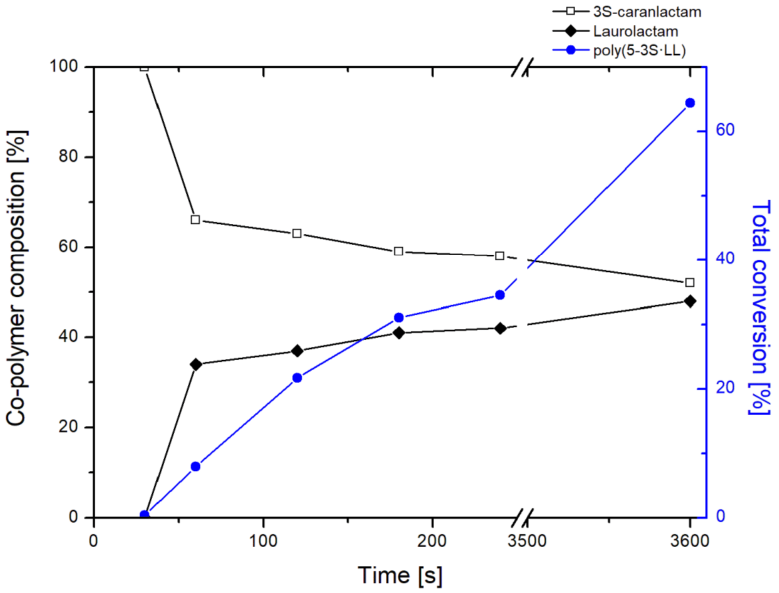

Supplementary Figure 29: Incorporation of **5-3S** and **LL** at different reaction times. Reaction conditions: 3S-caranlactam (**5-3S**, 2.39 g, 14.3 mmol), laurolactam (**LL**, 2.82 g, 14.3 mmol, NaH (60% on paraffin, 9.6 mg, 0.24 mmol) and **Bz5-3S** (56.0 mg, 0.23 mmol), 190 °C.

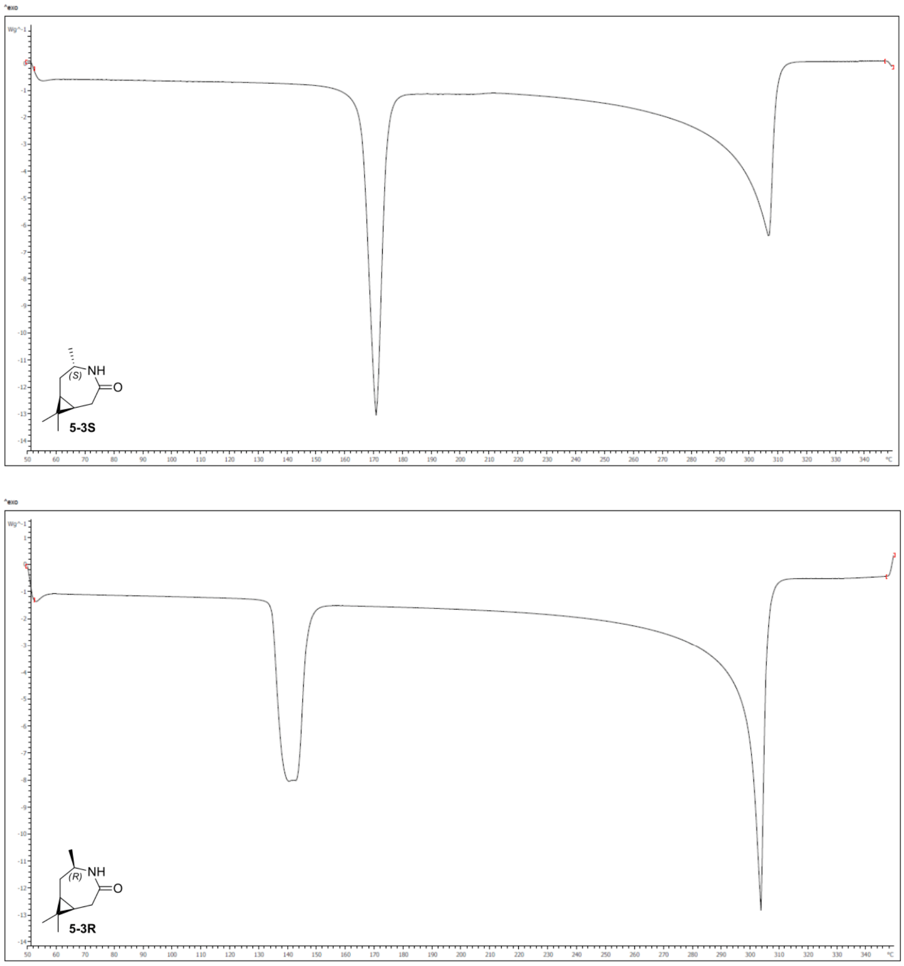

Supplementary Figure 30: DSC curves of **5-3S** (upper) and **5-3R** (lower).

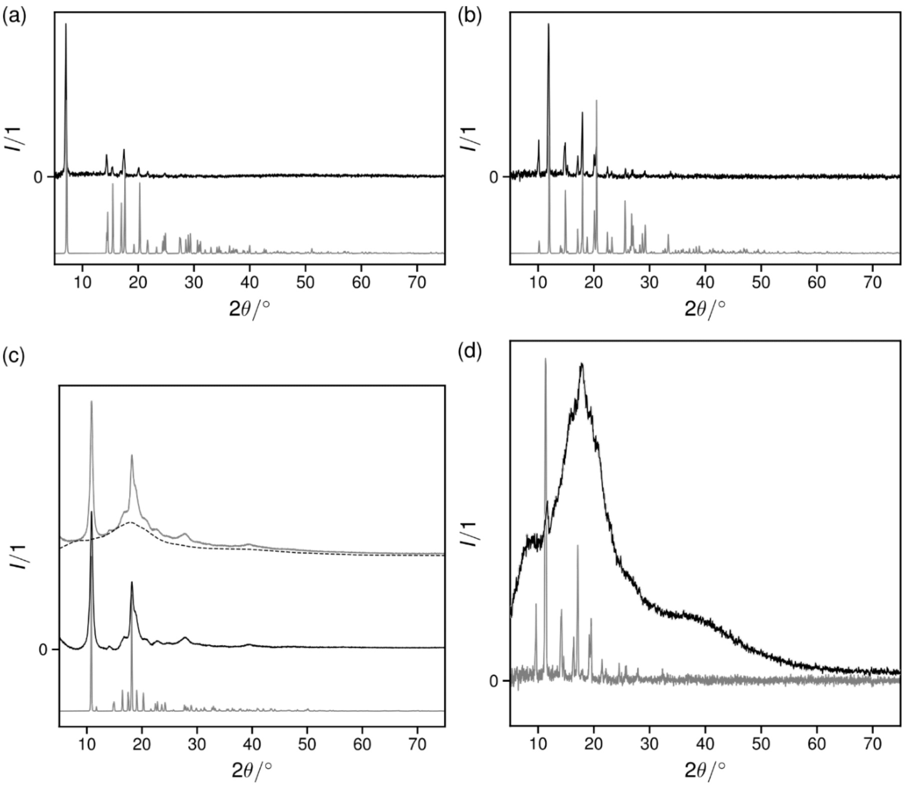

Supplementary Figure 31: Diffraction patterns (Cu Kα) from **5-3S** (a) and **5-3R** (b) and **poly5-3S** (c) S- and **poly5-3R** (d, black lines) with simulated diffractograms from the respective best-match crystal structures (lowest grey lines). In (c), the subtraction of the amorphous phase-diffractogram (dashed line) and the resulting purely crystalline pattern (black full line) are shown. In (d), instead of a best-match crystal pattern, the pattern from residual monomers, (b), is shown.

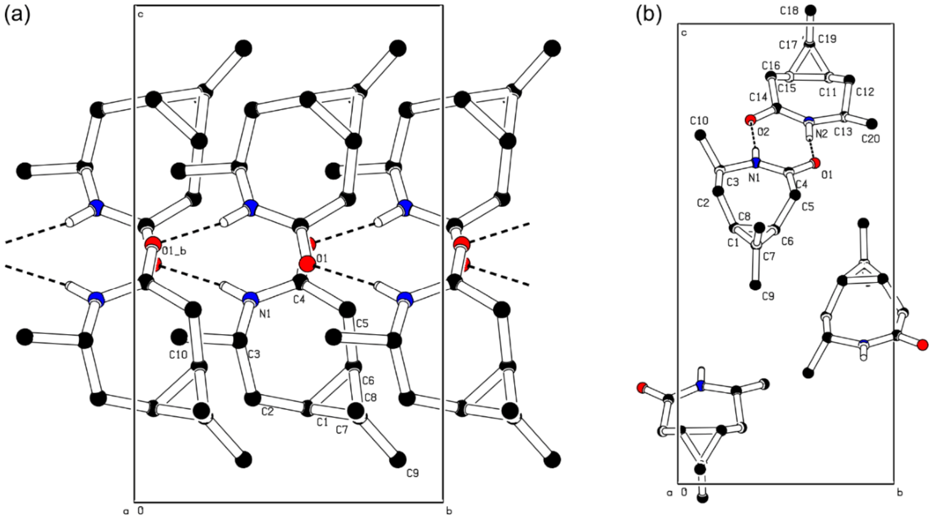
(a)
c
O1_b
O1
N1
C4
C5
C10
C3
C6
C8
C2
C1
C7
C9
a
0
b
(b)
C18
c
C17
C19
C16
C15
C11
C12
C14
C10
O2
N2
C13
C20
N1
O1
C3
C4
C2
C5
C8
C1
C6
C7
C9
a
0
b

Supplementary Figure 32: Structure of **5-3S** (left) and **5-3R** (right) with bonding hydrogens only, viewed in unit cell direction *a*.

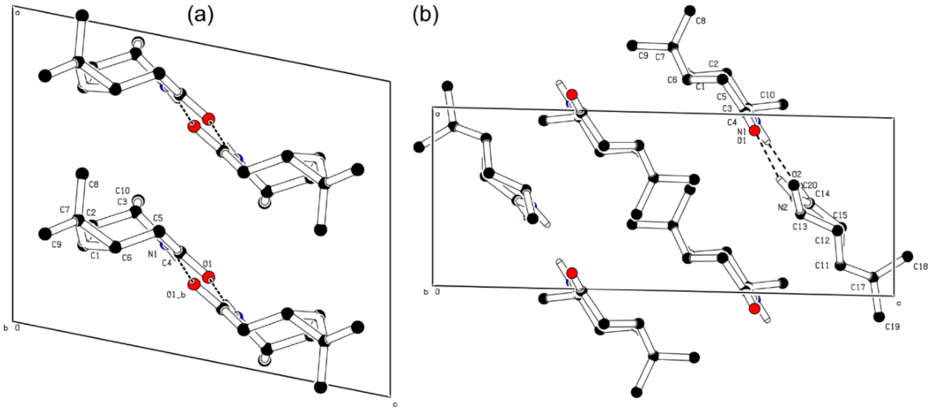
(a)
(b)
a
b 0
c
C8
C10
C7
C2
C3
C5
C9
C1
C6
N1
C4
O1
O1_b
C8
C9
C7
C2
C6
C1
C5
C10
C3
C4
N1
O1
O2
C20
C14
N2
C15
C13
C12
C11
C18
C17
C19

Supplementary Figure 33: Structure of **5-3S** (left) and **5-3R** (right) with bonding hydrogens only, viewed in unit cell direction *b*.

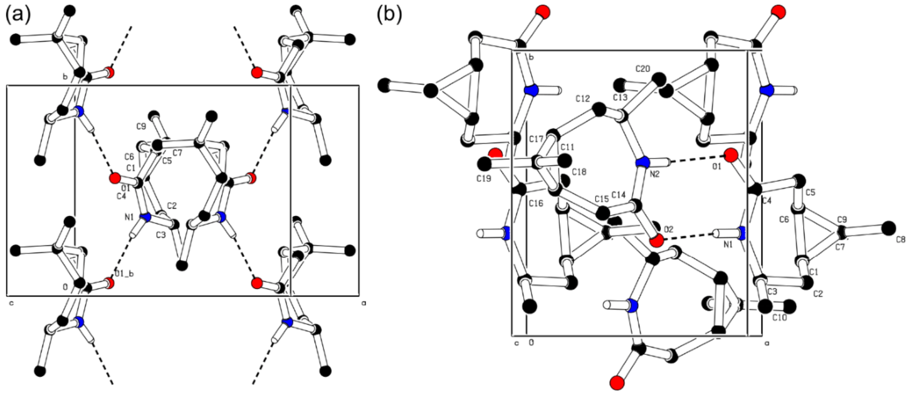
(a)
b
C9
C7
C6
C5
C1
O1
C4
N1
C2
C3
O1_b
c
0
a
(b)
b
C20
C12
C13
C17
C11
N2
O1
C19
C18
C16
C15
C14
C5
C4
C6
C9
O2
N1
C7
C8
C1
C2
C3
C10
c
0
a

Supplementary Figure 34: Structure of **5-3S** (left) and **5-3R** (right) with bonding hydrogens only, viewed in unit cell direction *c*.

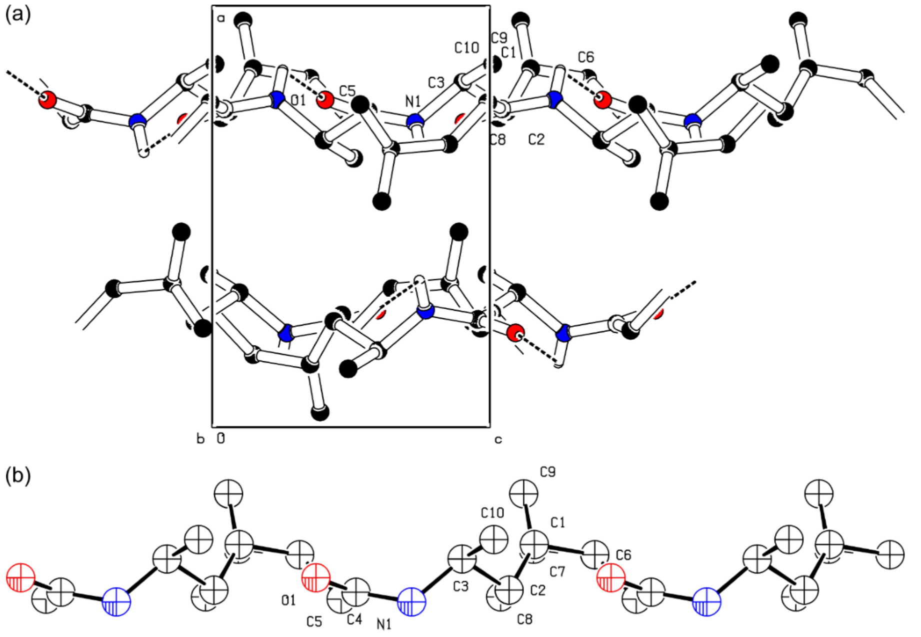
(a)
a
C10
C9
C1
C6
C3
C5
O1
N1
C8
C2
b
0
c
(b)
C9
C10
C1
C6
C7
C3
C2
O1
C5
C4
N1
C8

Supplementary Figure 35: Structure of **poly5-3S**, viewed in unit cell direction *b* (unit cell with bonding hydrogens only, the expanded repeating unit without hydrogens (lower).

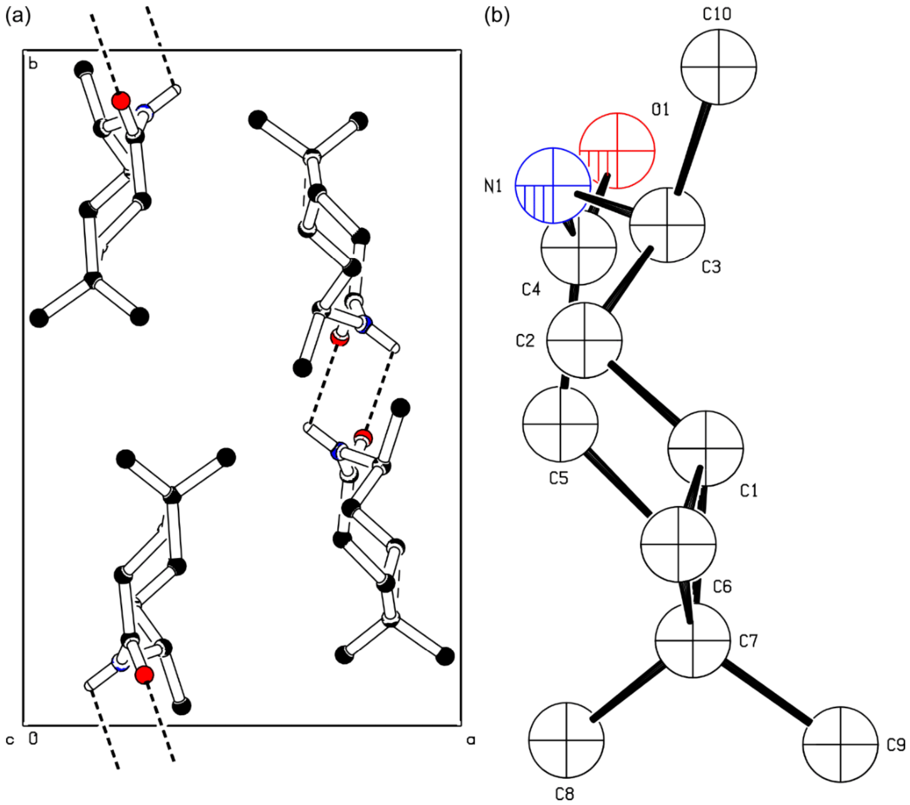
(a)
b
c
0
a
(b)
C10
O1
N1
C3
C4
C2
C5
C1
C6
C7
C9
C8

Supplementary Figure 36: Structure of **poly5-3S**, viewed in unit cell direction c; unit cell with bonding hydrogens only (left), the expanded repeating unit without hydrogens (right).

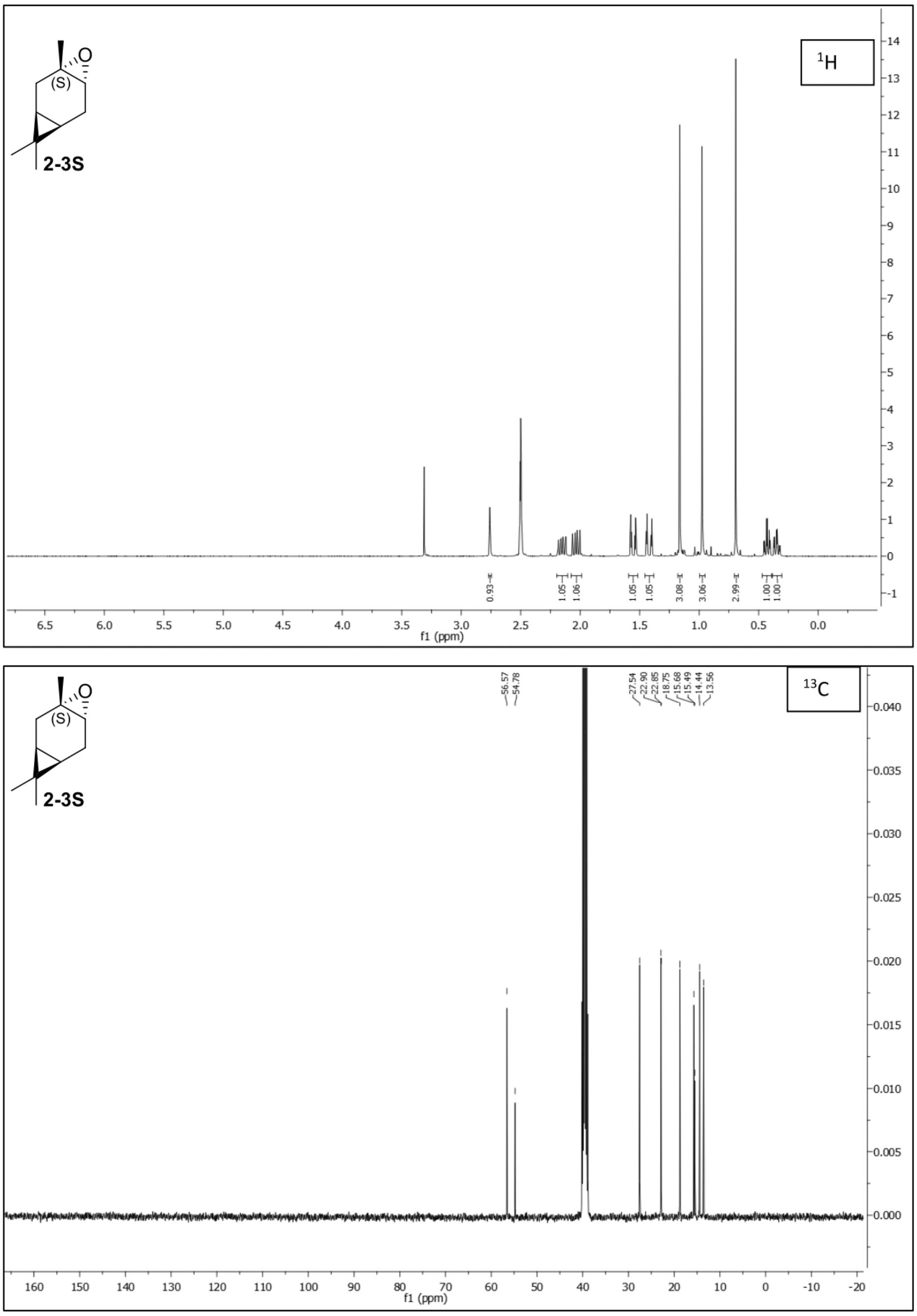

Supplementary Figure 37: NMR spectra of **2-3S**.

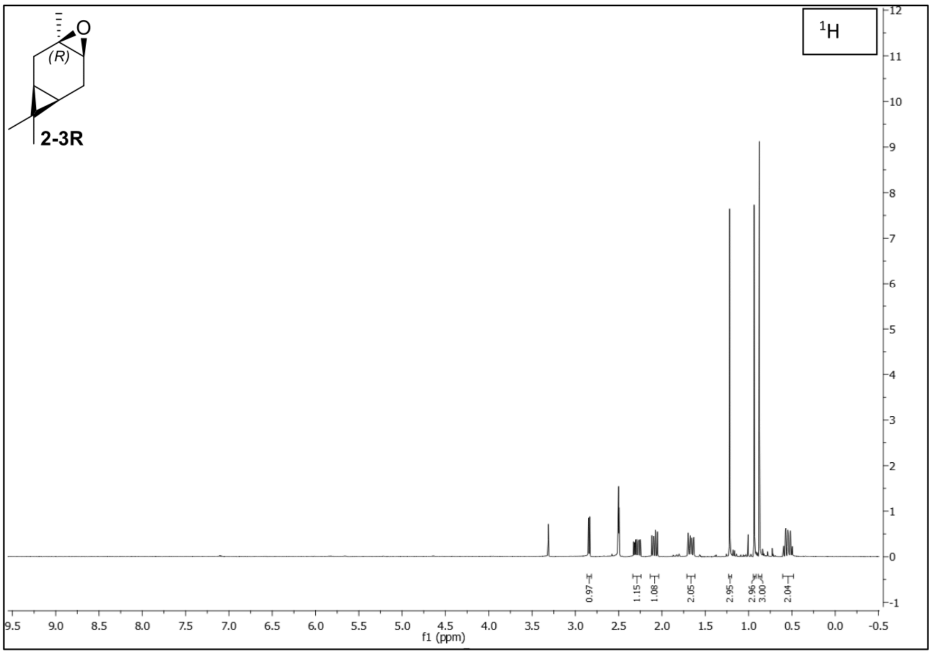

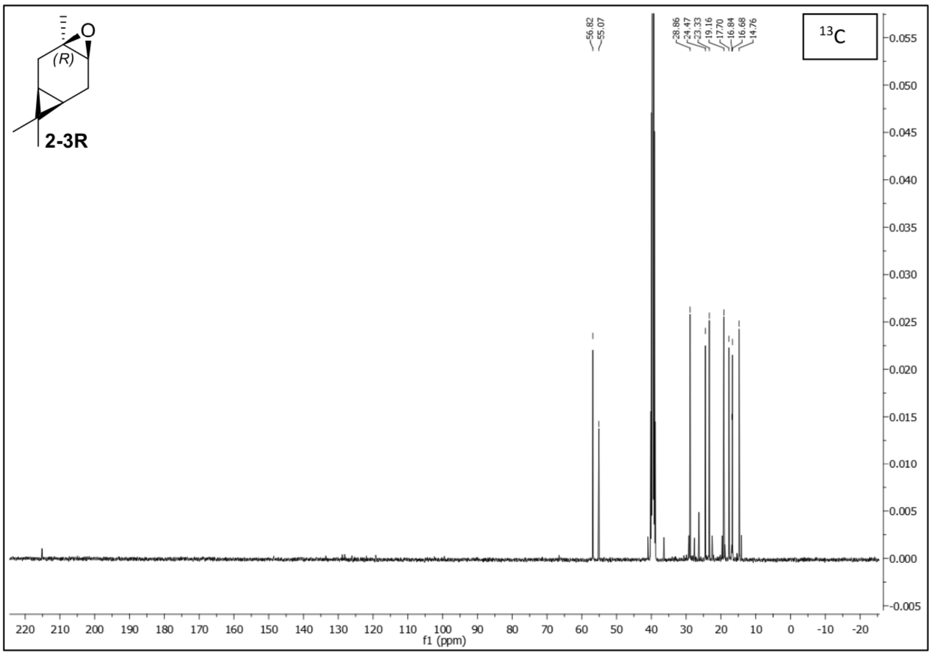

Supplementary Figure 38: NMR spectra of **2-3R**.

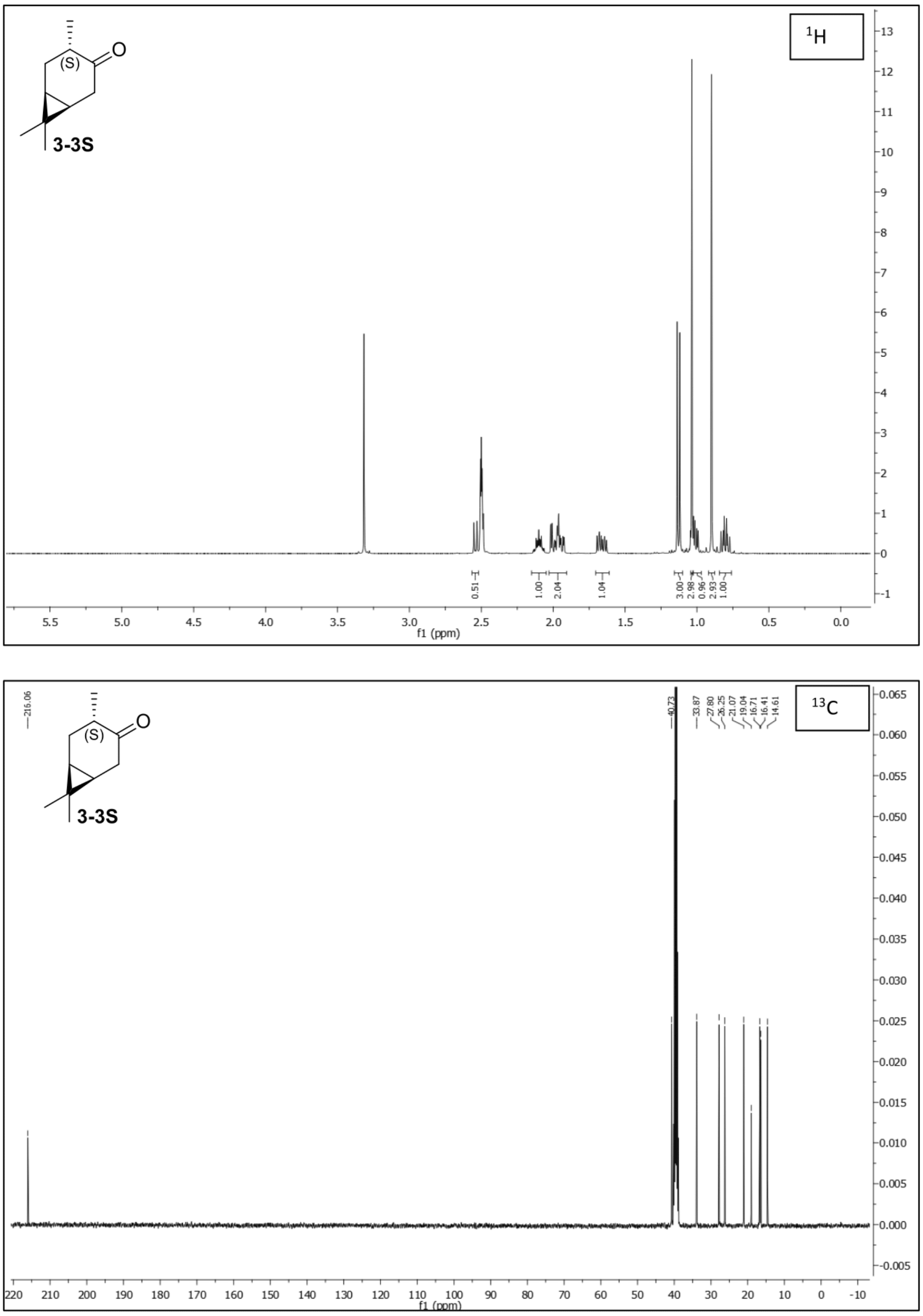

Supplementary Figure 39: NMR spectra of **3-3S**.

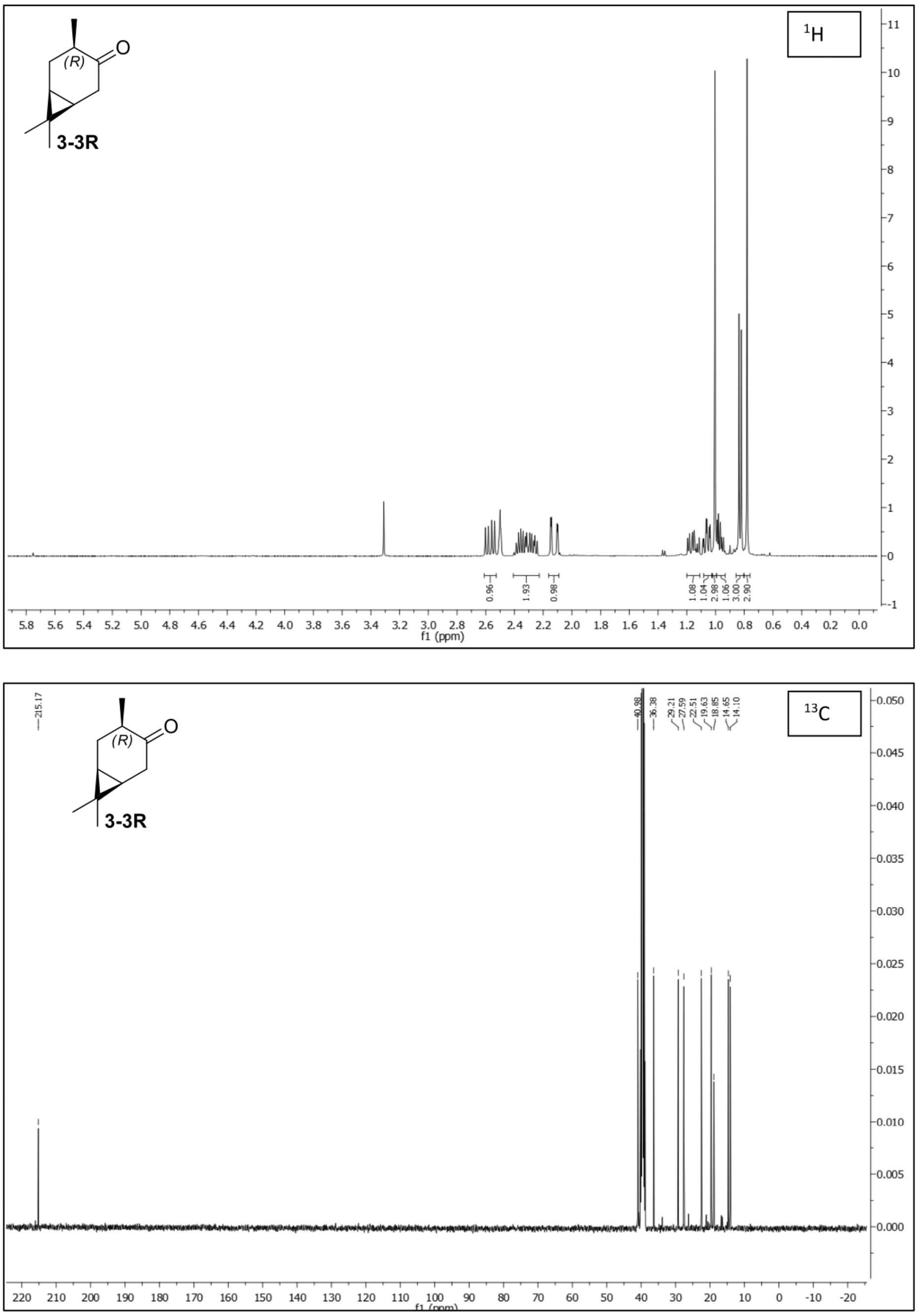

Supplementary Figure 40: NMR spectra of **3-3R**.

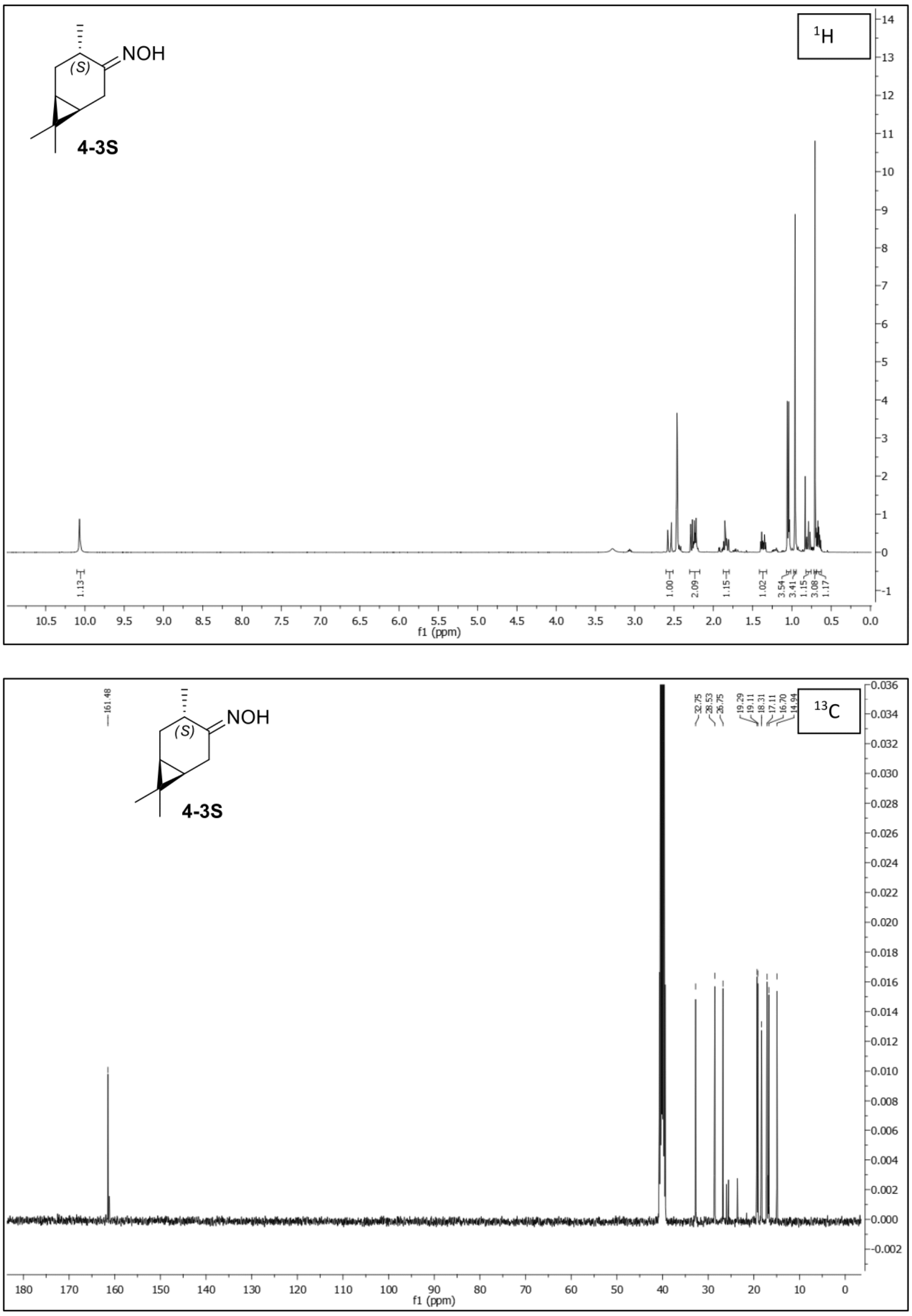

Supplementary Figure 41: NMR spectra of **4-3S**.

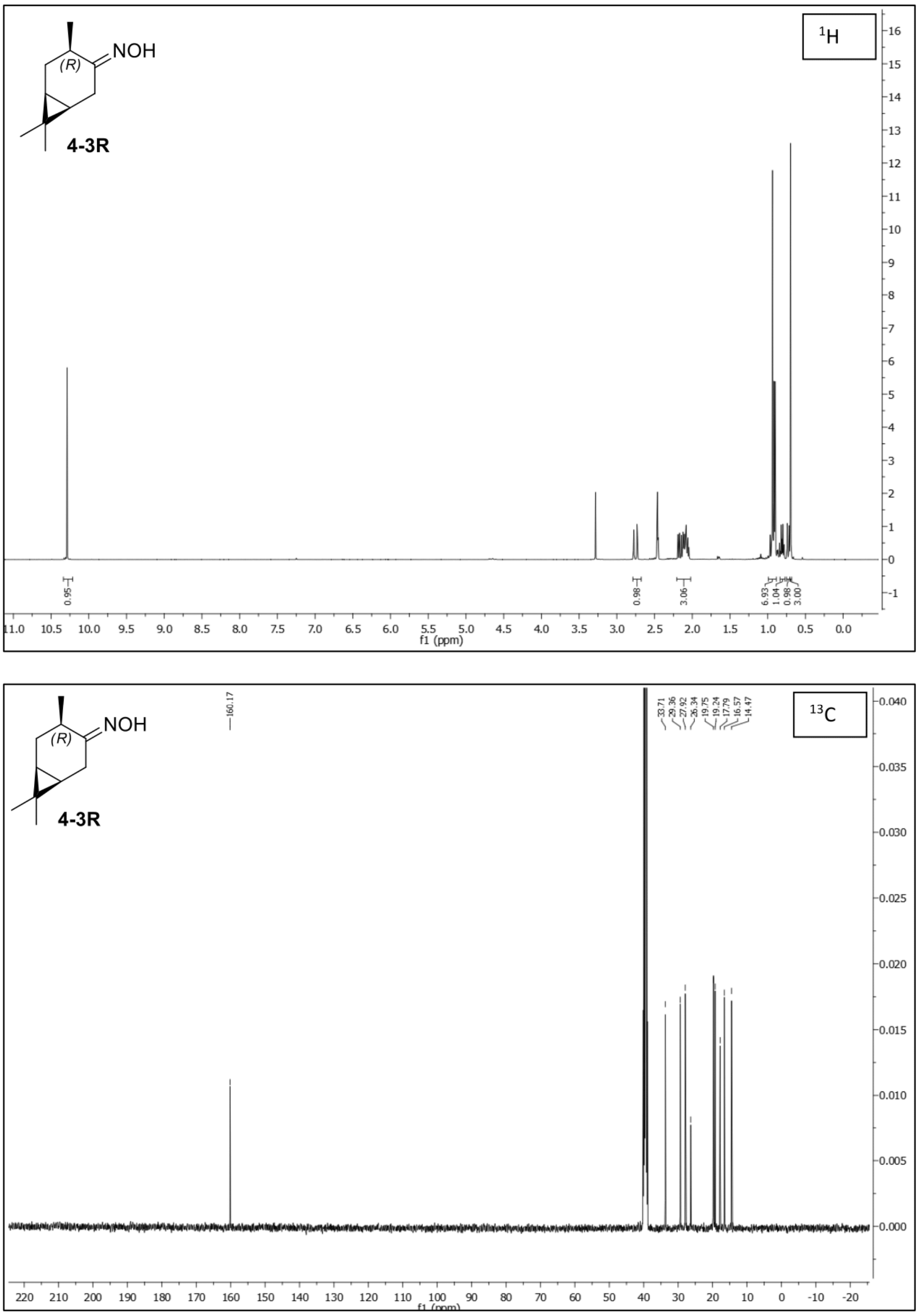

Supplementary Figure 42: NMR spectra of **4-3R**.

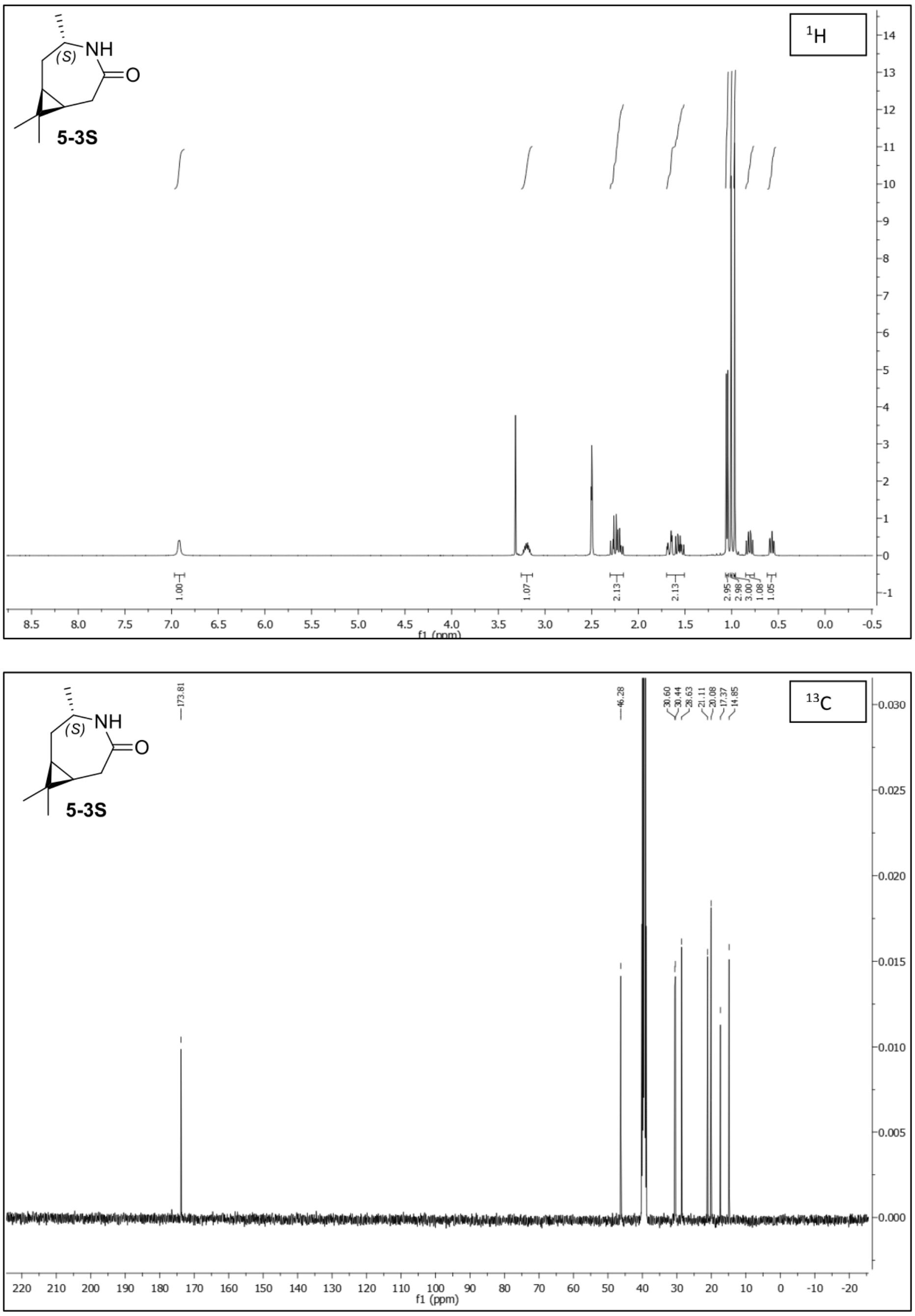

Supplementary Figure 43: NMR spectra of **5-3S**.

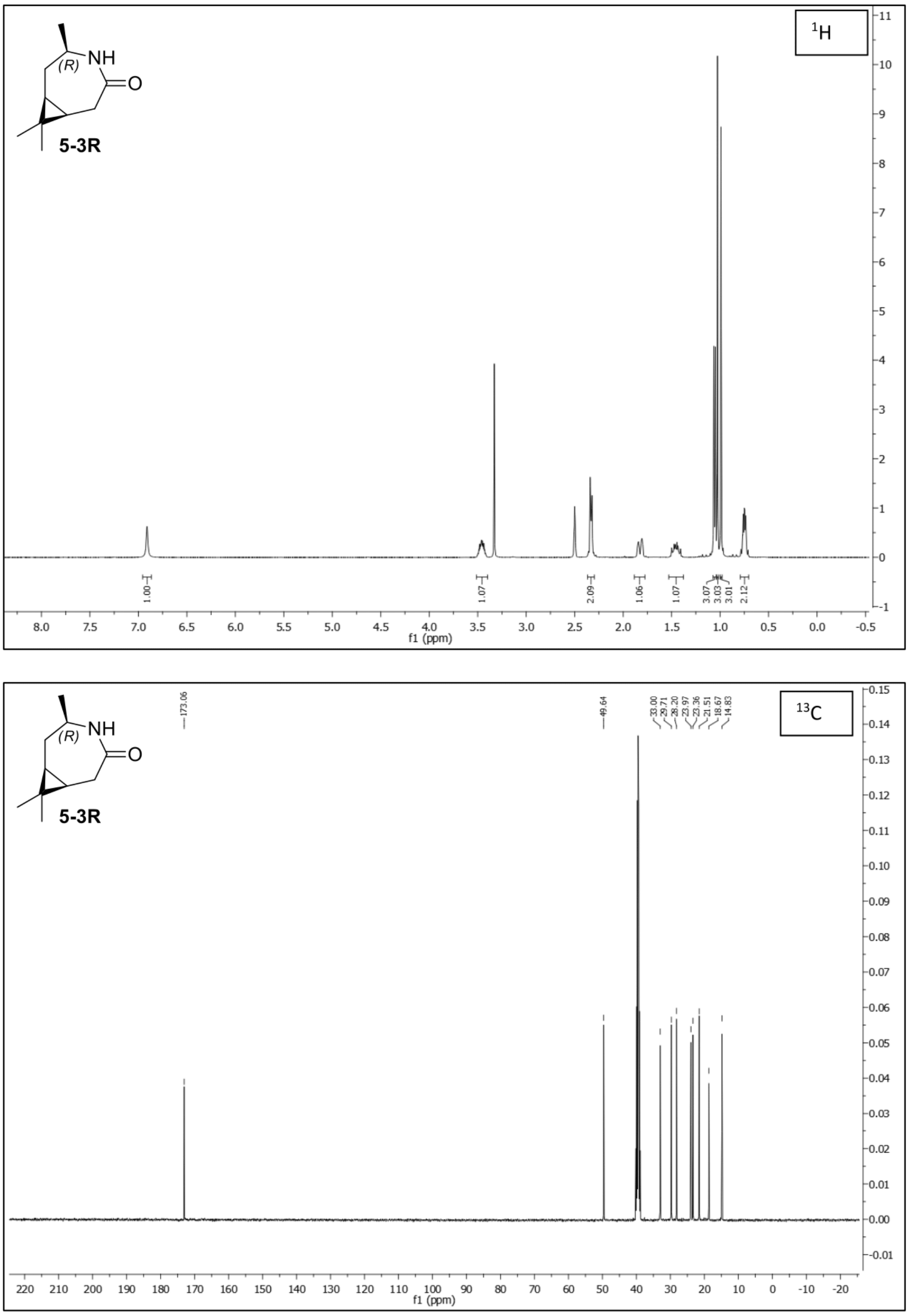

Supplementary Figure 44: NMR spectra of **5-3R**.

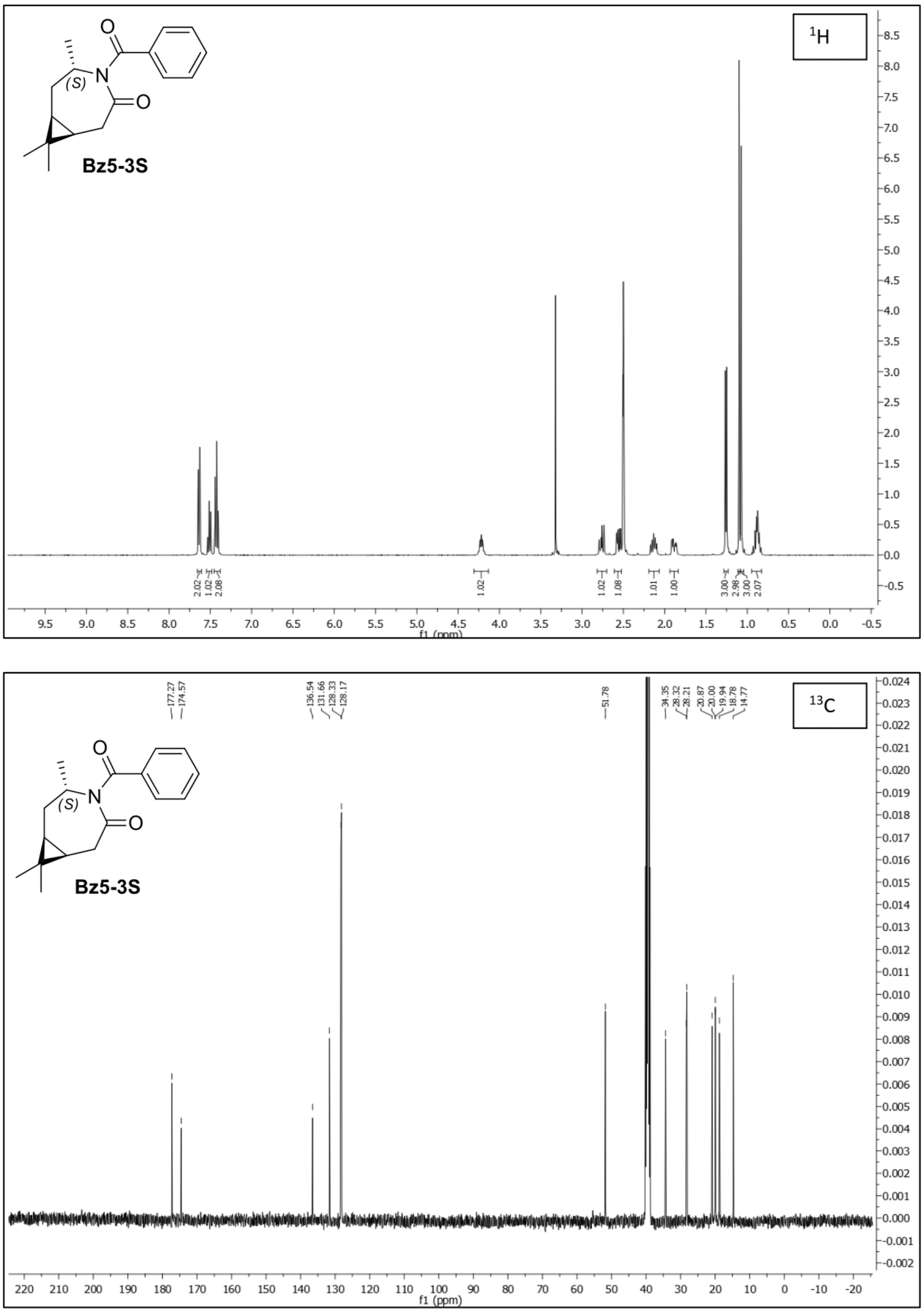

Supplementary Figure 45: NMR spectra of **Bz5-3S**.

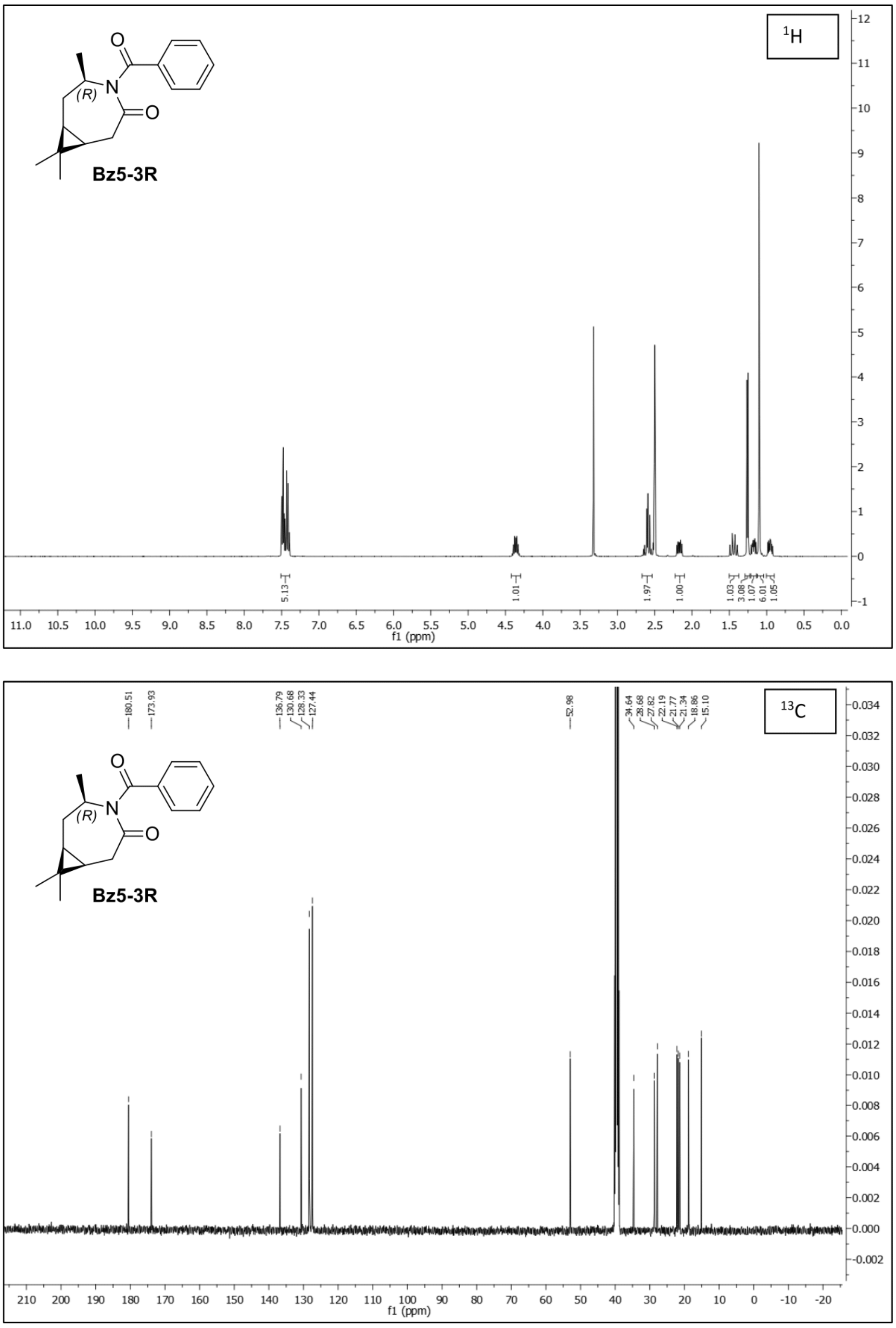

Supplementary Figure 46: NMR spectra of **Bz5-3R**.

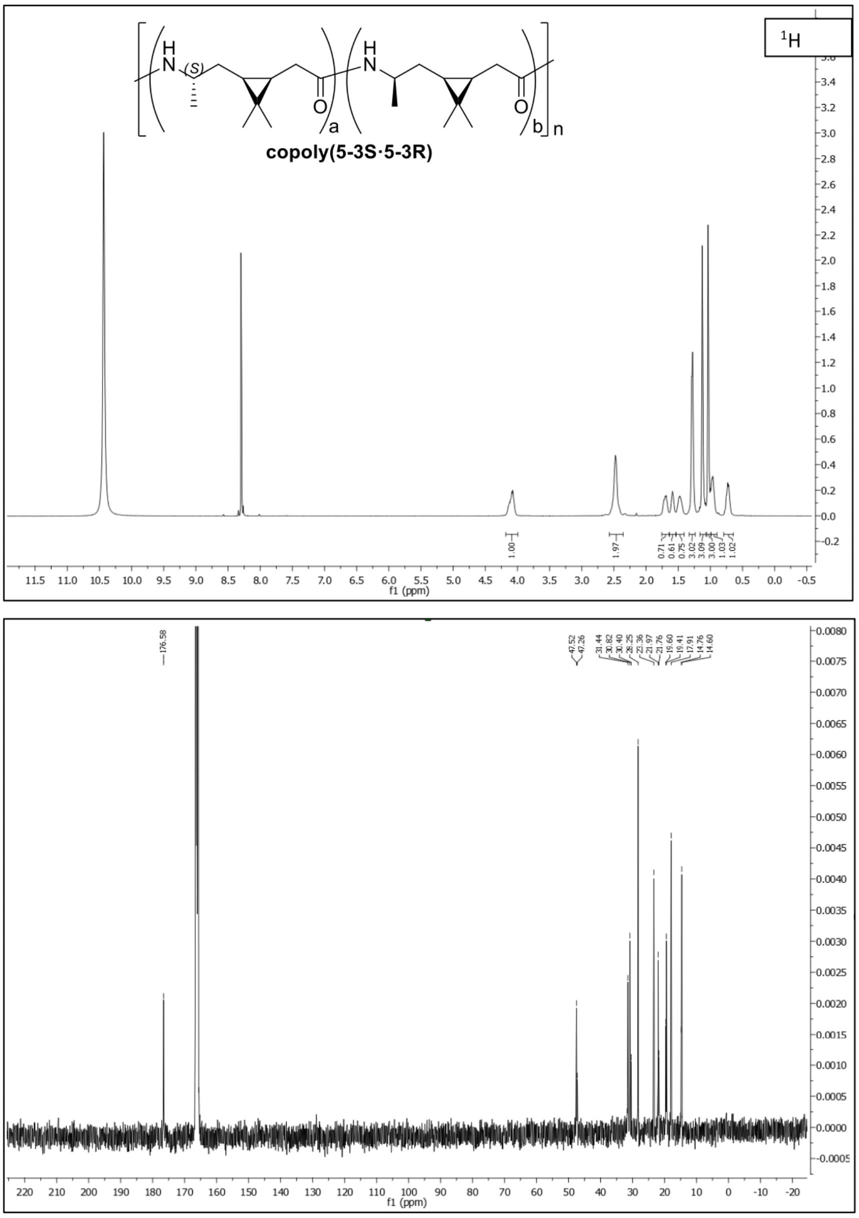

Supplementary Figure 47: NMR Spectra of 3S-caranlactam-3R-caranlactam-copolyamide (DCOOD, 1H 400 MHz, 13C 100 MHz)

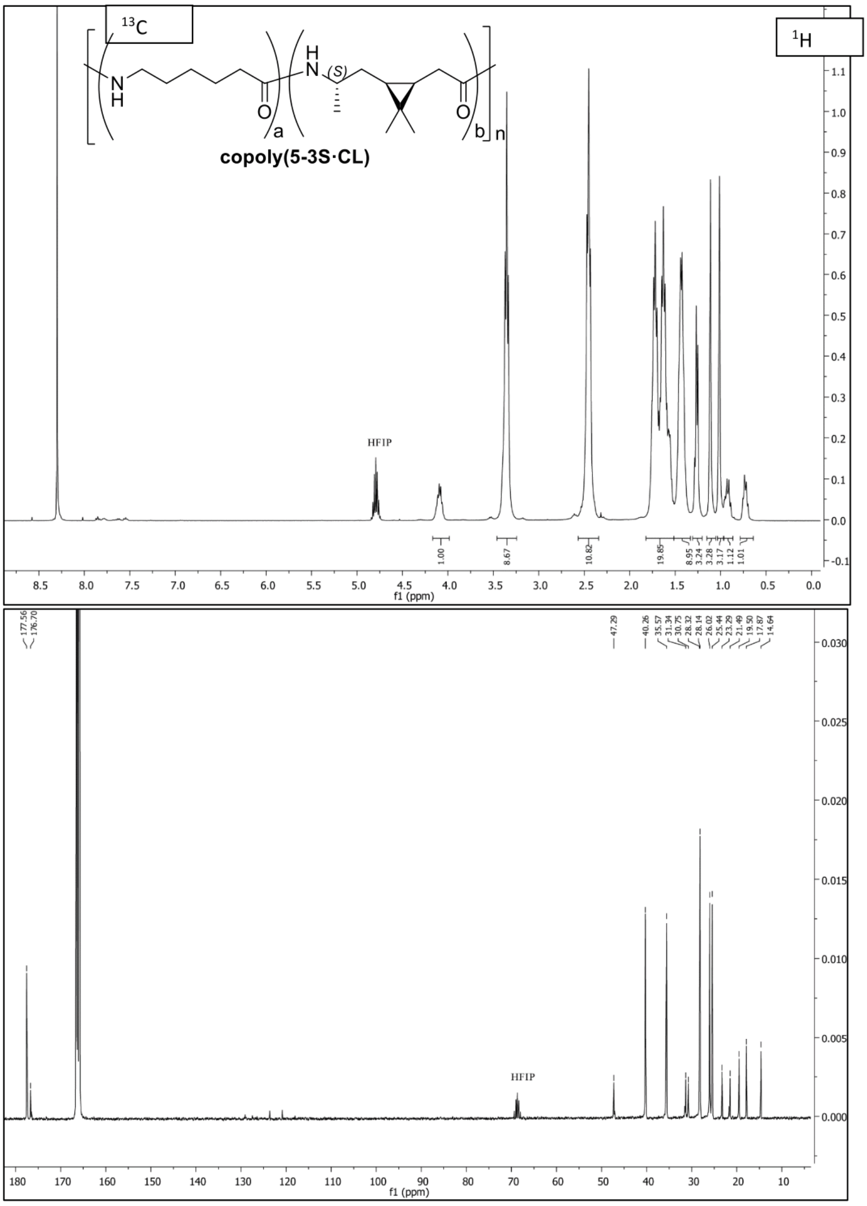

Supplementary Figure 48: NMR Spectra of 3S-caranlactam-caprolactam-copolyamide (DCOOD, ^{1}H 400 MHz, ^{13}C 100 MHz)

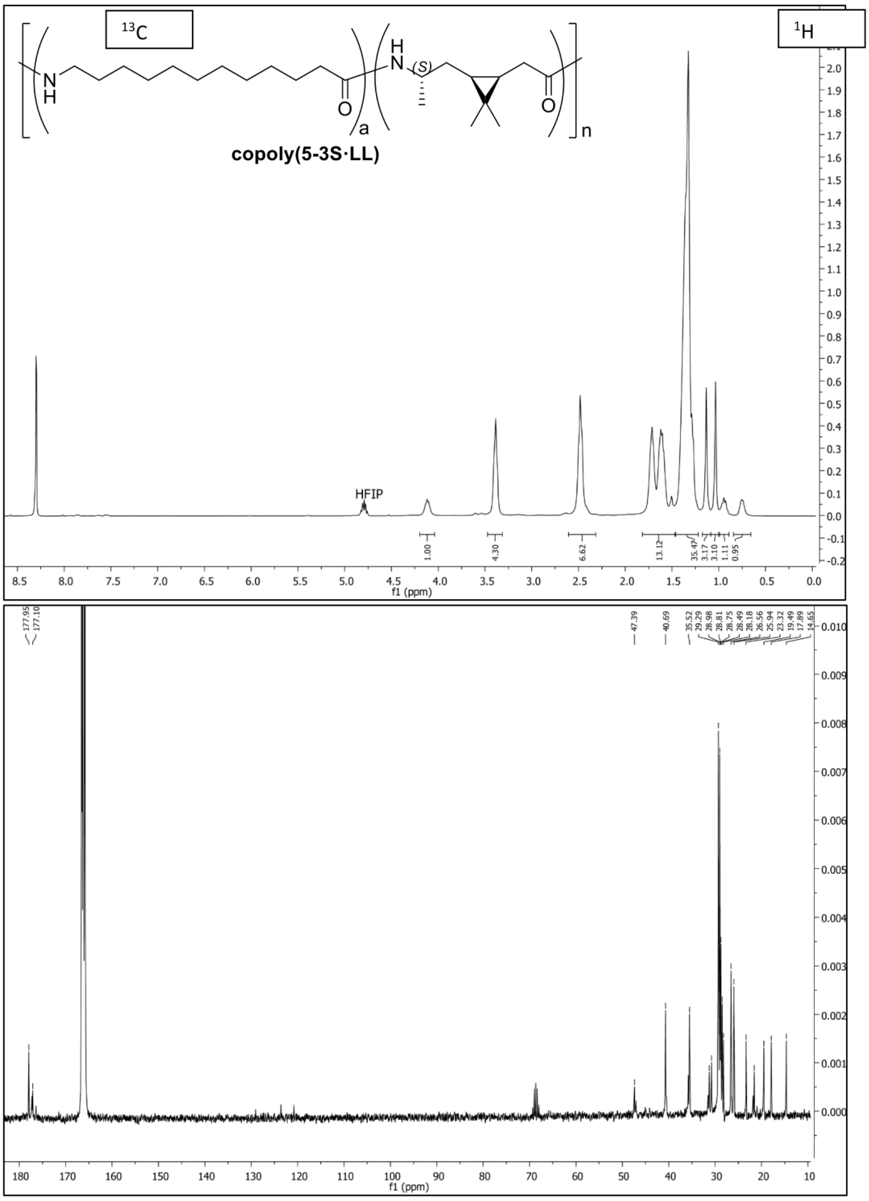

Supplementary Figure 49: NMR Spectra of 3S-caranlactam-laurolactam-copolyamide (DCOOD, ^{1}H 400 MHz, ^{13}C 100 MHz)

2. Supplementary Tables

Supplementary Table 1: Heating- and elution-parameters of the GC-MS analysis and retention times of the (+)-3-carene (**1**) derivatives

Parameters	Values
split rate	5
injection temperature	250 °C
carrier gas	helium
column flow-through	1.69 ml/min.
heating program	50 °C for 1 min.
	50-120 °C, heating 15 °C per min.
	120-170 °C, heating 5 °C per min.
	170-200 °C, heating 20 °C per min.
	200 °C for 7 min.
column	BPX5 (CS Chromatography), length 30 m,
	inner diameter 0.25 µm, diameter 0.25 mm

Substance	Retention time [min]	
(+)-3-carene (**1**)	5.7	-
3S-caranepoxide (**2-3S**)	7.3	-
3S-caranketone (**3-3S**)	8.2	-
3R-caranketone (**3-3R**)	8.0	-
3R-caranoxime (**4-3R**)	11.1 (trans, major)	11.0 (cis, minor)
3S-caranoxime (**4-3S**)	10.8 (trans, major)	10.9 (cis, minor)
3R-caranepoxide (**2-3R**)	7.2	-
3S-caranlactam (**5-3S**)	14.6 (major)	14.5 (minor)
3R-caranlactam (**5-3R**)	14.1 (major)	14.3 (minor)

Supplementary Table 2: Influence of solvent polarity on the rearrangement of 3S-caranepoxide (**2-3S**) to the R- and S-caranketone isomers. All experiments were carried out with a concentration of 1 M at 25 °C and 0.2% $Fe(ClO_4)_2 \cdot H_2O$ for 8 h. Conversion of 3S-caranepoxide (**2-3S**) was 100%. Data values refer to TIC of GCMS analytics (uncorrected values).

Entry	**Solvent**	**Relative polarity***	**Σ ketone [%]**	**3-3R [%]**	**3-3S [%]**
1	Cyclohexane	0.006	70	11	89
2	Hexane	0.009	64	13	87
3	Heptane	0.012	64	13	87
4	Toluene	0.099	71	14	86
5	2-Me-THF	-	66	26	74
6	THF	0.207	51	39	61
7	EtOAc	0.228	67	44	56
8	Chloroform	0.259	68	38	72
9	DCM	0.309	60	57	43
10	2-butanone	0.327	38	60	40
11	Acetone	0.355	24	61	39
12	Isopropanol	0.546	12	20	80
13	EtOH	0.654	26	50	50
14	MeOH	0.762	<1	-	-

* data retrieved from Christian Reichardt, Solvents and Solvent Effects in Organic Chemistry, Wiley-VCH Publishers, 3rd ed., 2003.

Supplementary Table 3: Screening of Lewis-acidic catalysts under various conditions. Data values refer to TIC-area of GCMS spectra (uncorrected values).

Entry	Catalyst [%]	Solvent	C [M]	T [°C]	Conversion [%]	Σ ketone [%]	3-3R [%]	3-3S [%]	t [h]
1	$ZnBr_2$ 10%	-	-	60	100	60	25	75	4
2	$Fe(OTf)_2$ 10%	EtOAc	0.05	60	100	57	30	70	1
3	ZSM-5 15 w%	EtOAc	1	45	100	54	34	66	1
4	$Zn(OTf)_2$ 10%	EtOAc	0.05	60	100	60	34	66	1
5	$ZnBr_2$ 100%	EtOAc	0.25	70	100	68	45	55	2
6	$ZnBr_2$ 10%	toluene	0.25	80	100	64	45	55	4
7	$ZnBr_2$ 10%	$CHCl_3$	0.25	80	100	66	45	55	4
8	$AlCl_3$ 100%	EtOAc	0.25	60	45	20	50	50	48
9	$FeCl_3 \cdot 6H_2O$ 100%	EtOAc	0.25	60	100	22	50	50	12
10	$ZnBr_2$ 100%	EtOAc	0.25	60	100	85	55	45	12
11	$Ti(BuO)_4$ 20%	EtOAc	0.2	50	0	0	0	0	12
12	$Sn(OAc)_2$ 10%	EtOAc	0.25	50	0	0	0	0	12
13	$CuCl_2$ 100%	EtOAc	0.25	60	0	0	0	0	12
14	$CeNO3 \cdot 6H_2O$ 100%	EtOAc	0.25	60	0	0	0	0	12
15	$ZnSO_4 \cdot 7H_2O$ 100%	EtOAc	0.25	60	0	0	0	0	12
16	$ZnCl_2$ 100%	EtOAc	0.25	60	0	0	0	0	12
17	$CoCl_2 \cdot 6H_2O$ 100%	EtOAc	0.25	60	0	0	0	0	12
18	CuI 100%	EtOAc	0.25	60	0	0	0	0	12
19	FeOAc 100%	EtOAc	0.25	60	0	0	0	0	12

Supplementary Table 4: Comparison of Fe- and Zn-Lewis acids at 60 °C in cyclohexane with a concentration of 1 M and 0.2% catalyst. Data values refer to TIC-area of GCMS spectra (uncorrected values).

Entry	Catalyst [%]	Conversion [%]	Σ ketone [%]	3-3R [%]	3-3S [%]	t [h]
1	$Zn(OAc)_2$	0	0	0	0	12
2	$Zn(OTf)_2$	48	70	9	91	40
3	$Zn(ClO_4)_2 \cdot H_2O$	73	78	13	77	4
4	$Fe(OAc)_2$	0	0	0	0	0
5	$Fe(OTf)_2$	91	73	15	85	0.5
6	$Fe(ClO_4)_2 \cdot H_2O$	100	82	15	85	0.5
7	$Fe(ClO_4)_3 \cdot H_2O$	100	81	16	84	0.5

Supplementary Table 5: Meinwald rearrangement of 3S-caranepoxide (**2-3S**) to ketones **3-3S** and **3-3R** using sulfonic acids. Data values refer to TIC-area of GCMS spectra (uncorrected values).

Entry	**Catalyst [%]**	**Solvent**	**C [M]**	**T [°C]**	**Conversion [%]**	**Σ ketone [%]**	**3-3R [%]**	**3-3S [%]**	**t [h]**
1	CF_3SO_3H 0.1%	toluene	1	25	100	73	13	87	1
2	CF_3SO_3H 0.1%	pentane	0.5	25	100	68	13	87	1
3	CF_3SO_3H 0.1%	hexane	0.5	50	100	67	15	85	1
4	CF_3SO_3H 0.1%	toluene	0.5	50	100	74	15	85	1
5	PTSA 1%	cyclohexane	1	60	100	69	17	83	12
6	CF_3SO_3H 0.1%	toluene	1	60	100	79	19	81	1
7	CF_3SO_3H 0.1%	toluene	1	85	100	73	22	78	1
8	CF_3SO_3H 0.1%	EtOAc	1	0	100	52	37	63	1
9	$MeSO_3H$ 20%	2-Me-THF	0.7	80	100	60	84	16	1
10	$MeSO_3H$ 7%	heptane	3	90	100	24	86	14	0.5
11	CSA 20 %	toluene	0.2	100	0	0	0	0	12

Supplementary Table 6: Influence of the amount of $Fe(ClO_4)_2 \cdot H_2O$ on the rearrangement of 3S-caranepoxide (**2-3S**) to the R- and S-caranketone isomers. All experiments were carried out with a concentration of 1 M at 25 °C for 5 h. Data values refer to TIC-area of GCMS spectra (uncorrected values).

Entry	**$Fe(ClO_4)_2 \cdot H_2O$ [mol%]**	**Conversion [%]**	**Σ ketone [%]**	**3-3R [%]**	**3-3S [%]**
1	0.1	90	71	20	80
2	0.25	95	69	14	86
3	0.5	98	67	15	85
4	1	100	63	15	85
5	5	100	54	28	72

Supplementary Table 7: Influence of the concentration of 3S-caranepoxide (**2-3S**) on the rearrangement to ketones **3-3S** and **3-3R**. All experiments were carried out with a concentration of 1 M at 25 °C and 0.2 % $Fe(ClO_4)_2 \cdot H_2O$ for 7 h. Data values refer to TIC-area of GCMS spectra (uncorrected values).

Entry	**$C_{S\text{-caranepoxide}}$ [M]**	**Conversion [%]**	**Σketone [%]**	**3-3R [%]**	**3-3S [%]**
1	0.1	<1	-	-	-
2	0.25	8	56	20	80
3	0.5	78	74	13	87
4	1.0	100	70	10	90
5	2.0	100	67	10	90
6	3.0	100	66	10	90

Supplementary Table 8: Comparison of temperature effects on combinations of Fe(ClO4)$_2$·H$_2$O (0.2%) in cyclohexane and CF_3SO_3H in hexane/pentane (0.1%).

Entry	**Catalyst [%]**	**Solvent**	**C [M]**	**T [°C]**	**Conversion [%]**	**Σ ketone [%]**	**3-3R [%]**	**3-3S [%]**	**t [h]**
1	$Fe(ClO_4)_2 \cdot H_2O$	cyclohexane	1	25	100	70	10	90	7
2	$Fe(ClO_4)_2 \cdot H_2O$	cyclohexane	1	60	100	82	15	85	0.1
3	CF_3SO_3H	pentane	0.5	25	100	68	13	87	1
4	CF_3SO_3H	hexane	0.5	50	100	67	15	85	1

Supplementary Table 9: Influence of the solvent on the isomerization of a 3S-caranketone (**3-3S**) enriched solution (purity 79%, R-caranketone 11%, S-caranketone 89%). All experiments were carried out with a concentration of 1 M and HCl (6.0%, from a 2 M solution) as isomerization agent. Samples were taken after stirring for 6 h at room temperature (a), additional 15 h at room temperature (b) and additional 48 h at 60 °C (c). Data values refer to TIC-area of GCMS spectra (uncorrected values).

Entry	**Solvent**	**Relative polarity***	**Σ ketone [%]**			**3-3R [%]**			**3-3S [%]**		
			a	b	c	a	b	c	a	b	c
1	Cyclohexane	0.006	77	77	70	20	20	74	80	80	26
3	Toluene	0.099	77	76	70	21	21	79	79	79	21
4	THF	0.207	76	76	73	78	85	78	22	15	22
5	EtOAc	0.228	77	77	73	55	85	78	45	15	22
6	Chloroform	0.259	77	77	73	21	21	23	79	79	77
7	Acetone	0.355	78	78	30	85	85	100	15	15	0
8	MeCN	0.460	78	78	20	80	82	100	20	18	0
9	EtOH	0.654	77	77	73	25	36	79	75	64	21
10	MeOH	0.762	78	78	70	33	57	76	77	43	24

* data retrieved from Christian Reichardt, Solvents and Solvent Effects in Organic Chemistry, Wiley-VCH Publishers, 3rd ed., 2003.

Supplementary Table 10: GPC-parameters applied for analysis of terpene-based polyamides.

Parameters	**Values**
column temperature	35 °C
flow	0.6 mL/min
elution solvent	0.05 M NaTFA in HFIP
sample concentration	1.0 mg/mL
injection volume	50 µL
elution time	30 min
elution volume	18.0 mL
column 1	PSS PFG pre-column
column 2	PSS PFG 100 Å
column 3	PSS PFG 1000 Å

Supplementary Table 11: Effect of the reaction temperature and the activator concentration on the molecular weights. Polymerization method A was applied. Conditions: 1.8 mmol **5-3S**, 2.0 – 5.5 mol% NaH on paraffin, 180 °C or 220 °C, 1 h, work up method A. M/A ratio = Monomer/Activator ratio. Molecular weights refer to masses over 1.0 kDa.

Entry	**M/A ratio**	**M_n** **[kDa]**	**M_w** **[kDa]**	**M_P** **[kDa]**	**P_D**	**T_g** **[° C]**	**T_m** **[° C]**
180 °C A)	90	10.2	16.2	14.0	1.59	115	250-280
180 °C B)	50	9.3	14.5	12.6	1.56	115	260-285
180 °C C)	46	9.1	14.1	12.5	1.55	113	255-285
180 °C D)	24	6.7	9.5	9.4	1.42	111	245-280
180 °C E)	16	5.9	8.3	8.4	1.41	105	245-280
220 °C F)	100	7.5	9.6	9.4	1.28	112	240-270
220 °C G)	96	7.1	9.0	9.0	1.27	112	230-270
220 °C H)	25	6.0	7.5	7.8	1.26	110	240-270
220 °C I)	16	5.6	7.3	7.4	1.30	108	230-270

Supplementary Table 12: DSC method B, method without tempering segment.

Segment	Temperature [°C] Start/End	heating rate [K/min]	N_2 [mL/min]
1	-20 (2 min)	isotherm	50
2	-20/320	10	50
3	320	isotherm	50
4	320/-20	10	50
5	-20 (1 min)	Isotherm	50
6	-20/320	10	50
7	320 (1 min)	Isotherm	50
8	320/-20	10	50
9	-20 (1 min)	Isotherm	50
10	-20/320	10	50

Supplementary Table 13: Impact of the activator concentration on the conversion. The conversion was verified by NMR (closed lactam -NH-C*H*CH$_3$-CH$_2$- compared to open lactam -NH-C*H*CH$_3$-CH$_2$-, see also Supplementary Figure 12) and GPC (M_n > 1.0 kDa). Conditions: 3.0 mmol **5-3S** or **5-3R**, 3.0 mol% NaH on paraffin, 190 °C, 1 h, polymerization method B, work-up method B. Conv. = conversion. M/A ratio = Monomer/Activator ratio. M/A CCR = Monomer/Activator conversion-correlated ratio [($n_{Monomer}$* conversion [%] * 100^{-1}) * $n_{Activator}^{-1}$].

Entry	**M/A ratio**	**GPC conv. [%]**	**NMR conv. [%]**	**M/A CCR**	**M_n [kDa]**	**M_w [kDa]**	**PD**	**T_g [° C]**
poly5-3R-E1	1250	45	39	500	19.9	32.9	1.65	119
poly5-3R-E2	789	57	53	418	20.2	43.8	2.17	120
poly5-3R-E3	330	84	85	281	19.6	45.6	2.33	117
poly5-3R-E4	158	84	88	134	15.2	36.3	2.38	116
poly5-3R-E5	107	86	88	93	13.5	31.8	2.35	115
poly5-3R-E6	79	86	91	69	13.1	29.7	2.27	117
poly5-3S-E7	150	1	1.5	5	3.3	7.3	2.22	-
poly5-3S-E8	107	19	19	24	6.6	13.7	2.08	-
poly5-3S-E9	79	65	64	54	8.6	16.9	1.97	-
poly5-3S-E10	54	71	69	43	8.4	15.2	1.81	-
poly5-3S-E11	38	87	88	36	7.6	13.9	1.83	-
poly5-3S-E12	27	85	84	26	7.1	12.8	1.79	-

Supplementary Table 14: Impact of the reaction time on the conversion and the state. Reaction conditions: 3S-caranlactam (**5-3S**, 1.80 mmol), NaH (60% on paraffin, 6.0 mg, 0.15 mmol) and **Bz5-3S** (15.0 mg, 0.06 mmol), 180 °C, polymerization method B.

Entry	**Reaction time [min]**	**Integral** 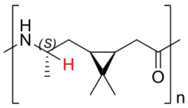 **poly5-3S**	**Integral** 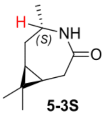 **5-3S**	**Conversion [%]**	**State**
A	5	1.00	1.03	49	viscous oil, yellow
B	15	1.00	0.63	61	very viscous oil, yellow
C	30	1.00	0.48	68	brittle solid, yellow
D	45	1.00	0.32	76	brittle solid, yellow
E	120	1.00	0.23	81	brittle solid, brown

Supplementary Table 15: DSC method A, method for thermal analysis of polyamides including a tempering segment (4).

Segment	**Temperature [°C] Start/End**	**heating rate [K/min]**	**N_2 [mL/min]**
1	20/350	20	50
2	350/20	-20	50
3	20/220	10	50
4	220 (20 min)	isotherm	50
5	220/0	-10	50
6	0/370	10	50
7	370/0	-10	50
8	0/440	10	50

Supplementary Table 16: Built-in was investigated by NMR. [*] = Application of Ac_2O and NaH for in-situ generated **Ac5-3S** as activator instead of **Bz5-3S**. [#] = detection limit insufficient.

					Reaction Conditions				
Entry	**5-3S [%]**	**53-R [%]**	**LL [%]**	**CL [%]**	**M/A ratio**	**T [°C]**	**t [min]**	**NaH [%]**	**Polymerization method**
E1	15	85			333	190	20	3.0	B
E2	50	50			64[*]	190	30	4.2	A[*]
E3	83	17			73	190	60	2.5	B
E4	30		70		50	170	30	1.6	A
E5	41		59		44	190	30	5.6	A
E6	37		63		400	190	30	1.6	A
E7	50		50		70	190	60	3.8	B
E8	85		15		20	190	60	2.0	A
E9	25			75	213	190	30	2.1	A
E10	50			50	86	190	60	3.0	B
E11	75			25	53	175	60	1.9	B

					Analytical Data				
Entry	**Built-in [%]**				**M_n [kDa]**	**M_w [kDa]**	**T_g [°C]**	**T_m [°C]**	**PD**
	5-3S	**53-R**	**LL**	**CL**					
E1	0[#]	100[#]			19.8	38.9	111	-	1.96
E2	30	70			no data	no data	111	-	no data
E3	75	25			10.4	15.0	109	210-250	1.43
E4	27		73		no data	no data	43	120-150	no data
E5	32		68		12.5	24.5	46	-	1.96
E6	33		67		30.2	60.1	49		1.99
E7	41		59		10.0	15.6	55	-	1.56
E8	83		17		no data	no data	82	220-240	no data
E9	18			82	15.2	31.1	62	160-190	2.04
E10	48			52	12.1	17.3	88	-	1.42
E11	73			27	no data	no data	94	-	no data

Supplementary Table 17: Incorporation of 5-3S in co-polymerization with CL or LL at different reaction times.

Poly(5-3S$_{50\%}$·CL$_{50\%}$)

Co-polymer composition [%]

Time [s]	Incorporated **5-3S**	Incorporated **CL**	Total conversion [%]
30	0	100	2.8
60	18	82	6.7
120	30	70	14.7
180	35	65	28.7
240	37	63	41
360	39	61	47.9
420	41	59	59.4
3600	49	51	84

Poly(5-3S$_{50\%}$·LL$_{50\%}$)

Co-polymer composition [%]

Time [s]	Incorporated **5-3S**	Incorporated **LL**	Total conversion [%]
30	100	0	0.39
60	66	34	7.9
120	63	37	21.7
180	59	41	31.1
240	58	42	34.5
3600	52	48	64.4

Supplementary Table 18: Outline of the determined crystal structures.

Name	SG	a, b, c [Å]	α, β, γ [°]	V [Å^3]	ρ [g cm^3]
5-3S	C121	10.302(10)	90.00	969.0(17)	1.147
		7.635(8)	101.37(4)		
		12.566(14)	90.00		
5-3R	P12$_1$1	6.716(4)	90.00	949.5(9)	1.171
		8.133(4)	91.38(2)		
		17.370(10)	90.00		
Poly5-3S	P2$_1$2$_1$2$_1$	9.79(6)	90.00	952(11)	1.167
		15.10(6)	90.00		
		6.44(6)	90.00		

3. Supplementary Methods

Analytical methods and instruments

Gas chromatography/Mass spectrometry (GC/MS). GC analysis was performed using GC-2010 Plus (Shimadzu) in combination with auto-injector AOC-5000 (Jain, Combi PAL). Separation was achieved via GC capillary column (BPX 5: 5% phenyl, 95% methyl polysilphenylene / siloxane; SGE). For coupled MS, MS-QP2010 Plus (Shimadzu) with electron ionization (70 eV) was used. Software analysis of measured data was accomplished with GC-MS Postrun Analysis (Shimadzu). Gathered data was compared with the National Institute of Standards and Technology database version 08. Supplementary Table 1 displays the used parameters and retention times.

Nuclear magnetic resonance (NMR) spectroscopy. All NMR-measurements were carried out on a JNM-ECA 400 MHz spectrometer from JEOL at 25 °C using standard pulse programs. Chemical shifts are reported as δ-values in ppm. Coupling constants (J-values) are given in Hertz (Hz). The DEPT135° technique was used to assign CH_2-signales. 2D NMR methods (COSY, HSQC, HMBC) were applied if useful. Chemical shifts are reported as follows: value (multiplicity, coupling constant(s) where applicable, number of protons). Only clearly identifiable peaks are assigned. For the characterization of observed signal multiplicities, the following abbreviations were applied: s (singlet), d (doublet), dd (double doublet), dt (double triplet), t (triplet), q (quartet), quint (quintet) and m (multiplet). The data was evaluated with JEOL Delta v5.0.4.4 or MestReNova 6.0.2. For polymer sample preparation, the polyamide (10-15 mg) was dissolved in 600 µL of DCOOD and shook until a homogenous, clear solution was obtained. The samples were measured immediately. As displayed in the spectra, the signals, as typical for polymers, are broadened. Therefore, no conclusive multiplet analysis was possible.

Thin layer chromatography (TLC). TLC was performed using aluminium plates coated with SiO_2 (Merck 60, F-254) and the spots were visualized with a $KMnO_4$ stain. Flash column was performed using SiO_2 (0.06-0.2 mm, 230-400 mesh ASTM) from Roth.

Size exclusion chromatography (SEC). SEC was performed by a SECcurity GPC system with an autosampler (1260 Infinity, Agilent Technologies) and a TCC6000 column oven (Polymer Standards Service, PSS). As columns, a system of three Novema GPC/SEC columns was used (1: 50x8 mm, 10 µm; 2: 300x8 mm, 10 µm, 100 Å; 3: 300x8 mm, 10 µm, 3000 Å). The data was evaluated using PSS WinGPC UniChrom (PSS). PMMA was chosen for narrow molar mass standard calibration and PA6 standards from a PSS ready-call-kit (M_w/M_n = 31400/17400 Da; 22000/13000 Da; 17200/11300 Da) for the broad calibration. For sample preparation, the polyamide was dissolved in a solution of 0.05 M sodium trifluoroacetate (NaTFA) and hexafluoro-iso-propanol (HFIP). Supplementary Table 10 displays the applied GPC parameters.

Differential Scanning Calorimetry (DSC). DSC was performed on a DSC 1 from Mettler Toledo with the software STARe V. 16.00. The samples (5-10 mg) were prepared in alumina crucibles. Supplementary Tables 15 and 11 displays the applied methods DSC method A and DSC method B. For method A, the segments 6 and 7 were used for verification of T_g and T_m if not otherwise stated. For method B, the last heating run was used for evaluation.

Matrix-assisted laser desorption/ionization – time-of-flight (MALDI-TOF). MALDI-TOF was conducted on a Bruker Ultra Flex TOF/TOF mass spectrometer. α-cyano-4-hydroxycinammic acid or dithranol was applied as the matrix. HFIP or formic acid were used as solvents.

Single crystal X-ray diffraction. Monomers were analysed by single-crystal X-ray diffractometry (SC-XRD, D8 Venture, Bruker AXS, Madison, WI, USA) equipped with a 4-circle goniometer (Kappa geometry), a CMOS detector (Photon 100, Bruker AXS), a rotating anode (TXS, Bruker AXS) with MoKα radiation (λ=0.71073 Å), and a multilayer mirror monochromator (HELIOS, Bruker AXS), using the APEX 2 software package (version 2008.4., Bruker AXS). The measurements were performed on single crystals coated with perfluorinated ether, frozen under a stream of cold nitrogen at 100 K. A matrix scan was used to determine the initial lattice parameters. Reflections were merged and corrected for Lorenz and polarization effects, scan speed, and background using a narrow-frame algorithm (SAINT version 7.56a, Bruker AXS). Absorption corrections were performed using SADABS (version 2008/1, Bruker AXS). Space group assignments were based upon systematic absences, E statistics, successful solution (using SHELXT [1]) and refinement of the structures. These were solved by direct methods with the aid of successive difference Fourier maps, and were refined against all data using SHELXL-2014[2] in conjunction with SHELXLE.[3] If not mentioned otherwise, non-hydrogen atoms were refined with anisotropic displacement parameters. Hydrogen atoms were placed in ideal positions using the SHELXL riding model. Full-matrix least-squares refinements were carried out by minimizing $\Sigma\, w(F^2{}_0\text{-}F^2{}_C)^2$ with the SHELXL-20142 weighting scheme. Neutral atom scattering factors for all atoms and anomalous dispersion corrections for the non-hydrogen atoms were taken from *International Tables for Crystallography*.[4] For 3S-caranlactam (**5-3S**), a clear colourless fragment-like specimen of $C_{10}H_{17}NO$, approximate dimensions 0.060 mm x 0.221 mm x 0.263 mm, was used. A total of 1228 frames were collected, for a total exposure time of 2.96 hours.

For 3R-lactam (**5-3R**), a clear colourless fragment-like specimen of $C_{10}H_{17}NO$, approximate dimensions 0.204 mm x 0.214 mm x 0.445 mm, was used. A total of 1420 frames were collected, for a total exposure time of 0.74 hours.

Powder X-ray diffraction. Polymers were assessed by powder X-ray diffraction in Bragg-Brentano geometry (PXRD, Miniflex, Rigaku, Japan, with silicon strip detector D/teX Ultra). Copper Kα radiation was used and sample holders rotated around the axis at half the scattering angle 2Θ to reduce effects of texture. Intensities were recorded in steps of Θ = 0.02°, using incident and receiving Soller slits with angular apertures of 2.5° and 1.0°. 3S- and 3R-polycaranamide (**poly5-3S**, **poly5-3R**) powders were compressed on low-background holders (cut silicon wafers) with flat recesses. Also, scattering patterns of solvent-cast thin films of **poly5-3S** were recorded. In the latter, crystallization was effectively quenched through rapid solvent evaporation, allowing to record amorphous reference patterns. For presentation, scattering patterns from S- and R-monomers, deposited from solution, were recorded. All patterns were corrected for their sample holder backgrounds.

For **5-3S**, the amorphous reference was scaled to give the volume fraction of crystalline phase, *fc* via the fractions of integral intensities. Its structure was determined by the direct space method simulated annealing (SA) in Expo2014.[5] In detail, molecular models retaining the hydrogen atoms at the three chiral centres were used. The distance between the bonding atoms C1-C6 was flexibly constrained to 1.54 pm, the distance between N1 and O1 to 2.85 pm. An initial selection of unit cells and space groups (SG) was made, based on reflex positions, indexed by N-TREOR09.[6] For each cell, ten SA runs were performed with a resolution of 1.8 Å. Each result was characterized by a figure of merit CF (lower meaning better match). The results were discriminated, based on the CF and the requirements that the obtained crystalline phases possess:

- Densities $\rho_{c,p}$ matching the density of the corresponding monomeric crystals $\rho_{c,m}$ as $\rho_{c,p} \in \rho_{c,m} \pm \rho_{c,m}/5$.

- Structures that are chemically plausible, in particular with respect to the bond angle between C1 and C6.

The cells yielding positive results were explored by additional 50 SA runs, with subsequently added hydrogens. They were then tested for their physical plausibility by semi-empirical geometry optimization by the Molecular Orbital Package (MOPAC, PM7 algorithm, singlet state).[7] As the final figure of merit (FOM), we multiplied the root mean square displacement (RMSD) between the results and their MOPAC-optimized geometries with their respective CF.

Synthetic procedures

Unless otherwise stated, all chemicals, solvents and starting materials were commercially available and used as received. All intermediates were separated from side products by distillation, column chromatography or crystallization until combined data of GCMS and NMR could verify the product and subsequent reactions could be performed satisfactorily. For the enzymatic epoxidation, Novozyme-435 (CALB lipase immobilized on acrylic resin) was applied.

Synthesis of 3S-caranepoxide (2-3S) ***(1S,3S,5R,7R)-3,8,8-trimethyl-4-oxatricyclo[5.1.0.03,5]octane*** **(Enzyme catalysis)**. (+)-3-carene (**1**) (92.2 g, 677 mmol, 1.00 equiv.) was dissolved in EtOAc (2.80 L) and heated under stirring to 50 °C. Novozyme-435 (20 g) was added followed by portions of H_2O_2 (35%, 80.4 mL, 918 mmol, 1.40 equiv., 13.4 mL every hour). The reaction mixture was stirred over night until full conversion of the substrate and the enzyme was removed by filtration. The organic phase was washed with Na_2HCO_3 (saturated solution, 1.50 L) Na_2SO_3 (saturated solution) until a peroxide test (*Quantofix peroxide 100*) was negative. The combined aqueous layers were extracted with toluene. The organic layers were dried using $MgSO_4$ and the organic solvent was removed under reduced pressure to give crude 3S-caranepoxide (**2-3S**, 98.5 g, 646 mmol, 96%) as yellow oil. The purity of the crude product was above 95% (GCMS, NMR) and could be used without further purification. The yield after distillation was 84%.

Synthesis of 3S-caranepoxide (2-3S) ***(1S,3S,5R,7R)-3,8,8-trimethyl-4-oxatricyclo[5.1.0.03,5]octane*** AcOOH (38%, 170 mL, 800 mmol 1.10 equiv.) were given to a solution of $NaOAc{\cdot}3H_2O$ (130 g, 950 mmol, 1.30 equiv.) in water 500 mL) and heated in an oil bath until the mixture reached a temperature of 30 °C. (+)-3-carene (**1**) (100 g, 730 mmol, 1.00 equiv.) was dropped to the solution within a period of 0.5 h under vigorous stirring. Without external heating, the temperature of the reaction mixture increased to 60 °C. The full conversion of (+)-3-carene (**1**) was reached after 1 h, as monitored by GCMS. After cooling to room temperature, pentane (200 mL) and NaCl (saturated solution, 200 mL) were added and the layers of the reaction mixture were separated. The organic layer was washed with NaOH solution (1 M, 2x250 mL), Na_2SO_2 (saturated solution, 1x250 mL) and water (1x250 mL) and dried over $MgSO_4$. All layers were tested for remaining peracid species. After the solvent was removed under reduced pressure, 100 g of the crude product were distilled (45 °C, 2 mbar) to yield 3S-caranepoxide (**2-3S**, 92 g,605 mmol, 82%) as colourless oil.

^{1}H NMR (400 MHz, DMSO-d6): δ/ppm = 2.76 (s, 1H, -CH$_2$-C*H*O-CCH$_3$O-), 2.15 (ddd, J = 16.3, 9.1, 1.9 Hz, 1H, -CCH$_3$O-C*H$_2$*-CH-), 2.03 (dd, J = 16.1, 9.1 Hz, 1H, -CHO-C*H$_2$*-CH-), 1.55 (dt, J = 16.3, 2.4 Hz, 1H, -CCH$_3$O-C*H$_2$*-CH-), 1.42 (dd, J = 16.1, 2.3 Hz, 1H, -CHO-C*H$_2$*-CH-), 1.16 (s, 3H, -CHC*H$_3$*-), 0.98 (s, 3H, -CCHCHC*H$_3$*CH$_3$-), 0.69 (s, 3H, 3H, -CCHCHCH$_3$C*H$_3$*-), 0.43 (td, J = 9.1, 2.3 Hz, 1H, -CHO-CH$_2$-C*H*-), 0.35 (td, J = 9.1, 2.4 Hz, 1H, -CCH$_3$O-CH$_2$-C*H*-).

^{13}C NMR (100 MHz, DMSO-d6): δ/ppm = 56.6 ($-\underline{C}CH_3O-$), 54.8 ($-\underline{C}HO-$), 27.5 ($-CCHCH\underline{C}H_3CH_3-$), 22.9 ($-CHO-\underline{C}H_2-CH-$), 22.9 ($-C\underline{C}H_3O-$), 18.8 ($-CCH_3O-\underline{C}H_2-CH-$), 15.7 ($-CHO-CH_2-\underline{C}H-$), 15.5 ($-\underline{C}CHCHCH_3CH_3-$), 14.4 ($-CCHCHCH_3\underline{C}H_3-$), 13.6 ($-CCH_3O-CH_2-\underline{C}H-$).

MS (EI, 70 eV): m/z (%) = 152.10 (0.94), 151.05 (0.48), 138.15 (3.64), 137.10 (34.48), 136.15 (0.79), 135.10 (0.77), 134.10 (2.37), 133.15 (0.37), 124.10 (1.81), 123.10 (14.74).

MS (EI, 70 eV): % (m/z) = 100.00 (43.05), 83.40 (67.10), 67.72 (41.10), 63.07 (109.10), 44.70 (81.10), 44.59 (39.10), 34.48 (137.10), 32.83 (79.10), 30.62 (55.05), 27.86 (95.10).

Synthesis of 3R-caranepoxide (2-3R) ***(1S,3R,5S,7R)-3,8,8-trimethyl-4-oxatricyclo[5.1.0.03,5]octane***. (+)-3-Carene (**1**, 50 g, 370 mmol, 1.00 equiv.) were dissolved in acetone (200 mL) and H_2O (200 mL) and cooled in an ice bath before N-bromsuccinimide (72.0 g, 400 mmol, 1.08 equiv.) were added portion-wise while the temperature of the reaction mixture was kept below 10 °C. After the addition was complete, the reaction was allowed to reach room temperature and was then stirred for 1 h before another portion of N-bromsuccinimide (5.00 g, 28.0 mmol, 0.08 equiv.) was added without cooling. When the conversion of (+)-3-carene (**1**) was complete, NaOH (5 M, 250 mL) were dropped to the reaction mixture and stirred at room temperature for 12 h. After extraction with hexane (2x200 mL), the combined organic layers were washed with Na_2SO_3 (saturated solution, 250 mL) and NaCl (saturated solution, 250 mL) and then dried over $MgSO_4$. The solvent was removed under reduced pressure and the crude product was purified by fractionated vacuum distillation (55-90 °C, 3 mbar) to yield 3R-caranepoxide (**2-3R**, 26.1 g, 170 mmol, 46 %, purity: 97 % 3R-caranepoxide (**2-3R**) and 3.0 % 3S-caranketone (**3-3S**) as verified by GCMS) as colourless oil.

^{1}H NMR (400 MHz, DMSO-d6): δ/ppm = 2.84 (d, J = 5.4 Hz, 1H, $-CCH_3CO-C\underline{H}O-CH_2-$), 2.29 (ddd, J = 16.7, 9.2, 5.4 Hz, 1H, $-CHO-C\underline{H_2}-CH-$), 2.08 (dd, J = 16.4, 9.2 Hz, 1H, $CCH_3O-C\underline{H_2}-CH-$), 1.71 – 1.61 (m, 2H, $-CHO-C\underline{H_2}-CH-$, $-CCH_3O-C\underline{H_2}-CH-$), 1.22 (s, 3H, $-CC\underline{H_3}O-$), 0.94 (s, 3H, $-CCHCHC\underline{H_3}CH_3-$), 0.88 (s, 3H, $-CCHCHC\underline{H_3}CH_3-$), 0.61 – 0.48 (m, 2H, $-CHO-CH_2-C\underline{H}-$, $-CCH_3O-CH_2-C\underline{H}-$).

^{13}C NMR (100 MHz, DMSO-d6): δ/ppm = 56.8 ($-\underline{C}HO-$), 55.07 ($-\underline{C}CH_3O-$), 28.86 ($-CCHCH\underline{C}H_3CH_3-$), 24.47 ($-C\underline{C}H_3O-$), 23.33 ($-CHO-\underline{C}H_2-CH-$), 19.16 ($CCH_3O-\underline{C}H_2-CH-$), 17.70 ($-CHO-CH_2-\underline{C}H-$), 16.84 ($CCH_3O-CH_2-\underline{C}H-$), 16.68 ($-\underline{C}CHCHCH_3CH_3-$), 14.76 ($-CCHCHCH_3\underline{C}H_3-$).

MS (EI, 70 eV): m/z (%) = 152.20 (1.27), 138.10 (1.91), 137.15 (17.91), 136.15 (0.53), 134.10 (1.17), 124.15 (1.31), 123.15 (10.85), 122.15 (1.08), 121.15 (2.56), 120.15 (1.05).

MS (EI, 70 eV): % (m/z) = 100.00 (79.10), 93.02 (43.05), 67.30 (67.10), 52.62 (41.05), 44.01 (109.10), 42.23 (94.10), 34.09 (81.10), 29.28 (93.10), 27.58 (39.05), 26.27 (95.10).

Synthesis of 3S-caranketone (3-3S) ***(1R,4S,6S)-4,7,7-trimethylbicyclo[4.1.0]heptan-3-one***. 3S-caranepoxide (**2-3S**, 43.6 g, 280 mmol, 1.00 equiv.) was dissolved in cyclohexane (230 mL) and heated to 60 °C. Fe(ClO$_4$)$_2$·H$_2$O (167 mg, 0.2 mol%) in EtOAc (1 mL) was added. The rearrangement was completed after 1.5 h. GCMS verified a *de* of 95%. The mixture was washed with HCl (2.0 M, 2x50 mL), NaHCO$_3$ (saturated solution, 100 mL) and water (100 mL). Cyclohexane was removed under reduced pressure and 15.0 g of the crude product were purified by fractional vacuum distillation (100 – 140 °C, 10 mbar) to yield 3S-caranketone (**3-3S**, 8.0 g, 53%) as colourless oil.

^{1}H NMR (400 MHz, DMSO-d6): δ/ppm = 2.56 – 2.47 (m, 1H, -CO-C$\underline{H_2}$-CH-, superposition by solvent peak), 2.10 (qdd, J = 7.3, 5.0, 2.7 Hz, 1H, -C$\underline{H}$CH$_3$-), 2.03 – 1.90 (m, 2H, -CHCH$_3$-C$\underline{H_2}$-CH-, -CO-C$\underline{H_2}$-CH-), 1.70 – 1.62 (m, 1H, -CHCH$_3$-C$\underline{H_2}$-CH-), 1.13 (d, J = 7.2 Hz, 3H, -CHC$\underline{H_3}$-), 1.04 (s, 3H, -CCHC$\underline{H_3}$CH$_3$-), 1.03 – 0.97 (m, 1H, -CO-CH$_2$-C$\underline{H}$-), 0.90 (s, 3H, -CCHCH$_3$C$\underline{H_3}$-), 0.80 (td, J = 8.9, 6.4 Hz, 1H, -CHCH$_3$-CH$_2$-C$\underline{H}$-).

^{13}C NMR (100 MHz, DMSO-d6): δ/ppm = 216.1 (-$\underline{C}$O-), 40.7 (-$\underline{C}$HCH$_3$-), 33.9 (-CO-$\underline{C}$H$_2$-CH-), 27.8 (-CCHCH$\underline{C}$H$_3$CH$_3$-, 26.3 (-CHCH$_3$-$\underline{C}$H$_2$-CH-), 21.1 (-CO-CH$_2$-$\underline{C}$H-), 19.0 (-$\underline{C}$CHCHCH$_3$CH$_3$-), 16.7 (-CH$\underline{C}$H$_3$-), 16.4 (-CO-CH$_2$-$\underline{C}$H-), 14.6 (-CCHCHCH$_3$$\underline{C}H_3$-).

MS (EI, 70 eV): m/z (%) = 153.10 (2.77), 152.10 (27.38), 138.10 (1.16), 137.10 (12.12), 135.15 (0.47), 134.10 (2.59), 125.15 (0.48), 124.10 (4.38), 123.10 (4.10), 121.10 (0.54).

MS (EI, 70 eV): % (m/z) = 100.00 (67.10), 83.36 (81.10), 69.63 (41.10), 45.24 (39.10), 44.25 (82.10), 33.71 (95.10), 32.68 (109.10), 30.74 (110.10), 27.40 (55.10), 27.38 (152.10).

Synthesis of 3R-caranketone (3-3R) ***(1R,4R,6S)-4,7,7-trimethylbicyclo[4.1.0]heptan-3-one*** **by rearrangement of 3R-caranepoxide (2-3R).** 3R-caranepoxide (**2-3R**, 10.0 g, 66 mmol, 1.00 equiv.) was dissolved in cyclohexane (55 mL) and heated to 60 °C before a solution of Fe(ClO$_4$)$_2$·H$_2$O (78 mg, 0.30 mmol, 0.005 equiv.) in EtOAc (0.5 mL) was dropped to the reaction mixture and stirred for 3 h. GCMS revealed a *de* of 100%. After complete conversion, Na$_2$SO$_3$ (saturated solution, 150 mL) was added and the layers were separated. The organic layer was washed with water (1x100 mL) and the solvent was removed under reduced pressure. Crude product (8.80 g) was purified by fractional vacuum distillation (105 °C, 30 mbar) to yield a mixture of caranketones (5.74 g, 57 % purity > 80% as confirmed by GCMS and NMR, R 82%, S 18%). As no 3S-caranketone (**3-3S**) was present before the distillation and a heat-induced isomerization was not observed for pure 3R-caranketone (**3-3R**), it is likely that the 3S-caranketone (**3-3S**) formation is promoted by residual bromide species that could not be removed by the washing steps.

Synthesis of 3R-caranketone (3-3R) ***(1R,4R,6S)-4,7,7-trimethylbicyclo[4.1.0]heptan-3-one*** **by isomerization of 3S-caranketone (3-3S) and subsequent enrichment of 3R-caranketone (3-3R) by reaction with HONH$_2$·HCl**. Freshly distilled 3S-caranepoxide (**2-3S**, 88.0 g, 580 mmol, 1.00 equiv.) was dissolved in cyclohexane (600 mL) and heated to 60 °C. FeClO$_4$·6H$_2$O (150 mg, 0.58 mmol, 0.001 equiv.) in EtOAc (1.0 mL) was added and stirred overnight until all 3S-caranepoxide (**2-3S**) was converted. After washing with Na$_2$SO$_3$ (2.0 w%, 2 x 400 mL), HCl (0.1 M, 500 mL) and NaCl (saturated solution, 500 mL) and drying under use of MgSO$_4$, the organic solvent was removed under reduced pressure to give crude 3S-caranketone (**3-3S**, 83.8 g) that was then dissolved in MeCN (500 mL). For the isomerization to 3R-caranketone (**3-3R**), HCl (2 M, 120 mL) was then dropped to the solution within 30 min under vigorous stirring and then stirred for 48 h until the equilibrium isomeric ratio of 4:1 in favour of the R-isomer was reached. As the S-isomer reacts faster to the corresponding oxime, a further enrichment of the R-isomer was possible. NaOAc·3 H$_2$O (6.56 g, 80.0 mmol) in water (200 mL) was given to the reaction mixture and stirred for 5 min before HONH$_2$·HCl (5.07 g, 73 mmol) was added portion-wise within an hour. After stirring for 4 h, the reaction mixture was investigated by GCMS. The whole process is displayed in Supplementary Figure 17. The layers were separated, and the aqueous phase was extracted with cyclohexane (3 x 100 mL). The combined organic phases were washed with NaHCO$_3$ (saturated solution, 300 mL) and NaCl (saturated solution, 300 mL) and dried using Na$_2$SO$_4$. The crude product was purified by vacuum distillation (60 → 100 °C, 3 mbar) to yield 3R-caranketone (**3-3R**, 41.3 g, 47%, purity > 90 % as confirmed by GCMS and NMR, isomeric ratio > 25:1).

^{1}H NMR (400 MHz, DMSO-d6): δ/ppm = 2.57 (dd, J = 17.6, 8.4 Hz, 1H, -CO-C$\underline{H_2}$-CH-), 2.41 – 2.23 (m, 2H, -C$\underline{H}$CH$_3$-CO-, -CHCH$_3$-C$\underline{H_2}$-CH-), 2.12 (dd, J = 17.6, 2.1 Hz, 1H, -CO-C$\underline{H_2}$-CH-), 1.20 – 1.10 (m, 1H, -CHCH$_3$-C$\underline{H_2}$-CH-), 1.06 (td, J = 8.8, 2.3 Hz, 1H, -CO-CH$_2$-C$\underline{H}$-), 1.00 (s, 3H, -CCHCHC$\underline{H_3}$CH$_3$-), 1.00 – 0.92 (m, 1H, -CHCH$_3$-CH$_2$-C$\underline{H}$-), 0.83 (d, J = 6.4 Hz, 3H, -CH$_2$-CHC$\underline{H_3}$-CO-), 0.78 (s, 3H, -CCHCHC$\underline{H_3}$CH$_3$-).

^{13}C NMR (100 MHz, DMSO-d6): δ/ppm = 215.2 (-$\underline{C}$O-), 41.0 (-$\underline{C}$HCH$_3$-), 36.4 (-CO-$\underline{C}$H$_2$-CH-), 29.2 (-CHCH$_3$-$\underline{C}$H$_2$-CH-), 27.6 (-CCHCH$\underline{C}$H$_3$CH$_3$-), 22.5 (-CO-CH$_2$-$\underline{C}$H-), 19.6 (-CHCH$_3$-CH$_2$-$\underline{C}$H-), 18.9 (-$\underline{C}$CHCHCH$_3$CH$_3$-), 14.7 (-CCHCHCH$_3$$\underline{C}H_3$-), 14.1 (-CH$\underline{C}H_3$-).

MS (EI, 70 eV): m/z (%) = 153.15 (3.05), 152.20 (28.19), 138.20 (1.46), 137.20 (14.60), 135.15 (0.64), 134.15 (2.69), 124.15 (4.17), 123.15 (4.72), 119.15 (3.62), 111.15 (3.35).

MS (EI, 70 eV): % (m/z) = 100.00 (67.10), 87.96 (81.15), 36.29 (41.10), 46.76 (82.15), 37.97 (39.10), 36.57 (95.15), 35.65 (109.15), 34.44 (110.15), 29.04 (55.10), 28.19 (152.20).

Synthesis of 3S- and 3R-caranoxime (4-3S and 4-3R) ***(1R,4S,6S)-4,7,7-trimethylbicyclo[4.1.0]heptan-3-one oxime*** **and** ***(1R,4R,6S)-4,7,7-trimethylbicyclo[4.1.0]heptan-3-one oxime***. 3-caranketone (**3-3S** or **3-3R**, 1.00 equiv.) was dissolved in MeCN (1.25 M) and NaOAc (1.40 equiv.) followed by HONH$_2$·HCl (1.20 equiv.) were added sequentially. The suspension was stirred overnight until full conversion was verified by GCMS. The volume was doubled by the addition of water and the layers were separated. The aqueous phase was extracted with EtOAc until no oxime was observed in the aqueous phase and the combined organic phases were washed with NaHCO$_3$ (saturated solution, equivoluminar) and NaCl (saturated solution, equivoluminar) and dried using Na$_2$SO$_4$. The solvent was removed under reduced pressure to give the respective oximes **4-3S** or **4-3R** as a mixture of cis- (15%) and trans-oximes (85%) as very viscous oil in a total yield of 90 %.

3S-caran-*trans*-oxime:

^{1}H NMR (400 MHz, DMSO-d6): δ/ppm = 10.07 (s, 1H, -NO*H*), 2.56 (dd, J = 18.6, 1.6 Hz, 1H, -CNOH-C*H*$_2$-CH-), 2.32 – 2.17 (m, 2H,-C*H*CH$_3$-, -CNOH-C*H*$_2$-CH-), 1.90 – 1.78 (m, J = 16.8, 8.1, 3.1 Hz, 1H, -CHCH$_3$-C*H*$_2$-CH-), 1.37 (dt, J = 14.4, 4.9 Hz, 1H, -CHCH$_3$-C*H*$_2$-CH-), 1.05 (d, J = 7.1 Hz, 3H, CH$_2$-CHC*H*$_3$-CNOH-), 0.96 (s, 3H, -CCHCHC*H*$_3$CH$_3$-), 0.79 (td, *J* = 8.9, 1.8 Hz, 1H, -CNOH-CH$_2$-C*H*-) 0.71 (s, 3H, -CCHCHCH$_3$C*H*$_3$-), 0.69 – 0.62 (m, 1H, CHCH$_3$-CH$_2$-C*H*-).

^{13}C NMR (100 MHz, DMSO-d6): δ/ppm = 161.5 (-*C*NOH-), 32.8 (-*C*HCH$_3$-), 28.5 (-CCHCH*C*H$_3$CH$_3$-), 26.8 (-CHCH$_3$-*C*H$_2$-CH-), 19.3 (CH$_2$-CH*C*H$_3$-CNOH-), 19.1 (-CNOH-CH$_2$-*C*H-), 18.3 (*C*CHCHCH$_3$CH$_3$), 17.1 (-CNOH-*C*H$_2$-CH-), 16.7 (-CHCH$_3$-CH$_2$-*C*H-), 14.9 (-CCHCHCH$_3$*C*H$_3$-).

MS (EI, 70 eV): m/z (%) = 168.05 (1.30), 167.00 (11.80), 166.05 (1.66), 153.10 (1.47), 152.05 (15.72), 151.05 (1.69), 150.05 (10.83), 149.05 (1.90), 148.10 (5.97), 139.10 (2.56).

MS (EI, 70 eV): % (m/z) = 100.00 (41.05), 51.40 (39.10), 47.59 (67.05), 43.19 (112.10), 42.42 (79.05), 41.89 (107.10), 40.65 (55.10), 39.11 (106.05), 38.33 (43.05), 29.88 (81.05).

3R-caran-*trans*-oxime:

^{1}H NMR (400 MHz, DMSO-d6): δ/ppm = 10.29 (s, 1H, -CNO*H*-), 2.75 (dd, J = 18.1, 1.6 Hz, 1H, -CNOH-C*H*$_2$-CH-), 2.21 – 2.02 (m, 3H, -CNOH-C*H*$_2$-CH-, -C*H*CH$_3$-, -CHCH$_3$-C*H*$_2$-CH-),0.97 – 0.86 [7H, 2xC*H*$_3$ 1xC*H*H: 0.94 (s, 3H, CCHCHC*H*$_3$CH$_3$-), 0.91 (d, J = 6.2 Hz, 3H, -CHC*H*$_3$-), superposition -CHCH$_3$-C*H*$_2$-CH-)] 0.85 – 0.77 (m, 1H, -CNOH-CH$_2$-C*H*-), 0.73 (dd, J = 9.0, 2.0 Hz, 1H, CHCH$_3$-CH$_2$-C*H*-), 0.70 (s, 1H, -CCHCHCH$_3$C*H*$_3$-).

^{13}C NMR (100 MHz, DMSO-d6): δ/ppm = 160.2 (-*C*NOH-), 33.7 (-*C*HCH$_3$-), 29.4 (-CHCH$_3$-*C*H$_2$-CH-), 28.0 (-CCHCH*C*H$_3$CH$_3$-), 19.8 (-CNOH-CH$_2$-*C*H-), 19.7 (CNOH-*C*H$_2$-CH-), 19.3 (-CNOH-CH$_2$-*C*H-), 17.8 (*C*CHCHCH$_3$CH$_3$), 16.6 (CH$_2$-CH*C*H$_3$-CNOH-), 14.5 (-CCHCHCH$_3$*C*H$_3$-).

MS (EI, 70 eV): m/z (%) = 168.15 (1.95), 167.15 (15.02), 166.15 (2.30), 153.15 (2.14), 152.15 (19.40), 151.20 (2.22), 150.20 (16.60), 149.20 (2.13), 148.15 (7.09), 139.15 (3.59).

MS (EI, 70 eV): % (m/z) = 100.00 (41.10), 59.79 (112.10), 57.23 (67.10), 54.27 (79.10), 51.43 (107.10), 48.84 (106.10), 48.75 (55.10), 48.26 (39.05), 42.55 (43.10), 37.77 (134.15).

Synthesis of 3S- and 3R-caranlactams (5-3S and 5-3R) ***(1R,5R,7S)-5,8,8-trimethyl-4-azabicyclo[5.1.0]octan-3-one*** **and** ***(1S,5S,7S)-5,8,8-trimethyl-4-azabicyclo[5.1.0]octan-3-one***. 3-caranoxime (**4-3S** or **4-3R**, 1.00 equiv.) was dissolved in MeCN (1 M) and cooled in an ice bath before NaOH (2 M, 3.10 equiv.) was dropped to the solution. The reaction mixture was stirred for 2 h and tosyl chloride (1.10 equiv.) was added slowly within 1.5 h. The ice bath was removed after additional stirring for 2 h and kept at room temperature overnight. The aqueous layer was extracted with EtOAc until no product was detected in the aqueous phase and the combined organic layers were then washed with NaHCO$_3$ (saturated solution, equivoluminar) and NaCl (saturated solution, equivoluminar) and dried using Na$_2$SO$_4$. The solvent was removed under reduced pressure and the remaining solid was recrystallized from EtOAc at -20 °C to yield pure 3-caranlactam as colourless crystals (3R-caranlactam **5-3R**: 74 %; 3S-caranlactam **5-3S**: 76 %).

3S-caranlactam (**5-3S**)
^{1}H NMR (400 MHz, DMSO-d6): δ/ppm = 6.92 (s, 1H, -CO-N$\underline{H}$-) 3.5 – 3.14 (m, 1H, -NH-C$\underline{H}$CH$_3$-CH$_2$-), 2.31 – 2.15 (m, 2H, -CO-C$\underline{H_2}$-CH-), 1.71 – 1.49 (m, 2H, -CH-C$\underline{H_2}$-CCHCH$_3$-), 1.05 (d, *J* = 6.4 Hz, 3H, -NH-CHC$\underline{H}_3$-), 1.01 (s, 3H, -CC$\underline{\mathrm{H}}$CHCH$_3$C$\underline{H_3}$-), 0.97 (s, 3H, -CCHCHC$\underline{H_3}$CH$_3$-), 0.85 – 0.76 (m, 1H, -CC$\underline{H}$CHCH$_3$CH$_3$-), 0.57 (td, *J* = 9.0, 2.1 Hz, 1H, -CCHC$\underline{H}$CH$_3$CH$_3$-).

^{13}C NMR (100 MHz, DMSO-d6): δ/ppm = 173.8 (-$\underline{C}$O-), 46.3 (-NH-$\underline{C}$HCH$_3$-), 30.6 (-CO-C$\underline{H_2}$-CH-), 30.4 (CH-C$\underline{H_2}$-CHCH3-), 28.6 (-CCHCH$\underline{C}$H$_3$CH$_3$-), 21.11 (-NH-CH$\underline{C}$H$_3$-), 20.1 (CO-CH$_2$-$\underline{C}$H-), 20.1 (-CHCH$_3$-CH$_2$-$\underline{C}$H-), 17.4 (-$\underline{C}$CHCHCH$_3$CH$_3$-), 14.9 (-CCHCHCH$_3$$\underline{C}H_3$-).

MS (EI, 70 eV): m/z (%) = 168.10 (1.05), 167.15 (8.33), 166.25 (0.70), 154.20 (0.30), 153.20 (4.44), 152.20 (44.99), 151.25 (0.22), 150.20 (0.23), 139.20 (1.42), 138.15 (1.09).

MS (EI, 70 eV): % (m/z) = 100.00 (44.10), 60.39 (67.10), 44.99 (152.20), 44.18 (81.10), 42.43 (82.10), 37.54 (110.15), 35.25 (41.05), 28.11 (57.10), 19.97 (39.05), 19.46 (55.10).

m.P.: 171 °C

3R-caranlactam (**5-3R**)
^{1}H NMR (400 MHz, DMSO-d6): δ/ppm = 6.90 (s, 1H, -CO-N$\underline{H}$-), 3.50 – 3.41 (m, 1H, -NH-C$\underline{H}$CH$_3$-CH$_2$-), 2.37 – 2.29 (m, 2H, -CO-C$\underline{H_2}$-CH-), 1.88 – 1.77 (m, 1H, -CH-C$\underline{H_2}$-CCHCH$_3$-), 1.51 – 1.40 (m, 1H, -CH-C$\underline{H_2}$-CCHCH$_3$-), 1.06 (d, *J* = 6.4 Hz, 3H, -NH-CHC$\underline{H}_3$-), 1.03 (s, 3H, -CC$\underline{\mathrm{H}}$CHCH$_3$C$\underline{H_3}$-), 0.99 (s, 3H, -CCHCHC$\underline{H_3}$CH$_3$-), 0.79 – 0.69 (m, 2H, -CC$\underline{H}$CHCH$_3$CH$_3$-, -CCHC$\underline{H}$CH$_3$CH$_3$-).

^{13}C NMR (100 MHz, DMSO-d6): δ/ppm = 173.1 (-$\underline{C}$O-), 49.6 (-NH-$\underline{C}$HCH$_3$-), 33.0 (-CO-C$\underline{H_2}$-CH-), 29.7 (CH-C$\underline{H_2}$-CHCH3-), 28.2 (-CCHCH$\underline{C}$H$_3$CH$_3$-), 24.0 (-NH-CH$\underline{C}$H$_3$-), 23.4 (CO-CH$_2$-$\underline{C}$H-), 21.5 (-CHCH$_3$-CH$_2$-$\underline{C}$H-, 18.7 -$\underline{C}$CHCHCH$_3$CH$_3$-), 14.8 (-CCHCHCH$_3$$\underline{C}H_3$-).

MS (EI, 70 eV): m/z (%) = 168.10 (1.42), 167.10 (13.20), 166.15 (1.41), 153.15 (3.19), 152.10 (32.36), 139.15 (1.90), 138.15 (1.66), 134.15 (0.71), 127.15 (0.55), 126.15 (5.91).

MS (EI, 70 eV): % (m/z) = 100.00 (44.05), 71.08 (67.05), 59.84 (110.10), 50.77 (81.10), 41.82 (41.05), 41.15 (82.10), 32.36 (152.10), 24.22 (57.10), 22.96 (55.10), 21.80 (99.10).

m.P.: 140 °C

Synthesis of N-benzoyl-3S-caranlactam (Bz5-3S) ***(1R,5S,7S)-4-benzoyl-5,8,8-trimethyl-4-azabicyclo[5.1.0]octan-3-one***. 2-Methyl-THF (30 mL) in a nitrogen atmosphere was cooled in an ice bath and NaH (540 mg 60 % on paraffin wax, 15.5 mmol, 2.60 equiv.) was added. After 10 min 3S-caranlactam (**5-3S**, 1.00 g, 6.0 mmol, 1.00 equiv.) was added portion-wise within 5 min; a rise of temperature was not observed. After stirring for 2 h, BzCl (1.00 mL, 7.80 mmol, 1.30 mmol) was slowly given to the mixture *via* syringe. The mixture was allowed to reach room temperature and was stirred over for 12 h before 20 g ice was added. After extraction with hexane (3x100 mL), the combined organic phases were washed with NaOH (2.0 M, 150 mL), $NaHCO_3$ (saturated solution, equivoluminar) and NaCl (saturated solution, equivoluminar) and dried using Na_2SO_4. The solvent was removed under reduced pressure and the crude product was crystallized from pentane/EtOAc (4:1) at -20 °C to give N-benzoyl-3S-caranlactam (**Bz5-3S**, 930 mg, 3.40 mmol, 57%) as colourless crystals.

^{1}H NMR (400 MHz, DMSO-d6): δ/ppm = 7.66 – 7.61 (m, 2H, *ortho*-C$\underline{H}$-), 7.54 – 7.48 (m, 1H, *para*-C$\underline{H}$-), 7.46 – 7.39 (m, 2H, *meta*-C$\underline{H}$-), 4.22 (pd, *J* = 6.6, 2.6 Hz, 1H, -C$\underline{H}$CH$_3$-), 2.76 (dd, *J* = 13.9, 10.1 Hz, 1H, -CO-C$\underline{H_2}$-CH-), 2.56 (dd, *J* = 13.9, 6.8 Hz, 1H, -CO-C$\underline{H_2}$-CH-), 2.19 – 2.06 (m, 1H, -CHCH$_3$-C$\underline{H_2}$-CH-), 1.94 – 1.83 (m, 1H, -CHCH$_3$-C$\underline{H_2}$-CH-), 1.26 (d, *J* = 6.6 Hz, 3H, -CHC$\underline{H_3}$-), 1.10 (s, 3H, -CCHCHC$\underline{H_3}$CH$_3$-), 1.07 (s, 3H, -CCHCHC$\underline{H_3}$CH$_3$-), 0.94 – 0.83 (m, 2H, -CHCH$_3$-CH$_2$-C$\underline{H}$-, -CO-CH$_2$-C$\underline{H}$-).

^{13}C NMR (100 MHz, DMSO-d6): δ/ppm = 177.3 (-CH$_2$-$\underline{C}$O-NBz-), 174.6 (-N-$\underline{C}$O-Ph), 136.5 (-N-CO-*ipso*-$\underline{C}_{Ph}$), 131.7 (2x *ortho*-$\underline{C}_{Ph}$), 128.3 (2x *meta*-$\underline{C}_{Ph}$), 128.2 (*para*-$\underline{C}_{Ph}$), 51.9 (-$\underline{C}$HCH$_3$-), 34.4 (-CO-$\underline{C}$H$_2$-CH-), 28.3 (-CHCH$_3$-$\underline{C}$H$_2$-CH-), 28.2 (-CCHCH$\underline{C}$H$_3$CH$_3$-), 20.9 (-CO-CH$_2$-$\underline{C}$H-), 20.0 (-CHCH$_3$-CH$_2$-$\underline{C}$H-), 19.9 (-$\underline{C}$CHCHCH$_3$CH$_3$-), 18.8 (-CH$\underline{C}$H$_3$-), 14.7 (-CCHCHCH$_3\underline{C}$H$_3$-).

MS (EI, 70 eV): m/z (%) = 273.20 (0.09), 272.10 (0.86), 271.10 (4.65), 270.10 (2.47), 257.05 (0.15), 256.10 (0.84), 253.10 (0.23), 244.15 (0.12), 243.10 (0.90), 242.10 (0.46).

MS (EI, 70 eV): % (m/z) = 100.00 (105.05), 35.39 (77.05), 14.02 (82.05), 12.28 (148.10), 10.27 (67.10), 9.19 (41.05), 9.01 (81.10), 8.20 (166.10), 7.90 (106.05), 6.34 (70.05).

Synthesis of N-benzoyl-3R-caranlactam (Bz5-3R) ***(1R,5R,7S)-4-benzoyl-5,8,8-trimethyl-4-azabicyclo[5.1.0]octan-3-one***. 2-Methyl-THF (50 mL) was cooled in an ice bath under nitrogen atmosphere and NaH (600 mg 60 % on paraffin wax, 17.2 mmol, 1.90 equiv.) and 3R-caranlactam (**5-3R**, 1.50 g, 9.00 mmol, 1.00 equiv.) was added after 5 min. The reaction mixture was stirred for 2 h before BzCl (1.5 mL, 11.7 mmol, 1.30 equiv.) was dropped to the mixture *via* syringe. The reaction mixture was allowed to reach room temperature and after stirring for 12 h, NaH (350 mg 60% on paraffin wax, 10.0 mmol, 1.10 equiv.) and BzCl (0.5 mL, 3.90 mmol, 0.40 equiv.) were added to complete the conversion within 4 h. The reaction was quenched by addition of water. The mixture was extracted with hexane (3x100 mL) and the combined organic layers were washed with NaOH (2.0 M, 150 mL), NaHCO$_3$ (saturated solution, equivoluminar) and NaCl (saturated solution, equivoluminar) and dried using Na$_2$SO$_4$. After several crystallizations (EtOAc : hexane/ 1 : 4), N-benzoyl-3R-caranlactam (**Bz5-3R**, 530 mg, 1.90 mmol, 17 %) was obtained as colourless crystals.

^{1}H NMR (400 MHz, DMSO-d6): δ/ppm = 7.51 – 7.39 (m, 5H, -*phenyl*-), 4.36 (dp, J = 12.7, 6.3 Hz, 1H, -C*H*CH$_3$-), 2.65 – 2.54 (m, 2H, -CHCH$_3$-C*H$_2$*-CH-), 2.17 (ddd, J = 15.0, 6.4, 5.1 Hz, 1H,-CO-C*H$_2$*-CH-), 1.44 (dt, J = 15.0, 12.1 Hz, 1H,-CO-C*H$_2$*-CH-), 1.26 (d, J = 6.3 Hz, 3H, -CHC*H$_3$*-), 1.18 (ddd, J = 10.7, 8.9, 6.5 Hz, 1H,-CO-CH$_2$-C*H*-), 1.10 (s, 3H, -CCHCHC*H$_3$*CH$_3$-), 1.10 (s, 3H, -CCHCHCH$_3$C*H$_3$*-), 0.95 (ddd, J = 12.1, 8.8, 5.1 Hz, 1H, -CHCH$_3$-CH$_2$-C*H*-).

^{13}C NMR (100 MHz, DMSO-d6): δ/ppm = 180.51 (-CH$_2$-*C*O-NBz-), 173.93 (-N-*C*O-Ph), 136.79 (-N-CO-*ipso*-*C*$_{\mathrm{Ph}}$), 130.68 (2x *ortho*-*C*$_{\mathrm{Ph}}$), 128.33 (2x *meta*-*C*$_{\mathrm{Ph}}$), 127.44 (*para*-*C*$_{\mathrm{Ph}}$), 52.98 (-*C*HCH$_3$-), 34.64 (-CO-*C*H$_2$-CH-), 28.68 (-CHCH$_3$-*C*H$_2$-CH-), 27.82 (-CCHCH*C*H$_3$CH$_3$-), 22.19 (-CH*C*H$_3$-), 21.77 (-CO-CH$_2$-*C*H-), 21.34 (-CHCH$_3$-CH$_2$-*C*H-), 18.86 (-*C*CHCHCH$_3$CH$_3$-), 15.10 (-CCHCHCH$_3$*C*H$_3$-).

MS (EI, 70 eV): m/z (%) = 272.15 (0.53), 271.15 (2.92), 270.15 (3.77), 257.10 (0.56), 256.10 (2.81), 253.10 (0.11), 245.15 (0.10), 244.10 (0.97), 243.15 (4.99), 242.15 (1.28).

MS (EI, 70 eV): % (m/z) = 100.00 (105.10), 34.01 (77.10), 10.07 (82.10), 8.97 (70.10), 8.25 (106.10), 7.47 (67.10), 7.15 (41.10), 6.72 (81.10), 6.55 (148.15), 5.82 (51.05).

Scale-up one-vessel four-step synthesis of 3S-caranlactam (5-3S).

a. **Enzyme catalyzed epoxidation**. (+)-3-carene (**1**, 240 mL, 1.50 mol, 1.00 equiv.) was transferred into the reactor and EtOAc (2.80 L) was added. A pre-washed standard nylon sock (enzyme bag) filled with Novozyme-435 (50 g) was immersed into the mixture and the temperature was set to 60 °C at a stirring rate of 100 rpm min^{-1}. H_2O_2 (30%, 1.65 mol, 1.10 equiv., 12 x 15 mL) was added within 5 h. After the addition was complete, the spent Novozyme-435 was exchanged by new Novozyme-435 (20 g). After another 3 h, the conversion surpassed 98% and the reaction was terminated by removing the enzyme bag. The organic layer was washed with NaOH solution (1.00 M, 2x250 mL), sodium sulphite (saturated solution, 250 mL) and H_2O (1x250 mL). Additional cyclohexane (1.00 L) was added for azeotropic distillation to remove all water residuals (T_{jacket} = 95 °C) until the remaining volume in the reactor was 1.25 L, consisting of crude 3S-caranepoxide (**2-3S**) and cyclohexane.

b. **Epoxidation with diluted AcOOH**. A solution of NaOAc (267 g, 3.25 mol, 1.30 equiv.) and AcOOH (38%, 570 mL 3.25 mol, 1.30 equiv.) in H_2O (1.70 L) was transferred into the reactor and (+)-3-carene (**1**, 341 g ,2.5 mol, 1.00 equiv.) was added portion-wise within 15 min and stirred at room temperature for 2 h. The temperature was set to 30 °C for another 2 h to complete the conversion to 3S-caranepoxide (**2-3S**). During the whole process the stirring speed was set to 300 rpm to guaranty sufficient mixing. After cooling to room temperature, cyclohexane (1.00 L) was added and the aqueous layer was separated *via* the bottom outlet. The organic layer remaining in the reactor was then washed with NaOH solution (1.00 M, 2x500 mL), sodium sulphite (saturated solution, 500 mL) and H_2O (1x500 mL). Additional cyclohexane (2.00 L) was added for azeotropic distillation to remove all water residuals (T_{jacket} = 95 °C) until the remaining volume in the reactor was 2.50 L, consisting of crude 3S-caranepoxide (**2-3S**) and cyclohexane.

c. **Meinwald rearrangement**. For the rearrangement of 3S-caranepoxide (**2-3S**) to 3S-caranketone (**3-3S**), the temperature was set to 60 °C and $Fe(ClO_4)_2 \cdot H_2O$ (1.28 g, 3.6 mmol, 0.002 equiv.) dissolved in EtOAc (5 mL) was dropped into the mixture within 3 min. The mixture was allowed to reach room temperature after two hours (80% conversion) and was stirred for 12 h to complete the reaction. The catalyst was removed by washing with HCl solution (1 M, 2x500 mL), $NaHCO_3$ (saturated solution, 1.00 L) and water (1.00 L) and cyclohexane was distilled off (T_{jacket} 90 °C – 125 °C).

d. **Oximation**. Acetonitrile (2.00 L) and water (1.00 L) were poured into the vessel and $NaOAc \cdot 3H_2O$ (238 g, 1.75 mol, 0.70 equiv.) was added. Then, $HONH_2 \cdot HCl$ (122 g, 1.75 mol, 0.70 equiv.) was added portion-wise within 10 min. After stirring for 2 h at 30 °C, the conversion was complete. The aqueous layer was separated and analysed by GCMS, revealing no significant amounts of 3S-caranoxime (**4-3S**).

e. **Beckmann rearrangement**. NaOH (260 g, 6.5 mol, 2.60 equiv.) dissolved in water (1.00 L) was slowly dropped to the reaction mixture within 2 h and the temperature was kept beneath 20 °C (T_{jacket} = 15 °C) during the process. After stirring for 1 h, TsCl (333 g, 1.75 mol, 0.70 equiv.) was added in aliquots (28 x 12 g) within 3 h while the temperature was kept beneath 25 °C. GCMS analysis showed that all 3S-caranoxime (**4-3S**) was consumed and NaCl (saturated solution, 200 mL) was added to support phase separation. The aqueous layer was removed and extracted with EtOAc (3 x 600 mL). The combined EtOAc extracts were poured back into the reaction vessel. After washing with $NaHCO_3$ (saturated solution, 500 mL) and NaCl (half-saturated solution, 500 mL) the solvent was removed until the remaining volume was approximately 1.5 L. The solution was cooled down to 15 °C and stirred for 12 h. The crystals were filtered off, washed with water and recrystallized from EtOAc. The mother liquor was cooled to -20 °C in the freezer for 12 h and the formed crystals were filtered off and washed with water. The crystal fractions were combined and recrystallized from EtOAc to give pure 3S-caranlactam (**5-3S**, 101 g, 30 w%, 24 mol%) as colourless crystals (Supplementary Figure 4).

NMR analysis of the polyamides

Poly-3S-caranamide (**poly5-3S**)

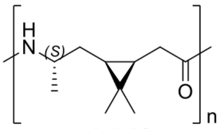

poly5-3S

^{1}H NMR (400 MHz, DCOOD): δ/ppm = 4.19 – 4.04 (1H, -NH-C*H*CH$_3$-CH$_2$-, repeating unit), 2.57 – 2.35 (2H, -HN-CO-C*H*$_2$-CH-, repeating unit), 1.66 – 1.53 (2H, -NH-CHCH$_3$-C*H*$_2$-CH-, repeating unit), 1.36 – 1.20 (3H, -NH-CHC*H*$_3$-CH$_2$-, repeating unit), 1.18 – 1.08 (3H, -CO-CH$_2$-CH-CCHCH$_3$C*H*$_3$-, methyl group facing carboxylic group, repeating unit), 1.05 – 1.00 (3H, -NH-CHCH$_3$-CH-CCHC*H*$_3$CH$_3$-, methyl group turned away from carboxylic group, repeating unit), 0.98 – 0.90 (1H, -CO-CH$_2$-C*H*-, repeating unit), 0.79 – 0.67 (1H, -NH-CHCH$_3$-CH$_2$-C*H*-, repeating unit).

^{13}C NMR (100 MHz, DCOOD): δ/ppm = 176.5 (-*C*O-), 47.3 (-NH-*C*HCH$_3$-), 31.5 (-CO-*C*H$_2$-), 30.9 (-CHCH$_3$-*C*H$_2$-), 28.2 (-CCHCH$_3$*C*H$_3$-, methyl group facing carboxylic group), 23.4 (-CO-CH$_2$-*C*H-), 21.8 (-CHCH$_3$-CH$_2$-*C*H-, 19.6 (-CH*C*H$_3$-), 17.9 (-*C*CHCHCH$_3$CH$_3$-), 14.7 (-CCH*C*H$_3$CH$_3$-, methyl group facing turned away from carboxylic group).

Poly-3R-caranamide (**poly5-3R**)

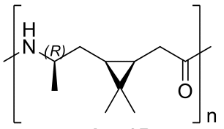

poly5-3R

^{1}H NMR (400 MHz, DCOOD): δ/ppm = 4.13 – 3.99 (1H, -NH-C*H*CH$_3$-CH$_2$-, repeating unit), 2.55 – 2.35 (2H, -HN-CO-C*H*$_2$-CH-, repeating unit), 1.77 – 1.60 (1H, -NH-CHCH$_3$-C*H*$_2$-CH-, repeating unit), 1.54 – 1.39 (1H, -NH-CHCH$_3$-C*H*$_2$-CH-, repeating unit), 1.32 – 1.22 (3H, -NH-CHC*H*$_3$-CH$_2$-, repeating unit), 1.18 – 1.07 (3H, -CO-CH$_2$-CH-CCHCH$_3$C*H*$_3$-, methyl group facing carboxylic group, repeating unit), 1.06 – 1.00 (3H, -NH-CHCH$_3$-CH-CCHC*H*$_3$CH$_3$-, methyl group turned away from carboxylic group, repeating unit), 0.99 – 0.88 (1H, -CO-CH$_2$-C*H*-, repeating unit), 0.76 – 0.64 (1H, -NH-CHCH$_3$-CH$_2$-C*H*-, repeating unit).

^{13}C NMR (100 MHz, DCOOD): δ/ppm = 176.6 (-*C*O-), 47.5 (-NH-*C*HCH$_3$-), 31.3 (-CO-*C*H$_2$-), 30.7 (-CHCH$_3$-*C*H$_2$-), 28.2 (-CCHCH$_3$*C*H$_3$-, methyl group facing carboxylic group), 23.3 (-CO-CH$_2$-*C*H-), 21.9 (-CHCH$_3$-CH$_2$-*C*H-), 19.3 (-CH*C*H$_3$-), 17.9 (-*C*CHCHCH$_3$CH$_3$-), 14.5 (-CCH*C*H$_3$CH$_3$-, methyl group facing turned away from carboxylic group).

3S-caranlactam-3R-caranlactam-copolyamide (**copoly(5-3S·5-3R)**)

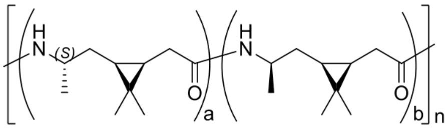

copoly(5-3S·5-3R)

^{1}H NMR (400 MHz, DCOOD): δ/ppm = 4.18 – 3.99 (1H, $-NH-C\underline{H}CH_3-CH_2-$), 2.58 – 2.36 (2H, $-HN-CO-C\underline{H_2}-CH-$), 1.77 – 1.64 (0.7 $H_{R\text{-isomer}}$, $-NH-CHCH_3-C\underline{H_2}-CH-$), 1.63 – 1.53 (0.6 $H_{S\text{-isomer}}$, $-NH-CHCH_3-C\underline{H_2}-CH-$), 1.52 – 1.41 (0.7 $H_{R\text{-isomer}}$, $-NH-CHCH_3-C\underline{H_2}-CH-$), 1.33 – 1.23 (3H, $-NH-CHC\underline{H_3}-CH_2-$), 1.17 – 1.07 (3H, $-CO-CH_2-CH-CCHCH_3C\underline{H_3}-$), 1.06 – 1.00 (3H, $-NH-CHCH_3-CH-CCHC\underline{H_3}CH_3-$), 0.99 – 0.89 (1H, $-CO-CH_2-C\underline{H}-$), 0.80 – 0.65 (1H, $-NH-CHCH_3-CH_2-C\underline{H}-$).

^{13}C NMR (100 MHz, DCOOD): δ/ppm = 176.6 ($-\underline{C}O-$), 47.5 ($-NH-\underline{C_R}HCH_3-$), 47.3 ($-NH-\underline{C_S}HCH_3-$) 31.4 ($-\underline{C_{R,S}}O-\underline{C}H_2-$), 30.8 ($-CHCH_3-\underline{C_{R,S}}H_2-$), 28.3 ($-CCHCH_3\underline{C_{R,S}}H_3-$), 23.4 ($-CO-CH_2-\underline{C_{R,S}}H-$), 22.0 ($-CHCH_3-CH_2-\underline{C_R}H-$), 21.8 ($-CHCH_3-CH_2-\underline{C_S}H-$), 19.6 ($-CH\underline{C_S}H_3-$), 19.4 ($-CH\underline{C_R}H_3-$), 17.9 ($-\underline{C_{R,S}}CHCHCH_3CH_3-$), 14.8 ($-CCH\underline{C_S}H_3CH_3-$), 14.6 ($-CCH\underline{C_R}H_3CH_3-$).

3S-caranlactam-caprolactam-copolyamide (**copoly(5-3S·CL)**)

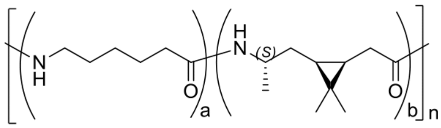

copoly(5-3S·CL)

In the ^{13}C-spectra, additional ^{13}C-signals were observed in close proximity to the expected signals. These signals can be interpreted as sign for a random built-in of small blocks of each monomer. The major ^{13}C-signal refers to the in-block carbons (+**5-3S**+**5-3S**+**5-3S**-; +**CL**+**CL**+**CL**+), whereas the minor signals are from the block-change units (+**CL**+**5-3S**+). A similar effect was not observed in the ^{1}H-spectra, probably due to the broad signals.

^{1}H NMR (400 MHz, DCOOD): δ/ppm = 4.17 – 4.01 ($-NH-C\underline{H}CH_3-CH_2-$), 3.46 – 3.26 ($-C\underline{H_2}-NH-$), 2.56 – 2.35 ($-HN-CO-C\underline{H_2}-CH-$; $-CO-C\underline{H_2}-CH_2-$), 1.85 – 1.51 ($-NH-CHCH_3-C\underline{H_2}-CH-$, $NH-CH_2-C\underline{H_2}-$, $-CO-CH_2-C\underline{H_2}-$), 1.50 – 1.34 ($CH_2-C\underline{H_2}-CH_2-$, 1.32 – 1.18 ($-NH-CHC\underline{H_3}-CH_2-$), 1.16 – 1.06 ($-CO-CH_2-CH-CCHCH_3C\underline{H_3}-$), 1.05 – 0.98 ($-NH-CHCH_3-CH-CCHC\underline{H_3}CH_3-$), 0.96 – 0.86 ($-CO-CH_2-C\underline{H}-$), 0.80 – 0.65 ($-NH-CHCH_3-CH_2-C\underline{H}-$).

^{13}C NMR (100 MHz, DCOOD): δ/ppm =

176.7 ($-\underline{C}O-$), 47.3 ($-NH-\underline{C}HCH_3-$), 31.3 ($-CO-\underline{C}H_2-$), 30.8 ($-CHCH_3-\underline{C}H_2-$), 28.3 ($-CCHCH_3\underline{C}H_3-$, methyl group facing carboxylic group), 23.3 ($-CO-CH_2-\underline{C}H-$), 21.5 ($-CHCH_3-CH_2-\underline{C}H-$, 19.5 ($-CH\underline{C}H_3-$), 17.9 ($-\underline{C}CHCHCH_3CH_3-$), 14.6 ($-CCH\underline{C}H_3CH_3-$, methyl group facing turned away from carboxylic group). (from **5-3S**, major ^{13}C signals).

177.6 (-*C*O-), 40.3 (-NH-*C*H$_2$-), 35.6 (-CO-*C*H$_2$-CH$_2$-), 28.1 (-NH-CH$_2$-*C*H$_2$-), 26.0 (-CO-CH$_2$-*C*H$_2$-), 25.4 (-CH$_2$-*C*H$_2$-CH$_2$-). (from **CL**, major signals).

3S-caranlactam (**5-3S**)-laurolactam-copolyamide (**copoly(5-3S·LL)**)

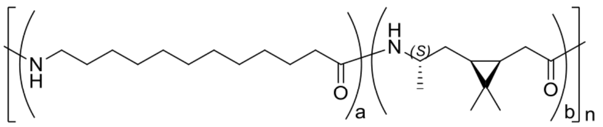

copoly(5-3S·LL)

In the ^{13}C-spectra, additional ^{13}C-signals were observed in close proximity to the expected signals. These signals can be interpreted as sign for a random built-in of small blocks of each monomer. The major ^{13}C-signal refers to the in-block carbons (+**5-3S**+**5-3S**+**5-3S**-; +**LL**+**LL**+**LL**+), whereas the minor signals are from the block-change units (+**LL**+**5-3S**+). A similar effect was not observed in the ^{1}H-spectra, probably due to the broad signals.

^{1}H NMR (400 MHz, DCOOD): δ/ppm = 4.18 – 4.03 (-NH-C*H*CH$_3$-CH$_2$-), 3.47 – 3.31 (-C*H$_2$*-NH-), 2.58 – 2.38 (-HN-CO-C*H$_2$*-CH-; -CO-C*H$_2$*-CH$_2$), 1.82 – 1.21 (-NH-CHCH$_3$-C*H$_2$*-CH-; -NH-CHC*H$_3$*-CH$_2$-; -C*H$_2$*-C*H$_2$*-), 1.19 – 1.10 (-CO-CH$_2$-CH-CCHCH$_3$C*H$_3$*-), 1.09 – 1.00 (-NH-CHCH$_3$-CH-CCHC*H$_3$*CH$_3$-), 0.99 – 0.87 (-CO-CH$_2$-C*H*-), 0.83 – 0.66 (-NH-CHCH$_3$-CH$_2$-C*H*-).

^{13}C NMR (100 MHz, DCOOD): δ/ppm =

177.1 (-*C*O-), 47.4 (-NH-*C*HCH$_3$-), 31.3 (-CO-*C*H$_2$-), 30.8 (-CHCH$_3$-*C*H$_2$-), 28.2 (-CCHCH$_3$*C*H$_3$-, methyl group facing carboxylic group), 23.3 (-CO-CH$_2$-*C*H-), 21.6 (-CHCH$_3$-CH$_2$-*C*H-, 19.5 (-CH*C*H$_3$-), 17.9 (-*C*CHCHCH$_3$CH$_3$-), 14.6 (-CCH*C*H$_3$CH$_3$-, methyl group facing turned away from carboxylic group). (from **5-3S**, major ^{13}C signals).

178.0 (-*C*O-), 40.7 (-NH-*C*H$_2$-), 35.5 (-CO-*C*H$_2$-CH$_2$-), 29.3 (2xC -*C*H$_2$-), 29.0 (-*C*H$_2$-), 28.8 (-*C*H$_2$-), 28.8 (-*C*H$_2$-), 28.5 (-*C*H$_2$-), 26.6 (-*C*H$_2$-), 25.9 (-*C*H$_2$-). (from **LL**, major signals).

4. Supplementary Notes

Supplementary Note 1. Single-crystal X-ray diffraction. For **5-3S** (CCDC 1938732), the integration of the data using a monoclinic unit cell yielded a total of 6057 reflections to a maximum Θ angle of 26.41° (0.80 Å resolution), of which 1959 were independent (average redundancy 3.092, completeness = 99.9 %, R_{int} = 2.65%, R_{sig} = 2.75%) and 1840 (93.93 %) were greater than $2\sigma(F^2)$. The final cell constants, Supplementary Table Supplementary **Table 1**8, are based upon the refinement of the XYZ-centroids of 4510 reflections above 20 σ(I) with 6.609° < 2Θ < 52.68°. The ratio of minimum to maximum apparent transmission was 0.862. The calculated minimum and maximum transmission coefficients (based on crystal size) are 0.9810 and 0.9960. The final anisotropic full-matrix least-squares refinement on F^2 with 117 variables converged at R1 = 3.00%, for the observed data and wR2 = 7.52% for all data. The goodness-of-fit was 1.081. The largest peak in the final difference electron density synthesis was 0.177 e$^-$/Å^3 and the largest hole was -0.157 e$^-$/Å^3 with an RMS deviation of 0.034 e$^-$/Å^3.

On the basis of the final model, the calculated density was 1.147 g/cm^3, and F(000) 368 e$^-$. For **5-3R** (CCDC 1938733 redetermination of CCDC 145220), the integration of the data using a monoclinic unit cell yielded a total of 25457 reflections to a maximum Θ angle of 28.31° (0.75 Å resolution), of which 4685 were independent (average redundancy 5.434, completeness = 99.7 %, R_{int}=2.96 %, R_{sig}=2.09 %) and 4541 (96.93 %) were greater than $2\sigma(F^2)$. The final cell constants, Supplementary Table Supplementary **Table 1**, are based upon the refinement of the XYZ-centroids of 9509 reflections above 2Θ σ(I) with 4.693° < 2Θ < 56.60°. The ratio of minimum to maximum apparent transmission was 0.922. The calculated minimum and maximum transmission coefficients (based on crystal size) are 0.6874 and 0.7457. The final anisotropic full-matrix least-squares refinement on F° with 232 variables converged at R1 = 2.89 %, for the observed data and wR2 = 7.74 % for all data. The goodness-of-fit was 1.081. The largest peak in the final difference electron density synthesis was 0.280 e$^-$/Å^3 and the largest hole was -0.155 e$^-$/Å^3 with an RMS deviation of 0.035 e$^-$/Å^3. On the basis of the final model, the calculated density was 1.171 g/cm^3, and F(000) 368 e$^-$.

Directional views of their structures were prepared as PLUTON periodic graphs, Supplementary Figures 32, 33 and 34.[8] The diffraction patterns obtained from **5-3S** and **5-3R** (from PXRD) showed narrow isolated Bragg reflexes without amorphous background, Supplementary Figures 31 (a) and (b).

Supplementary Note 2. Powder X-ray diffraction of poly5-3S. The diffraction patterns recorded from **poly5-3S** were characteristic of a semi-crystalline polymer, Supplementary Figure 31 (c). By scaling the amorphous reference patterns to match them at 2Θ values outside the range of Bragg peaks, we obtained *fc* = 0.43 from the ratios of the integrated intensities. Patterns from **poly5-3R** showed no distinct reflexes, save from residual monomer, Supplementary Figure 31 (d). Finding the structure of **poly5-3S** was impeded by the small number of distinct Bragg peaks. But, out of an initial selection of

13 tested unit cells and space groups, one met all three requirements for further assessment laid out in *Experimental*. The space group was Cambridge Structural Database entry 58438, Supplementary Table 17. The 50 SA runs performed on this structure then yielded a clear outcome: Three results presented distinctly lowest FOM. Of these, the one with the lowest CF simultaneously showed the most plausible atomic arrangement with regard to bonding angles, and the N-H···O bond arrangement. Directional views of its structure were prepared as periodic graphs, and as Oak Ridge thermal ellipsoid plots, Supplementary Figures 35,36, Figure 10.[8;9]

5. Supplementary References

[1] G. M. Sheldrick, “SHELXT – Integrated space-group and crystal-structure determination,” Acta Crystallographica Section A: Foundations and Advances, vol. 71, no. 1, pp. 3–8, 2015.

[2] G. M. Sheldrick, “Crystal structure refinement with SHELXL,” Acta Crystallographica Section C: Structural Chemistry, vol. 71, no. 1, pp. 3–8, 2015.

[3] C. B. Hübschle, G. M. Sheldrick, and B. Dittrich, “ShelXle: A Qt graphical user interface for shelxl,” Journal of Applied Crystallography, vol. 44, no. 6, pp. 1281–1284, 2011.

[4] A. Wilson, “International Tables for Crystallography, Vol. C, Tables 6.1. 1.4 (pp. 500–502), 4.2. 6.8 (pp. 219–222), and 4.2. 4.2 (pp. 193–199),” Kluwer Academic Publishers, Dordrecht, 1992.

[5] A. Altomare, N. Corriero, C. Cuocci, A. Falcicchio, A. Moliterni, and R. Rizzi, “Expo software for solving crystal structures by powder diffraction data: Methods and application,” Crystal Research and Technology, vol. 50, no. 9-10, pp. 737–742, 2015.

[6] A. Altomare, G. Campi, C. Cuocci, L. Eriksson, C. Giacovazzo, A. Moliterni, R. Rizzi, and P.-E. Werner, “Advances in powder diffraction pattern indexing: N- TREOR09,” *Journal of Applied Crystallography*, vol. 42, no. 5, pp. 768–775, 2009.

[7] J. Stewart, “MOPAC2016,” tech. rep., Stewart Computational Chemistry: Colorado Springs, Colorado, 2016.

[8] A. L. Spek, “PLATON SQUEEZE: A tool for the calculation of the disordered solvent contribution to the calculated structure factors,” Acta Crystallographica Section C: Structural Chemistry, vol. 71, no. 1, pp. 9–18, 2015.

[9] M. N. Burnett and C. K. Johnson, “ORTEP-III: Oak Ridge thermal ellipsoid plot program for crystal structure illustrations,” tech. rep., Oak Ridge National Laboratory report ORNL-6895, Tennessee, 1996.

[10] W. Astbury, “The hydrogen bond. The hydrogen bond in protein structure,” Transactions of the Faraday Society, vol. 36, pp. 871–880, 1940.

[11] W. L. Bragg, J. C. Kendrew, and M. F. Perutz, “Polypeptide chain configurations in crystalline proteins,” Proceedings of the Royal Society of London. Series A. Mathematical and Physical Sciences, vol. 203, no. 1074, pp. 321–357, 1950

[12] P. N. Stockmann, D. L. Pastoetter, M. Woelbing, C. Falcke, M. Winnacker, H. Strittmatter, V. Sieber, *Macromolecular rapid communications* **2019**, *40*, e1800903.

4.4 Methods section 2.5 “Limonene, α-pinene, and (+)-3-carene as precursor for diol monomers”

Synthesis of *6-oxo-3-(prop-1-en-2-yl)heptanal* (**8**)

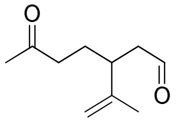

8

4-isopropyl-1-methyl-7-oxabicyclo[4.1.0]heptane (**5**, 6.4 g, 42 mmol) was added to a solution of MeCN (100 mL), H_2O (100 mL), and $NaIO_4$ (9.0 g, 42 mmol) at 25 °C. HCl (2 mmol) was added and the reaction was monitored by GCMS. After 90 min, the reaction mixture consisted of 1% **5**, 90% **8** and 9% of the opened epoxide **hydroxy-5**. The reaction was complete after another 90 min. The precipitate was isolated by filtration and dried under reduced pressure to give $NaIO_3$ (6.4 g, 32 mmol, 77%). EtOAc (100 mL) and a solution of saturated NaCl (100 mL) were added to the filtrate and the layers were separated. The aqueous layer was extracted with EtOAc (3 x 50 mL) and the combined organic phases were washed with a saturated solution of NaH_2CO_3 and brine. After drying over Na_2SO_4, the organic solvent was removed under reduce pressure. The crude oil was purified by fractional distillation (2.5 mBar, 90 °C) to give 6-oxo-3-(prop-1-en-2-yl)heptanal (**8**, 8.8 g, 28.6 mmol, 68%) as a clear, colorless oil.

^{1}H NMR (400 MHz, $CDCl_3$): δ/ppm = 9.67 (t, *J* = 2.2 Hz, 1H, -C*H*O), 4.84 – 4.82 (m, 1H, -CCH_3-CH*H*), 4.77 (s, 1H, CCH_3-C*H*H), 2.71 – 2.63 (m, 1H, -CH_2-C(*iso*-propenyl)*H*-CH_2-), 2.51 – 2.42 (m, 2H,-CH_2-CHO), 2.38 (t, *J* = 7.4 Hz, 2H, -CH_2-CO-CH_3), 2.12 (s, 3H, CH_3-CO-), 1.76 – 1.66 (m, 2H, -CO-CH_2-CH_2-), 1.63 (s, 3H, -CCH_2CH_3).

^{13}C NMR (101 MHz, $CDCl_3$): δ/ppm = 208.4 (-CO-), 201.9 (-C*H*O), 145.2 (-$CCHCH_2CH_3$), 113.4 (-$CCHCH_2CH_3$), 47.6 (-CH_2-CHO), 41.1 (-CH_2-CH_2-CO-), 40.9 (-CH_2-C(*iso*-propyl)H-CH_2-), 30.2 (CH_3-CO-), 26.6 (-CH_2-C(*iso*-propenyl)H-CH_2-), 18.5 (-$CCHCH_2CH_3$)

MS (EI, 70 eV): m/z (%) = 151 (0.24), 150 (2.0), 140 (0.11), 125 (2.4), 107 (32), 97 (5.1), 82 (14), 67 (22), 55 (19), 43 (100), 41 (27).

Synthesis of *4-isopropyl-1-methyl-7-oxabicyclo[4.1.0]heptane* (**9**)

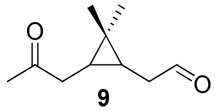

9

(1S,7R)-3,8,8-trimethyl-4-oxatricyclo[5.1.0.03,5]octane (**7**, 15.22 g, 100 mmol) was added to a solution of MeCN (200 mL), H_2O (200 mL), and $NaIO_4$ (21.4 g, 100 mmol), and HCl (2 mmol) at 25 °C. The conversion was complete after 4 h and the colorless precipitate ($NaIO_3$) was separated by filtration. EtOAc (200 mL) and a saturated solution of NaCl (200 mL) were added and the layers were separated. The aqueous layer was extracted with EtOAc (3 x 100 mL) and the combined organic phases were washed with a saturated solution of NaH_2CO_3 and a saturated solution of NaCl (200 mL). Purification by distillation (2.0 mBar, 85 °C) gave 6-oxo-3-(prop-1-en-2-yl)heptanal (**9**, 9.2 g, 54.7 mmol, 55%) as colorless oil

^{1}H NMR (400 MHz, d6-DMSO): δ/ppm = 9.63 (t, *J* = 1.6 Hz, 1H, $\text{-CH}_2\text{-C}\underline{H}\text{O}$), 2.37 – 2.31 (m, 4H, $\text{-C}\underline{H_2}\text{-CO-CH}_3$, $\text{-C}\underline{H_2}\text{-CHO}$), 2.04 (s, 3H, $\text{C}\underline{H_3}\text{-CO-}$), 1.03 (s, 3H, $\text{-CHCHCC}\underline{H_3}\text{CH}_3$), 0.83 – 0.75 (m, 5H, $\text{-CHCHCCH}_3\text{C}\underline{H_3}$, $\text{-CO-CH}_2\text{-C}\underline{H}\text{-}$, $\text{-C}\underline{H}\text{-CH}_2\text{-CHO}$).

^{13}C NMR (101 MHz, d6-DMSO): δ/ppm = 208.1 ($\text{CH}_3\text{-}\underline{C}\text{O-}$), 203.0 ($\text{-CH}_2\text{-}\underline{C}\text{HO}$), 39.0 ($\text{-}\underline{C}\text{H}_2\text{-CO-}$), 38.6 ($\text{-}\underline{C}\text{H}_2\text{-CHO}$), 29.5 ($\underline{C}\text{H}_3\text{-CO-}$), 28.4 ($\text{-CH}\underline{C}\text{H}_3\text{CH}_3$), 20.8 ($\text{-}\underline{C}\text{H-CH}_2\text{-CO-}$), 19.1 ($\text{-}\underline{C}\text{H-CH}_2\text{-CHO}$), 16.5 ($\text{-CHCH}\underline{C}\text{CH}_3\text{CH}_3$), 15.1. ($\text{-CH}\underline{C}\text{H}_3\text{CH}_3$)

MS (EI, 70 eV): m/z (%) = 168.15 (0.06), 153 (0.6), 139 (7.5), 125 (6.6), 111 (16), 93 (10.0), 81 (12), 67 (12), 55 (31), 43 (100).

Synthesis of *4-isopropyl-1-methyl-7-oxabicyclo[4.1.0]heptane* (**dihydro-5**)

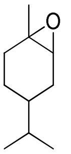

dihydro-5

1-methyl-4-(prop-1-en-2-yl)-7-oxabicyclo[4.1.0]heptane (**5**, 1.9 g, 9.2 mmol) was dissolved in EtOH (20 mL) and PtO_2 (0.09 mmol) was added. A hydrogen atmosphere was realized with a balloon. After stirring overnight, full conversion was observed by GCMS. The catalyst was separated by filtration and the solvent was removed under reduced pressure. 4-isopropyl-1-methyl-7-oxabicyclo[4.1.0]heptane (**dihydro-5**, 1.2 g, 7.8 mmol, 85%) was obtained as slightly yellow oil and used without further purification after the structure was confirmed by GCMS.

MS (EI, 70 eV): m/z (%) = 154 (1.2), 139 (15), 125 (12), 111 (49), 95 (11), 83 (18), 69 (40), 55 (30), 43 (100).

Synthesis of *3-isopropyl-6-oxoheptanal* (**dihydro-8**)

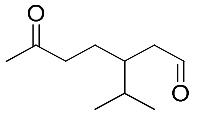

dihydro-8

4-isopropyl-1-methyl-7-oxabicyclo[4.1.0]heptane (**dihydro-5**, 1.0 g, 6.5 mmol) was dissolved in MeCN (15 mL), H_2O (15 mL), and $NaIO_4$ (1.4 g, 6.5 mmol) before HCl (0.2 mmol, 2 M HCl) was added. After 2.5 h, GCMS analysis verified full conversion. EtOAc (50 mL) and a saturated solution of NaH_2CO_3 (50 mL) were added, the layers separated, and the aqueous phase was extracted with EtOAc (3 x 50 mL). The combined organic layers were washed with a saturated solution of NaH_2CO_3 and brine. After drying over $NaSO_4$ and removing of the solvent under reduced pressure, 3-isopropyl-6-oxoheptanal (**dihydro-8**, 1.0 g, 5.8 mmol, 90%) was obtained as slightly yellow oil and used without further purification.

MS (EI, 70 eV): m/z (%) = 170 (0.27), 152 (0.86), 126 (6.8), 112 (10), 109 (17.6), 95 (7.3), 71 (19), 58 (26), 43 (100), 41 (20).

Synthesis of *3-(prop-1-en-2-yl)heptane-1,6-diol* (**11**)

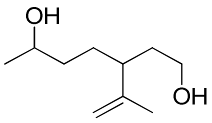

11

6-oxo-3-(prop-1-en-2-yl)heptanal (**8**, 5.0 g, 29.7 mmol) was dissolved in MeOH (60 mL) and cooled in an ice bath. $NaBH_4$ (1.13 g, 30 mmol) was added portion-wise within 30 min and the temperature was kept beneath 8 °C. After the addition was completed, GCMS verified that all substrate was consumed. After 30 min of additional stirring, NH_4Br (6.0 g, 61 mmol) dissolved in H_2O (50 mL) were carefully added. The mixture was stirred for 30 min before EtOAc (60 mL) and brine (50 mL) were added. The layers were separated, and the aqueous layer was extracted with EtOAc (3 x 60 mL). The combined organic phases were washed with a saturated solution of NaH_2CO_3 and brine. The organic solvent was removed under reduced pressure after drying under Na_2SO_4, and crude product was obtained (3.50 g). The purification was performed by column chromatography (EtOAc : hexanes = 1 : 1, 160 g silica, column diameter 3.5 cm) and pure 3-(prop-1-en-2-yl)heptane-1,6-diol (**11**, 3.30 g, 19.1 mmol, 64%) was obtained as a colorless oil.

Bp.: 280 °C (DSC).

^{1}H NMR (400 MHz, d6-DMSO): δ/ppm = 4.78 – 4.74 (m, 1H, CCH_3-CH*H*), 4.74 – 4.70 (m, 1H, CCH_3-C*H*H), 3.81 – 3.69 (m, 1H, CH_3-C*H*OH-), 3.64 – 3.51 (m, 2H,-CH_2-CHO), 2.26 –

2.12 (m, 1H, -CH_2-C(*iso*-propenyl)$\underline{H}$-CH_2-),), 1.63 – 1.55 (m, 5H, $C\underline{H}_3$-CHOH-, -CH_2-$C\underline{H}_2$OH), 1.51 – 1.27 (m, 4H, -$C\underline{H}_2$-CH_2-CHOH-, -CH_2-$C\underline{H}_2$-CHOH-), 1.16 (s, 1.5H, diastereo:$CCHCH_2C\underline{H}_3$), 1.15 (s, 1.5H, diastereo: $CCHCH_2C\underline{H}_3$).

^{13}C NMR (101 MHz, d6-DMSO): δ/ppm = 147.38, 147.33 (diastereo: -$\underline{C}CHCH_2CH_3$), 112.37, 112.34 (diastereo: -$CCH\underline{C}H_2CH_3$); 68.38, 67.86 (diastereo: CH_3-$\underline{C}$HOH-) 61.39, 61.35 (diastereo: -CH_2-$\underline{C}H_2OH$) 44.45, 43.99 (diastereo: -CH_2-$\underline{C}$(*iso*-propyl)H-CH_2-) 37.19, 36.85 (diastereo: -CH_2-$\underline{C}H_2$-CHOH-), 36.29, 36.27 (diastereo: -$\underline{C}H_2$-CH_2OH), 29.59, 29.12 (diastereo: -$\underline{C}H_2$-CH_2-CHOH-), 23.72, 23.59 (diastereo: $\underline{C}H_3$-CHOH-), 17.84, 17.80 (diastereo: -$CCHCH_2\underline{C}H_3$).

MS (EI, 70 eV): m/z (%) = 157 (1.7), 154 (0.7), 139 (6.0), 136 (3.6), 111 (31), 95 (87), 81 (70), 69 (99), 55 (87), 41 (100).

Synthesis of *1-(3-(2-hydroxyethyl)-2,2-dimethylcyclopropyl)propan-2-ol* (**12**)

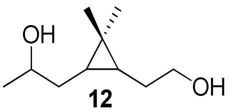

12

(1S,7R)-3,8,8-trimethyl-4-oxatricyclo[5.1.0.03,5]octane (**7**, 11.1 g, 73.0 mmol) was dissolved in MeCN (150 mL)and H_2O (150 mL) and $NaIO_4$ (15.6 g, 73.0 mmol) was added. The reaction mixture was stirred overnight. GCMS confirmed that the conversion was complete. $NaIO_3$ was filtered of, and EtOAc (200 mL) and H_2O (200 mL) were added. The layers were separated, and the aqueous phase was extracted with EtOAc (3 x 150 mL). The combined organic phases were washed with a saturated solution of NaH_2CO_3 and brine. After drying with Na_2SO_4, the solvent was removed under reduced pressure and crude 1-(3-(2-hydroxyethyl)-2,2-dimethylcyclopropyl)propan-2-ol (**12**, 10.4 g, 84%) were obtained as a yellow oil. The structure was determined by NMR and GCMS.

^{1}H NMR (400 MHz, d6-DMSO): δ/ppm = 4.41 – 4.25 (m, 2H, -$C\underline{H}$H-OH, -$C\underline{H}$H-CHOH-), 3.61 – 3.49 (m, 1H, CH_3-$C\underline{H}$OH-), 3.39 – 3.30 (m, 2H, $CH\underline{H}$-OH, -$CH\underline{H}$-CHOH), 1.37 – 1.22 (m, 2H, -CH-$C\underline{H}_2$-CH_2-OH), 1.04 – 0.98 (m, 3H, $C\underline{H}_3$-CHOH-), 0.97 – 0.93 (m, 3H, -$CHCHCC\underline{H}_3CH_3$), 0.81 (m, 3H, -$CHCHCCH_3C\underline{H}_3$), 0.52 – 0.31 (m, 2H, -CO-CH_2-$C\underline{H}$-, -$C\underline{H}$-CH_2-CH_2OH).

MS (EI, 70 eV): m/z (%) = 154 (0.38), 139 (2.4), 130 (14), 128 (25), 124 (1.4), 115 (36), 95 (82), 81 (51), 67 (91), 55 (100), 41 (70).

Synthesis of *3-isopropylheptane-1,6-diol* (**dihydro-10**)

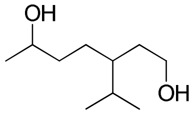

dihydro-10

3-isopropyl-6-oxoheptanal (**dihydro-8**, 6.0 g, 35.8 mmol) was dissolved in MeOH (100 mL) and cooled in an ice bath before $NaBH_4$ (1.02 g, 26.9 mmol) was portion-wisely given to the mixture. The conversion was 90% as confirmed by GCMS and another portion of $NaBH_4$ (110 mg, 0.5 mmol) was added. After stirring for another hour, acetone (40 mL) was carefully given to the mixture. The mixture could reach room temperature, and a saturated solution of NaH_2CO_3 (100 mL) and EtOAc (100 mL) were added. The layers were separated, the aqueous phase was extracted with EtOAc (3 x 100 mL) and the combined organic phases were washed with brine. The mixture was dried with Na_2SO_4 and the solvent was removed under reduced pressure to give crude product (5.7 g). 4.0 g of the crude oil were purified by column chromatography (EtOAc : hexanes gradient 6 : 1 to 2 : 1 , 160 g silica, column diameter 3.5 cm) and 3-isopropylheptane-1,6-diol (**dihydro-10**, 2.7 g, 15.5 mmol, 62%) was obtained as colorless oil.
^{1}H NMR (400 MHz, d6-DMSO): δ/ppm = 3.82 – 3.72 (m, 1H, CH_3-C$\underline{H}$OH-), 3.71 – 3.60 (m, 2H, -CH_2-C$\underline{H_2}$-OH), 1.72 – 1.65 (m, 1H,-CHC$\underline{H}$$CH_3CH_3$), 1.64 – 1.54 (m, 1H,-C$\underline{H}CHCH_3CH_3$), 1.48 – 1.22 (m, 6H, -CHOH-C$\underline{H_2}$-CH_2-, -CHOH-CH_2-C$\underline{H_2}$-, -C$\underline{H_2}$-CH_2OH), 1.19 (d, J = 6.3 Hz, 3H, C$\underline{H_3}$-CHOH-), 0.89 – 0.82 (m, 6H, -CHCHC$\underline{H_3}$CH_3).
^{13}C NMR (101 MHz, d6-DMSO): δ/ppm = 68.73, 68.42 (diastereo: CH_3-$\underline{C}$HOH-), 61.94, 61.90 (diastereo: -CH_2-$\underline{C}H_2$OH), 40.51, 40.14 (diastereo: -CH_2-$\underline{C}$(*iso*-propyl)H-CH_2-, 37.40, 37.11 (diastereo: -CH_2-$\underline{C}H_2$-CHOH-, 33.74, 33.58 (diastereo: -$\underline{C}H_2$-CH_2OH), 29.63, 29.59 (diastereo: -$\underline{C}H_2$-CH_2-CHOH-), 26.93, 26.75 (diastereo: -CH$\underline{C}$HCH_3CH_3), 23.74 ($\underline{C}H_3$-CHOH-), 19.55, 19.45 (diastereo: -CHCH$\underline{C}H_3CH_3$, 18.88, 18.81 (diastereo:-CHCH$CH_3$$\underline{C}H_3$).
MS (EI, 70 eV): m/z (%) = 156 (0.61), 141 (2.6), 138 (1.0), 131 (2.0), 111 (11), 95 (68), 83 (39), 69 (100), 55 (74), 43 (65).

Enzyme-catalyzed polymerization of *3-(prop-1-en-2-yl)heptane-1,6-diol* (**11**) with *dimethyl adipate* (**14**) to *poly(1-methyl-4-iso-propenyl adipate)* (**poly11-adipate**)

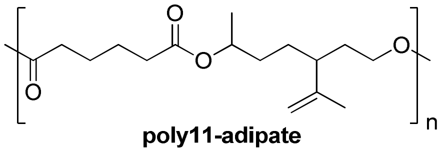

poly11-adipate

3-(prop-1-en-2-yl)heptane-1,6-diol (**11**, 78.6 mg, 0.50 mmol) and dimethyl adipate (**14**, 82.46 mg, 0.47 mmol) and CalB Lipase were stirred at 250 rpm, 50 °C and 50 mBar for 48 h. Then, the temperature was set to 70 °C and the pressure was decreased to 25 mBar. After 48 h, the viscosity of the mixture was strongly increased. NMR analytics in CDCl$_3$ revealed oligomerization.

^{1}H NMR (400 MHz, d6-DMSO): δ/ppm = 4.80 (m, 1H, -COO-C$\underline{H}$CH$_3$-), 4.73 (s, 1H, -CH-CC$\underline{H}$H-CH$_3$), 4.64 (s, 1H, -CH-CCH$\underline{H}$-CH$_3$), 3.93 (m, 2H, -CH$_2$-C$\underline{H_2}$-O-CO-), 2.26 (m, 4H, 2x -CH$_2$-C$\underline{H_2}$-CO-), 2.14 – 1.97 (m, 1H, CH$_2$-C$\underline{H}$C-CH$_2$-), 1.55 (m, 9H, -O-CHC$\underline{H_3}$-, 2x -C$\underline{H_2}$-CH$_2$-CO-O-, -O-CHCH$_3$-C$\underline{H_2}$-), 1.49 – 1.19 (m, 4H, -CH$_2$-C$\underline{H_2}$-CH-, -CHC-C$\underline{H_2}$-CH$_2$-O-), 1.17 – 1.11 (m, 3H, -CHCCH$_2$C$\underline{H_3}$).

Chemical polymerization of *3-(prop-1-en-2-yl)heptane-1,6-diol* (**11**) with *dimethyl terephthalate* (**15**) to *poly(1-methyl-4-iso-propenyl terephthalate)* (**poly11-terephthalate**)

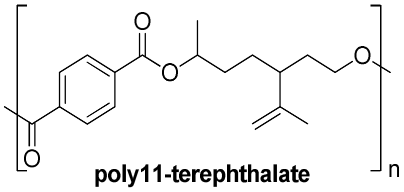

poly11-terephthalate

3-(prop-1-en-2-yl)heptane-1,6-diol (**11**, 227 mg, 1.44 mmol), dimethyl terephthalate (**15**, 279 mg, 1.437 mmol) and Sn(OAc)$_2$ (34.0 mg, 0.144 mmol) were stirred under a nitrogen atmosphere at 180 °C for 4.5 h. The temperature was set to 200 °C and the pressure was lowered to 2.5 mBar. After stirring for 2.5 h, it was heated to 220 °C and the pressure was reduced to 1.4 mBar. The viscosity was observed to increase noticeably. The reaction was cooled after another1.5 h and the mixture was slowly cooled to room temperature. After cooling, the obtained slightly orange solid was analyzed by NMR in CDCl$_3$ and DSC.

^{1}H NMR (400 MHz, CDCl$_3$): δ/ppm = 8.15 – 7.95 (m, 4H, terephthalic), 5.16 (m, 1H, -COO-C$\underline{H}$CH$_3$-), 4.83 (m, 1H, -CHC$\underline{H}$HCH$_3$), 4.77 (s, 1H, -CHCH$\underline{H}$CH$_3$), 4.37 – 4.16 (m, 2H, -CH$_2$-C$\underline{H_2}$OH), 2.33 – 2.19 (m, 1H, CH$_2$-C$\underline{H}$CCH$_2$-), 1.92 – 1.75 (m, 2H, -O-CHCH$_3$-C$\underline{H_2}$-CH$_2$-), 1.72 – 1.42 (m, 7H, CHCH$_3$-CH$_2$-C$\underline{H_2}$-, -CH-C$\underline{H_2}$-CH$_2$O-), 1.40 – 1.28 (m, 3H, -CH-CCH$_2$C$\underline{H_3}$).

NMR spectra of 6-oxo-3-(prop-1-en-2-yl)heptanal (**8**)

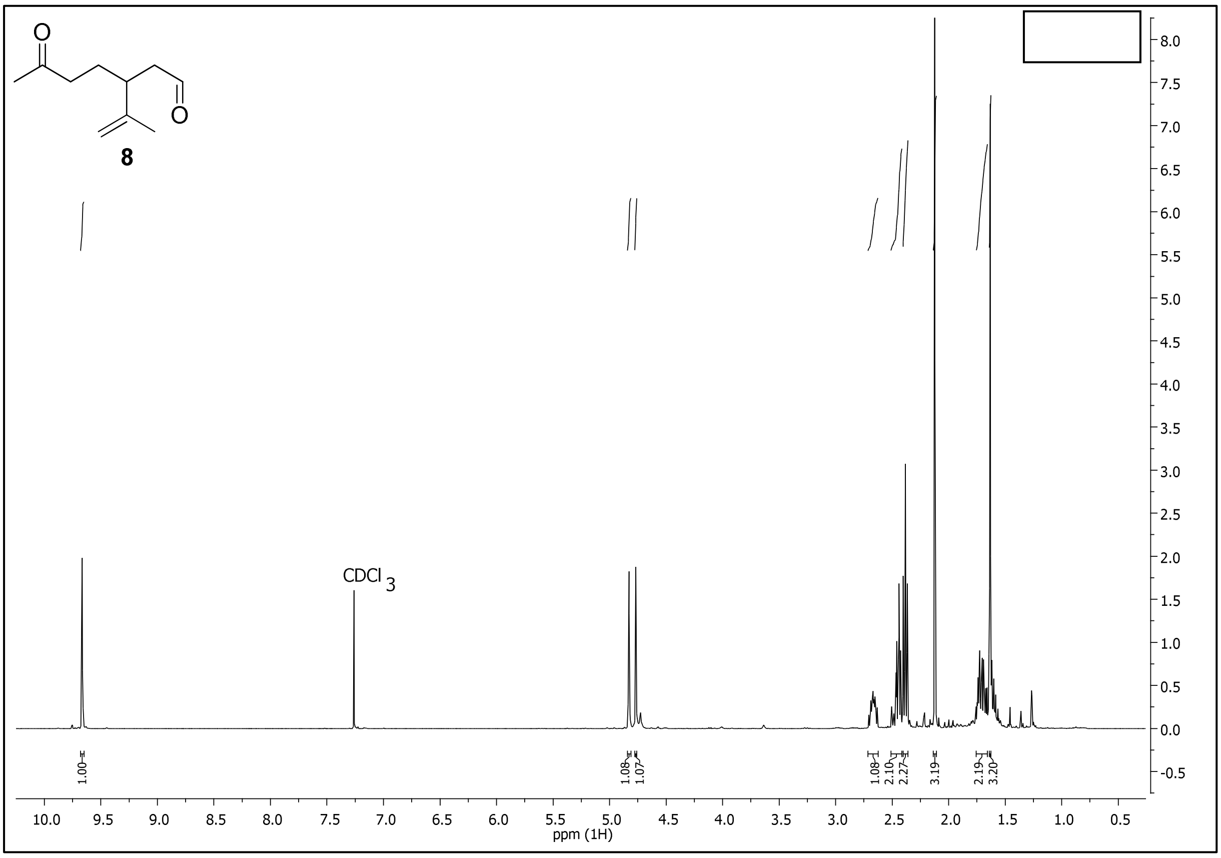

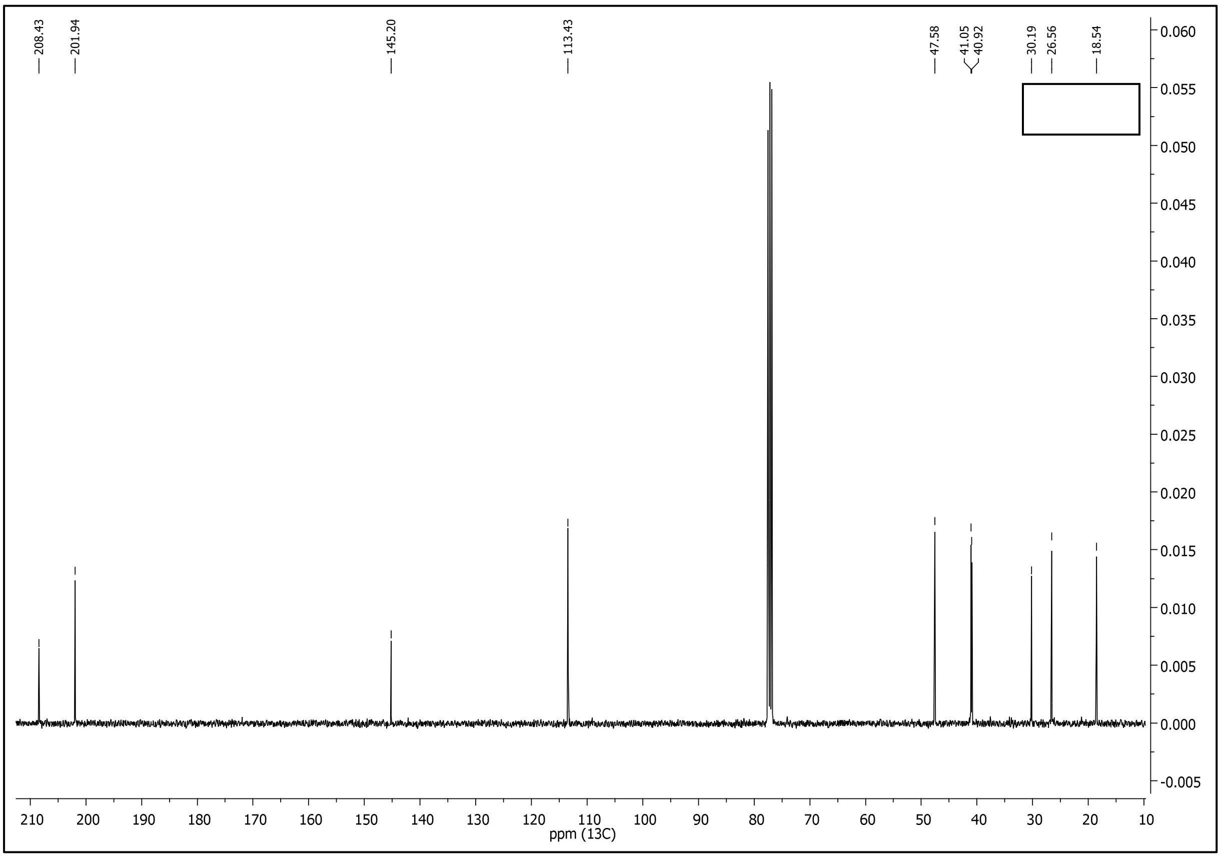

NMR spectra of 3-(prop-1-en-2-yl)heptane-1,6-diol (**11**)

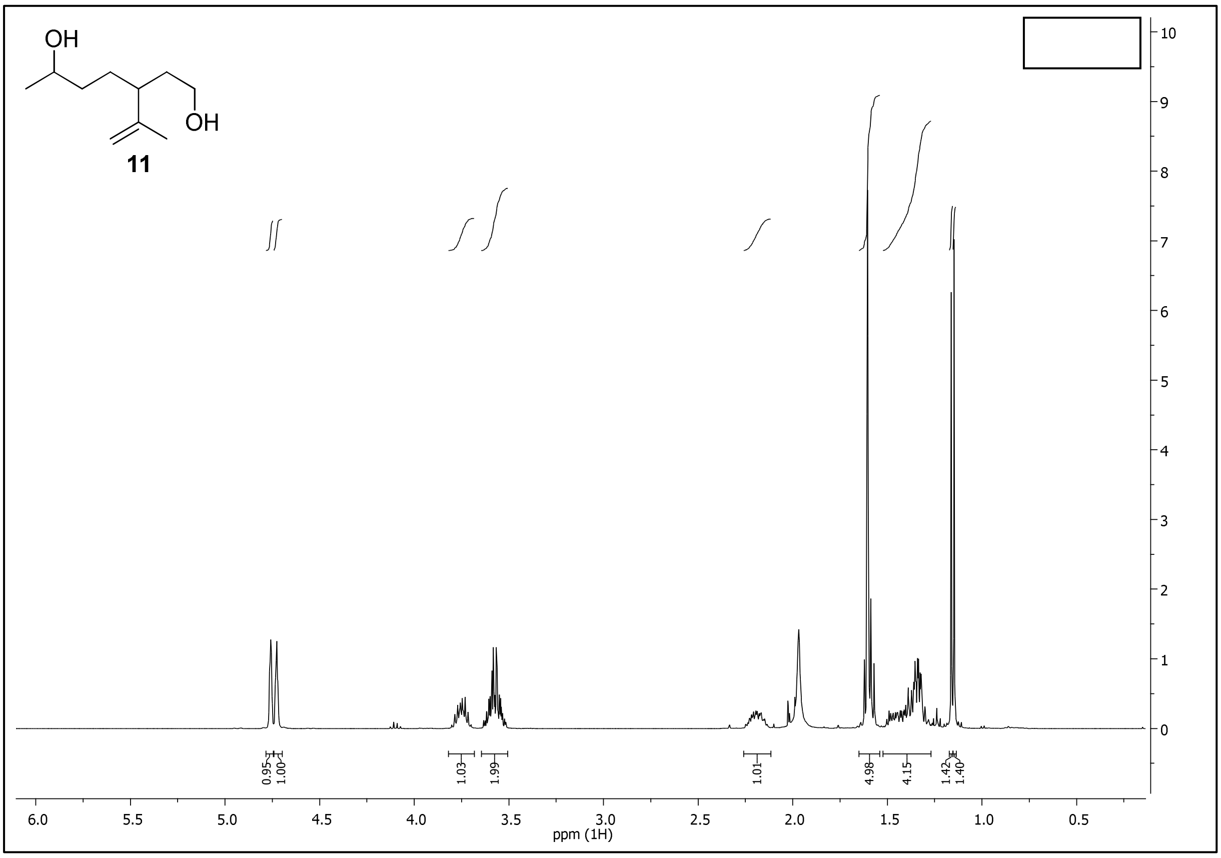

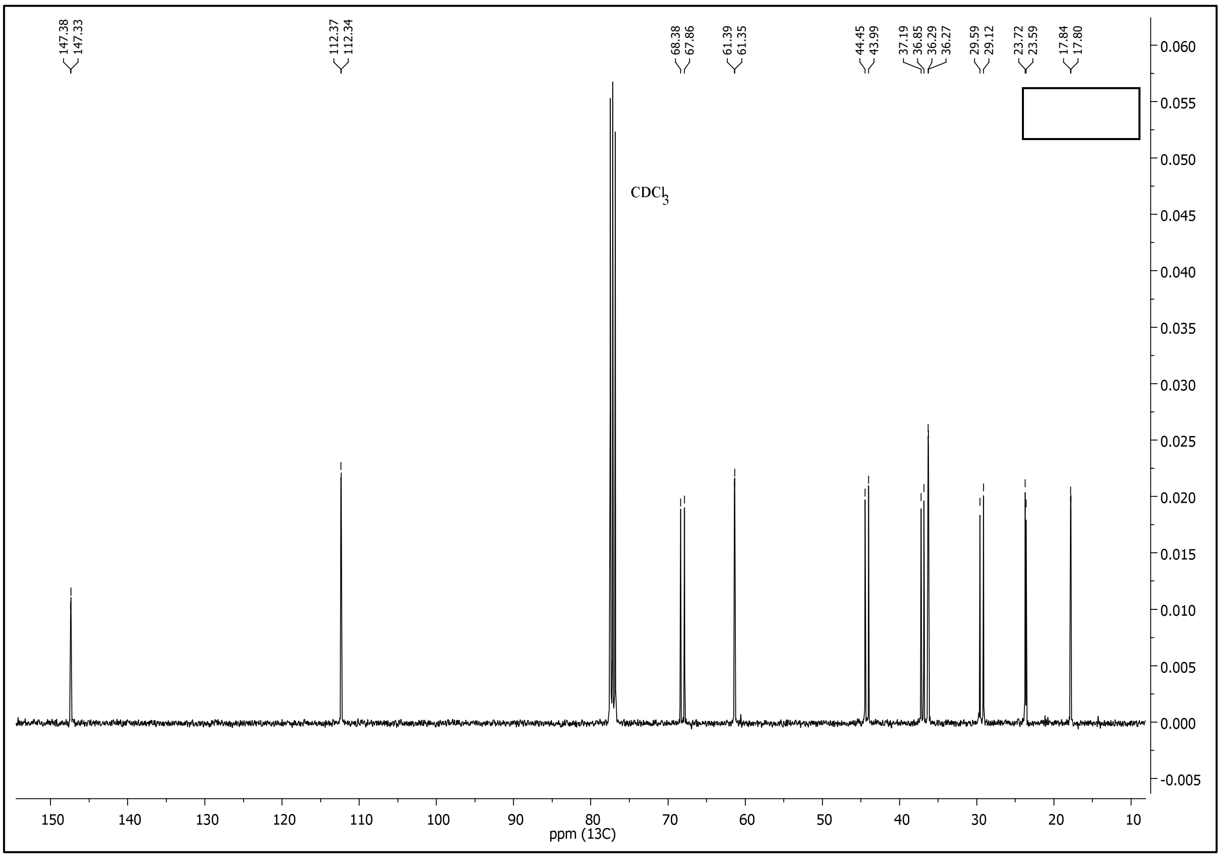

NMR spectra of 3-isopropylheptane-1,6-diol (**dihydro-10**)

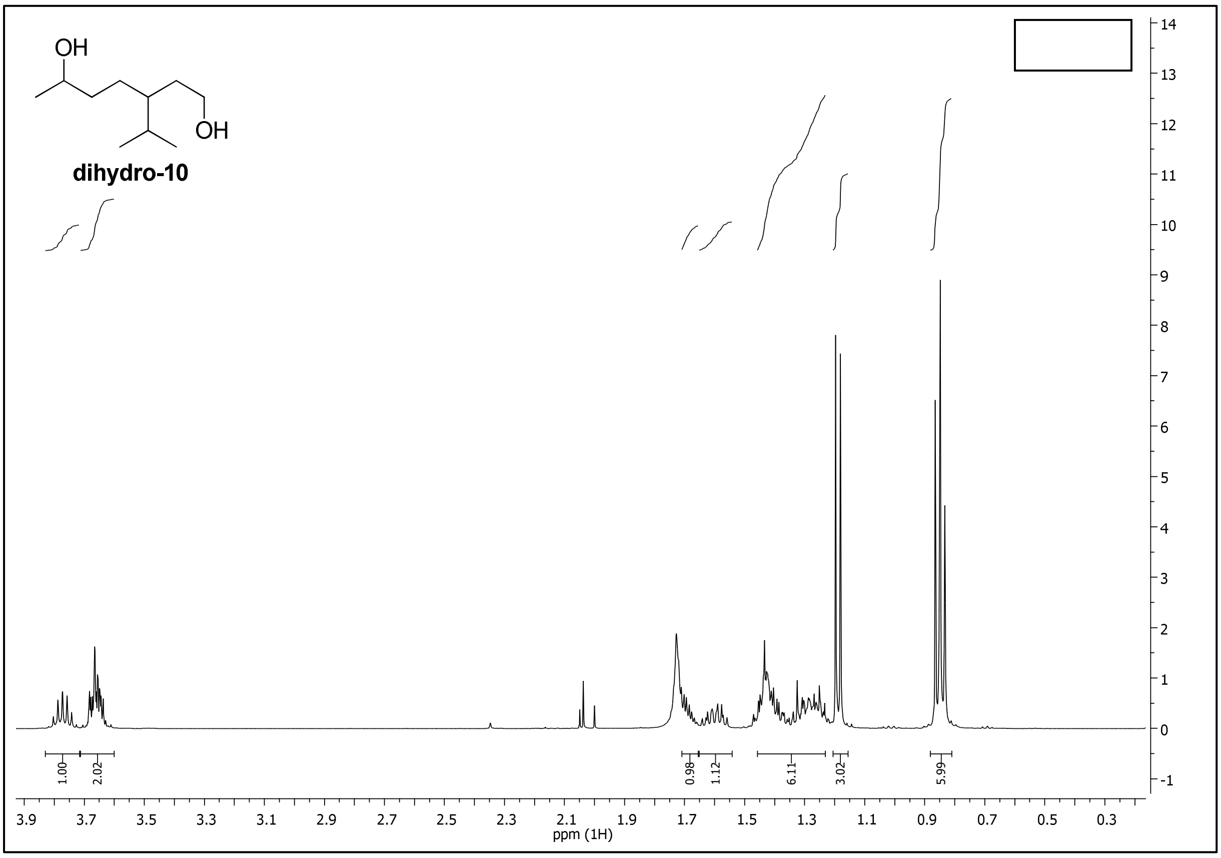

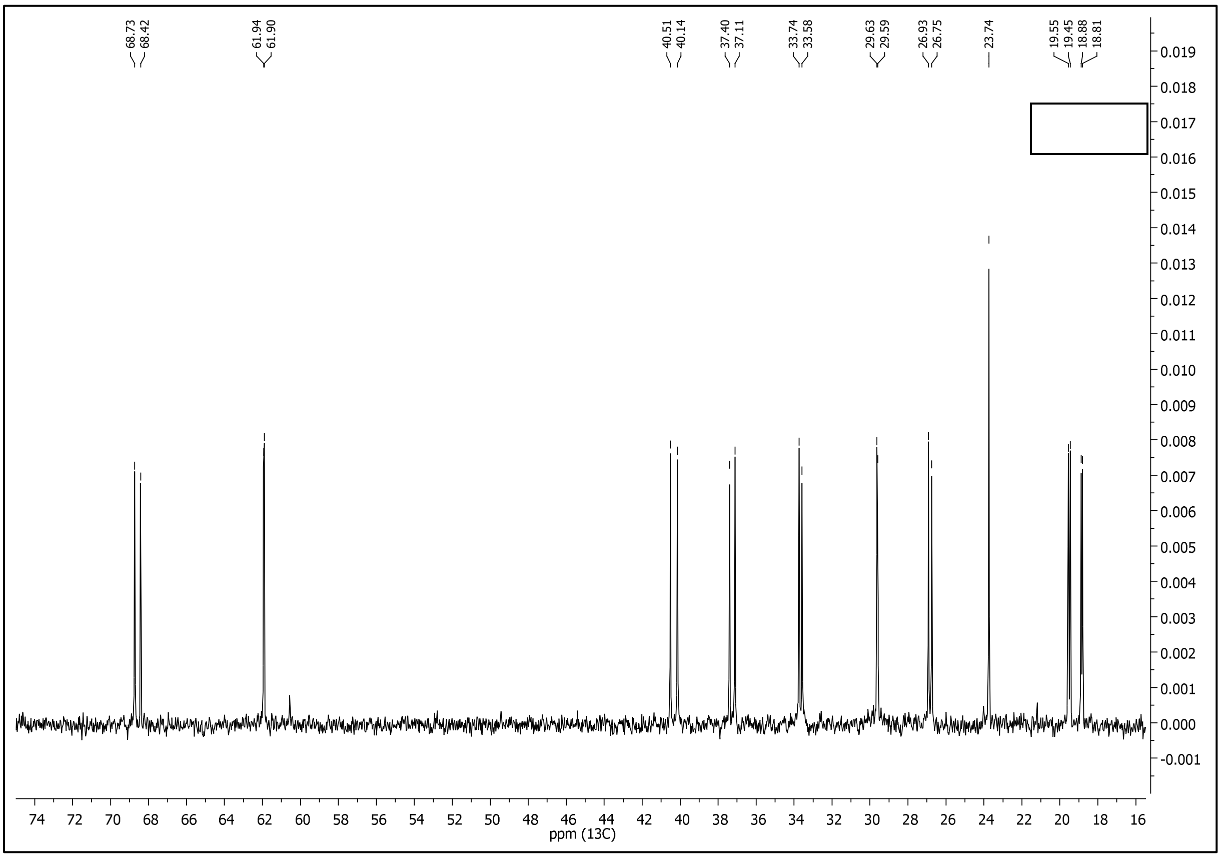

NMR spectra of 3-(prop-1-en-2-yl)heptane-1,6-diol (**11**)

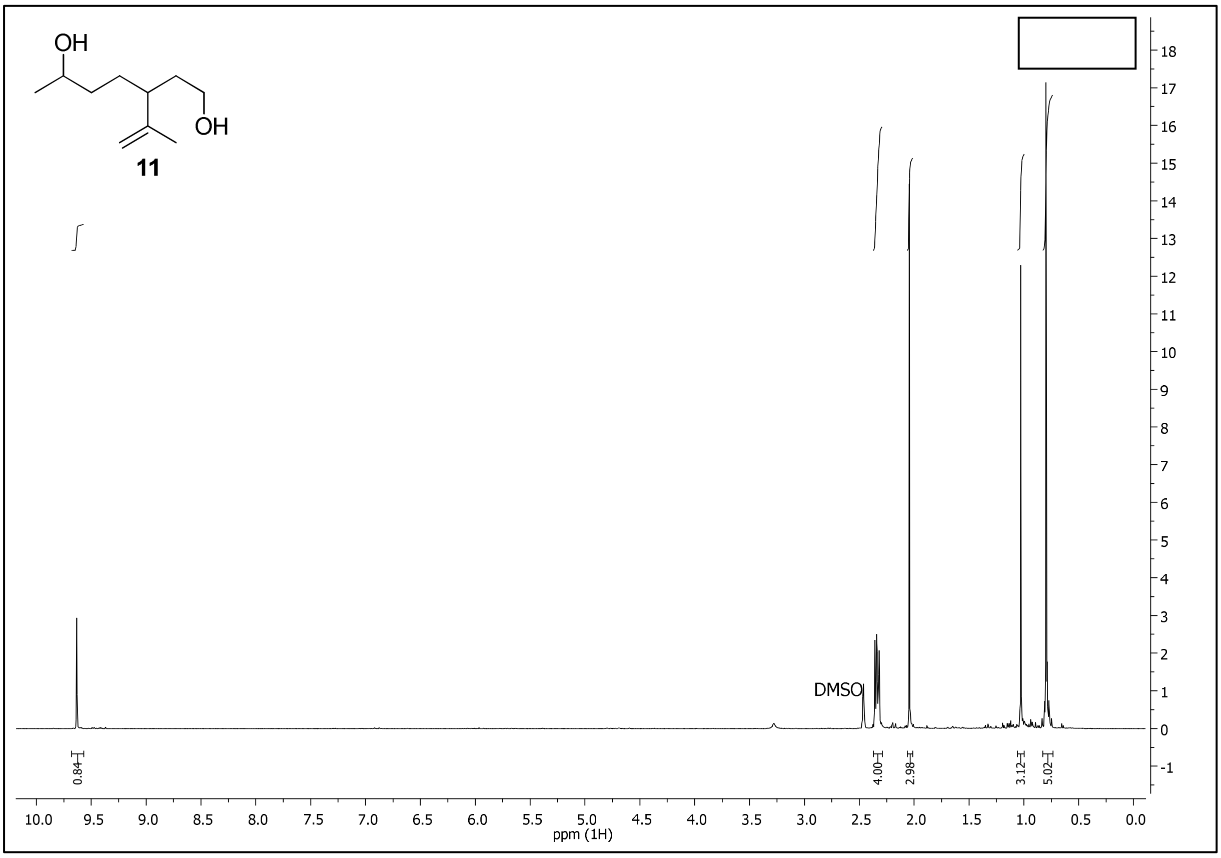

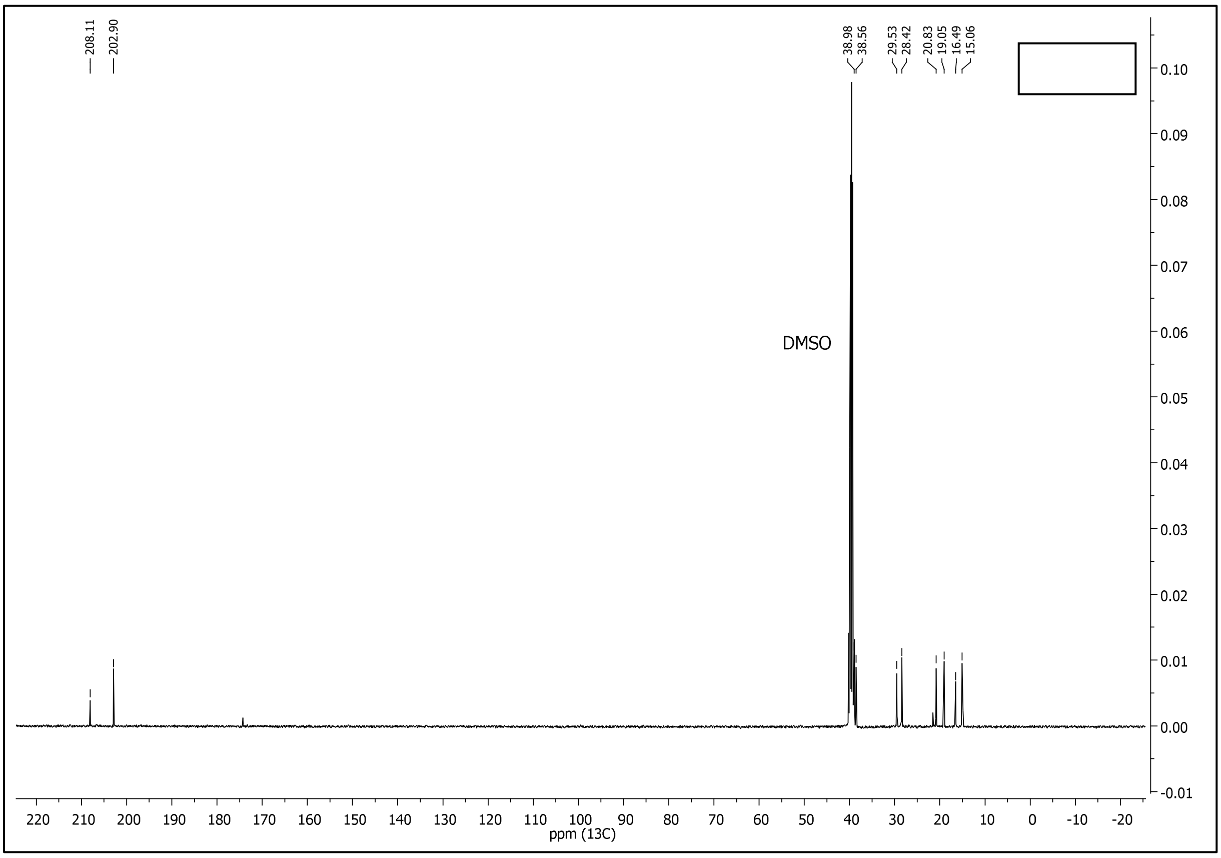

NMR spectra of 1-(3-(2-hydroxyethyl)-2,2-dimethylcyclopropyl)propan-2-ol (**12**)

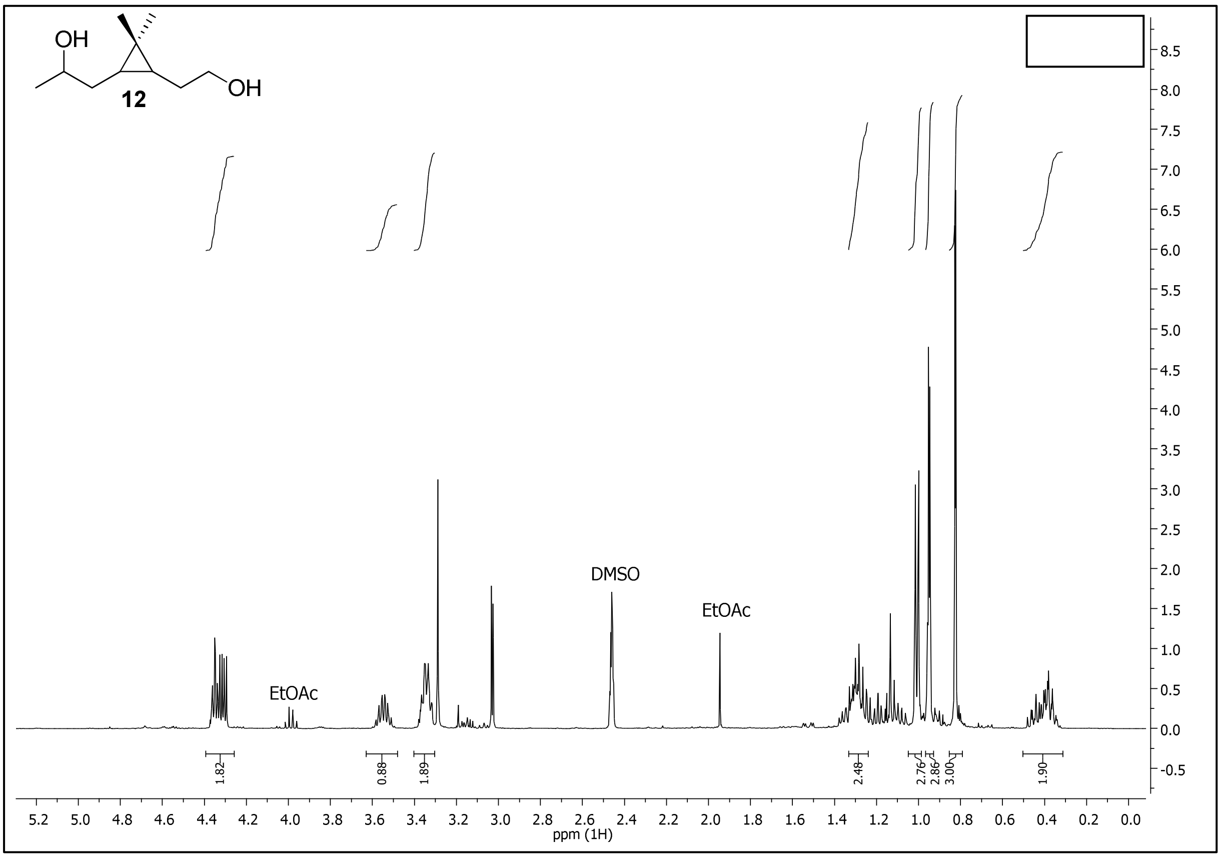

Poly(1-methyl-4-iso-propenyl adipate) **(poly11-adipate)**

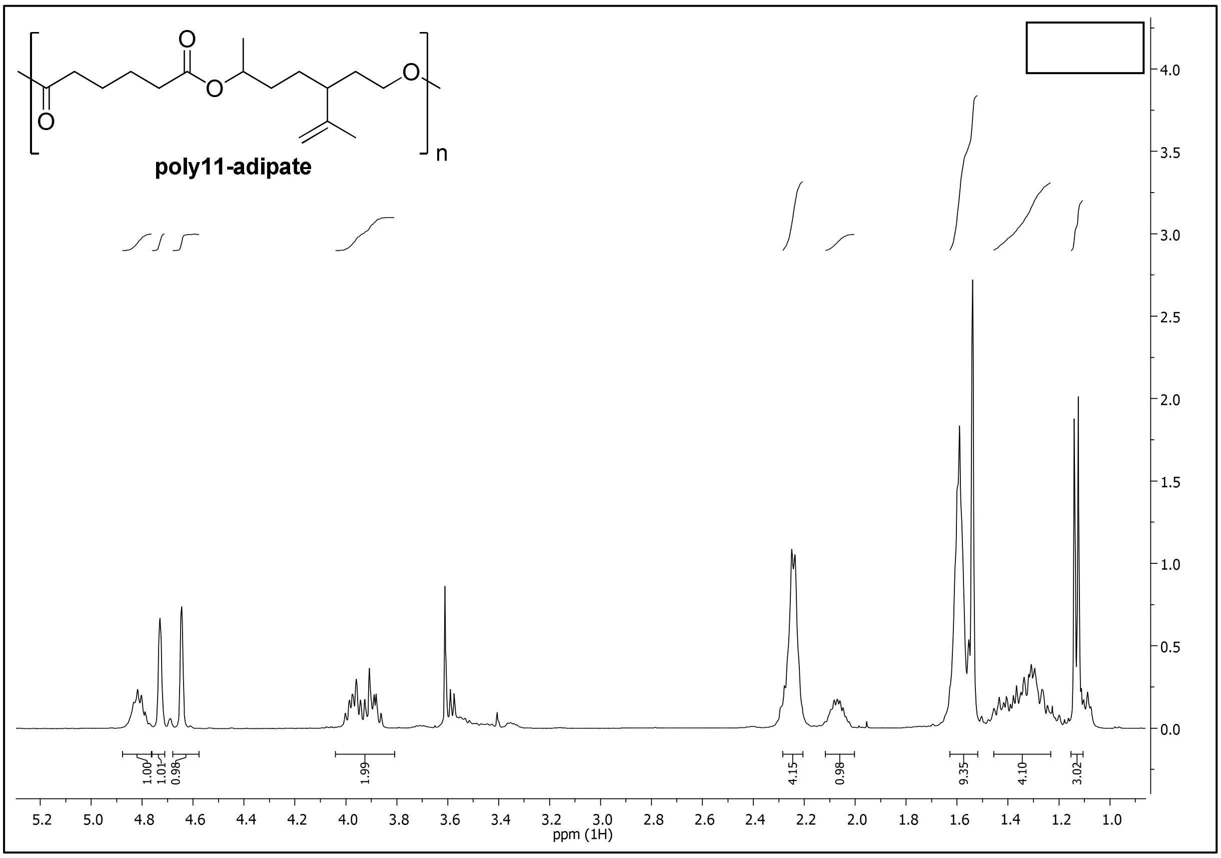

NMR spectra of poly(1-methyl-4-iso-propenyl terephthalate) (**poly11-terephthalate**)

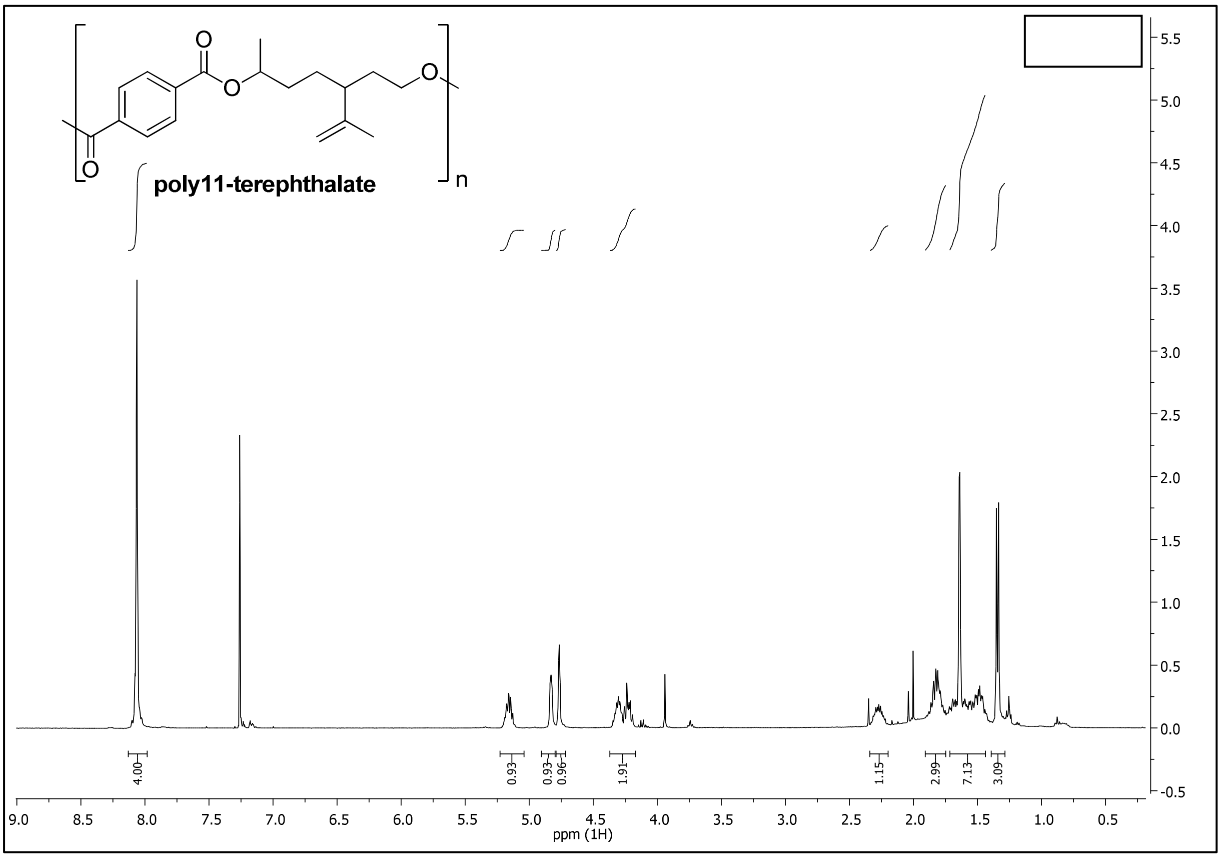

5 Lists

List of Schemes

Scheme 1.1 Biosynthesis of isoprene following the methylerythritol phosphate (MEP) and the mevalonate pathway (MVA). MEP: DXS 1-deoxyxylulose-5-phosphate synthase, DXR 1-deoxy-Dxylulose-5-phosphate reductoisomerase, CMK 4-diphophocytidyl-2-C-methyl-D-erythritol kinase, MCT 4-diphosphocytidyl-2-C-methyl-D-erythritol synthase, MDS 2-C-methyl-Derythritol 2,4-cyclodiphosphate synthase, HDS 1-hydroxy-2-methyl-2-(E)-butenyl 4-diphosphate synthase, HDR hydroxymethylbutenyl diphosphate reductase. MVA: AAT Acetyl-CoA C-acetyltransferase, HMGS hydroxymethylglutaryl-CoA synthase, HMGR hydroxymethylglutaryl-CoA reductase, MK mevalonate kinase,, PMK phosphomevalonate decarboxylase, MVD diphosphomevalonate decarboxylase.[2,7,9] 3
Scheme 1.2 Eurochim-method for the synthesis of isoprene from *i*C_4H_8 and formaldehyde. 5
Scheme 1.3 Synthesis of a terpene-based co-polyester starting from the Diels-Alder reaction of α-phellandrene with malic anhydride. 22
Scheme 1.4 Synthesis of terpene lactones from carvone (a),[76,77] menthone (b)[78] and β-pinene (c)[79] and subsequent ROP to polyesters. BHT = [4-[bis[4-[(3-sulfophenyl)amino]phenyl]methylidene]-1-cyclohexa-2,5-dienylidene]-(4-sulfophenyl)azanium. 24
Scheme 1.5 Synthesis of limonene-based AB- and AA/BB-type homo-polyesters. TEMPO = 2,2,6,6-tetramethylpiperidin-1-yl)oxyl; bpy = 2,2′-bipyridine; NMI = N-methylimidazole.[80] 25
Scheme 1.6 Synthesis of hydroxyborneol and polymerization with succinic acid to a chiral terpene-based polyester.[81] 26
Scheme 1.7 Synthesis of limonene-based poly(thioether amides). DMPA = 2,2-dimethoxy-2-phenylacetophenone (photoinitiator); TBD = 1,5,7-triazabicyclo-[4.4.0]dec-5-ene.[83] 26
Scheme 1.8 Synthesis of β-pinene based homopolyamides.[85] 27
Scheme 1.9 Synthesis and polymerization of a menthone-derived lactam by anionic ROP.[87,89] 28
Scheme 2.1 Reaction pathway for the synthesis of lactams **2-4** and lactones **5-6** as precursor for **dihydro-5/6**. 69
Scheme 2.2 AROP of lactam **2** to **poly2** with NaH and Ac_2O. 72
Scheme 2.3 Acetylation and tosylation of β-lactam **2**. 75
Scheme 2.4 General epoxidation via the chlorohydrine (a) and adjusted synthesis of **7** using in-situ generated HOBr (b). 78
Scheme 2.5. Hydrogenation of the double bond of **8** in MeOH (acetal formation) or THF. 107
Scheme 2.6 Meerwein-Ponndorf-Verley reaction for the selective reduction of aldehyde **8**. 108
Scheme 2.7 Reduction of the limonene (**1**)-based ketoaldehydes **8**, dihydro **8**, and the (+)-3-carene (**2**)-based **9** to the corresponding diols. 108

List of Figures

Figure 1.1 a) Important isoprene polymers and b) Several perfumes derived from isoprene.[17] 6
Figure 1.2 Polymer pyramid. Amorphous high-performance: Polyetherimide (PEI), poly(ether sulfone) (PES), polysulfone (PSU); Amorphous engineering: Cyclic olefin copolymer (COC), polycarbonate (PC); Amorphous commodity: Acrylonitrile butadiene styrene (ABS), poly(methyl methacrylate) (PMMA), polystyrene (PS), poly(vinyl chloride) (PVC); Semi-crystalline high-performance: Poly(tetrafluoro ethylene) (PTFE) , poly(ether ketone) (PEEK), poly(phenylene sulfide) (PPS); Semi-crystalline engineering: Polyamide 46 (PA46), polyamide 12 (PA12), poly(ethylene terephthalate) (PET), poly(*p*-phenylene oxide), poly(butylene terephthalate) (PBT), poly(oxy methylene), polyamide 6 (PA6), polyamide 66 (PA66); Semi-crystalline commodity: Polypropylene (PP), polyethylene high-density (PP-HD), polyethylene low-density (PP-LD);*Depending on polyurethane (PUR) type.[18–20] 8
Figure 1.3 Contribution of plastics for synthetic fibers (a) and engineering applications (b).[23] 9
Figure 1.4 Selection of typical diacids (a) and diols (b) for AA/BB-type polyester and AB-type monomers (c).[22] 9
Figure 1.5 Applications of polyamides.[28] 10
Figure 1.6 Dependence of T_m (upper) and the water uptake (lower) of the CH_2/CNOH ratio for various polyamides.[21,28] 11
Figure 1.7 Polycondensation of terephthalic acid and ethylene glycol to PET under release of water. 12
Figure 1.8 Graphs of Carothers' equation for differing r-values; $r = 0.5$ (red), $r = 0.9$ (orange), $r = 0.97$ (blue), $r = 1.0$ (dark blue). 13
Figure 1.9 Polymerization equilibrium of caprolactam and PA6.[38] 14
Figure 1.10 Initiation (dimer formation) and propagation of the activated aROP of caprolactam with acetyl-caprolactam as activator and sodium caprolactamate as initiator.[38] 15
Figure 1.11 Influence of a methyl substituent on $[M]_e$ at the α-ε positions in a bulk polymerization at 250 °C.[43] 17
Figure 1.12 Bio-based polymers and their fields of application.[50] 18
Figure 1.13 Global production capacities of bio-based polymers 2018 (only new economy plastics, without PUR). Poly(butylene succinate) (PBS); poly (butylene adipate terephthalate) (PBAT); poly (trimethylene terephthalate) (PTT); polyethylene (PE); poly (hydroxy alkanoate) (PHA).[47] 18
Figure 1.14 Synthesis pathway to bio-based ethylene glycol. Green: Land use; blue: Water use.[46] 19
Figure 1.15 Conversion of ricinoleic acid from castor oil to bio-PA11. Green: Land use; blue: Water use.[46] 20
Figure 1.16 Pathway from isoprene-precursors dimethylallyl pyrophosphate (DMAPP) and isopentenyl pyrophosphate (IPP) to hydroxylated and purely aliphatic linear, mono-cyclic, and bi-cyclic monoterpenes. 21
Figure 1.17 Synthesis of β-lactams and ε-lactams starting from (+)-3-carene and α-pinene. 30
Figure 1.18 Oxidative cleavage of limonene, (+)-3-carene, and α-pinene and subsequent conversion to diols. 30
Figure 2.1 Selected isoprene (**1**)-based building blocks for polymers. 67
Figure 2.2 Pathway from glucose to **dihydro-5/6** (a) and application of **dihydro-5/6** in a polysaccharide copolymer (b). 68
Figure 2.3 Various β-lactams which have successfully been polymerized to the corresponding poly-β-amides. 68
Figure 2.4 Proposed reaction pathway for the synthesis of lactam **8** from MTBE. 71
Figure 2.5 ^{13}C-NMR of **poly2** and signal-splitting of carbons attached to the chiral center as expected for an atactical polymer. 73
Figure 2.6 GPC curve (upper) and DSC curve (lower) of **poly2**. 74
Figure 2.7 Unsuccessful radical polymerization of β-lactam **2** with AIBN. 75
Figure 2.8 Possible side reactions of the isoprene (**1**) epoxidation. 78
Figure 2.20 Synthesis of ketoaldehydes **8**, **dihydro-8** and **9** starting from the corresponding epoxides. (a) = epoxidation; (b) hydrogenation; (c) epoxide opening to the corresponding diol; (d) oxidative C-C bond cleavage with $NaIO_4$. 106
Figure 2.21 GCMS chromatogram displaying the kinetic resolution of the *cis*/*trans* mixture of **5** by periodate cleavage. 107
Figure 2.22 NMR comparison of the monomers **11** and **14** with **poly11-adipate**. 109
Figure 2.23 DSC of **poly11-terephthalate** (second run). 110
Figure 2.24 NMR comparison of the monomers **11** and **15** with **poly11-terephthalate**. 111
Figure 3.1 Proposed mechanism for the formation of δ-lactones from a chlorosulfonyl-δ-lactam.[119,123] 114
Figure 3.2 Co-polymer of isoprene β-lactam and caprolactam, post-polymerization modifications and proposed effects. 115
Figure 3.3 Synthesis strategies for ketones that are used as precursors for lactams. 117
Figure 3.4 Synthesis approach of demethylated caranlactam starting from cyclohexa-1,4-diene under application of thio-ylide chemistry and enantioselective crystallization. 119
Figure 3.4 Terpene-based ketoaldehydes as platform chemicals for hydroxy carboxylic acids, amino acids, diamines, and diols. 123

List of Tables

Table 1.1 Isoprene (**1**)-based fine chemicals and their applications as commercialized by Kuraray Co., Ltd. 7
Table 1.2 Technical data of PET, PBT and PC.[21,25] 10
Table 1.3 Technical data of AA/BB and AB type polyamides.[21,25] ND = no data. 12
Table 1.4 Impact of the signs of ΔH_0 and ΔS_0 on the polymerization temperature. 15
Table 2.1 Influence of solvent polarity on the product distribution of the reaction of isoprene (**1**) with CSI. Reaction conditions: T = -70 – -30 °C, t = 2 – 3 h. *reaction temperature 0 °C. 71
Table 2.2 Lewis acids as catalysts for the synthesis of lactams **SO_2Cl-3** and **SO_2Cl-4** in relative comparison to a catalyst-free standard reaction. + = increased product formation; - = decreased product formation; / = no change. Reaction conditions: Isoprene (**1**) 2 mmol, 0.3 mmol Lewis acid, MeCN 5 mL, 50 °C, 3 h. 76
Table 3.1: The three bio-fuel generations and some of their characteristics.[147] 112
Table 3.1 Terpene-based polyamides and their properties. 120
Table 3.2 Bio-based polyamides from biomass other than terpenes and Ricinus oil and their properties. 121

List of abbreviations

$[M]_e$	monomer equilibrium concentration
9-BBN	9-Borabicyclo[3.3.1]nonane
Å	Angström
acac	acetyl acetonate
AH salt	hexamethylene diamine adipate
AIBN	azobisisobutyronitrile
AROP	anionic ring-opening polymerization
ATP	adenosine triphosphate
Bu	butyl-
Bz	benzoyl-
CALB	candida antarctica lipase B
CL	caprolactam
COD	1,5-cyclooctadiene
COSY	correlation spectroscopy
Cp	cyclopentadien
CSI	chlorosulfonyl isocyanate
DCM	dichlormethane
DEPT	distortionless enhancement by polarization transfer
DMAPP	dimethylallyl pyrophosphate
DMSO	diemthylsulfoxide
DSC	differential scanning chromatography
EG	ending group
Et-	ethyl
GCMS	gas chromatography mass spectrometry
HFIP	hexafluoroisopropanol
HH	head-to-head
HMBC	heteronuclear multiple bond coherence
HOSA	hydroxylamine sulfonic acid
HSQC	heteronuclear single quantum coherence
HT	head-to-tail
i	*iso-*
IL	ionic liquid
IPC	in-process control
IPP	isopentenyl pyrophosphate
*i*Pr-	*iso*-propyl
IR	infra-red
kDa	kilo Dalton
LL	laurolactam
MAO	methylaluminoxane
*m*CPBA	*meta* chlorobenzoic acid
Me-	methyl
MeCN	acetonitrile
MEP pathway	methylerythritol phosphate pathway
M_n	molecular number average weight

MTBE	methyl *t*-butyl ether
MVA pathway	mevalonate pathway
M_w	molecular mass average weight
NHC	N-heterocyclic carbene
NMR	nuclear magnetic resonance
NVP	N-vinylpyrrolidone
OAc	acetate
Oxone®	potassium hydrogen persulfate
p	conversion
p-	*para-*
PA	polyamide
PBT	poly (buthylene terephthalate)
PC	polycarbonate
PCL	polycaprolactone
PDI	polydispersity index
PEN	poly (ethylene naphthalate)
PET	poly (ethylene terephthalate)
Ph	phenyl
PHB	poly(hydroxy butyrate)
PLA	polylactic acid
Pn	average number degree of polymerization
PNNP	phosphor-nitrogen-nitrogen-phosphor
PNP	phosphor-nitrogen-phosphor
ppm	parts per million
pTSI	4-methylbenzenesulfonyl isocyanate
PUR	polyurethane
R	gas constant
RMS	residual monomer separation
ROP	ring-opening polymerization
SG	starting group
SI	supplementary information
SIS	styrene-isoprene-styrene
SLS	selective laser sintering
T	temperature
t	*tert-*
T_c	celling temperature
T_f	floor temperature
T_g	glass transition temperature
THF	tetrahydro furan
TLC	thin-layer chromatography
T_m	melting temperature
Ts	tosyl-
TT	tail-to-tail
vic	vicinal
XRD	X-ray diffraction
ZNc	Ziegler-Natta catalysts

ΔG	Gibbs free energy
ΔH_0	standard enthalpy
ΔS_0	standard entropy

7. References

1. Guenther, A. *et al.* Estimates of global terrestrial isoprene emissions using MEGAN (Model of Emissions of Gases and Aerosols from Nature). *Atmos. Chem. Phys.* **6,** 3181–3210; 10.5194/acp-6-3181-2006 (2006).
2. Ye, L., Lv, X. & Yu, H. Engineering microbes for isoprene production. *Metab. Eng.* **38,** 125–138; 10.1016/j.ymben.2016.07.005 (2016).
3. Morais, A. R.C. *et al.* Chemical and biological-based isoprene production. Green metrics. *Catal. Today* **239,** 38–43; 10.1016/j.cattod.2014.05.033 (2015).
4. Sharkey, T. D. & Loreto, F. Water stress, temperature, and light effects on the capacity for isoprene emission and photosynthesis of kudzu leaves. *Oecologia* **95,** 328–333; 10.1007/BF00320984 (1993).
5. Sharkey, T. D. & Singsaas, E. L. Why plants emit isoprene. *Nature* **374,** 769 EP -; 10.1038/374769a0 (1995).
6. Loreto, F. *et al.* Ozone quenching properties of isoprene and its antioxidant role in leaves. *Plant Physiol.* **126,** 993–1000 (2001).
7. Vickers, C. E., Gershenzon, J., Lerdau, M. T. & Loreto, F. A unified mechanism of action for volatile isoprenoids in plant abiotic stress. *Nat. Chem. Biol.* **5,** 283 EP -; 10.1038/nchembio.158 (2009).
8. Pollastri, S., Tsonev, T. & Loreto, F. Isoprene improves photochemical efficiency and enhances heat dissipation in plants at physiological temperatures. *J. Exp. Bot.* **65,** 1565–1570; 10.1093/jxb/eru033 (2014).
9. George, K. W., Alonso-Gutierrez, J., Keasling, J. D. & Lee, T. S. Isoprenoid drugs, biofuels, and chemicals--artemisinin, farnesene, and beyond. *Adv. Biochem. Eng./Biotechnol.* **148,** 355–389; 10.1007/10_2014_288 (2015).
10. Chaves, J. E. & Melis, A. Biotechnology of cyanobacterial isoprene production. *Appl. Microbiol. Biotechnol.* **102,** 6451–6458; 10.1007/s00253-018-9093-3 (2018).
11. Cervin, M. A. & Chotani, G. K., et al. *Compositions and methods for producing isoprene ,*
12. Biotechnology Innovation Organization (BIO). Advancing the Biobased Economy: Renewable Chemical Biorefinery Commercialization, Progress, and Market Opportunities, 2016 and Beyond. Available at https://www.bio.org/sites/default/files/BIO_Advancing_the_Biobased_Economy_2016.pdf (2016).
13. Dykman, A. S., Busygin, V. M., Gilmanov, H. H., Moiseev, I. I. & Fedortsova, E. V. Herstellung von Isopren - Ein Überblick. *GAK* **64,** 626–627 (2011).
14. Ezinkwo, G. O., Tretjakov, V. F., Talyshinky, R. M., Ilolov, A. M. & Mutombo, T. A. Overview of the Catalytic Production of Isoprene from different raw materials; Prospects of Isoprene production from bio-ethanol. *Catalysis for Sustainable Energy* **1**; 10.2478/cse-2013-0006 (2013).
15. Weitz, H. M. & Loser, E. *Ullmann's Encyclopedia of Industrial Chemistry: Isoprene* (Wiley-VCH Verlag GmbH & Co. KGaA, Weinheim, Germany, 2000).
16. EuroChim. Innovative high-efficiency resource ans energy saving technology for isoprene production frim isobutylene and formaldehyde by liquid-phase method. Available at http://www.eurochimgroup.com/upload/Presentations/Liquid-phase%20isoprene%20production_eng.pdf.
17. Funel, J.-A. & Abele, S. Industrial applications of the Diels-Alder reaction. *Angew. Chem. Int. Ed. Engl.* **52,** 3822–3863; 10.1002/anie.201201636 (2013).
18. Bonten, C. *Kunststofftechnik. Einführung und Grundlagen.* 1st ed. (Carl Hanser Fachbuchverlag, s.l., 2014).
19. Bonnet, M. in *Kunststofftechnik. Grundlagen, Verarbeitung, Werkstoffauswahl und Fallbeispiele,* edited by M. Bonnet (Springer Vieweg, Wiesbaden, 2016), Vol. 3, pp. 1–86.

20. Friedrich, K. Polymer composites for tribological applications. *Adv. Ind. Eng. Polym. Res.* **1,** 3–39; 10.1016/j.aiepr.2018.05.001 (2018).
21. Baur, E., Brinkmann, S., Osswald, T. A., Schmachtenberg, E. & Saechtling, H. *Saechtling Kunststoff Taschenbuch.* 30th ed. (Hanser, München, 2007).
22. Gubbels, E. *et al.* Polyesters. *Ullmann's encyclopedia of industrial chemistry*; 10.1002/14356007.a21_227.pub2 (2018).
23. Wesołowski, J. & Płachta, K. The Polyamide Market. *F&TinEE* **24,** 12–18; 10.5604/12303666.1221737 (2016).
24. Koltzenburg, S., Maskos, M. & Nuyken, O. *Polymere: Synthese, Eigenschaften und Anwendungen* (Springer Berlin Heidelberg, Berlin, Heidelberg, 2014).
25. Kern GmbH Kunststoffe. Polymer Technical Data Sheets. Available at https://www.kern.de/de/technische-datenblaetter-kunststoffe?lng=2.
26. Reglero Ruiz, J. A., Trigo-López, M., García, F. C. & García, J. M. Functional Aromatic Polyamides. *Polymers* **9**; 10.3390/polym9090414 (2017).
27. Bhat, G. ed. *Structure and properties of high-performance fibers* (WP Woodhead Publishing an imprint of Elsevier, Amsterdam, Boston, Cambridge, 2017).
28. Herzog, B., Kohan, M. I., Mestemacher, S. A., Pagilagan, R. U. & Redmond, K. Polyamides. *Ullmann's encyclopedia of industrial chemistry*; 10.1002/14356007.a21_179.pub3 (2013).
29. Carothers, W. H. & Arvin, J. A. STUDIES ON POLYMERIZATION AND RING FORMATION. II. POLY-ESTERS. *J. Am. Chem. Soc.* **51,** 2560–2570; 10.1021/ja01383a042 (1929).
30. Lenz, R. W. *Organic chemistry of synthetic high polymers* (Interscience Publ, New York, 1967).
31. Carothers, W. H. Polymerization. *Chem. Rev.* **8,** 353–426; 10.1021/cr60031a001 (1931).
32. Kauffman, G. B. Wallace Hume Carothers and nylon, the first completely synthetic fiber. *J. Chem. Educ.* **65,** 803; 10.1021/ed065p803 (1988).
33. Deopura, B. L., Alagirusamy, R., Joshi, M. & Gupta, B. *Polyesters and Polyamides.* 1st ed. (Elsevier Reference Monographs, s.l., 2008).
34. Kobayashi, S. Enzymatic ring-opening polymerization and polycondensation for the green synthesis of polyesters. *Polym. Adv. Technol.* **26,** 677–686; 10.1002/pat.3564 (2015).
35. Douka, A., Vouyiouka, S., Papaspyridi, L.-M. & Papaspyrides, C. D. A review on enzymatic polymerization to produce polycondensation polymers: The case of aliphatic polyesters, polyamides and polyesteramides. *Progress in Polymer Science* **79,** 1–25; 10.1016/j.progpolymsci.2017.10.001 (2018).
36. Han, Y.-K., Kim, S.-R. & Kim, J. Preparation and characterization of high molecular weight poly(butylene succinate). *Macromol. Res.* **10,** 108–114; 10.1007/BF03218299 (2002).
37. Sugihara, S., Toshima, K. & Matsumura, S. New Strategy for Enzymatic Synthesis of High-Molecular-Weight Poly(butylene succinate) via Cyclic Oligomers. *Macromol. Rapid Commun.* **27,** 203–207; 10.1002/marc.200500723 (2006).
38. Russo, S. & Casazza, E. in *Polymer science. A comprehensive reference,* edited by K. Matyjaszewski & M. Möller (Elseiver, Amsterdam, 2012), pp. 331–396.
39. Flory, P. J. *Principles of polymer chemistry.* 10th ed. (Cornell Univ. Pr, Ithaca, N.Y., 1978).
40. Dubois, P., Coulembier, O. & Raquez, J. M. eds. *Handbook of ring-opening polymerization* (Wiley-VCH, Weinheim, 2009).
41. Ricco, L., Russo, S., Orefice, G. & Riva, F. Anionic Poly(ε-caprolactam): Relationships among Conditions of Synthesis, Chain Regularity, Reticular Order, and Polymorphism. *Macromolecules* **32,** 7726–7731; 10.1021/ma9909004 (1999).
42. Bamford, C. H. & Tipper, C. F. H. eds. *Non-radical polymerisation* (Elsevier Scientific Pub. Co, Amsterdam, New York, 1976).
43. Šebenda, J. in *Non-radical polymerisation,* edited by C. H. Bamford & C. F. H. Tipper (Elsevier Scientific Pub. Co, Amsterdam, New York, 1976), pp. 379–471.

44. Uyama, H., Kikuchi, H., Takeya, K. & Kabayashi, S. Lipase-Catalyzed ring-opening polymerization and copolymerization of 15-pentadecanolide. *Acta Polym.* **47,** 357–360; 10.1002/actp.1996.010470807 (1996).
45. Hernández, N., Williams, R. C. & Cochran, E. W. The battle for the "green" polymer. Different approaches for biopolymer synthesis. Bioadvantaged vs. bioreplacement. *Organic & biomolecular chemistry* **12,** 2834–2849; 10.1039/c3ob42339e (2014).
46. Institute for Bioplastics and Biocomposites IfBB. Biopolymers facts and statistics 2018. Production capacities, processing routes, feedstock, land and water use; Hochschule Hannover IfBB - Institut für Biokunststoffe und Bioverbundwerkstoffe, Heisterbergallee 10A, 30453 Hannover. Available at https://www.ifbb-hannover.de/files/IfBB/downloads/faltblaetter_broschueren/Biopolymers-Facts-Statistics-2018.pdf (2018).
47. European Bioplastics. Report - Bioplastics Market Data 2018; European Plastics, Marienstraße 19-20, 10117 Berlin. Available at https://www.european-bioplastics.org/wp-content/uploads/2016/02/Report_Bioplastics-Market-Data_2018.pdf (2018).
48. Kabasci, S. *Bio-Based Plastics* (John Wiley & Sons Ltd, Chichester, UK, 2013).
49. PlasticsEurope. Plastics - the Facts 2018; PlasticsEurope AISBL, Rue Belliard 40, Box 16, 1040 Brussels, Belgium. Available at https://www.plasticseurope.org/application/files/6315/4510/9658/Plastics_the_facts_2018_AF_web.pdf (2018).
50. Carus, M. Bio-based Building Blocks and Polymers - Global Capacities, Production and Trends 2018-2013 (Short Version); nova-Institut GmbH, Chemiepark Knapsack, Industriestraße 300, 50354 Hürth, Germany. Available at http://bio-based.eu/download/?did=136226&file=0 (2019).
51. Jiang, Y. & Loos, K. Enzymatic Synthesis of Biobased Polyesters and Polyamides. *Polymers* **8**; 10.3390/polym8070243 (2016).
52. Buntara, T. *et al.* Caprolactam from renewable resources: catalytic conversion of 5-hydroxymethylfurfural into caprolactone. *Angewandte Chemie (International ed. in English)* **50,** 7083–7087; 10.1002/anie.201102156 (2011).
53. Castro-Aguirre, E., Iñiguez-Franco, F., Samsudin, H., Fang, X. & Auras, R. Poly(lactic acid)-Mass production, processing, industrial applications, and end of life. *Advanced drug delivery reviews* **107,** 333–366; 10.1016/j.addr.2016.03.010 (2016).
54. Martínez, L. M. T., Kharissova, O. V. & Kharisov, B. I. eds. *Handbook of ecomaterials* (Springer, Cham, Switzerland, 2019).
55. Breitmaier, E. *Terpene. Aromen, Dufte, Pharmaka, Pheromone* (Wiley-VCH, Hoboken, 2008).
56. Wallach, O. Zur Kenntniss der Terpene und ätherischen Oele. *Justus Liebigs Ann. Chem.* **238,** 78–89; 10.1002/jlac.18872380104 (1887).
57. Zebec, Z. *et al.* Towards synthesis of monoterpenes and derivatives using synthetic biology. *Curr. Opin. Chem. Biol.* **34,** 37–43; 10.1016/j.cbpa.2016.06.002 (2016).
58. Ruzicka, L. The isoprene rule and the biogenesis of terpenic compounds. *Experientia* **9,** 357–367; 10.1007/bf02167631 (1953).
59. Birladeanu, L. The Story of the Wagner-Meerwein Rearrangement. *J. Chem. Educ.* **77,** 858; 10.1021/ed077p858 (2000).
60. Sarkic, A. & Stappen, I. Essential Oils and Their Single Compounds in Cosmetics—A Critical Review. *Cosmetics* **5,** 11; 10.3390/cosmetics5010011 (2018).
61. Radbil', A. B., Zhurinova, T. A., Starostina, E. B. & Radbil', B. A. Preparation of High-Melting Polyterpene Resins from α-Pinene. *Russ. J. Appl. Chem.* **78,** 1126–1130; 10.1007/s11167-005-0464-z (2005).
62. Mildenberg, R., Collin, G. & Zander, M. *Hydrocarbon resins* (VCH, Weinheim, New York, 1997).
63. Pikh, Z. G., Nykulyshyn, I.Y., Rypka, A. M. & Chajkivska, R. T. Terpenes as Raw Materials for the Petroleum Resins Production. *SBUNFU* **26,** 268–274; 10.15421/40260134 (2016).

64. Hall, H. K. Synthesis and Polymerization of 3-Azabicyclo-[4.3.1]decan-4-one and 7,7-Dimethyl-2-azabicyclo[4.1.1]octan-3-one. *J. Org. Chem.* **28,** 3213–3214; 10.1021/jo01046a508 (1963).
65. Hall, H. K. Polymerization and Ring Strain in Bridged Bicyclic Compounds. *J. Am. Chem. Soc.* **80,** 6412–6420; 10.1021/ja01556a061 (1958).
66. Hall, H. K. Structural Effects on the Polymerization of Lactams. *J. Am. Chem. Soc.* **80,** 6404–6409; 10.1021/ja01556a059 (1958).
67. Hall, H. K. Synthesis and Polymerization of Atom-bridged Bicyclic Lactams. *J. Am. Chem. Soc.* **82,** 1209–1215; 10.1021/ja01490a044 (1960).
68. Hall, H. Synthesis and Polymerizability of Atom-Bridged Bicyclic Monomers. *Polymers* **4,** 1674–1686; 10.3390/polym4041674 (2012).
69. Zhao, J. & Schlaad, H. (Springer Berlin Heidelberg, Berlin, Heidelberg, 2012).
70. Corma, A., Iborra, S. & Velty, A. Chemical routes for the transformation of biomass into chemicals. *Chem. Rev.* **107,** 2411–2502; 10.1021/cr050989d (2007).
71. Winnacker, M. & Rieger, B. Recent progress in sustainable polymers obtained from cyclic terpenes: synthesis, properties, and application potential. *ChemSusChem* **8,** 2455–2471; 10.1002/cssc.201500421 (2015).
72. Winnacker, M. Pinenes. Abundant and Renewable Building Blocks for a Variety of Sustainable Polymers. *Angewandte Chemie (International ed. in English)* **57,** 14362–14371; 10.1002/anie.201804009 (2018).
73. Dakshinamoorthy, D., Weinstock, A. K., Damodaran, K., Iwig, D. F. & Mathers, R. T. Diglycerol-based polyesters: melt polymerization with hydrophobic anhydrides. *ChemSusChem* **7,** 2923–2929; 10.1002/cssc.201402249 (2014).
74. van Zee, N. J. & Coates, G. W. Alternating copolymerization of propylene oxide with biorenewable terpene-based cyclic anhydrides. A sustainable route to aliphatic polyesters with high glass transition temperatures. *Angewandte Chemie (International ed. in English)* **54,** 2665–2668; 10.1002/anie.201410641 (2015).
75. Peña Carrodeguas, L., Martín, C. & Kleij, A. W. Semiaromatic Polyesters Derived from Renewable Terpene Oxides with High Glass Transitions. *Macromolecules* **50,** 5337–5345; 10.1021/acs.macromol.7b00862 (2017).
76. Lowe, J. R., Tolman, W. B. & Hillmyer, M. A. Oxidized dihydrocarvone as a renewable multifunctional monomer for the synthesis of shape memory polyesters. *Biomacromolecules* **10,** 2003–2008; 10.1021/bm900471a (2009).
77. Lowe, J. R., Martello, M. T., Tolman, W. B. & Hillmyer, M. A. Functional biorenewable polyesters from carvone-derived lactones. *Polym. Chem.* **2,** 702–708; 10.1039/C0PY00283F (2011).
78. Wilson, J. A., Hopkins, S. A., Wright, P. M. & Dove, A. P. Synthesis and Postpolymerization Modification of One-Pot ω-Pentadecalactone Block-like Copolymers. *Biomacromolecules* **16,** 3191–3200; 10.1021/acs.biomac.5b00862 (2015).
79. Quilter, H. C., Hutchby, M., Davidson, M. G. & Jones, M. D. Polymerisation of a terpene-derived lactone: a bio-based alternative to ε-caprolactone. *Polym. Chem.* **8,** 833–837; 10.1039/C6PY02033J (2017).
80. Thomsett, M. R., Moore, J. C., Buchard, A., Stockman, R. A. & Howdle, S. M. New renewably-sourced polyesters from limonene-derived monomers. *Green Chem* **21,** 149–156; 10.1039/C8GC02957A (2019).
81. Roth, S., Funk, I., Hofer, M. & Sieber, V. Chemoenzymatic Synthesis of a Novel Borneol-Based Polyester. *ChemSusChem* **10,** 3574–3580; 10.1002/cssc.201701146 (2017).
82. Winnacker, M. & Rieger, B. Biobased Polyamides. Recent Advances in Basic and Applied Research. *Macromolecular rapid communications* **37,** 1391–1413; 10.1002/marc.201600181 (2016).

83. Firdaus, M. & Meier, M. A. R. Renewable polyamides and polyurethanes derived from limonene. *Green Chem* **15,** 370–380; 10.1039/C2GC36557J (2013).
84. Guy Donaruma, L. & Heldt, W. Z. in *Organic reactions,* edited by S. E. Denmark (Wiley, Hoboken, NJ, 2003-), pp. 1–156.
85. Winnacker, M., Sag, J., Tischner, A. & Rieger, B. Sustainable, Stereoregular, and Optically Active Polyamides via Cationic Polymerization of ε-Lactams Derived from the Terpene β-Pinene. *Macromolecular rapid communications* **38**; 10.1002/marc.201600787 (2017).
86. Winnacker, M. *et al.* Polyamide/PEG Blends as Biocompatible Biomaterials for the Convenient Regulation of Cell Adhesion and Growth. *Macromol. Rapid Commun.,* e1900091; 10.1002/marc.201900091 (2019).
87. Winnacker, M., Neumeier, M., Zhang, X., Papadakis, C. M. & Rieger, B. Sustainable Chiral Polyamides with High Melting Temperature via Enhanced Anionic Polymerization of a Menthone-Derived Lactam. *Macromolecular rapid communications* **37,** 851–857; 10.1002/marc.201600056 (2016).
88. Winnacker, M., Vagin, S., Auer, V. & Rieger, B. Synthesis of Novel Sustainable Oligoamides Via Ring-Opening Polymerization of Lactams Based on (−)-Menthone. *Macromol. Chem. Phys.* **215,** 1654–1660; 10.1002/macp.201400324 (2014).
89. Winnacker, M., Tischner, A., Neumeier, M. & Rieger, B. New insights into synthesis and oligomerization of ε-lactams derived from the terpenoid ketone (−)-menthone. *RSC Adv.* **5,** 77699–77705; 10.1039/C5RA15656D (2015).
90. Gregory, G. L., López-Vidal, E. M. & Buchard, A. Polymers from sugars: cyclic monomer synthesis, ring-opening polymerisation, material properties and applications. *Chem. Commun.* **53,** 2198–2217; 10.1039/c6cc09578j (2017).
91. Zhang, J. *et al.* Tough and Sustainable Graft Block Copolymer Thermoplastics. *ACS Macro Lett.* **5,** 407–412; 10.1021/acsmacrolett.6b00091 (2016).
92. Schneiderman, D. K. *et al.* Chemically Recyclable Biobased Polyurethanes. *ACS Macro Lett.* **5,** 515–518; 10.1021/acsmacrolett.6b00193 (2016).
93. Xiong, M., Schneiderman, D. K., Bates, F. S., Hillmyer, M. A. & Zhang, K. Scalable production of mechanically tunable block polymers from sugar. *PNAS* **111,** 8357–8362; 10.1073/pnas.1404596111 (2014).
94. Fahnhorst, G. W. & Hoye, T. R. Superabsorbent Poly(isoprenecarboxylate) Hydrogels from Glucose. *ACS Sustain. Chem. Eng. (ACS Sustainable Chemistry & Engineering)* **7,** 7491–7495; 10.1021/acssuschemeng.9b00218 (2019).
95. Kang, K.-S., Hong, Y.-K., Kim, Y. J. & Kim, J. H. Synthesis and properties of Nylon 4/5 copolymers for hydrophilic fibers. *Fibers Polym.* **15,** 1343–1348; 10.1007/s12221-014-1343-0 (2014).
96. Kricheldorf, H. R., Coutin, B. & Sekiguchi, H. 13C-NMR sequence analysis. 19. Anionic copolymerization of γ-butyrolactam, δ-valerolactam, and caprolactam at low temperatures. *J. Polym. Sci. Polym. Chem. Ed.* **20,** 2353–2370; 10.1002/pol.1982.170200901 (1982).
97. Liu, R. *et al.* Nylon-3 polymers with selective antifungal activity. *J. Am. Chem. Soc.* **135,** 5270–5273; 10.1021/ja4006404 (2013).
98. Liu, R. *et al.* Tuning the biological activity profile of antibacterial polymers via subunit substitution pattern. *J. Am. Chem. Soc.* **136,** 4410–4418; 10.1021/ja500367u (2014).
99. Mowery, B. P., Lindner, A. H., Weisblum, B., Stahl, S. S. & Gellman, S. H. Structure-activity relationships among random nylon-3 copolymers that mimic antibacterial host-defense peptides. *J. Am. Chem. Soc.* **131,** 9735–9745; 10.1021/ja901613g (2009).
100. Liu, R., Masters, K. S. & Gellman, S. H. Polymer chain length effects on fibroblast attachment on nylon-3-modified surfaces. *Biomacromolecules* **13,** 1100–1105; 10.1021/bm201847n (2012).
101. Dane, E. L. & Grinstaff, M. W. Poly-amido-saccharides: synthesis via anionic polymerization of a β-lactam sugar monomer. *J. Am. Chem. Soc.* **134,** 16255–16264; 10.1021/ja305900r (2012).

102. Zhang, J., Gellman, S. H. & Stahl, S. S. Kinetics of Anionic Ring-Opening Polymerization of Variously Substituted β-Lactams. Homopolymerization and Copolymerization. *Macromolecules* **43,** 5618–5626; 10.1021/ma1010809 (2010).

103. Zhang, J., Kissounko, D. A., Lee, S. E., Gellman, S. H. & Stahl, S. S. Access to Poly-β-Peptides with Functionalized Side Chains and End Groups via Controlled Ring-Opening Polymerization of β-Lactams. *J. Am. Chem. Soc.* **131,** 1589–1597; 10.1021/ja8069192 (2009).

104. Seebach, D., Beck, A. K. & Bierbaum, D. J. The world of beta- and gamma-peptides comprised of homologated proteinogenic amino acids and other components. *Chem. Biodivers.* **1,** 1111–1239; 10.1002/cbdv.200490087 (2004).

105. Chakraborty, S. *et al.* Ternary nylon-3 copolymers as host-defense peptide mimics. Beyond hydrophobic and cationic subunits. *J. Am. Chem. Soc.* **136,** 14530–14535; 10.1021/ja507576a (2014).

106. Bestian, H., Kaiser, E. & Korbanka, H. *Homo- and copolymers of 4-vinyl-4-methyl-azetidinone-2 and process for their manufacture ,*

107. Gramlich, W. M., Theryo, G. & Hillmyer, M. A. Copolymerization of isoprene and hydroxyl containing monomers by controlled radical and emulsion methods. *Polym. Chem.* **3,** 1510; 10.1039/c2py20072d (2012).

108. Fournier, L. *et al.* Facile and efficient chemical functionalization of aliphatic polyesters by cross metathesis. *Polym. Chem.* **7,** 3700–3704; 10.1039/C6PY00664G (2016).

109. Crivello, J. V. Vinyl epoxide accelerators for the photoinitiated cationic polymerization of oxetane monomers. *Polymer* **64,** 227–233; 10.1016/j.polymer.2015.01.019 (2015).

110. Ito, O. *et al.* Kinetics of ring-opening radical polymerization of vinyloxiranes. *Int. J. Chem. Kinet.* **23,** 853–860; 10.1002/kin.550231002 (1991).

111. Kanazawa, A. & Aoshima, S. Frequency control of crossover reactions in concurrent cationic vinyl-addition and ring-opening copolymerization of vinyl ethers and oxiranes: specific roles of weak Lewis bases and solvent polarity. *Polym. Chem.* **6,** 5675–5682; 10.1039/C5PY00152H (2015).

112. Kanazawa, A., Kanaoka, S. & Aoshima, S. Rational Design of Oxirane Monomers for Efficient Crossover Reactions in Concurrent Cationic Vinyl-Addition and Ring-Opening Copolymerization with Vinyl Ethers. *Macromolecules* **47,** 6635–6644; 10.1021/ma501707a (2014).

113. Graf, R. Reactions withN-Carbonylsulfamoyl Chloride. *Angew. Chem. Int. Ed. Engl.* **7,** 172–182; 10.1002/anie.196801721 (1968).

114. Graf, R. Umsetzungen mitN-Carbonyl-sulfamidsäurechlorid, III. Umsetzungen mit Olefinen und Aldehyden; über β-Lactame. *Justus Liebigs Ann. Chem.* **661,** 111–157; 10.1002/jlac.19636610109 (1963).

115. Cossio, F. P., Roa, G., Lecea, B. & Ugalde, J. M. Substituent and Solvent Effects in the [2 + 2] Cycloaddition Reaction between Olefins and Isocyanates. *J. Am. Chem. Soc.* **117,** 12306–12313; 10.1021/ja00154a033 (1995).

116. Deprès, J.-P., Greene, A. E. & Crabbé, P. β-Lactam prostaglandins. *Tetrahedron Lett.* **19,** 2191–2194; 10.1016/S0040-4039(01)86842-8 (1978).

117. Haug, T., Lohse, F., Metzger, K. & Batzer, H. Herstellung und Umsetzungen von β-Lactamen. *Helv. Chim. Acta* **51,** 2069–2089 (1968).

118. Hoffmann, H. & Diehr, H. J. Einwirkung von n-carbonyl-sulfamidsäurechlorid auf diene. *Tetrahedron Lett.* **4,** 1875–1879; 10.1016/S0040-4039(01)90933-5 (1963).

119. Moriconi, E. J. & Meyer, W. C. 1,2- and 1,4-cycloaddition of chlorosulfonyl isocyanate to dienes. *Tetrahedron Lett.* **9,** 3823–3827; 10.1016/S0040-4039(01)99111-7 (1968).

120. Dahn, H. *et al.* ber die Entstehung von ? -Keto-carbonium-Ionen bei der surekatalysierten Hydrolyse von Diazoketonen. (Vorlufige Mitteilung). *Helv. Chim. Acta* **51,** 2065–2069; 10.1002/hlca.19680510827 (1968).

121. Paul A. O'Gorman. Phd thesis. Univerity of Huddersfield (2009).
122. Hauser, F. M. & Ellenberger, S. R. A Superior Procedure for the Preparation of 2-Azetidinones From Volatile Olefins. *Synthesis* **1987,** 324; 10.1055/s-1987-27936 (1987).
123. Moriconi, E. J. & Meyer, W. C. Reaction of dienes with chlorosulfonyl isocyanate. *J. Org. Chem.* **36,** 2841–2849; 10.1021/jo00818a025 (1971).
124. Reichardt, C. *Solvents and Solvent Effects in Organic Chemistry.* 3rd ed. (Wiley-VCH, Weinheim, 2006).
125. Barrett, A. G. M., Betts, M. J. & Fenwick, A. Acyl and sulfonyl isocyanates in .beta.-lactam synthesis. *J. Org. Chem.* **50,** 169–175; 10.1021/jo00202a006 (1985).
126. Klimczak, U. K. & Zambroń, B. K. Effective 1,5-stereocontrol in Pd(0)/InI promoted reactions of chiral N-Ts-4-vinylazetidin-2-ones with aldehydes. An efficient entry into nonracemic semi-protected (3Z)-2,6-anti-enediols. *Chem. Commun.* **51,** 6796–6799; 10.1039/c5cc01485a (2015).
127. Socolsky, C. & Plietker, B. Total synthesis and absolute configuration assignment of MRSA active garcinol and isogarcinol. *Chem. Eur. J.* **21,** 3053–3061; 10.1002/chem.201406077 (2015).
128. Ranganathan, S., Gärtner, T., Wiemann, L. O. & Sieber, V. A one pot reaction cascade of in situ hydrogen peroxide production and lipase mediated in situ production of peracids for the epoxidation of monoterpenes. *J. Mol. Catal. B: Enzym.* **114,** 72–76; 10.1016/j.molcatb.2014.12.008 (2015).
129. Murphy, A., Dubois, G. & Stack, T. D. P. Efficient epoxidation of electron-deficient olefins with a cationic manganese complex. *J. Am. Chem. Soc.* **125,** 5250–5251; 10.1021/ja029962r (2003).
130. Broshears, W. C., Esteb, J. J., Richter, J. & Wilson, A. M. Simple Epoxide Formation for the Organic Laboratory Using Oxone. *J. Chem. Educ.* **81,** 1018; 10.1021/ed081p1018 (2004).
131. Dong, J. J. *et al.* Oxidation of Alkenes with H 2 O 2 by an in-Situ Prepared Mn(II)/Pyridine-2-carboxylic Acid Catalyst and the Role of Ketones in Activating H 2 O 2. *ACS Catal.* **2,** 1087–1096; 10.1021/cs3002226 (2012).
132. Vartzouma, C., Evaggellou, E., Sanakis, Y., Hadjiliadis, N. & Louloudi, M. Alkene epoxidation by homogeneous and heterogenised manganese(II) catalysts with hydrogen peroxide. *J. Mol. Catal. A: Chem.* **263,** 77–85; 10.1016/j.molcata.2006.08.025 (2007).
133. Cheung, S., McCarl, V., Holmes, A. J., Coleman, N. V. & Rutledge, P. J. Substrate range and enantioselectivity of epoxidation reactions mediated by the ethene-oxidising Mycobacterium strain NBB4. *Appl. Microbiol. Biotechnol.* **97,** 1131–1140; 10.1007/s00253-012-3975-6 (2013).
134. Choi, J., Oh, E.-T. & Koo, S. A chain extension method for apocarotenoids; lycopene and lycophyll syntheses. *Arch. Biochem. Biophys.* **572,** 142–150; 10.1016/j.abb.2014.12.028 (2015).
135. Macharla, A. K., Chozhiyath Nappunni, R. & Nama, N. Regio- and stereoselective hydroxybromination and dibromination of olefins using ammonium bromide and oxone®. *Tetrahedron Lett.* **53,** 1401–1405; 10.1016/j.tetlet.2012.01.026 (2012).
136. Kumar, M. A., Naresh, M., Rohitha, C. N. & Narender, N. Alkoxybromination of Olefins Using Ammonium Bromide and Oxone. *Synth. Commun.* **43,** 3121–3129; 10.1080/00397911.2012.761238 (2013).
137. Ishmuratov, G. Y. *et al.* Synthetic Approaches to Optically Active Macrolides Containing Hydrazide Fragments of L-(+)-Tartaric Acid from (+)-3-Carene, (+)-α-Pinene, and S-(–)-Limonene. *Chem. Nat. Compd.* **50,** 658–660; 10.1007/s10600-014-1046-1 (2014).
138. Dakdouki, S. C., Villemin, D. & Bar, N. On-Column Solvent-Free Oxidative Cleavage Reactions of Vicinal Diols by Silica Gel and Paraperiodic Acid: Application to In-Situ Sequential Oxidation and Knoevenagel Reactions. *Eur. J. Org. Chem.* **2012,** 780–784; 10.1002/ejoc.201101329 (2012).
139. Pérez, I. & Ávila-Zárraga, J. G. Synthesis of puleganic amides via a catalytically efficient two-step approach. *Tetrahedron Letters* **59,** 3077–3079; 10.1016/j.tetlet.2018.06.067 (2018).

140. Daeppen, C., Kaiser, M., Neuburger, M. & Gademann, K. Preparation of Antimalarial Endoperoxides by a Formal 2 + 2 + 2 Cycloaddition. *Organic letters* **17,** 5420–5423; 10.1021/acs.orglett.5b02773 (2015).

141. Brown, P. A. *et al.* Dialdehyde Production during Direct Dissociation of Energy-rich Criegee Intermediates Produced by Ozonolysis of Cycloalkenes. *Chem. Lett.* **45,** 916–918; 10.1246/cl.160294 (2016).

142. Spannring, P., Yazerski, V., Bruijnincx, P. C. A., Weckhuysen, B. M. & Klein Gebbink, R. J. M. Fe-catalyzed one-pot oxidative cleavage of unsaturated fatty acids into aldehydes with hydrogen peroxide and sodium periodate. *Chemistry (Weinheim an der Bergstrasse, Germany)* **19,** 15012–15018; 10.1002/chem.201301371 (2013).

143. in *Clinical guide to bioweapons and chemical agents,* edited by V. E. Friedewald (Springer London, London, 2008), pp. 367–370.

144. Cha, J. S. Recent Developments In Meerwein−Ponndorf−Verley and Related Reactions for the Reduction of Organic Functional Groups Using Aluminum, Boron, and Other Metal Reagents: A Review. *Org. Process Res. Dev.* **10,** 1032–1053; 10.1021/op068002c (2006).

145. Hesse, M. J., Butts, C. P., Willis, C. L. & Aggarwal, V. K. Diastereodivergent synthesis of trisubstituted alkenes through protodeboronation of allylic boronic esters: application to the synthesis of the Californian red scale beetle pheromone. *Angewandte Chemie (International ed. in English)* **51,** 12444–12448; 10.1002/anie.201207312 (2012).

146. Nicotra, F., Panza, L., Ronchetti, F., Russo, G. & Toma, L. Synthesis of enantiomerically pure 24-alkylsterol side chains, in both enantiomeric forms, starting from (R)-(+)-limonene. *J. Org. Chem.* **51,** 1272–1276; 10.1021/jo00358a020 (1986).

147. Oumer, A. N., Hasan, M. M., Baheta, A. T., Mamat, R. & Abdullah, A. A. Bio-based liquid fuels as a source of renewable energy: A review. *Renewable and Sustainable Energy Reviews* **88,** 82–98; 10.1016/j.rser.2018.02.022 (2018).

148. Wilson, J., Gering, S., Pinard, J., Lucas, R. & Briggs, B. R. Bio-production of gaseous alkenes. Ethylene, isoprene, isobutene. *Biotechnology for biofuels* **11,** 234; 10.1186/s13068-018-1230-9 (2018).

149. Wang, S. *et al.* Production of isoprene, one of the high-density fuel precursors, from peanut hull using the high-efficient lignin-removal pretreatment method. *Biotechnology for biofuels* **10,** 297; 10.1186/s13068-017-0988-5 (2017).

150. Riazi, B., Karanjikar, M. & Spatari, S. Renewable Rubber and Jet Fuel from Biomass. Evaluation of Greenhouse Gas Emissions and Land Use Trade-offs in Energy and Material Markets. *ACS Sustainable Chem. Eng.* **6,** 14414–14422; 10.1021/acssuschemeng.8b03098 (2018).

151. Beller, H. R., Lee, T. S. & Katz, L. Natural products as biofuels and bio-based chemicals. Fatty acids and isoprenoids. *Natural product reports* **32,** 1508–1526; 10.1039/c5np00068h (2015).

152. Chaves, J. E. & Melis, A. Engineering isoprene synthesis in cyanobacteria. *FEBS letters* **592,** 2059–2069; 10.1002/1873-3468.13052 (2018).

153. Pahima, E., Hoz, S., Ben-Tzion, M. & Major, D. T. Computational design of biofuels from terpenes and terpenoids. *Sustainable Energy Fuels* **3,** 457–466; 10.1039/C8SE00390D (2019).

154. Li, M. *et al.* Improvement of isoprene production in Escherichia coli by rational optimization of RBSs and key enzymes screening. *Microbial cell factories* **18,** 4; 10.1186/s12934-018-1051-3 (2019).

155. Lu, X. *Biofuels. From microbes to molecules* (Caister Academic Press, Norfolk, 2014).

156. Hauenstein, O., Agarwal, S. & Greiner, A. Bio-based polycarbonate as synthetic toolbox. *Nat. Commun.* **7,** 11862 EP -; 10.1038/ncomms11862 (2016).

157. Lochyński, S., Kułdo, J., Frąckowiak, B., Holband, J. & Wójcik, G. Stereochemistry of terpene derivatives. Part 2. Synthesis of new chiral amino acids with potential neuroactivity. *Tetrahedron: Asymmetry* **11,** 1295–1302; 10.1016/S0957-4166(00)00058-6 (2000).

158. Koltzenburg, S., Maskos, M., Nuyken, O., Mülhaupt, R. & Matyjaszewski, K. *Polymer chemistry* (Springer, Berlin, Heidelberg, 2017).

159. Shaabani, A. & Ameri, M. Oxidation of Benzylic and Secondary Alcohols to Carbonyl Compounds by NaBrO3–NH4Cl Reagent in Aqueous Acetonitrile†. *J. Chem. Res.,* 100–101; 10.1039/a701647f (1998).

160. Schulze, A., Pagona, G. & Giannis, A. Oxone/Sodium Chloride: A Simple and Efficient Catalytic System for the Oxidation of Alcohols to Symmetric Esters and Ketones. *Synth. Commun.* **36,** 1147–1156; 10.1080/00397910500514030 (2006).

161. Winnacker, M. & Sag, J. Sustainable terpene-based polyamides via anionic polymerization of a pinene-derived lactam. *Chemical communications (Cambridge, England)* **54,** 841–844; 10.1039/c7cc08266e (2018).

162. Musser, M. T. in *Ullmann's Encyclopedia of Industrial Chemistry* (Wiley-VCH Verlag GmbH & Co. KGaA, Weinheim, Germany, 2000).

163. Stockmann, P. Master thesis: Synthesis of α-pinene derived ε- and β-lactams and primary polymerization thereof. *Fraunhofer IGB, Bio, Electro and Chemocatalysis BioCat, Straubing branch* (2015).

164. Stockmann, P. N. *et al.* New Bio-Polyamides from Terpenes. A-Pinene and (+)-3-Carene as Valuable Resources for Lactam Production. *Macromol. Rapid Commun.* **40,** e1800903; 10.1002/marc.201800903 (2019).

165. Holmes, D. R., Bunn, C. W. & Smith, D. J. The crystal structure of polycaproamide: Nylon 6. *J. Polym. Sci.* **17,** 159–177; 10.1002/pol.1955.120178401 (1955).

166. Sousa, A. F. *et al.* Biobased polyesters and other polymers from 2,5-furandicarboxylic acid: a tribute to furan excellency. *Polym. Chem.* **6,** 5961–5983; 10.1039/C5PY00686D (2015).

167. Atta, A. M., Mansour, R. & Abdou, M. I. *Process for preparing a furan-bsaed polyamide, a furan-based oligomer and compositions and srticles comprising the furan-based polyamide* (2014).

168. Duursma, A., Aberson, R., Smith, D., Flores, J. & Gruter, G. J. M. *Process for preparing a furan-bsaed polyamide, a furan-based oligomer and compositions and srticles comprising the furan-based polyamide* (2014).

169. Day, M. & Wiles, D. M. Photochemical degradation of poly(ethylene terephthalate). II. Effect of wavelength and environment on the decomposition process. *J. Appl. Polym. Sci.* **16,** 191–202; 10.1002/app.1972.070160117 (1972).

170. Parvin, M. & Williams, J. G. The effect of temperature on the fracture of polycarbonate. *J Mater Sci* **10,** 1883–1888; 10.1007/BF00754478 (1975).

171. Matsuoka, S. & Ishida, Y. Multiple transitions in polycarbonate. *J. polym. sci., C Polym. symp.* **14,** 247–259; 10.1002/polc.5070140118 (1966).

172. Radzik, P., Leszczyńska, A. & Pielichowski, K. Modern biopolyamide-based materials: synthesis and modification. *Polym. Bull.* **77,** 501–528; 10.1007/s00289-019-02718-x (2020).

173. Kim, S. J. *et al.* Photoactive polyamideimides synthesized by the polycondensation of azo-dye diamines and rosin derivative. *J. Appl. Polym. Sci.* **79,** 687–695; 10.1002/1097-4628(20010124)79:4<687::AID-APP130>3.0.CO;2-9 (2001).

174. Atta, A. M., Mansour, R., Abdou, M. I. & Sayed, A. M. Epoxy resins from rosin acids: synthesis and characterization. *Polym. Adv. Technol.* **15,** 514–522; 10.1002/pat.507 (2004).

175. Moore, J. C., Pollard, D. J., Kosjek, B. & Devine, P. N. Advances in the enzymatic reduction of ketones. *Accounts of chemical research* **40,** 1412–1419; 10.1021/ar700167a (2007).